Influence of the Gravity System on the Seismic Performance of Special Steel Moment Frames

Francisco Xavier Flores Solano

Dissertation submitted to the faculty of the Virginia Polytechnic Institute and State University in partial fulfillment of the requirements for the degree of

Doctor of Philosophy
In
Civil Engineering

Finley A. Charney Chair
Diego López-García Gonzalez
Matthew R. Eatherton
Roberto T. Leon

March 2, 2015
Blacksburg VA

Keywords: Gravity System, Partially Restrained Connections, Special Moment Frames, Gravity Columns Continuity, Splices, FEMA P-695, Collapse Performance.

Influence of the Gravity System on the Seismic Performance of Special Steel Moment Frames

Francisco Flores

Abstract

This study investigates the influence of the gravity load resisting system on the collapse performance of Special Steel Moment Frames (SMFs). The influence was quantified using the FEMA P-695 methodology. The buildings used for this study were a 2-, 4- and 8-story SMFs taken from the ATC76-1 project where their collapse performance was already evaluated without the gravity system. The main work of this dissertation has been divided in two parts. The first part studies the influence of the gravity system when it is incorporated explicitly as part of the lateral resisting system. Aspects of the gravity frame that were investigated include the contribution of stiffness and strength of beam to column connections, and the location of splices in the gravity columns. Moreover, this research investigates the potential for the development of inelastic deformations in the gravity columns, and the effect of such deformations on structural response. The results show that gravity connections and gravity column's continuity profoundly affect the computed response and collapse probability. The inelastic behavior in gravity columns has a less important effect but should be included in the analysis.

The second part of the investigation looks more in depth at the role of the gravity columns on the collapse performance of SMFs. Using the 2-, 4- and 8-story SMFs, the gravity columns are incorporated using the approach where all the gravity columns are lumped into one elastic, pinned at the base and continuous element. The approach is first validated by checking different aspects such as: strength of gravity connections to induce yielding into gravity columns, difference between the explicit and lumping column approach, and required gravity column’s splices to provide continuity. The stiffness of the element representing the gravity columns was varied in order to find the influence of the gravity columns. At the end of the study it was found that they have a significant influence on the collapse performance of SMFs, especially on taller structures like the 8-story model. Moreover it was concluded that an adequate stiffness of the gravity columns could be found by performing nonlinear static pushover analysis.

Acknowledgments

First, I would like to thank God for so many blessings and opportunities throughout my life. I would especially like to thank my advisor, Dr. Finley Charney who turned into a close friend throughout this process. I will be eternally grateful for him giving me the opportunity to work with him and making it possible to accomplish the biggest achievement of my life. He helped me uncover what I am truly passionate about and set goals beyond what I had planned for myself. I want to thank him for teaching me how to find my own path to do research that allowed me to make his project my own. I am grateful for his patience, guidance, expertise and encouragement. I would also like to thank my advisor at the Pontifical Catholic University, Dr. Lopez-Garcia for his unconditional technical and personal support through this time. Thank you to my committee, Dr. Matthew Eatherton and Dr. Roberto Leon for their guidance and assistance while serving on my committee.

I want to thank my father and my mother, Francisco Flores Crespo and Ana Lucia Solano for encouraging me to complete this objective. For listening to me during difficult times, for giving me strength when I needed it and for showing so much interest in my research even though it was sometimes impossible to understand. I would have never achieved my goals without their example of hard work and life lessons. I want to especially thank my fiancé Alexandra Shourds for her infinite support and for waiting for me to complete my studies. Without the internal peace that I found since I met her it would have been very difficult to work on this degree. I am so grateful to my brother and sister for their support and for believe in me to pursue my Ph.D.

I would also like to thank Dr. Andy Hardyneic of Virginia Tech for his work creating the FEMA P-695 Toolkit. I am also appreciative of my colleagues Dr. Ozgur Atlayan, Jeena Jayamon and Johnn Judd for their contribution and collaboration.

Table of Contents

List of Figures

List of Tables

Chapter 1: Introduction

1.1 Overview and Motivation of Work

Advances in technology and computers have made it possible to analyze structures using improved and more detailed mathematical models. However, in spite of the drastic increase in computer speed and storage capacity over the past several decades, the modeling methodologies used in practice have just begun to adapt to these capabilities. A clear example is the seismic analysis of structures in which the analytical model takes into consideration only the main lateral load resisting system and neglects the gravity system. Recently, there is a trend taken by guidelines such as the PEER/ATC 72-1 [1], ASCE 41-13 [2] and the Appendix F of FEMA P-695 [3], where the gravity is encouraged to be included. The PEER/ATC 72-1 report states that the gravity system can provide significant benefits for lateral stability at large displacements and it can be included if desired. ASCE 41-13 requires the incorporation of secondary components (gravity system) to perform nonlinear static or nonlinear dynamic analysis. Appendix F of FEMA P-695 states that the collapse modes of the gravity system must be checked in the collapse assessment process, but leaves its incorporation as an option.

Regardless of the progress made by the aforementioned guidelines, ignoring the strength and stiffness of the gravity system is still typical in structural analysis. Addressing this issue should be a priority based on the reality from past earthquakes and from previous investigations which have shown that the gravity system can influence the response of the structure. During the Northridge earthquake in 1994, many steel frames presented brittle failures in critical beam-to-column connections, but the structures did not collapse. The most probable reason is that the buildings remained standing due to the gravity framing acting as a “backup system” preventing the structural collapse subsequent to the failure of the connections [4]. As a consequence of the

damage caused by this earthquake, great effort was made to evaluate the current state of practice in steel design [5-8]. One of the areas that researchers focused on was the cyclic capacity of simple gravity connections. Liu and Astaneh [9] studied these connections showing that their flexural capacity is not negligible and their rotation capacity is high.

Another investigation carried out as a consequence of the Northridge earthquake was performed by Gupta and Krawinkler [10]. One of the purposes of the study was to identify the influence of modeling details to evaluate the seismic response of Steel Special Moment Frames (SMFs). An important conclusion made by the authors is that gravity columns can increase significantly the post yield stiffness of structures. As a result of this, the seismic response of SMFs improves when they are subjected to large earthquakes. Additionally the authors concluded that the influence of simple connections is less important if the connections in the main lateral resisting system do not exhibit brittle failures.

Based on what was learned from past earthquakes and from different investigations on SMFs, it has been identified that the gravity system has an important role on the structural response when it is subjected to large earthquakes and undergoes large deformations. This suggests that the gravity system could have an important influence on the collapse performance of SMFs. Currently the FEMA P-695 methodology is the procedure developed to quantify the seismic response factors of a structural system. In the case of the SMFs, according to the ASCE7-10 [11], the response modification factor (R) is equal to 8, the deflection amplification factor (C_d) is equal to 5.5 and the overstrength factor is equal to 3. A key component to the application of the P-695 Methodology is an assessment of the probability of collapse of the system. In the existing version of P-695 the integration of the gravity system in the mathematical model is not permitted in analysis used to determine performance factors, and this is attributed to

the fact that gravity system configurations are highly variable cannot be predefined when analyzing generic archetypes. Thus it is clear that more research is necessary to determine the influence of the gravity system on the collapse performance and to develop or propose a generic way to include the gravity system in the analytical model. These two research needs are the main motivation for this study.

The ATC 76-1 project [12] was an extension of the investigation that resulted from the publication of the FEMA P-695 report. It expands the testing of the FEMA P-695 methodology to additional seismic force-resisting systems. One of these systems, Steel Special Moment Frames, were evaluated by Zareian et al. [13]. These structures were analyzed without the gravity system as required by the methodology. In the study presented herein, a variety of SMF buildings utilized in the ATC 76-1 project are analyzed with and without the gravity system to establish the influence on the seismic response. In order to evaluate the influence of the different components of the gravity system, the gravity columns, beams and gravity connections are explicitly modeled. The aspects investigated are: the influence of the gravity connections flexural strength, the influence of the gravity columns, yielding in gravity columns, and the influence of gravity columns splices.

The first part of the study is dedicated to study all the aforementioned parameters. In order to do so, multiple models were developed and thousands of analyses were performed. The investigation started with the influence of the gravity connections, where they are considered to be Partially Restrained (PR) with varying flexural strength capacities. Among the cases studies it is a case in which the PR connections are considered to have no flexural strength. This particular case is used to investigate the influence of only the gravity columns on the collapse performance of SMFs. The next step is to evaluate if yielding in the gravity columns is occurring and if it is

influencing the collapse performance of the structure. In this case, two different analyses are implemented: one with the gravity columns behaving elastically and another with the gravity columns modeled with the capability to capture any inelastic behavior. Finally, the influence of splices on the gravity columns is investigated by incorporating them into the model using two different patterns: leveled and staggered. The leveled splices are aligned at the same height within a given story and the staggered splices are placed at different heights within a story. The splices are modeled using a true hinge, representing a lower boundary result since it is known column splices do possess some flexural strength and stiffness.

The second part of the study investigates more in depth the effect of the gravity columns as they are considered the most important component of the gravity system [10]. The importance of the gravity columns relies on the continuous stiffness that they provide when they are continuous all over their height or if their splices provide full moment capacity. The continuous stiffness concept acknowledges that: "If columns are continuous over several stories of a structure, then the stiffness of the columns will limit the amount of drift concentration that can occur" [14]. Therefore, this concept could fulfill a current need presented in the ATC 76-1 project where it is stated that "there is a need to develop design concepts that prevent (or at least delay) the formation of partial mechanisms in lower stories of special SMF systems" [12].

Additionally if only the gravity columns are incorporated in the analysis, a generic approach of including them as part of the lateral resisting system is possible. The approach, called in this dissertation lumped column approach, lumps all the gravity columns into one elastic, continuous element pinned at the base of the structure. Thus this element can represent different configurations of the gravity system with a different number of columns or column sections. The performance of the buildings taken from ATC 76-1 is improved using the gravity

columns. To do so, the properties of the lumped column element are varied and the performance evaluated using the FEMA P-695 methodology.

The main outcome expected from this dissertation is to present the importance of analyzing a structure in a more realistic manner. Evaluating the influence of the different gravity system components will give insight to improved and more rational mathematical models when SMFs are and analyzed. In addition, as a result of the experience acquired from this study, a guideline to include the gravity system as part of the lateral resisting system is proposed.

The results of the investigation could be a deciding factor to conduct more research to modify the current seismic coefficient factors of SMFs.

1.2 Dissertation Organization

This dissertation is organized using the manuscript format, where some of the traditional chapters are replaced by articles that have been submitted to peer-reviewed journals or conferences. For this dissertation, two journal papers, supporting studies, and three conference papers are presented.

The dissertation begins with a literature review in Chapter 2 to provide additional background on numerous topics of interest, including: (1) Influence of Gravity System, (2) Continuous Stiffness of the Gravity Columns, and (3) Partially Restrained Connections. Chapter 3 summarizes the procedures and assumptions used to model the buildings analyzed in the dissertation. Chapter 4 is a manuscript published in the *Journal of Constructional Steel Research* titled "Influence of the Gravity Framing System on the Collapse Performance of Special Steel Moment Frames". Chapter 5 is a manuscript to be submitted also to the *Journal of Constructional Steel Research* and it is titled "The Influence of Gravity Column Continuity on the Seismic Performance of Special Steel Moment Frame Structures". Chapter 6 presents a

variety of supportive studies performed to complement this dissertation. Chapter 7 proposed guidelines to include the gravity system as part of the lateral resisting system in SMFs. Chapter 8 summarizes the results, gives overall conclusions, and provides recommendations for future work. For clarity purposes, references are provided at the end of each chapter. Finally, four appendices are provided. Appendix A is a conference paper titled "The Influence of Gravity Column Continuity on the Collapse Performance of Special Steel Moment Frames", which was presented in the *10th U.S. National Conference on Earthquake Engineering*. Appendix B is a conference paper titled "The Influence of the Gravity System Framing on The Seismic Performance of Special Steel Moment Frames", which was presented at the *10th U.S. National Conference on Earthquake Engineering*. Appendix C is a conference paper entitled "Seismic Performance of Special Steel Moment Frames Including the Gravity System", which has been submitted to the *11th Chilean Conference on Seismology and Earthquake Engineering*. Appendix D presents complementary results that could not be included in the published in the papers due to space limitations.

1.3 References

[1] PEER, Modeling and Acceptance Criteria for Seismic Design and Analysis of Tall Buildings (PEER/ATC 72-1), Richmond California, 2010.

[2] ASCE, Seismic Rehabilitation of Existing Buildings (ASCE/SEI 41-13), American Society of Civil Engineers Reston, Virginia, 2013.

[3] F. P695, Quantification of Building Seismic Performance Factors, Fededral Emergency Management Agency, Washington, D.C, 2009.

[4] R.T. Leon, Composite connections, Progress in Structural Engineering and Materials, 1 (1998) 159-169.

[5] S.J. Venture, State of the Art Report on Systems Performance of Steel Moment Frames Subject to Earthquakes, Report No. FEMA-355C, Washington (DC): Federal Emergency Management Agency (FEMA), 2000.

[6] S.J. Venture, State of the Art Report on Connection Performance, Report No. FEMA-355D, Washington (DC): Federal Emergency Management Agency (FEMA), 2000.

[7] S.J. Venture, State of the Art Report on Past Performance of Steel Moment-Frame Buildings in Earthquakes, Report No. FEMA-355E, Washington (DC): Federal Emergency Management Agency (FEMA), 2000.

[8] S.J. Venture, State of the Art Report on Performance Prediction and Evaluation of Steel Moment-Frame Buildings, Report No. FEMA-355F, Washington (DC): Federal Emergency Management Agency (FEMA), 2000.

[9] J. Liu, A. Astaneh-Asl, Cyclic testing of simple connections including effects of slab, Journal of Structural Engineering, 126 (2000) 32-39.

[10] A. Gupta, H. Krawinkler, Seismic demands for the performance evaluation of steel moment resisting frame structures, in, Stanford University, 1999.

[11] ASCE, Minimum design loads for buildings and other structures, American Society of Civil Engineers : Structural Engineering Institute, Reston, Va., 2010.

[12] NIST, Evaluation of the FEMA P-695 Methodology for Quantification of Building Seismic Performance Factors, National Institute of Standards and Technology, USA, 2010.

[13] F. Zareian, D. Lignos, H. Krawinkler, Evaluation of seismic collapse performance of steel special moment resisting frames using FEMA P695 (ATC-63) methodology, in: Proceedings of Structures Congress ASCE, New York, 2010.

[14] G.A. MacRae, The Continuous Column Concept-Development and Use, Proceedings of the Ninth Pacific Conference on Earthquake Engineering Building an Earthquake-Resilient Society, (2011).

Chapter 2: Literature Review

2.1 Introduction

This chapter of the dissertation provides background about several topics that are of special interest to this investigation. As described in the previous chapter, the main goal of this study is to evaluate the influence of the gravity system on the seismic performance of Special Steel Moment Frames (SMFs). However, it is recognized that the components of the gravity system that contribute the most to the performance are the gravity columns and the gravity connections which in turn depend on the beams. In the case of the gravity columns they can provide what is called continuous stiffness. Therefore, the literature provided in this section has been divided in three parts: 1) SMFs including the gravity system, 2) Gravity Connections and 3) Continuous Stiffness.

The first subsection summarizes different investigations on SMFs in which the gravity system has been incorporated as part of the main lateral load resisting system. The second part of this chapter reviews previous studies related to gravity connections. The last section of the chapter is dedicated to review the effect that continuous column stiffness has on structures.

2.2 Past Research on SMFs Including the Gravity System.

Several studies have been performed in the U.S. to evaluate the performance of SMFs. However, there are only a few studies where the gravity system is included and its influence is quantified. The study performed by Gupta and Krawinkler [1] was one of the investigations executed as a result of the of the Northridge earthquake consequences in 1994. The main objective of the investigation was to understand the inelastic behavior of SMFs. For this matter, topics such as P-Delta effects, the influence of accuracy in analytical modeling, and the influence of the gravity connection's strength, among others, were identified, addressed and quantified.

Structures of 3-, 9-, and 20-stories were analyzed in different locations within U.S., including Boston, Los Angeles and Seattle. Additionally, pre- and post- Northridge designs were evaluated to quantify the improvements of the changes made as a result of the earthquake.

To establish the importance of the analytical model, nonlinear static and dynamic analyses were performed on a variety of different models. The first model was a basic centerline model (M1), the second model included explicitly the strength and stiffness of the panel zone (M2). The third and fourth models included the gravity system. The third model (M2A(1) had a positive (top fibers in compression) and negative flexural strength equal to $0.4M_p$ and $0.2M_p$ respectively. On the other hand the fourth model (M2A(2)) had a positive and negative flexural strength equal to $0.2M_p$ and $0.1M_p$ respectively.

The gravity system was modeled using an equivalent one-bay frame placed parallel to the SMF. The stiffness and bending strength of the columns were computed depending on their bending axis orientation. The effect of all the gravity columns and the orthogonal moment resisting frame's columns were included. The gravity connections were defined with a simple rotational spring with an elasto-plastic behavior. The maximum flexural strength was achieved at a rotation of 0.02 radians under compression and 0.01 radians for tension.

After performing nonlinear static and dynamic analyses using the pre-Northridge models, the main findings of interest for this investigation were:

- The incorporation of the gravity system may have a substantial impact on the seismic response of the structure. The contribution is much more pronounced at high levels of ground shaking or when the building is susceptible to have problems due to P-Delta effects.

- The strength of the simple connections does not have major impact on the response of the models. However, gravity connections can become important if the moment resisting connections fracture.
- The effect of improving the model by incorporating the gravity system could be significant for taller structures. The main benefit provided by the gravity system was seen in the pushover curves where the slope of the post yield stiffness increased. The increase in was more pronounced in taller structures because are more prompt to be affected by P-Delta effects.

The Gupta and Krawinkler study also focused on the P-Delta effect. One of the problems of current codes is that the stability ratio is based on the elastic stiffness of the structure. According to this study, the stability ratio is based on the elastic stiffness due to the apparent lack of stability related failures and the to the good performance that has been attributed to the structure's overstrength. However, while it is true that displacements may be reduced by the overstrength, the dynamic P-Delta effects in an inelastic structure may be unacceptable, especially if the structure's post-yield stiffness is negative. In order to study the P-Delta effect in more detail, additional were created. One of these models was developed to evaluate the influence of the gravity columns on the structure's response. The main conclusion from this part of the study and of interest for this investigation was obtained from the pushover curves. These results showed that the gravity columns can increase the length of the strength plateau. As a result, the rotation at which the negative post-yield stiffness was reached for the model without the gravity columns was delayed. The improvement on the post-yield stiffness would solve the P-Delta problems that a structure could have. According to the authors, among all the members

and connections in the gravity system, the contribution of the gravity columns appeared to be the most important.

Lee and Foutch [2] evaluated Steel Special Moment Frames (SMFs) including the gravity system. The buildings were designed to fulfill code requirements imposed after the Northridge Earthquake in 1994. In order to assess the performance in a more realistic manner, the gravity system was incorporated as part of the mathematical model. The SMFs used Reduced Beam Section (RBS) connections and the gravity frames had simple connections with concrete slabs. The hysteretic behavior of the RBS and the simple connections was matched with laboratory tests and the analyses were performed using Drain 2DX. The objective of the study was to evaluate the performance of the structure at two different states: Immediate Occupancy (IO) at a hazard level of 50% in 50 year probability of exceedance and Collapse Performance (CP) at a 2% in 50 year probability of exceedance. A confidence factor that indicates if the structure satisfies the limit states was considered. The way this factor is computed is conceptually similar to the procedure used by FEMA P-695 Methodology [3] to establish if the probability of collapse is acceptable. The capacity of the structure is determined using Incremental Dynamic Analysis [4] and the demands for the 2% in 50 year hazard level are computed. The capacity is modified by uncertainties while the demand is adjusted by a resistance factor. Then, the confidence level is obtained by the ratio of these values. The results of the analysis showed that the designed buildings would perform well at the Maximum Considered Earthquake (MCE). Even though this study included the gravity system, their influence was not established because there was no comparison with the performance of the building considering only the main lateral resisting system.

The report NIST GCR 10-017-9 [5] presents the results of performing a nonlinear static pushover analysis using a SMF including the strength and stiffness of the gravity system. The analyzed structures were the same used by Zareian et al. [6] and the gravity system was modeled using simple shear tab connections including the effect of the concrete slab. The moment rotation curve of these connections was estimated from procedures and tests performed by Liu and Astaneh [7]. The hysteretic behavior of the gravity connections was simplified considerably and a simple elastic-perfectly plastic spring model was used. The conclusions stated in the report were that the benefits of incorporating the gravity system depends strongly on the structural configuration, but it could decrease drift demands and increase collapse capacity. Additionally, it is concluded that the gravity system could be effective in delaying or preventing dynamic instability because the gravity system increases the post-yield tangent stiffness [1].

A different prospective of the influence of the gravity system was studied by Jarret et al.[8]. In this investigation, two different structural systems one called Collapse Prevention Systems and Special Steel Moment Frames (SMFs) were studied with and without the gravity system. The effect of the gravity system was measured using the FEMA P58 [9] , which is a process that quantifies the performance of a structure in terms of casualties, repair cost, repair time and unsafe placards. The results of the study showed that including the gravity system reduces the expected average cost of repair significantly, particularly at higher intensity levels.

2.3 Gravity System Connections

This section of the chapter reviews the gravity connections. As already stated in the previous chapter, the gravity connections in this study are considered to be Partially Restrained (PR) connections.

Beam-column connections in structural analysis are usually considered to provide full moment capacity (fully restrained or fixed) or to have zero moment capacity (pinned). These assumptions make the analysis easier since the actual connections stiffness is not required to be incorporated. However, the real behavior of beam-column connections is between fixed and pinned, and they behave as partially restrained (PR) connections. The flexural behavior of these connections is commonly simulated by means of a nonlinear moment-rotation curve. Other effects such as torsion, shear, and axial deformations are neglected due to their small influence [10].

Analyzing structures with PR connections under seismic loads is still difficult. Even though extensive research has been done, the majority of laboratory tests have been executed under monotonic loads and few have been performed under cyclic loads. As a result of the monotonic tests different mathematical models that predict accurately enough the moment rotation curve of PR connections have been established. On the other hand, a phenomenological model (relatively easy to implement) that predicts the hysteretic behavior of PR connections is still required.

In order to establish whether a beam-column connection can be considered as pined, fixed or PR, building codes such as the AISC LRFD [11] have provided a classification which is based on connection strength and stiffness. The following subsections describe this classification.

2.3.1 AISC LRFD Beam-Column Classification

The classification of beam-column connections provided in different versions of the AISC has been changing. A brief description of these changes is summarized herein. The 1969 steel design specification [12] classified three types of construction:

- Type 1, or “Rigid Frames”: This construction assumes that the beam transfers the moment to the column.
- Type 2 or “Simple Frames”: This assumes that beams and girders connections transfer just the vertical shear reaction without bending moments when the structure is loaded with gravity loads.
- Type 3 or “Semi-Rigid Frames”: This assumes that the connection can transfer vertical shear and can transfer some moment.

The latter classification changed in the 1986 AISC specification [13]. Connections were designated as FR (Fully Restrained) and PR (Partially Restrained). The term “restrained” referred to the degree of moment transfer from the beam to the column. This specification also used the term “simple framing” for structures with “simple connections”. Even though the classification was modified it was equivalent to that used in 1969 (Type 1, 2 and 3). The current AISC LRFD [14] specification proposed a classification of connections based on connection stiffness, strength and ductility and is summarized in the following.

Connection Stiffness

Nonlinear behavior of connections starts at low levels of either vertical o lateral load. Therefore using the initial stiffness to classify the connection could be inaccurate. According to this specification [14], the secant stiffness (K_s) measured at service level is the factor to be used to establish the type of connection. Note that in order to establish the secant stiffness, the moment rotation curve that characterizes the connection is required. Once the secant stiffness has been defined, the beam stiffness is used as the parameter to be compared with to designate the type of connections. So, the rigidity of the connection is classified as follows:

$If \quad \frac{K_S L}{EI} \geq 20$ Fully Restrained Connection (FR)

$If \quad 1 \leq \frac{K_S L}{EI} \leq 20$ Partially Restrained Connection (PR)

$If \quad \frac{K_S L}{EI} < 1$ Simple Connection

Where L and EI are the length and bending rigidity of the beam, respectively.

Connection Strength

The strength classification of the connection is obtained by comparing the moment capacity of the connection with the plastic moment of the beam. The moment capacity of the connection is the peak moment (M_u) computed from the moment-rotation curve. If the response does not exhibit a peak, then the strength can be taken as the moment at a rotation of 0.02 radians. The strength of a connection then is classified as follows:

$If \quad M_u \geq M_{p(beam)}$ Full Strength (FS); otherwise is Partial Strength (PS) connection

Where :

M_u = Moment connection capacity

$M_{p(beam)}$ = Plastic moment capacity of the beam

Thus, a FS connection can develop the full plastic moment capacity ($M_{p(beam)}$) of the connected beam, while a PS connection can partially develop this plastic moment. A lower limit on strength has been also defined. Connections that transmit less than 20 percent of the fully plastic moment of the beam at a rotation of 0.02 radians are considered as simple connections.

Connection Ductility

If the connection strength is classified as full strength (FS), the beam controls the ductility of the system, so the moment-rotation curve for the connection is not required to be included in the analysis. However, if the connection is partial strength (PS), the ductility depends on the rotation of the connection. The ultimate rotation is measured when the strength of the

connection has reached the 80% of its maximum strength (post yield strength) value or it is measured at a rotation of 0.03 radians. So, the ductility of the connection can be classified as follows:

$If \quad \theta_u \geq 0.03 \ radians$ The connection is ductil, otherwise it is brittle

Where :

θ_u = Rotation measured when at a moment equal to 80% of maximum of moment capacity.

The aforementioned classification is used for structural systems not designed in seismic areas. The ductility of the connections according to the Seismic Design Manual [15] depends on the type of lateral resisting system. For completeness, the specific ductility requirements depending on the lateral resisting system are shown herein:

$If \quad \theta_u \geq 0.04 \ radians$ Special Steel Moment Frame is ductile

$If \quad \theta_u \geq 0.02 \ radians$ Intermediate Moment Frame is ductile

Where :

θ_u = Rotation measured when at a moment equal to 80% of maximum of moment capacity.

According to the Seismic Design Manual, even the Ordinary Moment Frame should be capable of provide at least an angle of 0.01 radians.

2.3.2 Modeling PR Connections

In order to analyze buildings with PR connections in seismic areas, the hysteretic behavior has to be defined. The accuracy or detail of this behavior depends on the type of analysis. Extensive research has been performed on PR connections. However, the majority of these tests were performed under mononotic load. Kishi and Chen [16] collected experimental data from different laboratory tests executed from 1936 to the time of the study, 1986. In this document it can be seen that moment rotation curves are available just for monotonic loads. The

same curves are reflected in Chen et al. [17]. These tests have been used to establish mathematical models that predict the PR connections behavior.

In the present, different methods are used to define the moment-rotation curves or the cyclic behavior of the PR connections. These methods are:

- Finite element analysis: modeling in detail the connection using the finite element technique.
- Mathematical models: the behavior is obtained by adjusting mathematical expressions with experimental tests.
- Mechanical models: sources of deformation in the connection are modeled individually using springs. The superposition of all these sources predicts the overall behavior of the connection.
- Experimental method: a predefined generalized hysteretic model is matched as close as possible with the cyclic behavior of a connection that has been computed in a laboratory test.

Additionally, the monotonic behavior of PR connections can also be predicted using analytical models. In this case, the curve is obtained from the geometry and mechanical properties.

2.3.2.1 Mathematical Models

This approach has been studied the most, especially for monotonic behavior. It uses parameters obtained on experimental tests. These parameters are then adjusted to mathematical expressions that predict the moment rotation curve of the beam-column connection. There are several models that have been suggested by different authors, the vast majority used to predict

monotonic behavior. Some of these models that predict the monotonic behavior of PR connections are:

a. Linear Model [18-20]
b. Multi-linear Model [21, 22].
c. Polynomial Model [23].
d. Cubic B-Spline Model [24].
e. Richard Model [25, 26].
f. Ramberg-Osgood Model [27]
g. Exponential Model [16]
h. AISC Design Guide 8 [28]
i. ASCE 41-13 [29]

Among all these mathematical models, the one chosen for this investigation is the one given by ASCE 41-13 and the methodology to implement it is described herein. In the case of the cyclic behavior of these connections, there are fewer mathematical methods, some of these are:

a. Model proposed by De Martino et al. [30].

2.3.2.1.1 Moment Rotation Curve (ASCE/SEI 41-13)

Partially restrained connections can be modeled using a moment-rotation behavior given by ASCE [38]. This model was defined from extensive laboratory tests performed on PR connections. According to this code, it can be used in lieu of relationships derived from experiments or analysis. The generalized load-deformation provided by this code is shown in Figure 2-1.

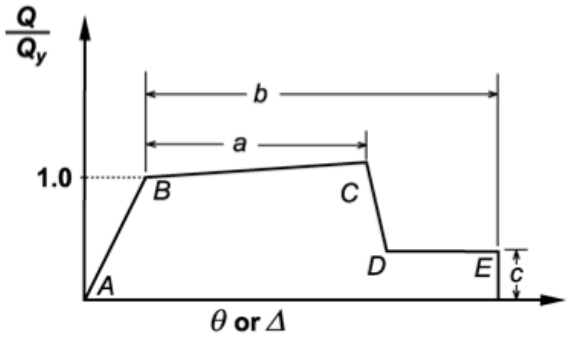

Figure 2-1 Generalized Moment-Rotation Curve for PR connections [29]

The moment strength (Q_y) of PR connections is used to compute the moment-rotation curve. This parameter depends on the type of connection and on the limit state (failure mode) that governs the strength of the analyzed connection. All the equations to compute the moment strength that control the connection behavior are determined according to Section 9.4.3.3 [29] and they are not summarized herein.

The parameters a, b and c shown in Figure 2-1 are defined in ASCE [29], Table 9-6. The Rotational stiffness (K_θ), for bare or composite PR connections, according to this document should be determined by experiment, by an approved rational analysis or by the following formula:

$$K_\theta = \frac{M_{CE}}{0.005}$$

Where

M_{CE} = Expected moment strength of PR connection (Q_y)

2.3.2.2 Mechanical Models

The mechanical or component method is the latest approach that researches are using to characterize the hysteretic behavior of PR connections. The attractiveness of this method is that it is somewhere in between the analytical model and finite element analysis. This approach is

used by the Eurocodes 3 [31] and Eurocode 4 [32] to predict monotonic behavior of connections but it has been expanded to cyclic behavior by different researchers [33-36].

The component method assembles a set of rigid and flexible elements modeled with springs. Each individual element represents a source of flexibility or deformation, including but not limited to angles, shear panel, column webs in compression, column webs in tension, and reinforcement in tension. The superposition of all these sources predicts the overall behavior of the connection. For example the main sources of deformation of a beam-to-column welded connection are the column web in compression, column web in tension and panel zone in shear.

A key point to compute the hysteretic behavior of a connection is to identify potential sources of deformation and potential failures of the connection. Once the sources are known a constitutive law is assigned to each spring (component). These constitutive laws represent force versus displacement relationships that can be obtained from laboratory tests, analytical analysis or finite element simulations. Different levels of refinement can be assigned to constitutive laws for each component, going from a simple elasto-plastic behavior to a force displacement relationship that includes strain hardening, strength and stiffness degradation. The accuracy of the overall connection's cyclic behavior depends on the complexity of these force displacement relationships. For instance the model created by Rassatti et al. [36] is capable of predicting the cyclic behavior of a PR connection with accuracy. However, this model was implemented in ABAQUS and it would be still difficult and computationally inefficient to incorporate as part of a full structural system to perform nonlinear analyses.

2.3.2.3 Experimental Method

This is a method that has been used extensively when nonlinear dynamic analysis is required. Because a phenomenological model, easy to be implemented, has not been established

for PR connections, it is a common approach to use past data from cyclic test of PR connections as the hysteretic behavior. Depending on the platform or software to be used, a predefined generalized hysteretic model is matched as close as possible with the cyclic behavior of the connection. A disadvantage of the method is that the sections used in the investigation to be performed must be the same as the ones used in the cyclic test.

A mixed approach was taken by Bozorgmehr [37] where a mathematical model for monotonic behavior and a generalized hysteretic model were used to match test results. The ascending branch of the backbone curve was defined with points obtained from a mathematical model and the descending branch was defined from experience.

2.4 Continuous Stiffness

The continuous stiffness or often called continuous columns concept acknowledges that: "If columns are continuous over several stories of a structure, then the stiffness of the columns will limit the amount of drift concentration that can occur"[38]. This effect has been investigated on different structural systems. A summary of these investigations is provided in this section of the chapter.

Tremblay and Stiemer [39] proposed the use of continuous columns as a back-up stiffness to mitigate P-Delta effects in a multi-story braced frame. Simple equations, obtained from simple models, were proposed to design the continuous columns. Assuming single-story and two-story mechanisms, the minimum stiffness required by the continuous columns to mitigate P-Delta effects was computed. Additionally, in the study, eight multi-story buildings with a height that varied from 2 to 12 stories were analyzed. The columns of these structures were designed using the proposed approach. The analyses considered four column modeling conditions for each building: pinned at each floor, pinned at each second floor, continuous over

the entire building with a pin-connection at the base and continuous over the entire building height with the base fixed.

The number of collapses, which were established when stability failure occurred, decreased considerably when the column's continuity was included. The worst case was the one that did not considers the continuity of columns (pinned at each floor) followed by the case pinned at each second floor. The best case according to the study was the one with the column continuous over the entire height and fixed at the base. The authors stated that it is an attractive and viable method but more research is required.

MacRae et al. [40] revealed that continuous stiffness provided by gravity columns could reduce the probability of having weak story mechanisms in concentrically braced frames (CBFs). CBFs are generally designed to resist the lateral forces by means of truss action. Thus, columns are designed to carry axial loads but the flexural demands are neglected. As a result of this assumption, CBFs present drift concentrations and are prompted to have soft story mechanisms when the mathematical models are analyzed. However, these kinds of failures are not generally seen after real earthquakes because columns are generally continuous and they have some flexural stiffness and strength. MacRae's study proposed closed form equations between drift concentration, column stiffness and strength for two story structures with uniform and variable strength over their height respectively. After performing nonlinear pushover and dynamic analyses, it was concluded that weak story mechanisms occurred due to current design provisions that did not consider the column flexural stiffness over the height of the frames. Moreover, it was shown that continuous columns belonging to the CBFs columns and the gravity columns reduced drift concentrations.

The study performed by Tagawa [41] had several objectives and one of them studied the influence of the gravity columns on special steel moment frames. The buildings analyzed were taken from the SAC project and they are representations of 3-, 9-, and 20-story steel moment frames in Los Angeles. The column continuity approach is used in this investigation to simulate the flexural behavior of columns in the moment frame. This is done to calibrate simpler shear-beam models that represent the steel frame. However, as one of the topics, the authors study the influence of the gravity columns on the performance of the special steel moment frames. By comparing the results obtained from a pushover and nonlinear dynamic analyses performed to the 9-story frame with and without the gravity columns, the following was found: the gravity columns increased the post-yield stiffness significantly preventing the plastic mechanism of the structure and improving the stability under the static pushover loading, the gravity columns have an important influence under large displacements when the dynamic analysis is performed. It was concluded by the author that gravity columns were likely to reduce the mean drift demand by 10% - 20% and reduce drift concentrations in taller buildings since they are more prompt to be more influenced by P-Delta effects. It is also mentioned that as the continuous stiffness increases, drift concentration decreases to a point where the structure deforms in a pure shear mode with respect to the base. It has to be mentioned that the author recommends as future research to evaluate the stability of the frames with beam-hinges that include stiffness and strength degradation since this study assumed a bilinear hysteretic moment-curvature. It is recommended also to include the capability of yielding in gravity columns.

Another study that investigated the influence of the gravity columns on concentrically braced frames (CBFs) was performed by Ji et al. [42]. In this study a three story structure was subjected to two sets of ground motions with a probability of exceedance of 10% and 2% in 50

years. One of the findings of the study was that the analyzed CBF was susceptible to drift concentrations in the first story under large earthquakes (2% in 50 years). These results were then compared with the ones obtained with the CBF that incorporates the gravity columns. The gravity columns were lumped into one elastic element with two different base conditions: pinned and fixed. According to the study, the fixed gravity columns improved more the response of the structure in comparison to the pinned gravity columns. However, in both cases, story drifts were distributed nearly uniformly along the height reducing in this way drift concentrations. Additionally, yielding in the gravity columns was checked and it was found that fixed gravity columns exceed the elastic limit more often than the pinned gravity columns. It was concluded, however, that nonlinearity of gravity columns would not have a significant influence on the response.

Zhe Qu [43] studied the concept of continuous column stiffness to improve the seismic performance of ductile reinforced concrete moment frames. The author states that the gravity columns in concrete frames do not provide continuous stiffness unlike steel structures. Therefore the solution taken in the investigation was to add a rocking wall frame. The moment of inertia of the wall was increased to improve the Drift Concentration Factor (DCF). This factor evaluates the amount of drift concentration that a building presents during an earthquake by obtaining the relation between the maximum inter-story drift and the roof drift. The DCF takes a value of 1.0 if the structure does not presents drift concentration. Thus the probability of having weak story mechanisms is lower. The chosen dimensions of the wall decreased the DCF closer but not equal to 1.0 because the size of the rocking wall would not have been realistic.

As part of this study, an 8-Story reinforced concrete moment frame was modeled with and without the rocking wall using fiber based elements on ABAQUS 6.8. The comparison

between the structure with and without the rocking wall was done by subjecting the structures to ten different earthquakes scaled according to Japanese seismic practice. The results of the nonlinear dynamic analyses showed how inter-story drifts and damage (measured as ductility demand) were decreased considerably when the rocking wall was incorporated.

The previous study [43] was the basis for designing a retrofit an eleven-story reinforced concrete frame on the campus of the Tokyo Institute of Technology in Japan. Qu et al. [44] presented the case of study where the seismic performance of this building was enhanced by incorporating rocking wall frames on the perimeter of the building. The retrofit aimed to enhance integrity of the structure and prevent weak story mechanisms in the existing moment-resisting frames. In addition, steel plates were placed connecting the extremes of the rocking wall to the columns of the moment frame in order to dissipate energy during an earthquake. This approach was possible to implement as a result of having the rocking wall because it uniforms the interstory drift and cause the structure to deflect in pure mode shape. Nonlinear dynamic analyses were performed before and after the retrofit in order to evaluate the seismic performance. Among the results presented in the study were the interstory drift ratio (IDR) and energy dissipation. The rocking walls created a much more uniform distribution of IDRs reducing drift concentrations drastically. Moreover, the steel plates (dampers) decreased the IDRs even more. The energy dissipation results presented in the paper showed that before the retrofit, dissipation occurred more on columns than beams. After the retrofit but when the dampers were not including, the dissipation of energy increased slightly on beams but the main dissipation was through columns as well. Finally, when the dampers were included the main dissipation was trough the devices installed in the building. These results proved that the pin-supported wall frame reduced IDRs drastically but acting alone (without energy dissipation

devices) it does not contribute to dissipate energy. However, it helps distributing damage along the height of the building.

Qu. et al. [45] investigated the effect of column continuity to mitigate drift concentrations in a two story steel plate shear wall (SPSW). The most desirable behavior of SPSWs occurs when all the stories yield simultaneously. However, this is unlikely to occur in practice even for a two story SPSW due the fact that the required plate thicknesses to achieve this behavior may not be available. According to U.S codes, the surrounding columns of the infill walls have to be designed to remain elastic with the exception of the plastic hinges at the column bases when the columns are fixed. The benefits of including and varying the stiffness of these columns were investigated in the study.

In order to evaluate the influence of the column's continuity, the authors performed nonlinear nonlinear static pushover analyses using finite element models. The authors state that conceptually if the columns are ideally rigid and pinned to the ground, yielding in the infill walls will occur simultaneously. On the other hand, if columns are relatively flexible, steel shear walls will yield progressively per story resulting in possible drift concentrations. This statement was proved after performing the analyses and the main conclusion was that drift concentrations are reduced considerably when the columns stiffness was increased.

Alavi and Krawinkler [46] proposed using fixed or hinged walls to distribute uniformly the story ductility over the height when the structure is subjected to near-field ground motions. Near-field ground motions may cause non-uniform distribution of story ductility demands due to their pulse components. The study analyzes twenty-story generic frames (concrete or steel) coupled with concrete rocking walls hinged and fixed at the base. Nonlinear dynamic analyses were performed using an equivalent pulse motion as a representation of near-fault ground

motions. In order to evaluate the influence of the wall dimensions, its stiffness was varied. The performance of the hinged and fixed walls was compared considering first the walls to behave elastically and then inelastically. The main conclusion of this investigation was that strengthening frame structures with hinged walls is more effective than fixed walls to reduce the maximum story drift demands. It creates a more uniform distribution of story drifts over the height of the structure. The three deformation components of the hinged wall are: flexural, shear, and rigid-body rotation about the base. If the stiffness of the wall is adequate compared to the frame, both bending and shear deformations will become small and the dominant displacement mode will be the rigid body rotation. As a result, the drift distribution over the height is uniform. In addition, elastic shear and moment demands are much lower on hinged walls than fixed walls.

One of the aspects studied by Lang [47] was the effect of the gravity columns on the effects of P-Delta on the behavior of moment-resisting frames in seismic regions. The analyzed buildings were taken from the SAC project and they are representations of 3-, 9-, and 20-story steel moment frames in Los Angeles. The design of these structures reflects buildings built prior to the 1994 Northridge earthquake. The mathematical models included plastic hinges at the end of beams and columns using bilinear hysteretic behaviors. In addition a leaning column was included to introduce P-Delta effects but unlike common analyses, this column incorporated the properties of the gravity columns.

The influence of the gravity columns was evaluated by varying the lumped gravity column stiffness. Different values were assigned to the P-Delta column to consider stiffer gravity columns and the analyses used to assess their influence were nonlinear static and dynamic analyses. The resulting deformed shape from the pushover analyses illustrated that drift concentrations are reduced for taller buildings such as the 9- and 20-story. However, because the

ground motions at which the structures were subjected to represented the design level earthquake, the improvement from the gravity column was not significant. The reason is because the effect of the gravity columns is important for large earthquakes.

2.5 Summary

The literature review presented in this dissertation summarized different studies where the gravity system was included as part of lateral resisting system. In addition a review of methodologies used to model PR connections was done. From the information described above, the following important facts and research needs were found:

Important Facts:

- The gravity system contributes more at high levels of ground shaking or when the building is susceptible to have problems due to P-Delta effects.
- Gravity connections can become important if the moment resisting connections fracture.
- Among all the members and connections in the gravity system, the contribution of the gravity columns appeared to be the most important.
- Gravity columns have an important effect on the post yield stiffness of the structure.
- Continuous stiffness provided by the gravity columns in SMFs decreases drift concentrations. As a result the likelihood of having weak story mechanisms reduces.
- An accurate and relatively easy model to define the parameters for the hysteretic behavior of a PR connection has not been yet defined and the most common approach used to perform nonlinear dynamic analysis is to match experimental results with a predefined hysteretic model.

Research Needs

- There is little information regarding the influence of the gravity system on the seismic performance of SMFs. Specific topics such as the effect of different gravity connections, effect of gravity columns, yielding in gravity columns have not been studied or limited investigations have been performed.

- Even though it has been stated that the gravity system contributes at high level intensity ground motions, there are no studies that evaluate the collapse performance of SMFs including in the gravity system.

- The influence of the gravity connections flexural strength in SMFs has not been evaluated.

- There is no information regarding the effect of splices in the gravity columns.

- A comprehensive study of the effect of the gravity columns in SMFs has not been executed.

From the literature and research needs presented, it can be seen that much more information is required to characterize the influence of the gravity system on the seismic performance of SMFs. This is why all the enlisted research needs are studied in in this dissertation. However, it has to be noted that some topics are studied more in depth than others.

2.6 References

[1] A. Gupta, H. Krawinkler, Seismic demands for the performance evaluation of steel moment resisting frame structures, in, Stanford University, 1999.

[2] K. Lee, D.A. Foutch, Performance evaluation of new steel frame buildings for seismic loads, Earthquake engineering & structural dynamics, 31 (2002) 653-670.

[3] F. P695, Quantification of Building Seismic Performance Factors, Fededral Emergency Management Agency, Washington, D.C, 2009.

[4] D. Vamvatsikos, C.A. Cornell, Applied incremental dynamic analysis, Earthquake Spectra, 20 (2004) 523.

[5] NIST, "Applicability of Nonlinear Multiple-Degree-of-Freedom Modeling for Design", National Institute of Standards and Technology, USA, 2010.

[6] F. Zareian, D. Lignos, H. Krawinkler, Evaluation of seismic collapse performance of steel special moment resisting frames using FEMA P695 (ATC-63) methodology, in: Proceedings of Structures Congress ASCE, New York, 2010.

[7] J. Liu, A. Astaneh-Asl, Cyclic testing of simple connections including effects of slab, Journal of Structural Engineering, 126 (2000) 32-39.

[8] J.A. Jarrett, J.P. Judd, F.A. Charney, Comparative evaluation of innovative and traditional seismic-resisting systems using the FEMA P-58 procedure, Journal of Constructional Steel Research, 105 (2015) 107-118.

[9] FEMA, Seismic Performance Assessment of Buildings, volume I - Methodology, FEMA P-58 Washington, D.C. Federal Emergency Management Agency, 2012.

[10] W.-F. Chen, Practical analysis for semi-rigid frame design, World Scientific Publishing Company, 2000.

[11] AISC, Steel construction manual, American Institute of Steel Construction, [Chicago, Ill.], 2005.

[12] AISC, Specification for the design, fabrication & erection of structural steel for buildings : [adopted] February 12, 1969, AISC, New York, 1969.

[13] AISC, Load and resistance factor design specification for structural steel buildings : September 1, 1986, American Institute of Steel Construction, Chicago, Ill., 1986.

[14] AISC, Specification for Structural Steel Buildings, AISC/ANSI 360-05, American Institute of Steel Construction, Chicago, Illinois, 2011.

[15] AISC, Seismic Provisions for Structural Steel Buildings, ANSI/AISC 341-05, American Institute for Steel Construction., Chicago, Ill., 2005.

[16] N. Kishi, W.-F. Chen, Data base of steel beam-to-column connections, Structural Engineering Area, School of Civil Engineering, Purdue University, 1986.

[17] W.-F. Chen, N. Kishi, M. Komuro, Semi-rigid connections handbook, J. Ross Publishing, 2011.

[18] J. Baker, A Note on the Effective Length of a Pillar Forming Part of a Continuous Member in a Building Frame, Second Report, (1934) 13-43.

[19] J.C. Rathbun, Elastic properties of riveted connections, American Society of Civil Engineers Transactions, (1936).

[20] J.E. Lothers, Elastic restraint equations for semi-rigid connections, Transactions of the American Society of Civil Engineers, 116 (1951) 480-494.

[21] P.D. Moncarz, K.H. Gerstl, Steel frames with nonlinear connections, Journal of the Structural Division, 107 (1981) 1427-1441.

[22] C. Poggi, R. Zandonini, Behaviour and strength of steel frames with semi-rigid connections, in: Connection Flexibility and Steel Frames, ASCE, 1985, pp. 57-76.

[23] M.J. Frye, G.A. Morris, Analysis of flexibly connected steel frames, Canadian Journal of Civil Engineering, 2 (1975) 280-291.

[24] S. Jones, P. Kirby, D. Nethercot, Effect of semi-rigid connections on steel column strength, Journal of Constructional Steel Research, 1 (1980) 38-46.

[25] M. Elsati, P. Richard, Derived moment rotation curves for partially restrained connections, Structural engineering review, 8 (1996) 151-158.

[26] R.M. Richard, B.J. Abbott, Versatile elastic-plastic stress-strain formula, Journal of the Engineering Mechanics Division, 101 (1975) 511-515.

[27] K. Ang, G. Morris, Analysis of three-dimensional frames with flexible beam-column connections, Canadian Journal of Civil Engineering, 11 (1984) 245-254.

[28] R.T. Leon, J.J. Hoffman, P. Staeger, Steel Design Guide Series 8: Partially Restrained Composite Connections, American Institute of St eel Construction, (1996).

[29] ASCE, Seismic Rehabilitation of Existing Buildings (ASCE/SEI 41-13), American Society of Civil Engineers Reston, Virginia, 2013.

[30] A. De Martino, C. Faella, F. Mazzolani, Simulation of beam-to-column joint behaviour under cyclic loads, Construzioni Metalliche, 6 (1984) 346-356.

[31] S. European Committee for, prEN 1993-1-8 : eurocode 3 : design of steel structures part 1-8 : design of joints, European Committee for Standardization, Brussels, 2003.

[32] S. European Committee for, Eurocode 4 : design of composite steel and concrete structures, CEN, Brussels, 1994.

[33] F.M. Elnashai, AS, A component-based model for beam-column connections, Earthquake Engineer 10th World, 8 (1992) 4495.

[34] M. De Stefano, A. De Luca, A. Astaneh-Asl, Modeling of cyclic moment-rotation response of double-angle connections, Journal of Structural Engineering, 120 (1994) 212-229.

[35] G. Rassati, S. Noè, R.T. Leon, PR Composite joints under cyclic and dynamic loading conditions: The component model approach, in: Proc. 4th AISC International Workshop on Connections in Steel Structures, Roanoke, 2000, pp. 213-222.

[36] G. Rassati, R. Leon, S. Noe, Component modeling of partially restrained composite joints under cyclic and dynamic loading, Journal of Structural Engineering, 130 (2004) 343-351.

[37] A. Bozorgmehr, Collapse Assessment of Partial Restraint Composite Connection Moment Frames, in: Department of Civil and Environmental Engineering, Chalmers Univeristy of Technology, 2011.

[38] G.A. MacRae, The Continuous Column Concept-Development and Use, Proceedings of the Ninth Pacific Conference on Earthquake Engineering Building an Earthquake-Resilient Society, (2011).

[39] R. Tremblay, S. Stiemer, Back-up stiffness for improving the stability of multi-storey braced frames under seismic loading, Proceedings of the 1994 SSRC Annual Technical Session, Bethlehem, Pa, (1994) 311-325.

[40] G.A. MacRae, Y. Kimura, C. Roeder, Effect of column stiffness on braced frame seismic behavior, Journal of Structural Engineering, 130 (2004) 381-391.

[41] H. Tagawa, Towards an understanding of seismic response of 3D structures-stability & reliability, Doctor Thesis, Washington: University of Washington, (2005).

[42] X. Ji, M. Kato, T. Wang, T. Hitaka, M. Nakashima, Effect of gravity columns on mitigation of drift concentration for braced frames, Journal of Constructional Steel Research, 65 (2009) 2148-2156.

[43] Z. Qu, L. Ye, A. Wada, Seismic damage mechanism control of RC ductile frames from a stiffness point of view, in: 8th International Conference on Urban Earthquake Engineering, Tokyo, Japan, 2011.

[44] Z. Qu, A. Wada, S. Motoyui, H. Sakata, S. Kishiki, Pin-supported walls for enhancing the seismic performance of building structures, Earthquake engineering & structural dynamics, 41 (2012) 2075-2091.

[45] B. Qu, X. Guo, M. Pollino, H. Chi, Effect of column stiffness on drift concentration in steel plate shear walls, Journal of Constructional Steel Research, 83 (2013) 105-116.

[46] B. Alavi, H. Krawinkler, Strengthening of moment-resisting frame structures against near-fault ground motion effects, Earthquake engineering & structural dynamics, 33 (2004) 707-722.

[47] K.A. Lang, Effects of P-Delta and gravity column stiffness on the behavior of moment-resisting frames in seismic regions, in, 1999.

Chapter 3: Mathematical Model

3.1 Introduction

In order to perform a nonlinear analysis, the hysteretic behavior of any component that could behave in an inelastic manner has to be modeled. This chapter describes the procedure followed to develop the mathematical models analyzed in this dissertation. The first section summarizes the buildings used throughout this investigation. The second and third parts of the chapter illustrates the approaches used to model the Special Steel Moment Frames (SMFs) and the gravity system respectively.

3.2 Buildings Overview

The buildings analyzed were taken from the ATC 76-1 project [1]. Complete information about the design and the nonlinear models can be found in the referenced document. However, a summary of the main information is provided herein. The SMFs that were evaluated in the ATC 76-1 project were designed and analyzed by Zareian et al. [2]. The design space considered buildings of 1, 2, 4, 8, 12 and 20 stories. Each building was designed and detailed in accordance with the strength design requirements in AISC 341-05 [3] and the seismic design requirements in ASCE 7-05 [4] requirements with the exception that the deflection amplification factor C_d was taken equal to the response modification factor, R, as specified in FEMA P-695 [5]. The gravity system was not included in the analysis as the P-695 procedure specifies.

Two different analysis methods were used to design the buildings: the Equivalent Lateral Force (ELF) method and the Modal Response Spectrum Analysis (RSA) method. All the SMFs were designed using reduced beam section connections (RBS) for a seismic design category D_{max} (S_s=1.5g, S_1=0.6g), for a typical gravity load, and considering Site Class D.

This investigation analyzes a subset of the buildings from the ATC 76-1 project. These are the 2-, 4-, and 8-story models designed using the RSA method. The base of the columns of the buildings were fixed for the 4- and 8-story models, and pinned for the 2-story model. The nomenclature that identified these structures in ATC 76-1 is: 2RSA (2 story), 3RSA (4 story) and 4RSA (8 story). Figure 3-1 shows the plan view for all the buildings. The bay width (center line dimensions) between columns of each SMF is 6.1m (20 ft). The height of the first story is 4.6 m. (15 ft) (to top of steel beam), and the height of all other stories is 4 m (13 ft). The design dead load (D) is 4.31 kN/m^2 (90 psf) uniformly distributed over each floor, and the cladding load is applied as a perimeter load of 1.2 kN/m^2 (25 psf). The unreduced design live load (L) is 2.4 kN/m^2 (50 psf) on all floors and 0.96 kN/m^2 (20 psf) on the roof. These loads were considered in the analysis in a combination of 1.0 D + 0.25 L.

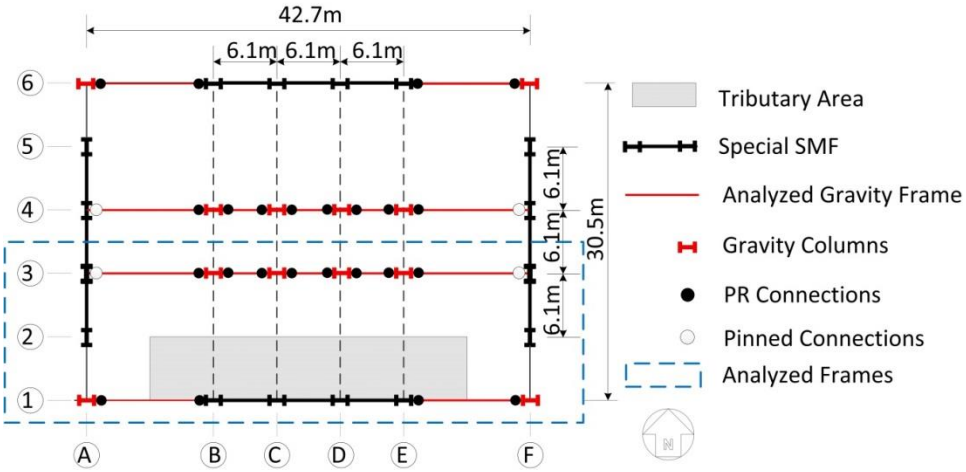

Figure 3-1 Typical Building Plan View

Figure 3-1 illustrates the configuration of the gravity system only in the direction to be analyzed (East-West). In this investigation, the gravity connections are considered to be Partially Restrained (PR) connections. The lateral strength of the SMF columns oriented on the weak axis

(A3, F3) is not considered because it is the influence of the gravity columns that is of interest in this study.

3.3 Modeling Special Steel Moment Frame

The numerical two-dimensional models idealized to perform the nonlinear analysis were created using OpenSees. Material and geometric nonlinearities were included in every model. In the case where the gravity system was not included, P-Delta effects were considered using a leaning column with no flexural stiffness placed parallel to the SMF. The load applied to this column represents half of the total load from the gravity system that was not tributary to the SMF columns. For the cases where the gravity system was included, a leaning column was not required because the loads were applied directly to the gravity columns.

The approach applied to model the frames was using elastic elements with the nonlinear inelastic behavior lumped into plastic hinges located at the ends of the members. The components of the SMF with nonlinear behavior are shown in Figure 3-2 and they are: panel zones, plastic hinges located at the RBSs of the beam and plastic hinges at the column ends. The complete procedure used to create the mathematical model in OpenSees is described in the following subsections.

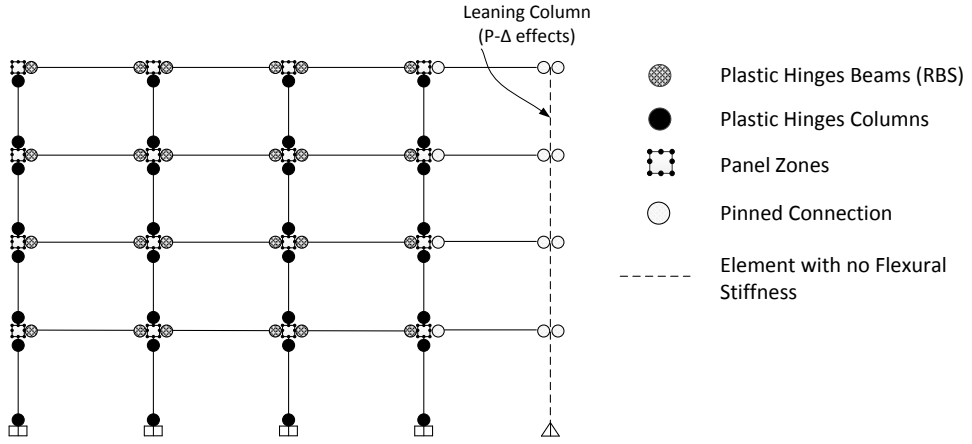

Figure 3-2. Special Steel Moment Frame Model

3.3.1 Plastic Hinges Beams

The hysteretic behavior of the reduced beam sections (RBS) was modeled using the Modified Ibarra Krawlinkler deterioration model [6]. This material has a hysteretic behavior as is shown in Figure 3-3.

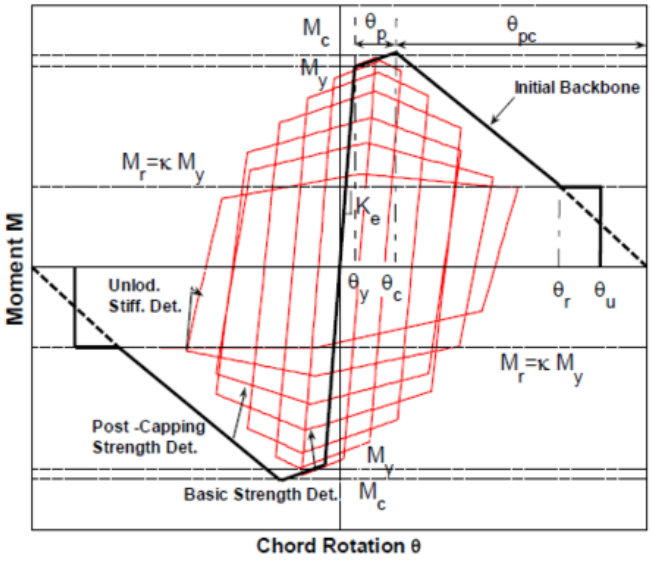

Figure 3-3. Modified Ibarra Krawlinkler Deterioration Model [7]

The parameters required to model the hysteretic behavior were computed following the recommendations of Lignos and Krawlinkler [8]. Figure 3-3 displays all the parameters that define the RBS cyclic behavior according to the referenced document. However, in order to incorporate this behavior within OpenSees, fewer parameters than shown in the figure have to be defined. These parameters are listed in Table 3-1 where the nomenclature for the parameters used by Lignos and Krawinkler [8] and the one used by OpenSees are also included.

Table 3-1 Parameters required by Modified Ibarra Krawlinkler Deterioration Model

OpenSees Nomenclature	**Lignos-Krawlinkler Nomenclature (Figure 3-2)**	**Definition**
K_o	K_e	Elastic Stiffness
as_plus	-	Strain hardening ratio for positive loading
My_plus	My	Effective yield strength for positive loading direction
Lamda_S	Λ_s	Cyclic deterioration parameter for strength deterioration
Lamda_C	Λ_p	Cyclic deterioration parameter for post-capping strength deterioration
Lamda_A	Λ_a	Cyclic deterioration parameter for acceleration reloading stiffness deterioration
Lamda_K	Λ_k	Cyclic deterioration parameter for unloading stiffness deterioration
theta_p_Plus	θ_p	Pre-capping rotation for positive loading direction (often noted as plastic rotation capacity)
theta_pc_Plus	θ_{pc}	Post-capping rotation for positive loading direction.
Res_Pos	κ	Residual strength ratio for positive loading direction
theta_u_Plus	θ_u	Ultimate rotation capacity for positive loading direction.

The parameters shown in Table 3-1 are for the positive side of the hysteretic curve, but the negative side is considered to be symmetric for this study since the influence of the concrete floor slab was not included.

3.3.1.1 RBS Hysteretic Behavior Parameters

A description of the Lignos and Krawinkler parameters used for modeling the RBS hinges is provided in the following subsections.

a) Elastic Stiffness (K_e)

As already mentioned, the inelastic behavior of the beam and column elements of the structure are modeled with plastic hinge rotational springs that are located near the ends of the elements. Thus beams are a series of sub-elements connected in the following order: elastic beam-column element, plastic hinge rotational spring (located at the RBS) and another beam-column element (these elements are symmetric for the other half of the beam). In the case of the

columns the order is: plastic hinge rotational spring at member ends and an elastic beam-column between the plastic hinges. As proposed by Ibarra and Krawinkler [9] (Appendix B), the elastic stiffness of the spring is modified with a factor (***n=10)*** . This is done to account for the assemblage of elements with different stiffness.

$$K_e = \frac{6 \cdot E \cdot I\_beam_{\text{mod}}}{L} \cdot n$$

$$I\_beam_{\text{mod}} = I\_beam \cdot \left(\frac{n+1}{n} \right)$$

Where :

$I\_beam_{\text{mod}} = \text{Modified moment of inertia of beam}$

$L = \text{beam length}$

$n = \text{stiffness multiplier for rotational spring.}$

b) Yielding Moment (M_y)

Yielding moment is obtained from the properties of the section. It is given by:

$$M_y = Z_{xx} F_y R_y$$

Where :

$Z_{xx} = \text{Plastic section modulus}$

$F_y = \text{Specified minimum yield stress of the steel section}$

$R_y = \text{Ratio of the expected yield stress to the specified minimun yield stress } F_y.$

c) Cyclic deterioration parameter (Λ)

The equation to compute the cyclic deterioration parameters for strength (Λ_s), post-capping strength (Λ_c), acceleration reloading stiffness (Λ_A) and unloading stiffness (Λ_k) were obtained experimentally by Lignos and Krawinkler [8]. The specimens considered were the ones that failed in a ductile manner and for which cyclic deterioration was clearly observed. All modes of cyclic deterioration (Λ_s Λ_c Λ_A Λ_k) are assumed to be defined by the same parameter (Λ). The equation proposed by Lignos and Krawinkler for predicting the cumulative rotation capacity Λ for beams with RBS is:

$$\Lambda = 585 \cdot \left(\frac{h}{t_w}\right)^{-1.14} \cdot \left(\frac{b_f}{2 \cdot t_f}\right)^{-0.632} \cdot \left(\frac{L_b}{r_y}\right)^{-0.205} \cdot \left(\frac{c_{unit}^2 F_y}{355}\right)^{-0.391}$$

Where :

h = fillet web depth

t_w = web thickness

b_f = flange width

t_f = flange thickness

L_b = Unbraced beam length

r_y = Radious of gyration about weak axis

c_{unit}^2 = Units conversion coefficient (6.895 if d is in inches and F_y in ksi)

d) Pre-capping rotation (θ_p)

Based on 72 test specimens of beams with RBS and with $d \geq 21$" the regressed equation for pre-capping rotation is given by:

$$\theta_p = 0.19 \cdot \left(\frac{h}{t_w}\right)^{-0.314} \cdot \left(\frac{b_f}{2 \cdot t_f}\right)^{-0.100} \cdot \left(\frac{L_b}{r_y}\right)^{-0.185} \cdot \left(\frac{L}{d}\right)^{0.113} \cdot \left(\frac{c_{unit}^1 d}{533}\right)^{-0.760} \cdot \left(\frac{c_{unit}^2 F_y}{355}\right)^{-0.070}$$

Where :

h = fillet web depth

t_w = web thickness

b_f = flange width

t_f = flange thickness

L_b = Unbraced beam span

L = Beam span

d = Beam depth

r_y = Radious of gyration about weak axis

c_{unit}^1 = Units conversion coefficient (25.4 if d is in inches)

c_{unit}^2 = Units conversion coefficient (6.895 if d is in inches and F_y in ksi)

e) Strain Hardening (as_plus)

Strain hardening has to be modified to account for the assemblage of elements as described for the elastic stiffness [9]. Strain hardening was computed as follows:

Strain hardening ratio of spring:

$$as = \frac{My \cdot (\frac{Mc}{My} ratio - 1)}{K_e \cdot \theta_p}$$

Modified strain hardening ratio of spring:

$$as\_plus = \frac{(n+1) \cdot as}{n+1-n \cdot as}$$

Where:

n = stiffness multiplier for rotational spring.

My = Yielding Moment

$\frac{Mc}{My} ratio = 1.10$; Maximum moment post-yielding over the effective yield moment

θ_p = Pre-capping rotation

K_e = Elastic stiffness

f) Post-capping rotation (θ_{pc})

The regression equation for θ_{pc} for beams with RBS is:

$$\theta_{pc} = 9.52 \cdot \left(\frac{h}{t_w}\right)^{-0.513} \cdot \left(\frac{b_f}{2 \cdot t_f}\right)^{-0.863} \cdot \left(\frac{L_b}{r_y}\right)^{-0.108} \cdot \left(\frac{c_{unit}^2 F_y}{355}\right)^{-0.360}$$

Where:

h = fillet web depth

t_w = web thickness

b_f = flange width

t_f = flange thickness

L_b = Unbraced beam span

r_y = Radious of gyration about weak axis

c_{unit}^2 = Units conversion coefficient (6.895 if d is in inches and F_y in ksi)

g) Residual strength ratio (κ)

A residual strength ratio of 0.4 is suggested from low cycle fatigue experiments. However, more experiments with very large deformations cycles need to be conducted [8].

h) Ultimate rotation capacity (θ_u)

For beams with RBS, an estimate of θ_u is 0.06 to 0.07 radians. For monotonic type of loading θ_u is on the order of three times as large as the values reported for symmetric cyclic loading.

i) Experimental data range

As mentioned previously these equations were obtained by experiments, so there is a range of sections that were tested. The experimental data with the following range of parameters were used for deriving the equations previously described:

Reduced Beam Section (RBS)

$$21 \le \frac{h}{t_w} \le 55$$

$$20 \le \frac{L_b}{r_y} \le 65$$

$$4.5 \le \frac{b_f}{2t_f} \le 7.5$$

$$2.3 \le \frac{L}{d} \le 6.3$$

$$21'' \le d \le 36''$$

3.3.2 Column Plastic Hinges

Currently, there is not a phenomenological element in OpenSees that represents the hysteretic behavior of a column including axial force – bending moment (P-M) interaction. Thus, the same hysteretic behavior used to represent the inelastic behavior of the beams is used for the columns, but the bending strength is decreased due to P-M interaction. Even though the decrease varies depending on the axial force, which changes during a dynamic analysis, the axial force is computed before the analysis and the bending strength is reduced accordingly. The axial force was obtained by performing a nonlinear static pushover analysis and was considered to be equal

to $P_{grav} + 0.5P_{E,max}$, where P_{grav} is the gravity load that the column is subjected to and $P_{E,max}$ is the maximum load that the column receives during the pushover analysis. The pushover analysis is performed until a reduction of 20% in the peak base shear, V_{max}, is reached. With the axial load determined, the reduced bending strength is computed using the AISC P-M interaction equation [23] and subsequently used in the models. The equations used to compute the parameters for the RBS hysteretic behavior are different in the case of the columns because the section is not reduced. These equations are not described herein but they can be found in the paper by Lignos and Krawinkler [8]. An example of the hysteretic behavior that characterizes the inelasticity of beams and columns is shown on Figure 3-4 (a) and (b).

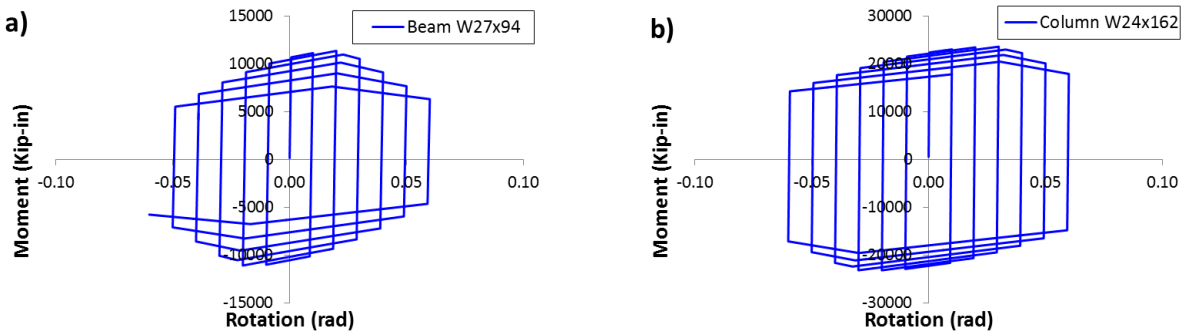

Figure 3-4 Hysteretic behavior a) Reduced Beam Section b) Column

3.3.3 Panel Zones

Panel zones are modeled using a rectangle region composed of eight very stiff elastic beam-column elements and one nonlinear rotational spring to represent shear distortions in the panel zone (Figure 3-5a) [10]. These deformations are due to shear yielding and column flange flexure yielding and are represented by a tri-linear backbone curve assigned to the rotational spring (Figure 3-5b).

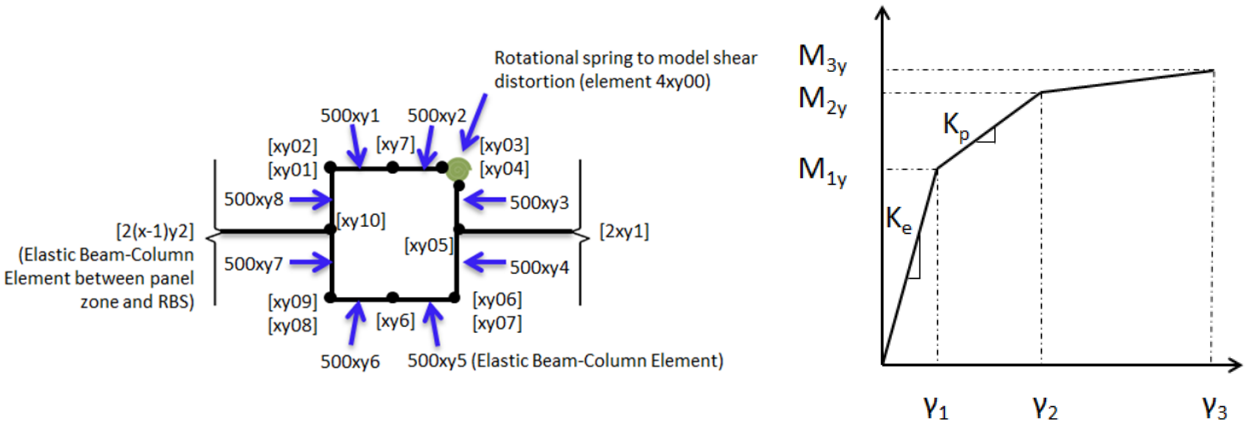

Figure 3-5 Modeling Panel Zones a) OpenSees Model [7]

b) Panel Zone Backbone Curve

The equations that define the tri-linear behavior are given by the following equations:

$$V_y = 0.55 \cdot Fy \cdot d_c \cdot t_p$$

$$K_e = 0.95 \cdot G \cdot t_p \cdot d_c$$

$$K_p = \frac{0.95 \cdot G \cdot bf_c \cdot tf_c^{\,2}}{d_b}$$

$$\gamma_1 = \frac{V_y}{K_e}; \qquad M_{1y} = \gamma_1 \cdot K_e \cdot d_b$$

$$\gamma_2 = 4 \cdot \gamma_1; \qquad M_{2y} = M_{1y} + K_p \cdot d_b \cdot (\gamma_2 - \gamma_1)$$

$$\gamma_3 = 100 \cdot \gamma_1; \qquad M_{3y} = M_{2y} + a_s \cdot K_e \cdot d_b \cdot (\gamma_3 - \gamma_2)$$

Where :

G = Shear modulus

Fy = Yield Strength

d_c = column depth

bf_c = column flange width

tf_c = column flange thickness

t_p = panel zone thickness

d_b = beam depth

a_s = assumed strain hardening (0.03)

3.4 Modeling Gravity System

The additional components modeled in the case where the gravity system was included are: PR connections and gravity columns modeled using fiber sections. The complete frame with the gravity system placed in parallel is shown in Figure 3-6. Before, the process of creating the mathematical model is described, a brief overview of the gravity system is done.

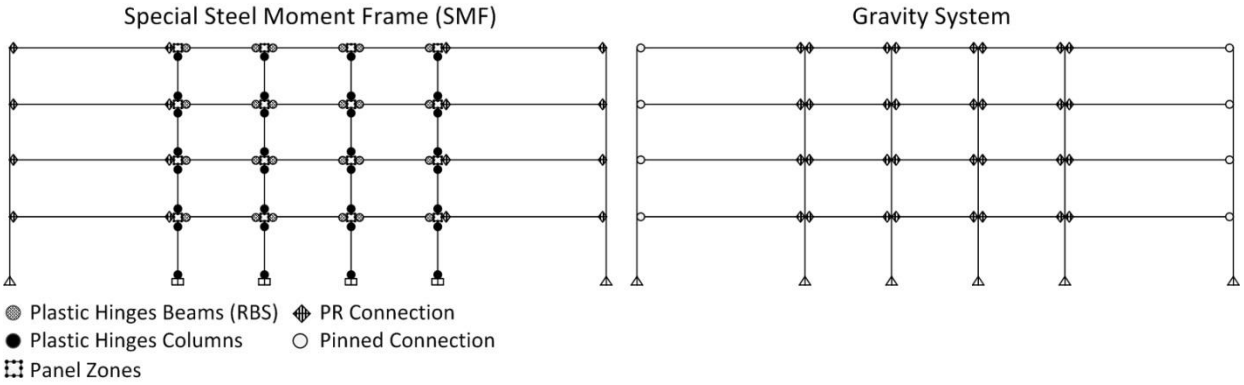

Figure 3-6 Elements of the models that include the gravity system

A typical design was conducted to obtain the size of beams and columns of the gravity framing. The system was designed using A992 steel and the same loads as previously mentioned for the SMF. For the purpose of member selection it was assumed that the gravity beams were non-composite and simply supported. The design was performed using SAP2000 and checked by hand. The size of the gravity framing members is provided in Table 3-2, with grid identifiers (e.g. A3) as referenced in Figure 3-1.

As Table 3-2 (a) (b) and (c) illustrate, the gravity system design chosen for the 8 story building has different steel sections than the 2 and 4 story buildings. Sections with more inertia (W18) were used in order to increase columns stiffness and to improve the effect of continuous stiffness provided by the gravity columns. For the lower stories W18 sections with a "column profile" were used (e.g. W18x143) and in the upper levels the 18 inch depth was maintained to facilitate splice construction.

Table 3-2 a) 2 Story b) 4 Story c) 8 Story Gravity System Member Sizes

a) 2 Story Model

Story	Columns				Beams		
	A1,F1	**A3,F3**	**B3, E3**	**C3, D3**	**A1 - B1, E1 - F1**	**A3 - B3, E3 - F3**	**B3-E3**
1	**W14x43**	W24x162	**W14x90**	**W14x61**	W24x62	W24x94	**W16x36**
2	**W14x43**	W24x162	**W14x90**	**W14x61**	W24x55	W24x84	**W16x36**

b) 4 Story Model

Story	Columns				Beams		
	A1,F1	**A3,F3**	**B3, E3**	**C3, D3**	**A1 - B1, E1 - F1**	**A3 - B3, E3 - F3**	**B3-E3**
1	**W14x43**	W24x103	**W14x90**	**W14x61**	W24x62	W24x94	**W16x36**
2	**W14x43**	W24x103	**W14x90**	**W14x61**	W24x62	W24x94	**W16x36**
3	**W14x30**	W24x62	**W14x90**	**W14x61**	W24x62	W24x94	**W16x36**
4	**W14x30**	W24x62	**W14x90**	**W14x61**	W24x55	W24x84	**W16x36**

c) 8 Story Model

Story	Columns				Beams		
	A1,F1	**A3,F3**	**B3, E3**	**C3, D3**	**A1 - B1, E1 - F1**	**A3 - B3, E3 - F3**	**B3-E3**
1	**W18x76**	W24x162	**W18x143**	**W18x76**	W24x62	W24x94	**W16x36**
2	**W18x76**	W24x162	**W18x143**	**W18x76**	W24x62	W24x94	**W16x36**
3	**W18x76**	W24x162	**W18x143**	**W18x76**	W24x62	W24x94	**W16x36**
4	**W18x50**	W24x162	**W18x76**	**W18x50**	W24x62	W24x94	**W16x36**
5	**W18x50**	W24x131	**W18x76**	**W18x50**	W24x62	W24x94	**W16x36**
6	**W18x50**	W24x131	**W18x76**	**W18x50**	W24x62	W24x94	**W16x36**
7	**W18x40**	W24x94	**W18x50**	**W18x40**	W24x62	W24x94	**W16x36**
8	**W18x40**	W24x94	**W18x50**	**W18x40**	W24x55	W24x94	**W16x36**

Note: Gravity farming shown in **bold** text.

3.4.1 Partially Restrained Connections

The flexural strength of the gravity connections was considered to be a percentage of the plastic moment strength (M_p) of the beam. Different strength levels were studied with the purpose of establishing their influence on the structure's response. Liu and Astaneh [11] performed cyclic tests on different simple connections and the range of flexural strength depend on the type of connection. For instance, shear tab connections with and without the contribution

of the concrete slab were able to develop a moment equal to 36%M_p and 18%M_p respectively. On the other hand, stronger connections developed moments up to 72%M_p. Based on these results, the percentages assigned to the PR connections were 0%, 35%, 50%, and 70%. The 0% represents the influence purely of the gravity columns, and the 35% is the minimum strength required by the connections to avoid yielding under gravity loads. Although probably too large, for practical applications, the 50% and 70% are included in the study in order to acquire an extended possible range of behavior.

Even though the cyclic behavior of the PR connections is complicated to characterize, it was considered that a simple model, such as the one given by ASCE 41-13 [12], was appropriate for this investigation. The model given by ASCE 41-13 was developed from experimental data and it depends on the type of PR connection and it is intended to be used for Nonlinear Static Pushover Analysis only. However, for the purpose of this research and considering that this model represents a conservative hysteretic behavior of the connection, it is used for the dynamic analysis. The model is conservative because PR connections tests have some strain hardening, and do not show the flat plateau and the maximum strength usually occurs at a larger rotation than the 0.005 radians as specified by this model. Two parameters are required to define this curve besides that observed in Figure 3-7, initial stiffness (K_{CE}) and moment capacity of the connection (Q_{CE}). The initial stiffness is computed according to ASCE 41-13 and is equal to the moment capacity of the connection divided by 0.005 radians. However, the moment capacity of the connection (Q_{CE}) depends on the type of connection and the limit state (failure mode) that controls the design. This value depends on the characteristics of the connections and is obtained by calculating the controlling failure mode. This failure mode is the minimum value computed from several equations given by ASCE 41-13, and they depend on the type of connection. The

rest of the parameters displayed in Figure 3-7 are given in Table 9-6 of ASCE 41-13 and they differ depending on the type of PR connection and on the limit state that controls the design. A "top and bottom clip angle connection" is chosen as a PR connection for this analysis, and the connection is configured so that the controlling limit state is flexural failure of the angles.

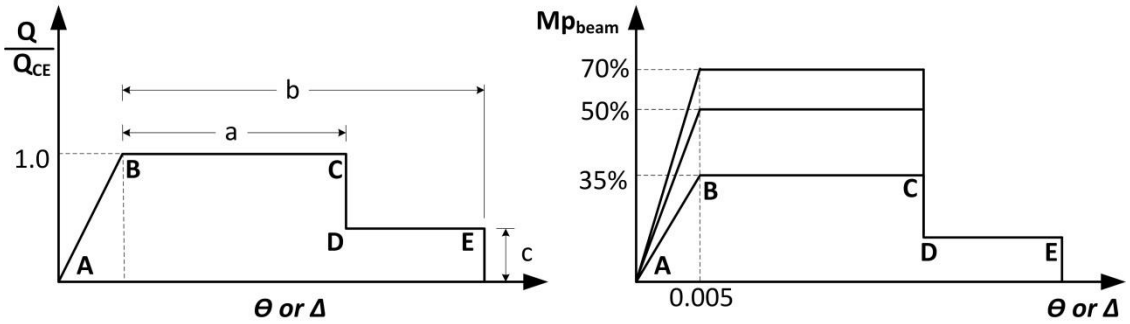

Figure 3-7 Moment Rotation Characterization Curve

ASCE 41-13 provides the backbone curve as already shown in Figure 3-7. The hysteretic behavior assigned to the PR connections using OpenSees is shown in Figure 3-8. It can be seen that the hysteretic behavior follows the backbone curve given by the ASCE 41-13 model. A more realistic model would gradually loose the flexural strength instead of losing most of it abruptly. However, as mentioned previously, for the purpose of the investigation, this model is considered to be good enough.

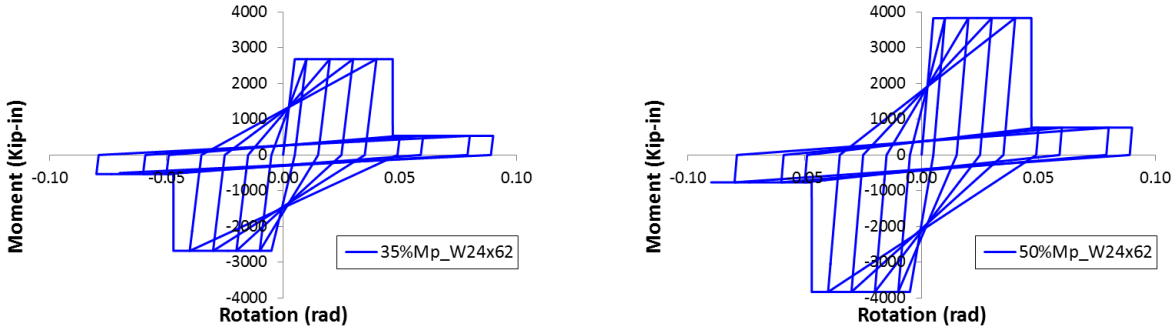

Figure 3-8 Partially Restrained Connections Hysteretic Behavior

a) 35%Mp b) 50%Mp

3.4.2 Gravity Columns

In order to account for any inelastic deformation that could occur in the gravity columns, they were modeled using force-based fiber elements with a bilinear material with strain hardening equal to 10% of the initial stiffness. The benefit of using fiber sections is that the axial-moment interaction is taken into account. However, because strength degradation is not included, the capability of the model to represent collapse is limited. This is why plastic hinges at columns of the SMFs were modeled using a phenomenological approach rather than with fiber elements.

3.5 Damping

For all the nonlinear dynamic response history analyses, a Rayleigh damping of 2.5% was assigned at the first mode period T_1 and at T=0.2T_1 in all cases. As proposed by Zareian and Medina [13], stiffness proportional damping was assigned to elements that remain elastic, and mass proportional damping was assigned to nodes or elements where mass is lumped. It has to be mentioned that the amount of damping introduced in the model was validated by performing a free-vibration analysis.

3.6 References

[1] NIST, Evaluation of the FEMA P-695 Methodology for Quantification of Building Seismic Performance Factors, National Institute of Standards and Technology, USA, 2010.

[2] F. Zareian, D. Lignos, H. Krawinkler, Evaluation of seismic collapse performance of steel special moment resisting frames using FEMA P695 (ATC-63) methodology, in: Proceedings of Structures Congress ASCE, New York, 2010.

[3] AISC, Seismic Provisions for Structural Steel Buildings, ANSI/AISC 341-05, American Institute for Steel Construction., Chicago, Ill., 2005.

[4] ASCE, Minimum design loads for buildings and other structures, American Society of Civil Engineers/Structural Engineering Institute, Reston, VA, 2006.

[5] F. P695, Quantification of Building Seismic Performance Factors, Fededral Emergency Management Agency, Washington, D.C, 2009.

[6] L.F. Ibarra, R.A. Medina, H. Krawinkler, Hysteretic models that incorporate strength and stiffness deterioration, Earthquake engineering & structural dynamics, 34 (2005) 1489-1511.

[7] F. McKenna, G. Fenves, M. Scott, OpenSees: Open system for earthquake engineering simulation, Pacific Earthquake Engineering Center, University of California, Berkeley, CA., http://opensees. berkeley. edu, (2006).

[8] D.G. Lignos, H. Krawinkler, Deterioration modeling of steel components in support of collapse prediction of steel moment frames under earthquake loading, Journal of Structural Engineering, 1 (2010) 279.

[9] L.F. Ibarra, H. Krawinkler, P.E.E.R. Center, Global collapse of frame structures under seismic excitations, Pacific Earthquake Engineering Research Center, 2005.

[10] F.A. Charney, J. Marshall, A Comparison of the Krawinkler and Scissors Models for Including Beam-Column Joint Deformations in the Analysis of Moment-Resisting Steel Frames, Engineering journal., 43 (2006) 31.

[11] J. Liu, A. Astaneh-Asl, Cyclic testing of simple connections including effects of slab, Journal of Structural Engineering, 126 (2000) 32-39.

[12] ASCE, Seismic Rehabilitation of Existing Buildings (ASCE/SEI 41-13), American Society of Civil Engineers Reston, Virginia, 2013.

[13] F. Zareian, R.A. Medina, A practical method for proper modeling of structural damping in inelastic plane structural systems, Computers & structures, 88 (2010) 45-53.

Chapter 4: "Influence of the Gravity Framing System on the Collapse Performance of Special Steel Moment Frames"

Francisco X. Flores[a] , Finley A. Charney[a*], and Diego Lopez-Garcia[b]

[a] *Dept. of Civil and Environmental Engineering, Virginia Tech, VA 24060, USA*

[b]*Dept. of Geotechnical and Structural Engineering, Pontifica Universidad de Catolica, Santiago, Chile*

Abstract

This paper investigates the influence of the gravity framing system on the seismic performance of Special Steel Moment Frames (SMFs). The buildings used in this study were taken from one of the examples that form part of the ATC-76-1 project, which used the FEMA P-695 Methodology to assess the collapse probability of SMF systems. Two, four and eight story SMFs were analyzed with and without the gravity frame to quantify their collapse performance. Aspects of the gravity frame that were investigated include the contribution of stiffness and strength of beam to column connections, and the location of splices in the gravity columns. Moreover, this research investigates the potential for the development of inelastic deformations in the gravity columns, and the effect of such deformations on structural response. The results show that gravity connections and gravity column's continuity profoundly affect the computed response and collapse probability. The inelastic behavior in gravity columns has a less important effect but should be included in the analysis.

Keywords: Special Moment Frames, Gravity Framing, Partially Restrained Connections, Column Splices, Continuous Stiffness, Seismic Performance, Collapse Probability

4.1 Introduction

The seismic performance of special steel moment frames (SMF) has been assessed analytically, experimentally, and through observation of performance during previous earthquakes. These different perspectives provide valuable insight into the likely behavior of SMF systems. Additional insight into behavior has recently been provided by Zareian, et al. [1] through collapse analysis carried out using the FEMA P-695 methodology [2]. The buildings used in the study ranged from 1 to 20 stories in height and were designed using ASCE 7-05 [3] and AISC 341-05 [4]. The strength and stiffness of the gravity system was not included in the Zareian et al. study because the P-695 methodology specifies that it not be included when assessing the collapse probability of "performance groups" of similar generic archetypes.

It is typical to ignore the strength and stiffness of a gravity system during structural analysis. However, as part of the experience gained from past earthquakes, the gravity system can profoundly influence response. For example, during the Northridge earthquake in 1994, many steel frames suffered brittle failures of critical beam-to-column connections, but the structures did not collapse. The most likely reason that the buildings remained standing is that the gravity framing acted as a "backup system," preventing structural collapse subsequent to the failure of the connections [5]. Presently, there are no published studies where the gravity system is explicitly modeled and a complete P-695 methodology has been performed to determine its influence on collapse probability.

Gupta and Krawinkler [6] addressed the response of SMFs at various seismic hazard levels. In this study, nonlinear static and dynamic analyses were performed on a variety of different models. The first model was a basic centerline model, and the second model explicitly included the strength and stiffness of the panel zone. There were two additional models that included the gravity system. Model 3 had simple composite connections with strength capacity equal to forty percent the plastic moment

capacity of the beam ($0.4M_p$) for positive bending (top in compression) and strength of twenty percent the plastic moment capacity of the beam ($0.2M_p$) for negative bending. Model 4 had half of the connection strength of model 3. The gravity connections were defined with a simple rotational spring in which the maximum strength was achieved at a rotation equal to 0.02 radians for positive bending and 0.01 radians for negative bending. The authors state from this study that significant response improvements might be achieved at large drifts when gravity frames are included. The potential for improvement depends on the number of gravity frames present, the properties of the gravity connections, the orientation of the columns, the column boundary conditions, and the magnitude of drift demand. However, among all of the members and connections in the gravity system, the contribution of the gravity column continuity appeared to be the most important, with the gravity connections playing a much less significant role. The main conclusion from the Gupta and Krawinkler investigation was that the gravity system can significantly increase the post-yield stiffness of the system, which in turn reduces the influence of P-delta effects under high intensity ground motion.

Lee and Foutch [7] performed an analysis using post-Northridge special steel moment frames including the gravity system. The objective of this study was to compute a confidence factor, λ, which indicates if the structure satisfies the collapse prevention (CP) limit state criteria at the Maximum Considered Earthquake (MCE) (with a 2% in 50-year probability of exceedance). The way this factor is computed is conceptually similar to, but predates that used in the P-695 Methodology. The capacity of the structure, which is the ultimate building capacity against total collapse, is determined using Incremental Dynamic Analysis [8], while the demand of the structure is determined with ground motions representing the 2% in 50-year hazard level. The capacity is modified by uncertainties while the demand is adjusted by a resistance factor. Then, the confidence level is obtained by the ratio of capacity to demand. The results of the analysis showed that the designed buildings would perform well at the

MCE hazard level. Even though this study included the gravity system, a comparison between the performances of the structure considering only the SMF with the one that includes the gravity system was not provided.

An example of a nonlinear static pushover analysis of special SMF performance including the strength and stiffness of the gravity system was reported by NIST [9]. The analyzed structures were the same used by Zareian et al. [1], and the gravity system connections were modeled using a simple elasto-plastic model. The conclusions from this study were that the benefits of incorporating the gravity system depends strongly on the structural configuration, but it could decrease drift demands and increase collapse capacity. Additionally, it is concluded that the gravity system could be effective in delaying or preventing dynamic instability if the gravity framing increases the post-yield tangent stiffness [10].

The studies described above give an insight of the influence of the gravity system. However, none of them specifically investigated the influence of the gravity system on the collapse performance. Gupta and Krawinkler [6] used a very simple model to quantify the simple connections, Lee and Foutch [7] did not differentiate the influence between the lateral resistant system acting alone and then with the gravity system included, and in the NIST study [9] a P-695 collapse analysis was not performed.

MacRae et. al. [11] revealed that continuous stiffness (no splices or splices provide full continuity) given by gravity columns can reduce story drift concentrations and prevent weak story failures in braced frames. This effect was also pointed out by Gupta and Krawinkler [6]. The effect of continuous stiffness in columns is studied in braced frames by Ji et al. [12] and in reinforced concrete structures by Qu et al. [13]. Tagawa [14] studied steel moment frames and the results of his investigation showed that continuous gravity columns improve stability and prevent plastic mechanisms.

4.2 Revised Analysis of SMF Including Gravity Systems

To add to the knowledge base on the influence of gravity framing on the collapse performance of SMF, the P-695 study performed by Zareian et al. [1], and analyzed further in NIST [9], has been extended to explicitly include the gravity framing. The first step in the new analysis was to validate the original analysis for the bare SMFs. This was followed by the new analysis in which the beams, columns, and connections of the gravity system are modeled explicitly. Beam-to-column connections are assumed to be partially restrained (PR). In addition, a variety of assumptions are explored to determine the influence of column continuity and splice locations in the gravity columns. The comparison is made by means of pushover curves and by performing a P-695 collapse analysis.

4.2.1 Evaluation and Model Validation

The ATC-76-1 project [15] is a continuation of the P-695 report where examples of the methodology are described. SMFs analyzed by Zareian et al. [1] form part of the examples illustrated in the report. In this study, buildings of 1, 24, 8, 12 and 20 stories were designed following ASCE/SEI 7-05 [3] requirements with the exception that the deflection amplifier C_d was taken equal to the response modification factor, R, as specified in FEMA P-695.

For the analyzed buildings, the strength and stiffness of the gravity frames were not considered, because as pointed out in the P-695 report, the configuration of gravity columns is highly variable and cannot be predefined when analyzing generic archetypes. It is noted, however, that several guidelines for performance based seismic design establish that the gravity system may be or must be included. PEER/ATC 72-1[16] report states that the gravity system can provide significant benefits for lateral stability at large displacements and it can be included if desired. ASCE 41-13[17] requires the incorporation of secondary components (gravity system) when performing nonlinear static or nonlinear dynamic analysis. Appendix F of FEMA P-695, which is used to assess the collapse performance of an

actual building with a known gravity system (instead of an archetype without a defined gravity system) leaves the incorporation of the gravity system to the discretion of the user.

All these procedures that allow the gravity frame to be included are applied to a specific building, so the gravity system is known and its strength and stiffness can be quantified. On the other hand, the P-695 methodology is used to compute the seismic response factors of a specific structural system. In this case, the gravity system is not known. Therefore, more research is necessary to determine a generic way to include the gravity system to be part of a lateral resisting system.

In the work presented herein, a subset of the buildings analyzed as examples for the ATC-76-1 project are reanalyzed including the gravity system. The chosen SMFs are the 2, 4 and 8 story buildings. These structures were designed using Response Spectrum Analysis (RSA) for a seismic design category D_{max} (S_s=1.5g, S_1=0.6g), and for a typical gravity load. The nomenclature that identifies these structures in ATC 76-1 is 2RSA (2 story), 3RSA (4 story) and 4RSA (8 story).

All the structural analyses for assessing the performance of the systems with and without gravity framing were performed in OpenSees [18] through NEEShub [19]. The approach used to characterize the nonlinear behavior of the main lateral load resisting structure is the same as used in the ATC-76-1 project. The method used for including the gravity system is described later in this paper. However, before a complete evaluation of the structures including the gravity system was performed, the structures without gravity framing were reanalyzed to validate the published results [15] and to form the basis for comparison of the systems with the gravity framing included.

4.2.2 Building Overview.

The 2, 4, and 8 story buildings have the same plan view and seismic design category (D_{max}) and were designed using the same approach (RSA). Connections at the base of the columns are considered fixed for the 4 and 8-story models and pinned for the 2-story model. The seismic force resistance of the

building is provided by a three-bay special SMF with prequalified reduced beam section (RBS) connections located on the perimeter of each side of the building. These SMFs provide lateral resistance to seismic forces and stability against P-Delta shears. Figure 4-1 shows the plan layout for all the buildings analyzed. In the figure the main lateral load resisting system is shown, as is the gravity framing that is considered in further analysis. Note that two of the SMFs columns that form part of the gravity frame are oriented on the weak axis. To be conservative and in order to evaluate just the effect of gravity columns, the lateral strength provided by the SMFs columns oriented on the weak axis is not considered. The shaded area in the figure represents the tributary area for gravity loading on the individual SMFs.

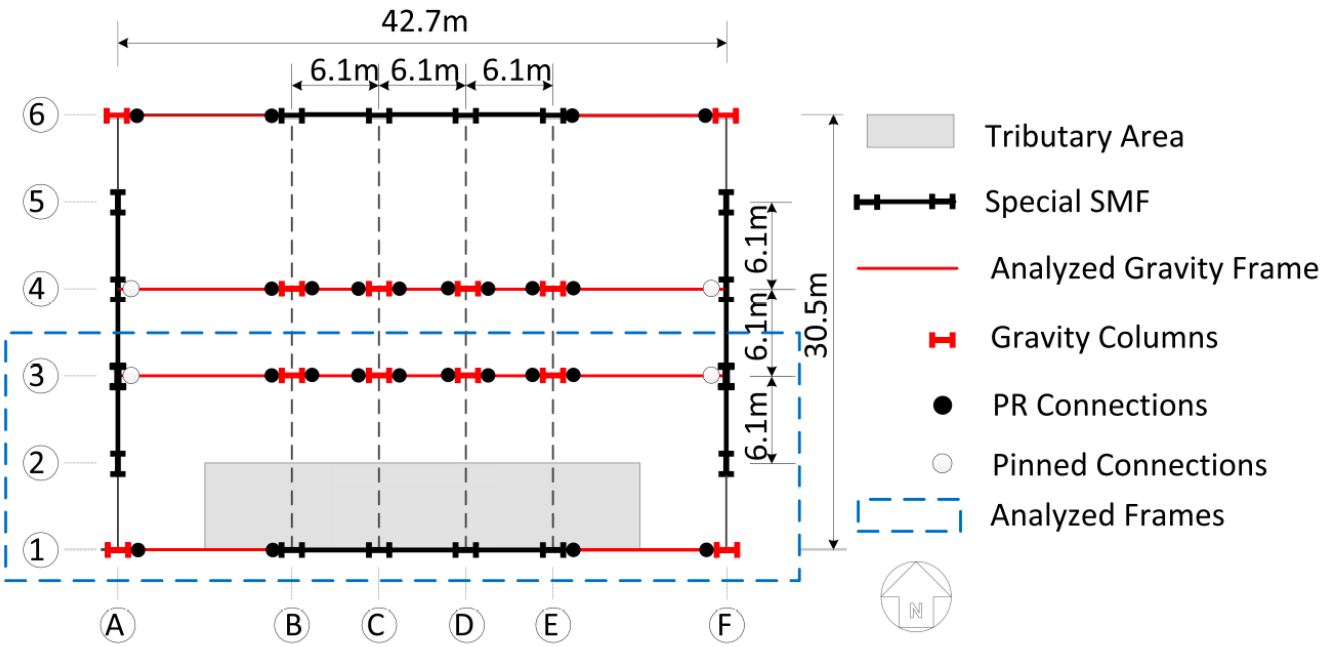

Figure 4-1 Buildings Plan View

The bay width (center line dimensions) between columns of each SMF is 6.1 m. The height of the first story is 4.6 m (to top of steel beam), and the height of all other stories is 4 m. The dead load is

4.31 kN/m^2 uniformly distributed over each floor, and the cladding load is applied as a perimeter load of 1.2 kN/m^2. The unreduced live load is 2.4 kN/m^2 on all floors and 0.96 kN/m^2 on the roof.

4.2.3 Modeling Methodology for the Special Moment Frame

In order to perform a nonlinear analysis, the hysteretic behavior of any component that could behave in an inelastic manner has to be modeled. This is accomplished by modeling components as elastic elements and lumping nonlinearities using phenomenological models into plastic hinges regions near the end of the elements.

The components that behave inelastically in the SMF are shown in Figure 4-2. These are: the plastic hinges located at the reduced beam section, the panel zones, the column bases, and the plastic hinges at the extremes of the columns that have moment resisting connections. A complete description of the inelastic behavior of each component can be found in the ATC 76-1 report [15]. However, a brief overview is provided herein. The Hysteretic behavior of the Reduced Beam Sections (RBS) in the beams is characterized with the "Bilin" material provided within OpenSees. The constitutive law of this material is based on the modified Ibarra-Krawlinkler deterioration model [20], and the parameters to define this model are described by Lignos and Krawinkler [21].

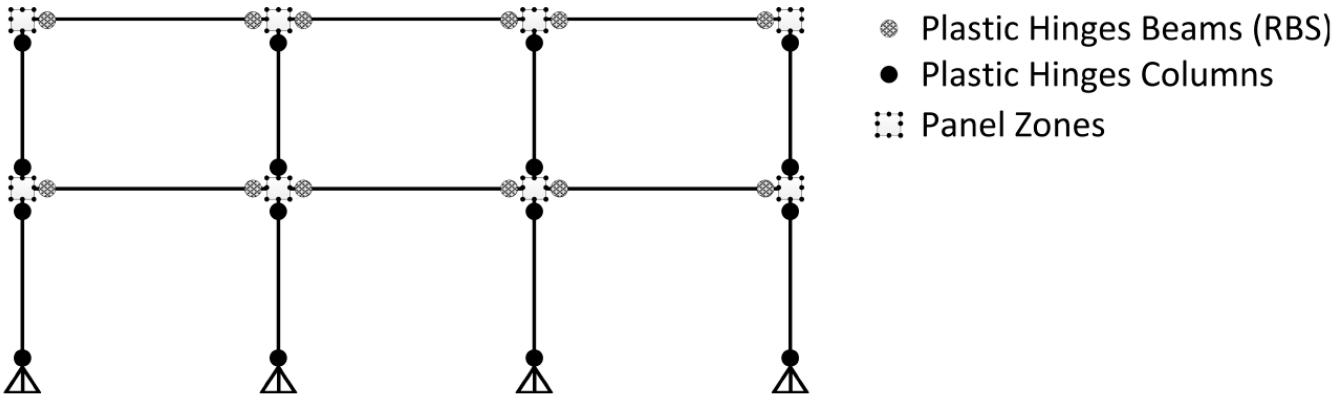

Figure 4-2 SMF 2-Story Model

Panel zones are modeled using a rectangle region composed of eight very stiff elastic beam-column elements and one nonlinear rotational spring to represent shear distortions in the panel zone [22]. These deformations are due to shear yielding and column flange flexure yielding and are represented by a tri-linear backbone curve assigned to the rotational spring.

Currently, there is not a phenomenological element in OpenSees that represents the hysteretic behavior of a column including axial force – bending moment (P-M) interaction. Thus, the same hysteretic behavior used to represent the inelastic behavior of the beams is used for the columns, but the bending strength is decreased due to P-M interaction. Even though the decrease varies depending on the axial force, which changes during a dynamic analysis, the axial force is computed before the analysis and the bending strength is reduced accordingly. The axial force was obtained by performing a nonlinear static pushover analysis and was considered to be equal to $P_{grav} + 0.5P_{E,max}$, where P_{grav} is the gravity load that the column is subjected to and $P_{E,max}$ is the maximum load that the column receives during the pushover analysis. The pushover analysis is performed until a reduction of 20% in the base shear, V_{max}, is reached. With the axial load determined, the reduced bending strength is computed using the AISC P-M interaction equation [23] and subsequently used in the models.

Although the strength and stiffness of the gravity system was not modeled in this analysis, a leaning column was used to represent the destabilizing (P-Delta influence) of the gravity load on the structure. Since the geometric transformation used for each element in the SMF includes the P-Delta effect, a load equal to $1.05D + 0.25L$ *o*n a tributary area equal to half of the plan area minus the shaded area (Figure 4-1) is applied on the leaning column. The leaning column has zero flexural stiffness and is placed parallel to the building. For the case where the gravity system is included the load is applied to the gravity beams. For the nonlinear dynamic response history analysis, a Rayleigh damping of 2.5% is assigned at the first mode period T_1 and at T=0.2T_1 in all cases. As proposed by Zareian (2010) [24],

stiffness proportional damping is assigned to elements that remain elastic, and mass proportional damping is assigned to nodes or elements where mass is lumped.

4.2.4 Performance Evaluation and Validation of Results

In this section, a comparison between ATC 76-1 project results and the results obtained by the authors is presented for the system modeled without gravity framing. For comparison purposes the buildings modeled by the author are called F&C models and the buildings taken from ATC-76-1 project are called ATC models. First, the pushover curves computed for the ATC models are compared with those computed independently by the authors. Next, as required by P-695 methodology, a complete Incremental Dynamic Analysis (IDA) is performed to obtain the collapse margin ratio (CMR), and these values are compared again with the values computed for ATC models.

4.2.5 Nonlinear Static Pushover Analysis

To ilustrate the similarity of results between the F&C models and the ATC models, the 2 and 8 story pushover curves are plotted in Figure 4-3. In addition, the procedure to calculate the FEMA P-695 period based ductility (μ_T) is shown in this figure. The 2 story model pushover curve of this investigation is the closest to the ATC models. The computed period of vibration for this structure is 0.94 s., which is very close to the ATC 2 story model (0.91 s.). The 8 story model, with computed period of vibration of 2.22 s. shows a slightly larger initial stiffness in the pushover curve. The period for the story ATC model is 2.29 s. It is important to note the proximity of the results even though the two studies were executed by different teams of analysts and using different software (DRAIN 2DX and OpenSees).

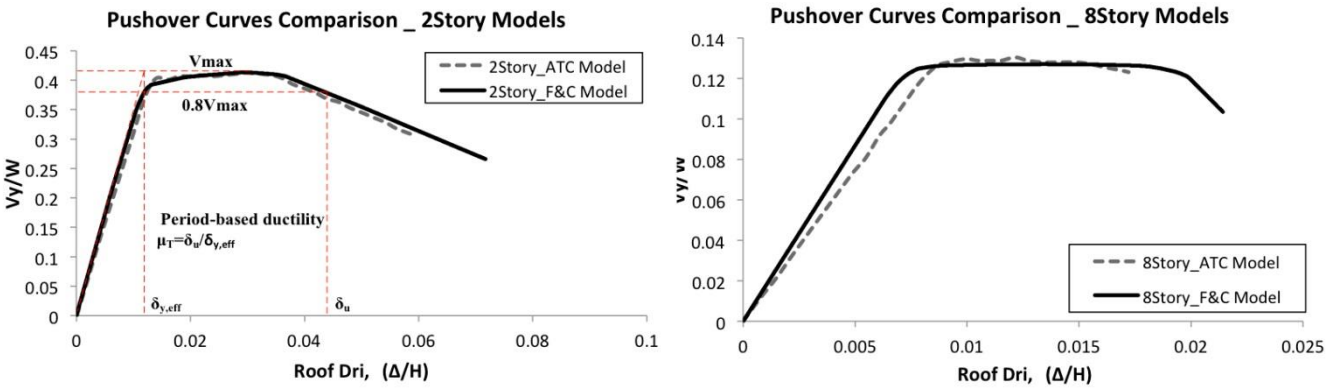

Figure 4-3 Pushover Curves Comparison

4.2.6 Collapse Performance Evaluation

Once the nonlinear static behavior was proven to be similar for both models, a FEMA P-695 collapse performance evaluation is performed to compare the nonlinear dynamic behavior. This comparison is made with the purpose of pointing out how two researchers working independently are able to get almost identical results. The collapse margin ratio (CMR), overstrength (Ω), and the period-based ductility (μ_T) are the main values to be compared because they come directly from the nonlinear dynamic and static analysis. The complete performance evaluation comparison is presented in Table 4-1. The collapse uncertainty, associated with the design-requirements, test data, and nonlinear models used for the evaluation is the same as specified in ATC76-1. The quality ratings assigned to the three uncertainties are: Design requirements (A=Very Good), test data (B=Good) and nonlinear models (B=Good).

Table 4-1 Performance Evaluation Comparison

Arch. Design IDA No.	Model	Design Configuration			Period T (s)	Computed Overstrength and Collapse Margin Parameters					Acceptance Check	
		No. of Stories	Gravity Loads	SDC		Static Ω	CMR	μ_T	SSF	ACMR	Accept. ACMR	Pass/Fail
2RSA	ATC Model	2	Typ.	D_{max}	0.91	3.94	2.22	4.02	1.23	2.73	1.52	Pass
2RSA	F&C Model	2	Typ.	D_{max}	0.94	3.90	2.15	4.27	1.24	2.67	1.52	Pass
3RSA	ATC Model	4	Typ.	D_{max}	1.62	2.21	1.46	4.84	1.33	1.95	1.52	Pass
3RSA	F&C Model	4	Typ.	D_{max}	1.60	2.28	1.48	5.09	1.34	1.99	1.52	Pass
4RSA	ATC Model	8	Typ.	D_{max}	2.29	3.27	1.42	2.74	1.30	1.85	1.50	Pass
4RSA	F&C Model	8	Typ.	D_{max}	2.22	3.26	1.48	3.23	1.34	1.99	1.52	Pass

Table 4-1 shows the results obtained for the ATC and F&C models. The difference in the results for the period, overstrength and CMR between the models is less than 4%. The difference in the ductility results is also less than 6%, with the exception of the 8 story model, where a difference of 17% was obtained. The values shown in the table, besides proving the proximity with the ATC models, are the baseline to obtain the influence of the gravity system when the P-695 procedure is applied.

4.3 Gravity System Influence

In this section of the study, the gravity system is incorporated as part of the lateral load resisting system. Traditionally, beam-to-column connections of gravity frames are modeled as pinned (zero moment resistance), even though it is known they provide strength and stiffness. Given that this strength and stiffness is likely to be less than that obtained for full moment connections, the gravity frame connections for this analysis are considered to be partially restrained (PR). In addition, the influence of gravity column continuity and potential inelastic behavior in gravity columns are investigated by consideration of a variety of splice locations and by explicitly modeling inelastic deformations in the columns.

Table 4-2 a) 2 Story b) 4 Story c) 8 Story Gravity System Member Sizes

a) 2 Story Model

Story	Columns				Beams		
	A1,F1	**A3,F3**	**B3, E3**	**C3, D3**	**A1 - B1, E1 - F1**	**A3 - B3, E3 - F3**	**B3-E3**
1	**W14x43**	W24x162	**W14x90**	**W14x61**	W24x62	W24x94	**W16x36**
2	**W14x43**	W24x162	**W14x90**	**W14x61**	W24x55	W24x84	**W16x36**

b) 4 Story Model

Story	Columns				Beams		
	A1,F1	**A3,F3**	**B3, E3**	**C3, D3**	**A1 - B1, E1 - F1**	**A3 - B3, E3 - F3**	**B3-E3**
1	**W14x43**	W24x103	**W14x90**	**W14x61**	W24x62	W24x94	**W16x36**
2	**W14x43**	W24x103	**W14x90**	**W14x61**	W24x62	W24x94	**W16x36**
3	**W14x30**	W24x62	**W14x90**	**W14x61**	W24x62	W24x94	**W16x36**
4	**W14x30**	W24x62	**W14x90**	**W14x61**	W24x55	W24x84	**W16x36**

c) 8 Story Model

Story	Columns				Beams		
	A1,F1	**A3,F3**	**B3, E3**	**C3, D3**	**A1 - B1, E1 - F1**	**A3 - B3, E3 - F3**	**B3-E3**
1	**W18x76**	W24x162	**W18x143**	**W18x76**	W24x62	W24x94	**W16x36**
2	**W18x76**	W24x162	**W18x143**	**W18x76**	W24x62	W24x94	**W16x36**
3	**W18x76**	W24x162	**W18x143**	**W18x76**	W24x62	W24x94	**W16x36**
4	**W18x50**	W24x162	**W18x76**	**W18x50**	W24x62	W24x94	**W16x36**
5	**W18x50**	W24x131	**W18x76**	**W18x50**	W24x62	W24x94	**W16x36**
6	**W18x50**	W24x131	**W18x76**	**W18x50**	W24x62	W24x94	**W16x36**
7	**W18x40**	W24x94	**W18x50**	**W18x40**	W24x62	W24x94	**W16x36**
8	**W18x40**	W24x94	**W18x50**	**W18x40**	W24x55	W24x94	**W16x36**

Note: Gravity farming shown in **bold** text.

4.3.1 Gravity System Overview

A typical design was conducted to obtain the size of beams and columns of the gravity framing. The system was designed using A992 steel and the same loads as previously mentioned for the SMF. For the purpose of member selection it was assumed that the gravity beams were non-composite and simply supported. The design was performed using SAP2000 [25] and checked by hand. The size of the gravity framing members is provided in Table 4-2, with grid identifiers (e.g. A3) as referenced in Figure 4-1.

As Table 4-2 (a) (b) and (c) illustrate, the gravity system design chosen for the 8 story building has different steel sections than the 2 and 4 story buildings. Sections with more inertia (W18) were used in order to increase columns stiffness and to improve the effect of continuous stiffness provided by the gravity columns. For the lower stories W18 sections with a "column profile" were used (e.g. W18x143) and in the upper levels the 18 inch depth was maintained to facilitate splice construction.

A nonlinear static pushover analysis was performed on the 8 story building to evaluate the performance when a gravity system designed with both W14 and W18 sections are used. The results, shown in Figure 4-4, demonstrate the benefits on the secondary stiffness when sections with more inertia are used in the design. In this analysis the strength of the gravity beam to column connections was taken as zero, so all of the influence of the gravity column is based on its inertia alone.

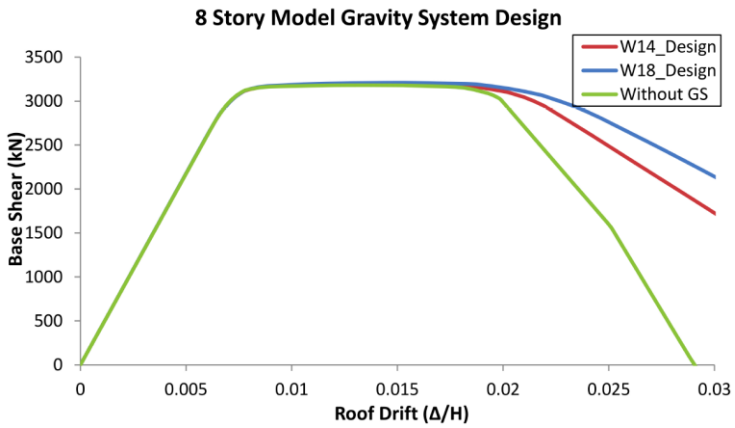

Figure 4-4 Pushover Curves Comparison

For the purpose of this analysis the floor and roof diaphragms were considered rigid in plane, allowing the modeling of the structure in two dimensions. As shown in Figure 4-1, the perimeter framing (on grid line 1 of Figure 4-1) and the interior framing (on grid line 2 of Figure 4-1) were modeled as a single planar frame. The columns of the gravity frame are considered pinned to the base. As an initial study, all the columns included as part of the gravity system are considered to be oriented in the strong axis, leaving for future research the influence of gravity columns with different orientations. The SMF with the gravity frame represent half of the full structure and they were modeled as shown in

Figure 4-5. Because every element stiffness directly includes P-Delta effects, a "leaner column" is not necessary when the gravity system is included. The connections in the gravity frame are taken into account in the analysis by modeling them as partially restrained (PR) connections. As part of this study, the gravity columns are checked for yielding by comparing the nonlinear static pushover curves of models that have the gravity columns behaving elastically with the models that allow the columns to yield. In addition the complete P-695 methodology is performed to quantify the effect of yielding in the gravity columns. When the columns are considered to behave elastically, the only nonlinearity that the gravity frame has is at the beam to column connections. The influence of the PR connections strength is investigated by assuming the connections to have different strengths with respect to the plastic moment capacity of the beam. The flexural strength of the gravity connections is considered to be a percentage of the plastic moment strength of the beam, and the percentages studied are 0% 35%, 50% and 70%. A detailed description of how the behavior of the connections was quantified is discussed later in this paper. The 0% strength is included to study the influence of the gravity column continuity and splice location, which as shown later in this paper, has a significant effect on the system behavior. The use of the 50% and 70% strength ratios may be somewhat unrealistic they are included in the analysis to provide a broad range of behaviors.

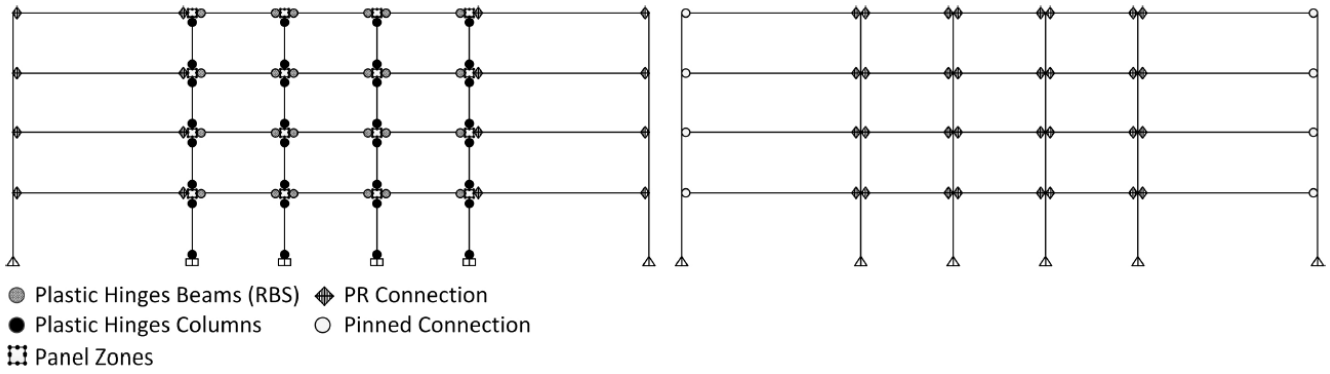

Figure 4-5 SMF with Gravity Frame

Different variations in the gravity frame are made with respect to column modeling in order to understand the influence of the gravity columns on the seismic performance. An initial analysis is performed by modeling the columns with elastic elements and with three assumptions made regarding splice locations. The splice assumption are (1) continuous columns without splices, (2) splices included and located at the same elevation (leveled splices) and (3) columns with splices at different levels (staggered splices). The analysis is then repeated by allowing the columns to behave in an inelastic manner. In this case, the columns are modeled using fiber elements with a bilinear material that has a strain hardening equal to 10% of the initial stiffness. Modeling columns with fibers makes possible to include the axial-moment interaction in the analysis but strength degradation is not considered. This is why plastic hinges at columns of the SMFs were modeled using a phenomenological approach.

The strength requirements for splices in SMF is that they have the same strength as the columns [4]. Thus, for this study it is considered that splices in the SMF provide full moment capacity and they are not explicitly included in the model. On the other hand, lower bound results are computed when the splices are included in the gravity system because they are considered to have no moment resistance. Actual gravity splices will have some stiffness, and this effect will be included in future studies. Wide flange sections have commercial lengths that vary from 10.6 m. to 19.8 m. This range is used as limit to locate the splices. Since the 2 story building has a total height lower than 9.1 m., no splices are required and the columns are continuous from top to bottom. Splices are placed in the 4 and 8 story model. In the case of the 4 story building, it was required to place one splice in each column, as shown in Figure **4-6**.

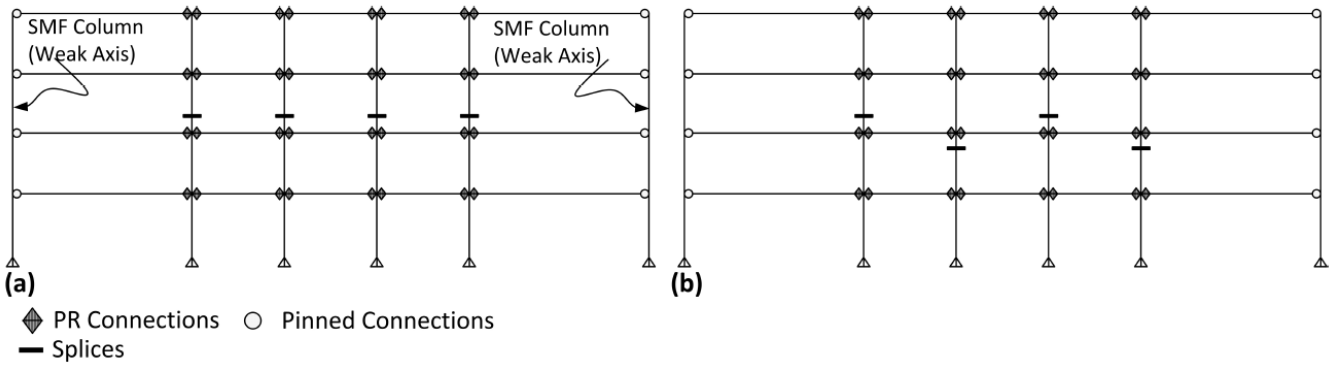

Figure 4-6 (a) 4-Story Model with Leveled Splices (b) 4-Story Model with Staggered Splices

Figure 4-6 (a) shows the 4-story model with leveled splices and Figure 4-6 (b) shows the model with staggered splices. As it was already mentioned the columns that are part of the SMF but oriented in the weak axis are considered to have no flexural strength, so they do not provide continuous stiffness. Splices on columns A-1 and F-1 (Figure 4-1) are located at the third of the height in the second story for the leveled and staggered case. As it was already mentioned the same analysis is repeated but dividing the columns in three elements and modeling these with fibers.

The splice location is an important factor to consider. In this study splices are located at two thirds of the column height. This is unusual in common construction but a nonlinear static pushover analysis was performed to determine if the traditional 1/3 height produces optimal performance. For instance, three different options were studied for the 8-story building: splices located at one third, middle and two thirds of the column height. The results of the splice location analyses are shown in Figure 4-7.

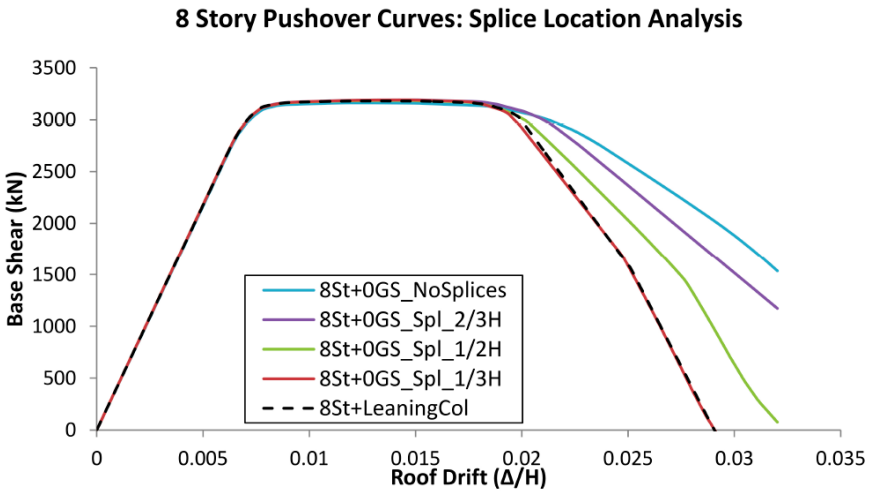

Figure 4-7 Effect of Splice Location on Pushover Response

It can be seen from the pushover curves that splice location is a very important factor in performance. The optimum case is when no splices are placed because continuous stiffness is provided. The worst location for the splices is at one third of the column height, which is the traditional location in construction. The gravity system in this case has no effect at all on the performance. The next best scenario occurs when splices are located at two thirds of the column height. Even though, this is not a common place to locate the splice, it is used for the analysis. It has to be mentioned that for the 8-story model, the location of the first splice above grade is the most important and in order to obtain the best performance, it should be located as far as possible from the base. This is because the continuity of gravity columns provides continuous stiffness that decreases drift concentrations in the first stories and reduces the probability of weak story mechanisms. The 8-story model requires three splices in each column. These are located in a leveled and staggered manner. The location is shown in Figure **4-8**.

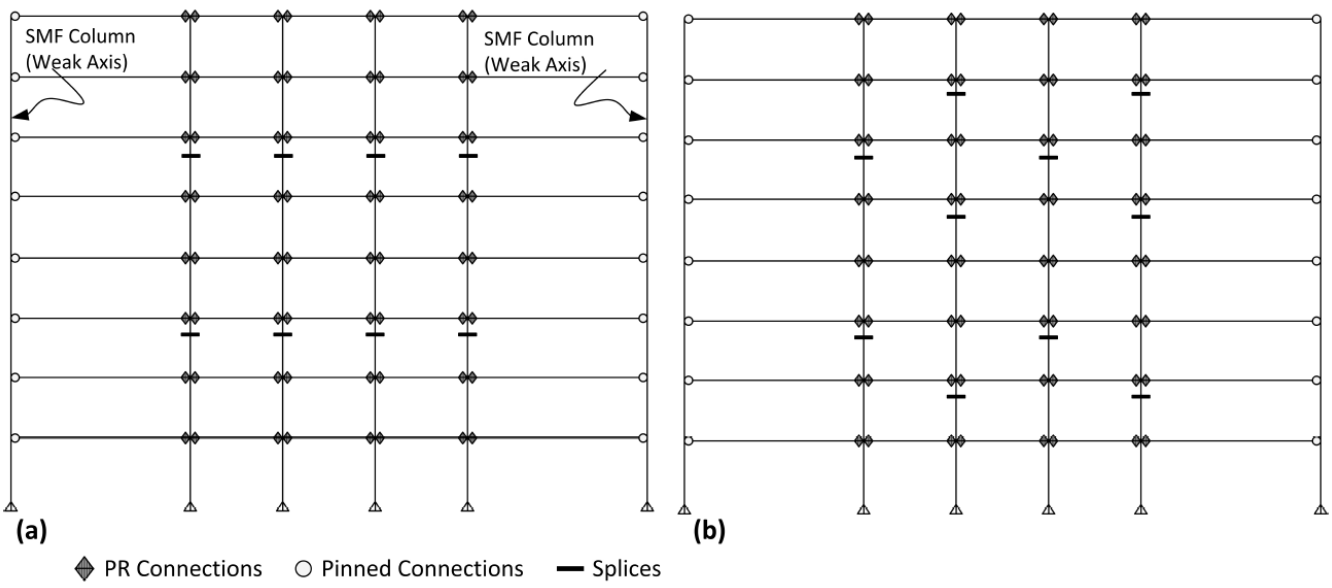

Figure 4-8 (a) 8-Story Model with Leveled Splices (b) 8-Story Model with Staggered Splices

Splices are located at the extreme columns (e.g. location A-1) of the special SMF as well. These columns are not part of the lateral resisting system as it was already mentioned. The location of these is at the same level and they are placed in the same position as the splices of the first (left) column of the gravity frame (Figure 4-8(a) and (b)).

4.3.2 Partially Restrained Connections

Partially restrained connections have the capability to sustain large deformations was demonstrated by Liu and Astanneh [26]. Unfortunately, an accurate and relatively easy model to define the parameters for the hysteretic behavior of a PR connection has not been yet defined and the most common approach used to perform nonlinear dynamic analysis is to match experimental results with a predefined hysteretic model. Another approach to obtain the cyclic behavior of a PR connection is using the component method, where the connection is decomposed in all possible limit states by using a variety of nonlinear springs. Each spring has a different constitutive law that represents the effect in question. A model created by Rassatti et al. [27] is capable of predicting the behavior with accuracy.

However, this model was implemented in ABAQUS and it is too cumbersome and computationally inefficient for implementation in a P-695 analysis of a complete moment frame. The objective of this investigation is to have a better insight of the influence of these connections on a performance evaluation using the P-695 methodology. Therefore, a simple hysteretic behavior given by ASCE 41-13 [17] is used (Figure 4-9).

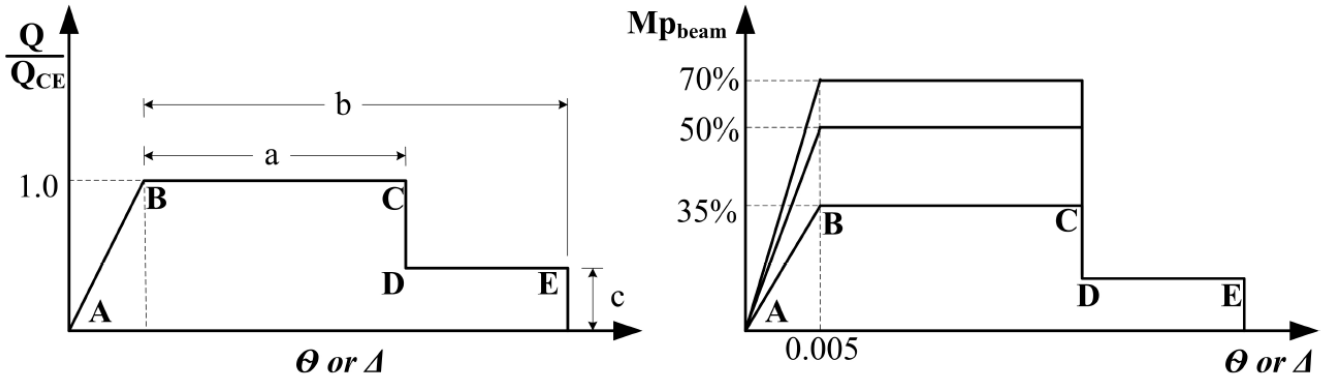

Figure 4-9 Moment Rotation Characterization Curve [17]

The model given by ASCE 41-13 was developed from experimental data and it depends on the type of PR connection and it is intended to be used for Nonlinear Static Pushover Analysis only. However, for the purpose of this research and considering that this model represents a conservative hysteretic behavior of the connection, it is used for the dynamic analysis. The model is conservative because PR connections tests have some strain hardening, and do not show the flat plateau and the maximum strength usually occurs at a larger rotation than the 0.005 radians as specified by this model. Two parameters are required to define this curve besides that observed in Figure 4-9, initial stiffness (K_{CE}) and moment capacity of the connection (Q_{CE}). The initial stiffness is computed according to ASCE 41-13 and is equal to the moment capacity of the connection divided by 0.005 radians. However, the moment capacity of the connection (Q_{CE}) depends on the type of connection and the limit state (failure mode) that controls the design. This value depends on the characteristics of the connections and

is obtained by calculating the controlling failure mode. This failure mode is the minimum value computed from several equations given by ASCE 41-13, and they depend on the type of connection. The rest of the parameters displayed in Figure 4-9 are given in Table 9-6 of ASCE 41-13 and they differ depending on the type of PR connection and on the limit state that controls the design. A "top and bottom clip angle connection" is chosen as a PR connection for this analysis, and the connection is configured so that the controlling limit state is flexural failure of the angles. The parameters extracted from ASCE 41-13 are shown in Table 4-3. The shaded row is the chosen limit state.

Table 4-3 Modeling Parameters PR connection [17]

Top and Bottom Clip Angle	**Plastic Rotation**		**Residual Force Ratio**
	a	**b**	**C**
a. Shear Failure of Rivet or Bolt	0.036	0.048	0.2
b. Tension Failure of Horizontal Leg of Angle	0.012	0.018	0.8
c. Tension Failure of River or Bolt	0.016	0.025	1
d. Flexural Failure of Angle	0.042	0.084	0.2

As it was stated, the main principle of PR connections is that its capacity is lower than the plastic moment of the connected beam. In the analysis presented herein the strength or capacity of the connection is assumed to be a percentage of the plastic moment of the beam and is not computed from the design. The percentages used to define the strength of the connections are 0, 35, 50 and 70% and they are assigned to every connection in the gravity frame. The lower bound strength of 35% considered for this analysis was determined as the minimum strength required to prevent the connections to reach a rotation of 0.005 radians (yielding point) under gravity loads. Modeling the connection in the simple manner described above will provide the required insight into the influence of gravity framing on the seismic performance of SMFs.

4.3.3 Nonlinear Analysis

Nonlinear analysis is required by P-695 methodology to evaluate the performance of the special SMF when the gravity system is incorporated. The results of the nonlinear static pushover analysis are used to compute overstrength (Ω) and period-based ductility (μ_T) of the each archetype. Incremental dynamic analysis (IDA) is then performed to compute the collapse margin ratio (CMR).

4.3.3.1 Nonlinear Static Pushover Analysis

Nonlinear static pushover analysis is performed on all the models in order to compute Ω and μ_T. The lateral load applied to the system corresponds to the fundamental mode shape and mass distribution of the system. A total of 59 pushover analyses were performed. The nomenclature used to differentiate the results among the analyses is: 8Story + 0GS_(Lev/Stg)_Spl_Fib

8Story:	Number of floors the building has.
0GS:	Percentage of strength assigned to PR connections (0%).
(Lev/Stg)_Spl:	Indicates that splices are used for that model. (Lev/Stg) describe if the splices are leveled or staggered.
Fib:	Indicates if gravity columns are modeled with fiber elements.

If the indicator "Fib" is not present in the name it means that the columns are modeled using elastic elements.

Pushover curves of the 2 story building are shown in Figure 4-10. As it was already mentioned, splices are not included in this model because the total height of the building allows the columns to be continuous.

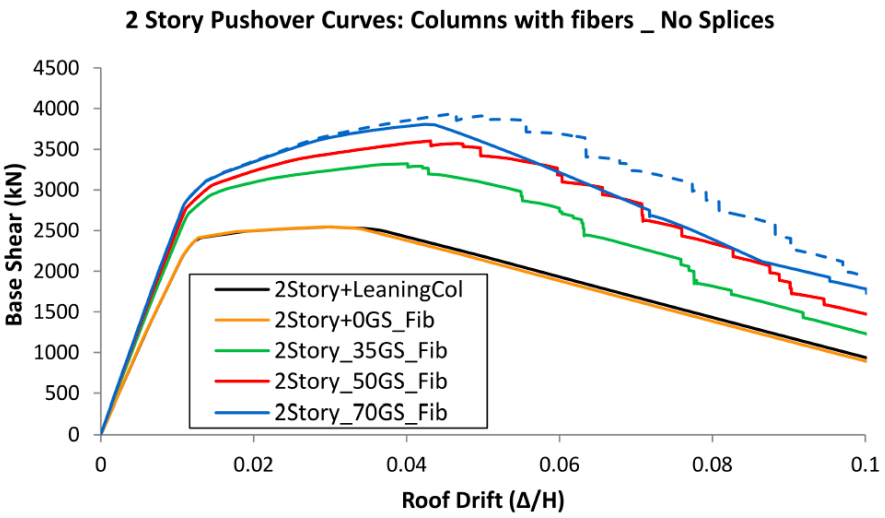

Figure 4-10 Pushover Curves 2 Story Model

The influence of PR connections can be seen in Figure 4-10 and it is significant even for the smallest percentage of strength assigned to the PR connections (35%). The influence of the gravity columns is illustrated when the PR connections strength is zero and is negligible as can be seen by the lowermost two pushover curves. The use of fibers allows the columns to yield if required. The difference between columns that behave elastically and inelastically for the 2-Story model is insignificant except for the case where PR connections have 70% strength. In this case, the lateral strength contribution of the gravity columns was lost because all the columns yielded in a point located at the same height. The elastic pushover curve for the case where PR connections have 70% strength is plotted with dotted lines using the same color as the case when fibers where used. The main data obtained from the nonlinear static analysis are summarized in Figure 4-11. These are: the overstrength (Ω) and period-based ductility (μ_T).

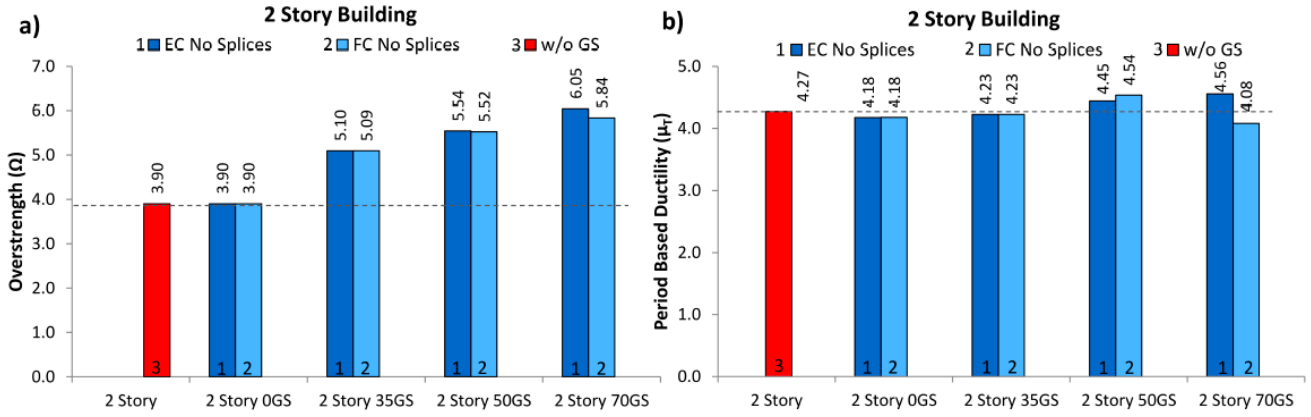

Figure 4-11 Results of 2 Story Model a) Overstrength b) Ductility

Figure 4-11 demonstrates the significant influence that PR connections strength have on overstrength. The maximum increment is around 50% when the 70% PR connections are used. The 2 story model period based ductility is not affected by the strength of the gravity connections and the period of vibration decreased around 10% for the strongest PR connections. Note that the results between the elastic and inelastic gravity columns are almost the same except for PR connections that have 70% strength for the reason already mentioned.

The results of the 4 story model are summarized herein. Figure 4-12 (a) shows the pushover curves for all the cases when no splices were considered and the columns of the gravity system can behave inelastically. This plot demonstrates the influence of the gravity system on the strength and ductility of the structure. As it was expected, the base shear capacity increases when more strength is assigned to the connections of the gravity system. Figure 4-12 (b), (c) and (d) display the pushover curves when the splices are placed in the gravity system. If the results of the case where the columns behave elastically or inelastically differ, the pushover curve for the elastic case is also included with a dotted line. The effect of yielding in the gravity columns is not significant but generally it decreases ductility. The use of splices in the gravity system decreases ductility drastically because continuous stiffness provided by columns of the gravity system is reduced, making the structure more vulnerable to

soft story mechanisms and inter-story drift concentrations. From Figure 4-12(b), (c) and (d) it can be seen that leveled splices provide almost the same strength and ductility to the system than staggered splices. Although ductility is decreased by the use of splices, it has to be emphasized that overstrength maintains virtually the same value as the case where no splices are added.

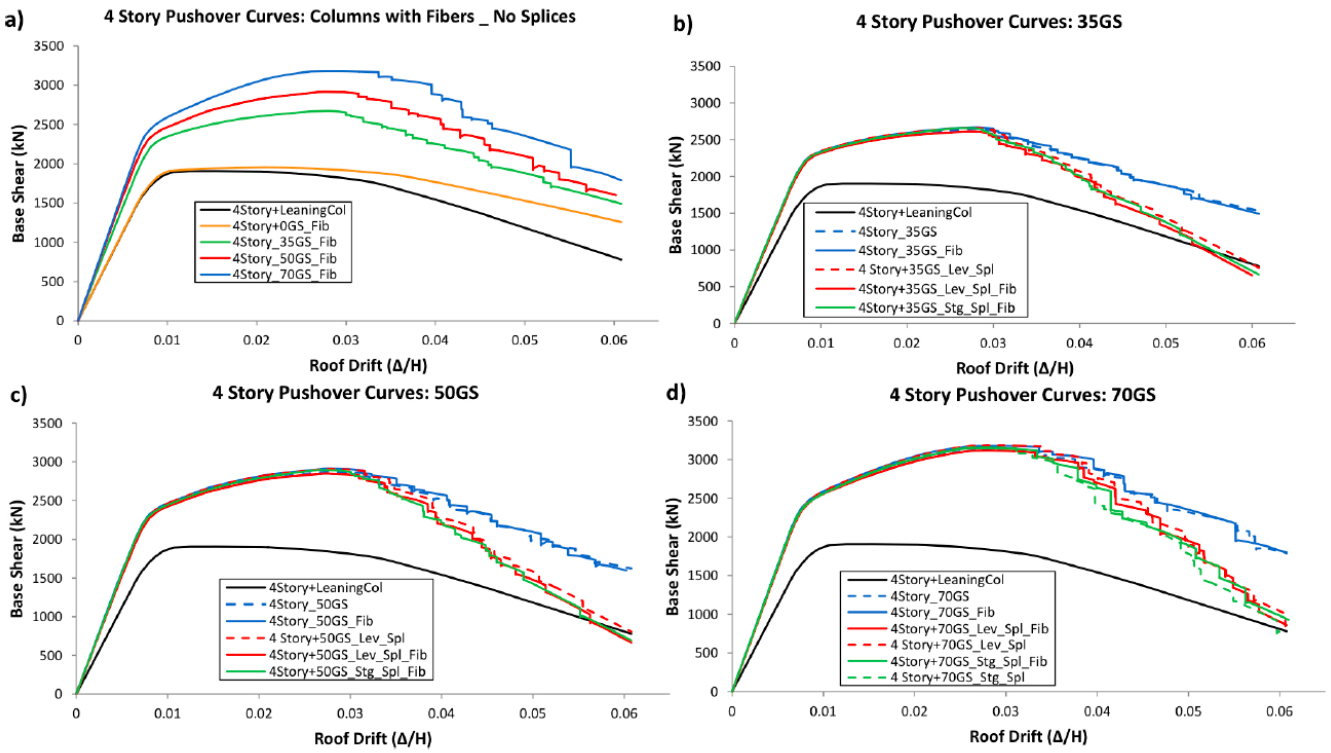

Figure 4-12 Pushover Curves 4 Story Model

The influence of the gravity system overstrength and period-based ductility for all the analyses is shown in Figure 4-13(a), (b). The overstrength in comparison to the SMF without the gravity system is almost the same when PR connections are pinned (0GS) but the ductility increases. On the other hand when strength of the PR connections increases the overstrength increases as well but the ductility decreases (Figure 4-13 b). For instance, the overstrength increases 40% but ductility decreases 11% when the PR connections have 35% strength and leveled splices are placed. The results when connections have no rotational strength and no splices are placed improved in comparison with the SMF by itself. For this case, the ductility increases 17% and the overstrength is the same. The period of

vibration of the structure increases 10%, 14% and 15% when PR connections have 35%, 50% and 75% strength respectively. Note again that the results of the analysis with elastic gravity columns are almost the same as the one with inelastic gravity columns.

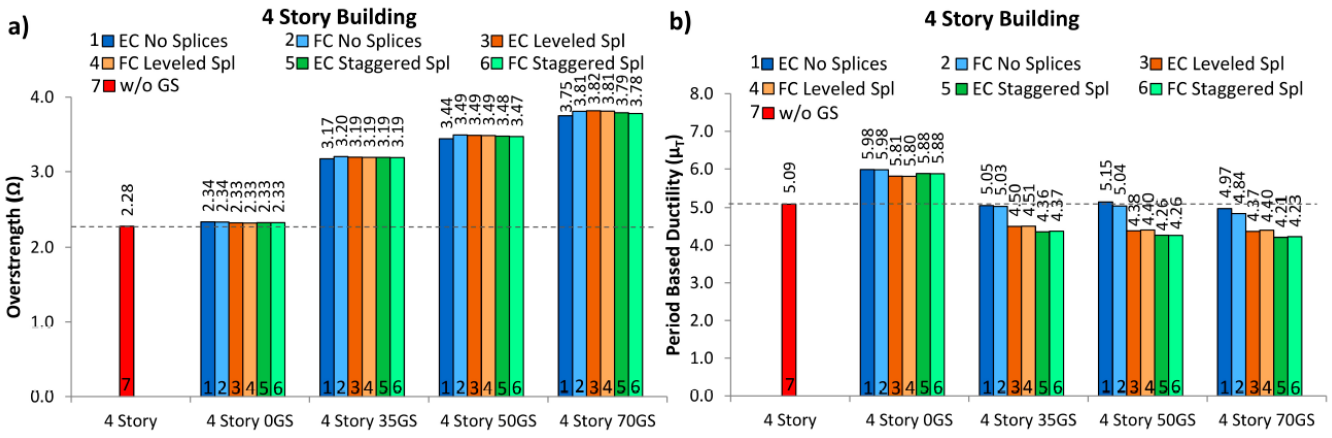

Note: EC: Elastic Columns, FC: Columns with Fibers

Figure 4-13 Results of 4 Story Model a) Overstrength b) Ductility

Pushover curves of the 8 story building, provided in Figure 4-14, show the same tendency as the 4 story building. Overstrength increases when PR connections strength increase and ductility decreases when splices are included. The effect of continuous stiffness, reflected in columns with no splices, have a positive and very important influence on ductility. This is because continuous stiffness reduces the probability of inter-story drift concentrations and soft story mechanisms to occur. Figure 4-14 (b), (c) and (d) show the effect of placing splices in the gravity columns. As it was already mentioned, dotted lines were used for the elastic cases when the elastic and inelastic analyses differ. As a result, it can be seen that columns yielded for the cases where no splices are placed and when staggered splices are used. Therefore, nonlinearity of columns in the gravity system is important to include in order to perform a correct analysis. Ductility decreases significantly for both cases where splices are included but the leveled splices show slightly better results.

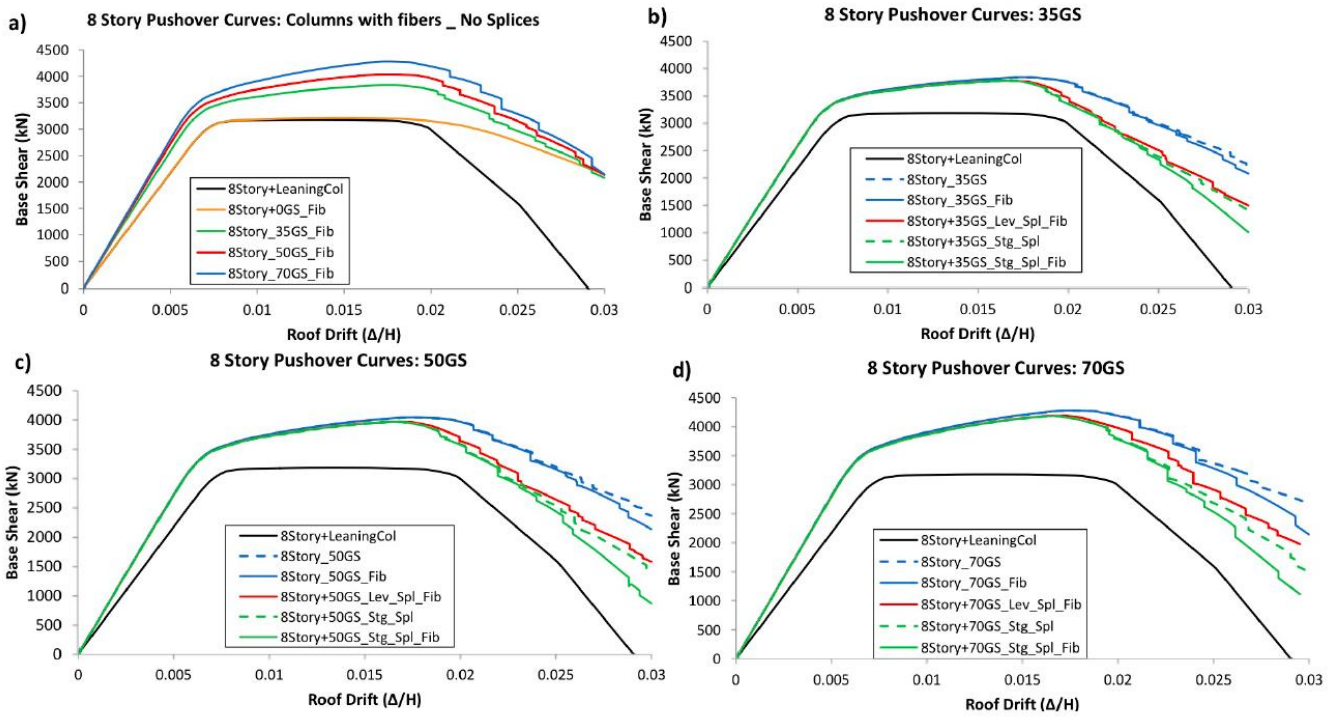

Figure 4-14 Pushover Curves 8 Story Model

The overstrength and period based ductility change depends on the type of analysis. The results for the 8 story model are shown in Figure 4-15. The overstrength increases 1%, 21%, 27% and 35% when the columns of the gravity system are considered to be continuous and the strength of the PR connections is 0%, 35%, 50% and 70% of the of the beams plastic moments respectively. On the other hand ductility for this case increases 22%, 11%, 10% and 5%. Hence, gaining strength represents a loss in ductility even though the lowest value is still 5% larger than the case without the gravity system. Note that overstrength is almost the same when splices are included for all the cases but they have a drastic effect on ductility. When leveled splices are included ductility increases 11% when PR connections have 0% strength, and 3% for the rest of PR connections strengths in comparison to the SMF by itself. The results for the staggered splices are close but worse than the leveled case. Even though yielding occurred in the gravity columns during the analysis, the results are very similar or the same. The period of the

structure is the same when strength of the connections is null but it decreases 7%, 9% and 10% when the PR connections have strength of 35%, 50% and 70% respectively.

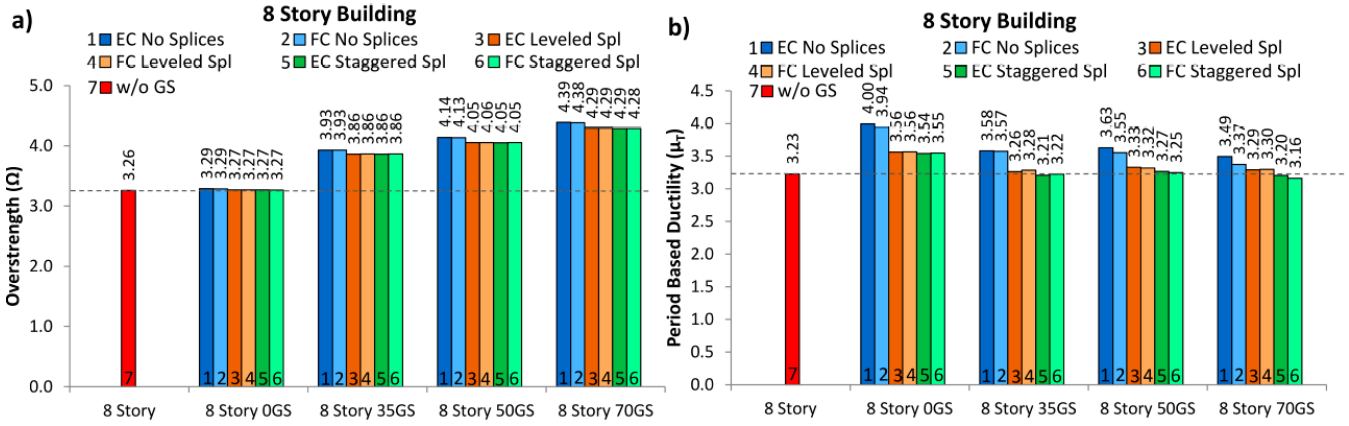

Note: EC: Elastic Columns, FC: Columns with Fibers

Figure 4-15 Results of 8 Story Model a) Overstrength b) Ductility

4.3.3.2 Collapse Performance Evaluation

In order to evaluate the collapse performance, according to P-695 procedure, performing an IDA is required. In this analysis each of the 44 different Far-Field ground motion is scaled to increasing intensities until the structure collapses. The collapse of the structures was established as defined in FEMA 350 [28]. According to this document, global stability capacity fails when the slope of the IDA curve is less than or equal to 20% of the elastic slope of the IDA curve, or when global drift reaches 0.1. Once the CMR is obtained, the performance evaluation following P-695 methodology is performed. The most important parameters are the CMR and probability of collapse because they show directly the influence of the gravity system. Since it was already determined that columns of the gravity frame should be modeled with capability to yield, all the results discussed in the following refer to the cases where columns are modeled with fibers. However, for comparison purposes the results for both cases are shown in all figures. The gravity connections strength has an important influence on the 2-story model and this is reflected in the CMR and probability of collapse shown in Figure 4-16(a) and (b). The CMR

goes from 2.15 to 2.80 when 70% strength is assigned to the connections. Continuous stiffness effect provided by the gravity columns also has an influence on the performance making the CMR increase from 2.15 to 2.40 (10%) which represents a reduction in the probability of collapse of 40% (Figure 4-16(b)). Even though the probability of collapse of this structure is low (2.49%), it is remarkable to see how this value decreases significantly when the gravity system is included. The effect of yielding in the gravity columns is clear for the case with 70% strength PR connections because the CMR decreased even more than the case where PR connections have 50% strength.

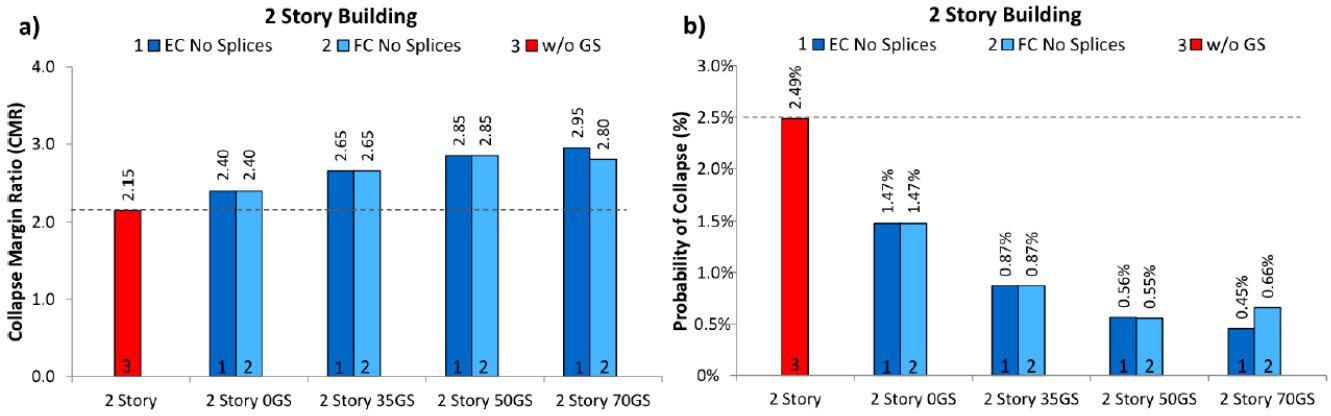

Note: EC: Elastic Columns, FC: Columns with Fibers

Figure 4-16 Results of 2 Story Building (a) CMR (b) Probability of Collapse

The parameters to quantify the influence of the gravity system on the 4 story model are also the CMR and the probability of collapse. Therefore, they are plotted for each model (Figure 4-17).

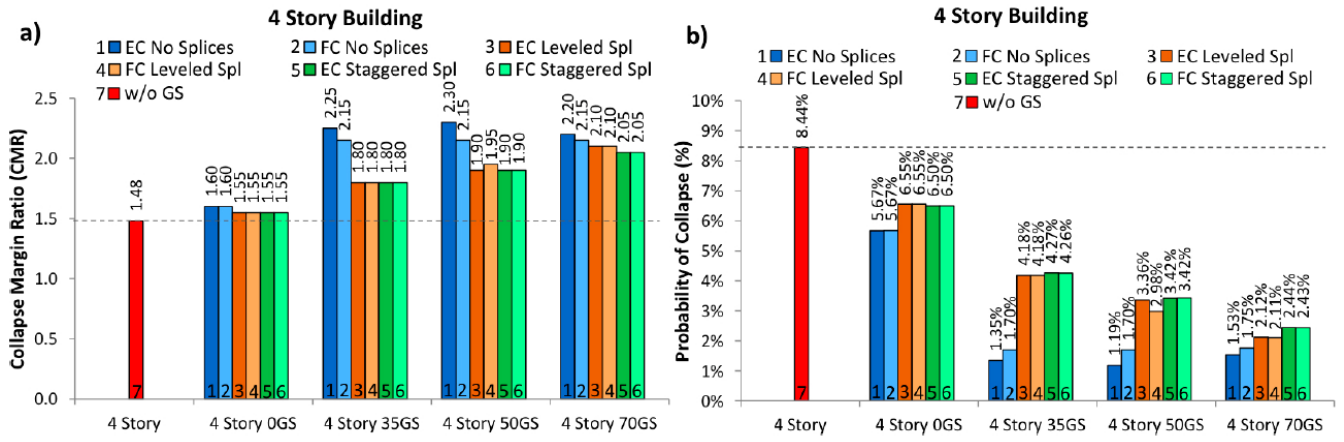

Note: EC: Elastic Columns, FC: Columns with Fibers

Figure 4-17 Results of 4 Story Building (a) CMR (b) Probability of Collapse

Figure 4-17 shows the CMR and probability of collapse of the 4 story building when the gravity system is included in the analysis. These figures clearly show the very significant influence of the gravity system on the performance. However, the main findings are listed herein. The CMR for the situation with no gravity column splices is increased by 8%for the cases with 0% PR strength and 45% for the rest of the PR strength cases. It is important to notice the important improvement in the results when 35% strength is assigned. However, the results do not improve at all when 50% or 70% strength is assigned. This is also reflected in the probability of collapse where PR connections with 0% strength reduces 33% and the rest of PR connections cases reduces 80% the probability of collapse. Therefore, the influence of PR connections strength to certain level is important in the 4-story model. Continuity of gravity columns improved 8% the CMR, so its influence is not as significant as gravity connections. When splices are included, the influence is diminished. The results when leveled and staggered splices are placed are comparable, but leveled splices produces slightly better results for most of the cases.

Figure 4-18 presents the influence of the gravity system in the CMR and probability of collapse of the 8-story building. The CMR increased and the probability of collapse decreased for all the studied cases. However, the most important findings are emphasized herein.

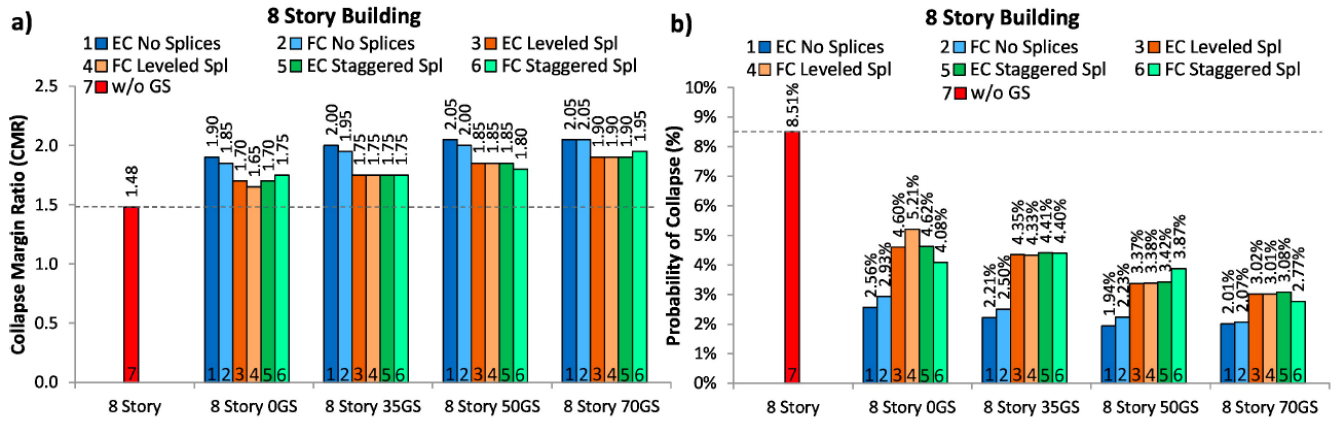

Note: EC: Elastic Columns, FC: Columns with Fibers

Figure 4-18 Results of 8 Story Building (a) CMR (b) Probability of Collapse

Starting for the case where no splices are included, it can be seen that the most important increment occurs when the gravity system is included with no strength in the connections, for this case the CMR goes from 1.48 to 1.85 (25% increment) and the probability of collapse goes from 8.51% to 2.93%. From this point, when strength is added to connections, the CMR is practically constant for all the cases. This proves once more the importance on performance that continuous stiffness brings through the columns of the gravity system with no splices and how the influence of strength of connections reduces for taller buildings. The use of splices decreases the CMR and the probability of collapse increases but it is still beneficial to include the gravity system in the analysis. From the results presented in Figure 4-18 (a) and (b), it can be seen that staggered and leveled splices improved the performance of the building basically in the same amount. The tendency of the case where splices are included is the same as when no splices are placed. The increment is larger when just the columns of the gravity system are included in the analysis and the results are almost the same for all the connections strengths tested.

4.4 Future work

The performed study demonstrates the influence of the gravity system in the performance of a structure. However, since several assumptions were made, future research is required to have a more in depth understanding of the influence. The first aspect to be investigated is the use of a more realistic and accurate model for the PR connections. The purpose of the current study was to evaluate the influence of these connections by assuming different strengths. Since the results obtained are promising, it justifies implementing a better PR connection hysteretic behavior. The second point to look at is the real orientation of the gravity system columns. As the presented results show, gravity columns have a very important influence on the performance. This study considered all the gravity columns oriented in the strong axis. As part of future research, the inertia required by the gravity columns to obtain a pushover curve with a secondary stiffness with a less steep slope in comparison to the SMF by itself should be computed.

Additional future studies should include more realistic modeling of gravity splice connections, and the column base connections as the stiffness and strength of these connections are likely to be influential in the computed response.

4.5 Conclusions

Including the gravity system requires more effort in modeling and time of analysis. However, after performing this study it can be concluded that including the gravity framing in the analysis is something that should be done to obtain an accurate assessment of the likely behavior of the structure. The findings from this investigation are:

1. Columns of the gravity system have an important influence in the performance, especially when they are considered to be continuous all their full height. This influence can be seen in every case where no strength is assigned to the PR connections and it is more beneficial for taller structures.

Columns with no splices provide continuous stiffness that improves the collapse performance of structures by decreasing the probability to have inter-story drift concentrations or soft story mechanisms.

2. Continuous stiffness provided by columns with no splices helps the structure to deform in the first mode and that is why drift concentrations and story mechanisms could be prevented.
3. Yielding in the columns of the gravity system cannot be predicted so it is required to include the nonlinear behavior, especially for cases where strength of gravity connections is considered.
4. The period of vibration of the analyzed structures decreases when the gravity system is considered to have strength in its connections. The increment varied depending on the structure but it can increase up to 15%.
5. Stronger PR connections increase overstrength and CMR, especially on smaller buildings.
6. In general, all the parameters measured in this study decreased when splices are included in the columns. However, the performance is still better than the SMF by itself.
7. The probability of collapse decreased significantly when the gravity columns continuity is included in the analysis. For instance, the 2, 4, and 8 story buildings had a reduction of 40%, 33% and 66% respectively for the case when PR connections have 0% strength.
8. The location of splices is an important factor to consider since CMR changes when leveled or staggered splices are used. In most cases leveled splices improved the performance more than staggered splices. But, columns with no splices showed the best results.
9. Incorporation of the gravity system generally improved the collapse capacity based on the FEMA P-695 methodology.

4.6 Recommendations

The performed study showed that performance of the SMFs improved when the gravity system is included in the analysis. This improvement, not included in traditional analysis, is considered to be an implicit factor of safety and that is why the gravity system is not traditionally considered. However, it could be safer if some critical aspects are considered in the analysis. These include the gravity columns continuity and splice locations in tall structures and the gravity connections strength in small structures. Having said this, the following specific recommendations are made:

1. In order to decrease the probability to have drift concentrations and soft story mechanisms in tall buildings, continuity of gravity columns should be considered.
2. Gravity connections strength could be included for small buildings to improve their seismic performance.
3. Nonlinearity in columns of the gravity system must be included when strength of gravity connections is considered.
4. Nonlinear pushover analysis should be performed to obtain the best location for placing the splices in gravity columns. From this study it is concluded that the first splice should be as far as possible from the ground as it influences the performance the most.

4.7 Acknowledgments

The work presented herein was possible through the support of the National Institute of Standards and Technology, award number 60ANB10D017. The authors would also like to acknowledge the contribution of Mr. Andy Hardyniec of Virginia Tech for his work creating the FEMA P-695 Toolkit and NeesHub for their help on conducting all the computations in their super computers.

4.8 References

[1] F. Zareian, D. Lignos, H. Krawinkler, Evaluation of seismic collapse performance of steel special moment resisting frames using FEMA P695 (ATC-63) methodology, in: Proceedings of Structures Congress ASCE, New York, 2010.

[2] FEMA, Quantification of Building Seismic Performance Factors (FEMA P-695), Fededral Emergency Management Agency, Washington, D.C, 2009.

[3] ASCE, Minimum design loads for buildings and other structures, American Society of Civil Engineers/Structural Engineering Institute, Reston, VA, 2006.

[4] AISC, Seismic Provisions for Structural Steel Buildings, ANSI/AISC 341-05, American Institute for Steel Construction., Chicago, Ill., 2005.

[5] R.T. Leon, Composite connections, Progress in Structural Engineering and Materials, 1 (1998) 159-169.

[6] A. Gupta, H. Krawinkler, Behavior of ductile SMRFs at various seismic hazard levels, Journal of Structural Engineering, 126 (2000) 98-107.

[7] K. Lee, D.A. Foutch, Performance evaluation of new steel frame buildings for seismic loads, Earthquake engineering & structural dynamics, 31 (2002) 653-670.

[8] D. Vamvatsikos, C.A. Cornell, Applied incremental dynamic analysis, Earthquake Spectra, 20 (2004) 523.

[9] NIST, "Applicability of Nonlinear Multiple-Degree-of-Freedom Modeling for Design", National Institute of Standards and Technology, USA, 2010.

[10] A. Gupta, H. Krawinkler, Dynamic P-delta effects for flexible inelastic steel structures, Journal of Structural Engineering, 126 (2000) 145-154.

[11] G.A. MacRae, Y. Kimura, C. Roeder, Effect of column stiffness on braced frame seismic behavior, Journal of Structural Engineering, 130 (2004) 381-391.

[12] X. Ji, M. Kato, T. Wang, T. Hitaka, M. Nakashima, Effect of gravity columns on mitigation of drift concentration for braced frames, Journal of Constructional Steel Research, 65 (2009) 2148-2156.

[13] Z. Qu, L. Ye, A. Wada, Seismic damage mechanism control of RC ductile frames from a stiffness point of view, in: 8th International Conference on Urban Earthquake Engineering, Tokyo, Japan, 2011.

[14] H. Tagawa, Towards an understanding of seismic response of 3D structures-stability & reliability, Doctor Thesis, Washington: University of Washington, (2005).

[15] NIST, Evaluation of the FEMA P-695 Methodology for Quantification of Building Seismic Performance Factors, National Institute of Standards and Technology, USA, 2010.

[16] PEER, Modeling and Acceptance Criteria for Seismic Design and Analysis of Tall Buildings (PEER/ATC 72-1), Pacific Earthquake Engineering Research Center, Richmond California, 2010.

[17] ASCE, Seismic Rehabilitation of Existing Buildings (ASCE/SEI 41-13), in, American Society of Civil Engineers Reston, Virginia, 2013.

[18] F. McKenna, G. Fenves, M. Scott, OpenSees: Open system for earthquake engineering simulation, Pacific Earthquake Engineering Center, University of California, Berkeley, CA., http://opensees. berkeley. edu, (2006).

[19] T.J. Hacker, R. Eigenmann, S. Bagchi, A. Irfanoglu, S. Pujol, A. Catlin, E. Rathje, The neeshub cyberinfrastructure for earthquake engineering, Computing in Science & Engineering, 13 (2011) 67-78.

[20] L.F. Ibarra, R.A. Medina, H. Krawinkler, Hysteretic models that incorporate strength and stiffness deterioration, Earthquake engineering & structural dynamics, 34 (2005) 1489-1511.

[21] D.G. Lignos, H. Krawinkler, Deterioration modeling of steel components in support of collapse prediction of steel moment frames under earthquake loading, Journal of Structural Engineering, 1 (2010) 279.

[22] F. Charney, J. Marshall, A comparison of the Krawinkler and scissors models for including beam-column joint deformations in the analysis of moment-resisting steel frames, Engineering Journal - American Institute of Steel Construction, 43 (2006) 31.

[23] AISC, Specification for Structural Steel Buildings, AISC/ANSI 360-05, American Institute of Steel Construction, Chicago, Illinois, 2011.

[24] F. Zareian, R.A. Medina, A practical method for proper modeling of structural damping in inelastic plane structural systems, Computers & structures, 88 (2010) 45-53.

[25] CSI, SAP2000 v14 Integrated Finite Element Analysis and Design of Structures, Computers and Structures, Berkeley, (2009).

[26] J. Liu, A. Astaneh-Asl, Cyclic testing of simple connections including effects of slab, Journal of Structural Engineering, 126 (2000) 32-39.

[27] G. Rassati, R. Leon, S. Noe, Component modeling of partially restrained composite joints under cyclic and dynamic loading, Journal of Structural Engineering, 130 (2004) 343-351.

[28] FEMA, Recommended seismic design criteria for new steel moment-frame buildings, FEMA 350 Report, 2000

Chapter 5: The Influence of Gravity Column Continuity on the Seismic Performance of Special Steel Moment Frame Structures

F. Flores[(1)], F. Charney[(2)], D. Lopez-Garcia[(3)]

[(1)] *Ph.D. Candidate, Department of Civil and Environmental Engineering, Virginia Tech, and Department of Structural and Geotechnical Engineering, Pontificia Universidad Catolica de Chile, ffloress@vt.edu*
[(2)] *Professor, Department of Civil and Environmental Engineering, Virginia Tech, fcharney@vt.edu*
[(3)] *Associate Professor, Department of Structural and Geotechnical Engineering, Pontificia Universidad Catolica de Chile, and National Research Center for Integrated Natural Disaster Management CONICYT/FONDAP/15110017, dlg@ing.puc.cl*

Abstract

This paper investigates the influence of the gravity columns on the collapse performance of Steel Special Moment Frames (SMFs). Using a simple approach where all the gravity columns are lumped into one elastic, continuous and pinned element, a two, four and eight story buildings taken from the ATC 76-1 project, were analyzed using the FEMA P-695 Methodology. Prior the use of what is called in this investigation the lumped column approach a complete validation of this method was carried out. In order to test the effect of having different number of gravity columns or different column sections, the inertia of the lumped column was used as a parameter that was varied and the influence on the collapse performance was evaluated for each variation. The results show that the gravity columns have a profound influence on the collapse performance of buildings, especially on taller structures such as the eight story. Moreover it was found that there seems to be a correlation between the nonlinear static pushover analysis and the collapse evaluation of the analyzed structure that would give insight into an optimal section of the lumped column which in turn will define the number or size of the gravity columns required by the structure to improve its performance.

Keywords: Special Moment Frames, Gravity Framing, Column Splices, Continuous Stiffness, Gravity Columns, Seismic Performance, Collapse Probability.

5.1 Introduction

Current design approaches do not account for the influence of the gravity framing system in the seismic performance of buildings, and instead rely exclusively on that part of the structural system that is specifically designed for lateral load resistance. While it is well known that the strength and stiffness of the gravity system provides enhanced performance under design level events, and reduces the probability of collapse under extremely rare ground motions, it is typically not included in the design and subsequent performance assessment of the structure. The main reason the gravity system is not considered is the difficulty of developing "full system" mathematical models that include the stiffness and strength of the numerous beams, columns, and beam-to-column connections in the gravity system. However, studies have shown that mainly the effect of the gravity columns provide significant benefits, primarily they delay or prevent the formation of story mechanisms that lead to premature collapse. In order to provide some quantification of the influence of gravity columns and to avoid complex analysis, this paper introduces a "Lumped Column" approach wherein a single column is used to represent all of the gravity columns in the structure. An important consideration in the assessment of the contribution of the gravity columns is the continuity of the columns, which is a function of the stiffness of the columns and the location, stiffness, and strength of splice connections. Where sufficient continuity is provided, the Lumped Column approach acknowledges that: “If columns are continuous over several stories of a structure, then the stiffness of the columns will limit the amount of drift concentration that can occur” [1].

The Lumped Column approach is demonstrated through the analysis of several Special Steel Moment Frames (SMFs) that were originally developed for use in the ATC-76-1 project [2]. Before this is done, some background is provided on influence of the gravity system on the

seismic performance of steel structures, and more specifically on the influence of the columns of the gravity system.

Tremblay and Stiemer [3] proposed the use of continuous columns as a backup stiffness to mitigate P-Delta effects on braced frames. The study performed nonlinear dynamic analyses looking for the influence of cthe continuous columns on the collapse of eight multi-story buildings that varied in height from two to twelve stories. The studied conditions were: columns with moment releases at the top and bottom of each floor (no continuous stiffness was provided), moment releases at the top and bottom of every two stories, and continuous over the entire building height. The last case was analyzed using pinned connections at the base of the columns and was repeated for fixed connections at the base of the columns. The results showed that the worst case (more collapses occurred) was when columns had moment releases at each level (no continuity) and the best case was when the columns were continuous over the entire height and fixed at the base. The authors concluded that the continuous stiffness concept is very attractive to mitigate P-Delta effects because it increases the post-yielding stiffness of the structure, but more research is required.

Qu et al. [4] investigated the influence of continuous column stiffness by adding a rocking wall frame to a ductile reinforced concrete moment frame. The results showed that interstory drift concentrations are reduced considerably when the rocking wall was incorporated. This was a supporting study for the retrofit of a 11-story reinforced concrete frame on the campus of the Tokyo Institute of Technology [5].

Tagawa [6] studied the continuous column effect on moment resisting frames when gravity columns are included in the analysis. Nonlinear static and dynamic analyses were performed using different buildings with and without the gravity columns. The results showed

that the post-yield stiffness increased in pushover response and that interstory drift concentrations predicted by the dynamic analysis were reduced when the gravity columns are added. The author concluded that continuous columns have a larger effect on taller structures (9- and 20-story buildings). It was also concluded that as continuous column stiffness increases, drift concentration decreases to a point where the columns rotate with respect to the base on a pure shear mode. The mathematical models of the moment frames used by Tagawa did not included stiffness and strength degradation in the inelastic components. As a result, one of the recommendations for future research made by this study is to incorporate the stiffness and strength degradation in beams and columns to obtain the influence of the continuous columns on SMFs.

Flores et al. [7] investigated the influence of the gravity system on the collapse performance of SMFs. This was a comprehensive study where various parameters such as the influence of the gravity columns and the influence of gravity beam-to-column connections on the collapse performance of SMFs were quantified using the FEMA P-695 methodology [8]. The analyzed buildings, 2, 4 and 8 stories in height, have the same configuration as used in the ATC 76-1 project [2], and were designed using the modal response spectrum analysis method (RSA). Their collapse performance was evaluated with and without the gravity system and several important results were described. Among the key findings from this research were: (1) that the gravity connections improved the collapse performance of the 2- and 4-story buildings but had almost no influence on the 8-story building, and (2) that the gravity columns had a very important influence on the taller 8-story building but that their influence decreased gradually for the shorter 4- and 2-story buildings. An important additional conclusion that Flores et al. [7] made, and it is the basis for the study performed herein, is that gravity columns are not likely to

yield unless the gravity beam-to-column connections have significant moment capacity (greater than 35% the beam plastic moment capacity of the gravity beam). It is noted that in the aforementioned study the gravity columns were modeled in two ways, using elastic elements and elements with the capability to yield, and the results indicated that the response was insensitive to the influence of yielding in the gravity columns.

In the new study reported herein, the influence of the gravity columns on the collapse performance of SMFs is evaluated using the Lumped Column approach. Unlike previous studies that have used this method [3, 4, 6], this investigation focuses first on proving the validity of the approach and then establishes the influence of the gravity columns on the collapse performance using the P-695 methodology [8]. Based on the assumption that gravity columns do not yield, the approach lumps all the gravity columns into a single elastic and continuous element. In this study, the same 2-, 4- and 8-story SMFs buildings used by Flores et al. [6] to investigate the behavioral improvements that the full gravity system provides are studied in more detail in order to quantify the influence of the continuous stiffness of the gravity columns. In order to evaluate the influence of having different number of gravity columns or different column sections, a very simple method is used, wherein the total moment of inertia provided by the gravity columns (per story) is assumed to be a percentage or ratio of the total moment of inertia provided by the SMFs (per story). Then, the FEMA P-695 methodology is used to quantify certain parameters that will evaluate the effect of continuous gravity column stiffness on SMF behavior.

5.2 Building Overview

The 2-, 4-, and 8-story buildings have the same floor plan, as shown in Figure 1. The connections at the base of the columns are fixed for the 4- and 8-story models and pinned for the 2-story model. As can be seen from Figure 1 the lateral resisting system of these buildings is

provided by three-bay SMFs located at the perimeter on each side of the building. These SMFs have prequalified reduced beam sections (RBS) connections [9] and are proportioned and detailed to resist the seismic forces and provide stability against P-Delta effects.

The bay width (center line dimensions) between columns of each SMF is 6.1 m. The height of the first story is 4.6 m (to top of steel beam), and the height of all other stories is 4.0 m. The dead load is 4.31 kN/m^2 uniformly distributed over each floor, and the cladding load is applied as a perimeter load of 1.2 kN/m^2. The unreduced live load is 2.4 kN/m^2 on all floors and 0.96 kN/m^2 on the roof.

The structures were analyzed in the East-West direction. The gravity frame is considered to be part of the system and it is also shown in Figure 5-1. In this study, the columns oriented on the weak axis (orthogonal SMFs columns) are not considered part of the lateral resisting system and they are modeled with moment releases at the top and bottom of each story so they do not provide any lateral resistance. While these columns would clearly add to the lateral resistance of the system, they were not included in the study as the intended focus was on gravity columns that are not part of the lateral system. The shaded area in the figure represents the tributary area for gravity loading on the individual East-West direction SMFs.

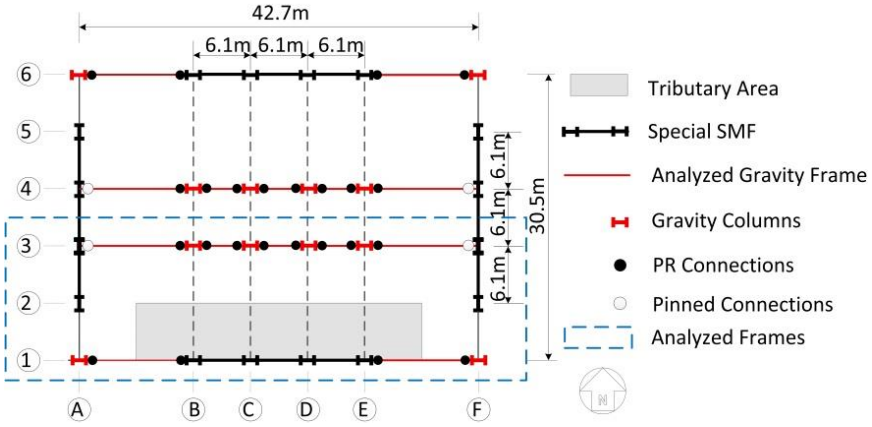

Figure 5-1 Building Overview

5.3 Modeling Approach

The numerical two-dimensional models idealized to perform the nonlinear analysis were created using OpenSees [10] and they include material and geometric nonlinearities. In the case where the gravity system was not included, P-Delta effects were considered using a leaning column with no flexural stiffness placed parallel to the SMF and the load applied to this column represents half of the total load from the gravity system that was not tributary to the SMF columns. For the cases where the gravity system was included, a leaning column was not required.

The approach applied to model the SMFs was using elastic beam elements and the nonlinear inelastic behavior was lumped into plastic hinges located at the ends of the members. The components of the SMF with nonlinear material behavior are shown in Figure 5-2 and they are: panel zones, plastic hinges located at the RBSs of the beam and plastic hinges at the column ends.

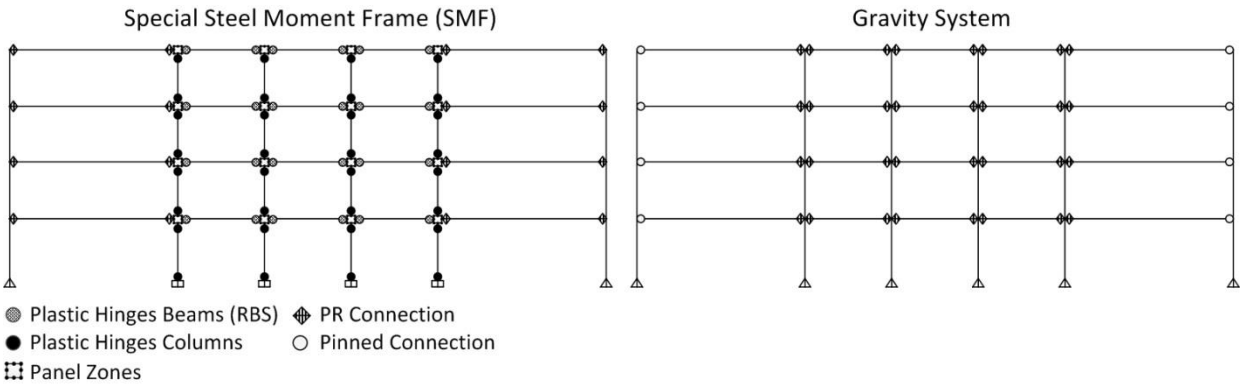

Figure 5-2 Model Components Including the Gravity System

A complete description of the inelastic behavior of each component can be found in the ATC 76-1 report. However, a brief overview is provided herein. The hysteretic behavior of the RBSs in the beams is modeled using a rotational spring. Using OpenSees, the behavior was

characterized by the material called “Bilin”. The constitutive law of this material is based on the modified Ibarra-Krawlinkler deterioration model [11], and the parameters to define it are described by Lignos and Krawinkler [12].

Panel zones are modeled using a rectangular region composed of eight very stiff elastic beam-column elements and one nonlinear rotational spring to represent shear distortions in the panel zone [13]. These deformations are due to column web shear yielding and column flange flexure yielding and are represented by a tri-linear backbone curve assigned to the rotational spring.

The phenomenological component used to characterize the nonlinear behavior of the SMF columns is the same as the one used for the beams. This approach was taken because, at the time the analysis was performed, OpenSees did not have a component with a hysteretic behavior that includes the axial force – bending moment (P-M) interaction. To account for the reduced bending strength of the columns due to the axial compressive force, a representative axial force was computed. Even though the axial force changes during a dynamic analysis, this representative axial force is computed before the analysis and the bending strength is reduced accordingly. The axial force used to determine the reduced strength was obtained by performing a nonlinear static pushover analysis and it was considered to be equal to $P_{grav} + 0.5\ P_{E,max}$, where P_{grav} is the gravity load that the column is subjected to and $P_{E,max}$ is the maximum load that the column receives during the pushover analysis. The pushover analysis was performed until a reduction of 20% in the base shear, V_{max}, is reached. With the axial load determined, the reduced bending strength is computed using the AISC P-M interaction equation [14] and subsequently used in the models.

For the nonlinear dynamic response history analysis, a Rayleigh damping of 2.5% is assigned to the first modal period T1 and to period T = 0.2 T1 in all cases. As proposed by Zareian and Medina [15], stiffness proportional damping is assigned to elements that remain elastic, and mass proportional damping is assigned to nodes or elements where mass is lumped.

5.4 Validation of the Models

The SMFs investigated in this study were previously analyzed by Zareian et al. [16] without the gravity system and the results were presented in the ATC 76-1 [2] project report. To validate the models that do not include the gravity system, a complete collapse evaluation of the 2-, 4- and 8-story models was performed and compared with the published results. The difference between the results reported by Zareian et al. and the ones found in this study was marginal. A more detailed description of the validation process can be found in [7].

5.5 Influence of Gravity Columns

In order to validate the approach where all the gravity columns are lumped into one elastic element, a number of supplemental analyses with the gravity system modeled explicitly are performed. This section of the study is devoted to show the influence of the gravity columns on the performance of SMFs. The gravity system is modeled explicitly as shown in Figure 5-2. The gravity columns are pinned at the base, continuous all over their height (splices considered to provide full moment capacity), and to capture yielding they were modeled using force-based fiber elements with a bilinear material with strain hardening equal to 10% of the initial stiffness. The material used has a yielding strength capacity equal to 414 Mpa (60 ksi). This value accounts for the expected material strength and strain hardening. Modeling columns with forced-based fiber elements makes possible to incorporate the axial-moment interaction in the analysis but strength degradation is not considered. This is why plastic hinges at columns of the SMFs

were modeled using a phenomenological approach. The gravity connections, are considered to be Partially Restrained (PR) connections and they are assumed to have no flexural strength because the sole influence of the gravity column continuity is to be evaluated.

A typical design was conducted to obtain the size of beams and columns of the gravity framing. The system was designed using A992 steel and the same loads as previously mentioned for the SMF. For the purpose of member selection it was assumed that the gravity beams were non-composite and simply supported. The design was performed using SAP2000 [17]. The size of the gravity framing members is provided in Table 5-1, with grid identifiers (e.g. A3) as referenced in Figure 5-1.

Table 5-1 a) 2-Story b) 4-Story c) 8-Story Gravity System Member Sizes

a) 2 Story Model

Story	Columns				Beams		
	A1,F1	**A3,F3**	**B3, E3**	**C3, D3**	**A1 - B1, E1 - F1**	**A3 - B3, E3 - F3**	**B3-E3**
1	**W14x43**	W24x162	**W14x90**	**W14x61**	W24x62	W24x94	**W16x36**
2	**W14x43**	W24x162	**W14x90**	**W14x61**	W24x55	W24x84	**W16x36**

b) 4-Story Model

Story	**Columns**				**Beams**		
	A1,F1	**A3,F3**	**B3, E3**	**C3, D3**	**A1 - B1, E1 - F1**	**A3 - B3, E3 - F3**	**B3-E3**
1	**W14x43**	W24x103	**W14x90**	**W14x61**	W24x62	W24x94	**W16x36**
2	**W14x43**	W24x103	**W14x90**	**W14x61**	W24x62	W24x94	**W16x36**
3	**W14x30**	W24x62	**W14x90**	**W14x61**	W24x62	W24x94	**W16x36**
4	**W14x30**	W24x62	**W14x90**	**W14x61**	W24x55	W24x84	**W16x36**

c) 8 Story Model

Story	Columns				Beams		
	A1,F1	**A3,F3**	**B3, E3**	**C3, D3**	**A1 - B1, E1 - F1**	**A3 - B3, E3 - F3**	**B3-E3**
1	**W18x76**	W24x162	**W18x143**	**W18x76**	W24x62	W24x94	**W16x36**
2	**W18x76**	W24x162	**W18x143**	**W18x76**	W24x62	W24x94	**W16x36**
3	**W18x76**	W24x162	**W18x143**	**W18x76**	W24x62	W24x94	**W16x36**
4	**W18x50**	W24x162	**W18x76**	**W18x50**	W24x62	W24x94	**W16x36**
5	**W18x50**	W24x131	**W18x76**	**W18x50**	W24x62	W24x94	**W16x36**
6	**W18x50**	W24x131	**W18x76**	**W18x50**	W24x62	W24x94	**W16x36**
7	**W18x40**	W24x94	**W18x50**	**W18x40**	W24x62	W24x94	**W16x36**
8	**W18x40**	W24x94	**W18x50**	**W18x40**	W24x55	W24x94	**W16x36**

Note: Gravity farming shown in **bold** text.

The 2-, 4- and 8-story models with and without the gravity columns were subjected to the 44 Far Field records provided by the FEMA P-695. The ground motions were scaled using the FEMA P-695 procedure. The intensity level at which the gravity columns are evaluated represent the Maximum Considered Earthquake (MCE) with 2% probability of occurrence in 50 years for the seismic design category D_{max}. The main nomenclature taken in this paper to indicate if the gravity column is included is: nStory + sGS, where n is the number of stories and s is the percentage of full strength assigned to the PR connections (if sGS is not included, the model does not include the gravity system, and instead includes a leaning column to account for P-Delta effects).

The observed influence of the gravity columns in the results is similar for the 2-, 4- and 8-story models. Drift concentrations at bottom stories and residual displacements were decreased considerably for the ground motions that caused large deformations in the building. However, it has to be mentioned that at MCE level the influence of the gravity columns is minimum and just some of the ground motions caused large deformations. Therefore, only the results of the nonlinear time history analyses that illustrate the influence of the gravity columns are shown in Figure 5-3.

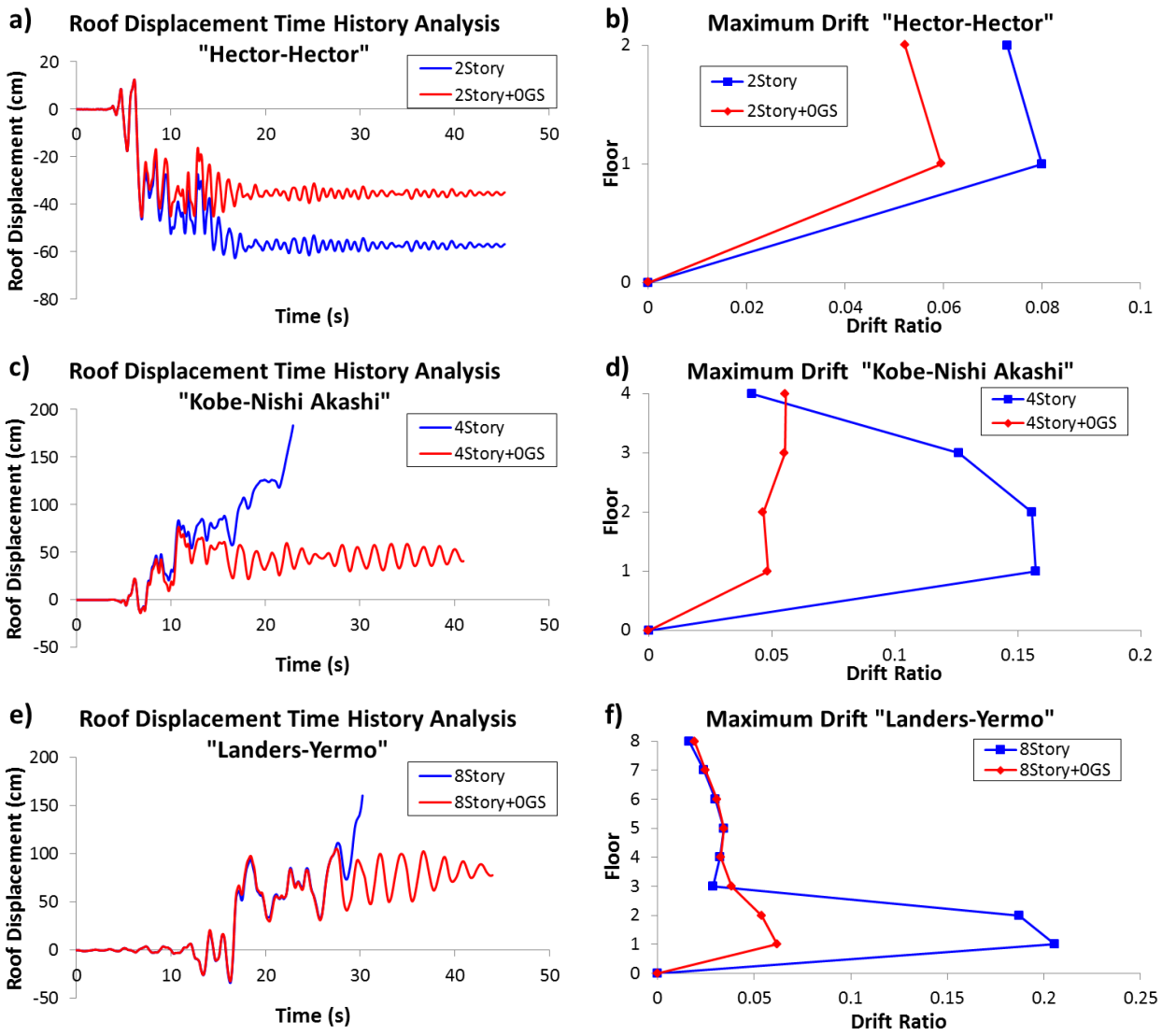

Figure 5-3. Residual Displacement and Maximum Story Drift at MCE level
a,b) 2-Story c,d) 4-Story e,f) 8-Story

Figure 5-3 illustrates the residual displacement and maximum interstory drifts for the 2-, 4- and 8-story buildings. Starting with the 2-story model (Figure 5-3(a) and (b)), it can be seen how the residual displacement is decreased when the gravity columns are included in the analysis and this is reflected directly in the maximum interstory drift. At MCE level, just one out of the 44 ground motions had this effect on the 2-story building while for the rest of ground motions, the gravity columns had a minimum effect on the response. Contrary to the 2-story model, the 4-

and 8- story models are more influenced by the gravity columns because taller buildings are more susceptible to have story drift concentrations at bottom stories. This is the case for the 4- and 8-story models without the gravity columns where drift concentrations at the bottom stories is causing the collapse as can be seen in Figure 5-3(c) and (d) and Figure 5-3 (e) and (f) respectively. These results verify what has been already observed by several authors: that continuous stiffness provided by gravity columns reduce interstory drift concentrations improving the seismic performance of buildings [3, 5, 6, 18].

5.6 "Lumped" Gravity Column Approach

Based on the assumption that the gravity columns do not yield even when the system undergoes large deformations, the Lumped Gravity Column approach combines all the gravity columns into one elastic element. However, in order to use this method two conditions have to be fulfilled: (1) the gravity columns are pinned at the base and continuous over their full height (splices provide full moment capacity), and (2) beam-to-column gravity connections have low flexural strength and high rotation capacity. If these conditions are not met the gravity columns may yield invalidating the method or the continuous elastic stiffness provided by the columns would not be achieved.

Figure 5-4 shows a sketch of a mathematical model that utilizes the lumped gravity column approach. The SMF is modeled with two vertical elements placed adjacent to it: (1) a "leaning column" that incorporates P-Δ effects, and (2) the lumped gravity column, which represents all the strong-axis oriented columns that are not part of the lateral load resisting system. It can be seen from this figure that the ratio of the sum of the moment of inertia of the gravity column (I_Gcol) to the moment of inertia provided by the columns of the SMF (I_SMF) has been computed, with the values shown to the right of the lumped gravity column. This value

simply provides a measure of the stiffness of the gravity columns relative to the stiffness of the SMF columns, and is used only to allow the comparison of results when the size of the gravity columns is increased.

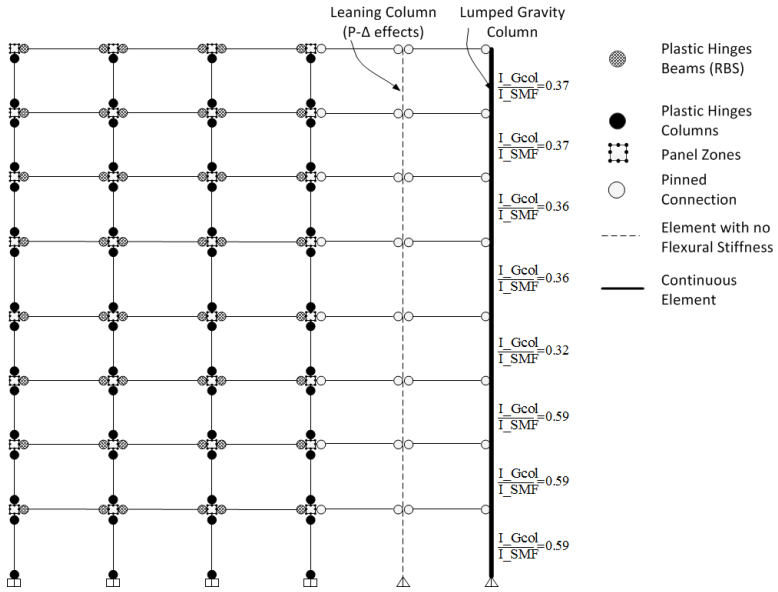

Figure 5-4 Mathematical Model Utilizing the Lumped Gravity Column Approach

Prior to demonstrate the influence on the performance that gravity columns bring, it is necessary to execute several preliminary analyses to investigate a variety of different issues that might arise regarding the method, including (1) are the gravity columns yielding, (2) what is the strength required by the gravity connections to induce yielding in the gravity columns, (3) what is the strength required by the gravity column's splices to provide continuity, and (4) are similar results obtained when a lumped column is used in lieu of modeling the individual columns? Each of these issues are investigated in the following subsections.

5.6.1 Yielding in Gravity Columns

The assumption that gravity columns remain elastic even when the structure is subjected to large displacements is fundamental to the concept that one elastic element with properties that

represent all the gravity columns will give the same results as a model with each individual gravity column included explicitly. In this section, the potential for yielding in the gravity columns is investigated by performing nonlinear static pushover and nonlinear dynamic analyses. In order to evaluate the sole influence of the gravity columns, the PR connections are considered to have no strength. However, since it is known that a perfectly pinned beam-to-column gravity framing connection is not possible in an actual building, yielding in the gravity columns is also studied when the PR connections have some strength.

The flexural strength of the PR connections is considered to be a percentage of the plastic moment strength (M_p) of the gravity beam. Depending on the type of connection, the flexural strength can be high but it is known that shear tab connections and other commonly used gravity connections do not have significant flexural strength capacity. Liu and Astaneh [19] carried out cyclic tests to evaluate the flexural capacity of simple connections. The results showed that shear tabs, which are common connections used as part of the gravity system, had a moment capacity approximately equal to 20% M_p if the contribution of the concrete slab is neglected and 35%M_p if it is considered. Therefore, it is assumed based on literature and other investigations, such as that performed by Gupta and Krawinkler [20], that a realistic value to represent the flexural strength of the gravity connection is 30% M_p. Another important characteristic that gravity connections must comply with is to have a high rotation capacity. The experimental results published by Liu and Astaneh [19] demonstrate that this characteristic can easily be achieved by simple connections. For instance, shear tabs reached a rotation that varied from 0.09 to 0.14 radians. It was also found that the composite action (contribution of the concrete slab) was lost due to damage at a rotation approximately equal to 0.04 radians. After this point the connection behaved the same as a bare connection.

Even though the cyclic behavior of the PR connections is complicated to characterize, a simple model, such as the one given by ASCE 41-13 [21], is accurate enough for the purpose of this study. One of the parameters given by this model is the rotation at which the PR connections yield (0.005 radians). The backbone curve of this model presents a plateau after the yielding point and it provides the rotation at which the connection losses the majority of its capacity. More information regarding the modeling of the PR connections can be found in Flores et al. [7].

To establish if the gravity columns yield, two analyses are performed: one where the material assigned to the fibers of the cross section that form part of the force-based elements used to model the gravity columns is elastic and the other one where the material assigned to the fibers is bilinear with strain hardening equal to 10% of the initial stiffness. The nonlinear static pushover analysis is performed on the 8-story building with and without the gravity system for the cases where the gravity columns behave elastically and inelastically. Additionally, nonlinear dynamic time history analysis is performed using eight ground motions chosen from the FEMA P-695 Far-Field record set. The ground motions used for this check were chosen arbitrarily and they are listed in Table 5-2. Incremental Dynamic Analysis [22] is used to systematically subject the building to increasing ground motion intensity, resulting in large displacements.

Table 5-2 Ground Motions Chosen From Far-Field Set

Component Name	Filename	npts	dt	PGA(g)
Manjil-Abbar	ABBAR--L.AT2	2676	0.02	0.407
Duzce-Bolu	BOL000.AT2	5590	0.01	0.458
Superstition Hills-Poe	B-POE270.AT2	2230	0.01	0.522
Loma Prieta-Capitola	CAP090.AT2	7991	0.005	0.483
Hector-Hector	HEC090.AT2	4531	0.01	0.367
Northridge-CC	LOS270.AT2	1999	0.01	0.400
Kobe-Nishi Akashi	NIS000.AT2	4096	0.01	0.525
San Fernando-LA	PEL090.AT2	2800	0.01	0.366

Figure 5-5 shows the results for the analyses performed on the 8-story building with gravity connections with no strength. From the pushover curves it could be inferred that the gravity columns are not yielding and it can be concluded that the gravity columns improve considerably the building's post-yield stiffness. A close investigation into the fibers behavior of the column's section confirmed that no yielding occurred in the gravity columns. For the dynamic analysis, the ground motions were scaled following the FEMA P-695 methodology. The ground motions are collectively scaled (or "anchored") to the ASCE7-05 [23] response spectrum (MCE level) such that the median spectral acceleration (S_a =0.55g) of the record set matches the target spectral acceleration at the fundamental period, (T=$C_u T_a$=1.64 sec) where C_u is a coefficient that represents an upper limit on the calculated period and Ta is an empirical approximation of the fundamental period. Note that this period is computed according to ASCE7-05 and is not the actual period of the structure. However, for the purpose of checking if yielding occurs in the gravity columns this is not relevant since the comparison is made at level intensities higher than the MCE level. The results from the nonlinear time history analysis shown in Figure 5-5(b) represent a level of intensity 1.8 times larger the MCE level intensity (S_a=0.99g). Based on the roof displacement time history results it appears that even at large deformations the gravity columns do not yield.

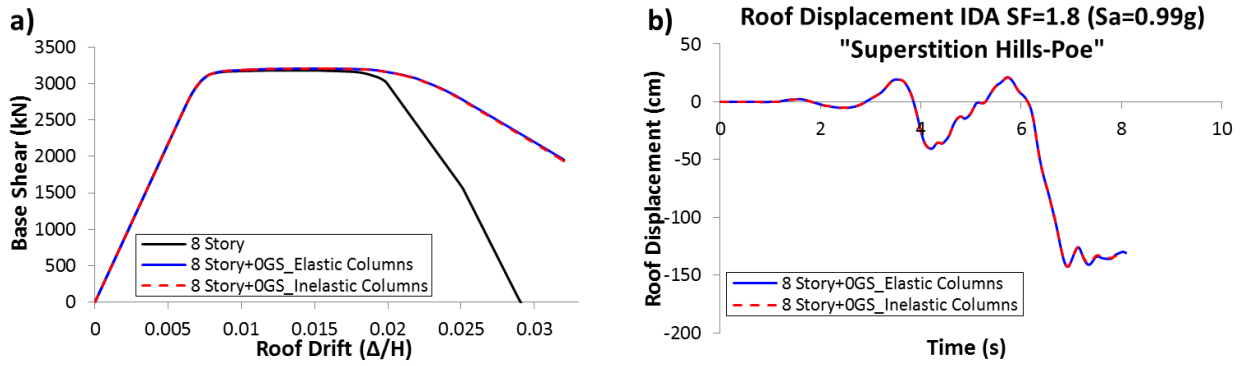

Figure 5-5 Checking Yielding on 8-Story Model a) Pushover Curves b) Nonlinear Dynamic Analysis (PR connections with no strength)

The next step required to validate the assumptions that the gravity columns do not yield is to assign a common flexural capacity to the PR connections. A flexural strength of 30% M_p has been chosen as a realistic value for shear connections. The same analyses performed for the case where the gravity connections have no strength are executed and the results are shown in Figure 5-6 (a) and (b). The pushover curves show that gravity columns are still not yielding since there is no difference in the response for the two cases. Again, this was confirmed by checking if the fibers reached the yielding point.

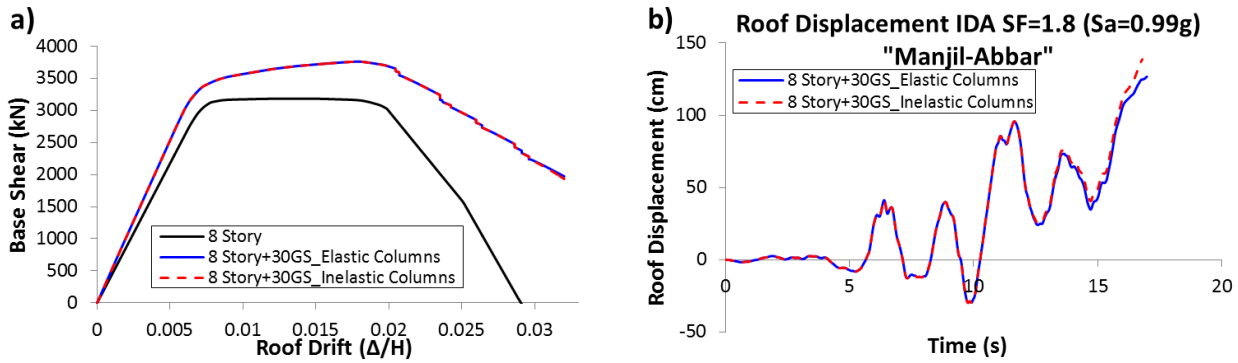

Figure 5-6 Checking Yielding on 8-Story Model a) Pushover Curves b) Nonlinear Dynamic Analysis (PR = 30%M_p)

On the other hand, the results for one of the cases for the dynamic analysis under large deformations (Figure 5-6 (b)) display a discrepancy between the elastic and inelastic results. A close inspection of fiber stresses in the column indicated that yielding occurred at 10% drift in the first story (Figure 5-7). This value of drift is very large and it is commonly considered collapse in steel moment frame structures [24].

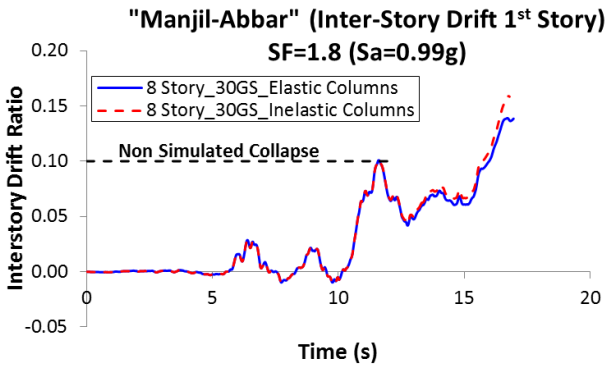

Figure 5-7. Inter-Story Drift 1st Story ("Manjil-Abbar") SF=1.8 S_a=0.99g

Even though yielding in the gravity columns occurred for one of the eight analyzed ground motions, it was for an earthquake with a hazard level much larger than the MCE and it occurred after the deformation exceeded 10%. Thus, it can be said that the gravity columns do not yield if the gravity connections have a low flexural strength capacity (less than 30%M_p). However, the following subsection will show that gravity connections will induce yielding if they have a significant moment capacity.

5.6.2 Yielding in Gravity Columns Induced by Gravity Connections

The previous section showed that the gravity columns do not go into the inelastic range when the gravity connections have a flexural capacity less or equal than 30% M_p. In this section PR connections with high flexural capacity are used to check if the gravity columns yield. Nonlinear static pushover analysis is used for this purpose. Whether or not yielding occurs is established by comparing the results obtained with gravity columns behaving in an elastic and inelastic manner. Furthermore yielding in the fibers of the sections was closely reviewed. Figure 5-8 shows the pushover curves obtained for the buildings with PR connections with strength equal to 50% and 70%M_p. The difference between the pushover curves indicate that yielding occurred in the gravity columns and this was validated by checking the stresses on the fibers of the sections. This demonstrates that high moment capacity connections induce yielding in the

gravity columns. Even though yielding occurred in the gravity columns at a large drift (0.025), it can be concluded that in order to use the method in question, the gravity connections must have a low flexural strength.

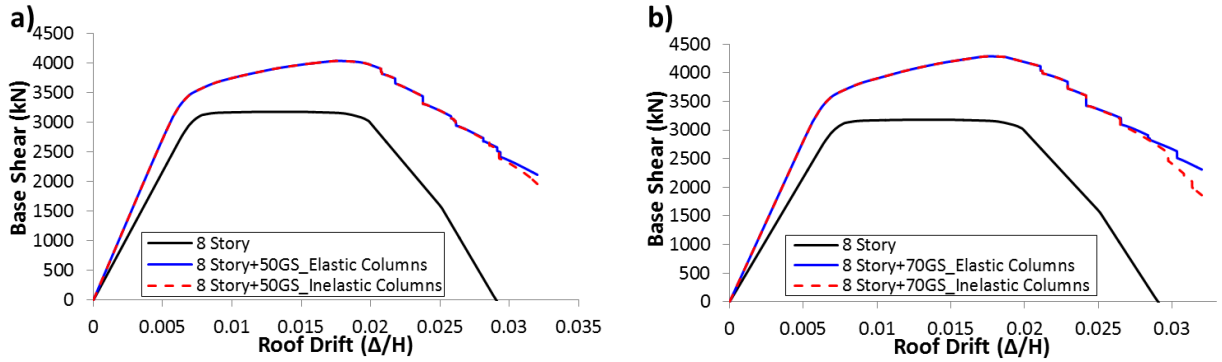

Figure 5-8 Inducing Yielding in Gravity Columns

5.6.3 Effect of Gravity Columns Splices

One of the most important issues when improving the seismic performance of SMFs using the gravity columns is that they have to provide continuous stiffness and this is achieved by making them continuous over the full height. However, in buildings taller than two stories, splices in the gravity columns are going to be necessary. Therefore, in order to use this approach the flexural strength provided by the splices has to be sufficient to simulate the continuity in the gravity columns.

Section J1.4 of the AISC Specification [14] says that compression splices in columns need to hold the parts secure in place. As a result of this requirement, AISC provides a series of standard column splices that can be found on Table 14-3 of the specification. Even though splices are not designed to carry moments, they can provide significant flexural capacity. There are two main sources of bending capacity for column splices: the first one, coming from the compression load in the column, is the bending moment required to cause tension in one of the column flanges and the second one is the moment capacity that splice plates and bolts provide [25]. The first source

depends on the compression load acting on the section and the second depends on the section depth and number of bolts. For instance, the gravity columns with section W18x143 located on axes B3 and E3 (Figure 5-1) have a 600 Kips compressive load from the gravity loads at the fourth story (splice location). The flexural capacity of a standard splice connection with eight A325N 3/4 diameter bolts will have a flexural capacity of 30%M_p, of which 12% comes from the moment required to induce tension in one of the flanges and 18% from the moment capacity that the bolts provide. The same connection could have a flexural strength of 53% M_p if twelve 7/8 diameter bolts and A325X are used. The capacity of the splices is much larger for lighter column sections and it was also found that due to larger lever arm, column splices provide more flexural capacity when W18 are used instead of W14 sections.

In this part of the study, the flexural strength of the gravity columns splices is investigated. Additionally, as a result of the study performed by Flores et al. [7] where it was found that the splice location is very important, four different configurations are used to investigate the influence of the splice location on the performance. The splices are located at the same level in all the gravity columns (including the two end gravity columns that are placed on the extremes of the SMF), but the number of splice locations along the height and story level(s) in which the splices are located is varied. The cases considered are shown in Figure 5-9 of which cases III and IV would require at least two levels of splices but the importance of the upper splices is to be evaluated using these cases.

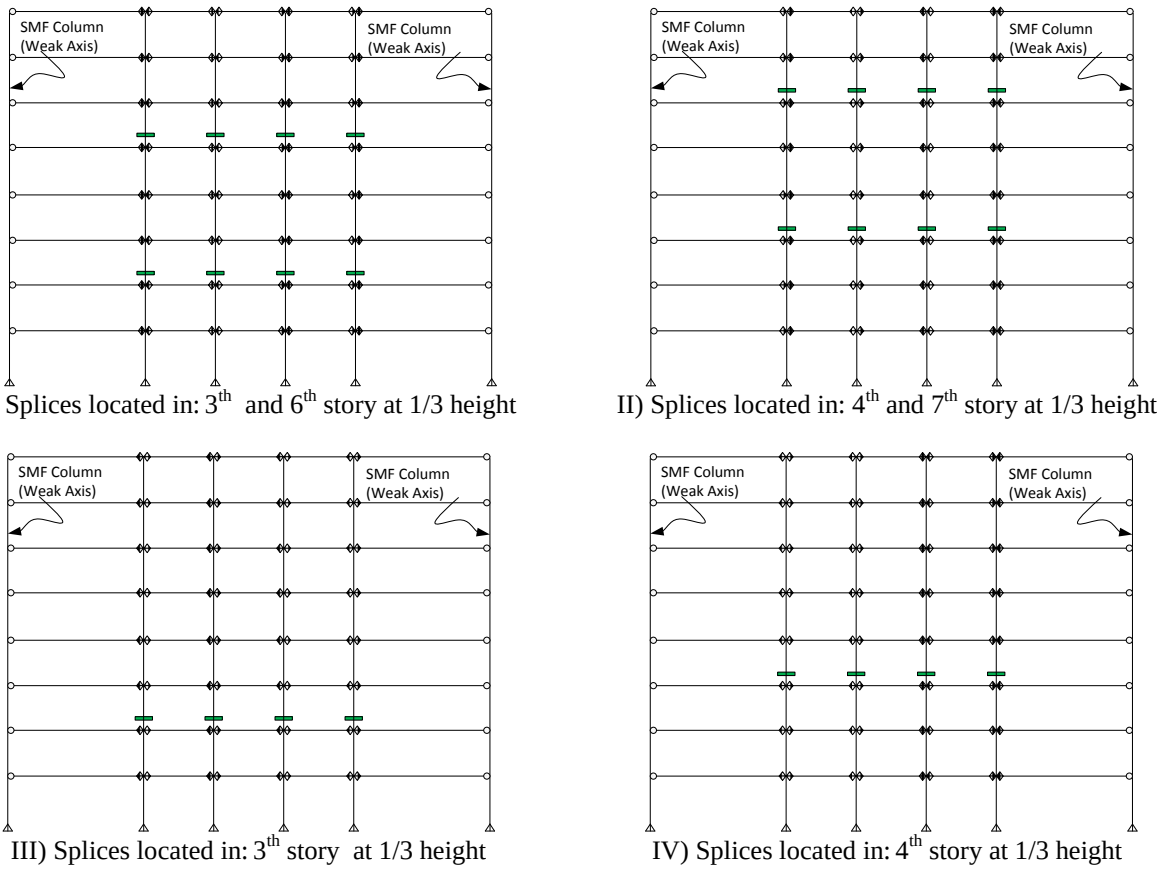

I) Splices located in: 3th and 6th story at 1/3 height

II) Splices located in: 4th and 7th story at 1/3 height

III) Splices located in: 3th story at 1/3 height

IV) Splices located in: 4th story at 1/3 height

Figure 5-9 Splice Location Cases

Initially, the splices are considered to have no flexural strength capacity so the results to be obtained represent a lower bound of the building performance. The influence of the splice location is quantified by means of nonlinear static pushover analysis. It can be seen from the cases to be studied that the difference between case I and III, and the cases II and IV, evaluates the influence of the upper story splices. On the other hand the difference between the cases I and II and the cases III and IV evaluates the influence of locating the splices at different stories.

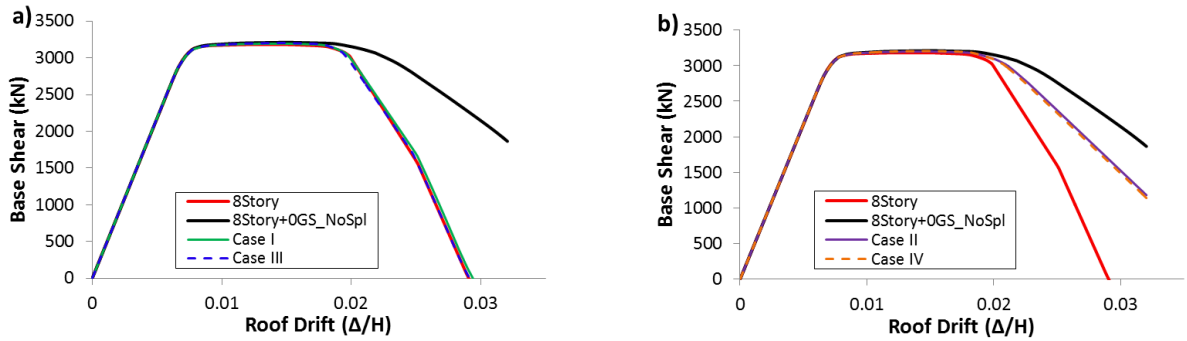

Figure 5-10 Influence of Splice Location (a) Cases I and III (b) Cases II and IV

Figure 5-10 (a) and (b) presents the results obtained from the nonlinear static pushover analyses. By observing the pushover curves for cases I and III and the cases II and IV it can be concluded that the upper story splices have almost no influence. However, the story where the splices are placed is very important and this is noticed by the difference in performance between cases I and II and cases III and IV. The main conclusion obtained from these analyses is that the first splice is the most important and it should be located as high as possible from the base of the building. Although this is true for the buildings investigated in this study, more research is required to generalize the conclusion to other structural systems.

Based on these results, the flexural strength required by the splices to provide continuity is investigated. Since the upper story splices have barely an influence on the performance, just the cases III and IV are considered. Figure 5-10 represents the lower bound performance of the building because the splices were modeled with zero flexural strength capacity. Thus, in this section a flexural strength capacity is assigned to the splices using an elasto-plastic hysteretic behavior and the influence on the behavior is analyzed. The stiffness of the splices do not have major incidence on the performance of the structure and that is why a rigid connection is used. A side study was performed to back up this finding and it also matches what was already stated by Ladani et al. [26] where a parametric study changing the splice stiffness was performed and the

variation on the results was minimum. The flexural strength capacity of the splice connections is considered the parameter to be studied and it is taken as a percentage of the plastic moment of the column. The flexural strength is varied and the performance compared with the performance obtained for the building with no splices

The required strength to be provided to the splices is computed by performing nonlinear static pushover analysis. Figure 5-11 presents the gravity column's splice strength requirements for cases III and IV in order to deliver continuity. It can be seen that if case III is used (Figure 5-11 (a)), the splice connection has to be fully restrained (around 90% M_p) while the case IV (Figure 5-11 (b)) requires splice connections with flexural strength equal to 50% the plastic moment capacity of the columns. This illustrates once more that the first splice should be located as far as possible from the ground because they provide more continuity and the strength requirements for the splices are reduced.

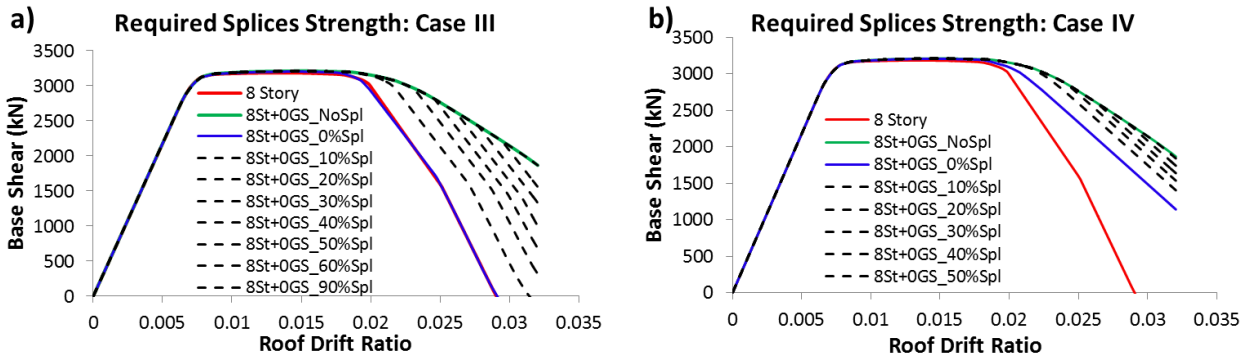

Figure 5-11 Gravity Columns Splices Required Flexural Strength a) Case III b) Case IV

5.6.4 Lumped vs Explicit Model

Once the assumptions of the approach have been proved to be correct, the final step, which is the comparison between the "lumped" and the explicit model is carried out and the results are described in this section. As already indicated, the lumped method utilizes one elastic

element with the combined properties of all the gravity columns that are in the strong axis, whereas the explicit model includes all the gravity columns and beams (with hinged connections for the beams).

The results of performing a nonlinear static pushover analysis and nonlinear dynamic analysis are shown in Figure 5-12. It can be seen that the pushover curves and the roof displacement time history are exactly the same even when the structure is subjected to large displacements. The outcome was the same for all the ground motions used for the analysis.

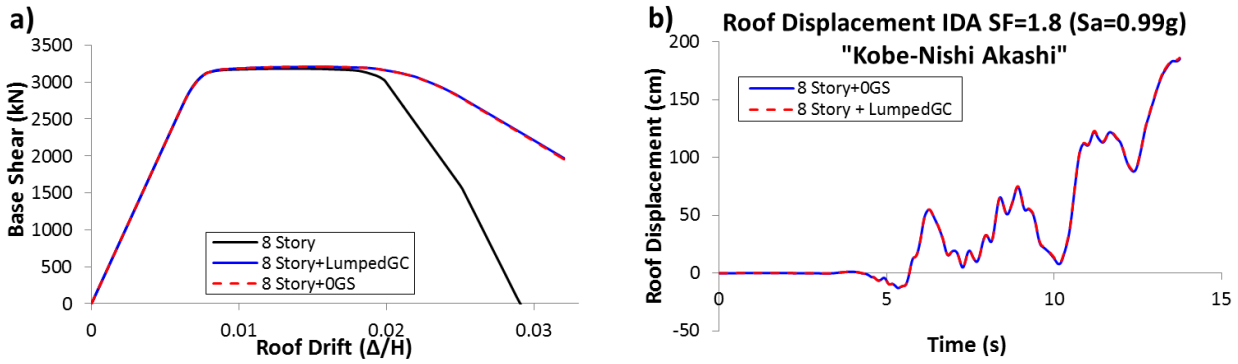

Figure 5-12 Modeling Gravity Columns Comparison a) Pushover Curves b) Nonlinear Dynamic Analysis

The discussion presented previously was dedicated to validate the concept that accumulating all the gravity columns that are in the strong axis into a single elastic, continuous and pinned base element is a valid approach to represent the behavior of all of the gravity columns in a structure. Since the influence of the gravity columns is most significant when the structure is subjected to large displacements, the collapse performance of SMFs including the gravity columns is evaluated in the following section of this investigation.

5.7 Collapse Performance of SMFs Including Gravity Columns

As known, in the present, SMFs are designed and analyzed without considering the gravity system as part of the lateral resisting system. One of the reasons is the complexity that modeling the gravity connections bring to the analysis. However, the previous sections in this paper were dedicated to prove that a relatively easy method to include at least the gravity columns in the analysis is possible. The improvement that these provide is reflected more when the structure undergoes large deformations and that is why the next section addresses the effect of the gravity columns on the collapse performance of SMFs using the FEMA P-695 methodology. The buildings to be analyzed with and without the gravity columns are the 2-, 4- and 8-story buildings from the ATC 76-1 project which were already described in previous sections.

The effect of the gravity columns on the collapse performance of the SMFs could be evaluated by analyzing different gravity systems with different gravity columns but it would not be practical. Instead, the lumped gravity column approach is used to study what it could be different designs and configurations of the gravity system which involves different number gravity columns or different column sections. The stiffness per story of the gravity columns was assumed to be a percentage or ratio of the stiffness per story of the SMF's columns. Therefore, as shown in equation Eq. (1), the moment of inertia of the gravity column, I_{Gcol}, is a constant (α) times the total moment of inertia provided by the columns in the SMF (I_{SMF}). The α values computed for the gravity system that form part of the 8-story building are shown in Figure 5-4. This is an approximate estimation of the SMF stiffness per story because it considers the beams of the SMF to be rigid. On the other hand the stiffness provided by the gravity columns, acting independently of the SMF, is null because the gravity connections have no strength and the

columns are pinned at the base. So the apparent stiffness of the gravity columns comes from the relative displacement (if exists) of the building's floors. A side study was performed to evaluate the actual influence of the gravity columns on the lateral stiffness per story. Even though the coefficient alpha can be large, it was found that the lateral stiffness per story provided by the gravity columns is significantly lower.

$$I_{Gcol} = \alpha \sum I_{SMFC} \tag{1}$$

Following this procedure, the total moment of inertia of the gravity columns per story was lumped in one continuous element placed in parallel to the SMF as is illustrated in Figure 5-4. Each story of the gravity column has a percentage (100 times α) of the total moment of inertia SMF's columns. In other words, instead of trying different number of gravity columns and different sections, an accumulated inertia per story was assigned and it was obtained as a percentage of the inertia per story of the SMF columns.

The approach taken herein is somewhat different from what other researchers have done in the past [4, 18]. The general trend is to compute a Drift Concentration Factor (DCF), which is the ratio between the maximum inter-story drift ratio and the roof drift ratio. The DCF is obtained from the nonlinear dynamic results and the closer the DCF gets to unity, the lower the possibility of developing drift concentrations. In order to decrease the DCF to a value that is considered acceptable the stiffness of the gravity column is varied using Eq. (2).

$$I_{Gcol} = \alpha \frac{EI}{kh^3} \tag{2}$$

where *EI* is the sectional bending stiffness of the continuous column, *h* is story height and *k* is story stiffness of the frame. The ratio α then is chosen by performing nonlinear dynamic analyses and the DCF is decreased to a value that is considered reasonable.

In order to avoid performing nonlinear dynamic analyses, this study does not use the DCF to establish the size of the gravity columns. The approach used instead is to assign the inertia to the gravity columns and then a nonlinear static pushover analysis is performed. From these results the most adequate or "optimal" stiffness is found by looking at the improvement on the post-yield stiffness. Even though this approach is somehow easier, more research is required to develop a simplified methodology or guideline that does not involve nonlinear analyses to obtain the "optimal" stiffness.

5.7.1 Nonlinear Static Pushover Analysis

One of the required steps in the FEMA P-695 procedure is to execute a nonlinear static pushover analysis. The parameters computed from this analysis are the overstrength (Ω) and period based ductility (μ_T). The overstrength measures the improvement on the building strength. On the other hand, the period based ductility is a measure of the post-yield stiffness improvement and from the FEMA-P695 perspective it has a direct effect on the Adjusted Collapse Margin Ratio (ACMR) which in turn is used to compute the probability of collapse. In order to evaluate the influence of the gravity columns on the aforementioned parameters, nonlinear static pushover analysis was performed on all the SMFs. The ratio of the inertia per story of the gravity columns was varied progressively from 10% to 100%. The results for the 2-story model are not included in this section because the influence of the gravity columns on the pushover curve is relatively not important since the P-Delta effect is insignificant for this building. The results of the pushover analyses and the influence on the period based ductility (μ_T) for the 4-story building are

shown in Figure 5-13 (a) and (b). These results are for the gravity columns with stiffness per story that varied from 5% (4Story +5%GSCol) to 100% (4Story +100%GSCol).

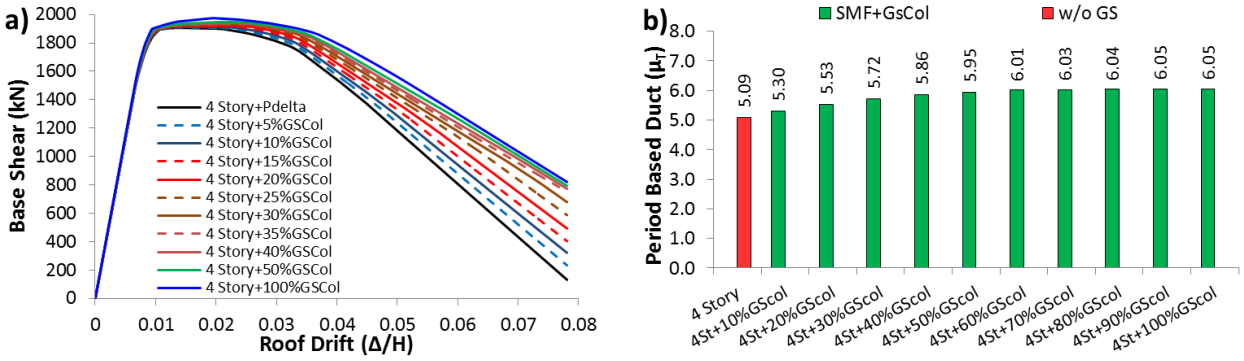

Figure 5-13a) Pushover curves 4-story model b) Period based ductility 4-story models**.**

Figure 5-13 (a) illustrates the influence of the gravity columns on the post-yield stiffness of the 4-story model. This influence is directly related to the period based ductility results shown in Figure 5-13 (b). The main conclusion from these figures is that it appears to exist an optimal performance that could be obtained when the gravity columns have the inertia per story in the neighborhood of 0.4 the inertia per story of the SMF. According to this analysis, it is not necessary to increase the gravity columns sections more than this ratio to improve the performance because the post-yield stiffness does not increase. Another aspect to point out is that the gravity columns have a minimum effect on the building overstrength.

The results of the pushover analyses and the calculated period based ductilities for the 8-story model are shown in Figure 5-14 (a) and (b). For these analyses, the inertia of the gravity columns was varied from 5% (8 Story + 5%GsCol) to 100% (8Story + 100%GsCol) the inertia of the SMF. In this case, the improvement is more noticeable than for the 4-Story model. The increase in the total moment of inertia per story of the gravity columns does not get saturated as in the case of the 4-story model, where after a ratio of 0.4 the results did not vary. To explain this behavior it has to be recalled the final effect of continuous stiffness on buildings. It makes the

structure rotate with respect to the base as a rigid body. In the case of smaller buildings the stiffness required by the gravity columns to accomplish this effect is lower than for taller buildings.

The influence of the gravity columns, when they are continuous, is important for the 8-story model. The benefits of improving the post-yield stiffness are directly related with dynamic stability since it counteracts the P-Delta effects. From Figure 5-14 (a), it can be seen that the post-yield stiffness improves faster when the gravity columns inertia vary from 5% to 50%. The period based ductility increases around 20% when the gravity columns have inertia per story equal to 50% the inertia per story of the SMF (Figure 5-14 (b)). So, this ratio could be the "optimal" to be used for the gravity columns. Additionally, the originally designed gravity system is shown in Figure 5-14 (a) to illustrate the behavior of this system relative to the ones where the influence of the columns is considered.

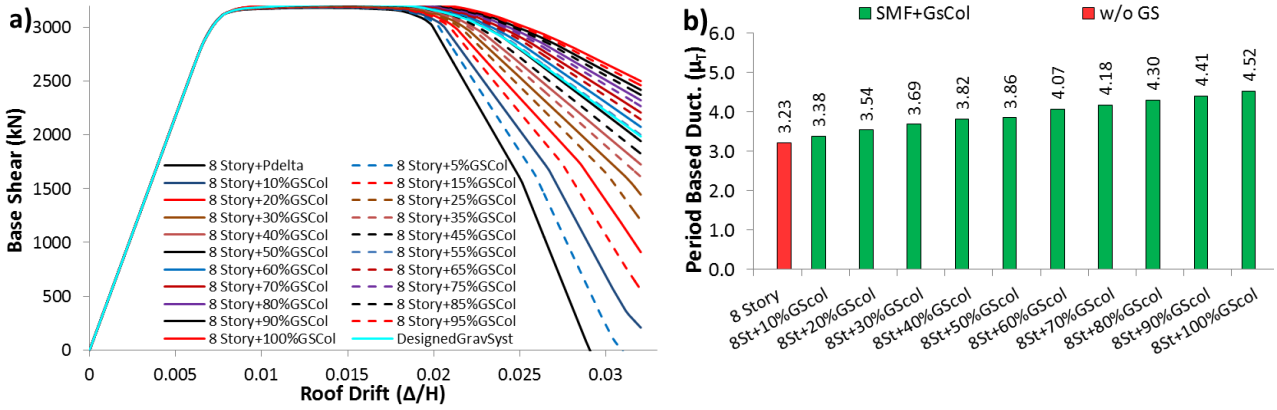

Figure 5-14 a) Pushover curves 8-story model b) Period based ductility 8-story models

5.7.2 Collapse Performance Evaluation

Following the P-695 methodology, the collapse performance of the structures is obtained performing nonlinear dynamic time history analyses, specifically using the incremental dynamic analysis (IDA) procedure [22]. Each of the 44 different far-field ground motions is scaled to

increasing intensities until the structure collapses which was considered to occur when the global drift is 0.1 or when the slope of the IDA curve is less than or equal to 20% the elastic slope of the IDA. This definition of collapse was established by FEMA 350 [24]. Once the IDA was performed, the collapse margin ratio (CMR) was obtained using the procedure defined in the P-695 methodology. The CMR is the ratio between the spectral acceleration that causes the median collapse (22 out of the 44 ground motions) to the spectral acceleration at MCE level.

The parameters to be used to evaluate the influence of the gravity columns on the performance of the SMFs are the Adjusted Collapse Margin Ratio (ACMR) and the probability of collapse. The ACMR is a ratio as described by P-695 that adjusts the CMR with the Spectral Shape Factor (SSF), which in turn accounts for the differences between the spectral shape that rare ground motions in California have with the design spectrum or a uniform hazard spectrum. The probability of collapse is computed at MCE level (ACMR=1). For further information regarding these parameters, the readers are referenced to the P-695 methodology [8] and to the study performed by Deierlein et. al [27].

The performance evaluation is carried out using a subset of the ratios (than the ones used for the pushover analysis) of the total moment of inertia per story of the gravity columns to the total moment of inertia of the SMF. The results of the analyses computed on the 2-story model are shown in Figure 5-15 (a) and (b).

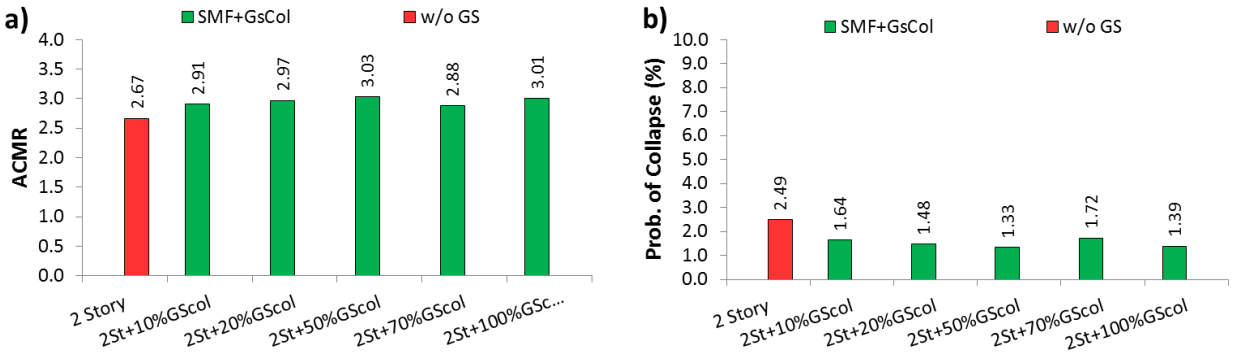

Figure 5-15 Results of 2-story building (a) CMR (b) Probability of collapse.

Figure 5-15 (a) illustrates the results of performing multiple IDAs to compute the ACMR of different models. Even though the gravity columns did not improve the post-yield stiffness on the pushover curves, it can be seen from Figure 5-15 (a) and (b) that they have some influence in the collapse performance. The ACMR increases slightly but in a regular manner until the gravity columns have a ratio of 0.5 with respect to the SMF per story stiffness. After this point the results are close but they do not necessarily keep increasing. The probability of collapse decreases from 2.49% to 1.33 % when the gravity columns stiffness per story ratio is 0.5. In general, the influence of the gravity columns is not as noticeable as it will be seen for the 4- and 8- story models. Moreover, the results fluctuate making difficult to establish an adequate inertia for the gravity columns.

The results of the analyses performed on the 4-story model are shown in Figure 5-16 (a) and (b). The ratios of the inertia per story of the gravity columns were chosen based on the results of the nonlinear static analysis. As Figure 5-13 displays, the post-yield stiffness improves progressively when the gravity columns are included until the ratio of the inertia per story is equal to 0.4. After this point the post-yield stiffness is the same and this is reflected in the results obtained from the collapse performance evaluation.

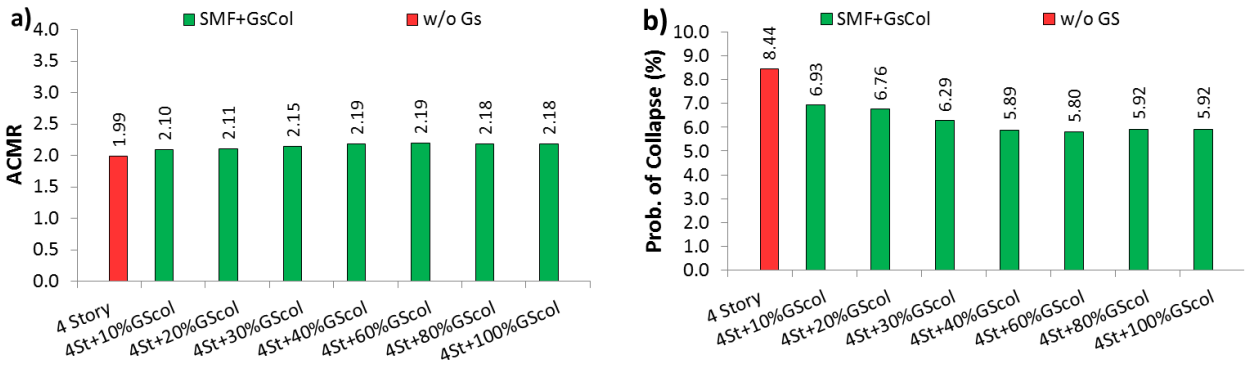

Figure 5-16 Results of 4-story building (a) ACMR (b) Probability of collapse.

It can be seen from Figure 5-16 (a) and (b) that the gravity columns improve the ACMR and the probability of collapse. However, in comparison to what it was found for the 8-story building the improvement is not drastic. It is important to note that having more gravity columns or increase their sections do not enhance the results after certain point. Probably the best ratio to use would be 0.4 because the ACMR goes from 1.99 to 2.10 (10% increment) and the probability of collapse decrease from 8.44% to 5.89%. Using larger ratios could represent an increase in the cost of the structure (more gravity columns or larger sections) and the improvements obtained are virtually the same. These results correlate with the results obtained in the pushover analysis where the post-yield stiffness improvement was saturated for ratios larger than 0.4.

The performance evaluation for the 8-story model is shown Figure 5-17 (a) and (b). As it was expected from the pushover curves, the improvement of the ACMR and probability of collapse is noticeable when gravity columns are included as part of the lateral resisting system. From Figure 5-17 (a) it can be seen that the ACMR goes from 1.99 for the 8-story building without the gravity column influence to 2.86 when the 8-story model includes the gravity columns with stiffness per story ratio equal to 1. It is interesting to note again the direct relation between the nonlinear dynamic with the nonlinear static results. Figure 5-14 shows how the post-yield stiffness improves progressively when the stiffness per story of the gravity columns

increases. Unlike the 4-story model the improvement does not reach a limit for ratios smaller than 1.

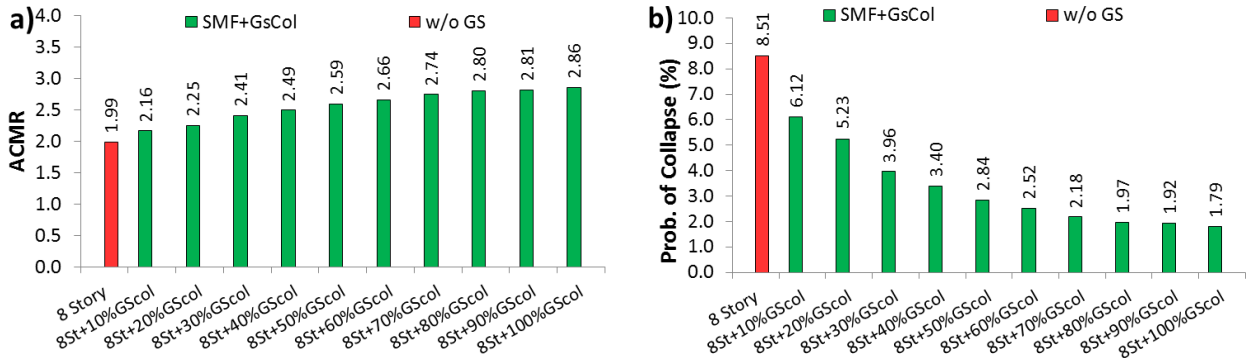

Figure 5-17 Results of 8-story building (a) ACMR (b) Probability of collapse.

Even though the use of larger gravity columns brings more benefits to the performance, it could be uneconomical. Therefore, a ratio that is considered to be the optimal has to be established. This ratio will benefit the performance and represent an economical solution. The pushover curves have an important role on determining this ratio. From Figure 5-14, it can be seen that the post-yield stiffness increases rapidly up to a point where the ratio of inertias is equal to 0.5. After this point, the post-yield stiffness still improves but in smaller increments. Thus, this ratio could be in this case considered to be the optimal for design. The ACMR for this ratio goes from 1.99 to 2.59 which represents an increase of 30.5%. On the other hand, the probability of collapse decreases from 8.51% to 2.84% which is a decrease of 66%.

5.7.3 Fragility Curves

Another method to present the results is using the collapse fragility curves. As indicated by the FEMA P-695 methodology, the collapse fragility curve is characterized by a lognormal cumulative distribution where the mean is the ACMR and the uncertainties are the standard deviation. More information can be found in the FEMA P-695 document or in the paper by

Deierlein et al. [27]. Figure 5-18 illustrates the fragility curves for the 2-, 4- and 8-story models. Noting that not all the analyzed cases are included, the curves represent the range of variation between not having gravity columns and having a ratio of inertia in the gravity columns equal to 100%. It can be seen how the probability of collapse decreases when the gravity columns are included in the analysis. However, it is clear from Figure 5-18 (c), the range of variation is significant in comparison to the 2-, and 4- story models, proving once more that this approach is more suitable for taller buildings.

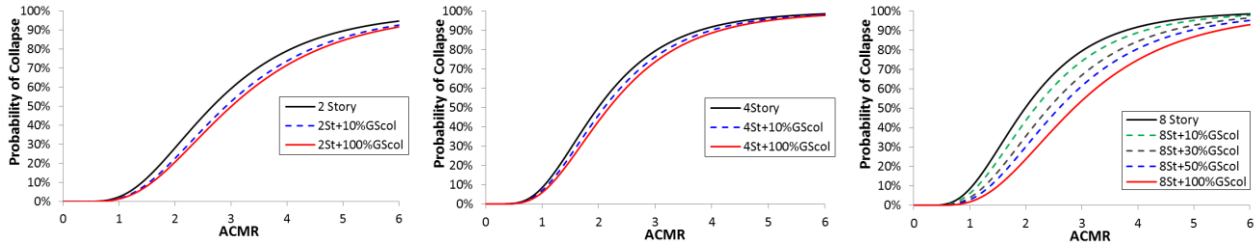

a) 2-Story b) 4-Story c) 8-Story

Figure 5-18 Collapse Fragility Curves

Figure 5-19 displays a portion of the fragility curves to illustrate the probability of collapse. As already mentioned this is computed at MCE level (ACMR=1) and it can be seen how it decreases for all cases but it is especially significant for the 8-Story model (Figure 5-19c).

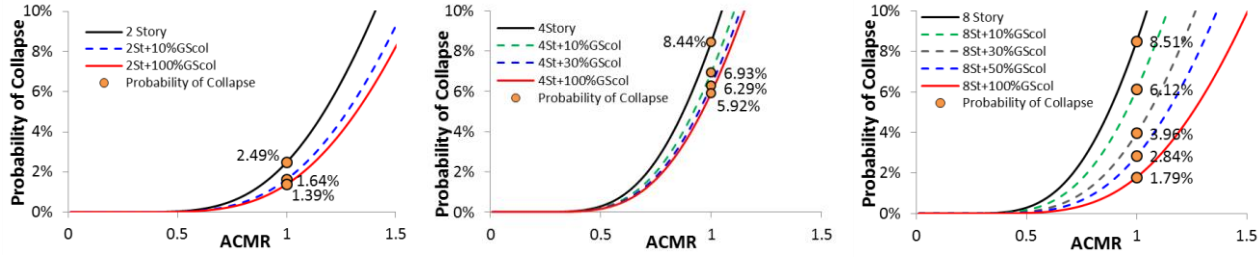

a) 2-Story b) 4-Story c) 8-Story

Figure 5-19 Adjusted Collapse Fragility Curves

5.8 Conclusions

The purpose of the investigation carried out herein was to improve the seismic performance of SMFs. For this purpose, the gravity columns were included as part of the lateral resisting system and the approach used to incorporate them was by lumping all the gravity columns that are located in the strong axis into one elastic, continuous element pinned at the base. The first part of this paper was dedicated to validating the approach used to include the gravity columns in the analysis. Then, in order to quantify the benefits of including the gravity columns, the collapse performance of SMFs including the gravity columns was evaluated and the conclusions obtained are:

- The gravity columns do not yield if the gravity connections have low flexural strength capacity (less than 30%M_p), and pinned at the base.
- The flexural capacity of the splices depends on the gravity column section, the compressive load, the number of bolts and the story location. Placing the column splices as far as possible from the ground is beneficial to decrease its flexural strength requirement to provide continuity.
- The influence of the gravity columns is beneficial for all three buildings. However, the improvement on the collapse performance that the 8-story model presents is significant in comparison to the other two buildings.
- It is known that continuous stiffness can prevent or reduce the probability of buildings to develop drift concentrations or weak story mechanisms. This was reflected in this study by reducing the probability of collapse of the structures.
- The stiffness to be assigned to the gravity columns in this study was taken as a ratio of the SMFs column's inertia. This was an arbitrary way of measuring the number of

gravity columns that the building could have. However, the adequate stiffness of the gravity columns could be obtained directly by performing nonlinear static pushover analysis.

- From the results, it can be seen that there seems to be a direct relation between the pushover curves and an adequate stiffness to be assigned to the gravity columns. However, in order to provide guidelines of how to compute this adequate stiffness without performing nonlinear static pushover analysis more research is required.
- The gravity system is considered to be an implicit factor of safety and that is why is not typically included in the analysis. However, if gravity columns are purposely made continuous and an adequate stiffness assigned to the gravity columns, the performance of the building could be enhanced considerably.
- One of the conclusions presented in the ATC 76-1 project was: "there is a need to develop design concepts that prevent (or at least delay) the formation of partial mechanisms in lower stories of special SMF systems" [2]. By observing how the collapse performance of SMFs improved in this study, it could be concluded that the gravity columns may be an option to fulfill this need.

5.9 Acknowledgements

The work presented herein was possible through the support of the National Institute of Standards and Technology, award number 60ANB10D017. Financial support was also provided by the Pontificia Universidad Catolica de Chile. The authors would also like to acknowledge the contribution of Mr. Andy Hardyniec of Virginia Tech for his work creating the FEMA P-695 Toolkit and NeesHub for their help on conducting all the computations in their supercomputers.

5.10 References

[1] G.A. MacRae, The Continuous Column Concept-Development and Use, Proceedings of the Ninth Pacific Conference on Earthquake Engineering Building an Earthquake-Resilient Society, (2011).

[2] NIST, Evaluation of the FEMA P-695 Methodology for Quantification of Building Seismic Performance Factors, National Institute of Standards and Technology, USA, 2010.

[3] R. Tremblay, S. Stiemer, Back-up stiffness for improving the stability of multi-storey braced frames under seismic loading, Proceedings of the 1994 SSRC Annual Technical Session, Bethlehem, Pa, (1994) 311-325.

[4] Z. Qu, L. Ye, A. Wada, Seismic damage mechanism control of RC ductile frames from a stiffness point of view, in: 8th International Conference on Urban Earthquake Engineering, Tokyo, Japan, 2011.

[5] Z. Qu, A. Wada, S. Motoyui, H. Sakata, S. Kishiki, Pin-supported walls for enhancing the seismic performance of building structures, Earthquake engineering & structural dynamics, 41 (2012) 2075-2091.

[6] H. Tagawa, Towards an understanding of seismic response of 3D structures-stability & reliability, Doctor Thesis, Washington: University of Washington, (2005).

[7] F.X. Flores, F.A. Charney, D. Lopez-Garcia, Influence of the gravity framing system on the collapse performance of special steel moment frames, Journal of Constructional Steel Research, 101 (2014) 351-362.

[8] F. P695, Quantification of Building Seismic Performance Factors, Fededral Emergency Management Agency, Washington, D.C, 2009.

[9] AISC, Seismic Provisions for Structural Steel Buildings, ANSI/AISC 341-05, American Institute for Steel Construction., Chicago, Ill., 2005.

[10] F. McKenna, G. Fenves, M. Scott, OpenSees: Open system for earthquake engineering simulation, Pacific Earthquake Engineering Center, University of California, Berkeley, CA., http://opensees. berkeley. edu, (2006).

[11] L.F. Ibarra, R.A. Medina, H. Krawinkler, Hysteretic models that incorporate strength and stiffness deterioration, Earthquake engineering & structural dynamics, 34 (2005) 1489-1511.

[12] D.G. Lignos, H. Krawinkler, Deterioration modeling of steel components in support of collapse prediction of steel moment frames under earthquake loading, Journal of Structural Engineering, 1 (2010) 279.

[13] F.A. Charney, J. Marshall, A Comparison of the Krawinkler and Scissors Models for Including Beam-Column Joint Deformations in the Analysis of Moment-Resisting Steel Frames, Engineering journal., 43 (2006) 31.

[14] AISC, Specification for Structural Steel Buildings, AISC/ANSI 360-05, American Institute of Steel Construction, Chicago, Illinois, 2011.

[15] F. Zareian, R.A. Medina, A practical method for proper modeling of structural damping in inelastic plane structural systems, Computers & structures, 88 (2010) 45-53.

[16] F. Zareian, D. Lignos, H. Krawinkler, Evaluation of seismic collapse performance of steel special moment resisting frames using FEMA P695 (ATC-63) methodology, in: Proceedings of Structures Congress ASCE, New York, 2010.

[17] E. Wilson, A. Habibullah, Sap 2000 Integrated Finite Element Analysis and Design of Structures Basic Analysis Refence Manual, Computers and Structures, Berkeley, (1998).

[18] G.A. MacRae, Y. Kimura, C. Roeder, Effect of column stiffness on braced frame seismic behavior, Journal of Structural Engineering, 130 (2004) 381-391.

[19] J. Liu, A. Astaneh-Asl, Cyclic testing of simple connections including effects of slab, Journal of Structural Engineering, 126 (2000) 32-39.

[20] A. Gupta, H. Krawinkler, Behavior of ductile SMRFs at various seismic hazard levels, Journal of Structural Engineering, 126 (2000) 98-107.

[21] ASCE, Seismic Rehabilitation of Existing Buildings (ASCE/SEI 41-13), American Society of Civil Engineers Reston, Virginia, 2013.

[22] D. Vamvatsikos, C.A. Cornell, Applied incremental dynamic analysis, Earthquake Spectra, 20 (2004) 523.

[23] ASCE, Minimum design loads for buildings and other structures, American Society of Civil Engineers/Structural Engineering Institute, Reston, VA, 2006.

[24] FEMA, Recommended seismic design criteria for new steel moment-frame buildings, FEMA 350 Report, 2000.

[25] A.R. Tamboli, L.S. Muir, W.A. Thornton, T. Kane, D.K. Miller, R.S. Funderburk, O.W. Blodgett, R.T. Leon, J.O. Malley, R.S. Pugliesi, Handbook of structural steel connection design and details, McGraw-Hill, 1999.

[26] F.T. Ladani, G. MacRae, G. Chase, C. Clifton, Effects of column splice properties on seismic demands in steel moment frames.

[27] G.G. Deierlein, A.B. Liel, C.B. Haselton, C.A. Kircher, K. Principal, ATC-63 methodology for evaluating seismic collapse safety of archetype buildings, in: ASCE-SEI Structures Congress, Vancouver, BC, 2008, pp. 24-26.

Chapter 6: Supporting Studies

This chapter of the dissertation presents supplemental studies that expand certain sections of the research done in the published papers [1, 2]. Additionally, results that were not included in the articles due to space limitations are shown herein. This chapter is divided into three subsections1) Influence of gravity column splice location and strength 2) Yielding in gravity columns and 3) Lumped vs Explicit Model.

6.1 Influence of Gravity Column Splice Location and Strength

6.1.1 Introduction

As a result of the analytical investigations reported in Chapters 4 through 5, it has been clearly demonstrated that the stiffness contributed by the continuity of gravity columns improves the seismic performance of special steel moment frames. The effect of the continuity is more important when the structure is subjected to large deformations. It decreases drift concentrations in the lower stories and reduces the likelihood of having weak story mechanisms develop in the building.

One of the disadvantages of using fully continuous gravity columns is that splices will have to be designed to have full moment capacity during the design stage. In this section of the chapter, two aspects of the splices that have an important role in providing continuous stiffness are studied: the location (story level and position within the story) and the splices flexural strength. These characteristics are investigated by analyzing systems with a variety of splice locations in the gravity columns, and by varying the splices strength. Two different configurations of splice locations are considered: “leveled” splices, where all of the splices are

located at a same level within the story height and “staggered” splices, where the splices are placed at different levels within the story.

The first step in the study is to analyze different arrangements of the leveled and staggered splices. The performance of the SMFs is evaluated by performing nonlinear static pushover analyses. The results are then compared with the pushover curves obtained for the building without the gravity system and for the building with the gravity system (continuous columns). Then, a subset of the splice configurations are investigated more in depth by computing the splice strength that is required to provide essentially full continuity, even though the provided strength is not equal to the full flexural strength of the columns at the splice locations.

6.1.2 Building Overview

One of the conclusions of the published studies [1, 2] is that the gravity columns continuity has a more of a significant effect on taller buildings (8-story model). For this reason, this supplemental study is focused just on the building that could be more influenced by the splices. The 8-story model taken from the ATC 76-1 [3] project is selected for this purpose.

6.1.3 Modeling Splices

As an initial study, a lower bound of the influence of the splices on the seismic performance of SMFs is computed by considering their flexural strength capacity to be null (zero). Therefore, a true hinge is located within the story where the splice is to be placed. Although the assumption of neglecting the splice flexural capacity is not realistic, it is the worst-case scenario and it will provide a clear idea of the influence on the performance. Later on in this study, the flexural strength of the splices is assumed to be a fraction of the column’s plastic

moment capacity. The moment rotation behavior assigned to the splices is rigid perfectly plastic (Figure 6.1 1.) and the flexural strength is the parameter to be varied.

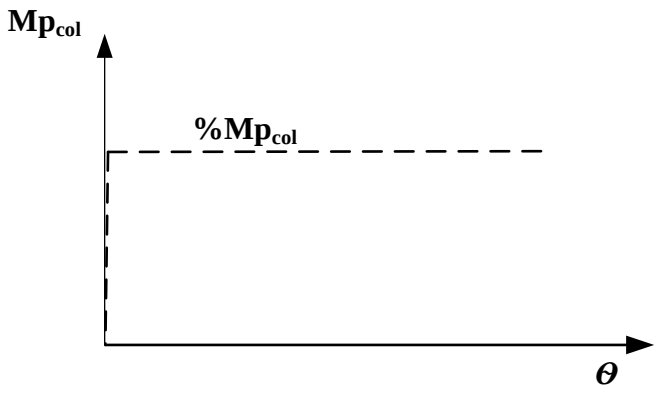

Figure 6.1-1 Gravity Column Splice Hysteretic Behavior

6.1.4 Levelled Splices

The splices were located just in the gravity columns and the number of cases depends on (1) the place within the column height where the splice is located and (2) in the story in which the splices are located. As already mentioned, the "leveled" splices are located at the same height in all stories. Twelve cases were investigated as shown from the Figure 6.1-2 to Figure 6.1-13.

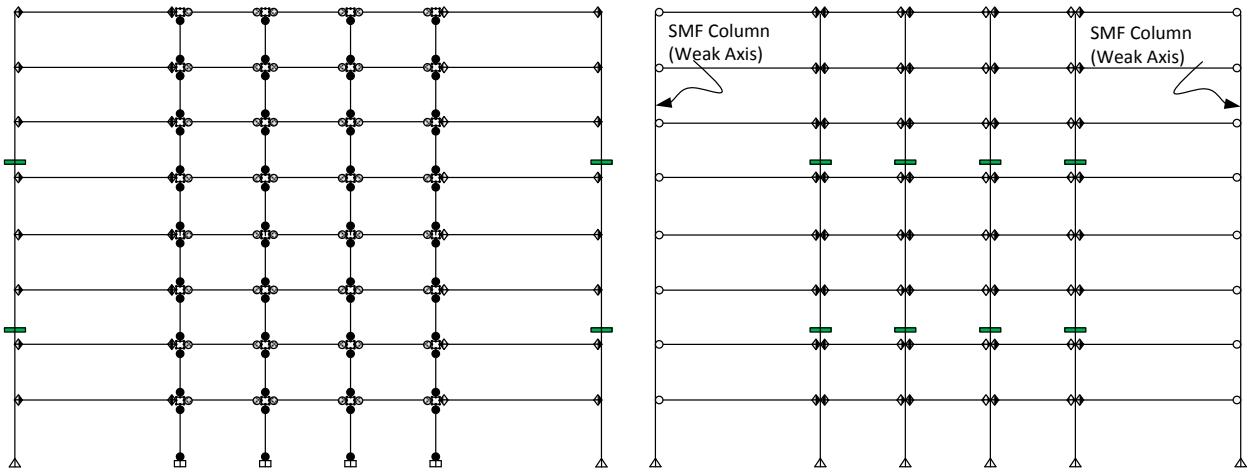

Figure 6.1-2 Case I_L: Splices located in 3rd and 6th story at 1/3 of column height

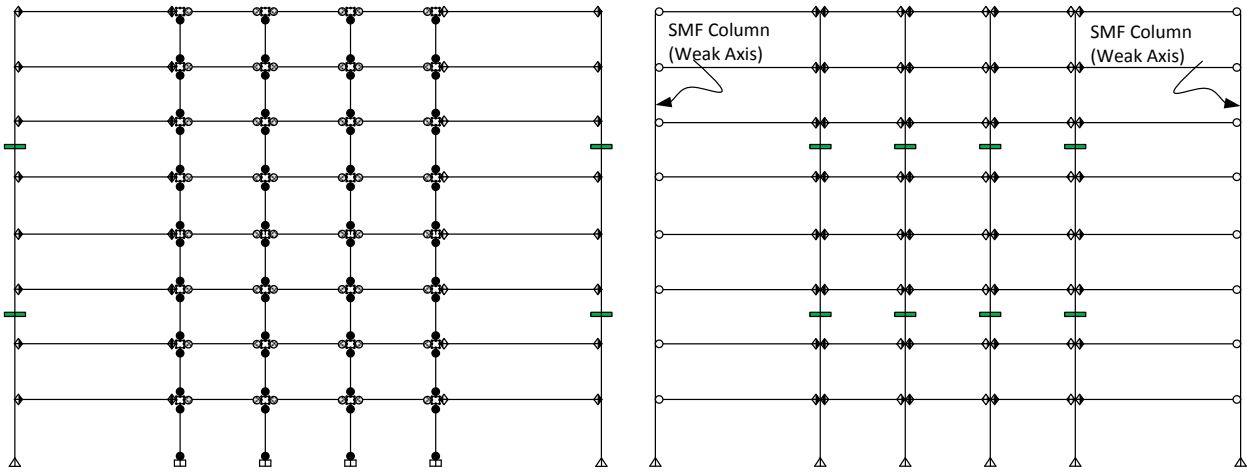

Figure 6.1-3 Case II_L: Splices located in 3rd and 6th story at 1/2 of column height

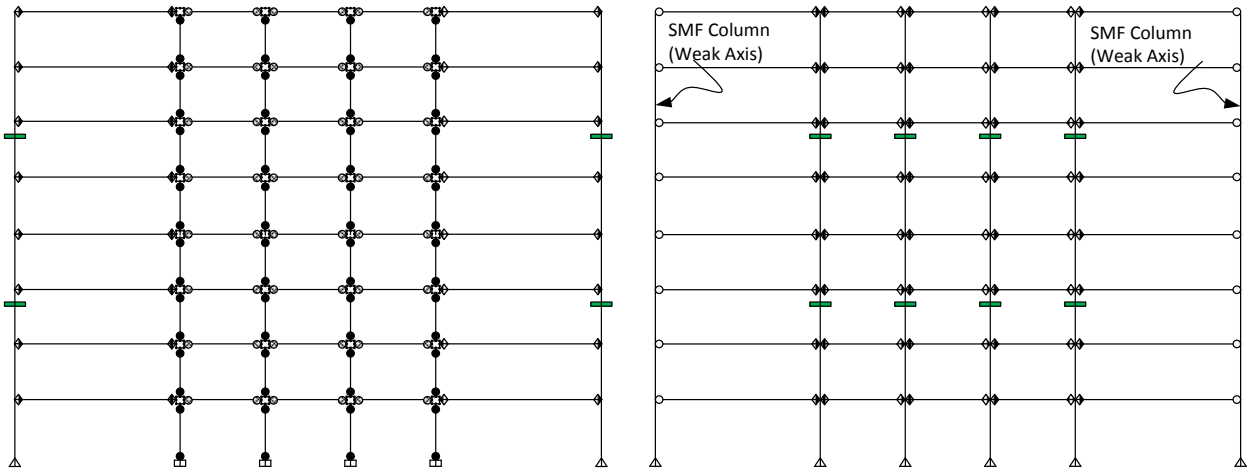

Figure 6.1-4 Case III_L: Splices located in 3rd and 6th story at 2/3 of column height

The cases I, II and III shown in Figure 6.1-2, Figure 6.1-3 and Figure 6.1-4 respectively have the splices in the 3rd and 6th story. However, what differentiates them from each other is the height within the story where the splices are placed. Cases I, II and III have the splices at 1/3, 1/2 and 2/3 of the column height. On the other hand, cases IV, V and VI shown in Figure 6.1-5 Figure 6.1-6 and Figure 6.1-7 respectively are similar to cases I, II and III with the difference being that they do not have splices in the 6th story. Even though, the length of the columns is too long to have one splice, these cases were created to evaluate the upper splice's effect.

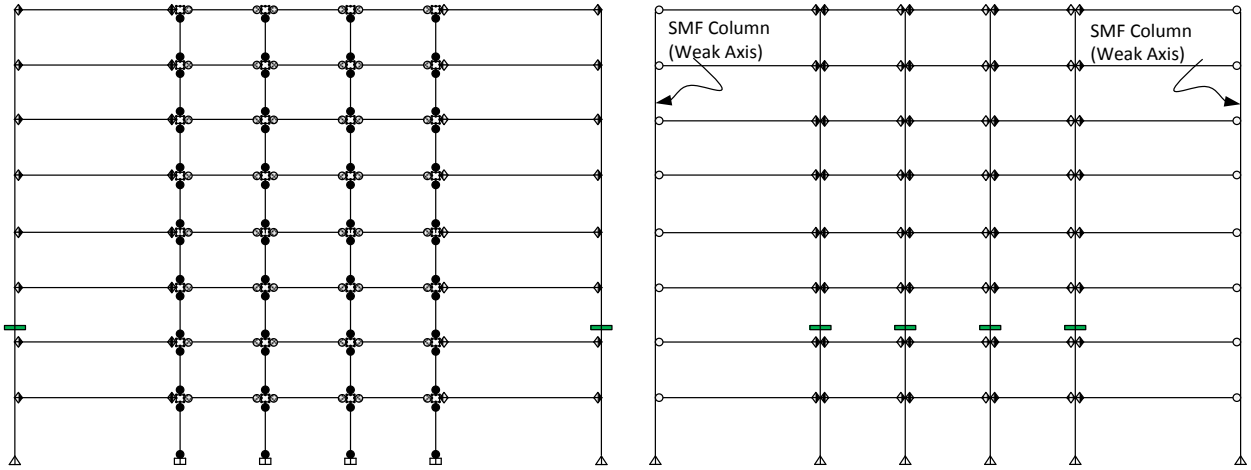

Figure 6.1-5 Case IV_L: Splices located in 3rd story at 1/3 of column height

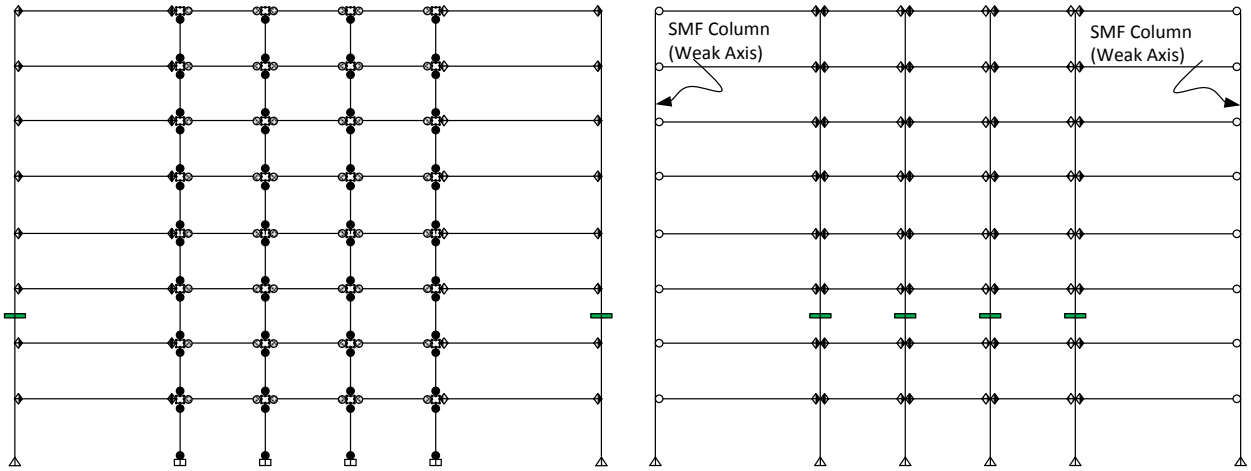

Figure 6.1-6 Case V_L: Splices located in 3rd story at 1/2 of column height

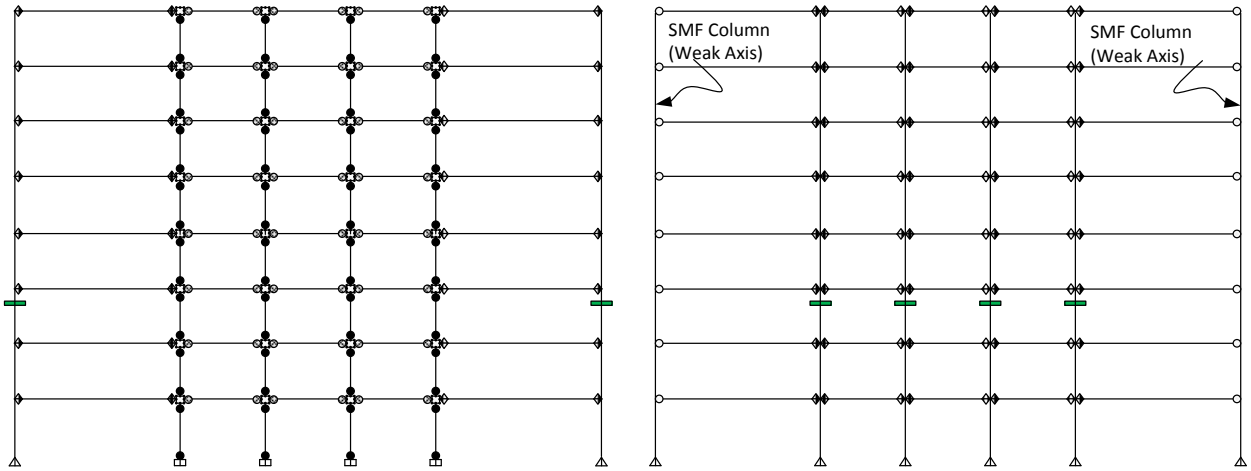

Figure 6.1-7 Case VI_L: Splices located in 3rd story at 2/3 of column height

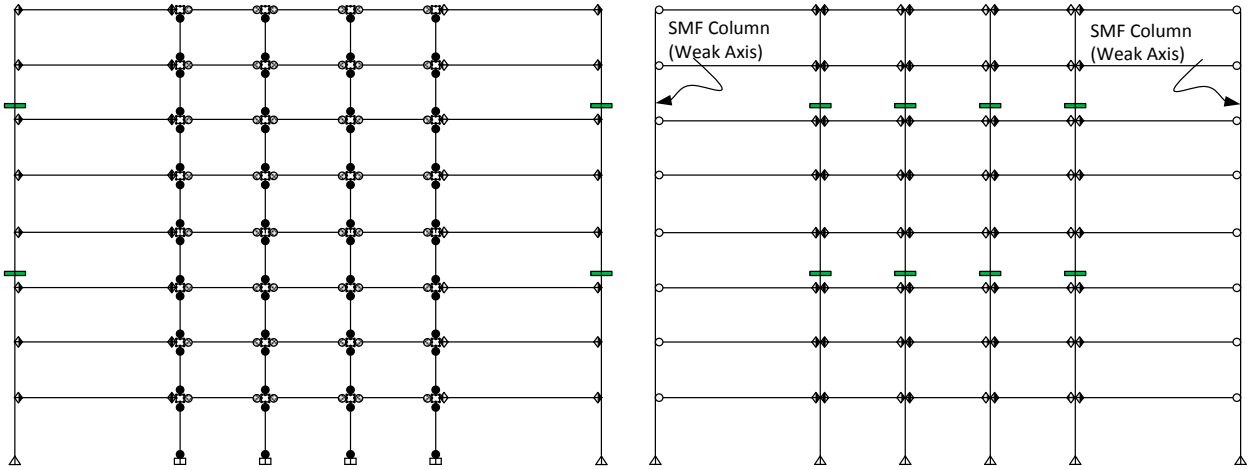

Figure 6.1-8 Case VII_L: Splices located in 4th and 7th story at 1/3 of column height

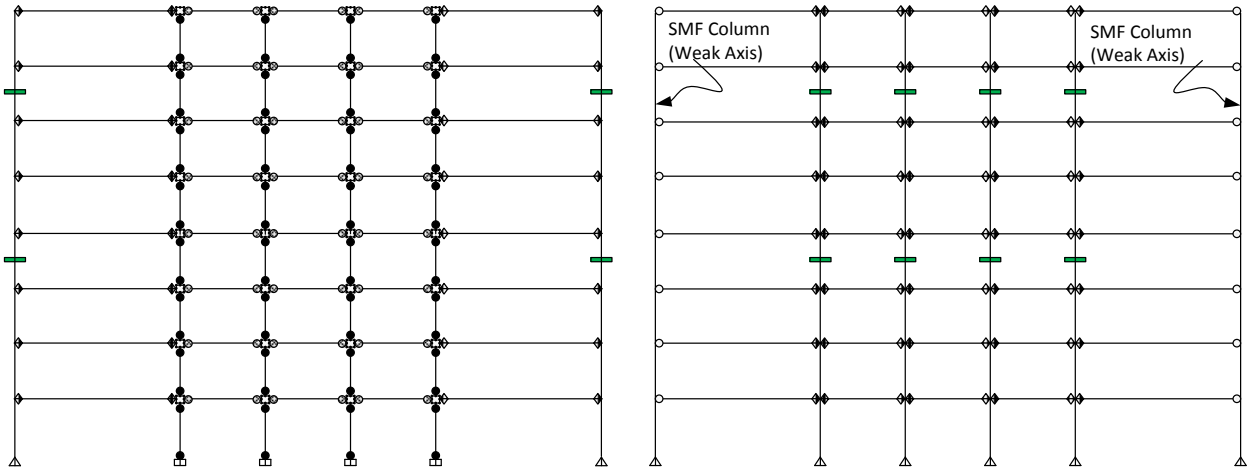

Figure 6.1-9 Case VIII_L: Splices located in 4th and 7th story at 1/2 of column height

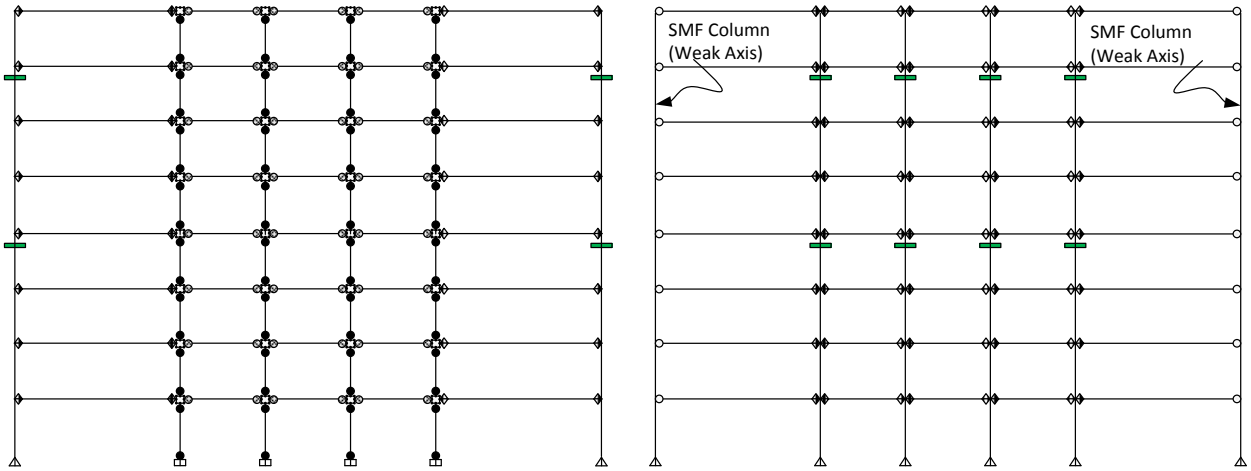

Figure 6.1-10 Case IX_L: Splices located in 4th and 7th story at 2/3 of column height

The cases VII, VIII and IX displayed in Figure 6.1-8, Figure 6.1-9 and Figure 6.1-10 respectively, have the splices in the 4th and 7th story. Again, what differentiates them from each other is the height within the story where the splices are placed. Cases VII, VIII and IX have the splices at 1/3, 1/2 and 2/3 of the column height. On the other hand, cases X, XI and XII shown in Figure 6.1-11, Figure 6.1-12 and Figure 6.1-13 respectively are similar to cases VII, VIII and IX with the difference that they do not have splices in the 7th story. The cases without the splices in the 7th story were also created to evaluate the upper splice's effect.

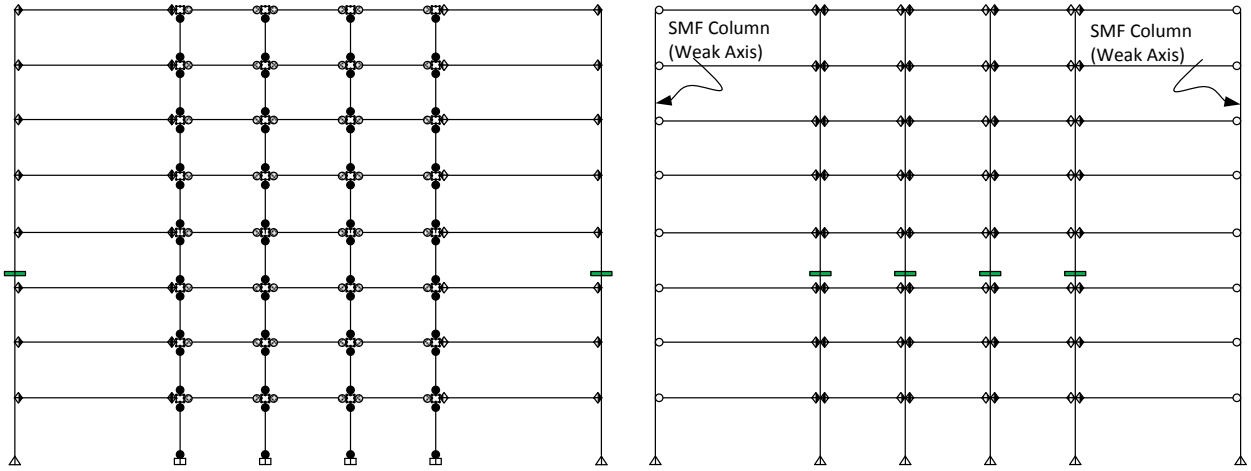

Figure 6.1-11 Case X_L: Splices located in 4th story at 1/3 of column height

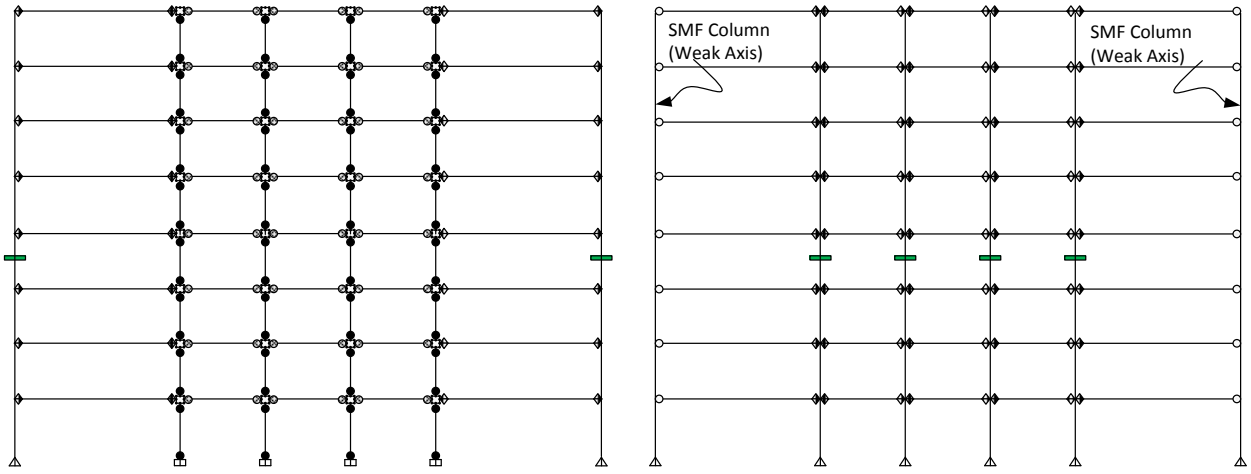

Figure 6.1-12 Case XI_L: Splices located in 4th story at 1/2 of column height

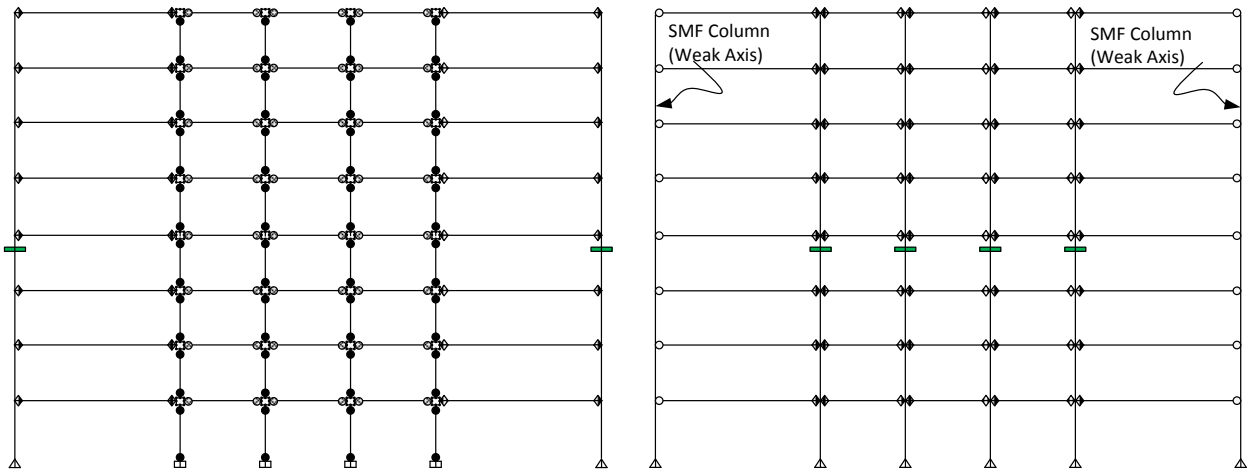

Figure 6.1-13 Case XII_L: Splices located in 4th story at 2/3 of column height

All the presented cases were created for the following purposes: 1) to establish the influence of placing the splices at different heights within the story 2) to evaluate the influence of the upper story splices and 3) to evaluate the influence of the splices placed in different story levels. The following subsections present the results of the analyses performed to evaluate the influence of the splices.

6.1.4.1 Influence of Splice Location within Column Height (Case I, II and III)

The splices for cases I, II and III are located at the same elevation across the 3rd and 6th story. The height where the splices for cases I, II and III are placed is 1/3, 1/2 and 2/3 of the column height respectively. The results are shown in Figure 6.1-14, and it can be seen how the performance improves progressively when the splices are placed farther from the bottom of the column in the spliced story. On the other hand, if the splices are placed in the 3rd story at 1/3 of the story height, the improvement is negligible. Thus it can be inferred that this location interrupted the continuous stiffness provided by the gravity columns. It is important to note that splices located at 2/3 of the column height is not a common practice in construction but this location improved the structure's performance the most.

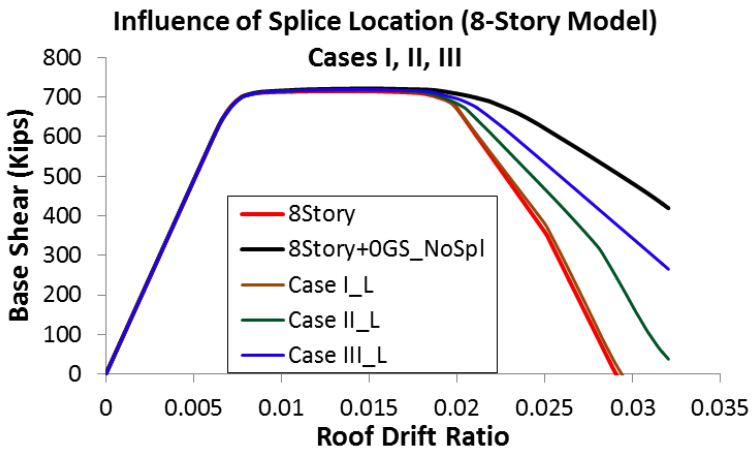

Figure 6.1-14 Pushover Curves Cases I, II, III (Levelled Splices)

6.1.4.2 Influence of Splice Location within Column Height (Case VII, VIII and IX)

The splices for cases VII, VIII and IX are located at the same story level across the 4th and 7th story. The column height where the splices for cases VII, VIII and IX are placed is 1/3, 1/2 and 2/3 of the height respectively. Unlike the results shown in Figure 6.1-14, the difference between the pushover curves obtained for splices located at different heights within the column is not relevant (Figure 6.1-15). Therefore, it can be said that the stiffness provided by the gravity columns is barely interrupted if the splices were located farther away from the column's base (4th and 7th story). It is important to point out that the improvement in the pushover curves arises from the prevention of drift concentrations on the bottom stories. Thus, the 8-story model is susceptible to have drift concentrations in the first three stories because if the gravity columns are continuous up to the 4th story, the continuous stiffness provided by these columns improved significantly the performance.

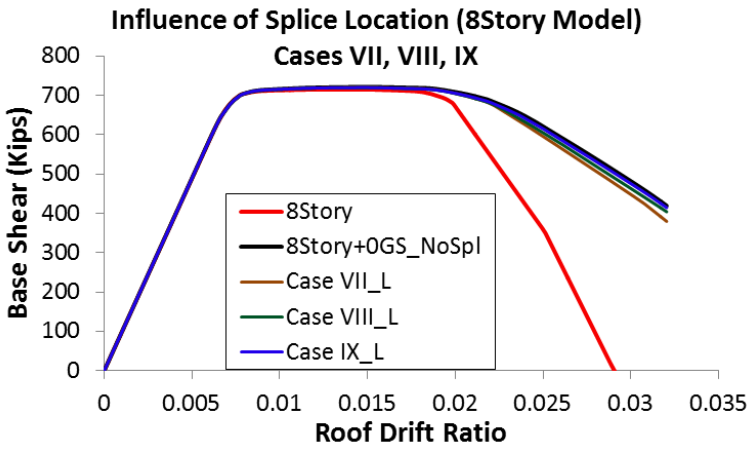

Figure 6.1-15 Pushover Curves Cases VII, VIII, IX (Levelled Splices)

6.1.4.3 Influence of Upper Splices (Case I vs IV, II vs V , III vs VI)

Figure 6.1-16 shows the comparison between cases I, II and III with the cases IV, V, and VI respectively. From this comparison, the influence of the splices located in the upper story (6^{th} story) is evaluated. The results display that for all the cases, the influence is minimum and it could be neglected. Thus the main splices are the ones located in the 3^{rd} story, and for these cases what controls the performance is how far away the splices are from the column's base within a given story.

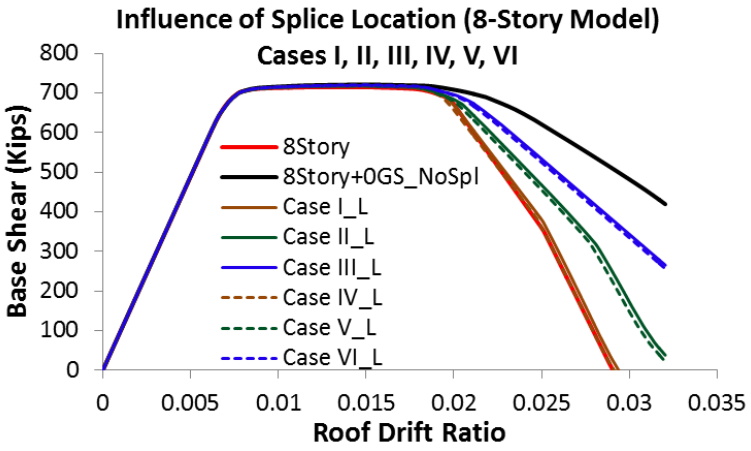

Figure 6.1-16 Influence of Upper Splices (cases I to VI)

6.1.4.4 Influence of Upper Splices (Case VII vs X, VIII vs XI, IX vs XII)

Figure 6.1-17 shows the comparison between cases VII, VIII and IX with the cases X, XI, and XII respectively. From this comparison, the influence of the splices located in the upper story (7^{th} story) is also evaluated and it can be seen again that for all the cases, the influence is minimum.

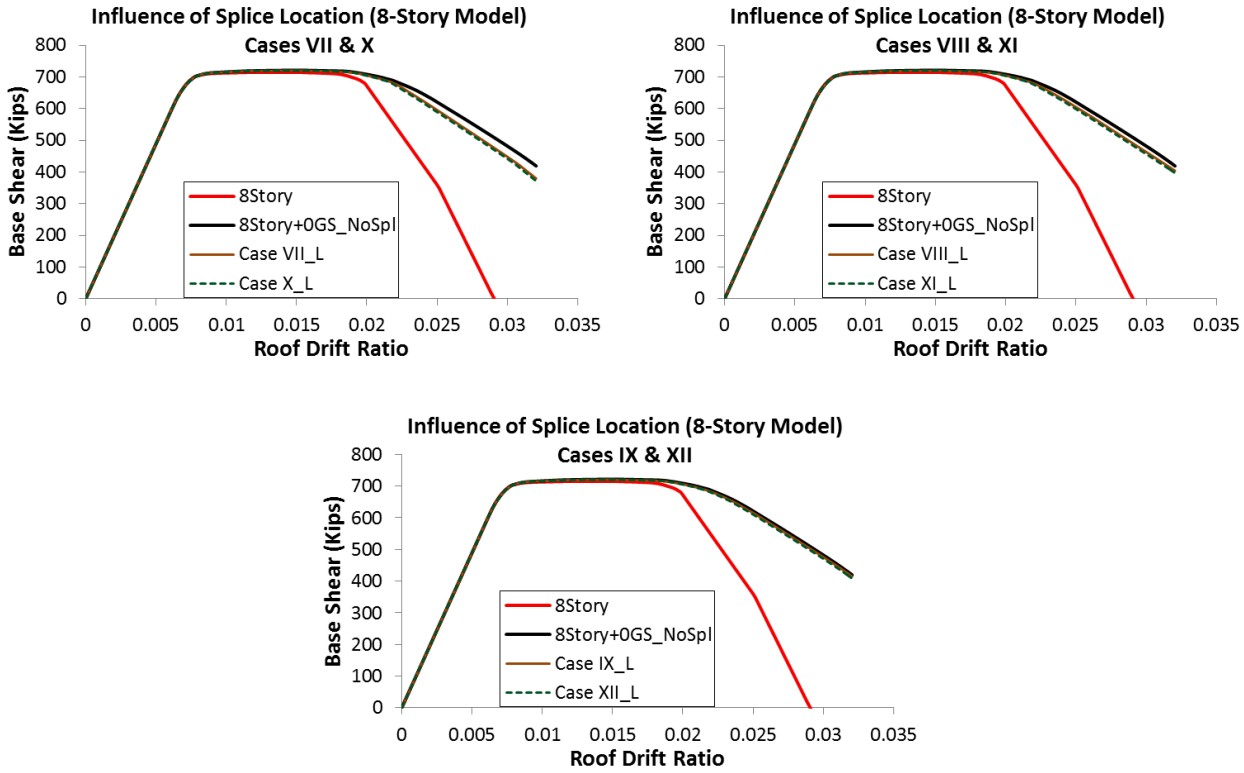

Figure 6.1-17 Influence of Upper Splices (cases VII to XII)

6.1.4.5 Influence of Story Level where Splices are Located

The pushover curves shown in Figure 6.1-18 represent the influence of the splices located in different story levels. The difference between the cases that are compared in each of the figures is that splices are placed in either the 3^{rd} and 6^{th} stories, or in the 4^{th} and 7^{th} stories. It was already demonstrated that the upper splices have a marginal influence on the seismic

performance. Thus it can be concluded from the figure that placing the splices in the 4th story instead of the 3rd story improves the performance drastically.

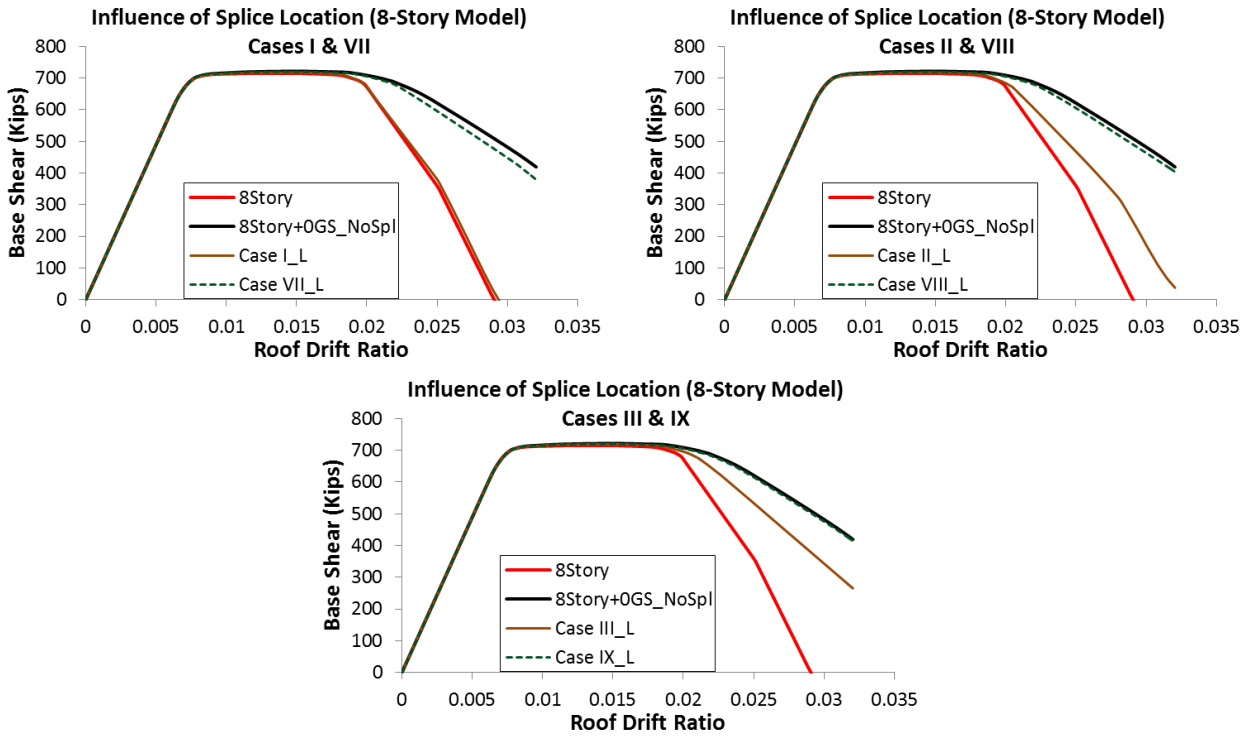

Figure 6.1-18 Influence of the story where splices are placed

6.1.5 Staggered Splices

The number of cases for the staggered splices depends on the place within the column height where the splices are located and in which story level. The purpose of studying the different cases is to establish any trend that indicates the improvement that staggering the splices could bring. However, from the results obtained for the "leveled" splices, it can be expected that the cases where the splices are located farther away from the column's base are going control the improvement in the seismic performance of the building. For the cases studied herein it has to be mentioned that the sections of the exterior gravity columns (B-3, E-3, Figure 3-1) in the gravity system are larger than the two interior ones (C-3, D-3, Figure 3-1). This is relevant for the cases with staggered splices because larger columns provide more stiffness. So, in the following cases

in addition to evaluating the location of the splices, the influence of the splices on larger columns is also quantified. The staggered cases to be studied are shown from the Figure 6.1-19 to Figure 6.1-28.

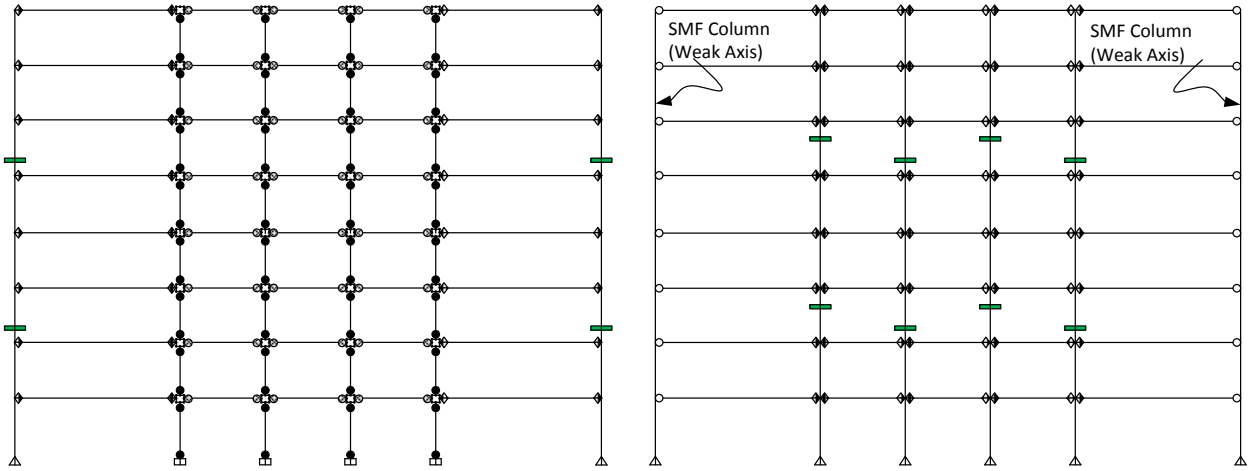

Figure 6.1-19 Case I_S: Splices located in 3rd and 6th story.

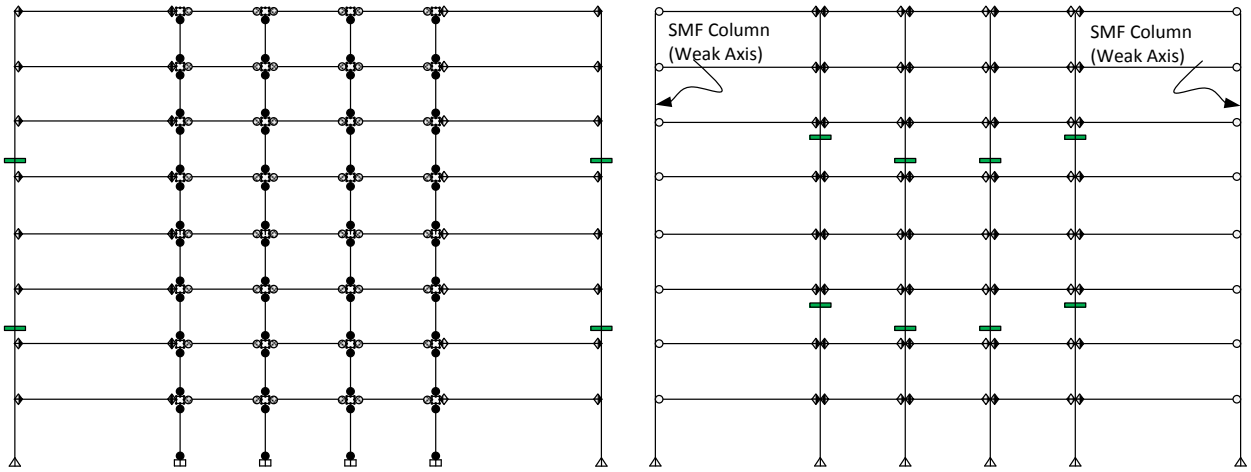

Figure 6.1-20 Case II_S: Splices located in 3rd and 6th story.

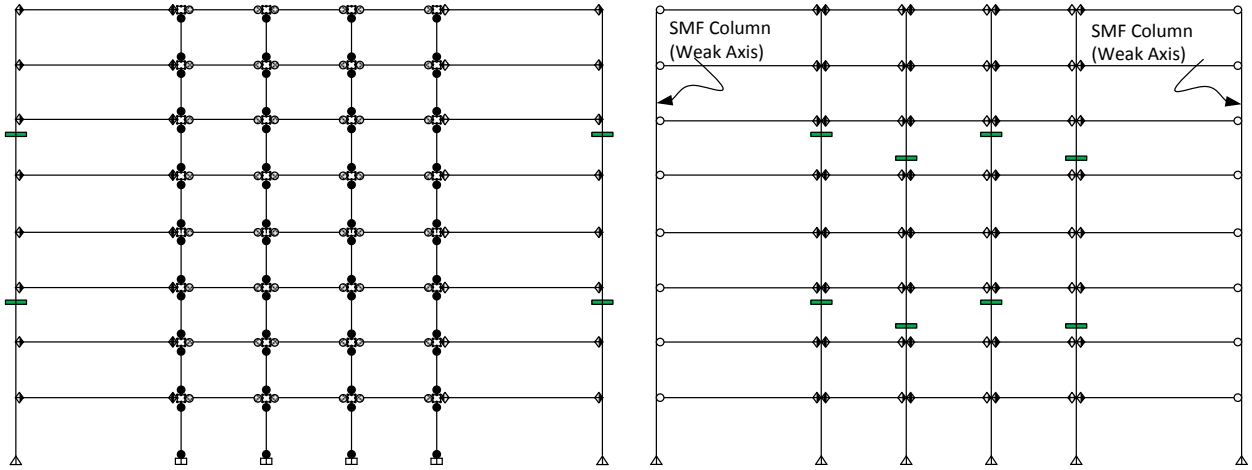

Figure 6.1-21 Case III_S: Splices located in 3rd and 6th story.

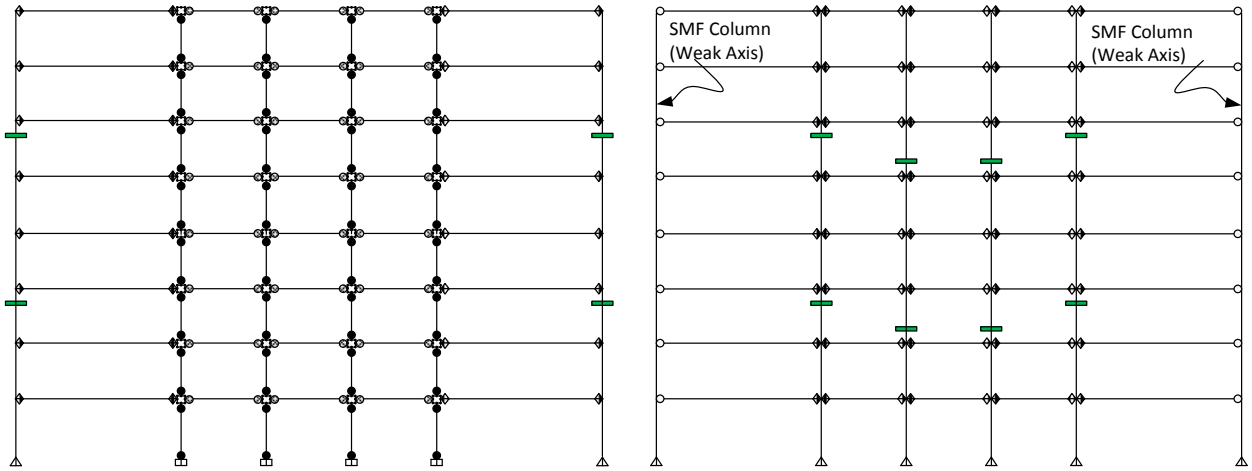

Figure 6.1-22 Case IV_S: Splices located in 3rd and 6th story.

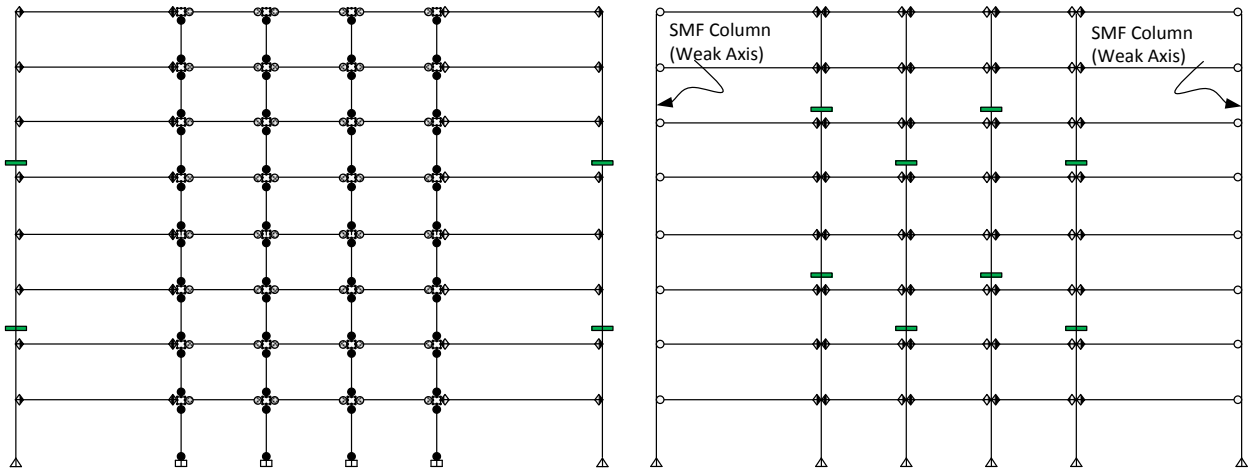

Figure 6.1-23 Case V_S: Splices located in 3rd, 4th and 6th ,7th story.

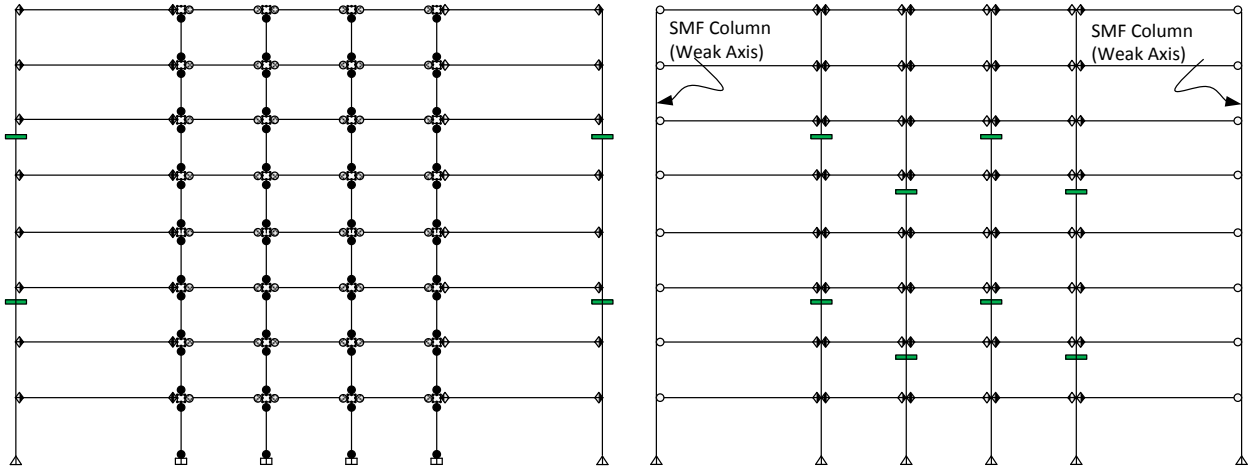

Figure 6.1-24 Case VI_S: Splices located in 2th, 3rd and 5th, 6th story.

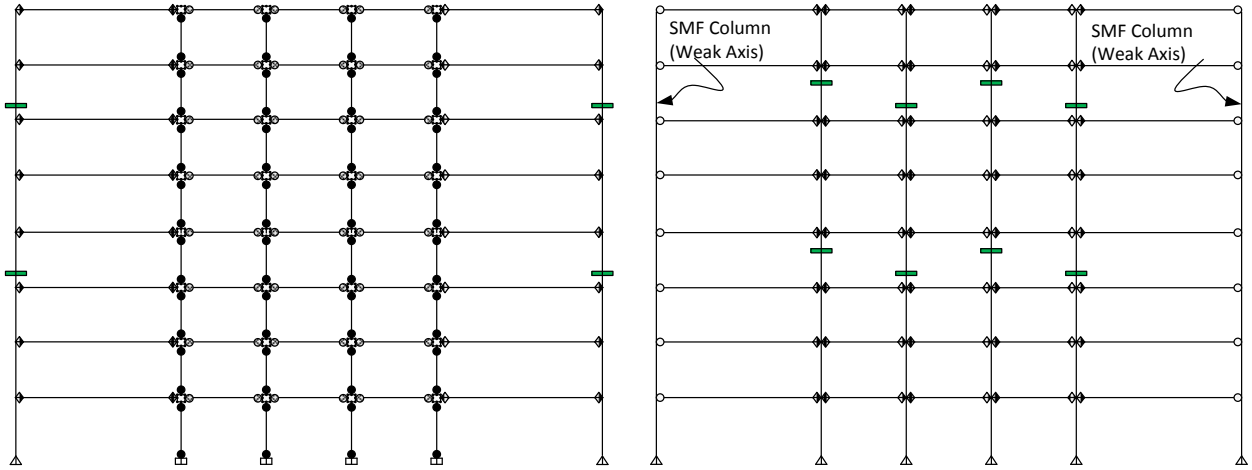

Figure 6.1-25 Case VII_S: Splices located in 4th and 7th story.

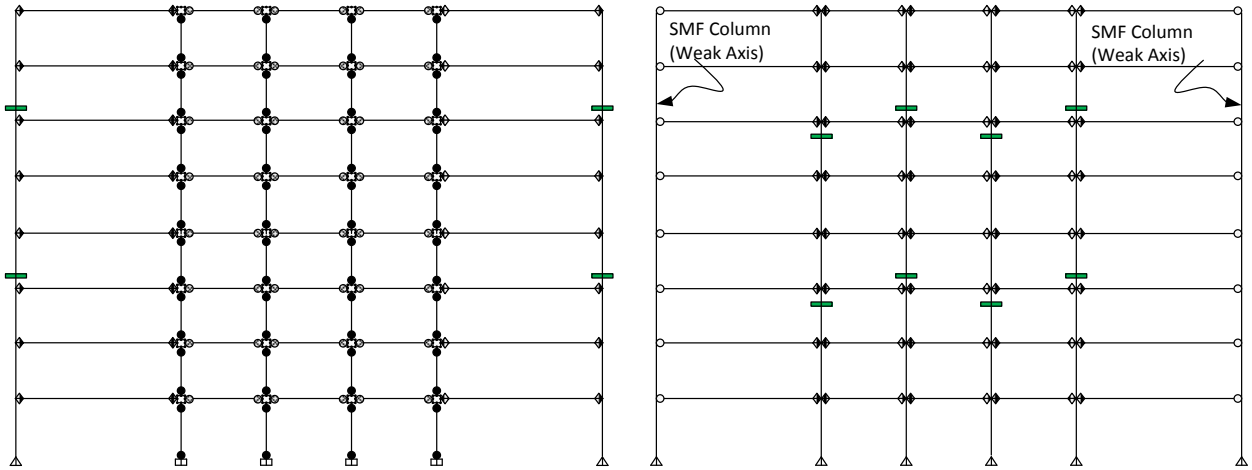

Figure 6.1-26 Case VIII_S: Splices located in 3rd, 4th and 6th, 7th story.

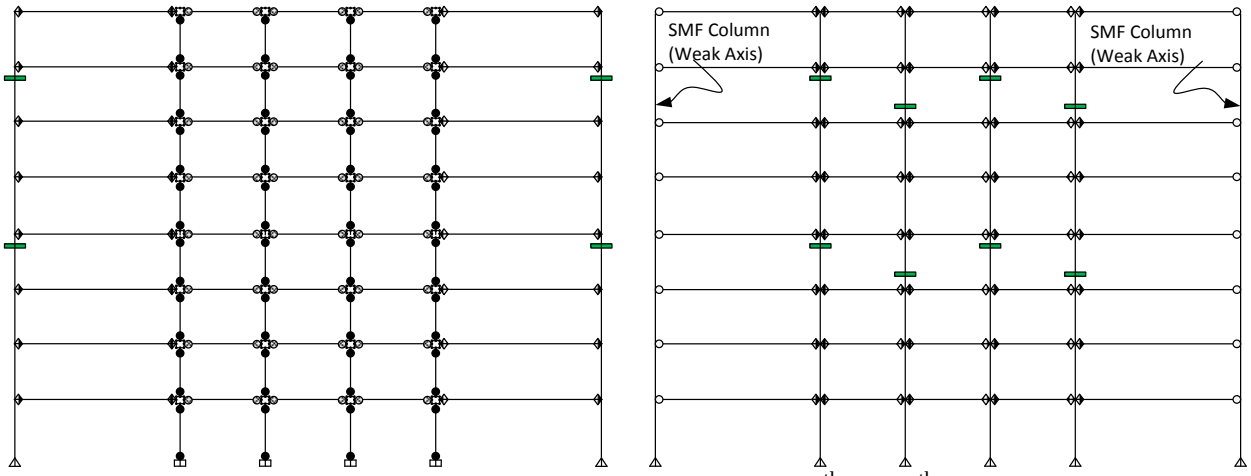

Figure 6.1-27 Case IX_S: Splices located in 4th and 7th story.

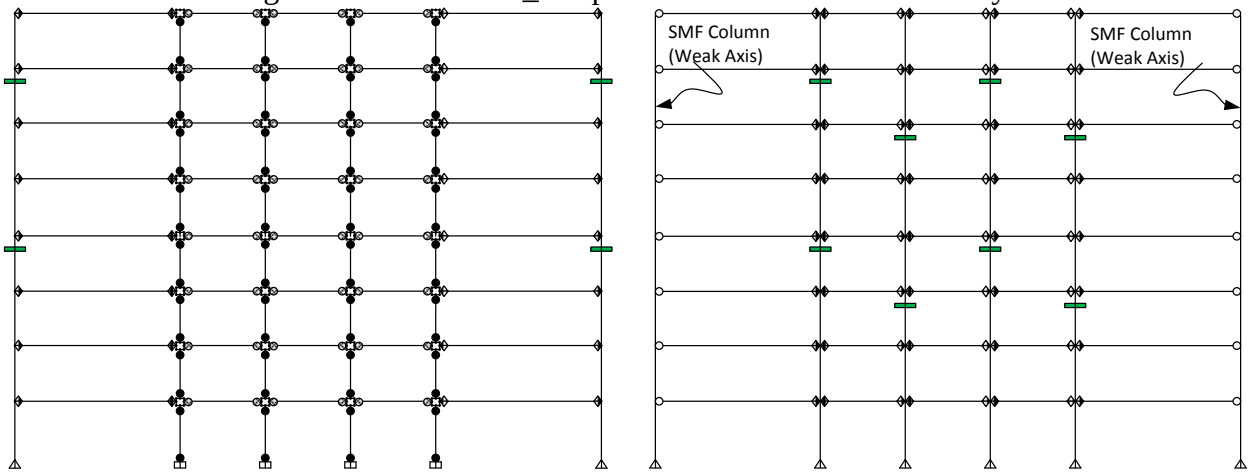

Figure 6.1-28 Case X_S: Splices located in 3rd, 4th and 6th, 7th story.

In the case of the splices placed in a staggered manner, it is difficult to see trends from the results, but some of the cases are compared herein. Figure 6.1-29 compares cases I through IV. The case that improves the performance the most is case IV because it has four splices located at 2/3 of the column height, but two of the columns are the extreme ones which have larger sections. The next best case among these is case III because it also has four splices located at 2/3 of the column height, but unlike case IV just one of the splices is located on an extreme column. Case II improves the behavior more than case I because the two splices located at the 2/3 of the column height are placed in the two extreme gravity columns.

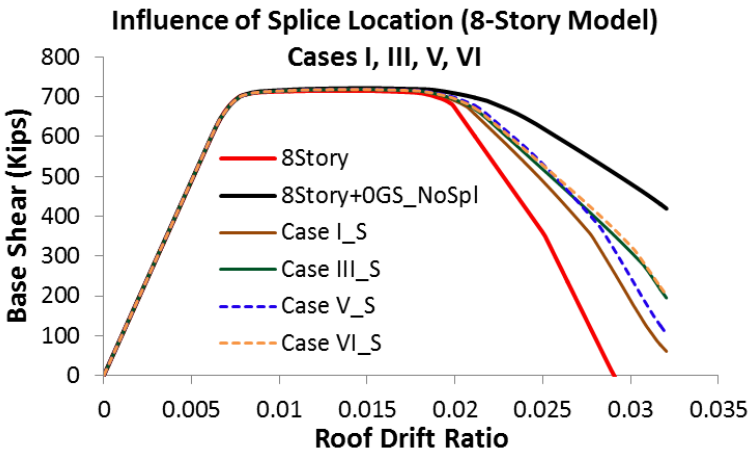

Figure 6.1-29 Pushover Curves Cases I, II, III and IV

Figure 6.1-30 shows different cases with comparable splice configurations. The main conclusion that can be made by comparing the cases I and V and the cases III and VI is that the performance is going to improve more if the splices are located farther from the column's base. Cases III and VI are almost the same because the splices located in the 3rd story and at 1/3 of the column height do not improve the performance of the structure since the continuity in the gravity column is lost almost completely.

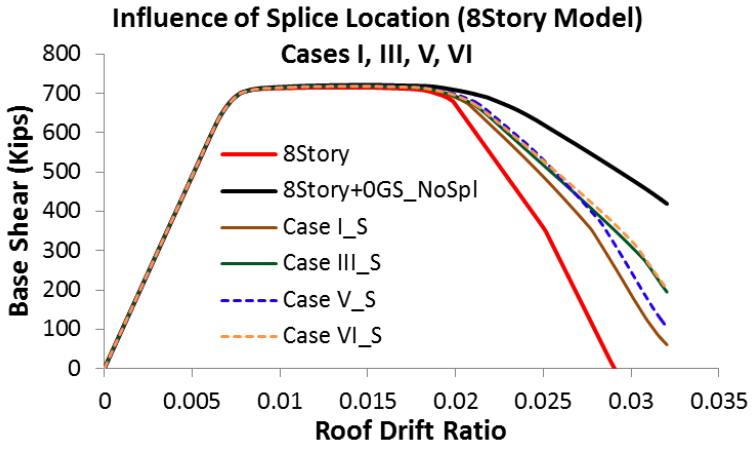

Figure 6.1-30 Pushover Curves Cases I, III, V, VI

Figure 6.1-31 shows the best seismic performances obtained from the staggered cases. All the cases displayed had almost the same performance because the majority of the splices were located in the 4th and 7th stories. However, among these cases the one that improved the seismic performance of the SMF the most is the case IX because it has more splices located farther from the ground.

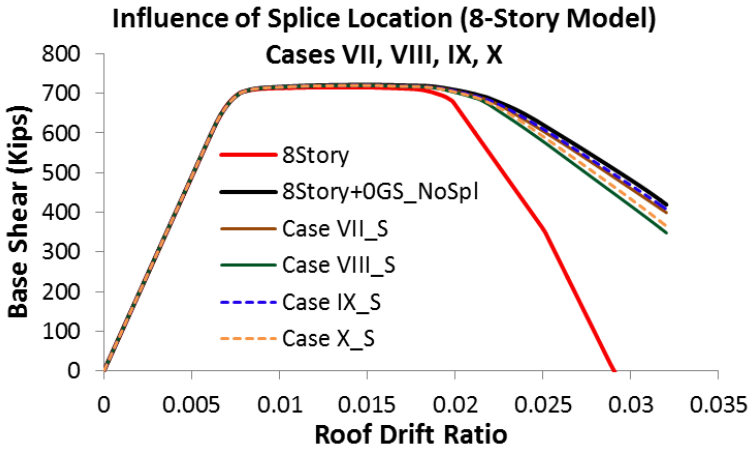

Figure 6.1-31 Pushover Curves Cases VII, VIII, IX, X

6.1.6 Summary and Conclusions

The importance of the splices in the gravity columns was addressed in this section of the dissertation. As known, the continuous stiffness provided in this case by the gravity columns have the effect of reducing drift concentrations and to lower the likelihood of having weak story mechanisms. As a result, the seismic performance of the SMFs improves drastically (in particular taller buildings like the 8-story). However, in order to acquire continuity, the splices in the gravity columns have to be designed to provide enough moment capacity.

It is common practice not to plan the layout of the splices in the gravity columns based on the performance of the building. This is a consequence of not including the gravity system as part of the lateral load resisting system. However, after performing several analyses, it was found

that the splice location within the column height and the story level have a significant influence on the seismic performance of the building. The main findings from this section of the dissertation are:

- The best way to define where the splices should be placed is by performing a nonlinear static pushover analysis.
- The continuous stiffness provided by the gravity columns prevents weak story mechanisms at bottom stories and that is why the first splice in every column should be placed as far as possible from the column's base.
- Splices located in the upper stories have negligible influence on the performance.
- From the results obtained herein, it can be concluded that there is no significant difference between staggered or levelled splices. The performance of the building improves depending on how far the splices are located from the ground.

Even though these conclusions are valid for the buildings studied in this dissertation, it should be mentioned that this is just a starting for future research in order to generalize the conclusions to all SMFs. Moreover, one of the conclusions is to perform a nonlinear static pushover analysis to establish the best splice's location in the building. However a more practical methodology needs to be studied.

6.1.7 Required Splice Strength

The previous section of this supplemental study considered the gravity column's splices strength to be null, so the obtained results represent a lower bound of the building seismic performance. From these lower bound results it was also seen that the performance depends directly on where the splices are located. However, it was concluded that the splices located in the upper stories have negligible influence on the performance and this is why in this part of the study just the cases with one splice along the length is considered.

In order to evaluate the effect of the splice's flexural strength on the continuity of gravity columns, a bilinear moment rotation behavior is assigned to the places where the splices are located. As already mentioned and shown in Figure 6.1-1 the flexural strength of the splices is considered to be a percentage of the column's plastic moment capacity. The cases to be studied herein are part of the "levelled" splices and they are the cases IV, VI and X.

6.1.7.1 Levelled Splices: Case IV

Case IV has the splices located in the 3rd story of the building and the relative height where they were placed is 1/3 the column height. Figure 6.1-16 showed that this is the worst-case scenario and the SMF performance does not improves at all. Recalling that splices had no flexural strength, in this section the required flexural strength to provide continuity in the gravity columns is studied. Figure 6.1-32 illustrates the results obtained from the nonlinear static pushover analysis. It can be seen how the performance improves progressively with the splices flexural strength. However, the required flexural strength to provide continuity in this case is equal to 90% the column plastic moment capacity of the column which is considered to be a fully restrained connection.

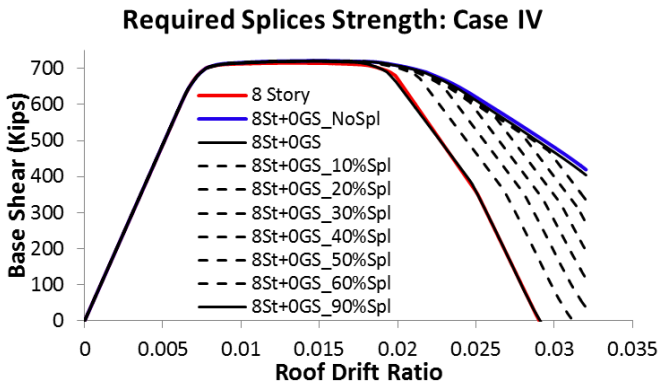

Figure 6.1-32 Splice's Required Flexural Strength: Case IV

6.1.7.2 Levelled Splices: Case VI

Case VI has the splices located in the 3rd story of the building and the relative height where they were placed is 2/3 of the column height. Figure 6.1-16 showed that this is the best-case scenario but the SMF performance is still not as good as having continuous columns. The splice's required flexural strength for this case is shown in Figure 6.1-33. According to the results shown in this figure, the performance of the building with splices is the same as having continuous columns when the splice's flexural strength is approximately equal to 50% the plastic moment of the columns.

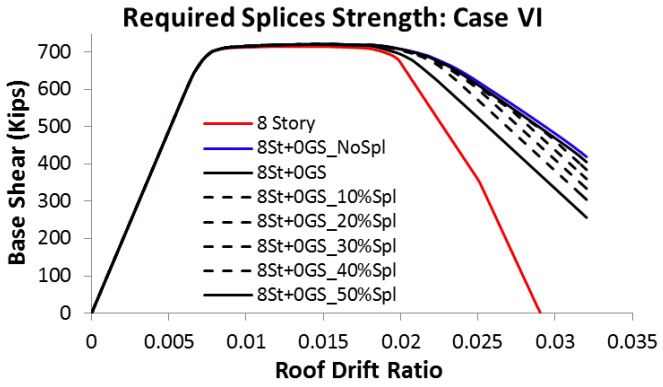

Figure 6.1-33 Splice's Required Flexural Strength: Case IV

6.1.7.3 Levelled Splices: Case X

Case X have the splices located in the 4th story of the building and the relative height where they were placed is 1/3 the column height. Even though the performance of this configuration is not as good as cases XI and XII the difference is minimum because the splices where located in the fourth story. In fact, the performance of the 8-story model with the splices in this configuration is almost the same as having no splices and that is why the required flexural strength to provide almost full effective continuity is only 20% of the column strength (Figure 6.1-34).

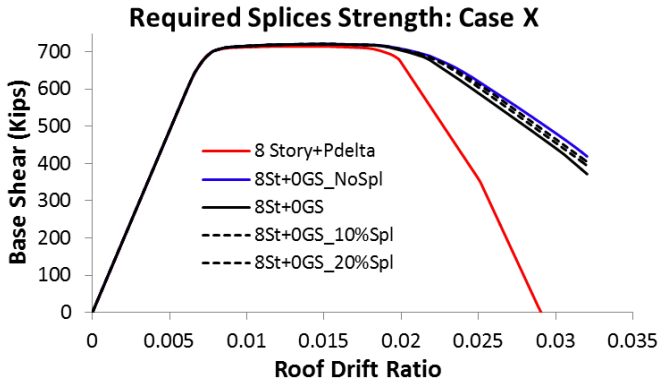

Figure 6.1-34 Splice's Required Flexural Strength: Case X

6.1.7.4 Summary and Conclusions

Using three of the levelled splices cases, the strength required by the splices to provide continuity to the gravity columns was studied herein. A simple bilinear moment rotation behavior was assigned to the splices and their flexural strength was increased until the performance of the building simulates the condition where the gravity columns are fully continuous. From the results obtained, the following conclusions can be made:

- The required splice's flexural strength to provide full effective continuity depends directly on where the splices are located.

- The worst case (IV) requires the splices to be fully restrained in order to provide continuity while case (X) requires a flexural strength of only 20% the plastic moment of columns. Therefore careful selection of splices location prevents the need for more detailed and stronger splice connections. However, this is a conclusion made by performing analyses on just one building. Thus more research is required to establish the best location for the splices.

6.1.8 References

[1] F.X. Flores, F.A. Charney, D. Lopez-Garcia, Influence of the gravity framing system on the collapse performance of special steel moment frames, Journal of Constructional Steel Research, 101 (2014) 351-362.

[2] F.X. Flores, F.A. Charney, D. Lopez-Garcia, The Influence of Gravity Column Continuity on the Seismic Performance of Special Steel Moment Frame Structures, Journal of Constructional Steel Research (To be published), (2015).

[3] NIST, Evaluation of the FEMA P-695 Methodology for Quantification of Building Seismic Performance Factors, National Institute of Standards and Technology, USA, 2010.

6.2 Yielding in Gravity Columns

6.2.1 Introduction

One of the topics of study in this dissertation was the influence of yielding in the gravity columns. The approach taken in Flores et al.[1] was to model the gravity columns using elastic elements and then repeat the same analysis using force-based elements with fiber sections made with a bilinear material. The difference between the results obtained for both analyses was the measure used to establish if yielding in the gravity columns occurred. One of the conclusions of this study was that gravity columns should be modeled with the capability of capturing yielding if the gravity connections are considered to have sufficient flexural strength.

In this supporting study, yielding in the gravity columns is studied more in depth. The first part focuses on the fact that gravity columns do not yield if the gravity connections do not have enough flexural strength to induce yielding. In order to demonstrate this hypothesis, nonlinear static pushover and nonlinear dynamic analyses are performed. The approach used to determine if the gravity columns yield is to model them first with elastic elements, and then with forced-based elements capable of capturing yielding during the analysis. The material assigned to the force based elements is bilinear and the yield strength assigned is equal to 60 ksi. Note the yield strength is the expected yield strength, and strain hardening is included.

The second part of this supporting study investigates the amount of flexural strength required by the gravity connections to induce yielding into the gravity columns. In order to establish if the gravity columns yielded, nonlinear static pushover analyses are performed.

The importance of establishing if the gravity columns are yielding is vital because one of the conditions required to apply the lumped column approach [2] is that the gravity columns

remain elastic. Moreover, the computational time required to analyze structures with the gravity columns behaving elastically is considerably shorter than the case where gravity columns are modeled with force- based elements.

6.2.2 Gravity Columns Remain Elastic

This section of the dissertation investigates if the gravity columns yield when the structure is subjected to large deformations. The building to be used is the 8-story model, and the columns of the gravity system have W18 sections (Chapter 3, Figure 3-1). The gravity connections are considered to be Partially Restrained (PR) connections as already described in [1]. Two cases are studied, one with gravity connections with zero flexural strength capacity and another with PR connections with strength equal to 30% the plastic moment capacity of the beams.

The analyses to be performed are: nonlinear static pushover and nonlinear dynamic analyses. The nonlinear dynamic analysis is executed using 8 out of the 44 Far Field Ground motions from the FEMA P-695 record set. The list of ground motions to be used is shown in Table 6.2-1.

Table 6.2-1 Ground Motions used to Perform Nonlinear Dynamic Analysis

	Component Name	Filename	npts	dt	PGA(g)
1	Manjil-Abbar	ABBAR--L.AT2	2676	0.02	0.406504
2	Duzce-Bolu	BOL000.AT2	5590	0.01	0.458376
3	Superstition Hills-Poe	B-POE270.AT2	2230	0.01	0.522201
4	Loma Prieta-Capitola	CAP090.AT2	7991	0.005	0.483189
5	Hector-Hector	HEC090.AT2	4531	0.01	0.367078
6	Northridge-CC	LOS270.AT2	1999	0.01	0.400062
7	Kobe-Nishi Akashi	NIS000.AT2	4096	0.01	0.524618
8	San Fernando-LA	PEL090.AT2	2800	0.01	0.365776

Incremental dynamic analysis then is implemented with each ground motion until the structure achieves large displacements. Then the results between the elastic and inelastic analysis are compared to establish if yielding was induced in the gravity columns.

6.2.3 Nonlinear Static Pushover Analysis

As already mentioned, two different cases are analyzed in this section: the gravity system with no gravity connection's flexural strength and the gravity system with PR connections strength equal to 30% the plastic moment capacity of the beams. The results of the nonlinear static pushover analyses for both cases are shown in Figure 6.2-1.

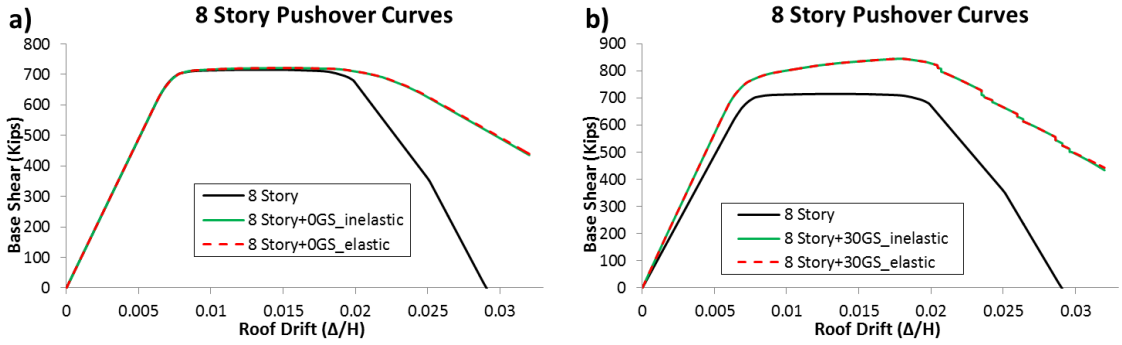

Figure 6.2-1 Pushover Curves a) PR connections with no strength (0GS)

b) PR connections with 30%M_p (30GS)

From the pushover curves shown in Figure 6.2-1 (a) and (b) the hypothesis that gravity columns do not yield has been proved. In addition the fibers of the sections were checked to confirm that the gravity columns did not yield. Thus it is concluded that the gravity columns do not yield even when the structure is subjected to large displacements. The requirement however, is that gravity connections do not have a significant amount of flexural strength (the strength must be less than or equal than 30%M_p).

6.2.4 Nonlinear Dynamic Analysis

The nonlinear dynamic analysis was executed using 8 of the 44 ground motions that form part of the Far Field ground motions set in the FEMA P695. Each ground motion was scaled following the FEMA P-695 procedure and then scaled again by performing an incremental dynamic analysis to subject the building to different intensity levels. FEMA P-695 scales the ground motions to the Maximum Considered Earthquake (MCE) spectrum which in turn represents a hazard level of 2% in 50 years. The spectral acceleration (S_a) for the 8-story model at MCE level is equal to 0.55g. However, the structure is subjected to larger hazard levels in order to check if the gravity columns yield. The scale factors used to analyze the buildings are 1.0 (S_a=0.55g), 1.5 (S_a=0.825g) and 1.8 (S_a=0.99g). In addition to the IDA scale factor 1.0 which represents the MCE level, the other two scale factors were chosen arbitrarily. However, the 1.8 scale factor is close to the factor that causes the median collapse of the structure. The results for the building with gravity connection with no strength, 20%, 25% and 30% the plastic moment of the beams are shown in Figure 6.2-2 (a), (b) and (c).

Gravity Connections with No Strength (8Story_0GS)

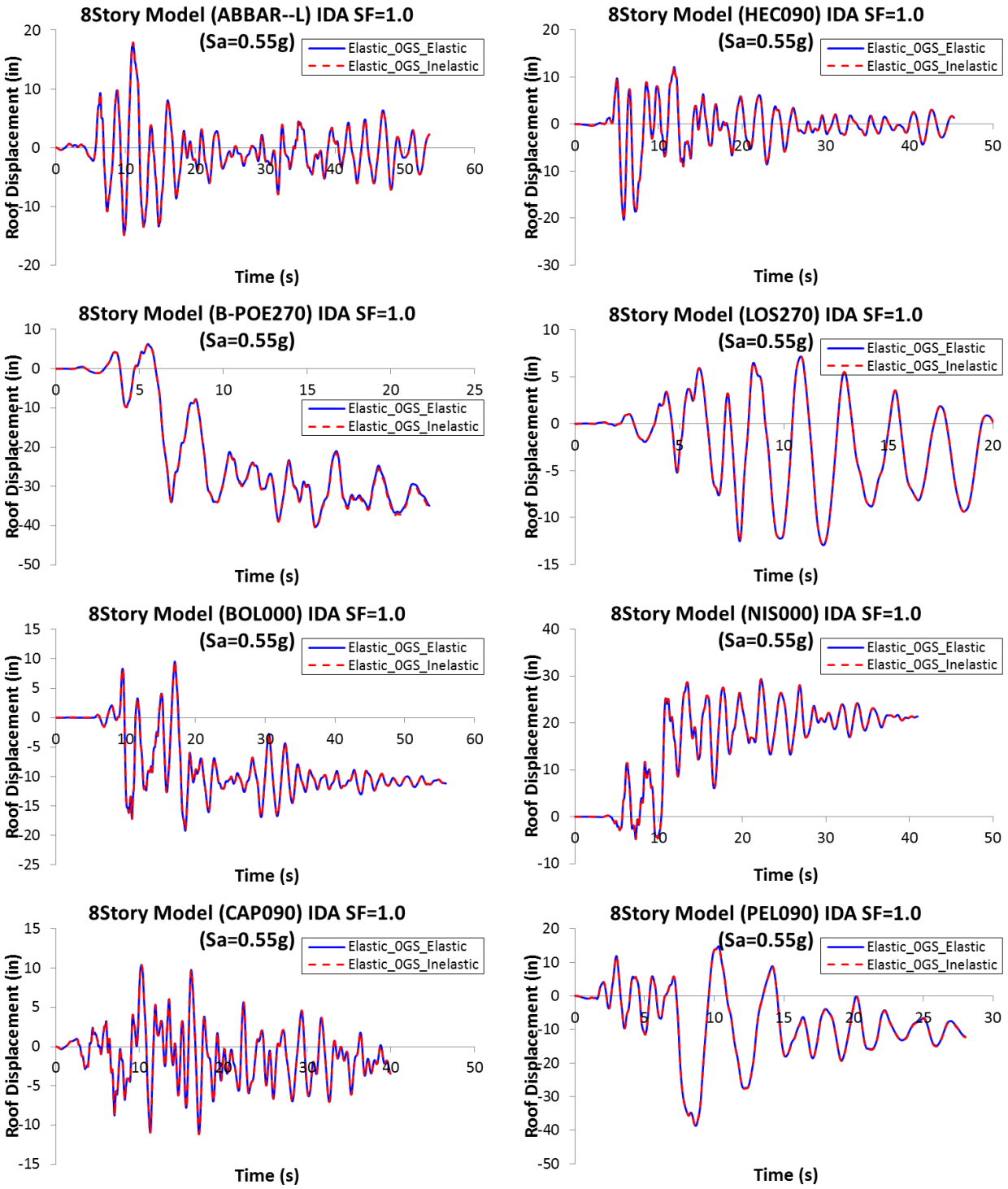

Figure 6.2-2 Nonlinear Dynamic Analyses 8Story_0GS a) Scale Factor =1 (MCE Level, S_a=0.55g)

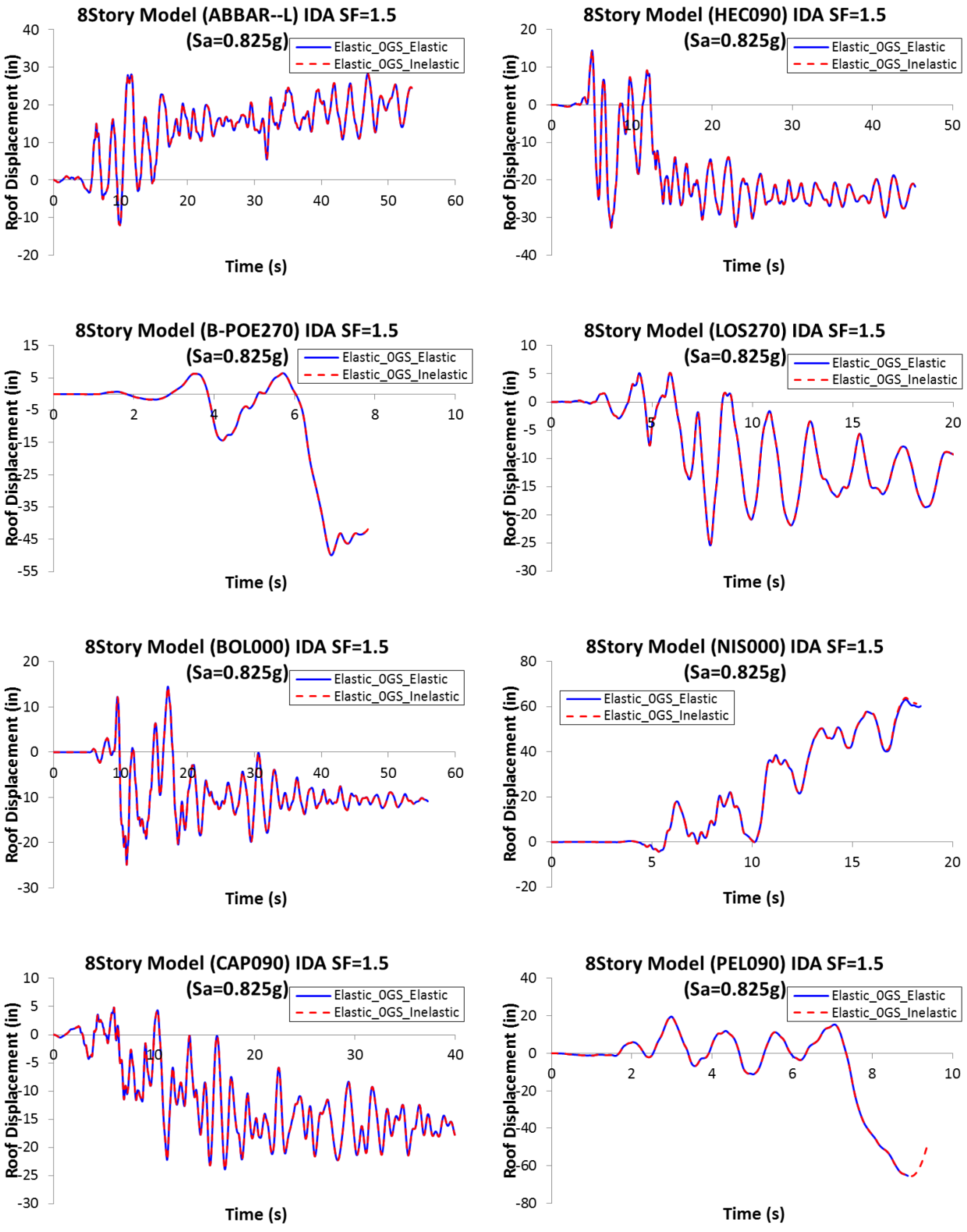

Figure 6.2-2 Nonlinear Dynamic Analyses 8Story_0GS b) Scale Factor =1.5 (S_a=0.825g)

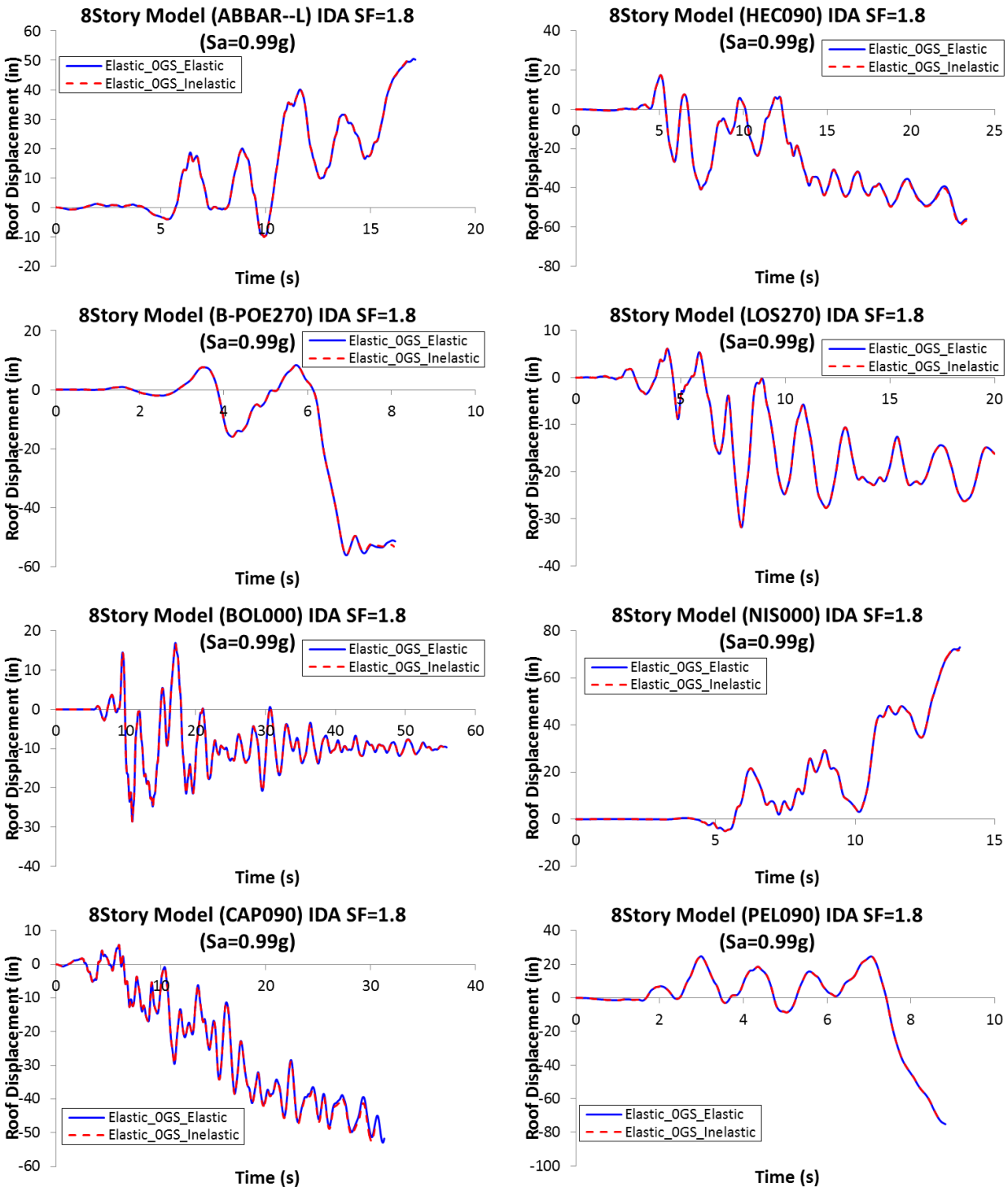

Figure 6.2-2 Nonlinear Dynamic Analyses 8Story_0GS c) Scale Factor =1.5 (S_a=0.99g)

Figure 6.2-2 (a) (b) and (c) illustrate the results obtained for the 8-Story model with zero strength gravity connections and the gravity columns behaving elastically and inelastically. It can be seen that for all the ground motions and for all the scale factors used, the results between the model with elastic and inelastic columns are the same. The only ground motion that shows a slight difference at very large displacement is "B-POE270". Because of this difference, additional results for this ground motion are shown in Figure 6.2-3. Floor accelerations in the first story in addition to the drift in the first and second story are presented in the figure. According to FEMA 350 [3], it is considered that a SMF collapses when an interstory drift is equal or larger than 10% is reached. Thus from Figure 6.2-3, it can be seen that the building is collapsing at 6.7 seconds. In order to show more detail of the acceleration history at 6.7 seconds a zoom view is provided. It can be seen then that after the 6.7 seconds there are some differences between the results in accelerations and drifts obtained using elastic and inelastic columns. Therefore it can be said that these gravity columns are not yielding prior to "collapse" even though the buildings have been subjected to large earthquakes and have large deformations.

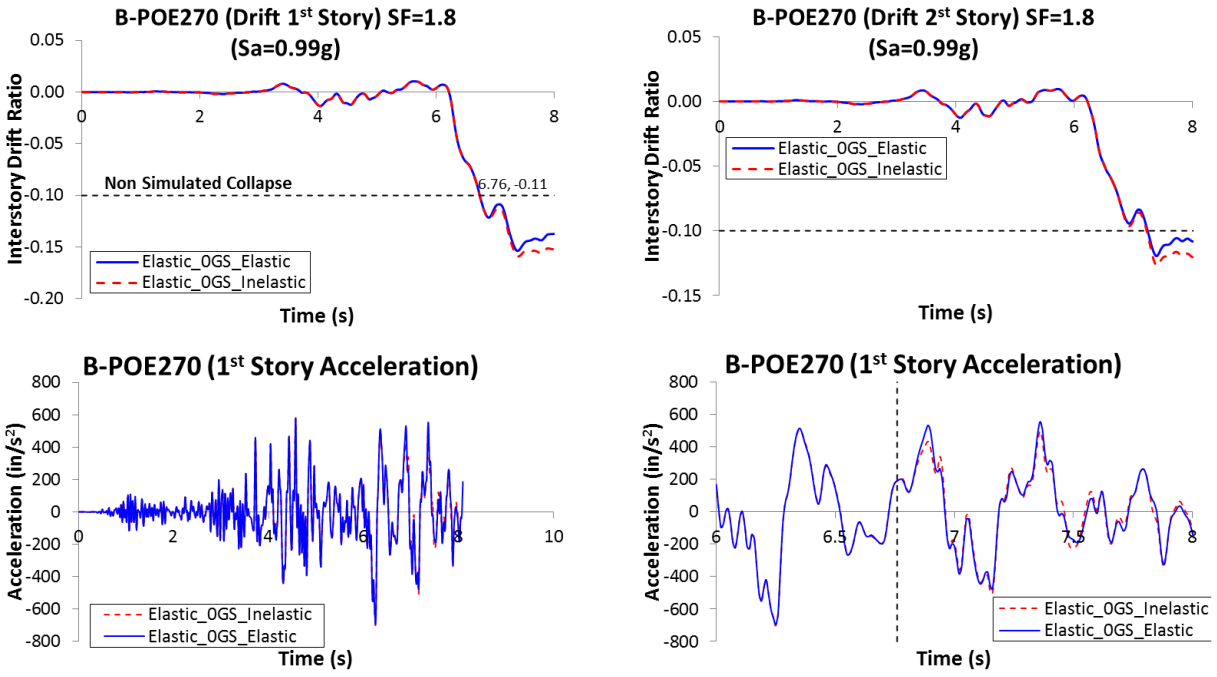

Figure 6.2-3 B-POE270 Results

.

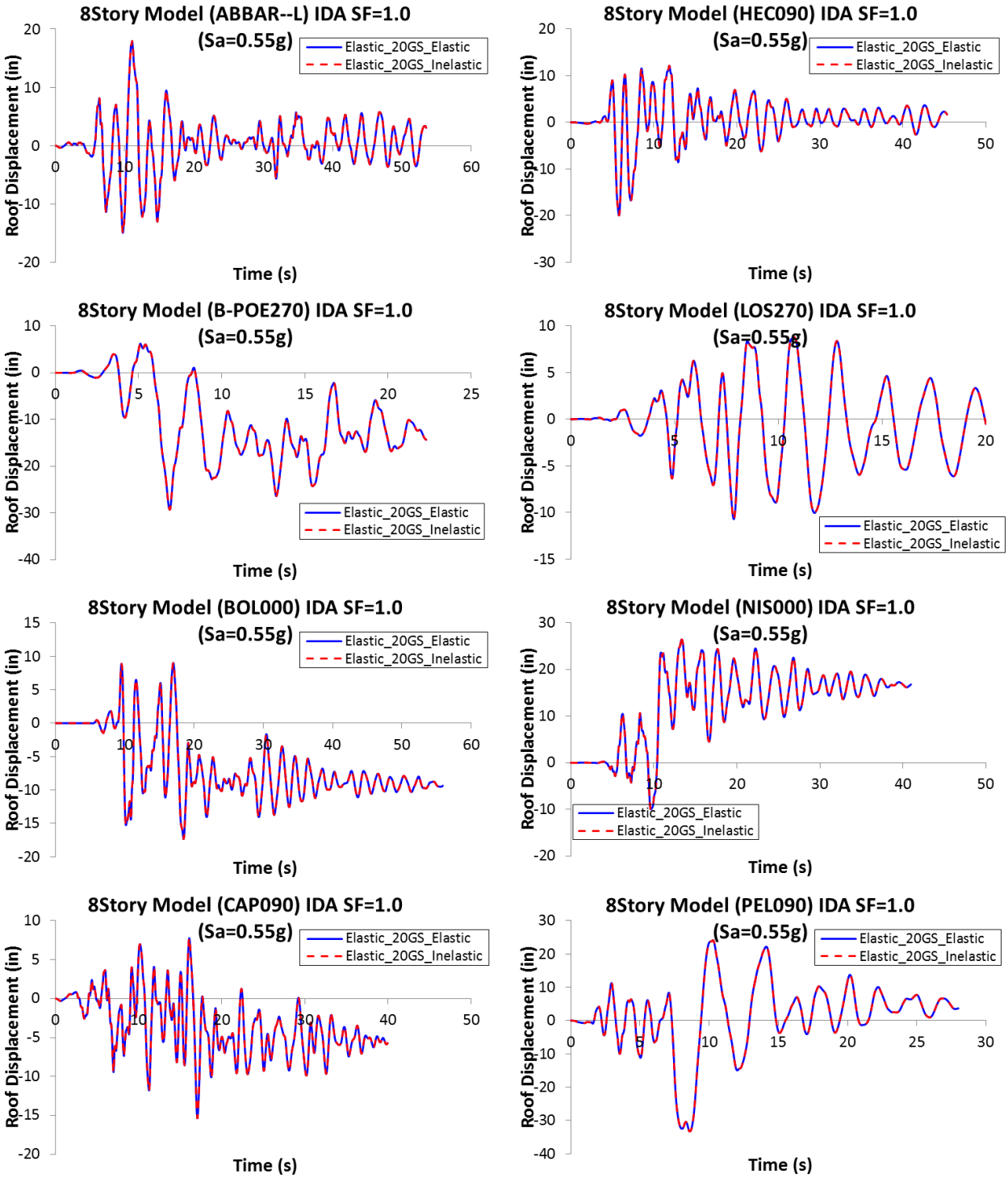

Figure 6.2-4 Nonlinear Dynamic Analyses 8Story_20GS a) Scale Factor =1 (MCE Level, S_a=0.55g)

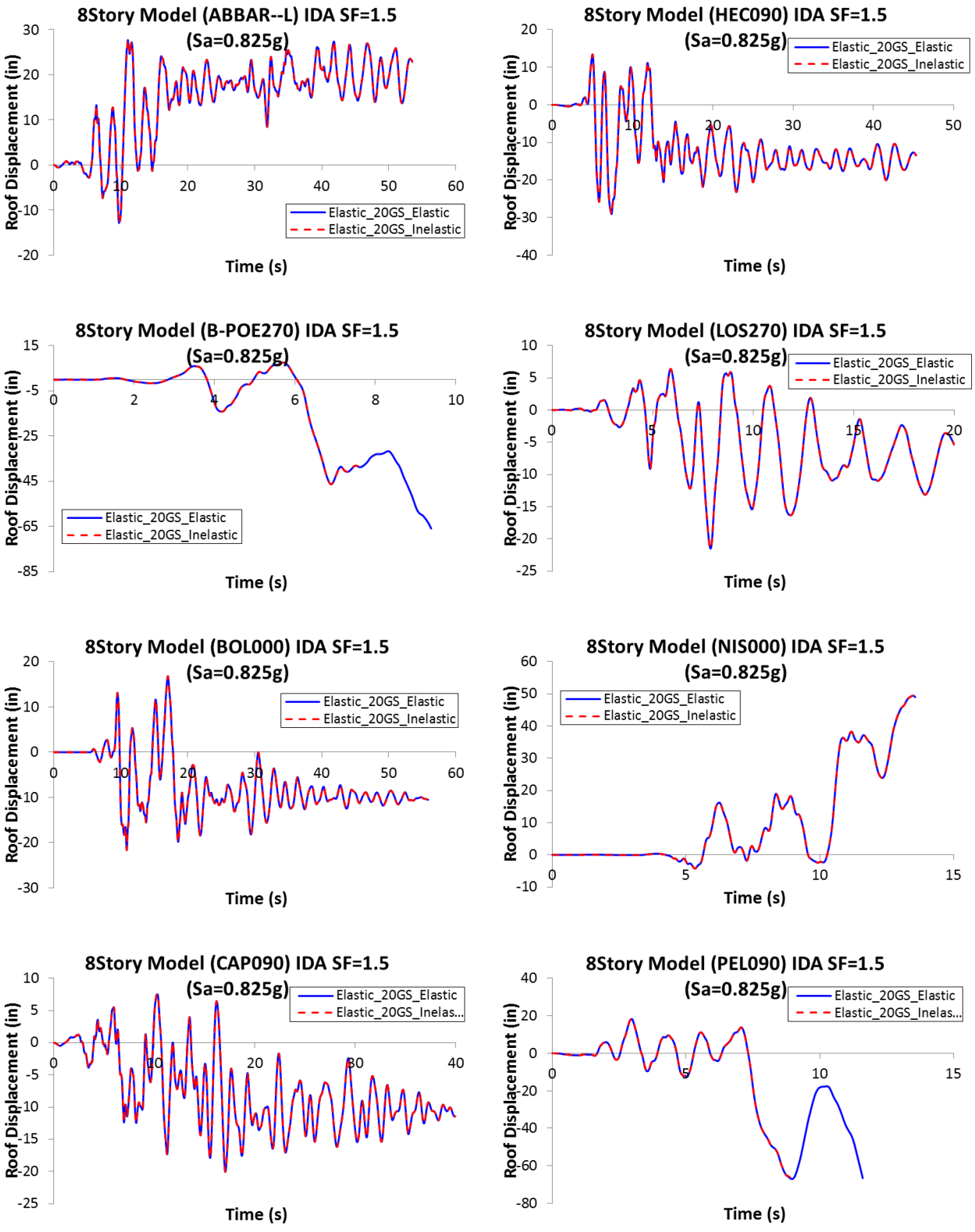

Figure 6.2-4 Nonlinear Dynamic Analyses 8Story_20GS b) Scale Factor =1.5 (S_a=0.825g)

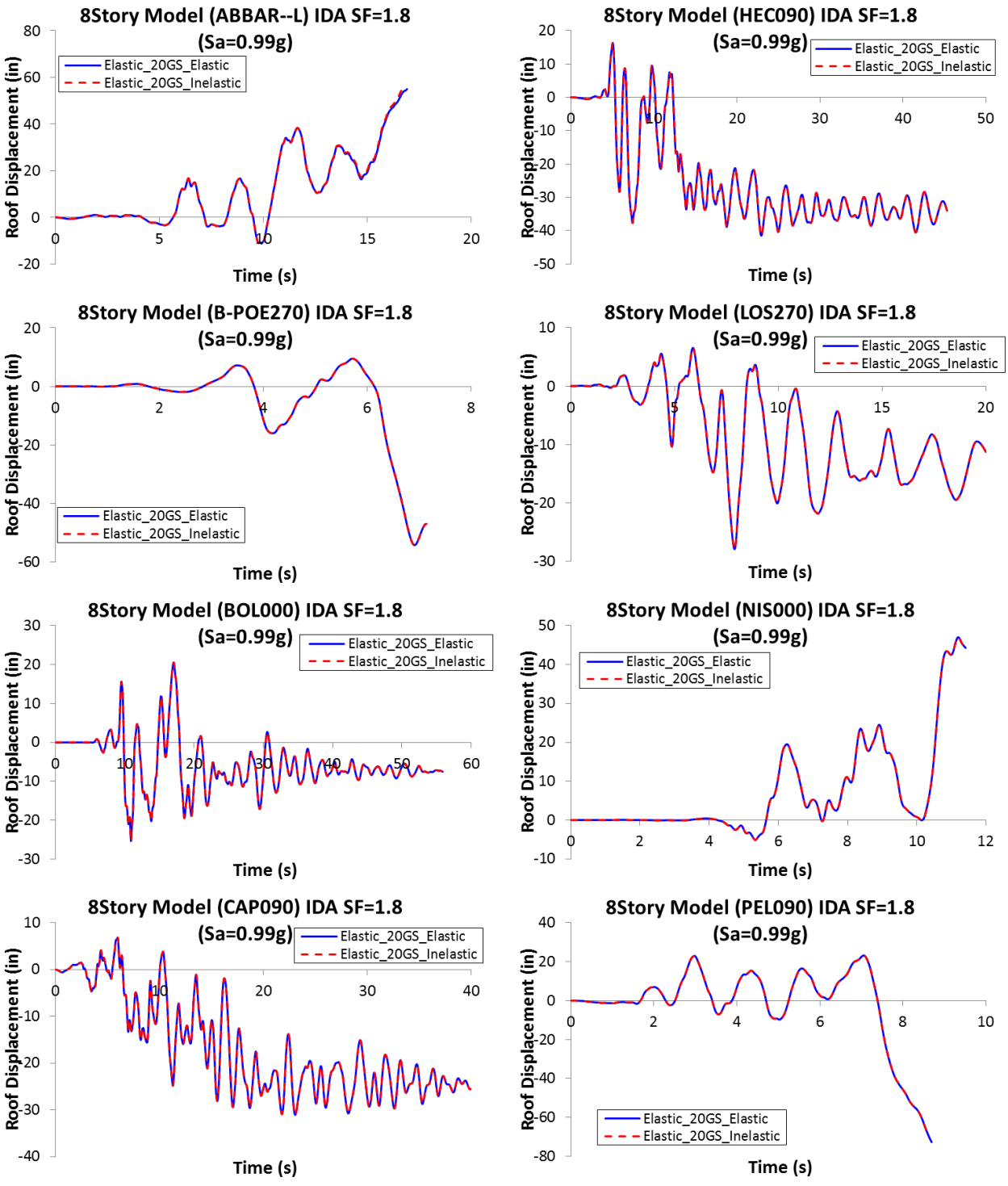

Figure 6.2-4 Nonlinear Dynamic Analyses 8Story_20GS c) Scale Factor =1.8 (S_a= 0.99g)

Figure 6.2-4 (a) (b) and (c) illustrate the results obtained for the 8-Story model with gravity connections with strength equal to 20% the plastic moment of the beams. These results show again that gravity columns are not yielding because the displacement time history analyses are the same for both models. However, there are a few ground motions at different scale factors that show some discrepancies between the results with elastic and inelastic gravity columns. These results are further analyzed by plotting the interstory drift in the first and second story (Figure 6.2-5). The first ground motion to check is "PEL090" at a scale factor of 1.5 which in turn has a spectral acceleration of 0.825g. This ground motion is causing the collapse of the structure at 8.33 seconds and after this point the results are considered not valid and all the differences appear after this point. This situation repeats for the ground motion "ABBAR--L" scaled at 1.8 (S_a=0.99g). After analyzing more in depth these results it can be concluded that the gravity columns are not yielding and if they are the structure has deformed beyond the point that is considered as collapse.

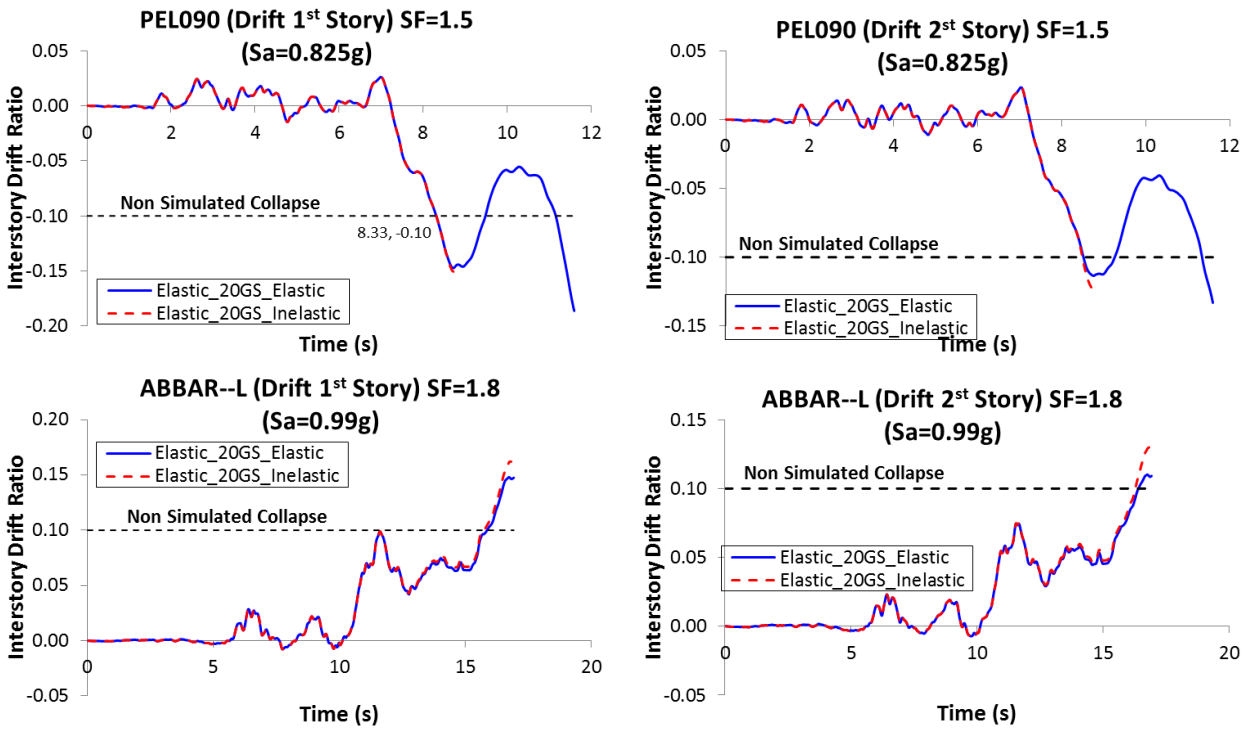

Figure 6.2-5 InterStory Drift: PEL090 and ABBAR—L

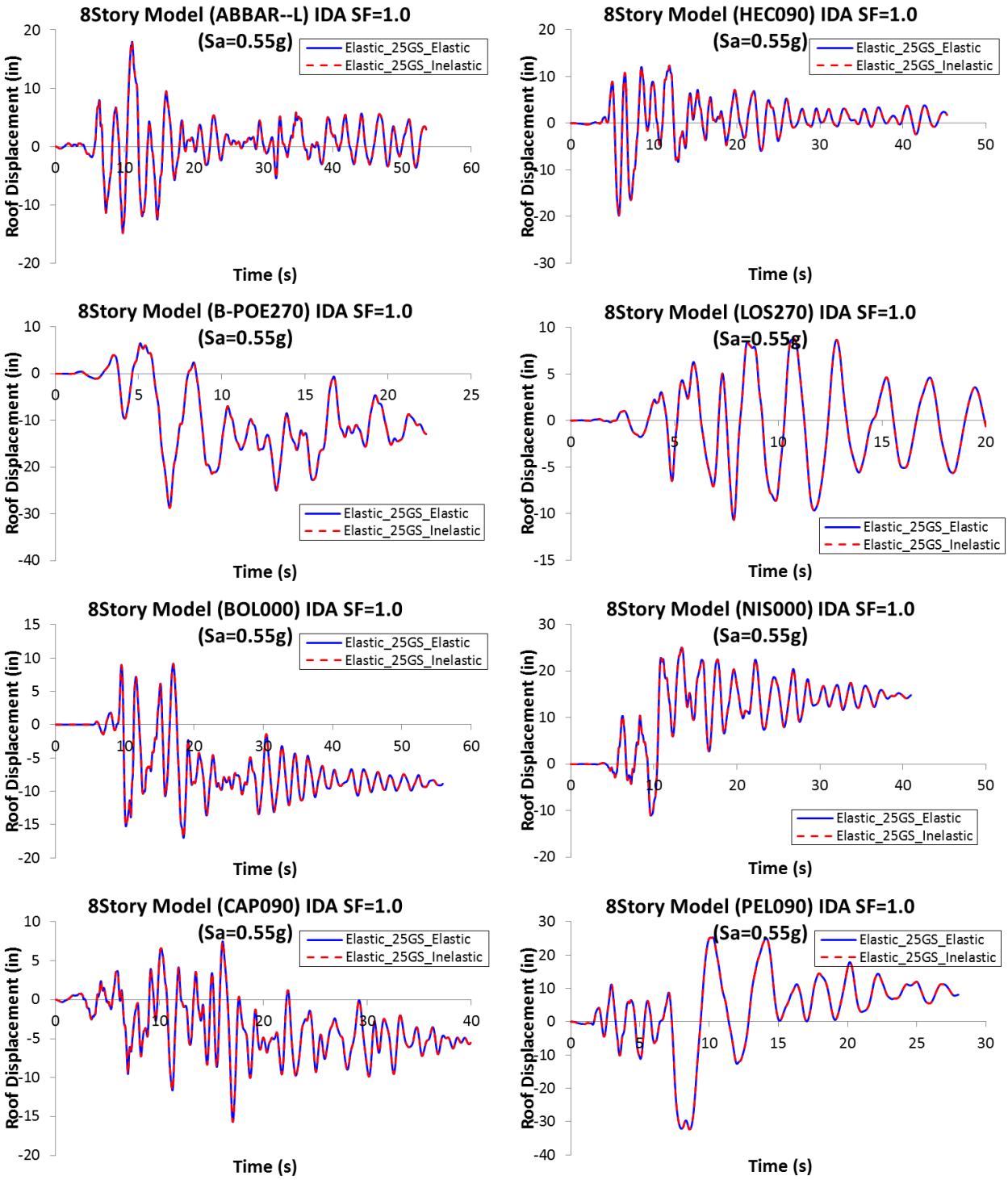

Figure 6.2-6 Nonlinear Dynamic Analyses 8Story_25GS a) Scale Factor =1.0 (MCE Level S_a=0.55g)

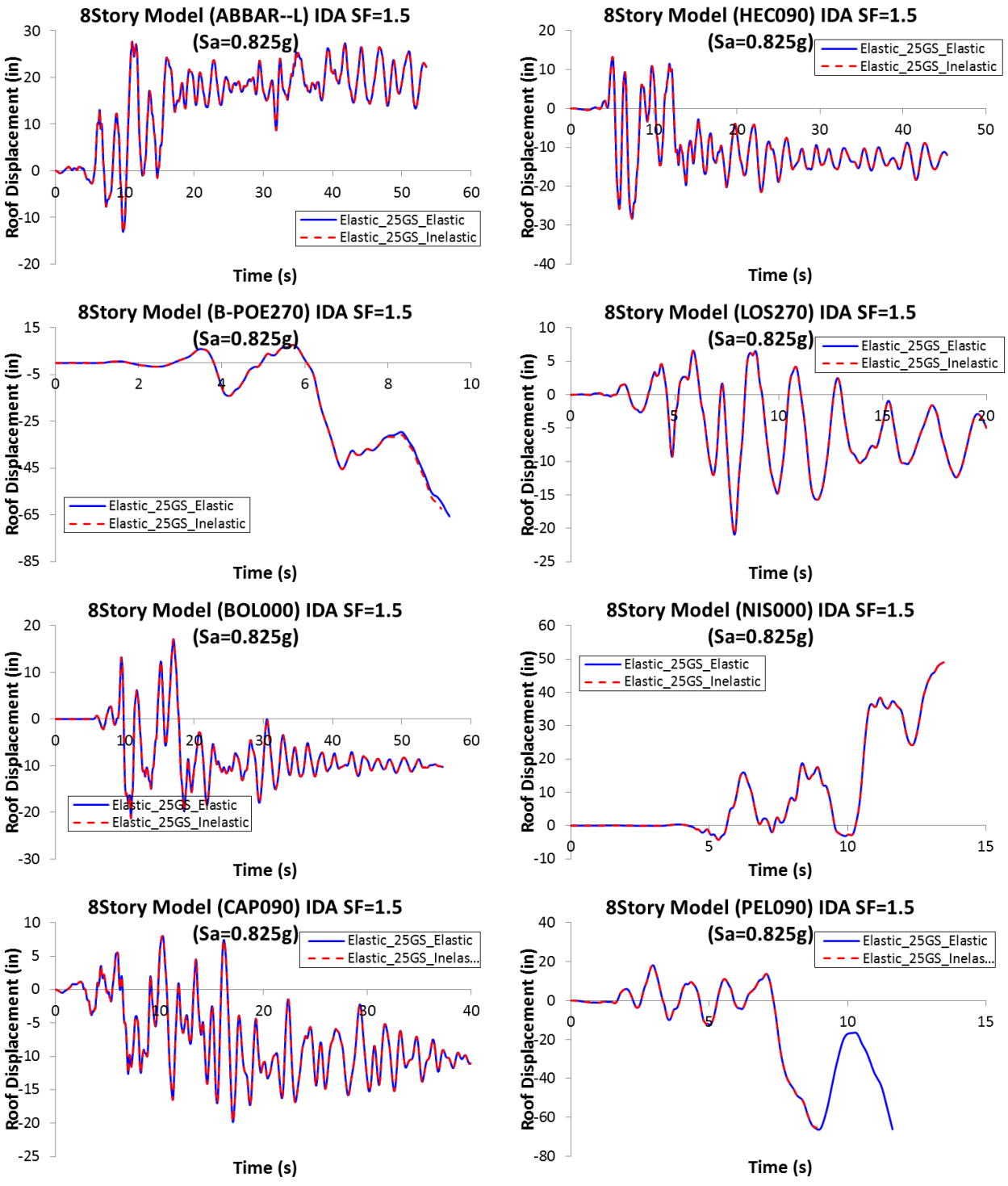

Figure 6.2-6 Nonlinear Dynamic Analyses 8Story_25GS b) Scale Factor =1.5 (S_a=0.825g)

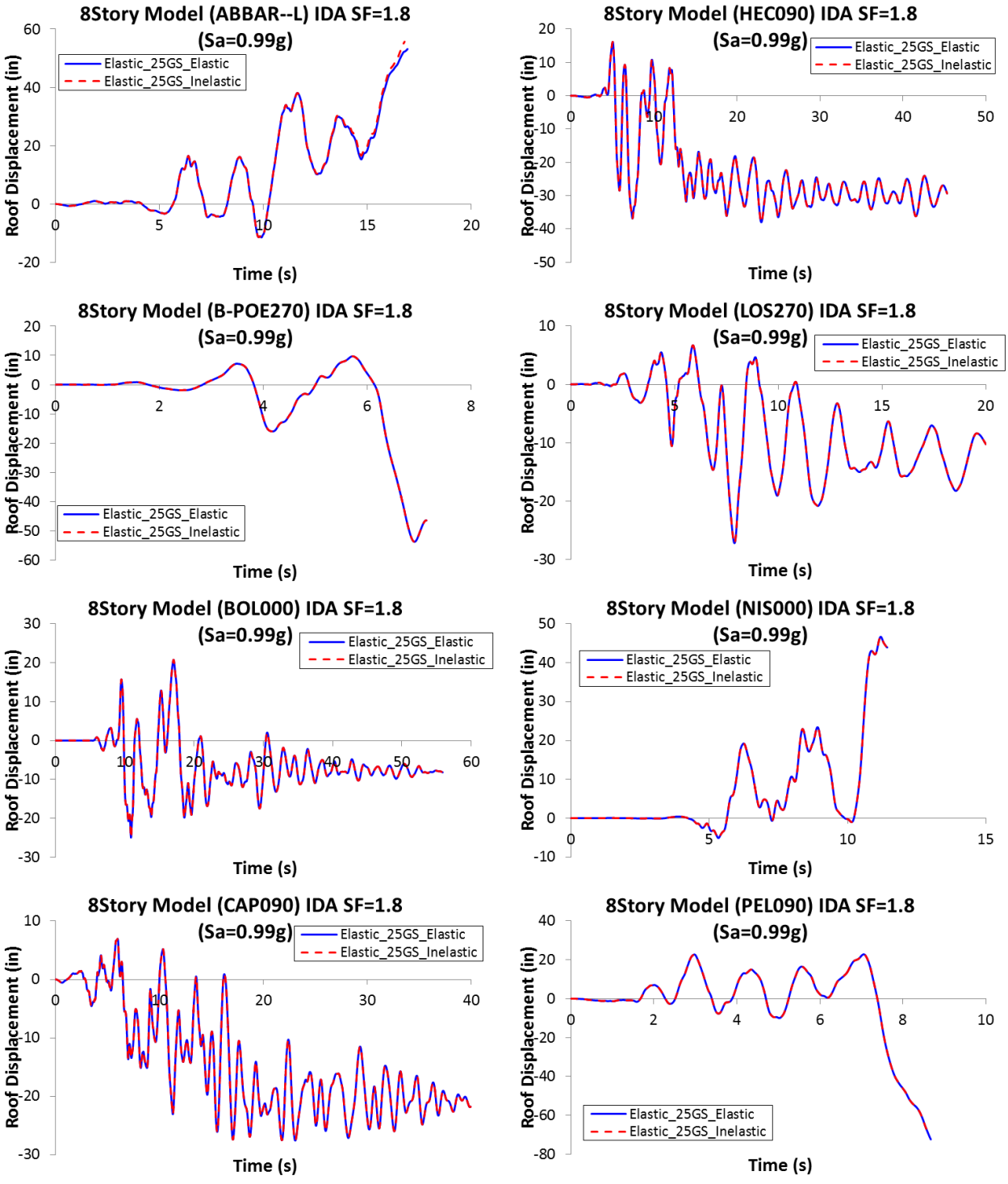

Figure 6.2-6 Nonlinear Dynamic Analyses 8Story_25GS c) Scale Factor=1.8 (S_a=0.99g)

Figure 6.2-6 displays the same trends already seen for buildings with weaker gravity connections. The same ground motions that showed discrepancy between the elastic and inelastic gravity columns in previous analyses are showing differences in this building too. Therefore more results are shown to prove that gravity columns are not yielding and if they are yielding it is because the structure already collapsed. Figure 6.2-7 shows the interstory drift for one of the ground motions that shows a slight difference between both results. However, it can be seen from this figure that the difference arises after the structure collapses. Therefore, the gravity columns of the structure with these gravity connections (25%M_p) are not yielding.

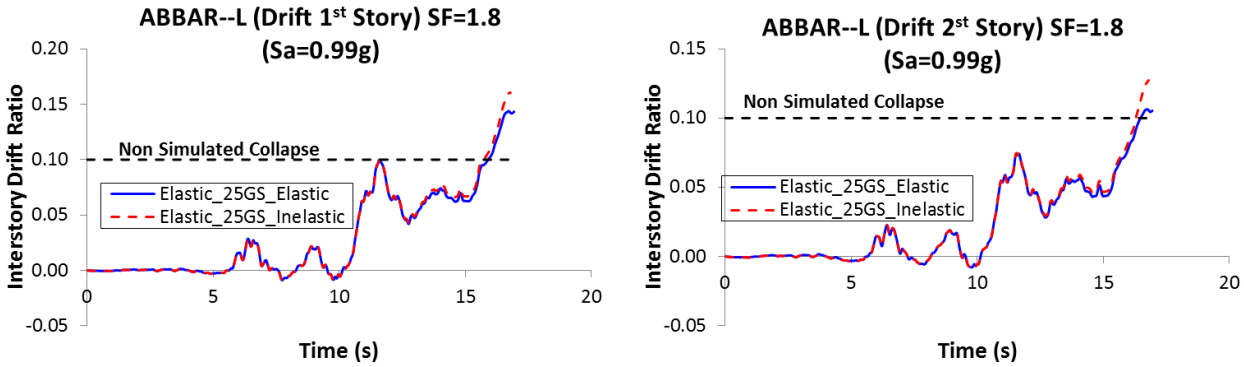

Figure 6.2-7 InterStory Drift: ABBAR--L

Gravity Connections with 30%M_{pbeam} (8Story_30GS)

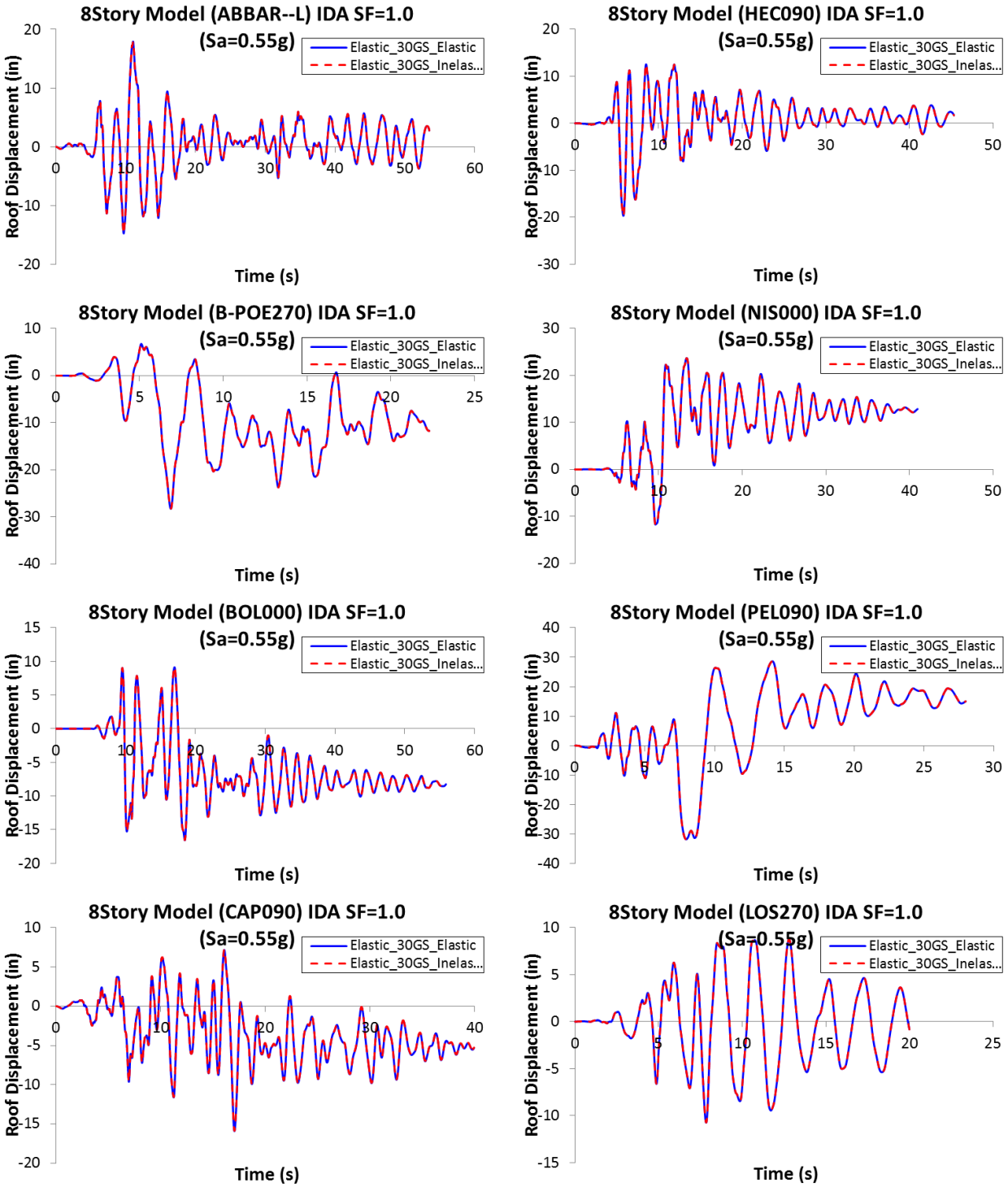

Figure 6.2-8 Nonlinear Dynamic Analyses 8Story_30 GS a) Scale Factor =1.0 (MCE Level S_a=0.55g)

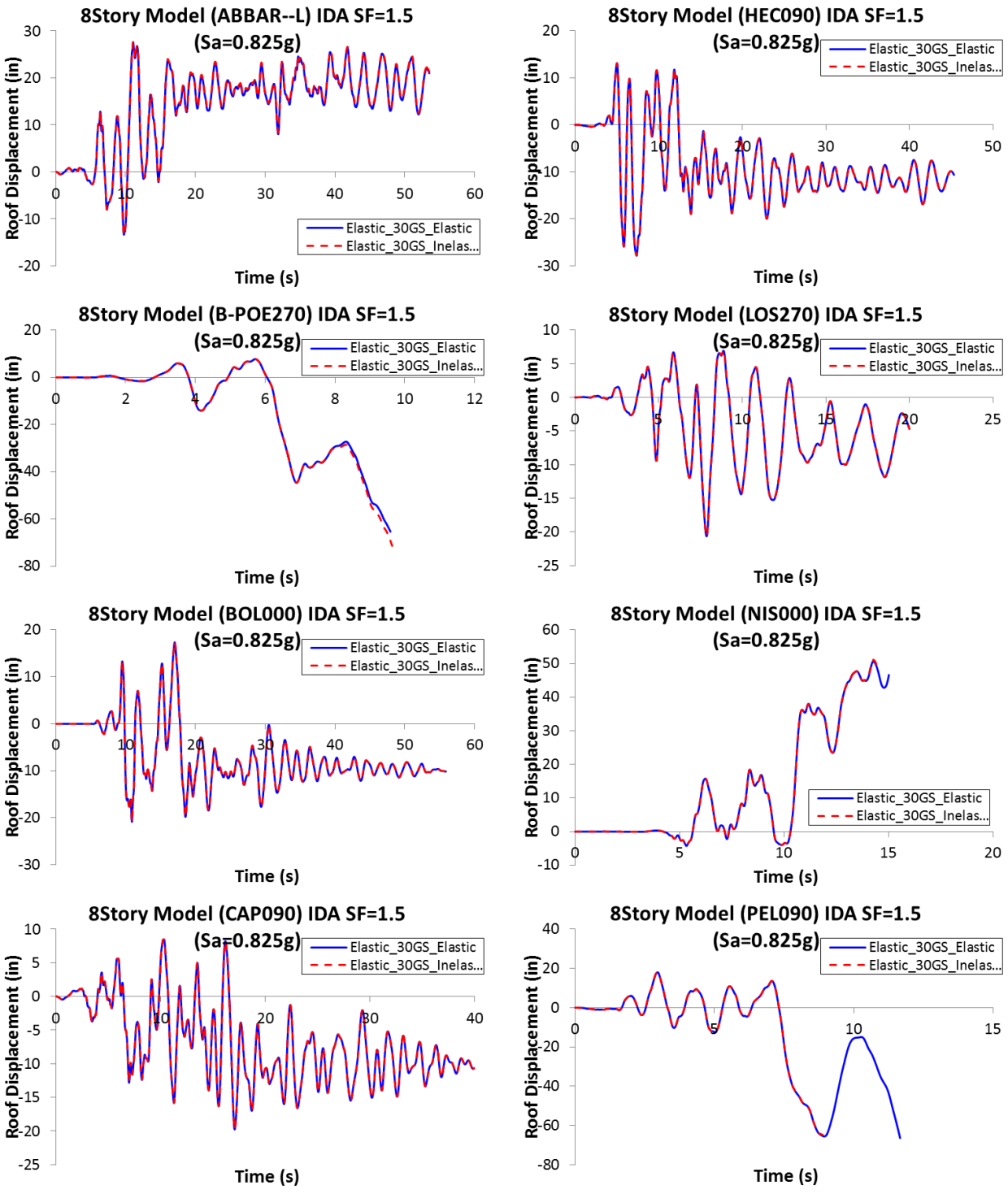

Figure 6.2-8 Nonlinear Dynamic Analyses 8Story_30 GS a) Scale Factor =1.5 (S_a=0.825g)

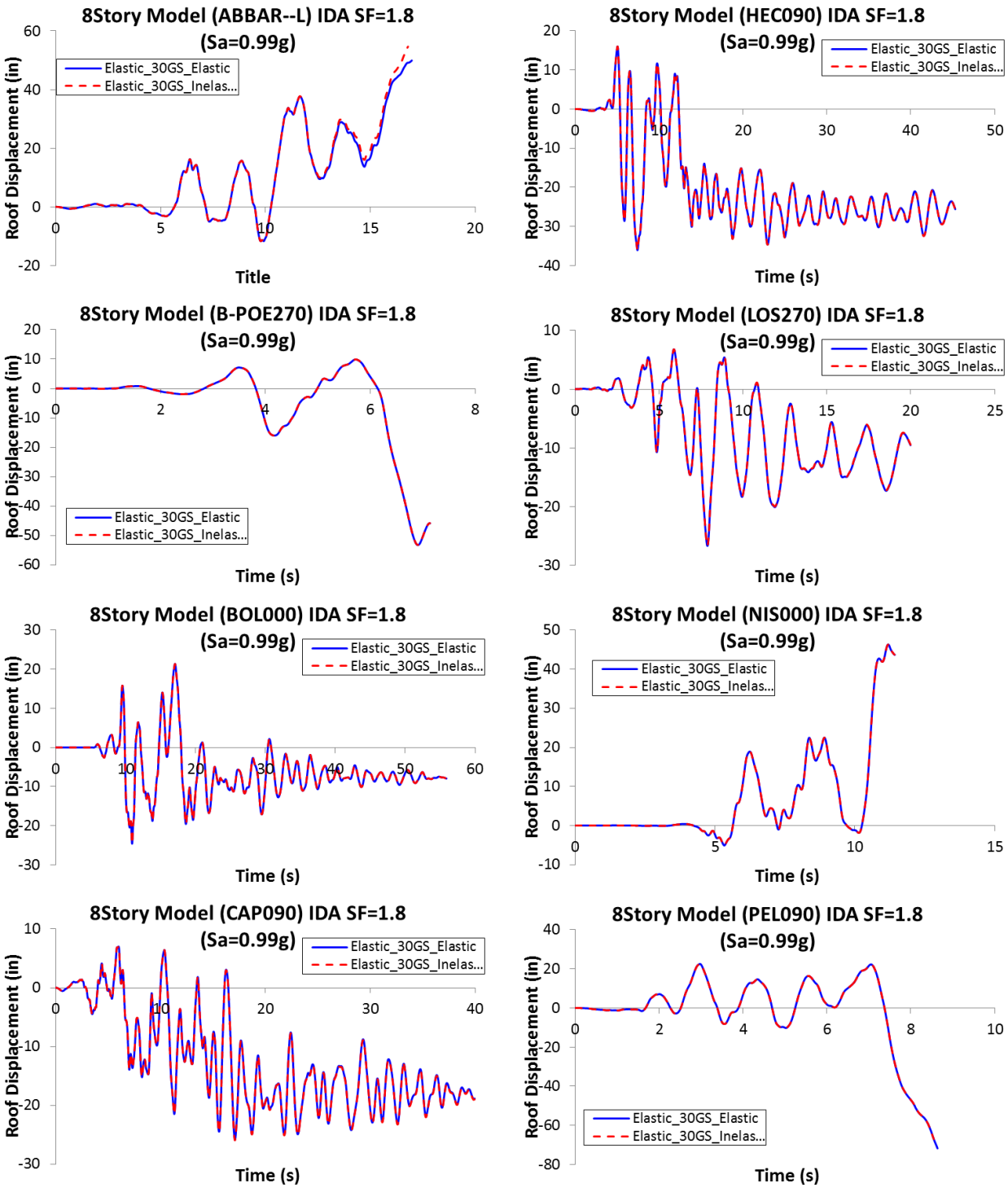

Figure 6.2-8 Nonlinear Dynamic Analysis 8Story_30 GS c) Scale Factor =1.8 (S_a=0.99g)

Figure 6.2-8 illustrates the results obtained for the 8-Story model with PR connections strength equal to 30% the plastic moment of the beams (30%M_p) and columns behaving elastically and inelastically. Even though these analyses included the gravity connections flexural strength there is no difference between the results obtained with the elastic and inelastic gravity columns unless the structure incurs an interstory drift larger than 10% (Figure 6.2-9). As a result, it can be concluded that the gravity columns are not yielding when the gravity connections have strength lower than or equal than 30% the plastic moment capacity of the beams regardless the ground motion intensity level.

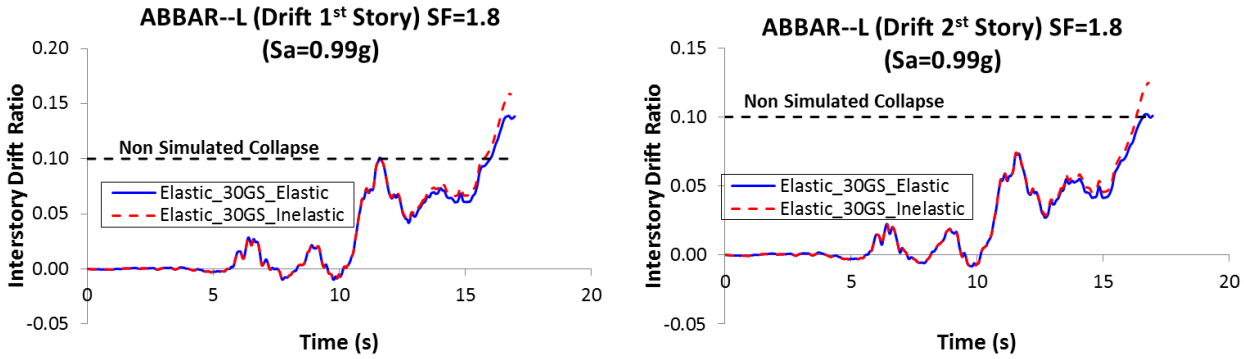

Figure 6.2-9 InterStory Drift: ABBAR--L

6.2.5 Summary and Conclusions

This section was devoted to prove that gravity columns can remain elastic even when the structure is subjected to large ground motion intensities. It is believed worthwhile to list again the gravity system characteristics of the models used in the analysis: gravity columns base connections considered to be pinned, W18 sections were used for the gravity columns, the assigned flexural strength of PR connections is a percentage of the beams plastic moment, and finally the gravity columns are continuous all over the height. After performing all the analyses, and for the conditions just mentioned, it can be concluded that the gravity columns are not

yielding even when the structure undergoes large displacements. This is an important conclusion because it is the basis of the approach used in the second paper of this dissertation where the gravity columns are lumped into one elastic element. However, it cannot be generalized for all systems and more research is required to establish a final conclusion.

6.2.6 Gravity Columns at Yielding

This section is dedicated to investigate the required gravity connections flexural strength to induce yielding in the gravity columns. For this purpose, the flexural strength assigned to the gravity connections is varied and it is considered to be a percentage of the plastic moment capacity of the beams. The procedure to establish if the gravity columns are yielding is the same as the one already used: the difference between the results obtained with gravity columns behaving elastically and inelastically will define if yielding occurred. The flexural strength assigned to the gravity connections is equal to 35%, 40%, 50% and 70% the plastic moment capacity of the beams. In order to establish the effect of the flexural strength, nonlinear static pushover analysis is performed for each case.

6.2.6.1 Nonlinear Static Pushover Analysis

A gravity system with stronger connections could induce yielding into the gravity columns. For this reason, the following study where the same building was tested using PR connections with different flexural strengths and the gravity columns modeled using elastic and inelastic elements is carried out. Nonlinear static pushover analysis was used to analyze the building. Figure 6.2-10 displays the results obtained for gravity connections with flexural strength equal to 35%, 40%, 50% and 70% the plastic moment capacity of the beam. This figure includes also the pushover curve of the SMF without the gravity system. It can be seen that gravity columns are showing signs of yielding when the PR connections have flexural strength

equal to 35%M_p. However, in this case the difference between the elastic and inelastic cases is minimum and it seems that yielding is not as significant as the cases with stronger PR connections.

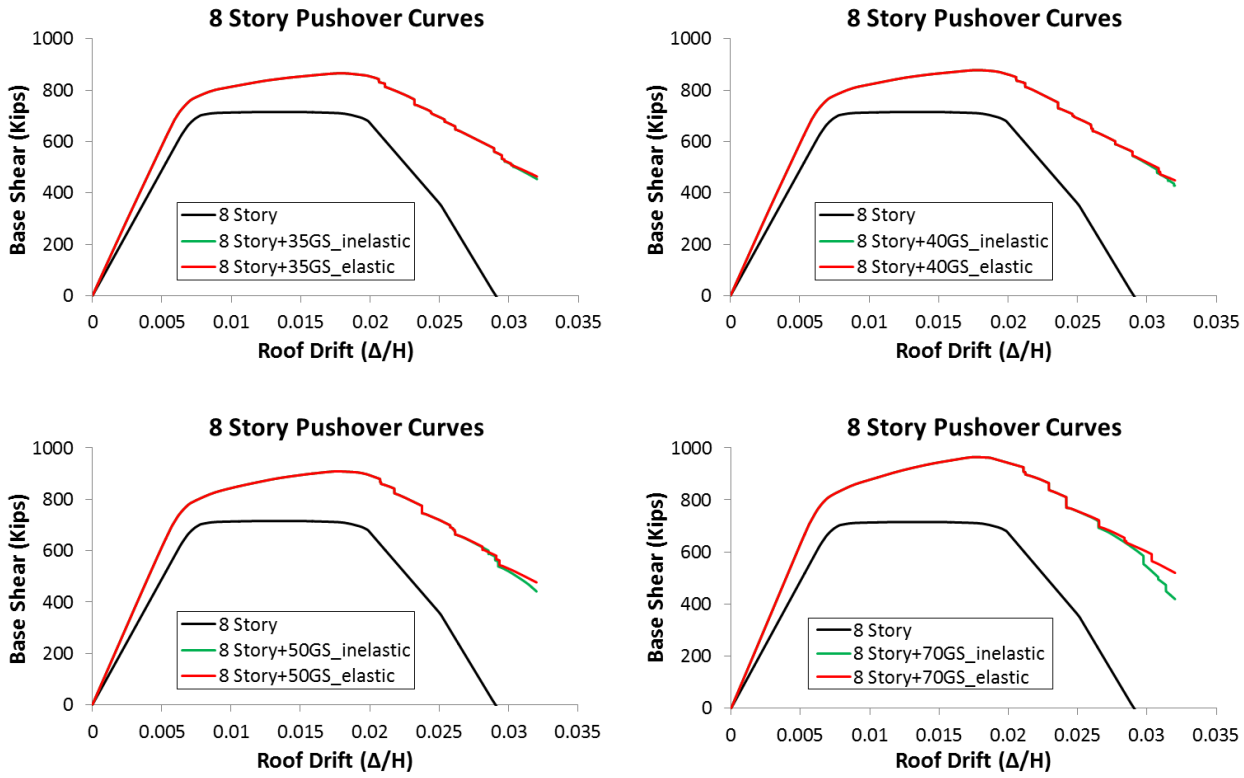

Figure 6.2-10 Pushover Curves for Different PR Connections Strengths

Even though the difference in the pushover curves demonstrates signs of yielding in the gravity columns, the specific location where the yielding occurred was investigated. For this matter, it was noted that the modelling approach is very important when specific results like checking if the fibers are yielding is required. The gravity columns were discretized in 3 elements along the height. Thus each element has a length of 52 in. On the other hand the way that sections were divided into fibers is shown in Figure 6.2-11.

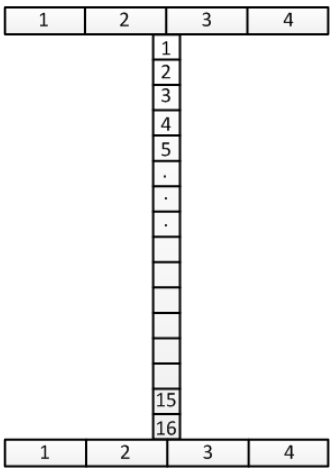

Figure 6.2-11. Gravity Column Section Divided in Fibers

After performing several analyses, it was found that the number of fibers used in the model is correct and the results do not change when the element and section is discretized more. However, when the stresses were obtained from the fibers, it was found that they did not exceed the yielding stress. The stresses reported by OpenSees are an average of the stresses computed along the volume of the fiber. Because, relatively long elements and small number of fibers were used, the stresses reported were not a good representation of what happened. Therefore the elements with higher stresses of the model with gravity connections strength of 50%M_p were divided in 8 elements of 6.5 in length each. The flange of the section was divided in 8 elements along their width and 20 elements along their thickness. Running all the analyses with this amount of detail is computationally expensive and it is not necessary because the results are the same. However, if yielding in the fibers is required to be checked, this procedure is necessary and it was found that the elements that surpass the yielding point are the ones showed in Figure 6.2-12.

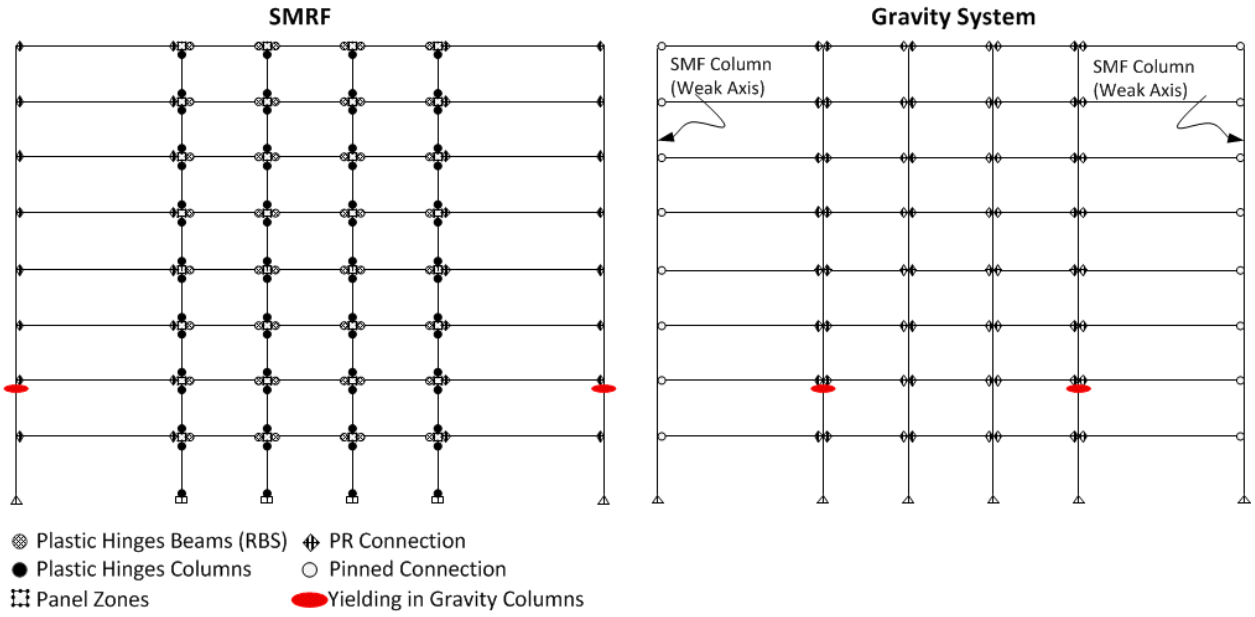

Figure 6.2-12. Yielding in Gravity Columns (8Story_50GS).

Once the elements and the sections were more discretized, OpenSees reported yielding in the fibers. Figure 6.2-12 shows the points were yielding occurred. It can be seen that this is happening where beams have longer spans, thus the beam sections are bigger and the gravity connections are stronger. This analysis and these results prove that the difference between the pushover curves with elastic and inelastic elements represent yielding in the gravity columns.

6.2.7 Conclusions

The objective of this supporting study was to validate the assumption that gravity columns remain elastic even when the structure is subjected to large intensity earthquakes. Moreover the required flexural strength in the gravity connections to induce yielding in the gravity columns is investigated.

In the first part of the study, nonlinear static pushover and nonlinear dynamic analyses were performed to buildings with gravity connections that have no flexural strength and that

have a flexural strength equal to 20%, 25% and 30%M_p. Yielding occurrence was measured by the difference between the results obtained when the gravity columns were modeled using elastic and inelastic elements. The conclusion from this part of the analysis is that gravity columns for the building in consideration are not yielding even when the connections have flexural strength equal to 30% the plastic moment capacity of the beam. However, some of the ground motions at very large intensity levels induced yielding into the gravity columns but the buildings had collapsed already by the time that yielding occurred. The collapse of the building was considered to occur when an interstory drift of 10% was reached.

The second part of the study focused on the required flexural strength on the connections to cause yielding in the gravity columns. Nonlinear static pushover analysis was performed to different buildings varying the flexural strength in the connections. The results obtained show that the gravity columns display very slight signs of yielding at the end of the pushover curves when the gravity connections have 35%. On the other hand yielding is definitely induced to the gravity columns when the gravity connections are stronger such as the case when the flexural strength is equal to 70%.

6.2.8 References

[1] F.X. Flores, F.A. Charney, D. Lopez-Garcia, Influence of the gravity framing system on the collapse performance of special steel moment frames, Journal of Constructional Steel Research, 101 (2014) 351-362.

[2] F.X. Flores, F.A. Charney, D. Lopez-Garcia, The Influence of Gravity Column Continuity on the Seismic Performance of Special Steel Moment Frame Structures, Journal of Constructional Steel Research (To be published), (2015).

[3] FEMA, Recommended seismic design criteria for new steel moment-frame buildings, FEMA 350 Report, 2000.

6.3 Lumped vs Explicit Model

6.3.1 Introduction

The second paper published as part of this dissertation [1] studies the influence of the gravity columns on the collapse performance of Special Steel Moment Frames (SMFs). The objective of the study was to improve the seismic performance of these systems. The buildings used were taken from the ATC 76-1 project and were the 2-, 4-, and 8-Story Special Steel Moment Frame buildings designed using the Response Spectrum Analysis method (RSA). The approach used to incorporate the gravity columns in the analysis was by lumping all the columns into one elastic and continuous element. This approach was based on the supporting studies (Sections 6.1 and 6.2) previously developed as part of this dissertation. Thus it was considered that gravity columns do not yield and splices supply enough flexural strength to provide continuity along the height.

This supplemental study has been developed to display all the analyses performed to demonstrate that the lumped column approach gives the same results as modeling all the elements of the gravity system (explicit model). In order to establish the equality between both methods, the results obtained with each method are compared. The building to be used for the comparison is the 8-story special moment frame and the analyses to be performed are nonlinear static pushover and nonlinear dynamic analyses.

6.3.2 Explicit Model

The explicit model incorporates all the columns and beams of the gravity system. The gravity connections have no strength (8Story_0GS) and it is assumed, based on the study performed by Liu and Astanneh [2], that these connections can accommodate large rotations.

Figure 6.3-1 shows the model where the gravity system is placed next to the SMF. This approach to model the structure considers the floors as rigid diaphragms and that is why it can be analyzed in two dimensions. However, it has to be mentioned that an important limitation that 2D models have is that torsion cannot be included. A different study about the influence of accidental torsion on the inelastic dynamic response of buildings was performed in conjunction with Pontifical Catholic University of Chile [3] where it is shown the importance of analyzing structures in 3D, especially if the they have torsional irregularities.

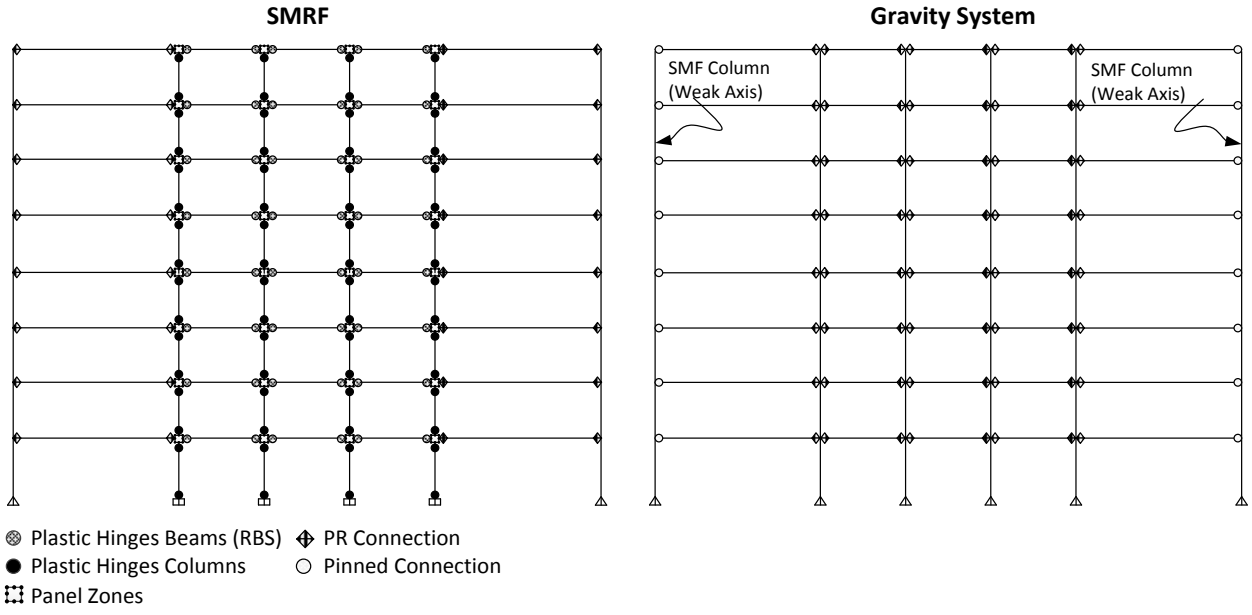

Figure 6.3-1 Explicit Model (8Story_0GS)

The gravity system was designed following common approaches and it has been already described in both of the papers that form part of this dissertation [1, 4]. However, for clarity purposes the layout of the building is shown again in Figure 6.3-2 and the sections obtained from the design for the 8-story model are shown in Table 6.3-1 (a).

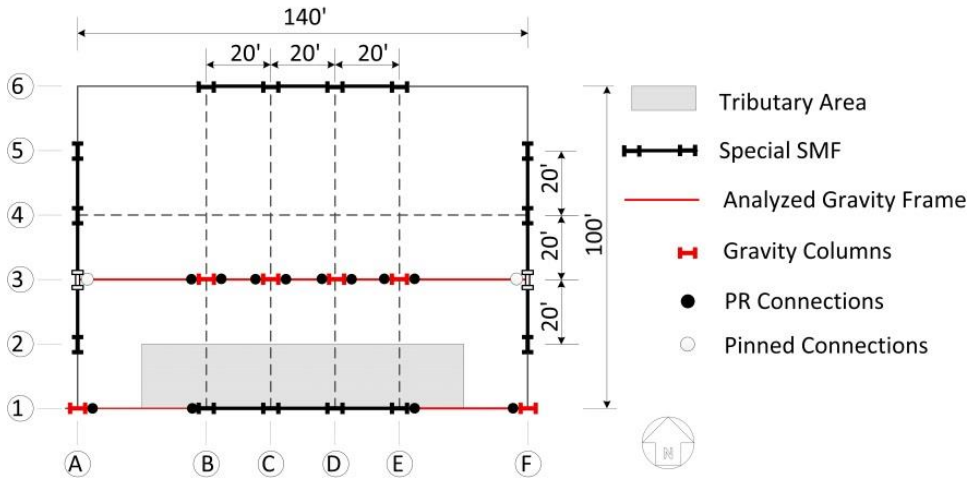

Figure 6.3-2 Buildings Layout

The sections of the gravity columns shown in Table 6.3-1 (a) are later on used to compute the inertia per story that the gravity system has with respect the inertia per story of the SMF columns.

Table 6.3-1 Gravity System Member Sizes

a) 8 Story Model

Story	Columns				Beams		
	A1,F1	A3,F3	B3, E3	C3, D3	A1 - B1, E1 - F1	A3 - B3, E3 - F3	B3-E3
1	**W18x76**	W24x162	**W18x143**	**W18x76**	W24x62	W24x94	**W16x36**
2	**W18x76**	W24x162	**W18x143**	**W18x76**	W24x62	W24x94	**W16x36**
3	**W18x76**	W24x162	**W18x143**	**W18x76**	W24x62	W24x94	**W16x36**
4	**W18x50**	W24x162	**W18x76**	**W18x50**	W24x62	W24x94	**W16x36**
5	**W18x50**	W24x131	**W18x76**	**W18x50**	W24x62	W24x94	**W16x36**
6	**W18x50**	W24x131	**W18x76**	**W18x50**	W24x62	W24x94	**W16x36**
7	**W18x40**	W24x94	**W18x50**	**W18x40**	W24x62	W24x94	**W16x36**
8	**W18x40**	W24x94	**W18x50**	**W18x40**	W24x55	W24x94	**W16x36**

Note: Gravity farming shown in **bold** text.

6.3.3 Lumped Model

The lumped column approach as called in this investigation accumulates all the gravity columns into one elastic element. The assumptions of the "lumped" method are:

- The gravity columns do not yield.
- The gravity columns are continuous all over their height.
- The base of the columns (at the foundation level) are pinned.
- Gravity connections have large rotation capacity and low flexural strength.

Based on these assumptions, which have been validated in analysis described previously, the moments of inertias per story of the gravity columns are computed and they are shown in Table 6.3-2. Arbitrarily, a ratio between the gravity column inertia per story (I_Gcol) and the inertia per story of the SMFs (I_SMF) was computed. This ratio was used in the second paper that form part of this dissertation [1] and is employed to represent different configurations of the gravity system (different number of gravity columns).

Table 6.3-2. Inertias and Areas per Story for the "Lumped" Model

Lumped Gravity Columns (Inertias)			
Inertia Per Story	**Inertia I_Gcol (in^4)**	**Inertia I_SMF (in^4)**	**Ratio I_GCcol/I_SMF**
1th Story	10820.00	18380.00	0.59
2nd Story	10820.00	18380.00	0.59
3th Story	10820.00	18380.00	0.59
4th Story	5860.00	18380.00	0.32
5th Story	5860.00	16080.00	0.36
6th Story	5860.00	16080.00	0.36
7th Story	4048.00	10800.00	0.37
8th Story	4048.00	10800.00	0.37

Figure 6.3-3 shows a sketch of the lumped approach where the SMF is modeled with two elements placed next to it: one that incorporates P-Δ effects and another that represents all the gravity columns. This figure shows the ratio already described, placed next to the lumped gravity column.

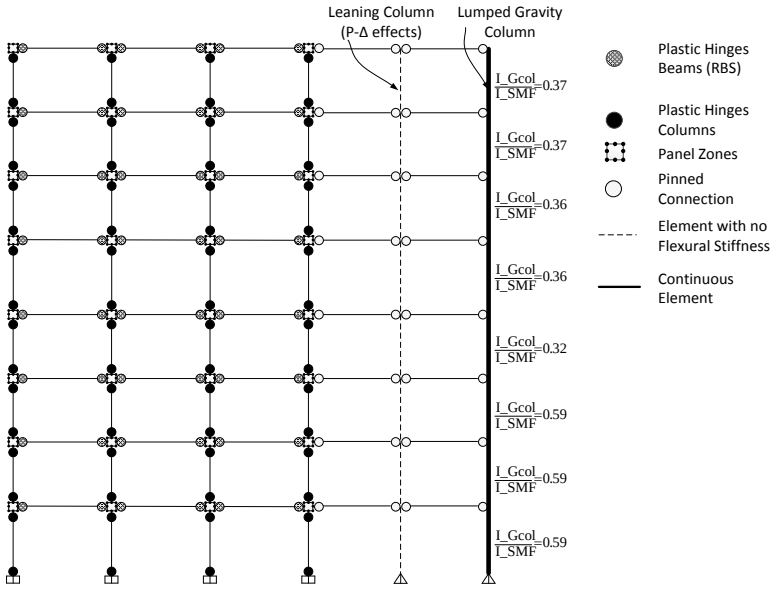

Figure 6.3-3 Lumped Model Approach

Once the methods have been described, nonlinear static pushover and nonlinear dynamic analyses are performed. The results obtained for the explicit and lumped model are then compared to establish their similarity. The ground motions and scale factors used in the dynamic analysis are the same as used in section 6.2 of this dissertation.

6.3.4 Nonlinear Static Pushover

The first step taken is to compare the nonlinear static pushover results obtained for the explicit and lumped model. Figure 6.3-4 illustrates the pushover curves of the lumped model (8Story+IGCol), the explicit model (8Story+0GS) and the model without the gravity system

(8Story). It is clear that the gravity system has an important effect on the building post-yield stiffness. Moreover, it can be concluded that the lumped model represents correctly the influence of the gravity columns because the results with the explicit model are the same even at large displacements.

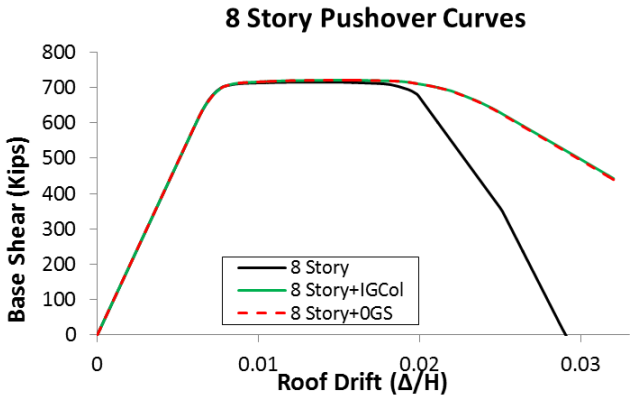

Figure 6.3-4 Nonlinear Static Pushover Curves "Lumped" vs "Explicit" Model

6.3.5 Nonlinear Dynamic Analysis

The nonlinear dynamic analysis was executed using 8 of the 44 ground motions that form part of the Far Field ground motions in the FEMA P695. Each ground motion was scaled following the FEMA P-695 procedure and then scaled again by performing an incremental dynamic analysis to subject the building to different intensity levels. FEMA P-695 scales the ground motions to the Maximum Considered Earthquake (MCE) spectrum which in turn represents a hazard level of 2% in 50 years. The spectral acceleration (S_a) for the 8-story model at MCE level is equal to 0.55g. However, the structure is subjected to larger hazard levels in order to check if the gravity columns yield. The scale factors used to analyze the buildings are 1.0 (S_a=0.55g), 1.5 (S_a=0.825g) and 1.8 (S_a=0.99g) and the results for the building with the gravity system modeled explicitly (8Story_0GS) and the lumped model (8Story_IGcol) are shown in Figure 6.3-5.

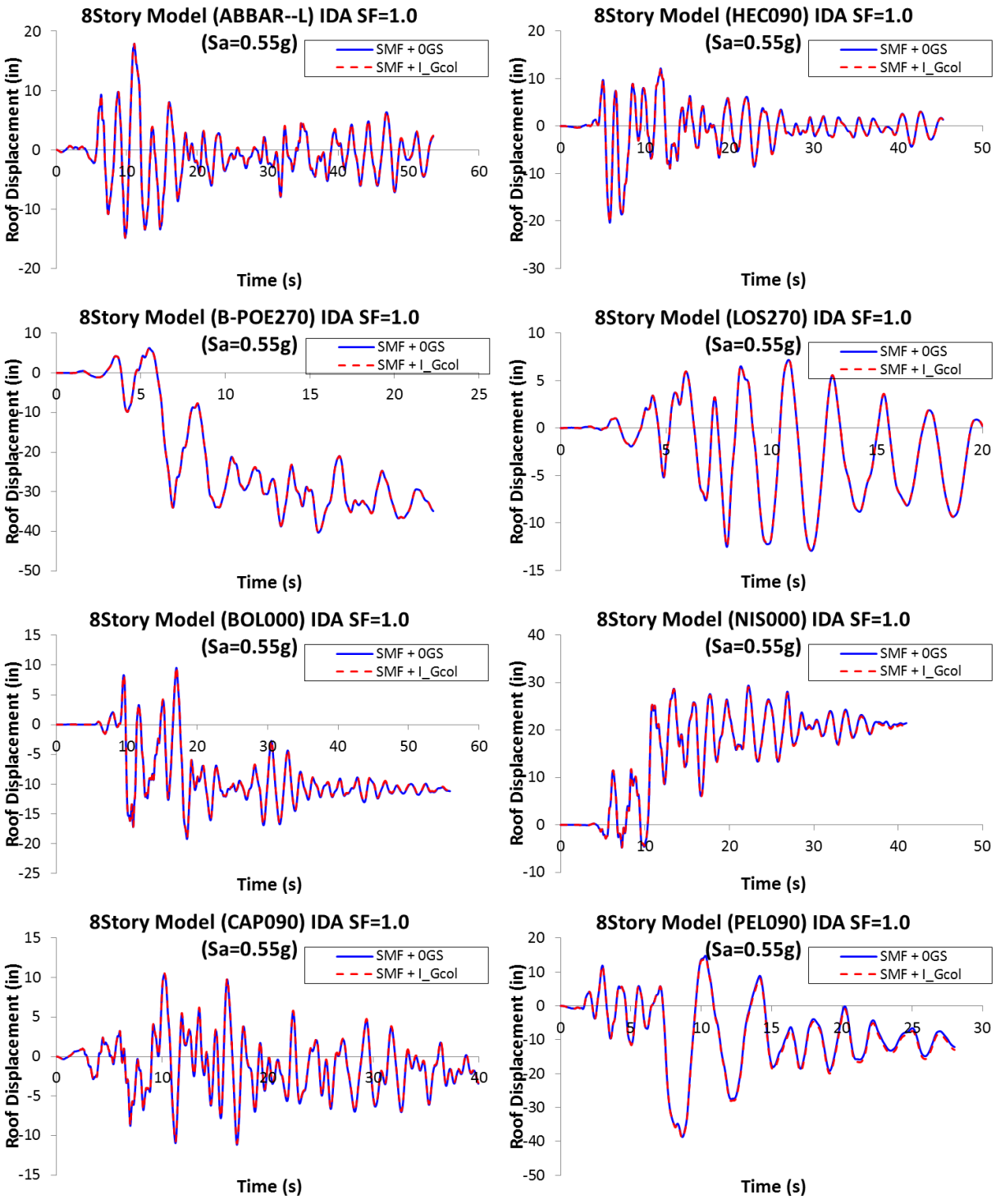

Figure 6.3-5 Nonlinear Dynamic Analyses Explicit vs Lumped Model a) Scale Factor =1.0

(MCE Level, S_a=0.55g)

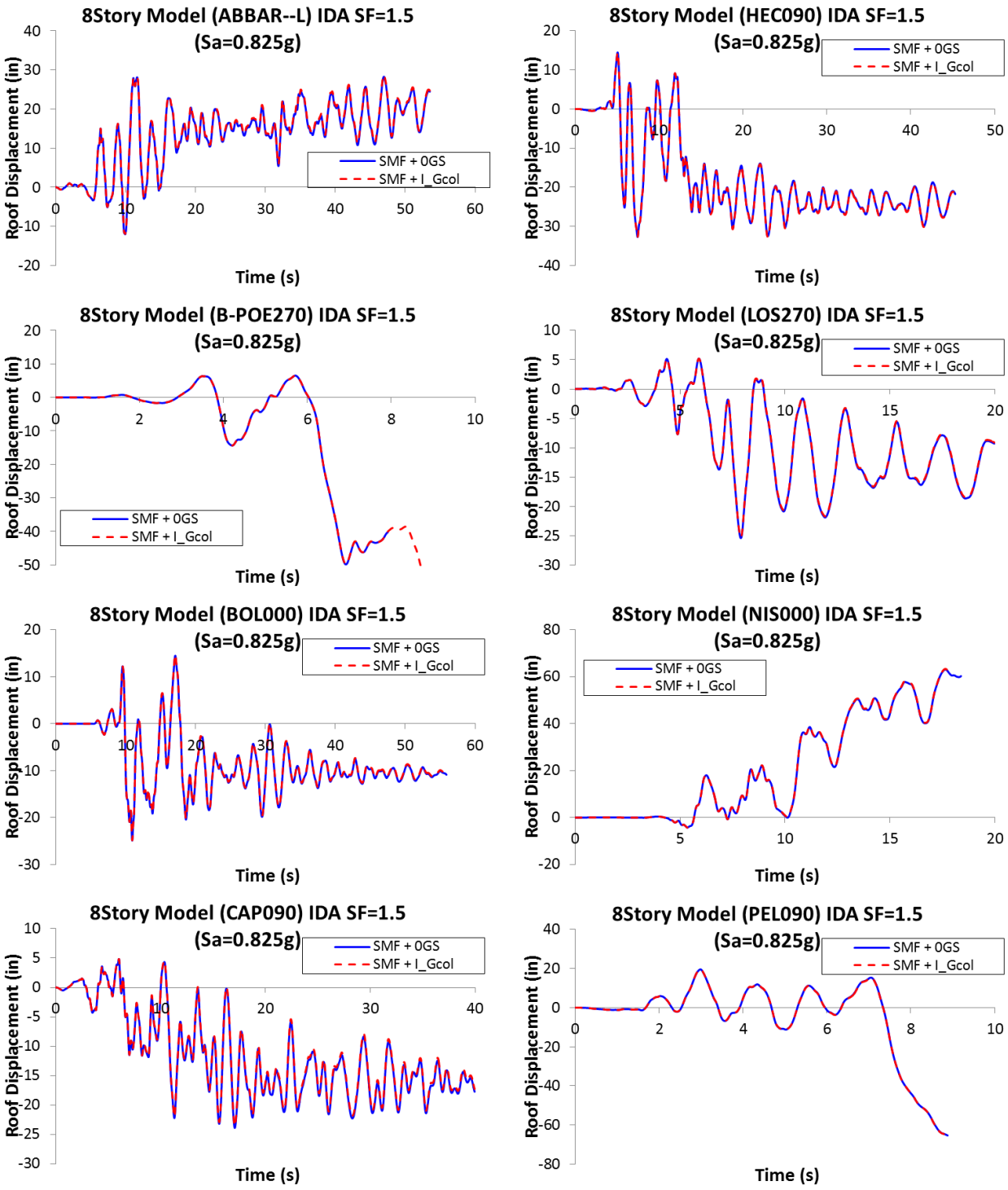

Figure 6.3-5 Nonlinear Dynamic Analyses Explicit vs Lumped Model b) Scale Factor =1.5 (S_a=0.825g)

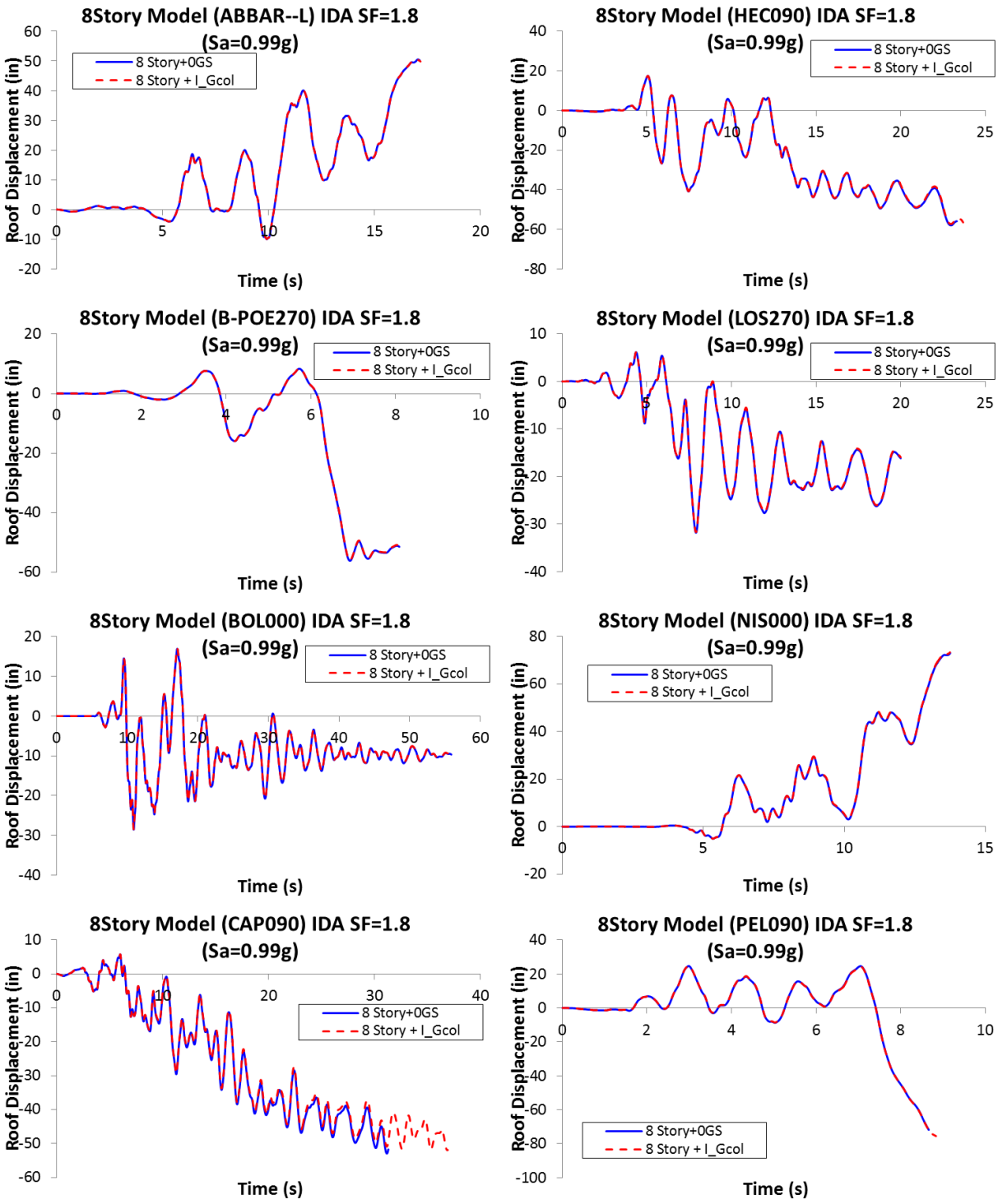

Figure 6.3-5 Nonlinear Dynamic Analyses Explicit vs Lumped Mode c) Scale Factor = 1.8 (S_a=0.99g)

Figure 6.3-5 shows the results obtained using both approaches to incorporate the gravity system as part of the lateral resisting system. Recalling the scale factor 1.0 represents the MCE intensity level, it can be seen that higher intensity levels were considered and for all of them the results between the explicit and lumped model are the same. Therefore, it can be concluded that the lumped column approach gives the same results as modeling the gravity system explicitly.

6.3.6 Summary and Conclusions

In this supporting study, a simple approach to include the gravity columns as part of the lateral resisting system of SMF was analyzed. The purpose of this section of the dissertation was to prove that placing one continuous element in addition to the leaning column next to the SMF is an accurate way to represent a gravity system with low flexural strength connections. For this matter a comparison between the 8-Story model with the gravity system modeled explicitly (8Story_0GS) and the 8-Story model with an extra element with properties that represent all the gravity columns, was carried out. The comparison was made by means of nonlinear static and nonlinear dynamic analyses.

The pushover curves showed that lumping all the gravity columns into one elastic element is the same as modeling the gravity system explicitly if the gravity connections have no strength and the gravity columns are pinned at the base. In addition, nonlinear dynamic analyses were performed using 8 Far Field ground motions from the FEMA P-695 methodology. The ground motions were scaled to higher intensity levels than the MCE level and the results obtained for the lumped and explicit model were the same. The results proved that this simple methodology could be used to incorporate the gravity columns as part of the lateral resisting system.

6.3.7 References

[1] F.X. Flores, F.A. Charney, D. Lopez-Garcia, Improving Seismic Performance of Steel Special Moment Frames Journal of Constructional Steel Research (To be published), (2015).

[2] J. Liu, A. Astaneh-Asl, Cyclic testing of simple connections including effects of slab, Journal of Structural Engineering, 126 (2000) 32-39.

[3] F.X. Flores, F.A. Charney, D. Lopez-Garcia, J.C. De La Llera, The Influence of Accidental Torsion on the Inelastic Response of Buildings During Earthquakes, 11th Chilean Conference on Seismology and Earthquake Engineering, (2015).

[4] F.X. Flores, F.A. Charney, D. Lopez-Garcia, Influence of the gravity framing system on the collapse performance of special steel moment frames, Journal of Constructional Steel Research, 101 (2014) 351-362.

6.4 Influence of PR connection Hysteretic Behavior

6.4.1 Introduction

This section demonstrates the importance of the hysteretic behavior assigned to the PR connections. As described in Chapter 3 of this dissertation, the backbone curve of the hysteretic behavior used for the PR connections was taken from the ASCE 41-13 [1] (Section 9.4.3 and Table 9-6). One of the objectives of the investigation reported in this dissertation was to establish the importance of the gravity connections strength. Even though the backbone curve was based on a double angle connection, the hysteretic behavior actually represents more a generic connection. It has to be clarified that the flexural strength of the PR connections was imposed and used as a variable of the study. Therefore, the backbone curve given by ASCE 41-13 is the same for all the types of PR connections specified in Table 9-4 (e.g. Composite Top and Clip angle Bottom, Top and Bottom Clip angles, shear tab connections) because the difference of the flexural strength of these connections depends on the limit state that controls the design of the connection. The parameters that control the rotation capabilities of the connection were chosen from Table 9-6 (ASCE 41-13) and these correspond to the double angle connection. According to this table, this connection could have the largest rotation capacity and that is why it was selected for the study. However, according to Liu and Astaneh [2], simple connections (shear tabs) have a large rotation capacity, so the chosen rotational parameters taken from ASCE 41-13 could represent these type of connections as well.

In order to show the effect of modeling the PR connections with a generic hysteretic behavior, this section analyzes the 8-story building with the PR connections modeled with a much more detailed hysteretic behavior. The building was designed using Partially Restrained Composite Connections (PR-CC) (Figure 6.4-1) [3]. This type of connections engage the

reinforcing steel of the concrete slab to form the top portion of the moment resting mechanisms. The bottom portion is typically provided by a steel seat angle with web angles providing the shear resistance [3]. The 8-story model with PR connections with different flexural strengths (0%, 35%, 50% and 70%M_p) and a generic hysteretic behavior are compared with the 8-story model with PR-CC by means of the FEMA P-695 methodology [4]. Specifically, the parameters to be compared are the overstrength (Ω), period based ductility (μ_T), collapse margin ratio (*CMR*) and probability of collapse. Additionally, the pushover curves are also compared.

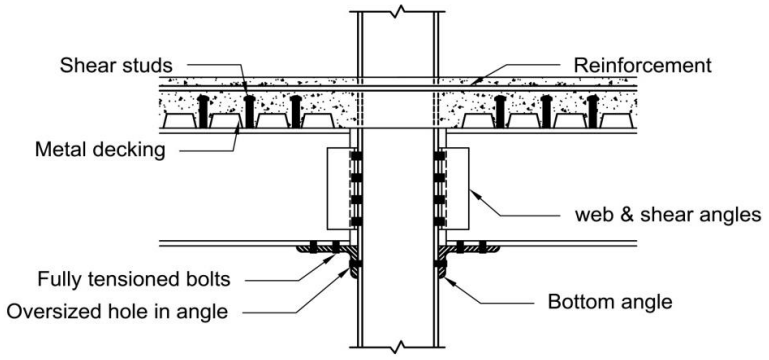

Figure 6.4-1 Partially Restrained Composite Connection [3]

6.4.2 PR-CC Calibration

The first step taken before modeling the PR-CC connection was to calibrate the hysteretic behavior. The method adopted was the same taken by Bozorgmehr [5] where a mathematical model for monotonic behavior and a generalized hysteretic model were used to match a specific test result. The ascending branch of the backbone curve was defined with points obtained from a mathematical model and the descending branch was defined from experience. The envelope of the hysteretic behavior is computed as follows:

1) The ascending and descending branch of the backbone curve is computed using the mathematical equations for monotonic behavior given by AISC Design Guide 8 [3]. This is done up to a rotation equal to 0.02 radians.
2) From the point where a rotation of 0.02 radians is attained the moment capacity decreases linearly to the point of rotation equal to 0.07 radians and moment equal to 20% the maximum moment capacity. Beyond this point the moment capacity is constant and equal to 20% the maximum moment.

Once the backbone curve is determined, the hysteretic model used to calibrate the behavior of PR is the "Pinching 4" model from OpenSees. The parameters for this model were calibrated with the test performed by Ammerman [6]. The computations performed to obtain the backbone curve are shown in Appendix E.

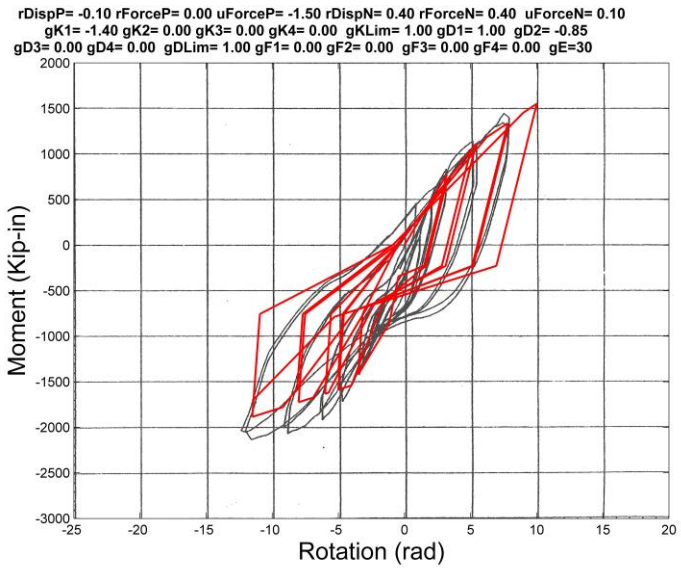

Figure 6.4-2 PR-CC Calibration Model (Test Results (Black) [6] vs OpenSees Model (red))

The results of the calibration are provided in Figure 6.4-2 shows the comparison between the OpenSees model and the test results. The text on the top of the graph displays all the values

used to calibrate the material ("Pinching 4"). The complete hysteretic behavior and the backbone curve are shown in Figure 6.4-3. It can be seen from this figure that the backbone curve is not the same for positive and negative deformations because the concrete slab has been incorporated as part of the connection.

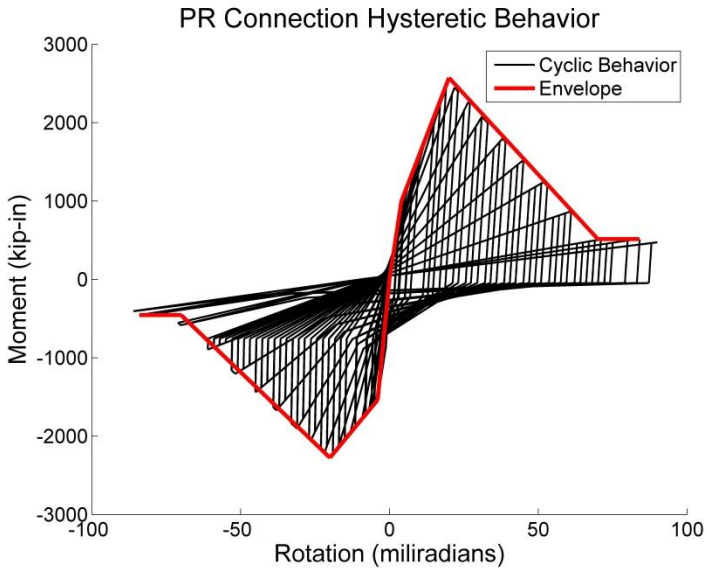

Figure 6.4-3 PR-CC Hysteretic Behavior

6.4.3 PR-CC Design

The connections for the 8-story model were designed following Example 9-78 of the manual of steel construction AISC-LRFD second edition [7] and then using the AISC Design Guide 8 [3]. The details are shown in Appendix E. The moment capacity that the connection was designed for was equal to 25% M_p of the connected beam. Once the design of the connection was complete, the backbone curve was computed using the AISC Design Guide 8 [3].

The final design of the connections and their respective moment rotation curves computed using the AISC design guide are shown from Figure 6.4-4 to Figure 6.4-7. The backbone curve is compared with the one computed using the ASCE 41-13 and a flexural

strength equal to 35% M_p. These figures display the similarity on the initial stiffness between the two models. However, the more realistic behavior has a different backbone curve in comparison to the one given by the ASCE 41-13. The main differences are that the PR-CC backbone curve is not symmetric due to the effect of the concrete slab and that the PR-CC has gradual strength degradation.

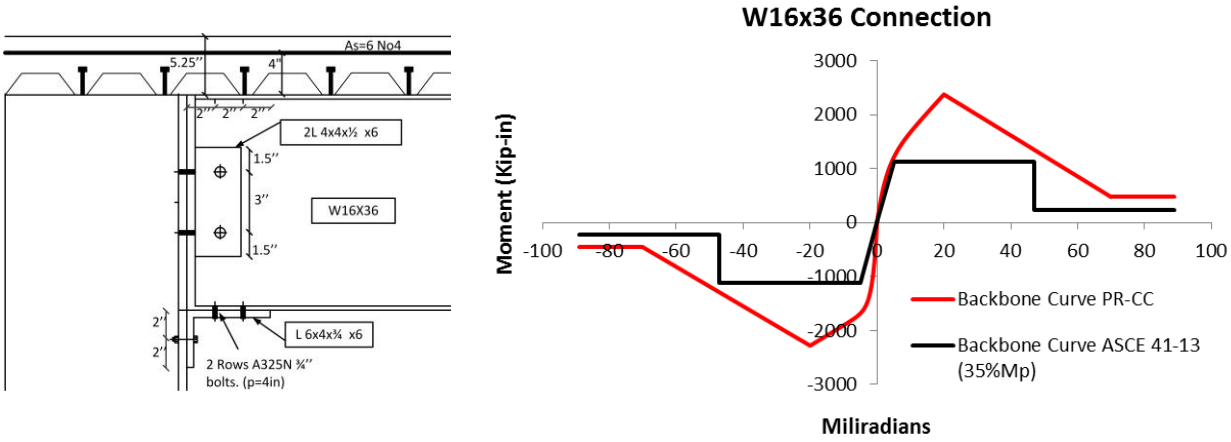

Figure 6.4-4 PR-CC W16x36

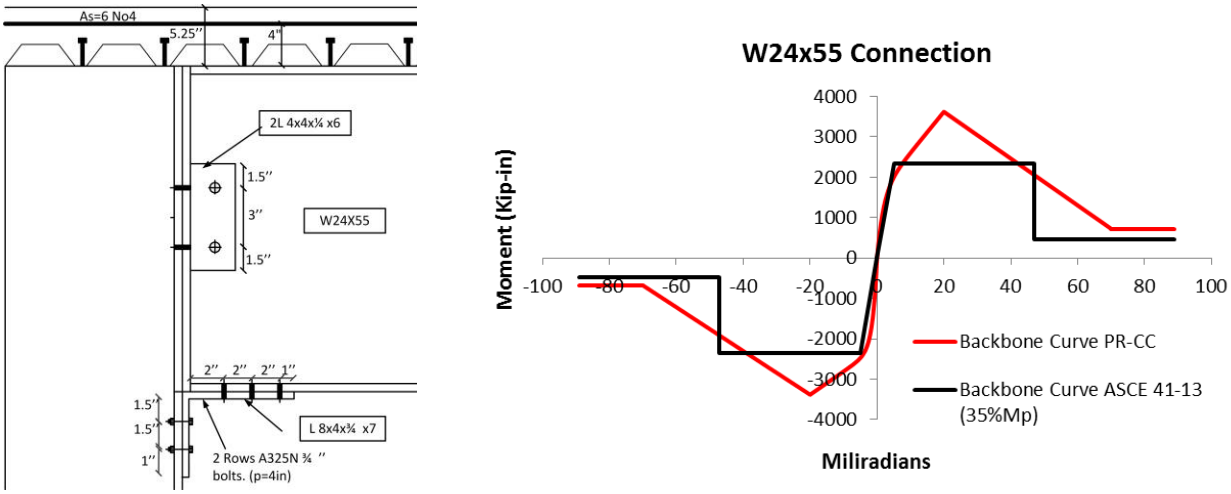

Figure 6.4-5 PR-CC W24x55

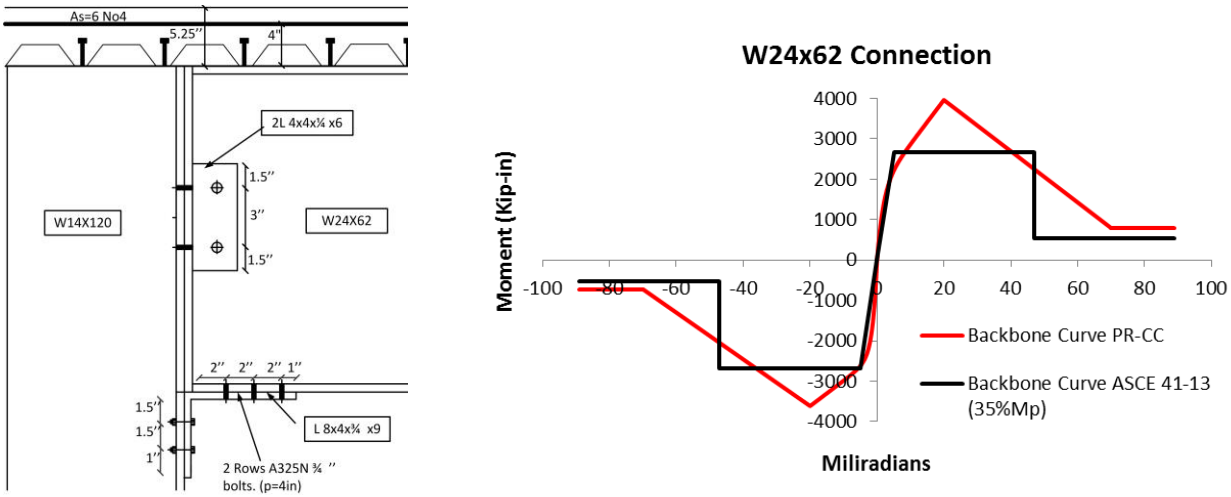

Figure 6.4-6 PR-CC W24x62

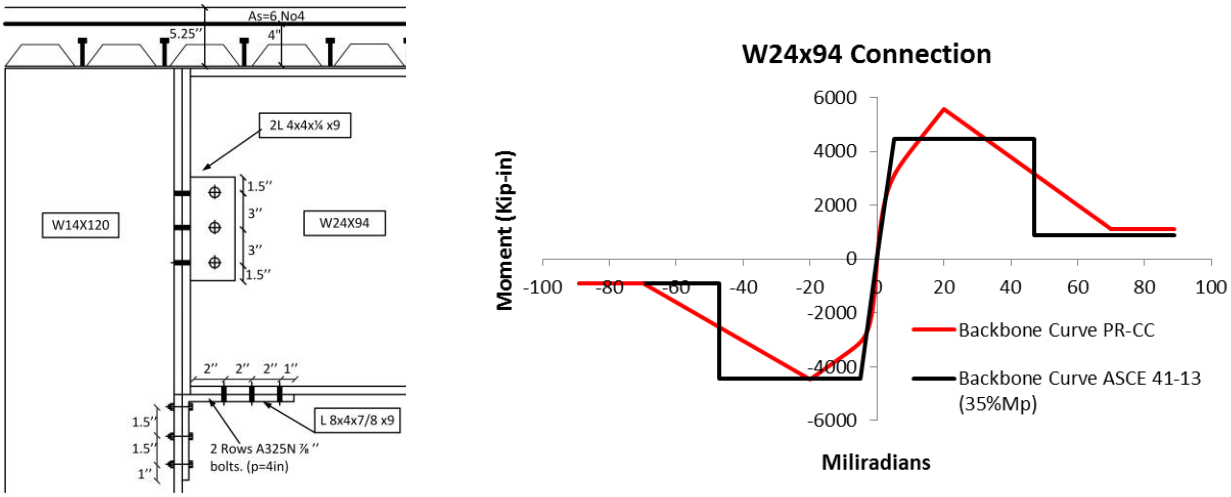

Figure 6.4-7 PR-CC W24x94

6.4.4 Hysteretic Behavior Comparison (PR-CC vs ASCE 41-13)

In this subsection of the dissertation a comparison of the hysteretic behavior computed for the PR-CCs and ASCE 41-13 is presented. Figure 6.4-8 displays the cyclic behavior for all the connections that form part of the gravity system. The hysteretic curves on the left side represent PR-CCs and they were computed using the methodology described herein. On the other hand the hysteretic curves on the right side represent a generic connection and their cyclic behavior does not follow a specific trend.

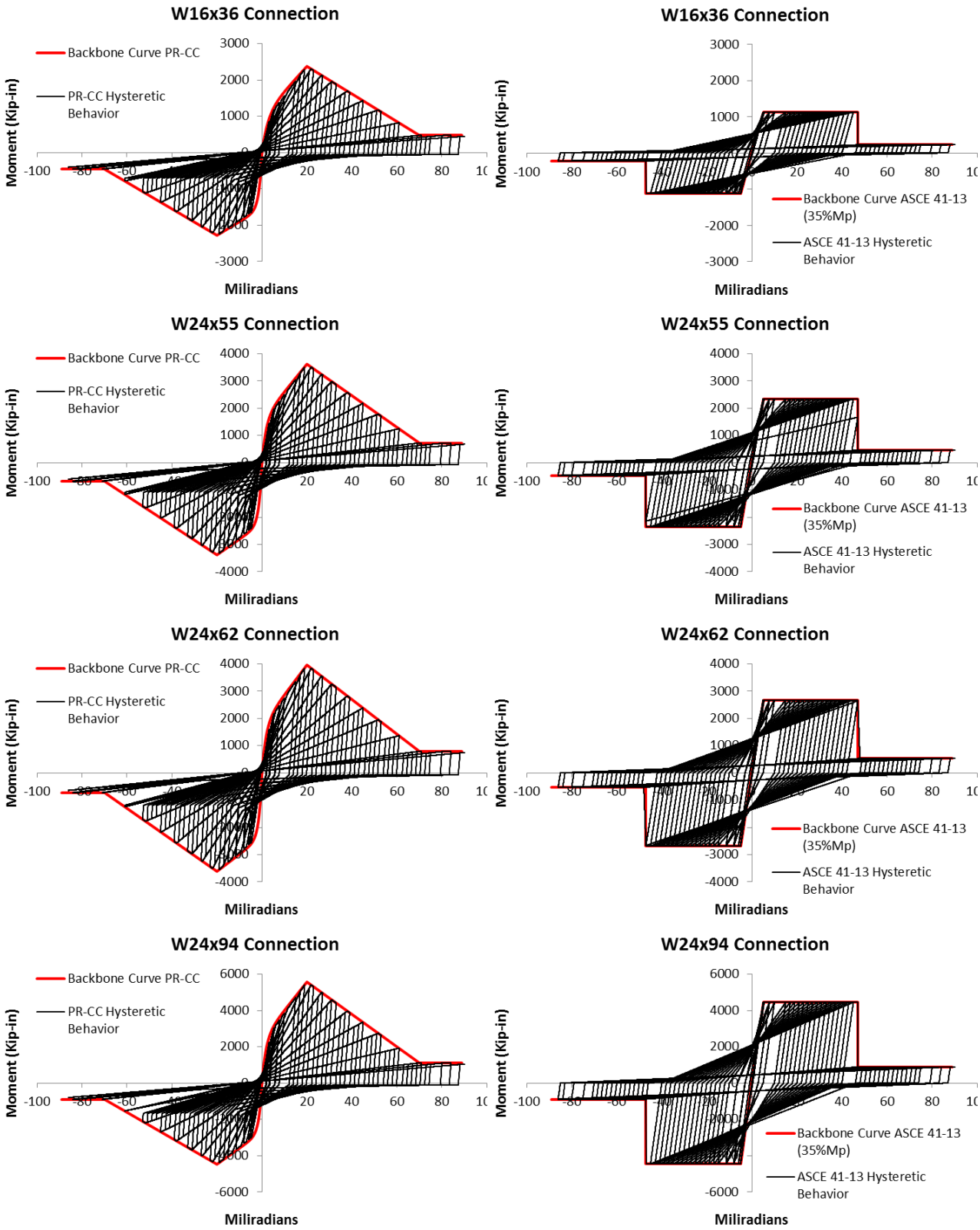

Figure 6.4-8 Hysteretic Behavior: PR-CC vs ASCE 41-13

From Figure 6.4-8 it can be seen that despite the differences between the two models, it is difficult to establish which one will dissipate more energy although it appears that the ASCE 41-13 connections are more conservative and dissipate less energy than the PR-CC.

6.4.5 Nonlinear Static Pushover Results

In order to compare the performance of the 8-story model with more detailed PR connections a nonlinear static pushover analysis is executed. The pushover curves obtained for the models with no splices and the gravity columns modeled using force-based fiber sections are shown in Figure 6.4-9.

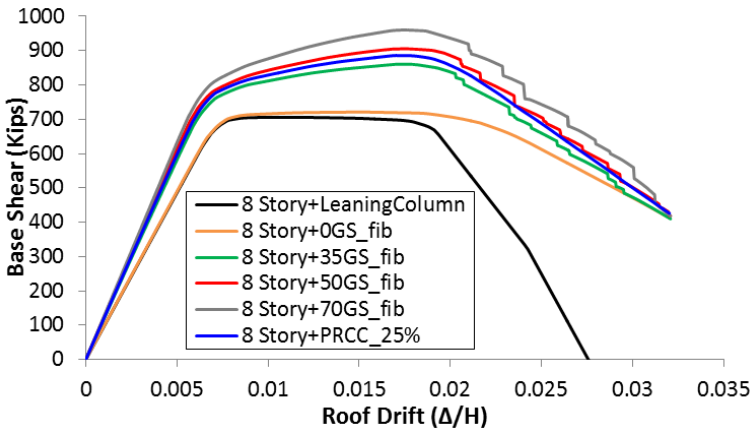

Figure 6.4-9 Pushover Curves Comparison (8-Story Model)

Figure 6.4-9 displays the pushover curves obtained for the models with the PR connections with different flexural strengths (0%, 35%, 50% and 70%M_p). In addition the pushover curve computed using the PR-CC with 25% of the girder strength is shown. From the figure, it can be seen that the model with PR-CC response is somewhere between the response of the model with PR connections with flexural strength equal to 35%M_p and 50%M_p. Because the PR-CCs have a gradual decrease in the flexural strength, the pushover curves is smooth in comparison to the other models. From the figure it can be concluded that the performance of the

8-Story model with PR-CCs is similar to the ones with the PR connections modeled using the ASCE 41-13. However, the hysteretic behavior does not have any contribution in the computed performance when nonlinear static pushover analysis is performed. Thus, nonlinear dynamic analysis needs to be performed in order to establish the importance of a more detailed PR connection model.

6.4.6 Performance Evaluation

The following step to evaluate the influence of a more detailed PR connection hysteretic model is to perform nonlinear dynamic analyses and quantify the collapse performance using the FEMA P-695 methodology. One of the conclusions from Chapter 4 was that the gravity connections do not have a major influence on the collapse performance of the 8-Story model. For this reason, a general comparison is done between the building with PR-CC and the buildings with the ASCE 41-13 PR connections. Table 6.4-1 displays a comparison of the results of the performance evaluation. By looking at the overstrength (Ω), ductility (μ_T) and collapse margin ratio (*CMR*) values, it can be concluded that they are very similar and at least for this building (8-Story), the complexity of the hysteretic behavior of the PR connections did not have major influence

Table 6.4-1 Performance Evaluation Comparison

Model			T (sec)	Vmax (Kips)	Overstrength Ω	Ductility μ	CMR	SSF	ACMR
	P-Delta	8 Story	2.22	715.11	3.21	3.13	1.48	1.33	1.98
Columns modeled with ealstic Fibers	No Splices	8 Story 0GS	2.22	721.08	3.24	3.82	1.85	1.38	2.56
		8 Story 35GS	1.97	860.55	3.85	3.51	1.95	1.36	2.66
		8 Story 50GS	1.94	905.48	4.04	3.48	2.00	1.36	2.72
		8 Story 70GS	1.91	960.18	4.29	3.40	2.05	1.35	2.78
		8 Story PR-CC	2.05	885.94	4.03	3.51	2.05	1.36	2.79

The CMR and probability of collapse for all the compared models are shown in Figure 6.4-10 (a) and (b) respectively. These figures show clearly that the cyclic behavior of the PR connections did not have a significant influence on the collapse performance.

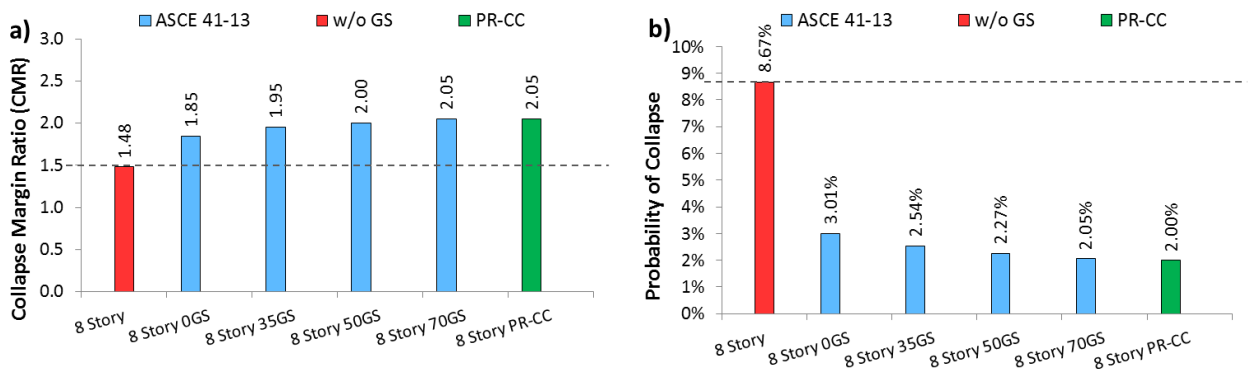

Figure 6.4-10 Result of 8-story building. (a) CMR. (b) Probability of collapse.

As Figure 6.4-10 illustrates that the CMR and probability of collapse have a minimum variation when the flexural strength on the PR connections was varied. Additionally, it is shown in this section that a more detailed hysteretic behavior did not influence the results.

6.4.7 Conclusions

As already mentioned as part of the conclusions in Chapter 4, the gravity connections did not have a major influence on the collapse performance of SMFs. This was one of the motives to perform the following investigation in Chapter 5, where the only component from the gravity system considered was the gravity columns. This section was devoted to quantify the importance of having a more detailed and realistic hysteretic model assigned to the PR connections. This was done to validate the procedure taken in this dissertation where the hysteretic behavior of a generic PR connection was used with the backbone curve taken from ASCE 41-13. The results of the performance evaluation demonstrated that at least for the 8-story model a more detailed hysteretic behavior did not have an impact on the results. Thus, it can be concluded that the PR connections model used in throughout this dissertation are valid in the context of that analysis performed and the results obtained in Chapter 4 and 5 contribute to have a better understanding of the influence of the gravity system on the seismic performance of structural systems that utilize SMFs.

6.4.8 References

[1] ASCE, Seismic Rehabilitation of Existing Buildings (ASCE/SEI 41-13), American Society of Civil Engineers Reston, Virginia, 2013.

[2] J. Liu, A. Astaneh-Asl, Cyclic testing of simple connections including effects of slab, Journal of Structural Engineering, 126 (2000) 32-39.

[3] R.T. Leon, J.J. Hoffman, P. Staeger, Steel Design Guide Series 8: Partially Restrained Composite Connections, American Institute of St eel Construction, (1996).

[4] F. P695, Quantification of Building Seismic Performance Factors, Fededral Emergency Management Agency, Washington, D.C, 2009.

[5] A. Bozorgmehr, Collapse Assessment of Partial Restraint Composite Connection Moment Frames, in: Department of Civil and Environmental Engineering, Chalmers Univeristy of Technology, 2011.

[6] D.J. Ammerman, Behavior and design of frames with semi-rigid composite connections, in, 1988.

[7] AISC, Manual of steel construction. Load & resistance factor design, American Institute of Steel Construction, Chicago, IL, 1994.

Chapter 7: Guidelines for Incorporating the Gravity System in Nonlinear Analysis

Traditionally, the gravity framing has not been considered as part of the lateral load resisting system when structures are subjected to seismic ground motions, even though it has been shown during past earthquakes that the gravity system can contribute significantly to the seismic resistance. One reason for ignoring the gravity system is the perception that significant effort and computer resources are required to include it. Additionally, in the case of structures incorporating SMFs as the main lateral system, little was known about the influence of the gravity system on the computed performance. The research summarized in the previous chapters has shown, however, that explicit inclusion of the gravity system provides clear benefits when assessing seismic performance and that in some cases the benefits can be realized by use of analytical models that are only marginally more complex than those used in the past.

This chapter has been created to propose guidelines on how to include the gravity system in mathematical models used for nonlinear seismic analyses of building structures. The experience and the outcomes obtained from the analyses presented in Chapters 4, 5, and 6 of this dissertation provided the motivation to create this chapter. The chapter is divided into different important sections. The first section summarizes the scope of the guideline. The following two sections discuss the importance of modeling in 3-D vs 2-D and the importance of the gravity system on lateral floor accelerations. Finally, guidelines and preliminary guidelines are presented for modeling the gravity system on special steel moment frame buildings in 2-D and 3-D respectively. The main guidelines are intended to be used in two-dimensional mathematical models because that was the methodology used in this investigation. Even though the trend of codes (e.g. ASCE7 [1]) in the present is to model the full system, procedures like the FEMA P-695 [2] or codes like the ASCE41-13 [3] still allow 2-D modeling.

7.1 Scope

The investigation performed in this dissertation brought up important conclusions regarding the influence of the gravity system on the seismic performance of SMFs. However, because of the amount of nonlinear dynamic analyses and computational time required to evaluate the collapse performance of structures using the FEMA P-695 methodology [2], a limited number of SMFs were studied. The buildings investigated were taken from the ATC 76-1 project [4] and they consist of 2-, 4- and 8-story SMFs. Only three basic SMF configurations were studied because of the multiple permutations required to investigate the influence of the gravity connections, gravity columns, splices and yielding in the gravity columns. Given these variations, the collapse performance of a total of 71 structures was investigated, requiring approximately 30,000 nonlinear dynamic analyses. The large variation in structural systems that were studied made it possible to establish different trends and define important effects that the gravity system provides where the principal lateral system is a SMF. However, because the maximum number of stories of the analyzed structures is eight, the conclusions of this investigation cannot be generalized for high rise buildings and this limited the scope of this dissertation. As a result, the guidelines to be provided herein are to be used with SMFs up to 10 stories.

Another important limitation of the investigation arises from analyzing the structures in 2-D instead of 3-D. Even with the drastic increase in computer speed and storage capacity over the past several decades, evaluation of the collapse performance of structuctures in 3-D is difficult. However, it is undeniable the importance of including effects such as torsion in the analysis, and the only way to do this is using 3-D models. Thus, the scope of this study is limited to structures that do not have torsional irregularities, so they can be analyzed in 2-D. A study

performed in conjunction with the Pontifical Catholic University of Chile (PUC) [5] is briefly described in this chapter to show the importance of modeling in 3-D and including effects such as accidental torsion.

7.2 Modeling Structure in 3-D vs 2-D

This section is dedicated to show the importance of modeling structures in 3-D in order to incorporate torsion in the analysis. Moreover, it is shown the essential importance of explicitly including all the gravity columns to capture correctly all the P-Delta effects. For this matter some of the results of the study performed in conjunction with the PUC [5] are shown herein. In the referenced investigation, a 9-story steel building with Buckling Restrained Braces (BRBs) was studied. Three versions of the building (system A, B and C) were considered, wherein the only difference is the plan location of individual braced frames (Figure 7-1). The variation in plan location produces different levels of torsional irregularity. For System A, BRBs in the N-S direction were positioned only along gridlines 4 and 6 as shown in Figure 7-1. System B has N-S BRBs only on gridlines 3 and 7, and system C has N-S BRBs only on gridlines 2 and 8. Based on ASCE 7-10 [1] definitions, System A has a Type-1b (extreme) torsional irregularity, System B has a Type 1a torsional irregularity, and system C is not torsionally irregular.

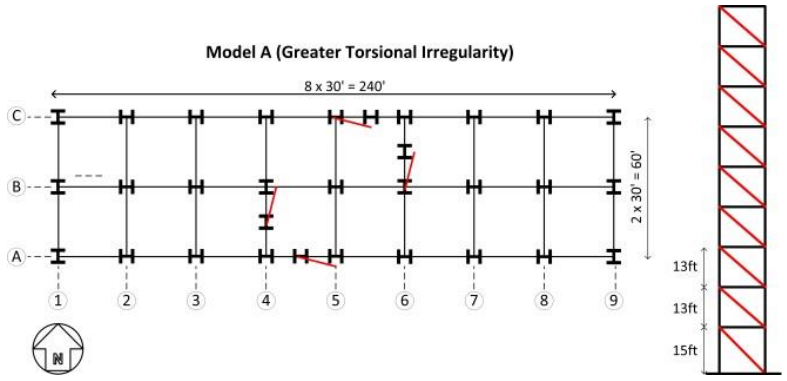

Figure 7-1 Building Overview [5]

The results to be displayed in this section of the chapter are related to the importance of including the gravity columns to capture P-Delta (P-Δ) effects and the effect that accidental torsion could have. In the mentioned study, two different ways of including P-Δ effects were considered: one where only one leaning column that includes P-Δ transformations was placed at the center of mass of the building and another where all the columns including the gravity columns incorporated the P-Δ transformations. In contrast to what it has been done in this dissertation, the gravity columns did not have flexural stiffness or strength, they were provided only as a mechanism for spatial distribution of destabilizing P-Delta forces. The total gravity load was applied to the leaning column in the first case and the tributary load per column was applied to the individual columns in the second case. Modeling one leaning column will capture correctly P-Δ effects caused by a translational deformation but in the case where the building is subjected to torsion, this model will not be able to capture the additional torsional loads created by the P-Δ effect. These additional torsional loads that arise as a result of P-Δ effects are called P-Theta (P-Θ) effects in the referenced paper [5]. Thus the difference between both analyses when the structure is subjected to torsional forces illustrates the importance of including P-Θ effects.

The three systems were subjected to both components of 11 ground motions which were scaled to represent the MCE level shaking. The amount of accidental torsion was imposed by modifying the diaphragm mass distribution until the desired mass eccentricity was achieved. The results from response history analysis of system A as subjected to the Kocaeli-Duzce ground motion are shown in Figure 7-2 (a) and (b).

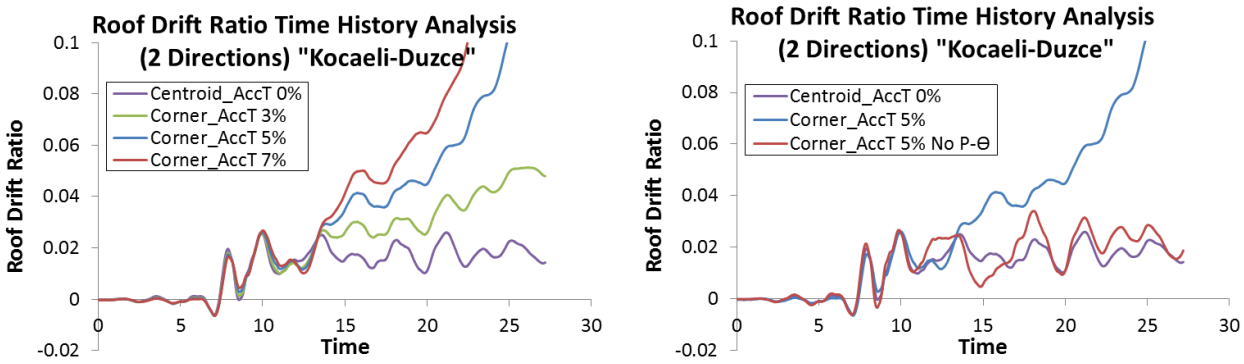

(a) Bidirectional loading (with P-Theta) (b) Bidirectional loading (w & w/o P-Theta)

Figure 7-2 Response histories of roof drift for System A [5]

Figure 7-2 (a) shows the effect that accidental torsion could have on a building that has an extreme torsional irregularity. It can be seen from this figure that the building is collapsing for an accidental torsion resulting from a mass offset equal to or larger than 5% of the longer building. On the other hand Figure 7-2 (b) illustrates the importance of P-Θ effects by showing how System A does not collapses if this effect is not included in the analysis. Similar results were obtained for the building with torsional irregularity Type 1a (System B) with the only difference that fewer collapses occurred relative to System A when P-Θ effects are included. However, System C which was not torsionally irregular, did not collapse for any of the ground motions and the P-Θ effects did not play a role in predicting collapse performance as important as it did for the other two systems that have torsional irregularities. In is noted, however, that inclusion of P-Θ effects was important for all systems when computing displacements at the edge of the building (as will be required for nonlinear analysis in ASCE 7-16).

The main conclusion from the study is the importance of modeling and analyzing structures in 3-D and to represent geometric nonlinearities on a column-by-column basis. It can be seen from the results that accidental torsion can influence the collapse performance of a structure. However, the importance of including torsion effects into the analysis arises when the

building presents a torsional irregularity (based on ASCE 7-10 definitions). Therefore it can be concluded, that analyzing structures in 2-D using the FEMA P-695 methodology would be adequate as long as the building has no torsional response (which is virtually impossible for a real structure).

Another relevant conclusion from the presented study is the necessity of explicitly including all the gravity columns in order to include P-Θ effects. Chapter 5 of this dissertation presented the approach where all the gravity columns are lumped into one element. This approach would not be possible to use in 3-D unless more research is carried out to define a minimum number and arrangement of lumped columns to incorporate correctly P-Θ effects.

7.3 Importance of Gravity System on Floor Accelerations

The analysis of seismic demands in nonstructural components is a topic often overlooked in earthquake engineering. Another investigation performed in conjunction with PUC studied the lateral floor accelerations developed during earthquakes in SMF systems [6]. The study focused on the importance of the structure's inelastic behavior and the importance of including the gravity system on the accelerations demands on Nonstructural Components (NSCs). The accelerations demands on NSCs were evaluated and compared with the accelerations given by ASCE 7-10. The structures were subjected to the 44 Far Field ground motions from FEMA P-695 scaled to represent the Design Earthquake (DE) level of intensity. The buildings used in the study are the same 2-, 4- and 8-story SMFs analyzed in this dissertation and the gravity system had different PR connections with different flexural strength capacity (0%, 35%, 50% and 70% M_p). In order to show the importance that the gravity system has on floor accelerations some of the results of the referenced study are presented herein.

Figure 7-3 (a) and (b) illustrate the peak floor accelerations computed for the 8-story SMF behaving elastically and inelastically respectively. The Peak Floor Acceleration (PFA) is the maximum total acceleration measured at a given floor, and is equal to the acceleration demand on a rigid NSC located at that floor. From these figures it can be seen that the inelastic response has a significant influence on PFAs and that accelerations computed using ASCE 7 are considerably overestimated. In regard to the gravity system however, the influence on the accelerations is negligible.

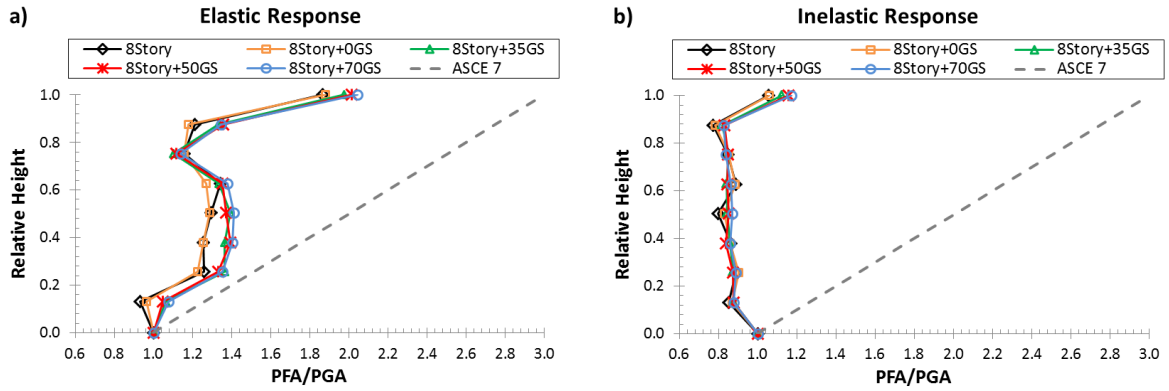

Figure 7-3 Normalized Peak Floor Acceleration (PFA/PGA): 8-Story Model [6]

The study concludes that the influence of the gravity columns is negligible and that the strength of the PR connections has some influence on accelerations computed for flexible NSCs. However, for rigid NSCs the effect of the gravity connections strength is negligible.

As a result of the findings obtained in the referenced study, it is determined that the importance of the gravity system to evaluate accelerations on NSCs is not essential. Thus, the gravity system could be neglected from the analysis. It has to be mentioned that floor accelerations are computed at a level of intensity equal to the design level earthquake (10% in 50 years) and as it has been stated multiple times throughout this dissertation, the gravity system has more influence at higher level ground motions.

7.4 Guidelines to include the gravity system (2-D)

The previous sections overviewed the importance of modeling in 3-D including the gravity system and the importance of including the gravity system to evaluate the accelerations demands on NSCs. The conclusion obtained from the referenced studies [5, 6] is that modeling in 2-D is adequate if the structures have negligible torsional response and that the gravity system can be neglected when quantifying floor accelerations.

guidelines and preliminary guidelines are presented for modeling the gravity system on special steel moment frame buildings in 2-D and 3-D respectively

Once that these two important topics have been described, guidelines and preliminary guidelines for modeling the gravity system on special SMF buildings in 2-D and 3-D respectively are proposed. Based on the results obtained in this dissertation, the guideline has been divided depending on the number of stories of the building: one for buildings with four stories or less, and another for buildings between four and ten stories. The differentiation between these two types of structures that depends on the number of stories arises from the influence of different components of the gravity system. For buildings with 4 stories or less the components of the gravity system that influence the performance the most are the gravity connections and beams. Gravity connections have basically the same strength along the height of a building, regardless of the number of stories. Thus, in terms of the influence on gravity connection strength, this will logically diminish as buildings become taller because the gravity connection strength relative the SMF strength reduces. On the other hand, buildings taller than 4 stories are more influenced by the gravity columns. The reasons why the response of these buildings is dominated by the gravity columns are because the gravity columns will increase in

size with the height of the building and because taller structures are more susceptible to have drift concentrations.

7.4.1 Buildings with four stories or less

Prior to describing the steps to model the gravity system in SMFs with 4 stories or less, the importance of the gravity connections and gravity columns is briefly summarized. The importance of these two components is shown first by means of the pushover curves obtained for the 4-story model.

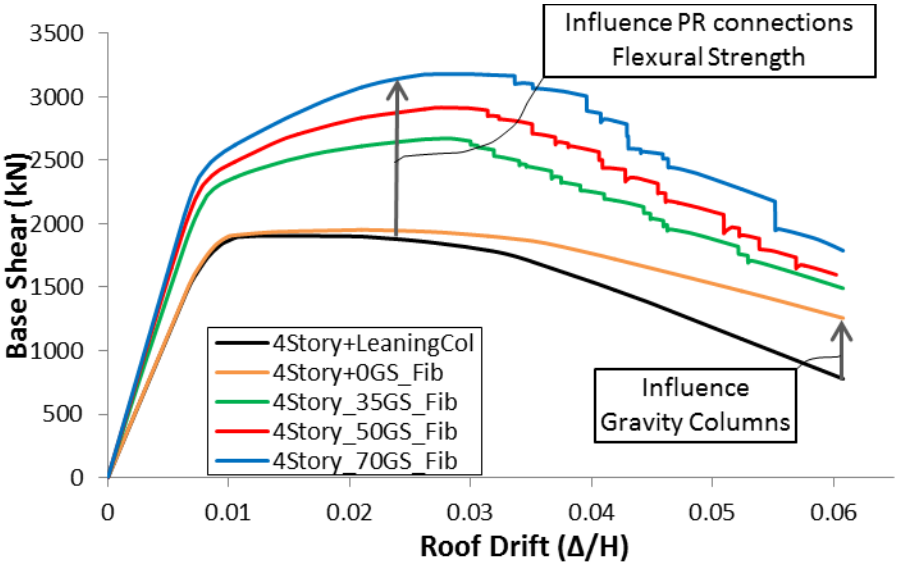

Figure 7-4 Pushover Curves 4Story model (Gravity Columns Continuous)

Figure 7-4 shows the pushover curves obtained for the 4-Story SMF. The gravity system was modeled using PR connections with varying flexural strengths. The gravity columns were modeled using force-based fiber sections and they were continuous all over their height. From this figure it can be seen that the flexural strength of the gravity connections has a significant influence on the structure's strength (overstrength). On the other hand, the influence of the gravity columns is measured on the improvement that these bring to the structure's post-yield stiffness. It can be seen that the influence of the gravity columns is not major. These results are

further demonstrated by illustrating the collapse performance of the 4-story model. Figure 7-5 presents the probability of collapse computed using the FEMA P-695 methodology. From these results it can be seen again that the major benefit on the performance comes from the gravity connections and not from the gravity columns. However it has to be pointed out that the amount of flexural strength in the gravity connection has very little influence on the performance. This was not the case for the 2-story model where the flexural strength had a significant influence.

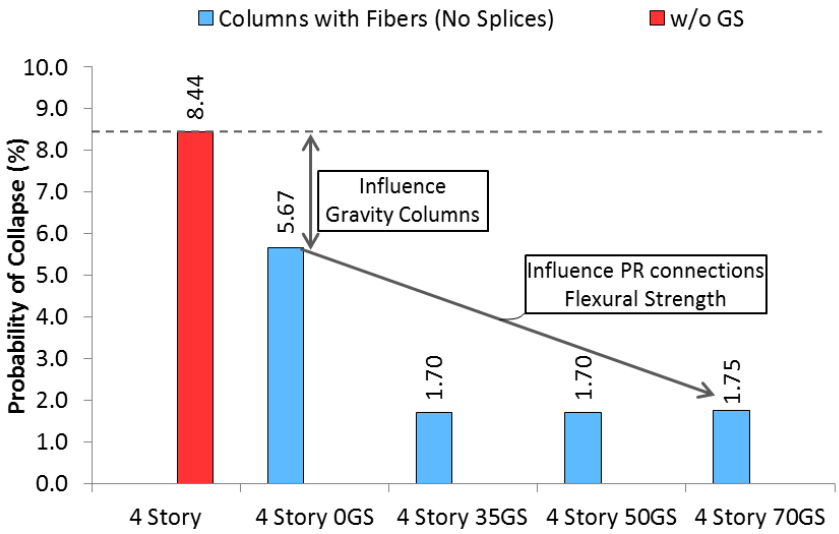

Figure 7-5 Probability of Collapse 4-Story Model (Gravity Columns Continuous)

Once the importance of the gravity connections and gravity columns were briefly overviewed, the following recommendations are given to include the gravity system on structures smaller than 4 stories:

- Gravity connections play an important role in decreasing residual displacements at DBE and reducing the probability of collapse when the structure is subjected to large earthquakes. Therefore, special care should be taken to the gravity connections in smaller structures.

- The gravity connections could be included in the model using a simple moment-rotation curve such that the one provided by ASCE 41-13, especially to perform nonlinear static pushover analyses. The backbone curve of this model could be used to perform nonlinear dynamic analysis too. For this investigation the hysteretic behavior within the backbone curve given by ASCE41-13 was characterized using the material named "Hysteretic" in OpenSees. The flexural strength of the connection should not be larger than 30% M_p of the beam to avoid yielding in the gravity columns and to be conservative since a simple model is being used. In this dissertation, a parametric investigation about the influence of strength or stiffness degradation in the gravity connections was not executed. Thus, a recommendation about these parameters cannot be done and it is recommended for future research to investigate the effect of different hysteretic behaviors in the gravity connections on structures with three or less stories.
- The effect of the gravity columns is not significant on these structures but it would be preferable to have gravity columns that do not have splices or that have splices as far away as possible from the base of the column.
- Perform nonlinear static pushover to evaluate the effect of the connections and the gravity columns is recommended.

7.4.2 Buildings between four and ten stories

As stated in the scope in this chapter, the recommendations to be given in this section apply to SMFs shorter than ten stories. The gravity system has a profound influence on the performance of these structures. The components that influence the system most are the gravity columns. Figure 7-6 shows the pushover curves obtained for the 8-story model. The gravity system was modeled using PR connections with different flexural strengths. The gravity

columns were modeled using force-based fiber sections and they were continuous all over their height.

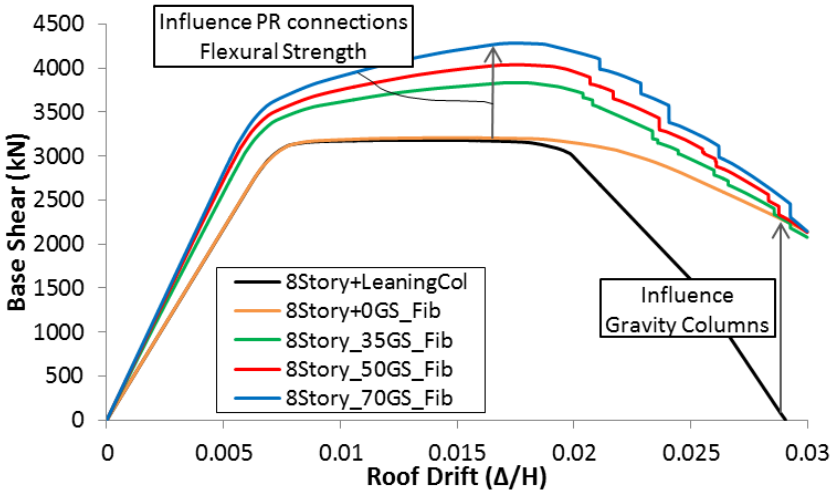

Figure 7-6 Pushover Curves 4Story model (Gravity Columns Continuous)

Figure 7-6 shows the influence that gravity columns have on the post yield stiffness of the structure. This benefit delays or prevents dynamic instability which improves the collapse performance of the building. Note that gravity columns are continuous all over their height. As a result, splices have to provide enough flexural strength to simulate continuity in the gravity columns. A procedure to evaluate this flexural strength was given in Chapter 6 (section 6.1) of this dissertation. Even though splices with partial strength will also improve the performance, it is recommended to design them with enough flexural strength to provide continuity. The gravity connections strength has some influence on the overstrength of the building but it is not as important as it was for the 4-story model.

The aforementioned statements are resembled in the collapse performance of the structure. The probability of collapse was computed using the FEMA P-695 methodology and the results are shown in Figure 7-7.

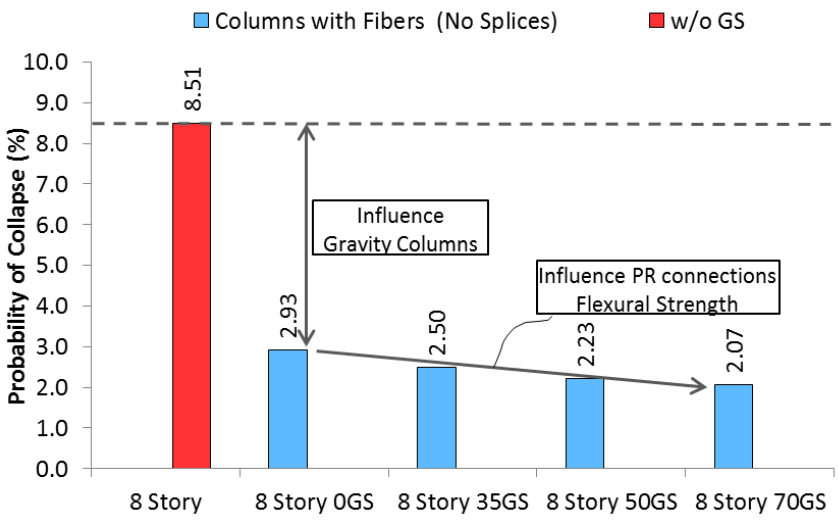

Figure 7-7 Probability of Collapse 8-Story Model (Gravity Columns Continuous)

Figure 7-7 illustrates again the important influence on the collapse performance that the gravity columns have. On the other hand, it can be seen that gravity connections have a negligible effect on the structure's performance.

Once the importance of the gravity columns and gravity connections for structures taller than 4 stories were overviewed, the following recommendations are given to include the gravity system:

- Unlike smaller buildings, the gravity connections on these systems are not as relevant and they could be neglected from the analysis. If these connections are modeled, a simple model like that provided in ASCE 41-13 could be used but as it was seen in this dissertation, their influence is not significant.
- Special focus has to be considered to the gravity columns of these structures. In order to improve the performance the most, a nonlinear static pushover analysis is should be executed to establish the amount of stiffness required by the gravity columns. Using the lumped column approach this stiffness can be found as shown in this dissertation.

- Special care should be taken to the splice's location in the gravity columns. In order to find the best location within the gravity columns, a nonlinear static pushover analysis considering the splices as a true hinge should be performed. The decision of the best location should be based on the improvement of the structure's secondary stiffness.
- The flexural strength required by the splices to provide continuity to the gravity columns depends directly on the splices location and it can be estimated as shown in this dissertation (Chapter 6).
- It is recommended to use pinned connections at the base of the gravity columns to prevent yielding. This recommendation applies to all structures.

7.5 Preliminary guidelines to include the gravity system (3-D)

Despite the fact that all the analyses performed in this investigation used two-dimensional mathematical models, different recommendations to model the gravity system in 3-D can be done as a result of the trends obtained herein and as a result of the investigation performed at PUC [5]. The preliminary guidelines to include the gravity system when modeling SMFs are:

- The gravity columns influence profoundly the response of buildings with more than four stories. In addition, it is required to include the gravity columns in a 3-D model to capture P-Delta effects correctly. Therefore, all the gravity columns should be included in the model and their stiffness should be considered. Moreover, performing a nonlinear static pushover analysis would be required to quantify the improvement that gravity columns bring to the system.
- The flexural strength of the columns that bent about the weak axis should not be incorporated in the analysis. This is done by locating hinges at the bottom and top of the column in each story. In this investigation it was proven that the gravity columns that

bent about the strong axis do not yield when the gravity connections do not have a significant flexural strength (less than 30%M_p). However, more research is required to establish if yielding would occur in the columns on the weak axis.

- The gravity connections could be included in the model using a simple model like the one given by the ASCE41-13. However, it is important to note again that no research was done herein regarding the gravity connections that frame into the weak axis of the columns. Therefore these connections should be excluded from the analysis.

Every column in the building should include P-Delta transformations in order to quantify correctly torsion. •

7.6 References

[1] ASCE, Minimum design loads for buildings and other structures, American Society of Civil Engineers : Structural Engineering Institute, Reston, Va., 2010.

[2] F. P695, Quantification of Building Seismic Performance Factors, Fededral Emergency Management Agency, Washington, D.C, 2009.

[3] ASCE, Seismic Rehabilitation of Existing Buildings (ASCE/SEI 41-13), American Society of Civil Engineers Reston, Virginia, 2013.

[4] NIST, Evaluation of the FEMA P-695 Methodology for Quantification of Building Seismic Performance Factors, National Institute of Standards and Technology, USA, 2010.

[5] F.X. Flores, F.A. Charney, D. Lopez-Garcia, J.C. De La Llera, The Influence of Accidental Torsion on the Inelastic Response of Buildings During Earthquakes, 11th Chilean Conference on Seismology and Earthquake Engineering, (2015).

[6] F.X. Flores, D. Lopez-Garcia, F.A. Charney, Assessment of floor accelerations in special steel moment frames, Journal of Constructional Steel Research, 106 (2015) 154-165.

Chapter 8: Summary, Conclusions and Future Work

The purpose of the research described in this dissertation was to evaluate the influence of the gravity framing system on the seismic performance of Special Steel Moment Frames (SMFs). In the first section of the study, very detailed 2D models that included the gravity system were analyzed. The objective was to quantify the importance of different component attributes, such as: the flexural strength of gravity beam-to-column connections, the influence of gravity columns where the beam-to-column connections are assumed to have zero strength, yielding in the gravity columns, and the influence of splices in the gravity columns. Using the FEMA P-695 [1] methodology, the collapse performance of the structures was evaluated. One of the most important conclusions obtained was the profound effect that gravity columns have on the response of SMFs, especially on the 8-story model.

As a result of the aforementioned conclusion, the second part of the investigation focused more in depth on the effect that gravity columns have on the seismic performance of SMFs. Using what is called in this study the "lumped column" approach, the gravity columns were accumulated into one continuous elastic element and pinned at the base. It was proved that this approach can be used if the gravity connections do not have a significant flexural strength and if the splices in the gravity columns have enough flexural capacity to provide effectively full continuity to the column. Moreover, this approach could be utilized in the FEMA P-695 methodology to provide insight into the role of the gravity system on computed performance factors. The high variability of the gravity system configuration is resolved with this approach, so generic archetypes with the gravity framing would be able to be analyzed.

The major findings from the research are presented in two journal and one conference articles, and are summarized below:

Paper: Influence of the Gravity Framing System on the Collapse Performance of Special Steel Moment Frames, *Journal of Constructional Steel Research.*

- The simple model taken from ASCE41-13 [2] used to evaluate the gravity connections was sufficient for the purpose of this study. The most important advantage of the model was that it allowed an evaluation of the influence of the flexural strength possessed by the gravity connections. As a result it was found that gravity connections do not play an essential role on taller buildings (8-story model) but they had a profound influence on smaller buildings (2-story model).

- Stronger PR connections increase overstrength and the Collapse Margin Ratio (CMR), especially on smaller buildings such as the 2- and 4-story buildings. However, the amount of flexural strength (35%M_p, 50% M_p or 70%M_p) barely influenced the results of the 4- and 8-story models.

- The period of vibration of the analyzed structures decreases depending on the gravity connections flexural strength. The reduction varied depending on the structure but it can be up to 15%.

- The columns of the gravity system have a relevant influence on the performance, especially when they are continuous (splices provide enough flexural strength). The continuous stiffness delivered by the columns reduced drift concentrations and the likelihood to have weak story mechanisms. This effect was more beneficial in taller structures and it was reflected in the results of the collapse evaluation.

- The probability of collapse decreased significantly when just the gravity columns (continuous over their height) were included as part of the lateral resisting system.

- Yielding in the columns of the gravity system occurred for the cases where the gravity connections have significant flexural strength (greater than about 30% of the plastic moment capacity of the gravity beam). Even though the results were not highly influenced by yielding it is necessary to analyze structures including the nonlinear behavior of the gravity columns when the connections have significant strength.

- In general, the improvement caused by the gravity system decreases when the splices are considered in the analysis. However, in spite of the reduction, the performance was still better than the SMFs by themselves.

- The location of the splices is an important factor to consider because it interrupts the continuity provided by the gravity columns. The FEMA P-695 Collapse Margin Ratio changed depending on the pattern used for the splices. In most cases leveled splices improved the performance more than staggered splices. But, columns with no splices showed the best results.

- In general the incorporation of the gravity system improved the collapse capacity of SMFs based on the FEMA P-695 methodology.

Paper: The Influence of Gravity Column Continuity on the Seismic Performance of Special Steel Moment Frame Structures, *Journal of Constructional Steel Research.*

- The gravity columns do not yield if the gravity connections have low flexural strength capacity (less than 30%M_p), and pinned at the base.

- A disadvantage of improving the response of SMFs is that the gravity column's splices are recommended to have full moment capacity. However, the flexural capacity depends on the splice location within the gravity columns.

- The gravity columns if they are continuous (splices provide enough flexural strength), have a direct effect on the post yield stiffness of the structure. The slope of the secondary stiffness increases reducing the likelihood of having excessive residual deformation and dynamic instabilities.

- The influence of the gravity columns is beneficial for all the 2-, 4- and 8-story buildings analyzed. However, the improvement on the collapse performance that the 8-story model presents is significant in comparison to the other two buildings.

- It is known that continuous stiffness can prevent or reduce the probability of buildings to develop drift concentrations or weak story mechanisms. This was reflected in this study by reducing the probability of collapse of the structures.

- The stiffness to be assigned to the gravity columns in this study was taken as a ratio of the SMFs column's inertia. This was an arbitrary way of measuring the number of gravity columns that the building should have. However, the adequate stiffness of the gravity columns could be obtained directly by performing nonlinear static pushover analysis.

- There is a direct relation between the effects of the gravity columns on the pushover curves and an adequate stiffness to be assigned to the gravity columns. The benefit behind this finding is that once the adequate stiffness is established, it can be used to

establish the stiffness needed by the gravity columns or to obtain the number of gravity columns required by the gravity system.

- The continuous stiffness provided by continuous gravity columns helps the structure deform in a pure shear mode. As a result drift concentrations and the likelihood of story mechanisms are decreased during an earthquake.

- One of the conclusions presented in the ATC 76-1 [3] project was that "there is a need to develop design concepts that prevent (or at least delay) the formation of partial mechanisms in lower stories of special SMF systems". By observing how the collapse performance of SMFs improved in this study and by knowing the effect that gravity columns have on the performance, it could be concluded that they are an option to fulfill this need.

- The lumped column approach is an interesting proposal to overcome the problem of incorporating the gravity system to perform the FEMA P-695 methodology which for the foreseeable future will utilize 2D models.

Paper: The Influence of the Gravity System Framing on the Seismic Performance of Special Steel Moment Frames, *Proceedings of the 10th National Conference in Earthquake Engineering.*

- It was found that in general, the strength of the gravity connections reduces the residual displacement at DBE and MCE level. However, as already stated the effect is less important in taller buildings.

- Continuous gravity columns reduced residual displacement at DBE or MCE intensities primarily when the structure was subjected to large deformations. This was reflected in

the interstory drift, where drift concentrations were reduced preventing the collapse. The influence of gravity columns is more important in the taller buildings such as the 8-story frame.

- Base shear increases more when the gravity system is included in short structures because the strength of the gravity connections has more influence.

8.1 Future Work

The investigation performed as part of this dissertation covered a wide spectrum of aspects regarding the influence of the gravity system on the collapse performance of SMFs. However, as a result of some of the findings and because of the limited scope of the research, future research is required to fully understand the importance of the gravity frame. The recommendations for future investigations are:

- Perform analyses in 3D to include torsion and look into the effect of the gravity system. Despite the fact that the mathematical models analyzed in this study were very detailed, they are not capable to represent other important effects such as torsion and secondary P-Delta effects since they were modeled in 2D. Moreover

- A study to implement the lumped column approach when 3D analysis is performed should be investigated. Having one lumped column does not incorporate the torsional P-Delta effects into the analysis which is of extreme importance as demonstrated by Flores et al. [4]. Thus, a study to establish a minimum number of lumped gravity columns required to satisfactorily include these torsional effects needs to be carried out.

- Investigate the influence of more realistic gravity connections on low rise buildings.

- Study the influence of a more accurate model of the base connections rather than consider them to be pinned or fixed.

- Perform laboratory tests of gravity column splices to characterize their real flexural capacity and hysteretic behavior.

- Perform an investigation to establish an optimal location for the gravity column's splices.

- Investigate the possibility to establish seismic modification coefficient (*R*) values that are dependent on the gravity columns. The improvement on the post yield stiffness that gravity columns bring to the structure is directly related to the collapse performance of the structure. However, this improvement depends on the amount of stiffness provided by the gravity columns. Thus, a seismic modification coefficient (*R*) value could be established depending on the amount of stiffness provided by the gravity columns. The major issue to overcome would be the minimum base shear imposed by ASCE 7-10 because with this barrier, the *R* value cannot increased significantly beyond the current maximum of *R*=8.

- Study the possibility of modifying the strong column weak beam requirements by incorporating the gravity columns as part of the lateral resisting system.

- Evaluate the influence of the gravity columns in high rise buildings.

- Based on the results obtained in this dissertation, one can conclude that using the lumped gravity column approach is a good alternative to analyze generic archetypes. The influence of the gravity columns should be studied in different structural systems.

8.2 References

[1] F. P695, Quantification of Building Seismic Performance Factors, Fededral Emergency Management Agency, Washington, D.C, 2009.

[2] ASCE, Seismic Rehabilitation of Existing Buildings (ASCE/SEI 41-13), American Society of Civil Engineers Reston, Virginia, 2013.

[3] NIST, Evaluation of the FEMA P-695 Methodology for Quantification of Building Seismic Performance Factors, National Institute of Standards and Technology, USA, 2010.

[4] F.X. Flores, F.A. Charney, D. Lopez-Garcia, J.C. De La Llera, The Influence of Accidental Torsion on the Inelastic Response of Buildings During Earthquakes, 11th Chilean Conference on Seismology and Earthquake Engineering, (2015).

Tenth U.S. National Conference on Earthquake Engineering
Frontiers of Earthquake Engineering
July 21-25, 2014
Anchorage, Alaska

Appendix A
THE INFLUENCE OF THE GRAVITY SYSTEM FRAMING ON THE SEISMIC PERFORMANCE OF SPECIAL STEEL MOMENT FRAMES

F. X. Flores[1] and F. A. Charney[2]

ABSTRACT

It is common practice to neglect the gravity framing system when seismic analysis is performed on building structures. Yet, past earthquakes such as the 1994 Northridge earthquake have demonstrated that the gravity system can act as an essential back up system when the main lateral resisting frame loses strength. This study focuses on the benefits of including the gravity system on the expected seismic performance of special steel moment frames (SMFs).

The 2-, 4- and 8-story SMFs from the ATC 76-1 project are reanalyzed with and without the gravity system using the FEMA P-695 procedure. The gravity system is incorporated using partially restrained (PR) connections idealized using ASCE 41-13, a bilinear hysteresis model, and assuming that the strength of the PR connections is a percentage (0, 35, 50 and 70%) of the plastic capacity of the beam. Nonlinear dynamic (response history) analysis is used to compare the influence of the gravity system on the interstory drifts, residual displacements and base shear for the Maximum Considered (MCE) and Design Basis (DBE) Earthquakes, as well as the influence of the gravity system on the collapse margin ratio (CMR). The results indicated that the gravity system has a significant impact on drifts, residual displacements, and the probability of collapse, even when a minimum strength in the gravity framing connections is assumed.

[1] Ph.D. Candidate - Via Department of Civil and Environmental Engineering, Virginia Tech, VA 24060,
Ph.D. Candidate - Pontificia Universidad Católica de Chile , Santiago-Chile
[2] Professor, Department of Civil and Environmental Engineering, Virginia Tech, VA 24060, USA

Flores FX, Charney FA. The Influence of Gravity Sistem Framing on the Seismic Performance of Special Steel Moment Frames. *Proceedings of the 10th National Conference in Earthquake Engineering*, Earthquake Engineering Research Institute, Anchorage, AK, 2014.

Tenth U.S. National Conference on Earthquake Engineering
Frontiers of Earthquake Engineering
July 21-25, 2014
Anchorage, Alaska

The Influence of the Gravity System Framing on the Seismic Performance of Special Steel Moment Frames

F. X. Flores[1] and F. A. Charney[2]

ABSTRACT

It is common practice to neglect the gravity framing system when seismic analysis is performed on building structures. Yet, past earthquakes such as the 1994 Northridge earthquake have demonstrated that the gravity system can act as an essential back up system when the main lateral resisting frame loses strength. This study focuses on the benefits of including the gravity system on the expected seismic performance of special steel moment frames (SMFs).

The 2-, 4- and 8-story SMFs from the ATC 76-1 project are reanalyzed with and without the gravity system using the FEMA P-695 procedure. The gravity system is incorporated using partially restrained (PR) connections idealized using ASCE 41-13, a bilinear hysteresis model, and assuming that the strength of the PR connections is a percentage (0, 35, 50 and 70%) of the plastic capacity of the beam. Nonlinear dynamic (response history) analysis is used to compare the influence of the gravity system on the interstory drifts, residual displacements and base shear for the Maximum Considered (MCE) and Design Basis (DBE) Earthquakes, as well as the influence of the gravity system on the collapse margin ratio (CMR). The results indicated that the gravity system has a significant impact on drifts, residual displacements, and the probability of collapse, even when a minimum strength in the gravity framing connections is assumed.

Introduction

Seismic performance of structures is often quantified neglecting the influence of the gravity system and analyzing just the main lateral load resisting system of the structure. Special Steel Moment Frames (SMFs) have been studied analytically and through experience, and performance has not always been acceptable. One event that caused researchers to look more in depth at the design and analysis of SMFs was the 1994 Northridge California earthquake. During this earthquake several SMFs connections failed. However, the buildings did not collapse after the failure of the main connections, suggesting that the gravity system provides a reserve strength mechanism within the structure [1].

After the Northridge earthquake, several studies were performed to evaluate SMFs and the connections of the gravity system. Liu and Astanneh [2] performed cyclic tests on different types of simple connections to characterize their hysteretic behavior. One of the conclusions was

[1] Ph.D. Candidate - Via Department of Civil and Environmental Engineering, Virginia Tech, VA 24060,
Ph.D. Candidate - Pontificia Universidad Católica de Chile, Santiago-Chile.
[2] Professor, Department of Civil and Environmental Engineering, Virginia Tech, VA 24060, USA

Flores FX, Charney FA. The Influence of Gravity Column Continuity on the Seismic Performance of Special Steel Moment Frames. *Proceedings of the 10th National Conference in Earthquake Engineering*, Earthquake Engineering Research Institute, Anchorage, AK, 2014.

that these connections have large rotation capacity and their strength can vary depending of the type of configuration.

There has been extensive experimental and analytical research on the seismic behavior of SMFs, but there are relatively few studies that include the gravity system in the analysis. Gupta and Krawinkler [3] studied the response of SMFs at various seismic hazard levels. Different models were used to perform nonlinear static and dynamic analyses. The authors concluded that the seismic behavior of the structures improves at large drifts when the gravity system is included. However, a number of factors such as the number of gravity frames, the properties of the gravity connections, boundary conditions and major-minor axis orientation of columns, and the magnitude of drift demand have an influence on the performance. Among these factors, according to Gupta and Krawinkler [3], the contribution of the gravity columns is the most important, with the gravity connections playing a much less significant role. The main finding or conclusion from the study was that the gravity system could increase the post-yield stiffness, thereby reducing the influence of P-Delta effects under high intensity ground motions.

Lee and Foutch [4] used post-Northridge SMFs incorporating the gravity system as part of an analytical research program. The objective of the investigation was to determine if the analyzed structure satisfies the collapse prevention (CP) limit state criteria at the Maximum Considered Earthquake (MCE). A procedure to evaluate if the structure satisfies this limit state is proposed in the investigation, and the results showed that SMFs analyzed including the gravity system would perform well at the MCE. The contribution of the gravity system to performance was not quantified, however, because the analysis was not performed with and without the contribution from the gravity frame.

Another important property that the gravity system provides to the structure is the continuous stiffness of the columns in the gravity system. MacRae et al. [5] revealed that this effect could reduce story drift concentrations and prevent weak story mechanisms in braced frames. The effect was also noticed by Gupta and Krawinkler [3]. Continuous column stiffness is provided by elements in the structure that are continuous all over the height (no splices or splices provide full continuity). Tagawa [7] studied the continuous stiffness provided by the gravity columns on SMFs. One of the conclusions made by the author was that continuous columns decrease drift concentrations when dynamic analysis is performed. An extensive investigation can also be found in the companion paper about the influence of columns continuity on the collapse performance of SMFs [6].

A new and different investigation was executed by Zareian et al. [9] as part of the ATC 76-1 project [10]. SMFs were studied using the P-695 methodology [11] to assess their collapse performance. The analyzed buildings ranged from 1 to 20 stories in height and they were designed complying with the minimum requirements established by the ASCE 7-05 [12] and AISC 341-05 [13] with the exception that the deflection amplification factor (C_d) was taken to be equal to the response modification coefficient (R), as specified in the FEMA P-695 methodology. The analytical basis for the design of the systems was the equivalent lateral load procedure (ELF) and Response Spectrum Analysis procedure (RSA). Since the objective of the study was

to evaluate the collapse probability of "performance groups" of generic buildings, the P-695 methodology specifies that the strength and stiffness of the gravity system is not included. The results of the Zareian investigation show that one of the performance groups designed using the RSA and for seismic design category D_{max} *(S_s=1.5g, S_1=0.6g),* do not satisfy the collapse requirements.

From these past studies, it can be observed that the influence of the gravity system on the seismic performance has not been investigated in detail. Therefore, to better clarify the influence of the gravity system on seismic response, the 2, 4 and 8-Story buildings taken from the study performed by Zareian et al. [9] are reanalyzed with and without the gravity system. Using the same Far-Field ground motions specified by the FEMA P-695 methodology, the structures are subjected to different hazard level earthquakes. The parameters to be compared at the Design Based Earthquake (DBE) and Maximum Considered Earthquake (MCE) are residual displacement, interstory drift, base shear, and the Collapse Margin Ratio. A more detailed study of the collapse performance of these buildings is presented in Flores and Charney [8].

Building Overview

The 2, 4, and 8-story buildings have the same plan geometry. The chosen buildings were the ones designed using the RSA approach. The connections at the base of the columns are fixed for the 4 and 8-story models and pinned for the 2-story model. Fig. 1 shows the plan layout for all the buildings analyzed. The SMFs have prequalified reduced beam sections (RBS) connections and have been designed to resist the seismic forces and provide stability against P-Delta shears.

The structures were analyzed in the East-West direction. The gravity frame considered to be part of the system is shown also in Fig. 1. In order to evaluate the influence of just the gravity system, the SMFs columns (A-3, F-3) oriented on the weak axis are considered to have zero lateral strength (continuous stiffness effect is neglected and beam to column connections are pinned). The shaded area in Fig. 1 represents the tributary area for gravity loading on the individual SMFs. The gravity connections were considered as pinned for the gravity beam design, and they are assumed to be PR connections for lateral load analysis. The design of the gravity system was performed in SAP2000 using A992 steel material for the members. The section sizes and other pertinent information can be found in Flores and Charney [8].

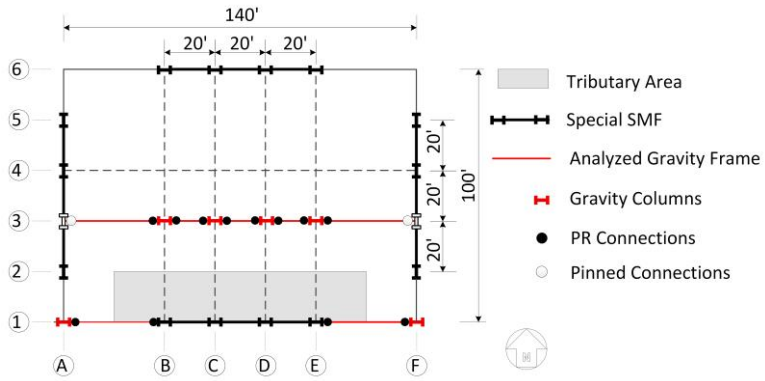

Figure 1. Buildings plan view.

The bay width (center line dimensions) between columns of each SMF is 20'. The height of the first story is 15' (to top of steel beam), and the height of all other stories is 13'. The dead load is 90 psf uniformly distributed over each floor, and the cladding load is applied as a perimeter load of 25 psf. Unreduced live load is 50 psf on all floors and 20 psf on the roof.

Modeling the Special Moment Frame

The nonlinearities incorporated into the analysis include rotational plastic hinges in the RBS regions of the beams, rotational plastic hinges at the ends of the columns and inelastic shear deformation in the panel zones. The platform used to perform the analysis was OpenSees [14]. The procedure used to model the structure was the same as described in the ATC 76-1 report [10]. The P-Delta effect was included in the analysis by adding a leaning column when the SMF was analyzed by itself. The leaning column has zero flexural stiffness and is placed parallel to the structure. The load applied to this column represents the destabilizing load that comes from the gravity load and is equal to $1.05D + 0.25L$ on a tributary area equal to half of the plan area minus the shaded area (Fig. 1). When the gravity system is included in the analysis, the P-Delta effects are modeled using geometric stiffness for all columns in the structure.

A Rayleigh damping of 2.5% is assigned at the first mode period T_1 and at $T=0.2T_1$ in all cases. As proposed by Zareian (2010) [15], stiffness proportional damping is assigned to elements that remain elastic, and mass proportional damping is assigned to nodes or elements where mass is lumped.

Modeling the Gravity System

The gravity system was modeled explicitly in the analysis. It was placed parallel to the SMF because it was assumed that every floor acted as rigid diaphragm. The nonlinearities modeled in the gravity frame were the plastic hinges at the connections and possible plastic hinges along the height of the columns. The gravity columns usually are considered to behave elastically. However, as demonstrated by Flores and Charney [8], gravity columns can yield when the gravity connections have strength. Therefore, for this study the gravity columns were

modeled using fiber elements with a bilinear material that has a strain hardening equal to 10% of the initial stiffness. Using fibers to model the columns bring up an important benefit that is the inclusion of the P-M interaction in the analysis. A disadvantage of the fiber approach is that the strength degradation is not considered, and this is why the columns of the SMFs were modeled as described in the ATC 76-1 report.

Modeling PR Connections

Partially restrained connections have the capability to sustain large deformations as was demonstrated by Liu and Astanneh [2]. Unfortunately a hysteretic behavior that represents the cyclic characteristics of these connections has not yet been defined. The most common approach to use these connections when nonlinear analysis is required is by matching experimental results with a predefined hysteretic model. More difficult techniques like the component method or finite element analysis are still computationally expensive. The aim of this study is to evaluate the gravity system on the seismic performance at different hazard levels, so using a simple hysteretic behavior to characterize the connections is considered to be a good start. The model used for the analyses was taken from ASCE 41-13 [16] and the details of modeling this connection can be found in [16]. However, an important assumption made for this study is that the limit state that controls the failure of the PR connections is the "Flexural Failure of Angle".

One of the most important advantages of using this model is that strength of the connection can be a parameter of study. For this investigation, the strength or capacity of the PR connections was assumed to be a percentage of the plastic moment of the beam (M_p). The percentages used to define the strength of the connections are 0, 35, 50 and 70% and they are assigned to every connection in the gravity frame. The PR connections with no strength (0%) were defined to assess the influence of the gravity columns. The lower bound strength of 35% considered for this analysis was determined as the minimum strength required to prevent the connections to reach a rotation of 0.005 radians (yielding point) under gravity loads.

The following sections illustrate the results of different parameters when the SMFs analyzed with and without the gravity system are subjected to ground motions scaled to the DBE and MCE. The parameters to be compared are Residual Displacement, Interstory Drift and Base Shear. The nomenclature used to identify the buildings with the gravity system is placing the percentage of PR connections strength next to the model name. For instance, 8Story_0GS is the structure that includes the gravity system with PR connections that have zero strength.

Residual Displacement at DBE and MCE

The residual displacement is measured at the roof of the building and it is the unrecovered deformation that the structure suffered after being subjected to an earthquake. In this section the 2, 4 and 8-story buildings are analyzed using the 44 ground motions from P-695. The ground motions were scaled to the DBE and MCE and the results are presented in the following sections. The influence of the gravity system at DBE and MCE for the 2-story model is similar. In general, the strength of the connections reduces the residual displacements. The

results for almost all the ground motions are very similar between the 2 story model without the gravity frame and the one that includes the gravity system. However, when the ground motion caused large roof displacement, the effect of the gravity system is important. This is the case of the ground motion "HEC090" shown in Fig. 3 (b), where the gravity system could be preventing the collapse of the structure. PR connections have a significant influence reducing the residual displacement in almost every case.

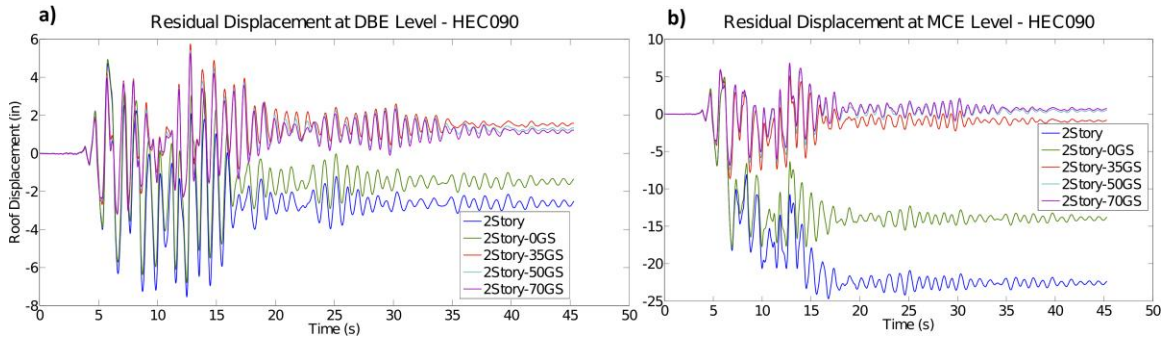

Figure 3. Residual displacement 2-story model a) DBE level b) MCE level.

The results of the residual displacement for the 4-story building show the same trend as the 2-story building. The influence of the gravity columns (PR connections with no strength) is minimal at DBE and MCE except for large drifts. The gravity connections have an important impact reducing the residual displacement. Fig. 4 (a) and (b) shows the residual displacements for the same ground motion at DBE and MCE level. It can be observed from Fig. 4 (b) that the ground motion "NIS000" caused the collapse of the 4-story building when gravity connections are not modeled. However, the structure performs better when the gravity system is incorporated. The gravity columns (gravity connections with zero strength) prevented the collapse and the PR connections reduced the residual displacement significantly.

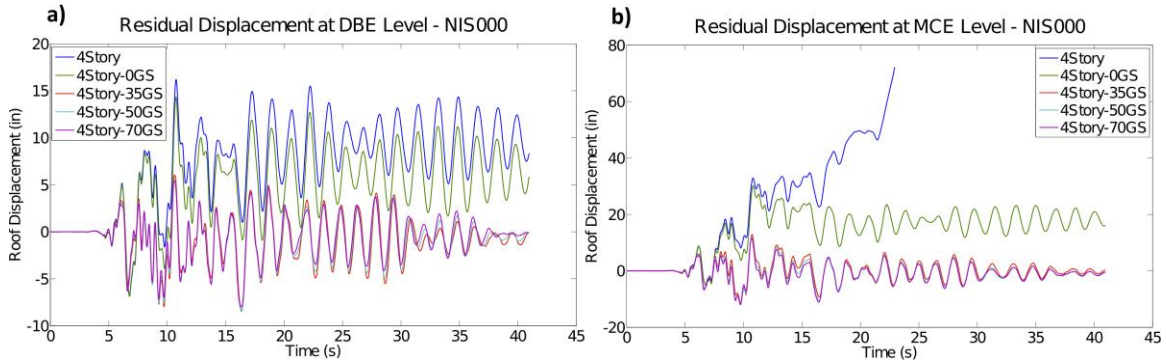

Figure 4. Residual displacement 4-story model a) DBE level b) MCE level

The 8-story model results have also similar trends to those already presented for the 2 and 4-story models. The gravity columns have almost no effect when the displacement demand is

small and the PR connections reduce the residual displacement in almost every case (Fig. 5 (a)). However, the 8-story model is more vulnerable to have drift concentrations that could lead to collapse under the MCE level earthquake and this is when the gravity system plays an important role. As it was already mentioned, the gravity columns have a decisive effect on large displacements. Among the 44 ground motions, 1 caused collapse to all the buildings and 3 caused the collapse of the 8-story model without the gravity system.

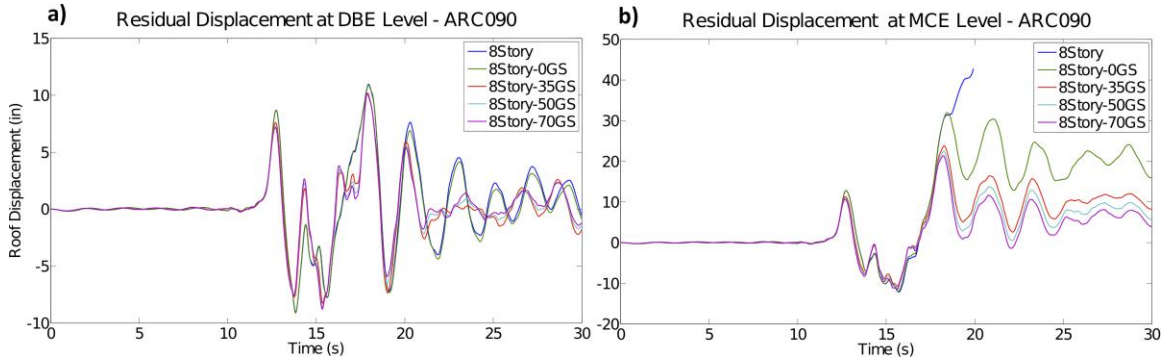

Figure 5. Residual displacement 8-story model a) DBE level b) MCE level.

Fig. 5 (b) presents the results of the 8-story model subjected to a ground motion scaled to the MCE level earthquake. This figure demonstrates the importance of the gravity system to prevent collapse in SMFs. The influence of the gravity columns, represented by the gravity system with zero strength connections, is very important to control excessive displacements that could lead to collapse. On the other hand the PR connections strength helped to reduce the residual displacement.

Interstory Drift at DBE and MCE

Another parameter used to compare the performance of SMFs with and without the gravity system is the interstory drift. This parameter is computed as the difference in displacement between two adjacent floors of the building divided by the story height that separates the floors. Since the structures were analyzed for 44 ground motions, the median values of the interstory drift are presented. The median was chosen because of two reasons: to be consistent with the P695 procedure when the ground motions are scaled and because some of the interstory drifts were very large due to collapses of the structure. It has to be mentioned that the median and mean values are close if the values when the structure collapse are dismissed. Fig. 6 (a) and (b) presents the 2-story building interstory drift at DBE and MCE level respectively while Fig. 6 (c) presents the interstory drift for the ground motion displayed in Fig. 3 (b). This ground motion caused large deformation in the building. From these results, it can be seen the important effect that gravity connections have on the roof residual displacement. The gravity columns (PR connections with zero strength) have almost no effect for this building on DBE and MCE hazard levels except when large displacements occurred in the structure (Fig 6 (c)).

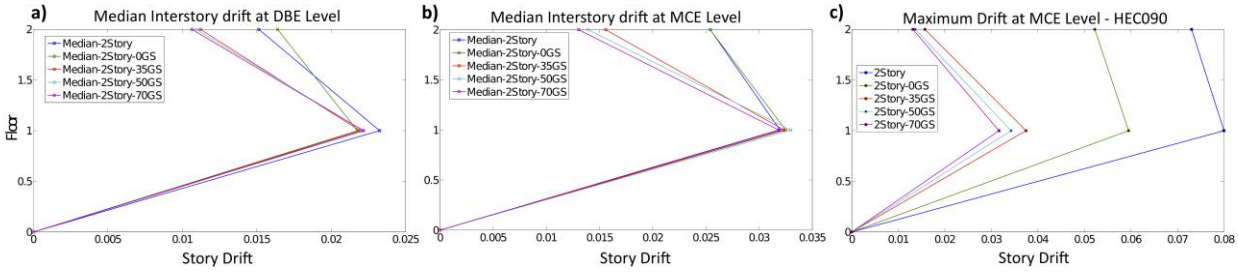

Figure 6 Median interstory drift 2-story model a) DBE level b) MCE level c) Large demand

Figs. 7 (a), (b) presents the median interstory drift at DBE and MCE level results for the 4-story model while Fig. 7 (c) displays the interstory drift for the ground motion presented in Fig. 4 (b). At both hazard levels, the gravity connections reduced the interstory drift considerably. The gravity columns have almost no effect at DBE and MCE level when the structure does not experience large demands. However, from Fig. 7 (c) it can be seen how the gravity columns (4-Story 0GS) reduce drift concentrations in the first story and prevents the structure from collapse.

Figs. 8 (a) and (b) presents the median interstory drift at DBE and MCE level results for the 8-story model and Fig. 8 (c) displays the interstory drift for the ground motion presented in Fig 5. (b). From these figures it can be seen that at DBE and MCE level the effect of the gravity system is not as important as it was for the 2 and 4-story models.

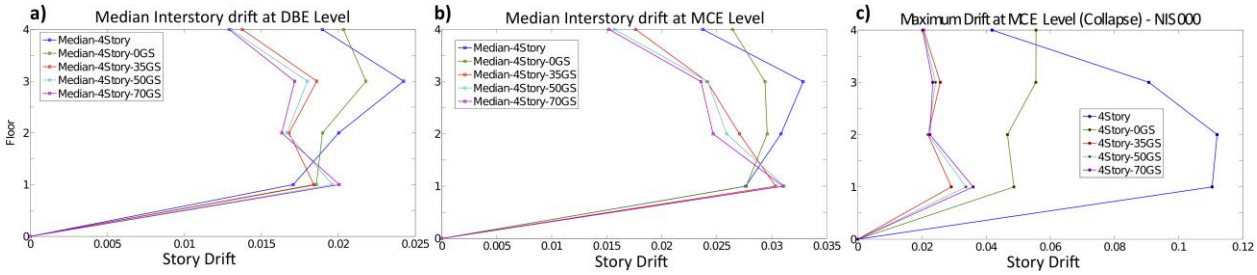

Figure 7 Median interstory drift 4-story model a) DBE level b) MCE level c) Collapse.

The influence of the gravity connection strength has been diminished for tall buildings. However, the effect of the gravity columns (8-Story 0GS) is more important at MCE level when the structure collapses (Fig. 8 (c)). It reduces the drift concentrations on the first floor in a manner that avoids collapse.

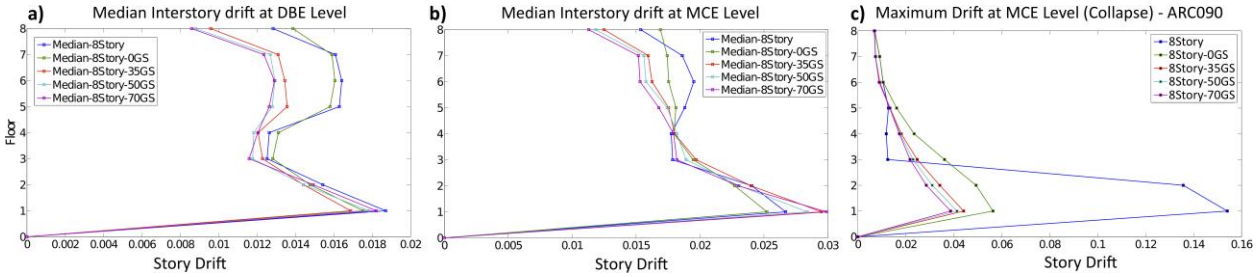

Figure 8 Median interstory drift 8-story model a) DBE level b) MCE level c) Collapse.

Base Shear at DBE and MCE

Base shear is the last parameter to be compared when the gravity system is included in the analysis. The median base shear for the 44 ground motions at DBE and MCE level was computed and it is shown in Fig. 9. From this figure, several observations can be made. The base shear increases at MCE level but not significantly. As it was expected, the base shear increases when the gravity system is included. The base shear for the 2-story model, at DBE and MCE levels increases around 6, 22, 25 and 30% when the gravity system have connections with 0, 35, 50 and 70% respectively. On the other hand the 4 and 8-story base shear increased around 4, 12, 16 and 19% when the gravity system have connections with 0, 35, 50 and 70% strength.

Collapse Performance Using FEMA P-695 Methodology

The gravity system, as it was already shown in the previous results, has the potential of improving the seismic performance. The influence of the gravity system is more important at MCE than DBE level. In this part of the study, the collapse performance of the structures is evaluated using the FEMA P-695 procedure. The parameters to be compared from this methodology are the collapse margin ratio (CMR) and the probability of collapse. Note that the CMR for the 2,4 and 8 story models are almost the same as computed by Zareian et al. [9].

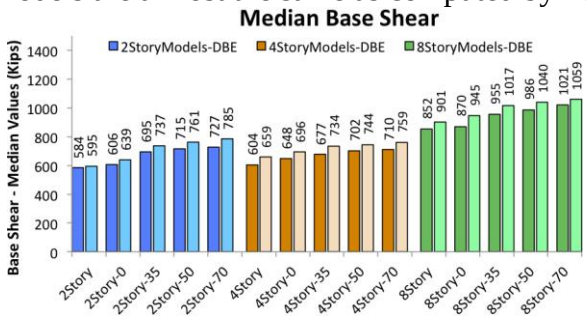

Figure 9. Median base shear at DBE and MCE levels.

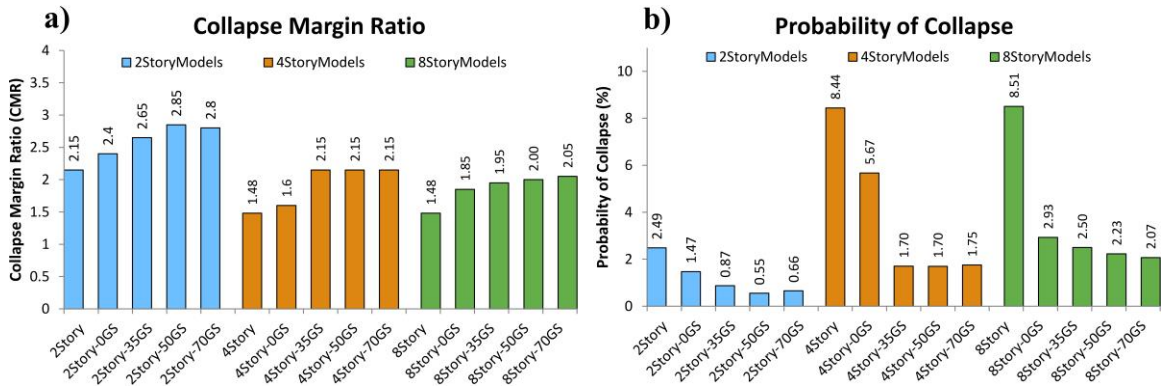

Figure 10. Collapse performance a) CMR b) Probability of collapse.

Fig. 10 a) presents the results of obtaining the CMR's for all the analyzed models. It can be seen from this figure the effect of the gravity connections strength is more important for the 2 and 4-story models. However, the 4-story model has the same collapse performance for all the different PR connections strengths. The 8-story model CMR improves considerably when the gravity columns are included in the analysis but the effect of the gravity connections strength is minimal. These statements are reflected directly in Fig. 10 b) where the probabilities of collapse were computed. For instance the probability of collapse for the 8-story building goes from 8.51% to 2.93% when the gravity columns are included in the analysis.

Conclusions

After performing this study, the following conclusions can be made regarding the influence of the gravity system on the seismic performance of SMFs.

- In general, the strength of the gravity connections reduces the residual displacement at DBE and MCE. The effect is less important in taller buildings.
- Continuous gravity columns (Gravity connections with no strength) reduced residual displacement at DBE or MCE primarily when the structure was subjected to large deformations. This was reflected in the interstory drift, where drift concentrations were reduced preventing collapse. The influence of gravity columns is more important in the taller buildings such as the 8-story frame.
- Base shear increases more when the gravity system is included in short structures because the strength of the gravity connections has more influence.
- Collapse performance of SMFs improved considerably with the gravity system.

Acknowledgments

The work presented herein was possible through the support of the National Institute of Standards and Technology, award number 60ANB10D017.

References

[1] R.T. Leon, Composite connections, *Progress in Structural Engineering and Materials*, 1 (1998) 159-169.

[2] J. Liu, A. Astaneh-Asl, Cyclic testing of simple connections including effects of slab, *Journal of Structural Engineering*, 126 (2000) 32-39.

[3] A. Gupta, H. Krawinkler, Behavior of ductile SMRFs at various seismic hazard levels, *Journal of Structural Engineering*, 126 (2000) 98-107.

[4] K. Lee, D.A. Foutch, Performance evaluation of new steel frame buildings for seismic loads, *Earthquake engineering & structural dynamics*, 31 (2002) 653-670.

[5] G.A. MacRae, Y. Kimura, C. Roeder, Effect of column stiffness on braced frame seismic behavior, *Journal of Structural Engineering*, 130 (2004) 381-391.

[6] Flores F. X., Charney F. A. The Influence of Gravity Column Continuity on the Seismic Performance of Special Steel Moment Frames. *Proceedings of the 10th National Conference in Earthquake Engineering*, Earthquake Engineering Research Institute, Anchorage, AK, 2014.

[7] H. Tagawa, Towards an understanding of seismic response of 3D structures-stability & reliability, Doctor Thesis, Washington: University of Washington, (2005).

[8] F. Flores, F. Charney, Influence of the Gravity Framing System on the Collapse Performance of Special Steel Moment Frames, *Journal of Constructional Steel Research* (To be published), (2013).

[9] F. Zareian, D. Lignos, H. Krawinkler, Evaluation of seismic collapse performance of steel special moment resisting frames using FEMA P695 (ATC-63) methodology, in: *Proceedings of Structures Congress ASCE*, New York, 2010.

[10] NIST, Evaluation of the FEMA P-695 Methodology for Quantification of Building Seismic Performance Factors, National Institute of Standards and Technology, USA, 2010.

[11] FEMA P695, Quantification of Building Seismic Performance Factors, Fededral Emergency Management Agency, Washington, D.C, 2009.

[12] ASCE, Minimum design loads for buildings and other structures, American Society of Civil Engineers/Structural Engineering Institute, Reston, VA, 2006.

[13] AISC, Specification for Structural Steel Buildings, AISC/ANSI 360-05, American Institute of Steel Construction, Chicago, Illinois, 2011.

[14] F. McKenna, G. Fenves, M. Scott, OpenSees: Open system for earthquake engineering simulation, Pacific Earthquake Engineering Center, University of California, Berkeley, CA., http://opensees. berkeley. edu, (2006).

[15] F. Zareian, R.A. Medina, A practical method for proper modeling of structural damping in inelastic plane structural systems, *Computers & structures*, 88 (2010) 45-53.

[16] ASCE, Seismic Rehabilitation of Existing Buildings (ASCE/SEI 41-13), in, American Society of Civil Engineers Reston, Virginia, 2013.

Tenth U.S. National Conference on Earthquake Engineering
Frontiers of Earthquake Engineering
July 21-25, 2014
Anchorage, Alaska

Appendix B
THE INFLUENCE OF GRAVITY COLUMN CONTINUITY ON THE COLLAPSE PERFORMANCE OF SPECIAL STEEL MOMENT FRAMES

F. X. Flores[1] and F. A. Charney[2]

ABSTRACT

It is known that the continuous stiffness of columns has the potential to decrease interstory drift concentrations in steel moment frames. In this study, the influence of continuity in gravity columns is evaluated by analyzing the 2-, 4- and 8-story special steel moment frames (SMFs) previously developed as part of the ATC-76-1 project.

The influence of the gravity columns continuity is evaluated by adding an elastic element placed in parallel to the SMF. This element represents all the gravity columns of the system. In this investigation the stiffness of this element was varied to establish an adequate stiffness that the gravity columns should have to enhance the performance. The variation was made by considering the stiffness per story of the gravity columns to be a ratio of the stiffness per story of the SMF. For all analyses the gravity beam-to-column connections are idealized as pinned connections, with adequate rotational capacity to carry the gravity loads prior to the failure of the SMF.

The influence of gravity column continuity on collapse behavior is determined using the P-695 methodology. The results demonstrate that gravity columns continuity enhance the collapse performance of all the buildings. However, the improvement is very important for the 8-story model since taller structures are more likely to have drift concentrations and weak story mechanisms.

[1] Ph.D. Candidate - Via Department of Civil and Environmental Engineering, Virginia Tech, VA 24060, USA
Ph.D. Candidate – Pontificia Universidad Católica de Chile, Santiago-Chile.
[2] Professor, Department of Civil and Environmental Engineering, Virginia Tech, VA 24060, USA

Flores FX, Charney FA. The Influence of Gravity Column Continuity on the Seismic Performance of Special Steel Moment Frames. *Proceedings of the 10th National Conference in Earthquake Engineering*, Earthquake Engineering Research Institute, Anchorage, AK, 2014.

Tenth U.S. National Conference on Earthquake Engineering
Frontiers of Earthquake Engineering
July 21-25, 2014
Anchorage, Alaska

The influence of Gravity Column Continuity on the Collapse Performance of Special Steel Moment Frames

F. X. Flores[1] and F. A. Charney[2]

ABSTRACT

It is known that the continuous stiffness of columns has the potential to decrease interstory drift concentrations in steel moment frames. In this study, the influence of continuity in gravity columns is evaluated by analyzing the 2-, 4- and 8-story special steel moment frames (SMFs) previously developed as part of the ATC-76-1 project.

The influence of the gravity columns continuity is evaluated by adding an elastic element placed in parallel to the SMF. This element represents all the gravity columns of the system. In this investigation the stiffness of this element was varied to establish an adequate stiffness that the gravity columns should have to enhance the performance. The variation was made by considering the stiffness per story of the gravity columns to be a ratio of the stiffness per story of the SMF. For all analyses the gravity beam-to-column connections are idealized as pinned connections, with adequate rotational capacity to carry the gravity loads prior to the failure of the SMF.

The influence of gravity column continuity on collapse behavior is determined using the P-695 methodology. The results demonstrate that gravity columns continuity enhance the collapse performance of all the buildings. However, the improvement is very important for the 8-story model since taller structures are more likely to have drift concentrations and weak story mechanisms.

Introduction

Current design approaches neglect the influence of the gravity system on the seismic performance of buildings because it is considered an inherent factor of safety. However, experience and past studies have demonstrated that the gravity system could take an important role, especially improving the collapse performance [1].

One of the most important benefits provided by the gravity system in Special Steel Moment Frames (SMFs) is the continuous stiffness of the gravity columns. The continuous column or stiffness concept acknowledges that: “If columns are continuous over several stories

[1] Ph.D. Candidate - Via Department of Civil and Environmental Engineering, Virginia Tech, VA 24060, USA
Ph.D. Candidate – Pontificia Universidad Católica de Chile, Santiago-Chile.
[2] Professor, Department of Civil and Environmental Engineering, Virginia Tech, VA 24060, USA

Flores FX, Charney FA. The Influence of Gravity Column Continuity on the Seismic Performance of Special Steel Moment Frames. *Proceedings of the 10th National Conference in Earthquake* Engineering, Earthquake Engineering Research Institute, Anchorage, AK, 2014.

of a structure, then the stiffness of the columns will limit the amount of drift concentration that can occur" [2].

Tremblay and Stiemer [3] proposed the use of continuous columns as a backup to mitigate P-Delta effects on braced frames. The study analyzed collapses on 8 multi-story buildings that varied in height from 2 to 12 stories. The studied conditions were: columns were pinned at each floor (no continuous stiffness was provided), pinned at each second floor, and continuous over the entire building height. The last case was analyzed using pinned and fixed connections at the base of the columns. The results showed that the worst case (more collapses) was when columns were pinned at each level (no continuity) and the best case was when the columns were continuous over the entire height and pinned at the base because the columns did not yield. The authors concluded that the continuous stiffness concept is very attractive to mitigate P-Delta effects but more research is required.

Qu et al. [4] investigated the influence of continuous stiffness by adding a rocking wall frame to a ductile reinforced concrete moment frame. The results showed that interstory drift concentrations are reduced considerably when the rocking wall was incorporated. This study was applied later on to retrofit an eleven-story reinforced concrete frame in Japan [5].

Tagawa [6] studied the continuous column effect on moment resisting frames when gravity columns are included in the analysis. Nonlinear static and dynamic analyses were performed using different buildings with and without the gravity columns. The results showed that the post-yield stiffness increases in the pushover analysis when gravity columns are added and drift concentration is reduced in the dynamic analysis. The author concluded that continuous columns have a larger effect on taller structures (9 and 20 story buildings). It was also concluded that as continuous column stiffness increases, drift concentration decreases to a point where the structure moves with respect to the base as a rigid body. The study recommends as future research to evaluate the stability of the frames with plastic hinges that include stiffness and strength degradation.

In the new study reported herein, the influence of gravity columns is evaluated on the basis of collapse performance of SMFs using the P-695 methodology [7]. The buildings to be analyzed are the 2-, 4- and 8-story SMFs previously developed as part of the ATC 76-1 project [8]. These buildings were studied by Zareian et al. [9]. In order to quantify the influence of continuous stiffness, the total moment of inertia provided by the gravity columns (per story) is assumed to be a percentage or ratio of the total moment of inertia provided by the SMFs (per story). Then, a complete P-695 methodology is performed to quantify the effect of continuous stiffness on SMFs.

Building Overview

The 2, 4, and 8 story buildings have the same floor plan. The chosen buildings from the ATC 76 -1 project were the ones designed using the Response Spectrum Analysis (RSA) approach. The connections at the base of the columns are fixed for the 4 and 8-story models and

pinned for the 2-story model. Fig. 1 shows the plan layout for all the analyzed buildings. It can be seen from this figure that the lateral resisting system of these buildings is provided by three SMFs bays located at the perimeter. These SMFs have prequalified reduced beam sections (RBS) connections and have the purpose to resist the seismic forces and provide stability against P-Delta shears.

The structures were analyzed in the East-West direction. The gravity frame is considered to be part of the system and it is shown also in Fig. 1. The sizes of these gravity columns are established by considering their stiffness per story to be a ratio of the stiffness per story of the columns in the SMFs. The shaded area in the figure represents the tributary area for gravity loading on the individual SMFs.

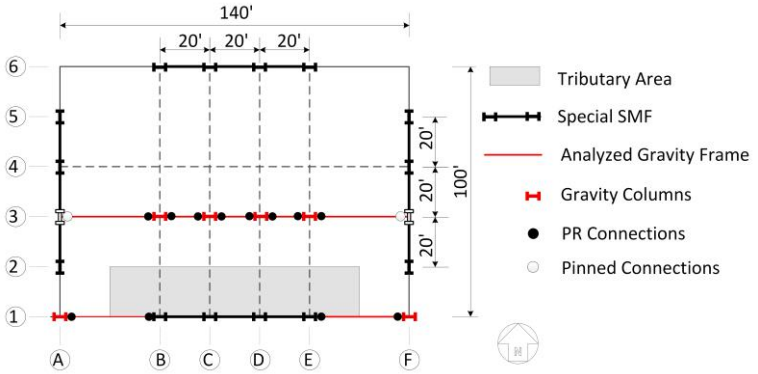

Figure 1. Buildings plan view.

The bay width (center line dimensions) between columns of each SMF is 20’. The height of the first story is 15’ (to top of steel beam), and the height of all other stories is 13’. The dead load is 90 psf uniformly distributed over each floor, and the cladding load is applied as a perimeter load of 25 psf. Unreduced live load is 50 psf on all floors and 20 psf on the roof.

Modeling Special Moment Frames

The nonlinearities incorporated into the analysis include rotational plastic hinges in the RBS regions of the beams, rotational plastic hinges at the ends of the columns and inelastic shear deformation in the panel zones. Fig. 2 shows the SMF model with its respective nonlinearities.

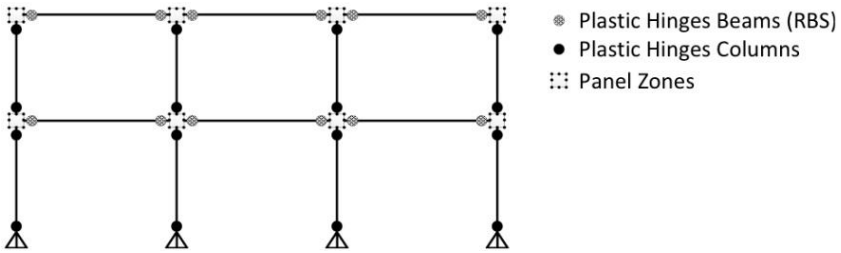

Figure 2. SMF 2-story model.

The platform used to perform all the analyses was OpenSees [10] and the way nonlinearities were represented is described briefly herein. More detailed descriptions of modeling the SMF can be found in the ATC 76-1 report [8]. The hysteretic behavior of the beams was modeled using the modified Ibarra-Krawinkler [11] deterioration model. The parameters to define this model were taken from Lignos and Krawinkler [12]. The panel zones were modeled using eight very stiff beam-column elements with one nonlinear rotational spring [13]. The nonlinearity of the panel zone comes from shear yielding and column flange flexure yielding and they were represented by a tri-linear backbone curve. The hysteretic behavior of the plastic hinges located at the extreme of the columns was modeled in the same way as the beams because currently there is not a phenomenological element in OpenSees that includes the axial force – bending moment (P-M) interaction. However, to overcome this problem, a representative axial force was computed from the gravity loads and the pushover analysis [8]. Using this load and the AISC P-M interaction equation [14] the bending strength of the column was decreased.

In order to include the P-Delta effect in the analysis, a leaning column was incorporated. The leaning column has zero flexural stiffness and is placed parallel to the structure. The load applied to this column represents the destabilizing load that comes from the gravity load equal to $1.05D + 0.25L$ on a tributary area equal to half of the plan area minus the shaded area (Fig. 1).

A Rayleigh damping of 2.5% is assigned at the first mode period T_1 and at $T=0.2T_1$ in all cases. As proposed by Zareian (2010) [15], stiffness proportional damping is assigned to elements that remain elastic, and mass proportional damping is assigned to nodes or elements where mass is lumped.

Modeling Gravity Columns

In this study, the gravity system was not designed explicitly. Instead another approach was taken to evaluate the influence of the gravity columns. The stiffness per story of the gravity columns was considered to be a percentage or ratio of the stiffness per story of the SMF's columns. Therefore, as shown in equation Eq. (1), the moment of the gravity column, I_{GC}, is a constant (α) times the total moment of inertia provided by the columns in the SMF. Note that this is an approximate estimation of the SMF stiffness per story because it considers the beams to be rigid.

$$I_{GC} = a \sum I_{SMFC} \tag{1}$$

Following this procedure, the total moment of inertia of the gravity columns per story was lumped in one continuous element placed in parallel to the SMF as is illustrated in Fig. 3. Each story of the gravity column has a percentage (100 times α) of the total moment of inertia SMF's columns.

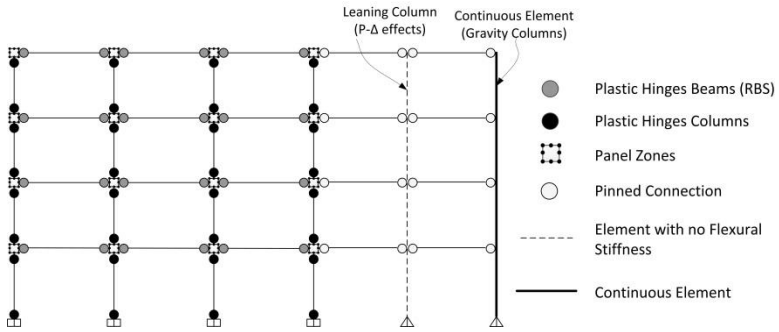

Figure 3. Modeling gravity columns.

As it reported in Flores and Charney [1], the gravity columns do not yield when the gravity connections have zero strength. Therefore, the gravity column element is considered to behave elastically. Under the studied scenarios the columns did not yield. However, more research needs to be done to verify that this assumption is generally accurate.

Nonlinear Static Pushover Analysis

One of the required steps in the FEMA P-695 procedure is to execute a nonlinear static pushover analysis. The parameters computed from the pushover analysis are the overstrength and period based ductility (μ_T). In order to evaluate the influence of the gravity columns on the aforementioned parameters, nonlinear static pushover analysis was performed to all the SMFs. The ratio of the inertia per story of the gravity columns was varied progressively from 10% to 100%. As it is already known, the gravity columns have an effect on the post-yield stiffness of the structure and this is why it is important to compare the period based ductility. The results for the 2-Story model are not included in this section because the influence of the gravity columns on the pushover curve is relatively insignificant. The reason is because the P-Delta effect is low on this building, so the gravity columns do not have any influence on the post-yield stiffness. The results of the pushover analysis and the influence on the period based ductility (μ_T) for the 4-story building are shown in Fig. 4 (a) and (b). The results shown in these figures are for the gravity columns with stiffness per story that varied from 10% (4Story +10GsCol) to 100% (4Story +100GsCol).

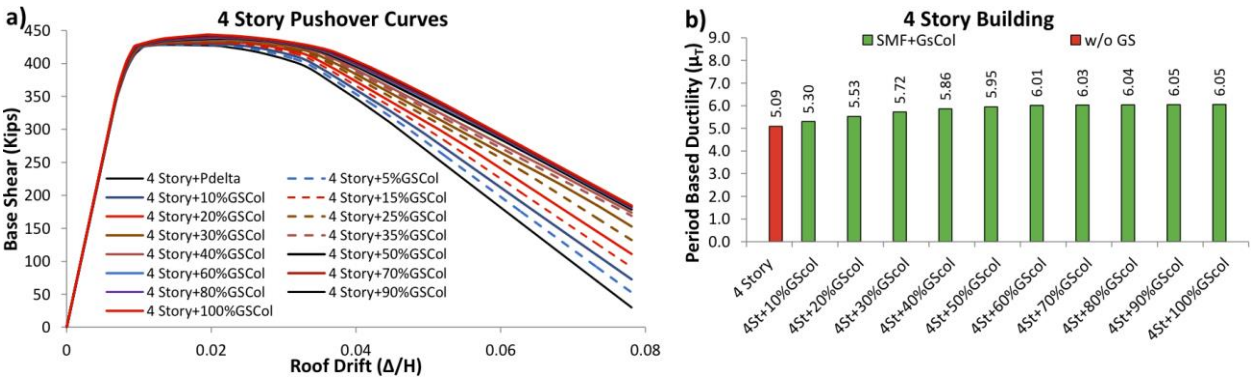

Figure 4. a) Pushover curves 4-story model b) Period based ductility 4-story models.

Fig. 4 (a) illustrates the influence of the gravity columns on the post-yield stiffness of the 4-story model. This influence is directly related with the period based ductility results shown in Fig. 4 (b). The main conclusion from these figures is that the optimal performance is obtained when the gravity columns have the inertia per story equal to 0.4 the inertia per story of the SMF. According to this analysis, it is not necessary to increase the gravity columns sections more than a ratio of 0.4 to improve the performance. It can also be seen that overstrength is not influenced at all (or only marginally) by the gravity columns.

The results of the pushover analyses and the calculated period based ductilities for the 8-story model are shown in Fig. 5 (a) and (b). For these analyses, the inertia of the gravity columns was varied from 10% (8 Story + 10%GsCol) to 100% (8Story + 100%GsCol) the inertia of the SMF. In this case, the improvement is more noticeable than for the 4-Story model. The increase in the total moment of inertia per story of the gravity columns does not get saturated as in the case of the 4-story model, where after a ratio of 0.4 the results did not vary.

The influence of the gravity columns, when they are continuous, is important for the 8-story model. The benefits of improving the post-yield stiffness are directly related with dynamic stability because it counteracts the P-Delta effects. From Fig. 5 (a), it can be seen that the post-yield stiffness improves faster when the gravity columns inertia vary from 5% to 50%. The period based ductility increases around 20% when the gravity columns have inertia per story equal to 50% the inertia per story of the SMF (Fig 5. (b)).

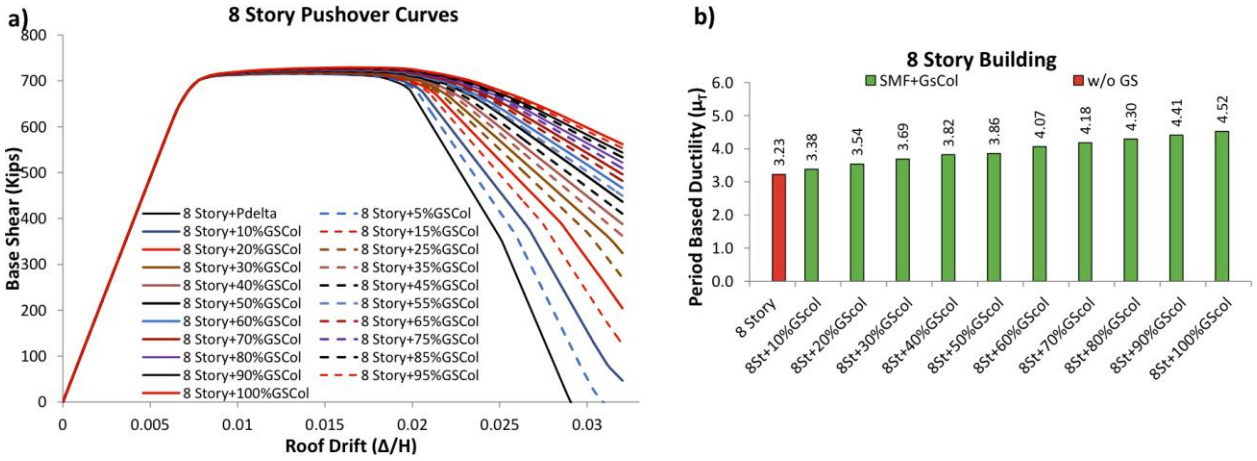

Figure 5. a) Pushover curves 8-story model b) Period based ductility 8-story models.

Collapse Performance Evaluation

Following the P-695 methodology, the collapse performance of the structures is obtained by means of nonlinear dynamic time history analyses, specifically using the incremental dynamic analysis (IDA) procedure [16]. In this analysis each of the 44 different far-field ground motions is scaled to increasing intensities until the structure collapses. The collapse of the structures was considered to occur when the global drift is 0.1 or when the slope of the IDA curve is less than or equal to 20% the elastic slope of the IDA. This definition of collapse was established by FEMA 350 [17]. Once the IDA was performed and the collapse margin ratio (CMR) obtained using the procedure defined in the P-695 methodology, the performance evaluation is executed. The quality ratings assigned to the uncertainties are the same as the ones considered for the ATC 76-1 project. The parameters to be compared are the CMR and the probability of collapse because they represent directly the influence of the gravity columns. In this part of the study, different ratios of the total moment of inertia per story of the gravity columns to the total moment of inertia of the SMF were considered for each building. The results of the analyses performed on the 2-story model are shown in Figs. 6 (a) and (b).

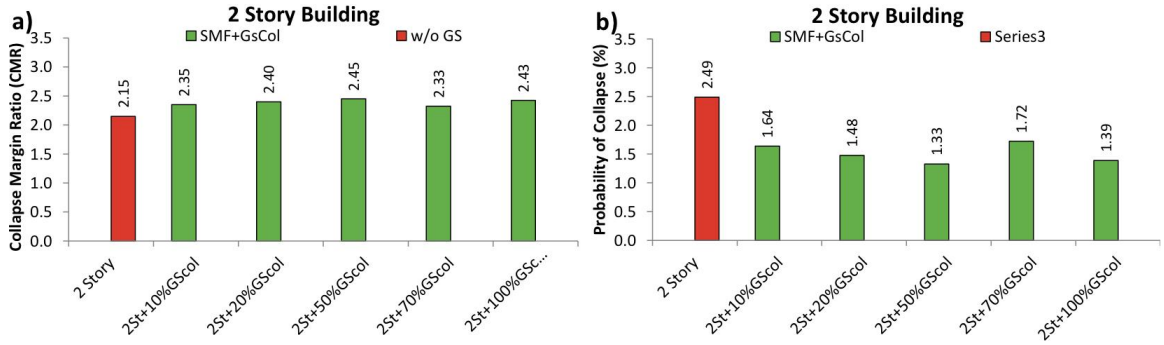

Figure 6. Results of 2-story building (a) CMR (b) Probability of collapse.

Fig. 6 (a) illustrates the results of performing multiple IDAs to compute the CMR of different models. In the case of the 2-story model, fewer increments of the variation of the gravity columns stiffness were analyzed. Even though the gravity columns did not improve the post-yield stiffness in the pushover analysis, it can be seen from Fig. 6 (a) and (b) that they have some influence in the collapse performance. From these results it can be seen that the CMR increases slightly but in a regular manner until the gravity columns have a ratio of 0.5 with respect to the SMF per story stiffness. After this point the results are close but they do not necessarily keep increasing. The probability of collapse decreases from 2.49% to 1.33 % when the gravity columns stiffness per story ratio is 0.5. In general, the influence of the gravity columns is not significant for the 2-story model and that is why the results can fluctuate.

The results of the analyses performed to the 4-story model are shown in Fig. 7 (a) and (b). The ratios of the inertia per story of the gravity columns were chosen based on the results of the nonlinear static analysis. As Fig. 4 displays, the post-yield stiffness improves progressively

when the gravity columns are included until the ratio of the inertia per story is equal to 0.4. After this point the post-yield stiffness is the same.

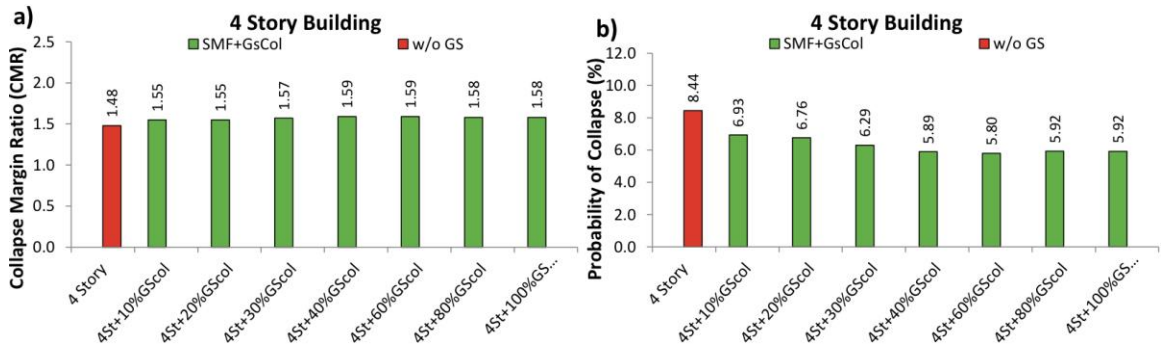

Figure 7. Results of 4-story building (a) CMR (b) Probability of collapse.

It can be seen from Fig. 7(a) and 7(b) that the gravity columns do not significantly influence the CMR or the probability of collapse. The probability of collapse depends on the period based ductility, and this is why the values change even when they have the same CMR. It is important to note that using gravity columns with larger sections do not enhance the results.

Probably the best ratio to use would be 0.4 because the CMR goes from 1.48 to 1.59 (7.43% increment) and the probability of collapse decrease from 8.44% to 5.89%. Using larger ratios will increase the cost of the structure and the results are virtually the same. These results corroborate with the results obtained in the pushover analysis where the post-yield stiffness improvement stopped for ratios larger than 0.4.

The results obtained for the 8-story model are shown Fig. 8 (a) and (b). As it was expected from the pushover curves, the improvement of the CMR and probability of collapse when gravity columns are included as part of the lateral resisting system, is notable. From Fig. 8 (a) it can be seen that the CMR goes from 1.48 for the 8-story building without the gravity column influence to 2.00 when the 8-story includes the gravity columns with stiffness per story ratio equal to 1. It is interesting to note the direct relation of the nonlinear dynamic results with pushover curves. Fig. 5 shows how the post-yield stiffness improves progressively when the stiffness per story of the gravity columns increases. Unlike the 4-story model the improvement does not reach a limit for ratios smaller than 1.

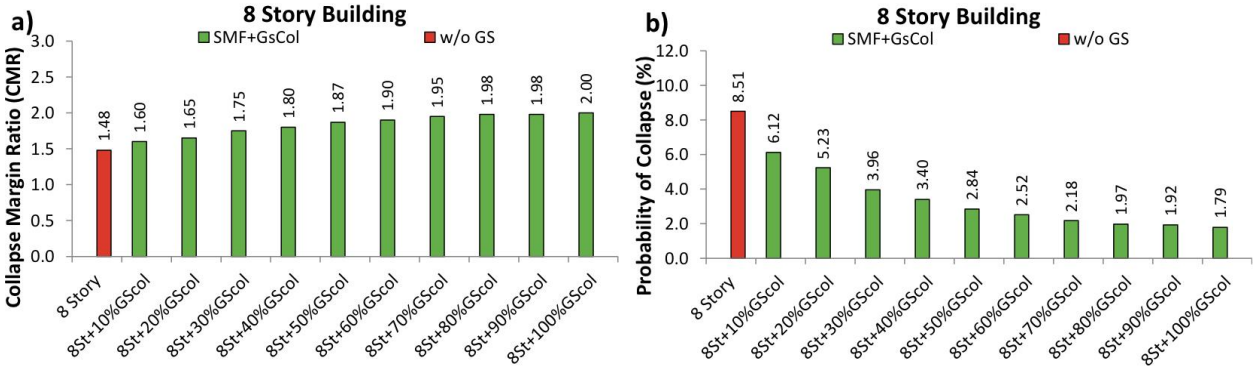

Figure 8. Results of 8-story building (a) CMR (b) Probability of collapse.

Even though the use of larger gravity columns brings more benefits to the performance, it could be uneconomical. Therefore, a ratio that is considered to be the optimal has to be established. This ratio will benefit the performance and represent an economical solution. The pushover curves have an important role on determining this ratio. From Fig. 5, it can be seen that the post-yield stiffness increases rapidly up to a point where the ratio of inertias is equal to 0.5. After this point, the post-yield stiffness still improves but in smaller increments. Therefore, this ratio is considered to be the optimal for design. The CMR for this ratio goes from 1.48 to 1.87 which represents an increase of 20%. On the other hand, the probability of collapse decreases from 8.51% to 2.84% which is a decrease of 66%.

Conclusions

In this study, a simple approach was used to include the gravity columns into the analysis. The variation of the stiffness per story helped to have a better insight of the influence of columns continuity on the collapse performance of the analyzed buildings. The findings from this investigation are:

- The influence of the gravity columns is beneficial for all three buildings. However, the improvement on collapse performance that the 8-story model presents is significant in comparison to the other two buildings.
- It is known that continuous stiffness can prevent or reduce the probability of buildings to develop drift concentrations or weak story mechanisms. This was reflected in this study by reducing the probability of collapse of the structures.
- From this investigation it can be concluded that there is a direct relation between the pushover curves and the most adequate stiffness ratio to be assigned to the gravity columns.

- The proposed approach to assign the inertia per story to the gravity columns equal to a ratio of the inertia per story of the SMFs seems to be adequate for estimating the influence of the gravity columns on the computed results. Moreover this could be an extra step to take when gravity columns are designed.
- The gravity system is considered to be an implicit factor of safety and that is why is not typically included in the analysis. However, if gravity columns are purposely made continuous and the stiffness per story is considered to be a ratio of the stiffness per story of the SMF, the performance of the building could be enhanced considerably.
- One of the conclusions presented in the ATC 76-1 project was that "there is a need to develop design concepts that prevent (or at least delay) the formation of partial mechanisms in lower stories of special SMF systems" [1]. From this study, by observing how the collapse performance of SMFs improved, it could be concluded that the gravity columns may be an option to fulfill this need.

The effect of gravity columns continuity is diminished when splices with marginal moment resistance are placed along the length of the columns. A comprehensive study was performed by Flores and Charney [1] on this matter.

Acknowledgments

The work presented herein was possible through the support of the National Institute of Standards and Technology, award number 60ANB10D017. The authors would also like to acknowledge the contribution of Mr. Andy Hardyniec of Virginia Tech for his work creating the FEMA P-695 Toolkit that was used in the analysis. Additionally it should be acknowledged that much of the analysis was performed using computer resources available through NeesHub.

References

[1] F. Flores, F. Charney, Influence of the Gravity Framing System on the Collapse Performance of Special Steel Moment Frames, *Journal of Constructional Steel Research* (To be published), (2013).

[2] G.A. MacRae, The Continuous Column Concept-Development and Use, (2011).

[3] R. Tremblay, S. Stiemer, Back-up stiffness for improving the stability of multi-storey braced frames under seismic loading, *Proceedings of the 1994 SSRC Annual Technical Session*, Bethlehem, Pa, (1994) 311-325.

[4] Z. Qu, L. Ye, A. Wada, Seismic damage mechanism control of RC ductile frames from a stiffness point of view, in: *8th International Conference on Urban Earthquake Engineering*, Tokyo, Japan, 2011.

[5] Z. Qu, A. Wada, S. Motoyui, H. Sakata, S. Kishiki, Pin supported walls for enhancing the seismic performance of building structures, *Earthquake engineering & structural dynamics*, 41 (2012) 2075-2091.

[6] H. Tagawa, Towards an understanding of seismic response of 3D structures-stability & reliability, *Doctor Thesis*, Washington: University of Washington, (2005).

[7] FEMA P695, Quantification of Building Seismic Performance Factors, Fededral Emergency Management Agency, Washington, D.C, 2009.

[8] NIST, Evaluation of the FEMA P-695 Methodology for Quantification of Building Seismic Performance Factors, National Institute of Standards and Technology, USA, 2010.

[9] F. Zareian, D. Lignos, H. Krawinkler, Evaluation of seismic collapse performance of steel special moment resisting frames using FEMA P695 (ATC-63) methodology, in*: Proceedings of Structures Congress ASCE*, New York, 2010.

[10] F. McKenna, G. Fenves, M. Scott, OpenSees: Open system for earthquake engineering simulation, Pacific Earthquake Engineering Center, University of California, Berkeley, CA., http://opensees. berkeley. edu, (2006).

[11] L.F. Ibarra, R.A. Medina, H. Krawinkler, Hysteretic models that incorporate strength and stiffness deterioration, *Earthquake engineering & structural dynamics*, 34 (2005) 1489-1511.

[12] D.G. Lignos, H. Krawinkler, Deterioration modeling of steel components in support of collapse prediction of steel moment frames under earthquake loading, *Journal of Structural Engineering*, 1 (2010) 279.

[13] F. Charney, J. Marshall, A comparison of the Krawinkler and scissors models for including beam-column joint deformations in the analysis of moment-resisting steel frames, *Engineering Journal - American Institute of Steel Construction*, 43 (2006) 31.

[14] AISC, Specification for Structural Steel Buildings, AISC/ANSI 360-05, American Institute of Steel Construction, Chicago, Illinois, 2011.

[15] F. Zareian, R.A. Medina, A practical method for proper modeling of structural damping in inelastic plane structural systems, *Computers & structures*, 88 (2010) 45-53.

[16] D. Vamvatsikos, C.A. Cornell, Applied incremental dynamic analysis, *Earthquake Spectra*, 20 (2004) 523.

[17] FEMA, Recommended seismic design criteria for new steel moment-frame buildings, FEMA 350 Report, 2000.

Appendix C

SEISMIC PERFORMANCE OF SPECIAL STEEL MOMENT FRAMES INCLUDING THE GRAVITY SYSTEM

F. Flores[(1)], F. Charney[(2)], D. Lopez-Garcia[(3)]

[(1)] *Ph.D. Candidate, Department of Civil and Environmental Engineering, Virginia Tech, and Department of Structural and Geotechnical Engineering, Pontificia Universidad Catolica de Chile, ffloress@vt.edu*
[(2)] *Professor, Department of Civil and Environmental Engineering, Virginia Tech, fcharney@vt.edu*
[(3)] *Associate Professor, Department of Structural and Geotechnical Engineering, Pontificia Universidad Catolica de Chile, and National Research Center for Integrated Natural Disaster Management CONICYT/FONDAP/15110017, dlg@uc.cl*

Abstract

Current practice in the U.S. neglects the gravity framing system as part of the lateral load resisting system when designing for seismic effects. Yet, past earthquakes such as the 1994 Northridge earthquake, have demonstrated that the gravity system contributed to the collapse resistance of some structures after their main lateral resisting system failed. In this study, the influence of the gravity system on the collapse performance of Special Steel Moment Frames (SMFs) is evaluated by means of the FEMA P-695 methodology. The analyzed buildings are 2-, 4- and 8-Story systems that were previously analyzed without gravity system contribution in the ATC 76-1 project. In order to quantify the influence of the gravity system, the collapse evaluation of the structures is reanalyzed with and without the gravity system. Two different approaches are used to include the gravity system in the analysis. One approach explicitly quantifies the importance of the full gravity system, including beams, columns, and connections, and the other approach considers only the influence of the gravity columns. At the conclusion of the investigation it was found that the influence of the gravity system is very important on the collapse performance of SMFs. The complete gravity system (especially the connections) have an important role on the performance of the 2- and 4-Story buildings, while the gravity columns are more relevant in the response of the 8-Story building.

Keywords: Special Steel Moment Frames, Collapse Assessment

1 Introduction

Seismic performance of structures is often quantified neglecting the influence of the gravity system. Special Steel Moment Frames (SMFs) have been studied analytically and through experience, and performance has not always been acceptable. One event that caused researchers to look more in depth at the design and analysis of SMFs was the 1994 Northridge California earthquake. During this earthquake several SMFs connections failed. However, buildings did not collapse after the failure of the SMF connections, suggesting that the gravity system provides a reserve strength mechanism within the structure [1]. After the Northridge earthquake, several studies were performed to evaluate the SMFs, and more specifically the beam to column connections used in the gravity system. In one of these studies Liu and Astanneh [2] performed cyclic tests on different types of simple gravity framing connections to characterize their hysteretic behavior. One of the main conclusions of Liu and Astanneh's research was that these connections have large rotation capacity and their strength can vary depending on the specific connection detail used.

There has been extensive experimental and analytical research on the seismic behavior of SMFs, but there are relatively few studies that include the gravity system in the analysis. Gupta and Krawinkler [3] studied the response of SMFs at various seismic hazard levels. Different models were used to perform nonlinear static and dynamic analyses. The authors concluded that the seismic behavior of the structures improves at large drifts when the gravity system is included. However, a number of factors such as the number of gravity frames, the properties of the gravity connections, column base connection details, major-minor axis orientation of columns, and the magnitude of drift demand have an influence on the performance. Among these factors, according to Gupta and Krawinkler [3], the contribution of the gravity columns is the most important, with the gravity connections playing a much less significant role. The main finding or conclusion from the study was that the gravity system contributes to and thereby increases the system's post-yielding stiffness, thereby reducing the influence of P-Delta effects under high intensity ground motions.

Another important property that the gravity system provides to the structure is the continuous stiffness of the columns in the gravity system. Continuous column stiffness is provided by gravity columns that have no splices, or where splices provide full moment capacity. This effect could be able to reduce story drift concentrations and prevent weak story mechanisms [4]. The effect was also noticed by Gupta and Krawinkler [3]. Tagawa [5] studied the continuous stiffness provided by the gravity columns on SMFs. One of the conclusions made by the author was that continuous columns decrease drift concentrations when dynamic analysis is performed.

A new and different investigation was executed by Zareian et al. [6] as part of the ATC 76-1 project [7]. SMFs were studied using the P-695 methodology [8] to assess their collapse performance. Following the FEMA P-695 procedure, this study did not include the gravity system in the collapse evaluation of the SMFs. The analyzed buildings ranged from 1 to 20 stories in height and they were designed complying with the minimum requirements established by ASCE 7-05 [9] and AISC 341-05 [10] with the exception that the deflection amplification factor (C_d) was taken to be equal to the response modification coefficient (R), as specified in the FEMA P-695 methodology.

From these past studies, it can be observed that the influence of the gravity system on the seismic performance has not been investigated in detail. Therefore, to better clarify the influence of the gravity system on seismic response, the 2, 4 and 8-Story buildings taken from the study performed by Zareian et al. [6] are reanalyzed with and without the gravity system. Two different approaches are used to incorporate the gravity framing into the analysis. The first approach, henceforth referred to as the "explicit" method, includes all the gravity columns and gravity connections. The second approach, from now on called the "lumped" method, incorporates just the gravity columns into the analysis. In

order to quantify the influence of the gravity system and to compare the benefits of each approach, the collapse evaluation of the buildings is performed using the FEMA P-695 methodology and the parameters used for the quantification are the Collapse Margin Ratio (CMR) and probability of collapse.

2 Building Overview

The 2, 4, and 8-Story buildings have the same plan geometry. The buildings selected for further study were those that were designed for the ATC 76-1 work using modal response spectrum analysis. The connections at the base of the columns are fixed for the 4- and 8-Story models and pinned for the 2-Story model. Fig. 1 shows the plan layout for all the analyzed buildings. The SMFs have prequalified reduced beam sections (RBS) connections and have been designed to resist the seismic forces and provide stability against P-Delta shears. The structures were analyzed in the East-West direction. The gravity frame considered to be part of the system is also shown in Fig. 1. In order to evaluate the influence of just the gravity system, the SMFs columns (A-3, F-3) oriented on the weak axis are considered to have zero lateral strength (continuous stiffness effect is neglected and beam to column connections are pinned). The shaded area in Fig. 1 represents the tributary area for gravity loading on the individual SMFs. The gravity connections were considered as pinned for the gravity beam design, and they are assumed to be partially restrained (PR) connections for lateral load analysis. The design of the gravity system was performed in SAP-2000 using A992 steel material for the members. The section sizes and other pertinent information can be found in Flores et al. [11].

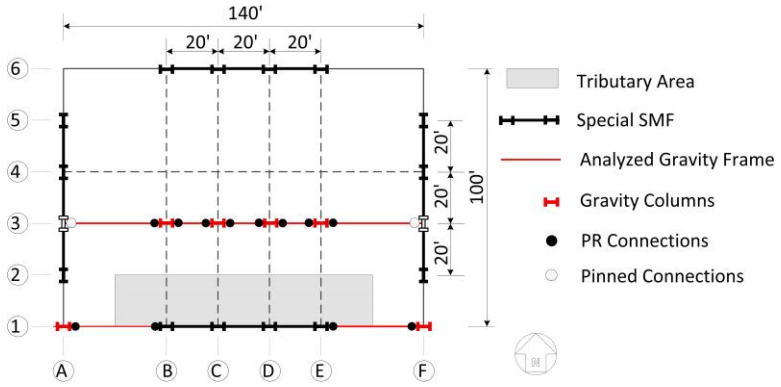

Fig. 1 - Buildings plan view

The bay width (center line dimensions) between columns of each SMF is 20’. The height of the first story is 15’ (to top of steel beam), and the height of all other stories is 13’. The dead load is 90 psf uniformly distributed over each floor, and the cladding load is applied as a perimeter load of 25 psf. Unreduced life load is 50 psf on all floors and 20 psf on the roof.

3 SMF Model

The material nonlinearities incorporated into the analysis include rotational plastic hinges in the RBS regions of the beams, rotational plastic hinges at the ends of the columns, and inelastic shear deformation in the panel zones. The platform used to perform the analysis was OpenSees [12]. The procedure used to model the structure was the same as described in the ATC 76-1 report [7]. The P-Delta effect was included in the analysis by adding a leaning column when the SMF was analyzed by itself. The leaning column has zero flexural stiffness and is placed parallel to the structure. The load applied to this column represents the destabilizing load that comes from the gravity load and is equal to 1.05 D + 0.25 L on a tributary area equal to half of the plan area minus the shaded area (Fig. 1). When

the gravity system is included explicitly in the analysis, the P-Delta effects are modeled using geometric stiffness for all columns in the structure.

Rayleigh damping of 2.5% is assigned at the first mode period T_1 and at $T = 0.2\ T_1$ in all cases. As proposed by Zareian (2010) [15], stiffness proportional damping is assigned to elements that remain elastic, and mass proportional damping is assigned to nodes or elements where mass is lumped.

4 Explicit Gravity System Model

The gravity system was modeled explicitly in the analysis. It was placed parallel to the SMF assuming the floors act as rigid diaphragms. The material nonlinearities modeled in the gravity frame were the plastic hinges at the connections and possible plastic hinges along the height of the columns. The gravity columns may be considered to behave elastically if the gravity connections do not provide a significant moment capacity, and this will be shown with different analyses in this study. However, as demonstrated by Flores et al. [11], the gravity columns can yield when the gravity connections have significant strength. Therefore, the gravity columns were modeled using fiber elements with a bilinear material that has a strain hardening equal to 10% of the initial stiffness. Using fibers to model the columns provide an important benefit which is the inclusion of the P-M interaction in the analysis. A disadvantage of the fiber approach is that the strength degradation is not considered. Degradation is essential in the modeling of the main SMFs, and this is why the columns of the SMFs were modeled using concentrated plasticity and approximate P-M interaction as described in the ATC 76-1 report.

4.1 Gravity Connections

The gravity connections are considered to be partially restrained (PR) connections, which according to the study performed by Liu and Astanneh [2], have the capability to sustain large deformations. A simple yet very accurate hysteretic behavior for this type of connections has not been defined. The most common approach to model these connections when nonlinear analysis is required is matching experimental results with a predefined hysteretic model. More difficult techniques like the component method or finite element analysis are still computationally expensive. In this study, a simple hysteretic model taken from ASCE 41-13 [13] is used because it is considered to be of appropriate accuracy for the aim of this study. The model was developed based on experimental data and the parameters that define the backbone curve depends on the PR connection type. The strength varies with the type of connection as well, but the rotation at yielding is the same for all (0.005 radians). The connection used in this investigation is the "top and bottom clip angle connection" and the limit state that controls failure is assumed to be the "Flexural Failure of Angle". The parameters that define the model change depending on the limit state that controls the connection. More information regarding the modeling can be found in [13].

One of the most important advantages of using this model is that the strength of the connection can be a parameter of study. For this investigation, the strength or capacity of the PR connections was assumed to be a percentage of the plastic moment of the beam (M_p). The percentages used to define the strength of the connections are 0, 35, 50 and 70% and they are assigned to every connection in the gravity frame. Even though some of these percentages are high (50% and 70%) it is worthwhile to evaluate their influence. The PR connections with no strength (0%) were defined to assess the influence of the gravity columns alone. The lower bound strength of 35% considered for this analysis was determined as the minimum strength required to prevent the connections from reaching a rotation of 0.005 radians (yielding point) under gravity loads.

The main nomenclature used to identify if the SMF includes or not the gravity system and the strength of the PR connections is as follows: n_Story+sGS, where n is the number of stories and s is the

percentage of full strength assigned to the PR connections (if sGS is not included, the model does not include the gravity system, and instead includes a leaning column to account for P-Delta effects).

4.2 Results for Elastic or Inelastic Gravity Columns

In this section, yielding in the gravity columns is checked by performing nonlinear static pushover and nonlinear dynamic analyses. The approach used was to model the gravity columns elastically and then repeat the same analysis but modeling the gravity columns using fiber sections. It has already stated by Flores et al. [11] that gravity columns yield when the gravity connections have sufficient strength and this is proven herein. However, as Fig. 2 displays, when the gravity connections have strength less than or equal to 30% of M_p the gravity columns do not yield. The difference between the elastic and inelastic analysis is minimal in the pushover curves, Fig. 2 (a), and there is virtually no difference in the results obtained when the nonlinear dynamic analysis, Fig. 2 (b), even though the hazard level used in the analysis was larger than the MCE level,

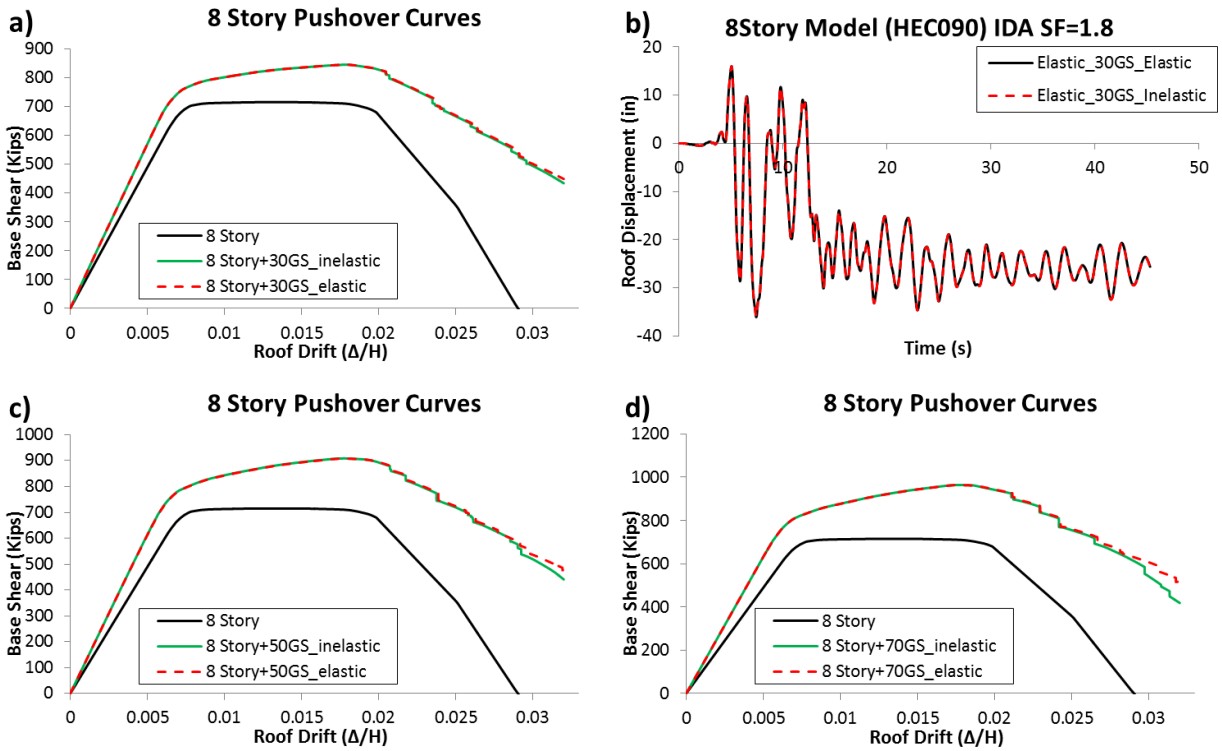

Fig. 2 - Different analyses results to check yielding in gravity columns (8-Story building)

Fig. 2 (c) and (d) show the pushover curves obtained when the gravity system connections have strength equal to 50% and 70% of M_p, respectively. From these curves, it is clear that there is a difference between the results for columns that behave elastically and inelastically. Therefore, it can be concluded that the gravity columns are yielding when the gravity connections have a significant moment capacity and this is why the gravity columns are modeled using fiber sections capable to capture yielding.

4.3 Explicit Model at DE, MCE and collapse evaluation

The main influence of the gravity system is measured by evaluating the collapse performance of the SMF with and without the gravity system. However, as part of the evaluation, the residual displacement is also quantified at the roof of the building and compared at different hazard levels such as Design Earthquake (DE) and Maximum Considered Earthquake (MCE). In this section, the 2-, 4- and 8-Story

buildings with and without the gravity system are analyzed using the 44 Far Field ground motions from FEMA P-695. Based on the results obtained in the previous section, the columns in the gravity system for these buildings are modeled using force based elements. So, they are able to capture any inelastic behavior that can occur during the analysis. The ground motions were scaled to the DE and MCE and the results are presented.

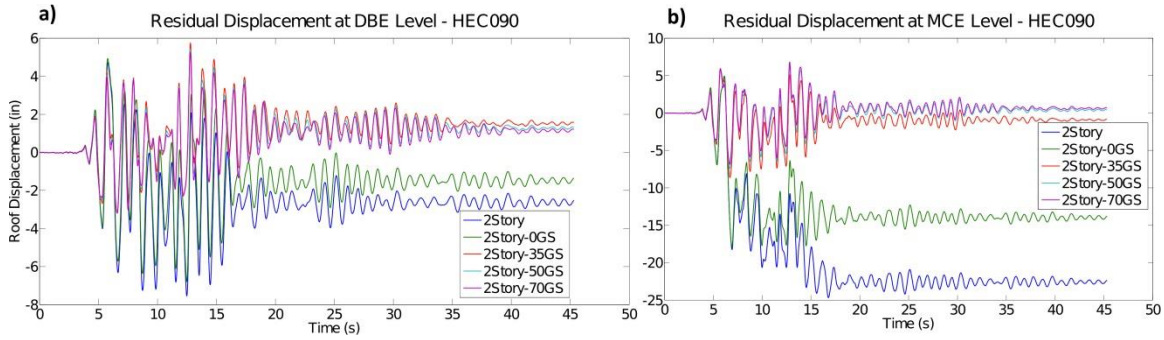

Fig. 3 - Nonlinear Dynamic Analyses at DE and MCE Level (2-Story Model)

The influence of the gravity system at DE and MCE for the 2-Story model is similar for all the ground motions. In general, the strength of the connections reduces the residual displacements and the effect of the gravity system is important when the structure is subjected to large drifts. This is the case of the ground motion "HEC090" shown in Fig. 3 (b), where the gravity system could be preventing the collapse of the structure.

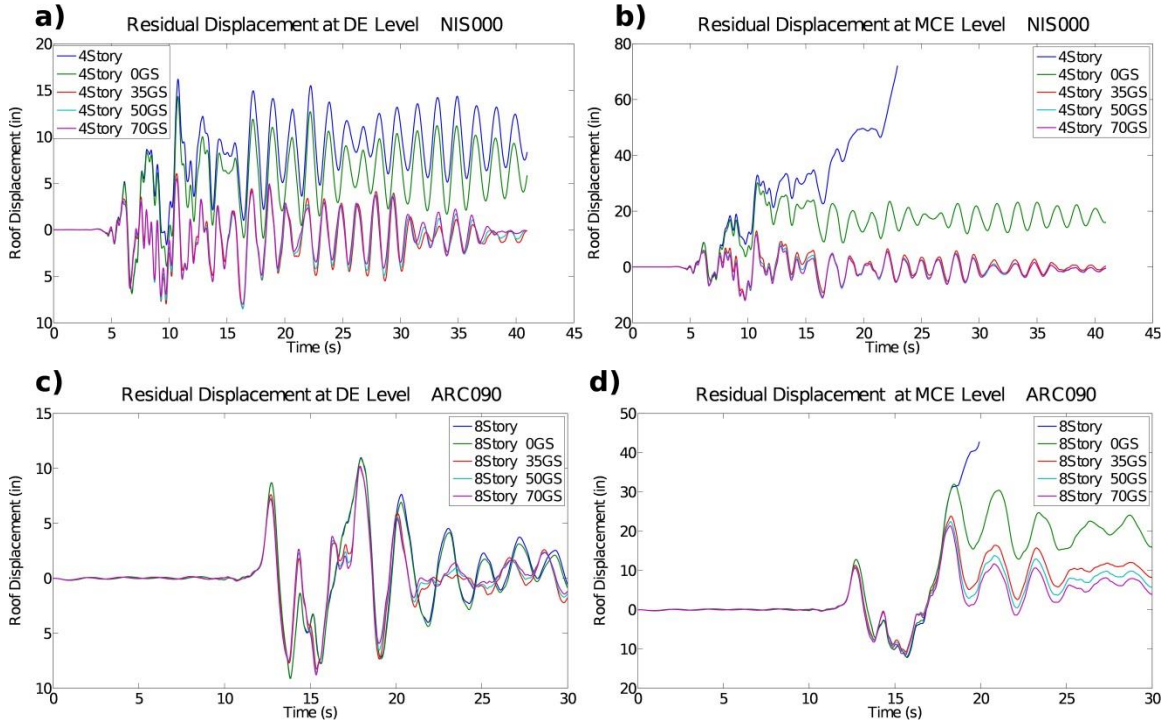

Fig. 4 - Nonlinear Dynamic Analyses at DE and MCE Level (4-, 8-Story models)

The residual displacements computed for the 4- and 8-Story buildings show the same trend as the 2-Story building except the effect of the gravity connections strength decreases as the building gets taller. Fig 4. (a) and (c) shows the results at DE level shaking, where it can be seen how the gravity system have almost no influence with the exception that the gravity connection reduce the residual displacement for the 4-story model. The influence of the gravity columns (PR connections with no

strength) is minimal at DE and MCE level shaking unless the building is subjected to large deformations. It can be observed from Fig. 4 (b) and (d) that the ground motions "NIS000" and "ARC090" caused the collapse of the 4-, and 8-Story buildings, respectively, when the gravity system is not included. The 8-Story model is more vulnerable to drift concentrations that could lead to collapse under the MCE level earthquake and this is when the gravity system (especially the gravity columns) plays an important role. Among the 44 ground motions, only one caused collapse to all the models while three caused the collapse just to the 8-Story model without the gravity system.

The gravity system, as it was already shown in the previous results, has the potential of improving the seismic performance. The influence of the gravity system is more important at MCE than DE at level because, as already mentioned, the structure is subjected to large deformations. In this part of the study, the collapse performance of the structures is evaluated using the FEMA P-695 procedure. The parameters to be compared from this methodology are the collapse margin ratio (CMR) and the probability of collapse. The quality ratings assigned to the uncertainties are the same as the ones considered for the ATC 76-1 project. Note that the CMR for the 2-, 4- and 8-Story models are almost the same as the ones presented in the ATC 76-1 project report [7].

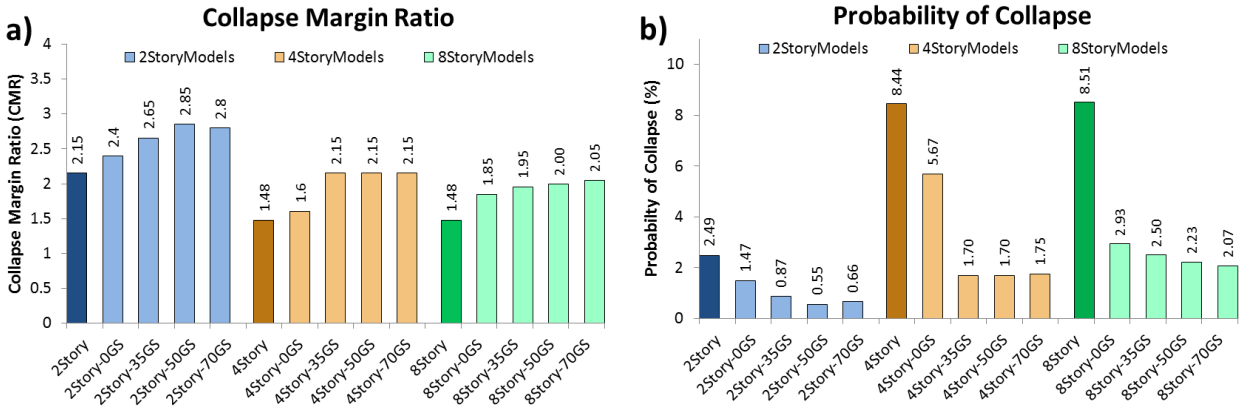

Fig. 5 - Collapse Performance Evaluation (Explicit Models)

Fig. 5 (a) presents the CMR obtained for all the analyzed models where it can be seen that the effect of the gravity connection strength is more important for the 2- and 4-Story models than for the 8-Story model. However, something to point out is that the 4-Story model has the same collapse performance for all the different PR connections strengths. The 8-Story model CMR improves considerably when the gravity columns are included in the analysis but the effect of the gravity connections strength is almost negligible. These statements are reflected directly in Fig. 5 (b) where the probabilities of collapse were computed. For instance the probability of collapse for the 8-Story building goes from 8.51% to 2.93% when the gravity columns are included in the analysis.

5 Simple Gravity System Model ("Lumped" Model)

As a second approach to incorporate the gravity system, a "lumped" model is developed where just the influence of the gravity columns is included in the analysis. This approach is analogous to the model with the gravity connections with no strength in the "explicit" model. Based on the fact that the gravity columns do not yield when the gravity connections have a low moment strength capacity (less than 30% M_p), this approach lumps the gravity columns stiffness per story into one elastic continuous element. The first step to be taken in this part of the study is to justify that the "lumped" model is accurate and it represents the gravity system correctly. The gravity system however has to comply with the following characteristics: gravity connections with no strength and gravity columns that are continuous all over the height and pinned at the base. Fig. 6 shows an illustration of the SMF with two

additional vertical elements; one that incorporates P-Δ effects and another that represents all the gravity columns. It can be seen from this figure that a ratio between the inertia of the gravity column (I_Gcol) to the inertia provided by the columns of the SMF (I_SMF) is computed. The inertia of the gravity columns was obtained from the designed sections. More information of the gravity system sections can be found in Flores et al. [11].

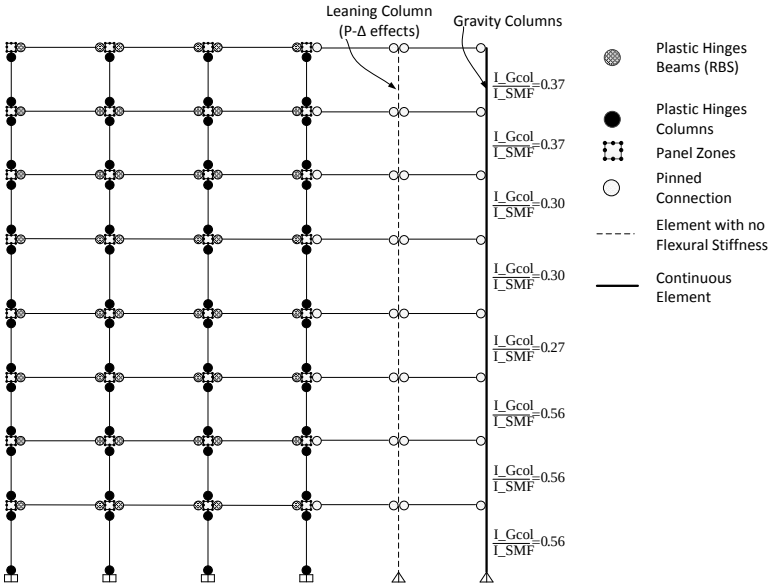

Fig. 6 - Lumped Model Approach

After justifying the method, the influence of the gravity columns is evaluated by varying the stiffness per story of the "lumped" element. The stiffness per story of the gravity columns was considered to be a percentage or ratio of the stiffness per story of the SMF's columns. The purpose of this is to compute the effect of having stronger gravity columns as part of a structure. The way the inertia per story of the gravity columns is varied is shown in Eq. (1): the moment of the gravity column, I_GCol, is considered to be a constant (α) times the total moment of inertia provided by the columns in the SMF. Note that this is an approximate estimation of the SMF stiffness per story because it considers the beams to be rigid.

$$I\_GCol = \alpha \sum I\_SMF \tag{1}$$

5.1 Gravity Columns Lumped into one element: Justification

Even though it was shown in section 4.2 that the gravity columns do not yield when the structure is subjected to large deformations unless the gravity connections have large moment strength capacity, it is necessary to show that the "lumped" approach sufficiently represents the gravity columns. For this reason the explicit model is compared with the lumped model. The comparison is made by performing nonlinear static pushover and nonlinear dynamic analysis. Fig. 7 shows the pushover curves obtained for the explicit model (8Story+0GS_elastic), the lumped model (8Story+LumpedGC) and the SMF without the gravity system (8Story). From these curves it can be seen that there is no difference between the explicit and the lumped model. However, to further justify the approach, the structures were subjected to different ground motions and to different hazard levels. One of the results obtained in the nonlinear dynamic analysis is shown in Fig. 7 (b) and it is clear that there is no difference between the explicit and the lumped model even though the scale factor is close to the one that causes collapse

to the structure. These results justify the use of this approach to represent just the gravity columns and neglect the gravity connections strength.

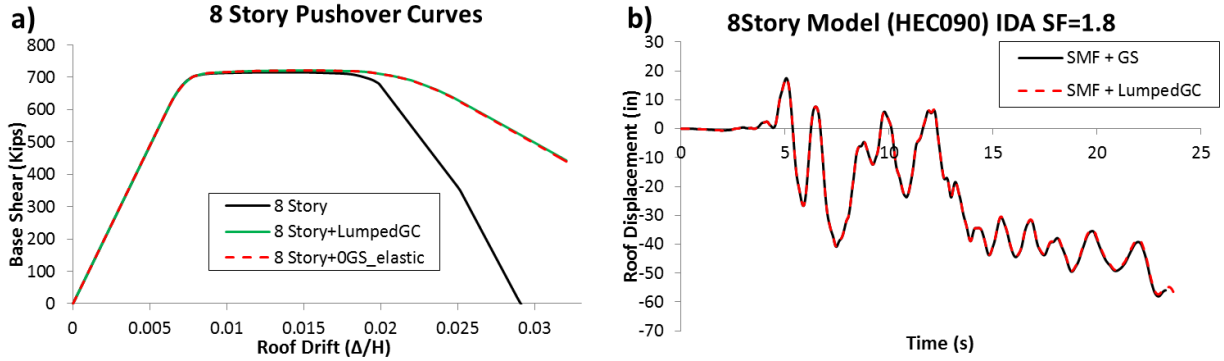

Fig. 7 - Lumped vs. Explicit Models

5.2 Collapse Evaluation

One of the required steps in the FEMA P-695 procedure is to execute a nonlinear static pushover analysis. The results of the nonlinear static pushover analyses are shown herein because it shows clearly the gravity column influence on the seismic performance of SMFs. The ratio of the inertia per story of the gravity columns was varied progressively from 5% to 100%. As it is already known, the gravity columns have an effect on the post-yielding stiffness of the structure improving considerably the period based ductility. Period based ductility is defined in the FEMA P-695 methodology and the reader is referenced to this document for more information.

The results for the 2-Story model are not included in this section because the influence of the gravity columns on the pushover curve is relatively insignificant. The reason is because the P-Delta effect is low on this building, so the gravity columns do not have any influence on the post-yielding stiffness. The results of the pushover analysis for the 4- and 8-Story buildings are shown in Fig. 8 (a) and (b). The results shown in these figures are for the gravity columns with stiffness per story that varied from 5% to 100%.

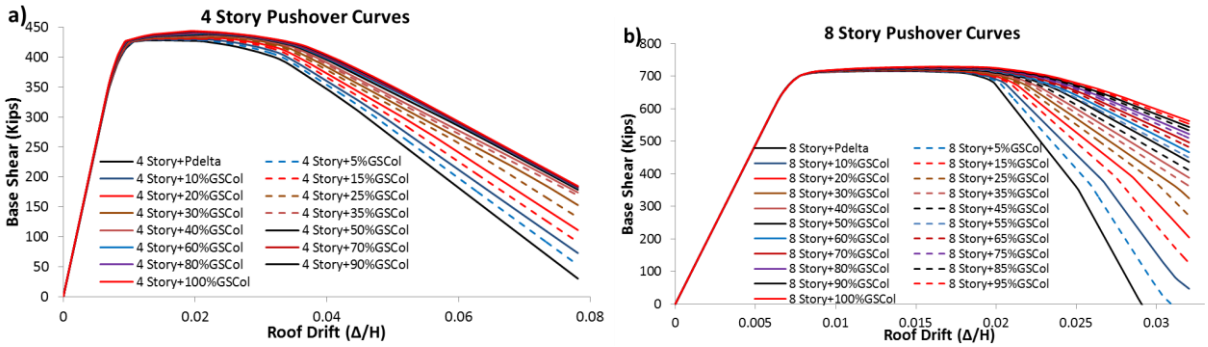

Fig. 8 - Nonlinear Static Pushover Curves (4-, 8-Story Models)

It is clear from Fig. 8 that the that gravity columns provide a very important and useful post-yielding stiffness to the SMFs. This enhancement is directly related to the prevention of dynamic instability because it counteracts the P-Delta effects. However, it can be seen that the influence is more significant for high rise buildings such as the 8-Story model in comparison to low rise buildings such as the 4- or 2- story models. The main finding that these pushover curves provide is that an optimal performance could be obtained depending on how large the gravity columns inertia is. For instance, this “optimal”

inertia ratio for the 4- and 8- story buildings seems to be 0.4 and 0.5 respectively because for larger ratios the buildings post-yielding stiffness do not increase significantly.

Following the P-695 methodology, the collapse performance of the structures is obtained by performing nonlinear dynamic time history analyses, specifically using the incremental dynamic analysis (IDA) procedure [14]. Each of the 44 different far-field ground motions is scaled to increasing intensities until the structure collapses. The collapse of the structures was considered to occur when the global drift is 0.1 or when the slope of the IDA curve is less than or equal to 20% the elastic slope of the IDA. This definition of collapse was established by FEMA 350 [15]. Once the IDA was performed and the collapse margin ratio (CMR) was obtained using the procedure defined in the P-695 methodology, the performance evaluation is executed. The parameters to be compared are the CMR and the probability of collapse because they represent directly the influence of the gravity columns. In this part of the study, different ratios of the total moment of inertia per story of the gravity columns to the total moment of inertia of the SMF were considered for each building. The results of the analyses performed on the 2-, 4- and 8-Story models are shown in Fig. 9 (a) and (b).

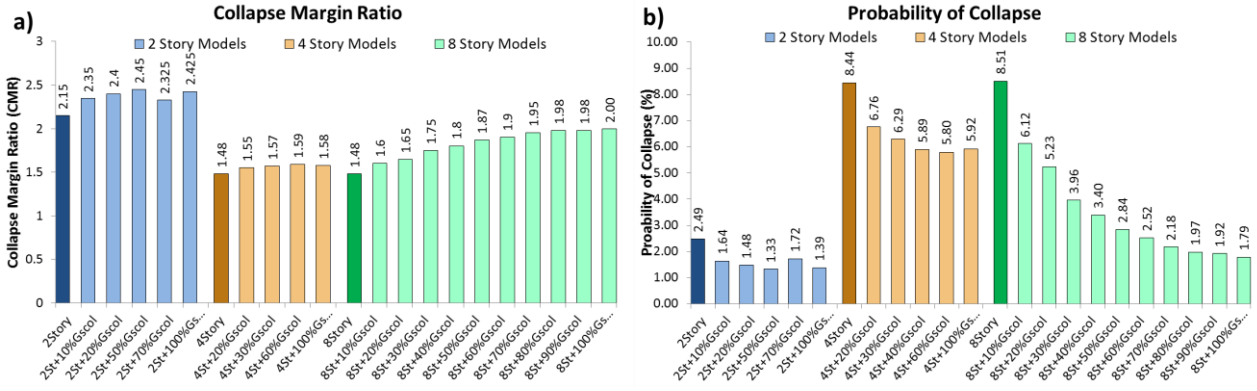

Fig. 9 - Collapse Performance Evaluation (Lumped Models)

In the case of the 2-Story model, fewer increments of the variation of the gravity columns stiffness were analyzed. Even though the gravity columns did not improve the post-yielding stiffness in the pushover analysis, it can be seen from the figure that they have some influence in the collapse performance. From these results it can be seen that the CMR increases slightly but in a regular manner until the gravity columns have a ratio of 0.5 with respect to the SMF per story stiffness. After this point the results are close but they do not necessarily keep increasing. The probability of collapse decreases from 2.49% to 1.33 % when the gravity columns stiffness per story ratio is 0.5. In general, the influence of the gravity columns is not significant for the 2-Story model and that is why the results can fluctuate. It has to be pointed out that the gravity connections improved the structure performance when they were included in the analysis (explicit model).

The ratios of inertia per story of the gravity columns for the 4-Story model were chosen based on the results of the nonlinear static analysis. It can be seen from Fig. 9 (a) and (b) that the gravity columns do not significantly influence the CMR or the probability of collapse. The probability of collapse depends on the period based ductility, and this is why the values change even when they have the same CMR. It is important to note that using gravity columns with larger sections do not enhance the results, which is why probably the best ratio to use could be 0.4. With this ratio the CMR goes from 1.48 to 1.59 (7.43% increment) and the probability of collapse decreases from 8.44% to 5.89%. Using larger ratios will increase the cost of the structure and the results are virtually the same. These results corroborate with the results obtained in the pushover analysis where the post-yielding stiffness improvement stopped for ratios larger than 0.4. Again, the explicit model could be justified for this structure because the gravity connection had some influence on its seismic performance.

The results obtained for the 8-Story model are shown in the Fig. 9 (a) and (b) as well, and as it was expected from the pushover curves, the improvement of the CMR and probability of collapse when the gravity columns are included as part of the lateral resisting system, is notable. The CMR goes from 1.48 for the 8-Story building without the gravity columns influence to 2.00 when the 8-Story model includes the gravity columns with stiffness per story ratio equal to 1. It is interesting to note the direct relation between the nonlinear dynamic results and the pushover curves. Fig. 8 (b) shows how the post-yielding stiffness improves progressively when the stiffness per story of the gravity columns increases.

6 Conclusions

This study had the purpose of evaluating the influence of the gravity system on the collapse performance of SMFs. Two different approaches were considered to this endeavor: an explicit model that incorporated the effect of the gravity columns and gravity connections and a lumped model that included just the effect of the gravity columns into the analysis. After performing the respective analyses, the following conclusions can be reached:

- The gravity columns do not yield unless the gravity connections have moment capacity strength (larger than 30% M_p).
- The influence on the collapse performance of SMFs that the gravity system brings when the explicit model is used is very important. However, the strength of the gravity connections influenced importantly just the 2-Story model, has a minor effect on the 4-Story, and has an almost negligible effect on the 8-Story model.
- In general, the strength of the gravity connections reduces the residual displacement at DBE and MCE. The effect is less important in taller buildings.
- Continuous gravity columns (gravity connections with no strength) reduced residual displacements at DE or MCE level shaking primarily when the structure was subjected to large deformations. The influence of the gravity columns is more important in taller buildings such as the 8-Story frame.
- The results of the lumped and explicit model are the same if the gravity system has connections with no strength and the gravity columns do not yield.
- The lumped model can be used if the gravity columns are continuous all over their height (splices provide full moment capacity) and they are pinned at the base.
- It is known that continuous stiffness can prevent or reduce the probability of buildings to develop drift concentrations or weak story mechanisms. This was reflected in this study by reducing the probability of collapse of the structures
- The influence of the gravity columns is significant on the 8-Story model and improves the collapse performance significantly.
- It was found that there is a relation between the post-yielding stiffness and the dynamic performance of the SMFs when the lumped model is used. Therefore an “optimal” lumped inertia could be found by performing nonlinear static pushover analysis.

7 Acknowledgements

The work presented herein was possible through the support of the National Institute of Standards and Technology, award number 60ANB10D017, and of the National Research Center for Integrated Natural Disaster Management CONICYT/FONDAP/15110017. The authors would also like to acknowledge the contribution of Mr. Andy Hardyniec of Virginia Tech for his work creating the

FEMA P-695 Toolkit and NeesHub for their help on conducting all the computations in their super computers.

8 References

[1] R.T. Leon, Composite connections, Progress in Structural Engineering and Materials, 1 (1998) 159-169.

[2] J. Liu, A. Astaneh-Asl, Cyclic testing of simple connections including effects of slab, Journal of Structural Engineering, 126 (2000) 32-39.

[3] A. Gupta, H. Krawinkler, Behavior of ductile SMRFs at various seismic hazard levels, Journal of Structural Engineering, 126 (2000) 98-107.

[4] G.A. MacRae, The Continuous Column Concept-Development and Use, Proceedings of the Ninth Pacific Conference on Earthquake Engineering Building an Earthquake-Resilient Society, (2011).

[5] H. Tagawa, Towards an understanding of seismic response of 3D structures-stability & reliability, Doctor Thesis, Washington: University of Washington, (2005).

[6] F. Zareian, D. Lignos, H. Krawinkler, Evaluation of seismic collapse performance of steel special moment resisting frames using FEMA P695 (ATC-63) methodology, in: Proceedings of Structures Congress ASCE, New York, 2010.

[7] NIST, Evaluation of the FEMA P-695 Methodology for Quantification of Building Seismic Performance Factors, National Institute of Standards and Technology, USA, 2010.

[8] F. P695, Quantification of Building Seismic Performance Factors, Fededral Emergency Management Agency, Washington, D.C, 2009.

[9] ASCE, Minimum design loads for buildings and other structures, American Society of Civil Engineers/Structural Engineering Institute, Reston, VA, 2006.

[10] AISC, Seismic Provisions for Structural Steel Buildings, ANSI/AISC 341-05, American Institute for Steel Construction., Chicago, Ill., 2005.

[11] F.X. Flores, F.A. Charney, D. Lopez-Garcia, Influence of the gravity framing system on the collapse performance of special steel moment frames, Journal of Constructional Steel Research, 101 (2014) 351-362.

[12] F. McKenna, G. Fenves, M. Scott, OpenSees: Open system for earthquake engineering simulation, Pacific Earthquake Engineering Center, University of California, Berkeley, CA., http://opensees. berkeley. edu, (2006).

[13] ASCE, Seismic Rehabilitation of Existing Buildings (ASCE/SEI 41-13), in, American Society of Civil Engineers Reston, Virginia, 2013.

[14] D. Vamvatsikos, C.A. Cornell, Applied incremental dynamic analysis, Earthquake Spectra, 20 (2004) 523.

[15] FEMA, Recommended seismic design criteria for new steel moment-frame buildings, FEMA 350 Report, 2000.

Appendix D: Incremental Dynamic Figures

Model: 8Story

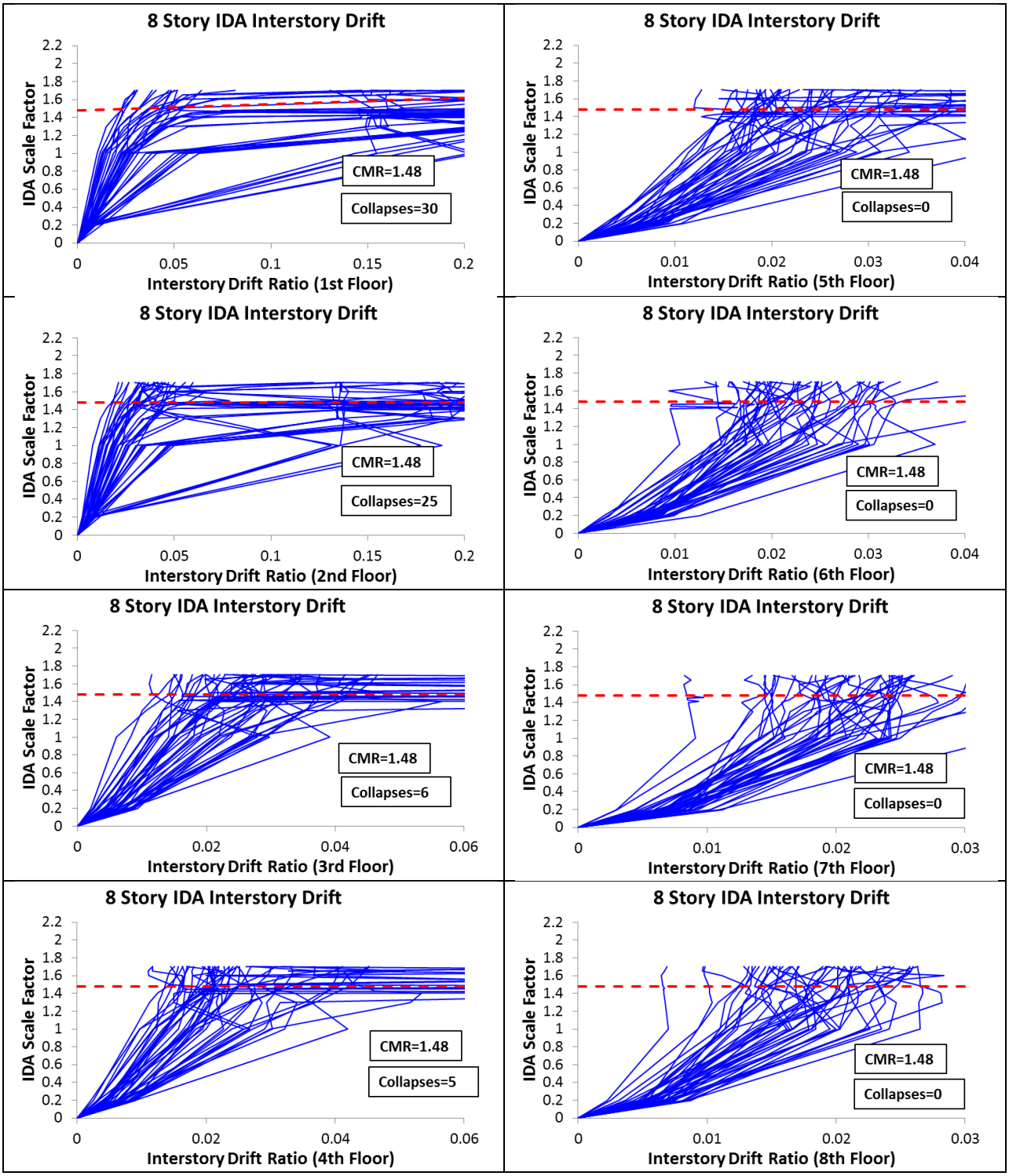

Model: 8Story_0GS (Elastic)

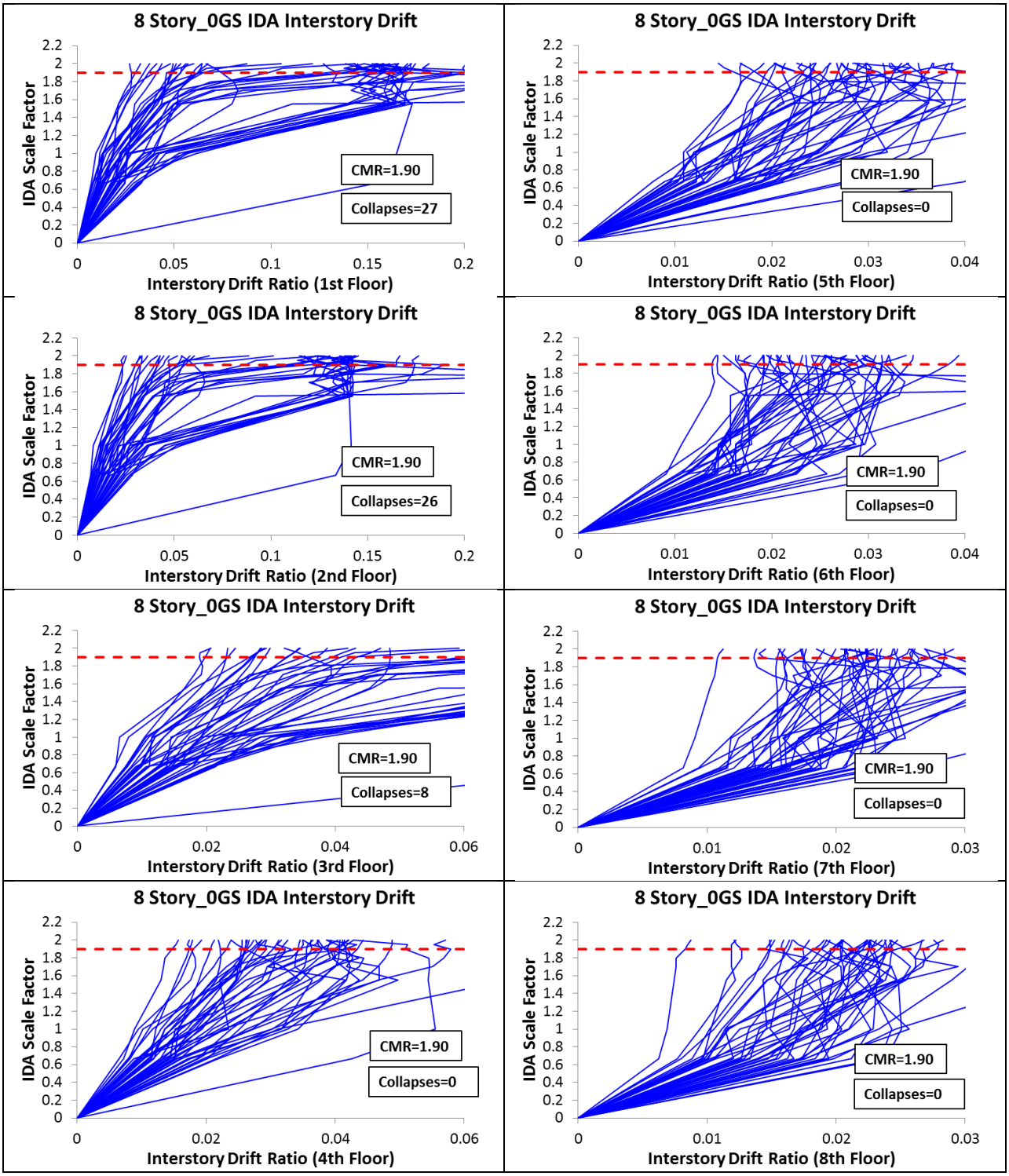

Model: 8Story_0GS (Fibers)

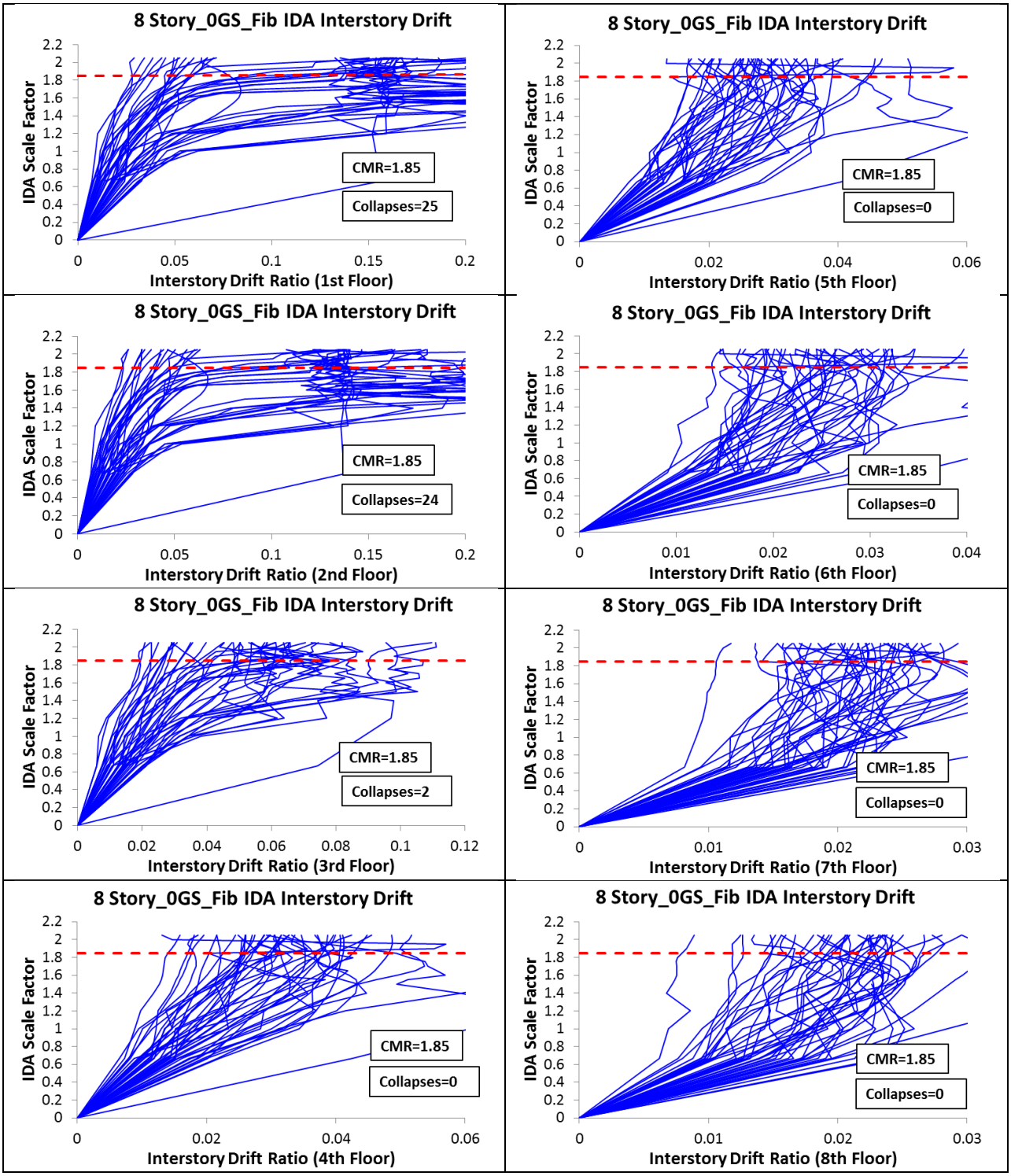

Model: 8Story_35GS (Elastic)

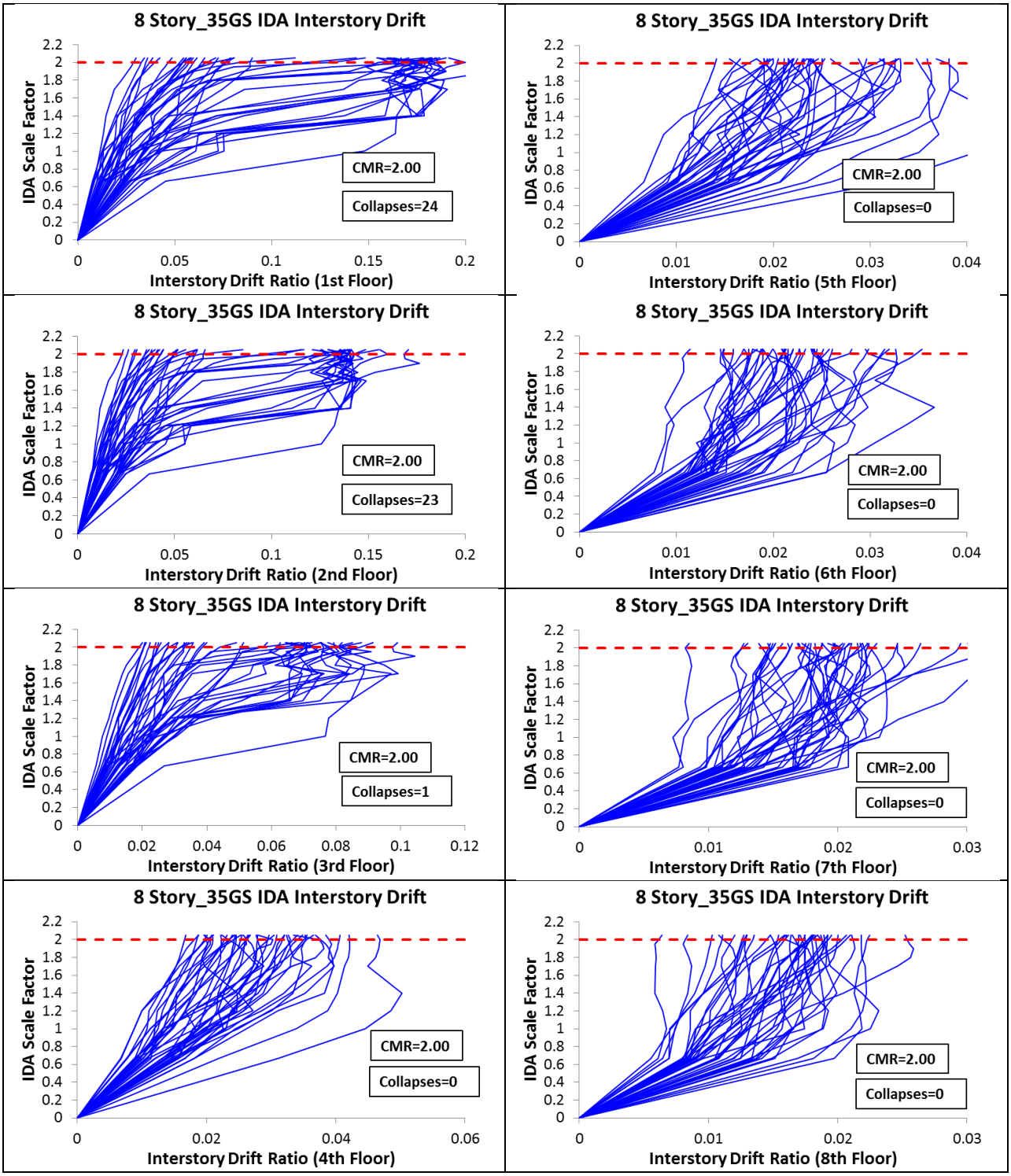

Model: 8Story_35GS (Fibers)

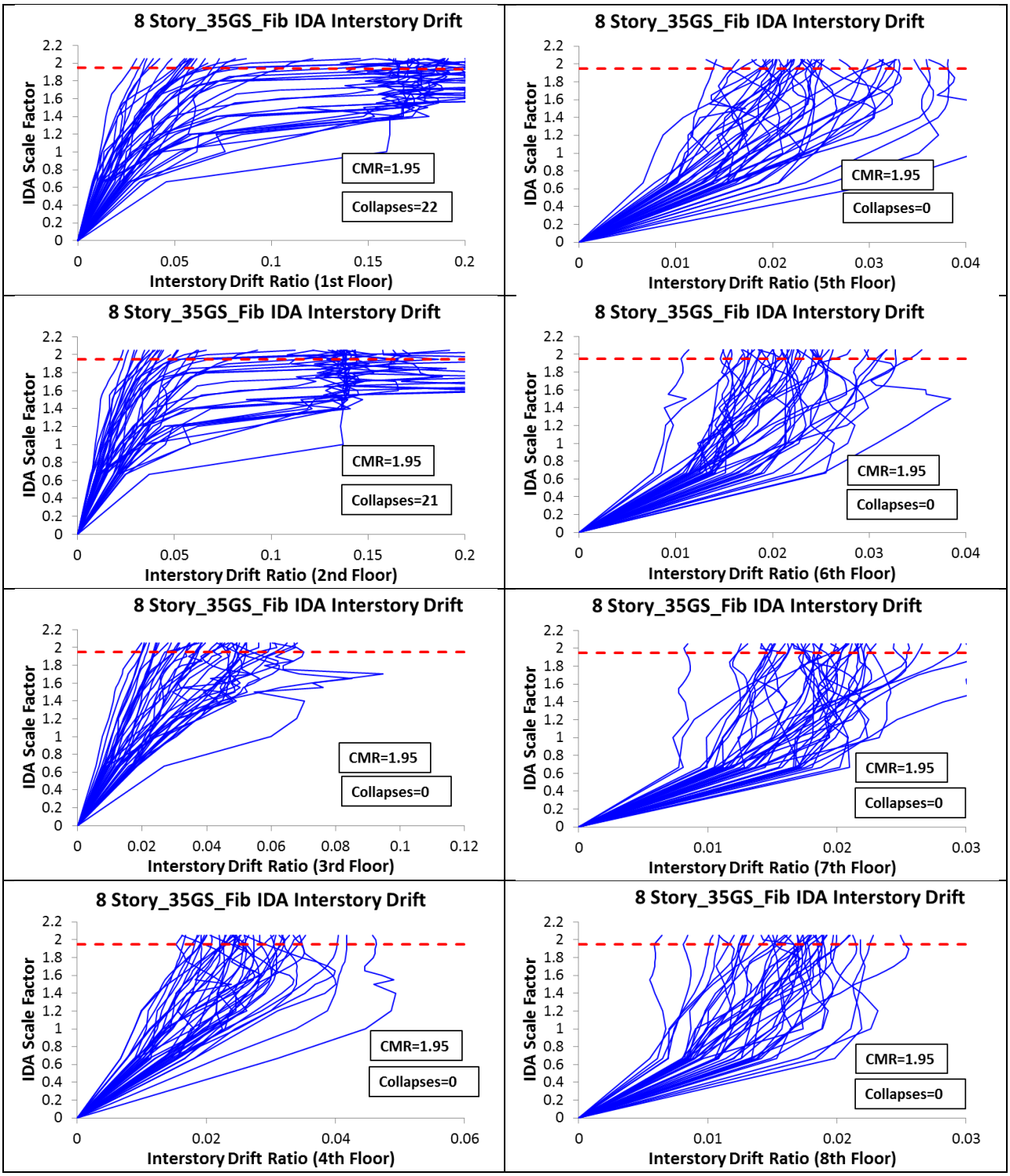

Model: 8Story_50GS (Elastic)

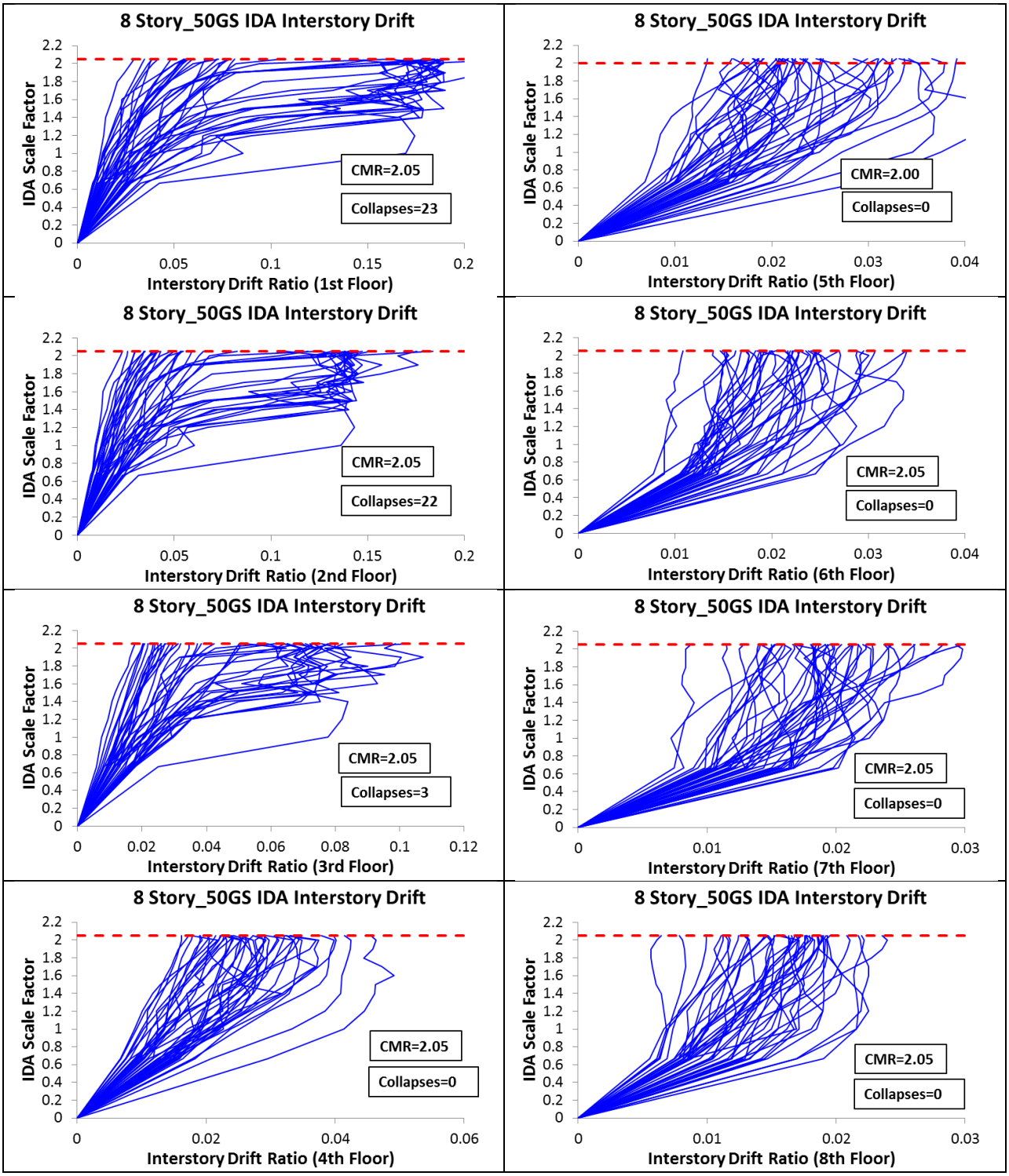

Model: 8Story_50GS (Fibers)

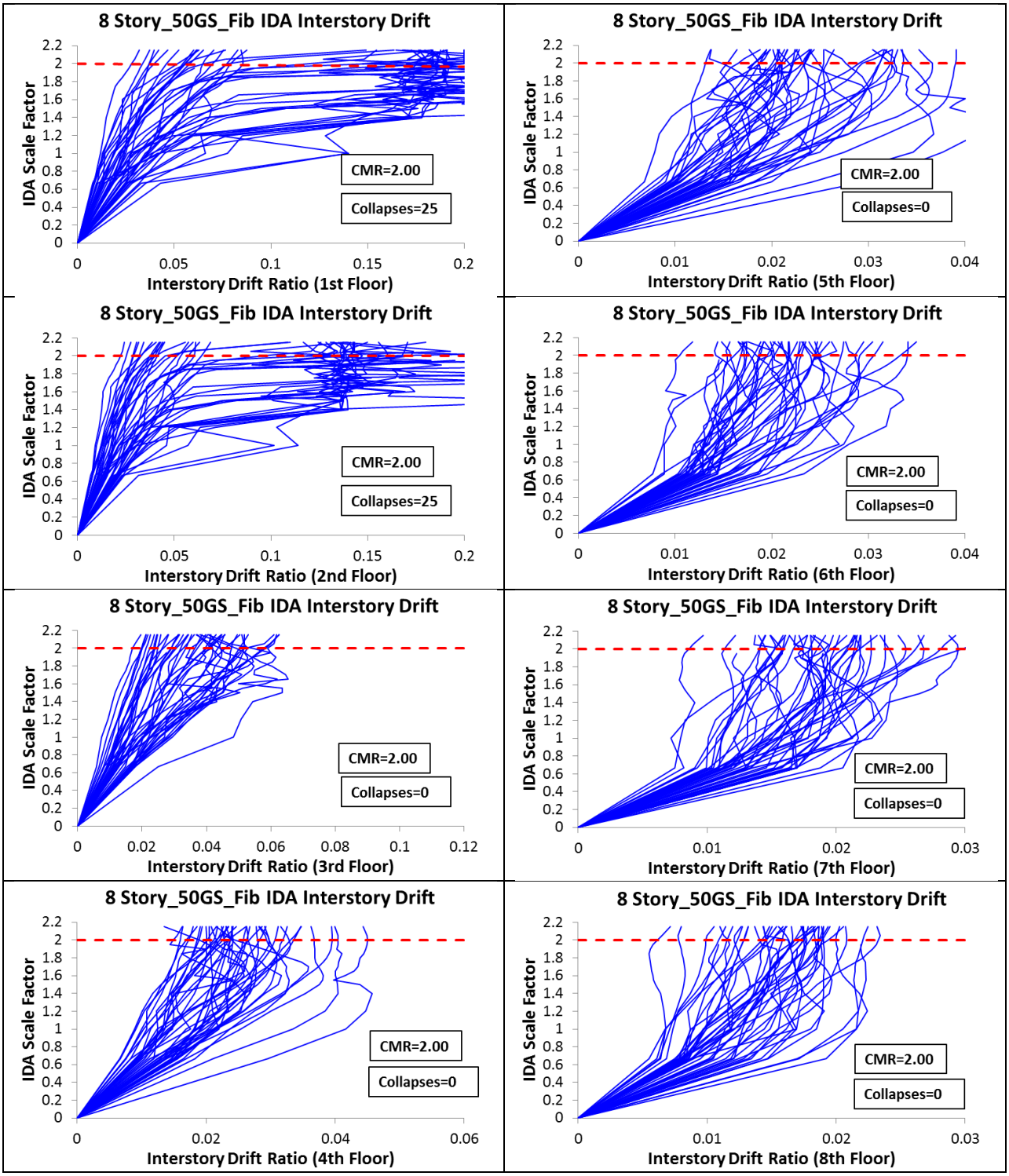

Model: 8Story_70GS (Elastic)

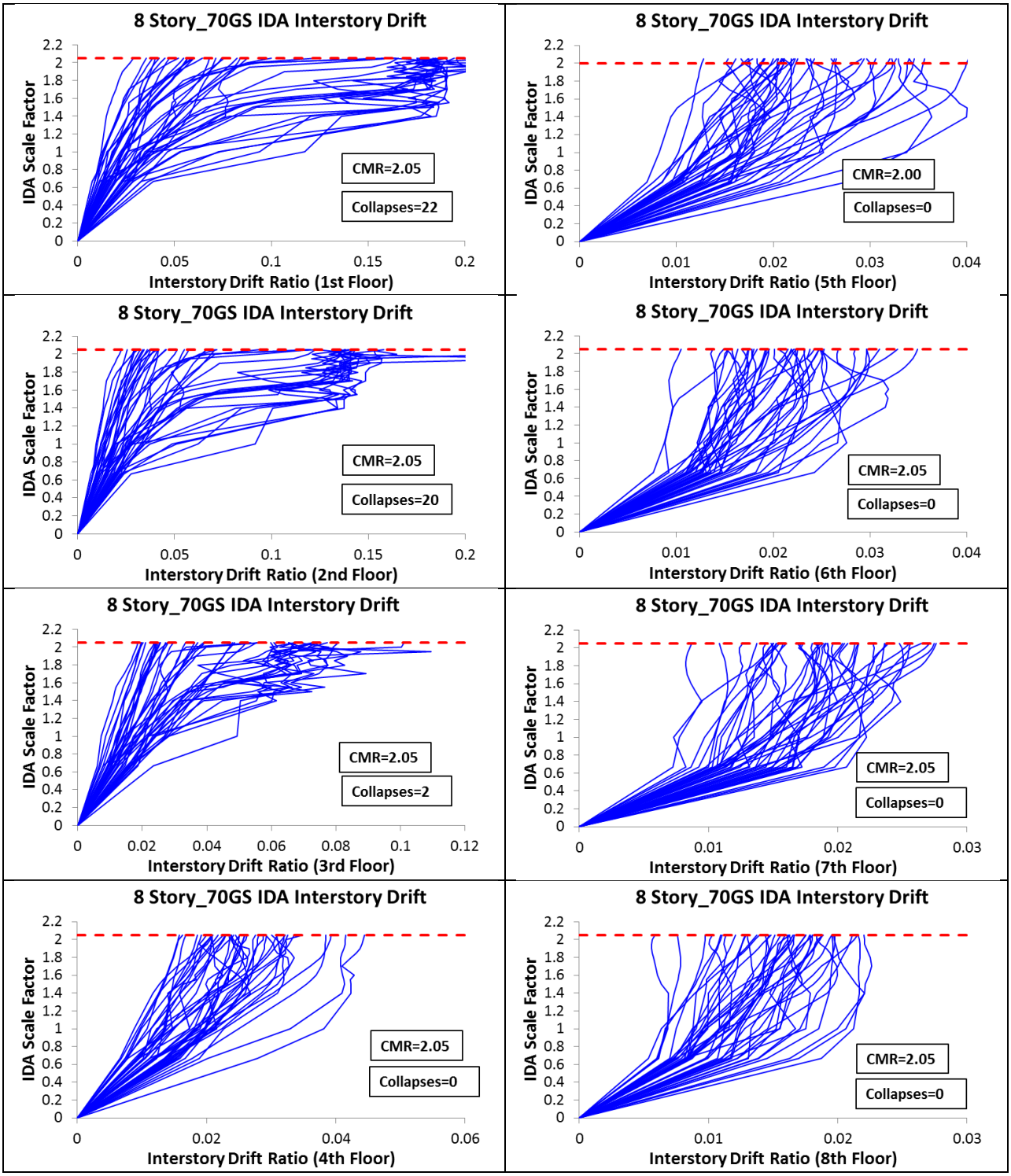

Model: 8Story_70GS (Fibers)

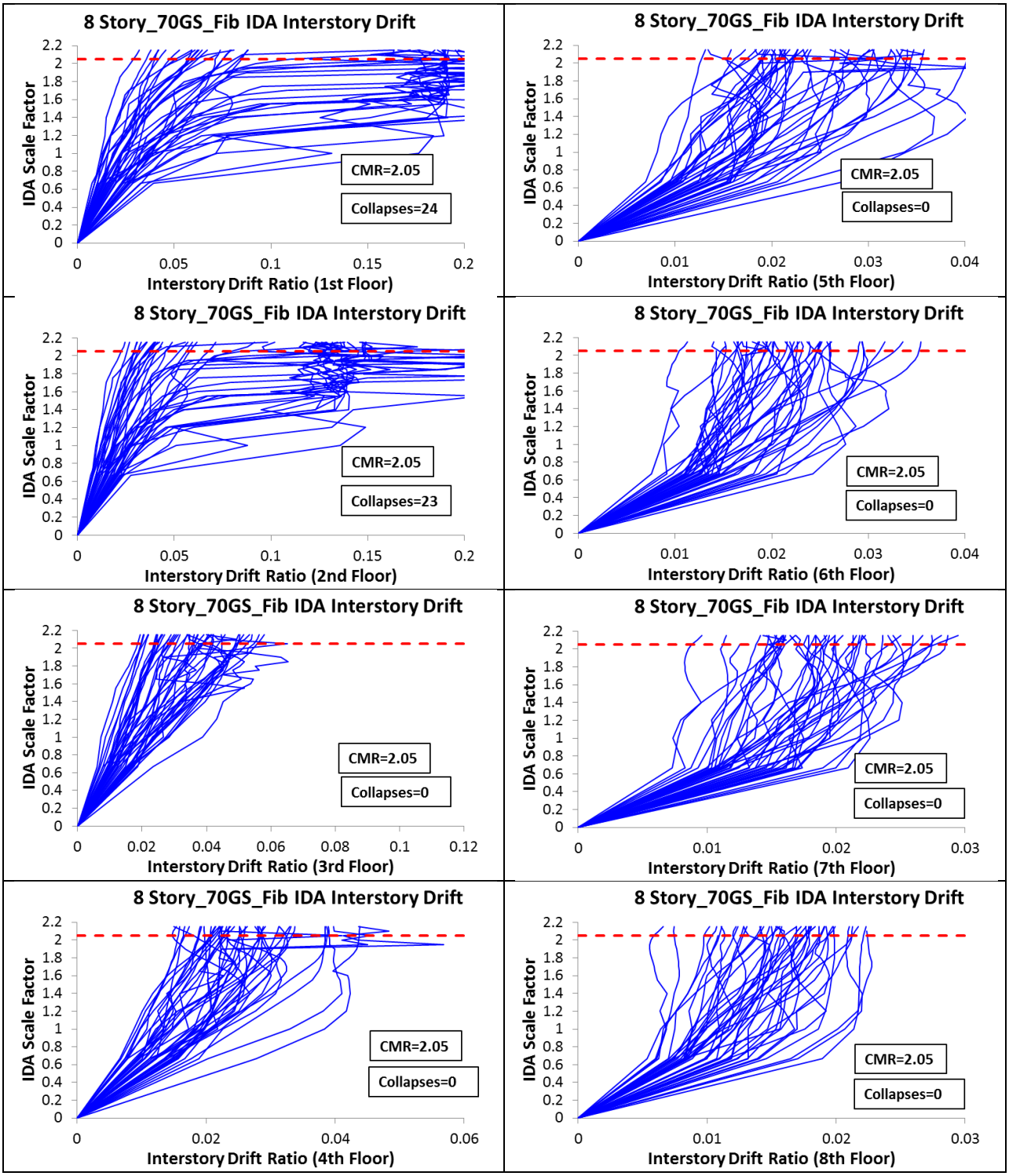

Scale Factors that Caused Collapse										
Far Field Ground Motions			Gravity Columns - Elastic Sections				Gravity Columns - Fiber Sections			
		8 Story	8 Story_0GS	8 Story_35GS	8 Story_50GS	8 Story_70GS	8 Story_0GS	8 Story_35GS	8 Story_50GS	8 Story_70GS
		CMR=1.48	CMR=1.90	CMR=2.00	CMR=2.05	CMR=2.05	CMR=1.85	CMR=1.95	CMR=2.00	CMR=2.05
Northridge-BH	MUL009									
Northridge-BH	MUL279									
Northridge-CC	LOS000	1.48	1.8	2	2.05		1.8		2	2.05
Northridge-CC	LOS270									
Duzce-Bolu	BOL000									
Duzce-Bolu	BOL090	1.3						1.95		
Hector-Hector	HEC000									
Hector-Hector	HEC090	1.48	1.9				1.85			
Imperial Valley-Delta	H-DLT262	1	1.55	1.4	1.4	1.4	1.2	1.2	1.4	1
Imperial Valley-Delta	H-DLT352	1	0.666	1	1	1	0.666	1	1	1
Imperial Valley-EC	H-E11140	1.4	1.8	1.9	2	2.05	1.7	1.85	1.9	1.95
Imperial Valley-EC	H-E11230	1.43	1.7	1.9	2	2.05	1.7	1.85	1.95	2
Kobe-Nishi Akashi	NIS000	1.3	1.55	1.4	1.5	1.55	1.55	1.4	1.4	1.55
Kobe-Nishi Akashi	NIS090	1.43	1.9				1.85			
Kobe-Shin Osaka	SHI000	1.3	1.55	1.7	1.6	1.6	1.5	1.5	1.5	1.6
Kobe-Shin Osaka	SHI090									
Kocaeli-Duzce	DZC180	1.3	1.55	1.4	1.5	1.4	1.4	1.4	1.4	1.4
Kocaeli-Duzce	DZC270	1.3	1.55	1.7	1.6	1.6	1.4	1.5	1.5	1.6
Kocaeli-Arcelik	ARC000									
Koaceli-Arcelik	ARC090	1	1.55	1.2	1.4	1.4	1.2	1.2	1.4	1.4
Landers-Yermo	YER270	1	1.55	1.4	1.4	1.5	1.2	1.4	1.4	1.55
Landers-Yermo	YER360			2	2.05	2.05			2	
Landers-Coolwater	CLW-LN									
Landers-Coolwater	CLW-TR									
Loma Prieta-Capitola	CAP000									
Loma Prieta-Capitola	CAP090		1.9							
Loma Prieta-Gilroy	G03000									
Loma Prieta-Gilroy	G03090	1.48	1.8	1.9	2	2.05	1.8	1.85	1.9	1.95
Manjil-Abbar	ABBAR--L	1.48	1.8	1.8	1.9	1.85	1.75	1.7	1.75	1.8
Manjil-Abbar	ABBAR--T	1.3	1.9	1.7	1.7	1.7	1.85	1.65	1.6	1.65
Superstition Hills-EC	B-ICC000	1.3	1.55	1.7	1.7	1.8	1.5	1.6	1.65	1.7
Superstition Hills-EC	B-ICC090									
Superstition Hills-Poe	B-POE270	1	1.55	1.4	1.4	1.4	1.2	1.4	1.4	1.4
Superstition Hills-Poe	B-POE360	1.3	1.55	1.4	1.4	1.4	1.5	1.4	1.4	1.4
Cape Mendocino-Rio Dell	RIO270									
Cape Mendocino-Rio Dell	RIO360									
Chi Chi-CHY	CHY101-E	1.3		1.9	2	2		1.9	1.9	1.9
Chi Chi-CHY	CHY101-N	1.3	1.55	1.4	1.5	1.55	1.4	1.4	1.4	1.4
Chi Chi-TCU	TCU045-E	1.3	1.55	1.7	1.6	1.6	1.4	1.5	1.5	1.55
Chi Chi-TCU	TCU045-N									
San Fernando-LA	PEL180	1.4	1.55	1.7	1.6	1.6	1.5	1.5	1.55	1.6
San Fernando-LA	PEL090	1	1.55	1.4	1.4	1.4	1.2	1.4	1.4	1.2
Friuli-Tolmezzo	A-TMZ000									
Friuli-Tolmezzo	A-TMZ270									
Number of Colapses		25	24	23	23	22	23	22	23	22

Model: 8Story_0GS_Levelled_Splices (Elastic)

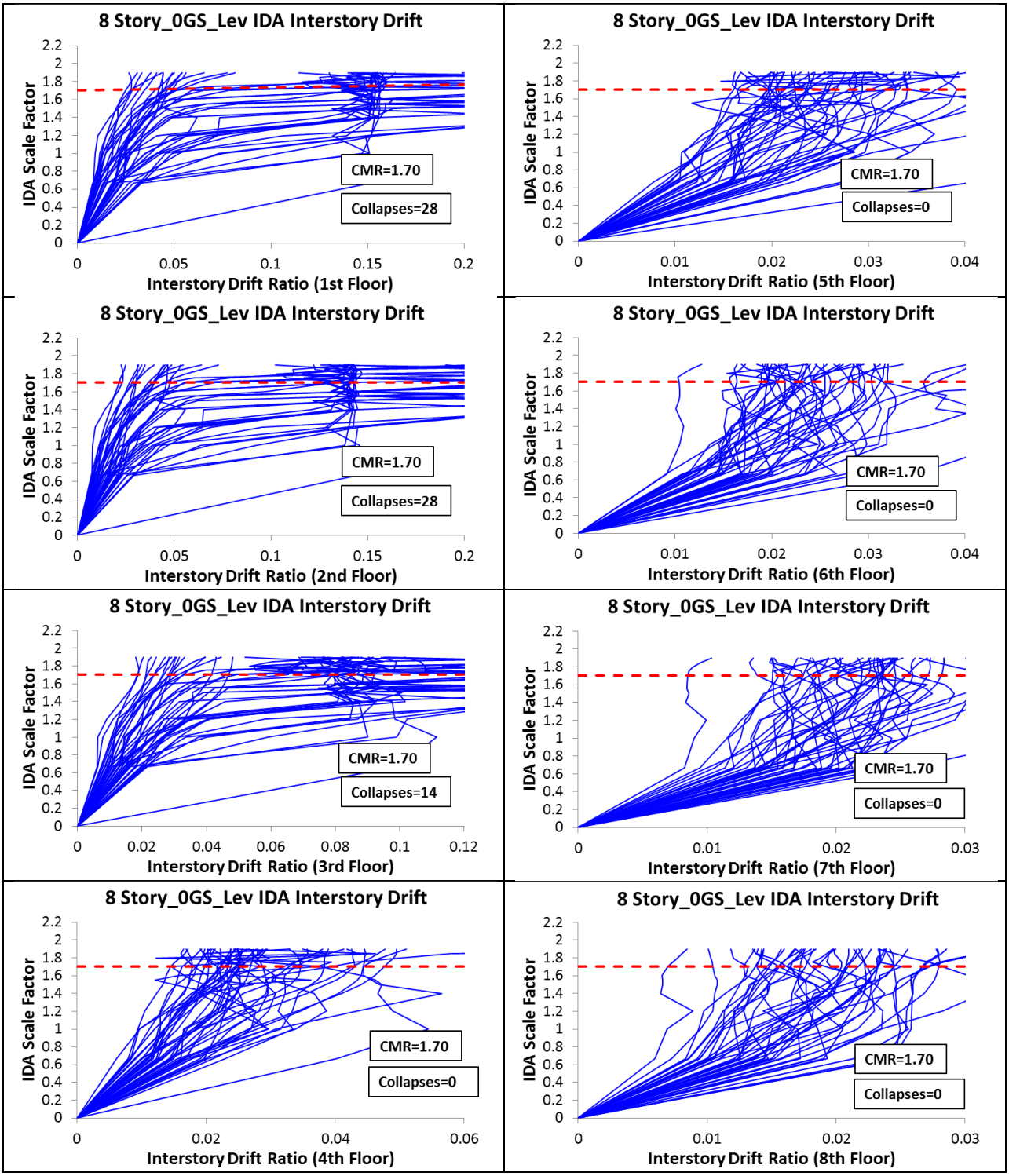

Model: 8Story_0GS_Levelled_Splices (Fibers)

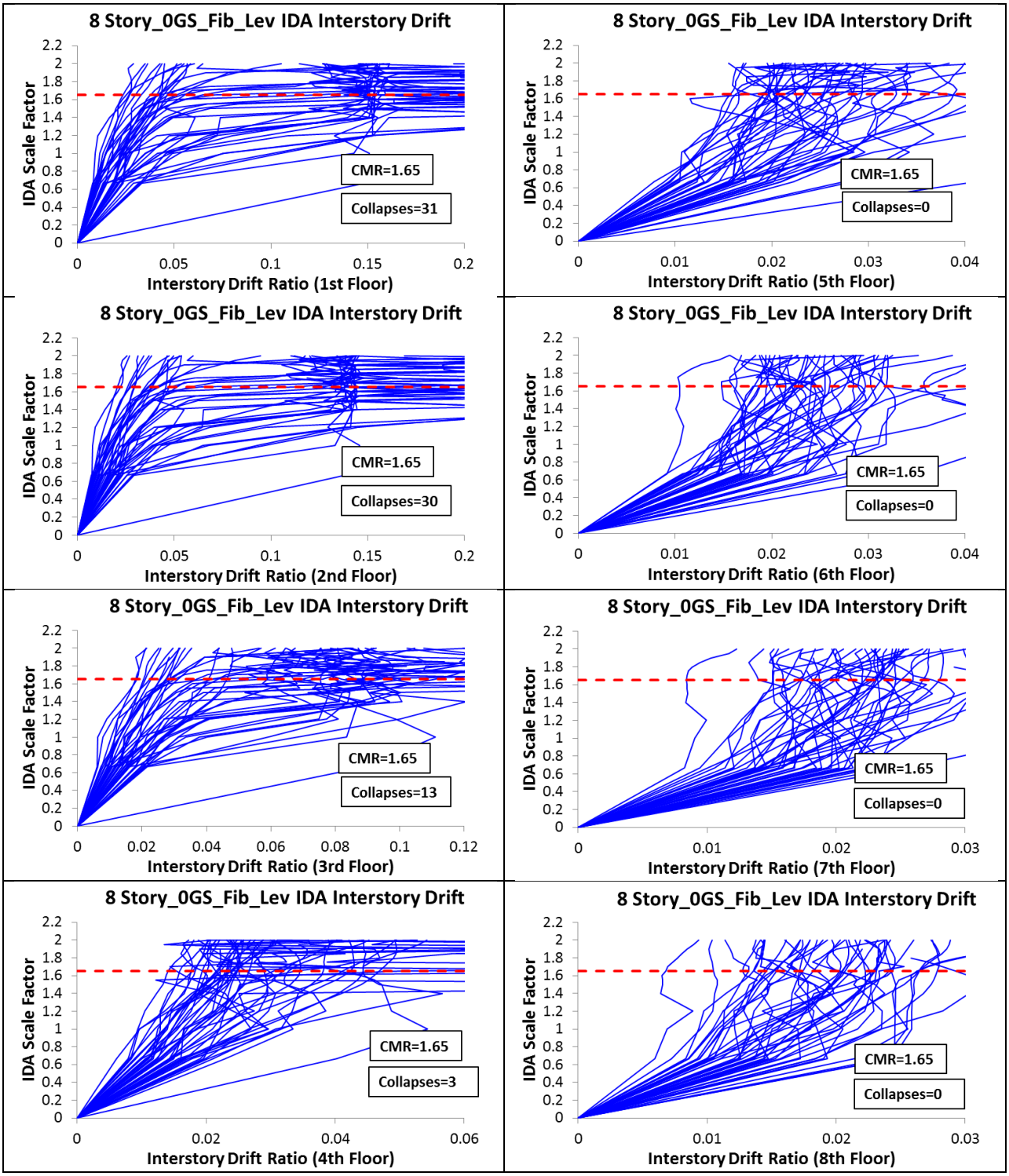

Model: 8Story_35GS_Levelled_Splices (Elastic)

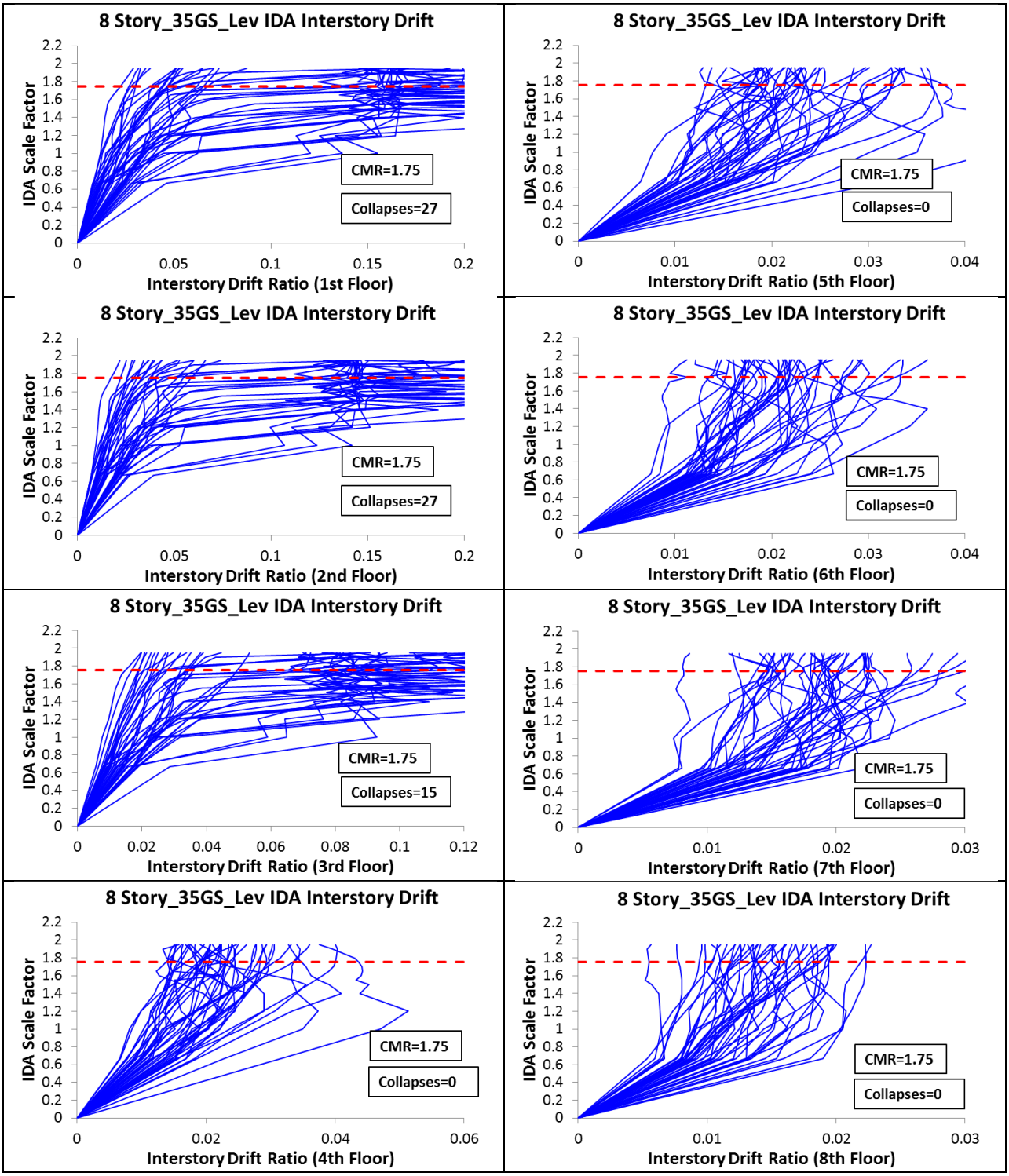

Model: 8Story_35GS_Levelled_Splices (Fibers)

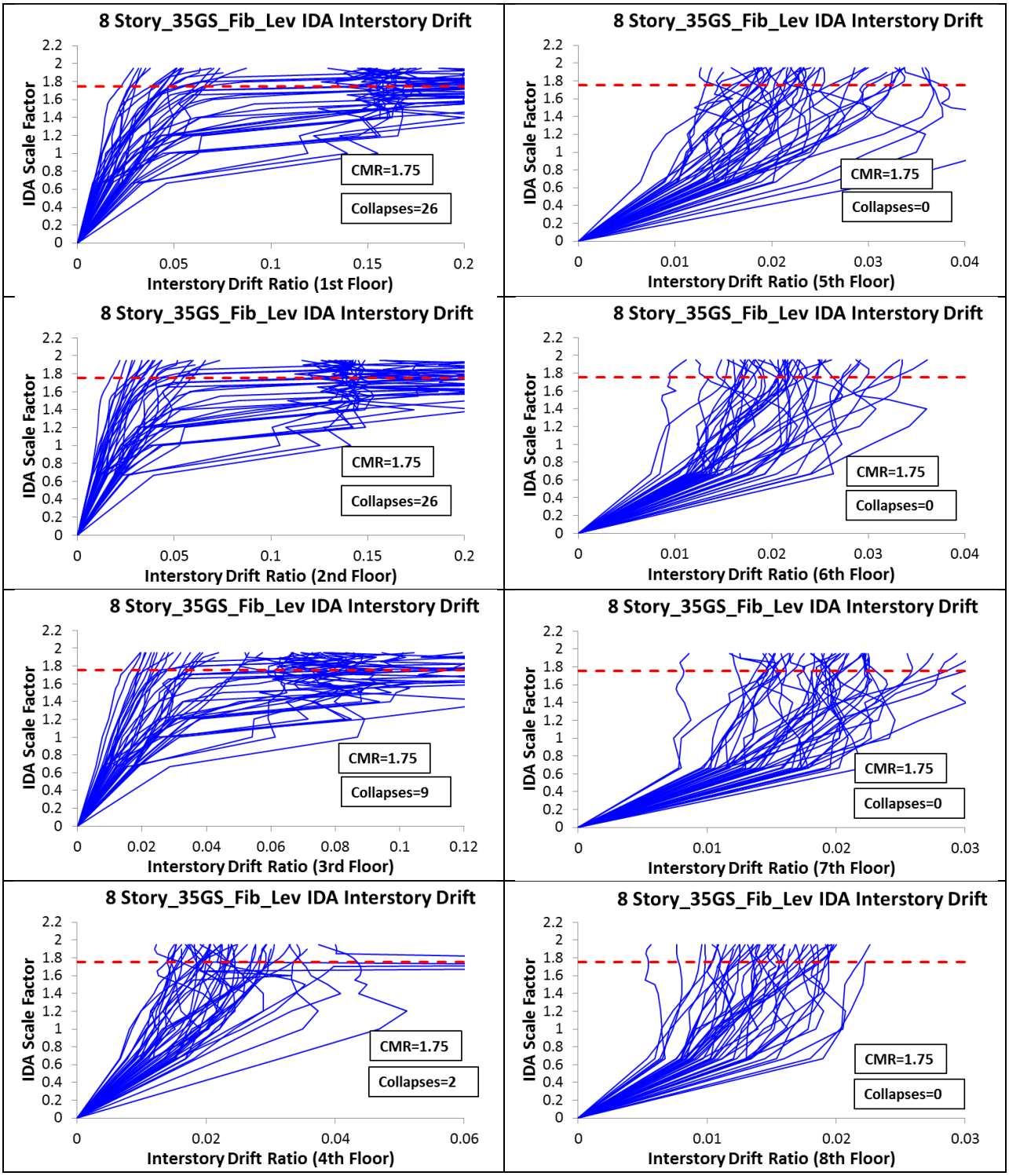

Model: 8Story_50GS_Levelled_Splices (Elastic)

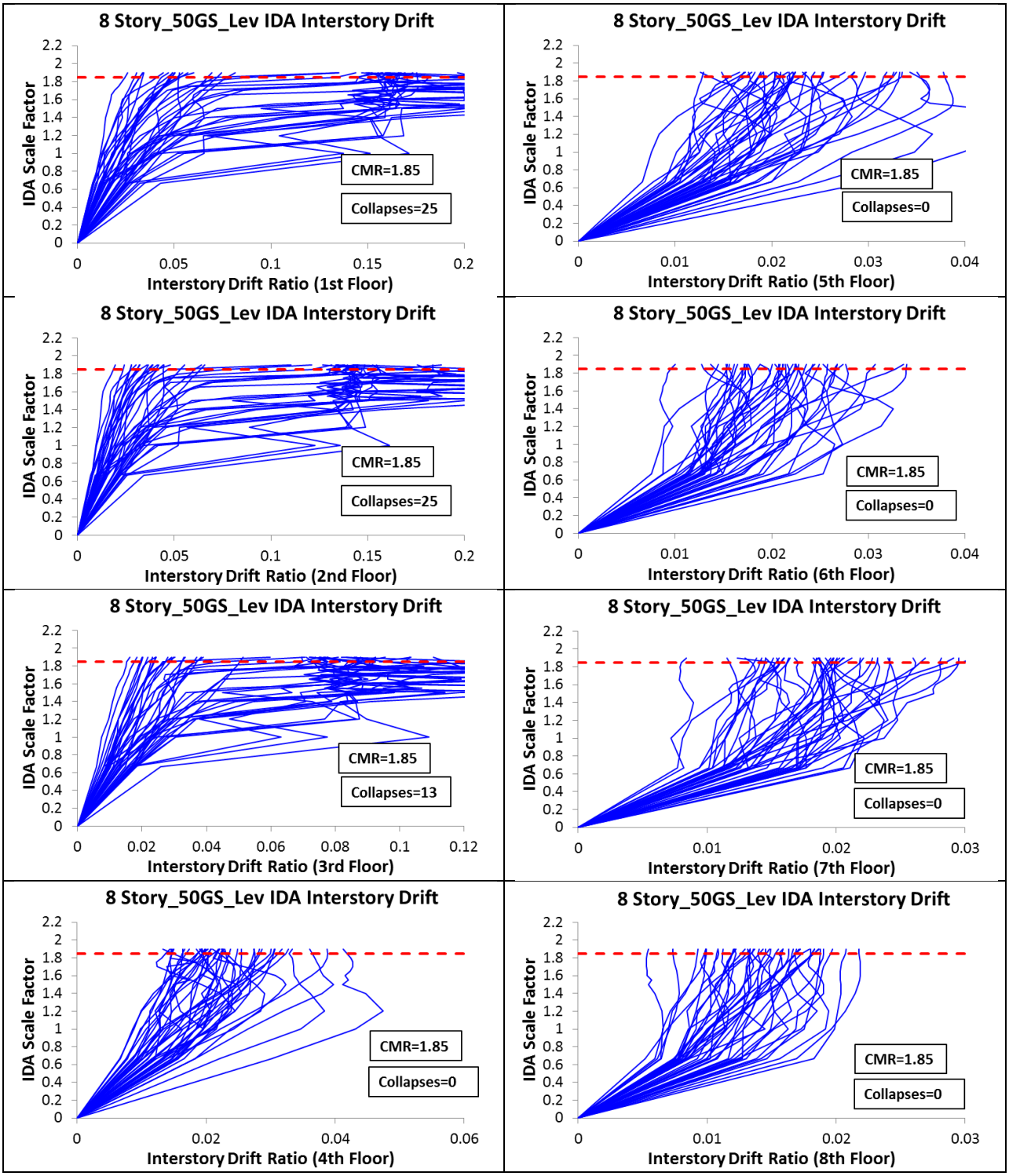

Model: 8Story_50GS_Levelled_Splices (Fibers)

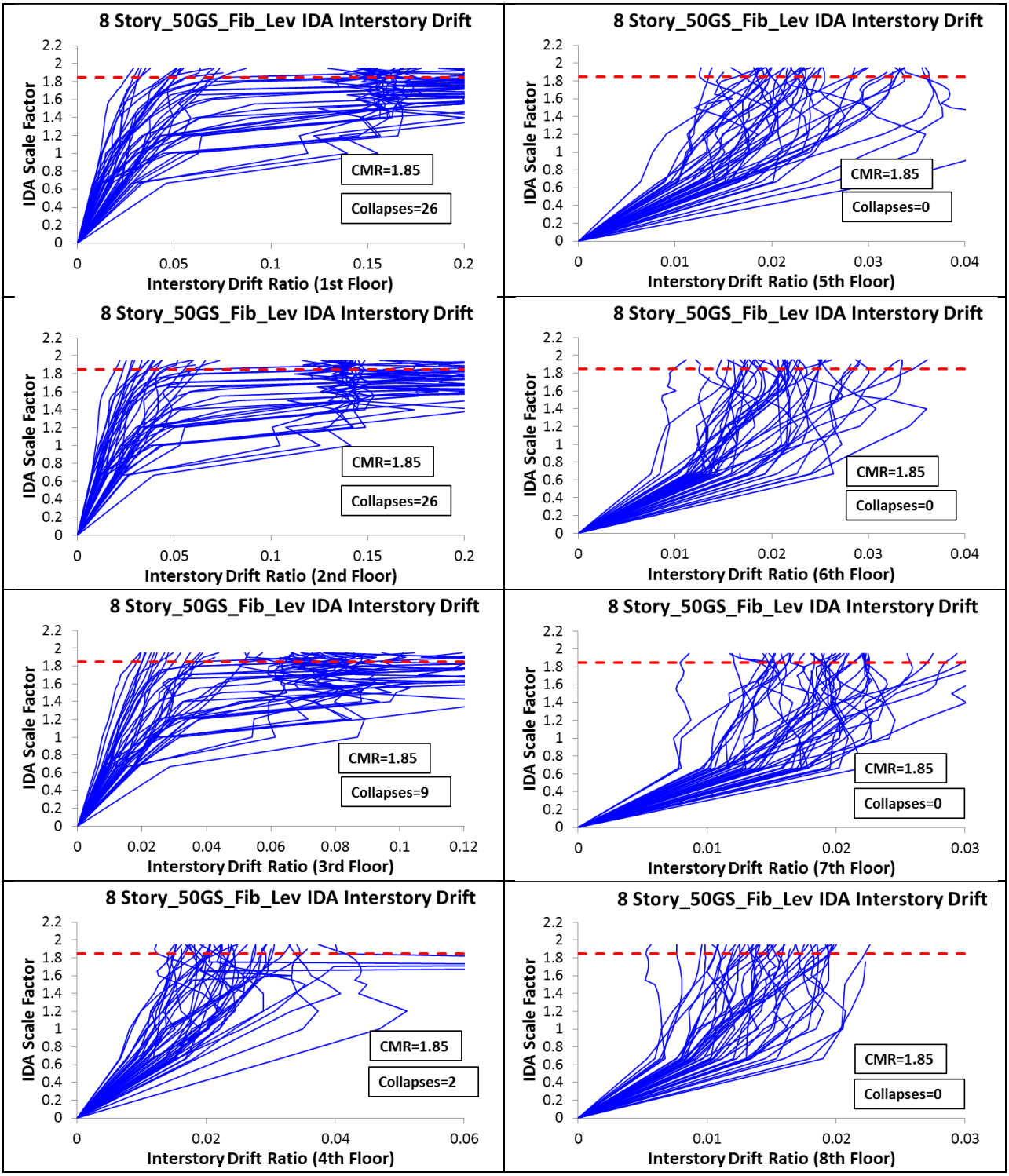

Model: 8Story_70GS_Levelled_Splices (Elastic)

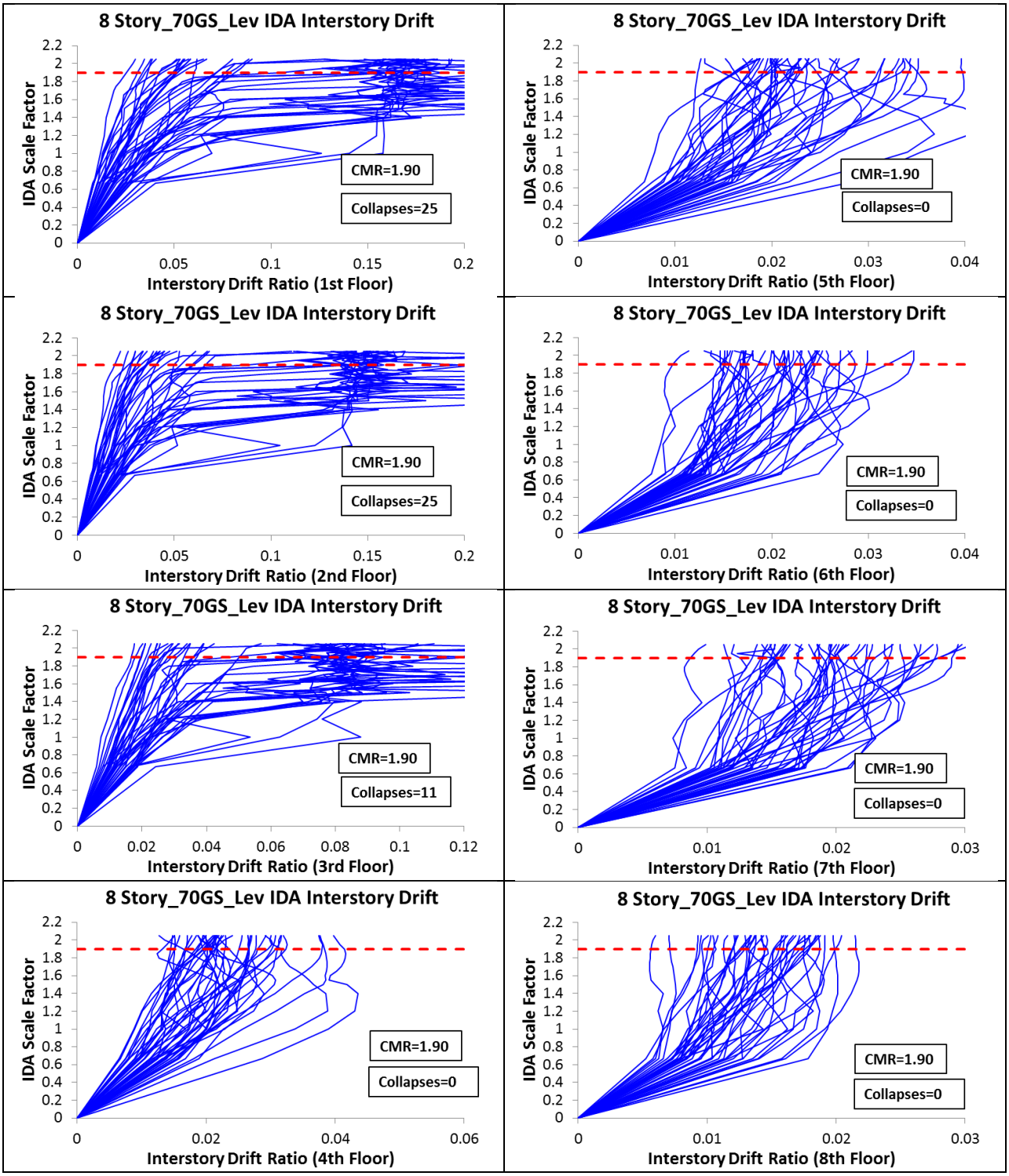

Model: 8Story_70GS_Levelled_Splices (Fibers)

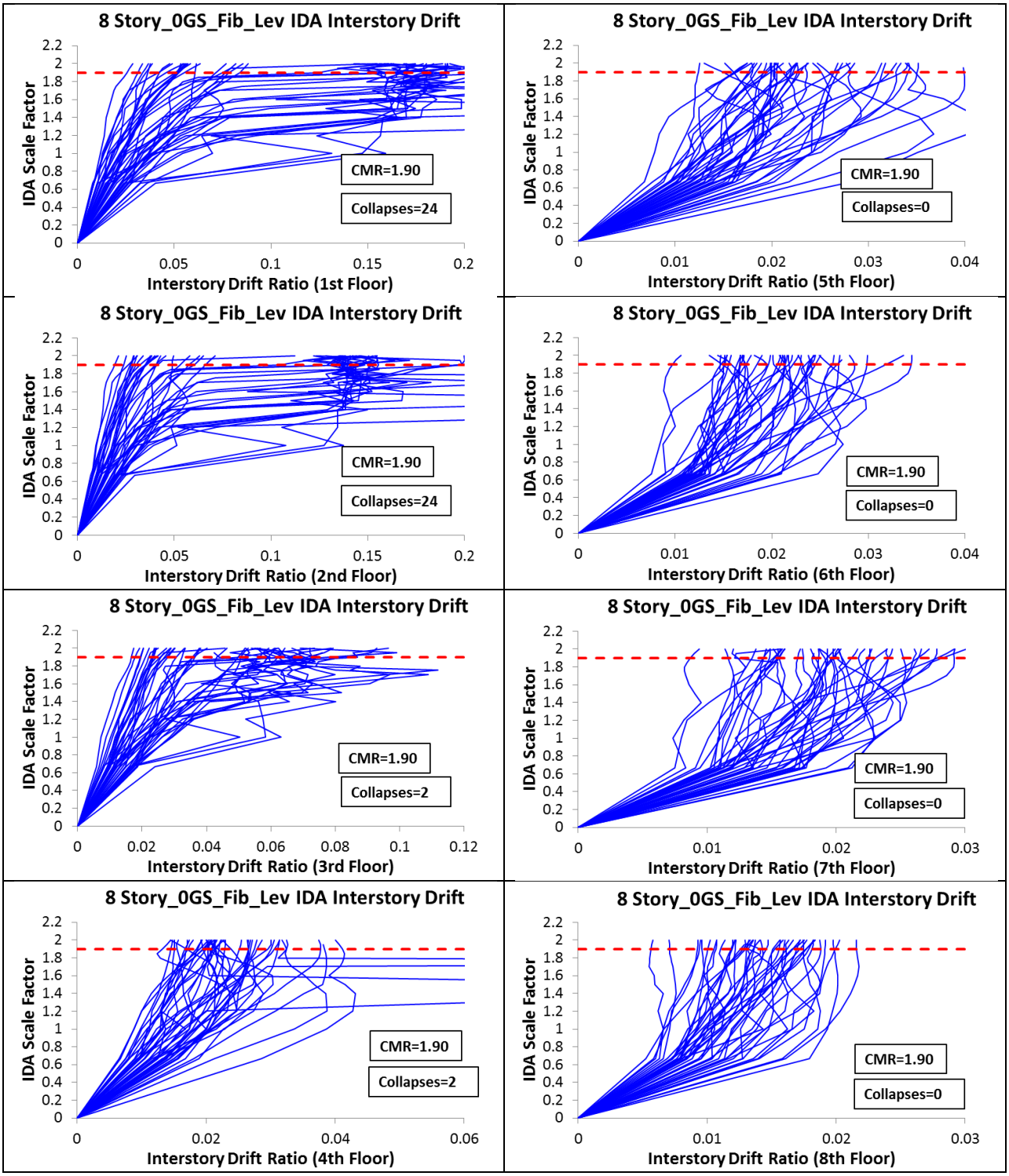

Scale Factors that Caused Collapse									
Far Field Ground Motions		Levelled Splices: Gravity Columns Elastic Sections				Levelled Splices: Gravity Columns with Fiber Sections			
		8 Story_0GS	8 Story_35GS	8 Story_50GS	8 Story_70GS	8 Story_0GS	8 Story_35GS	8 Story_50GS	8 Story_70GS
		CMR=1.70	CMR=1.75	CMR=1.85	CMR=1.90	CMR=1.65	CMR=1.75	CMR=1.85	CMR=1.90
Northridge-BH	MUL009								
Northridge-BH	MUL279								
Northridge-CC	LOS000	1.6	1.7	1.75	1.8	1.6	1.7	1.7	1.8
Northridge-CC	LOS270								
Duzce-Bolu	BOL000								
Duzce-Bolu	BOL090	1.4	1.6	1.75		1.55	1.6	1.6	
Hector-Hector	HEC000								
Hector-Hector	HEC090								
Imperial Valley-Delta	H-DLT262	1	1	1	1	1	1	1	1.6
Imperial Valley-Delta	H-DLT352	0.666	1	1	1	0.666	1	1	1
Imperial Valley-EC	H-E11140	1.5	1.75	1.85	1.9	1.5	1.75	1.75	1.9
Imperial Valley-EC	H-E11230	1.6	1.75	1.8	1.9	1.6	1.75	1.75	1.9
Kobe-Nishi Akashi	NIS000	1.4	1.2	1.4	1.4	1.4	1.2	1.2	1.4
Kobe-Nishi Akashi	NIS090	1.7						1.85	2
Kobe-Shin Osaka	SHI000	1.2	1.4	1.4	1.5	1.4	1.4	1.4	1.5
Kobe-Shin Osaka	SHI090								
Kocaeli-Duzce	DZC180	1.2	1.4	1.4	1.4	1.2	1.4	1.4	1.4
Kocaeli-Duzce	DZC270	1.4	1.4	1.4	1.5	1.4	1.4	1.4	1.5
Kocaeli-Arcelik	ARC000								
Koaceli-Arcelik	ARC090	1.2	1.2	1.2	1.4	1.2	1.2	1.2	1.4
Landers-Yermo	YER270	1	1.4	1.4	1.5	1.2	1.4	1.4	1.5
Landers-Yermo	YER360				1.9			1.85	1.9
Landers-Coolwater	CLW-LN								
Landers-Coolwater	CLW-TR								
Loma Prieta-Capitola	CAP000	1.7				1.65			
Loma Prieta-Capitola	CAP090								
Loma Prieta-Gilroy	G03000								
Loma Prieta-Gilroy	G03090	1.6	1.65	1.7	1.75	1.6	1.65	1.65	1.75
Manjil-Abbar	ABBAR--L	1.55	1.5	1.55	1.65	1.55	1.5	1.5	1.7
Manjil-Abbar	ABBAR--T		1.5	1.5	1.55		1.5	1.5	1.6
Superstition Hills-EC	B-ICC000	1.4	1.55	1.55	1.65	1.4	1.55	1.55	1.7
Superstition Hills-EC	B-ICC090								
Superstition Hills-Poe	B-POE270	1	1.2	1.2	1.4	1	1.2	1.2	1.4
Superstition Hills-Poe	B-POE360	1.4	1.2	1.2	1.4	1.4	1.2	1.2	1.4
Cape Mendocino-Rio Dell	RIO270								
Cape Mendocino-Rio Dell	RIO360								
Chi Chi-CHY	CHY101-E	1.4	1.7	1.75	1.85	1.4	1.7	1.7	1.85
Chi Chi-CHY	CHY101-N	1.5	1.4	1.4	1.5	1.5	1.4	1.4	1.5
Chi Chi-TCU	TCU045-E	1.4	1.4	1.5	1.5	1.4	1.4	1.4	1.5
Chi Chi-TCU	TCU045-N								
San Fernando-LA	PEL180	1.4	1.5	1.5	1.55	1.4	1.5	1.5	1.6
San Fernando-LA	PEL090	1.2	1	1.4	1.55	1.2	1	1	1
Friuli-Tolmezzo	A-TMZ000								
Friuli-Tolmezzo	A-TMZ270								
Number of Colapses		24	23	23	23	23	23	25	24

Model: 8Story_0GS_Staggered_Splices (Elastic)

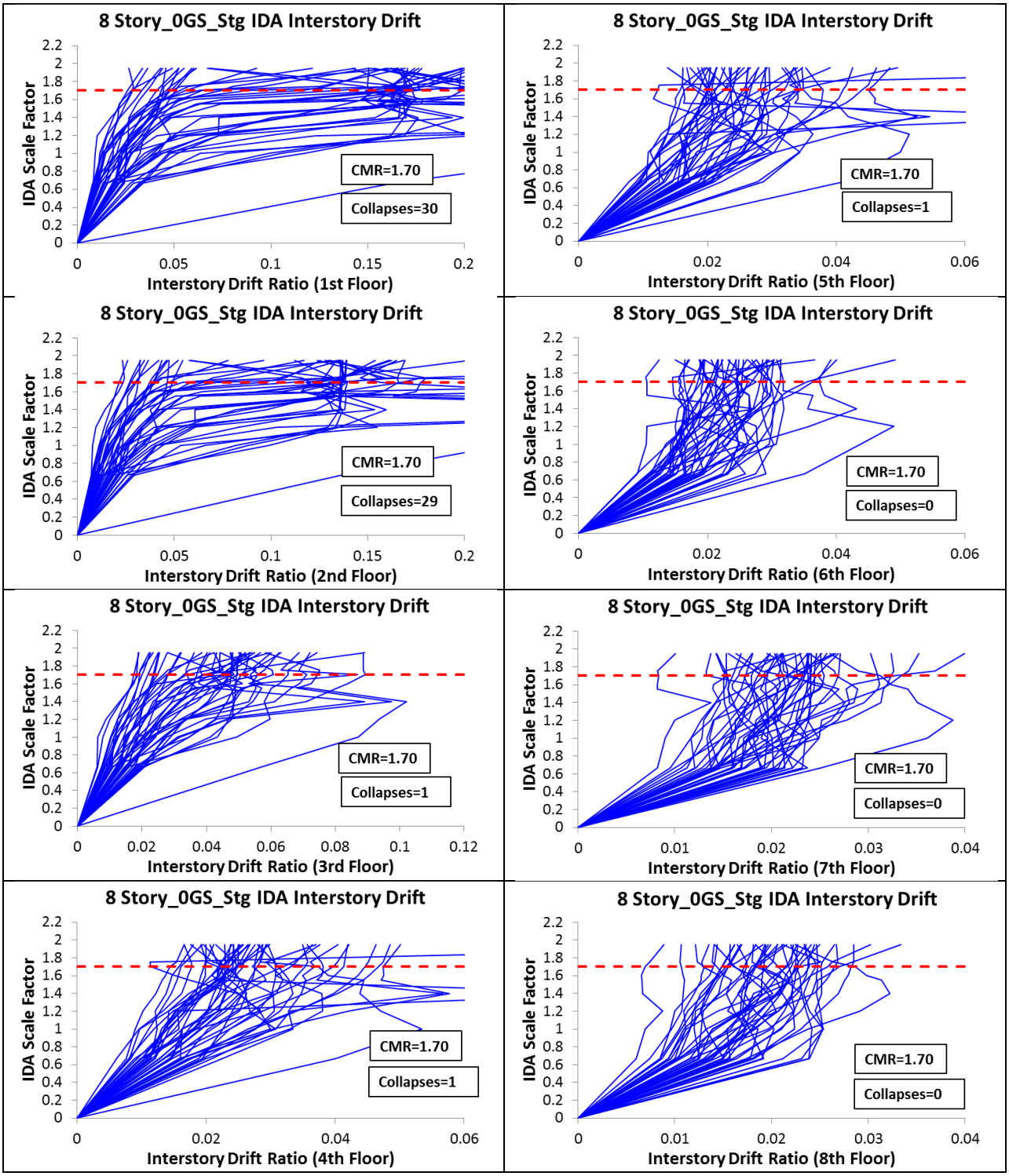

Model: 8Story_0GS_Staggered_Splices (Fibers)

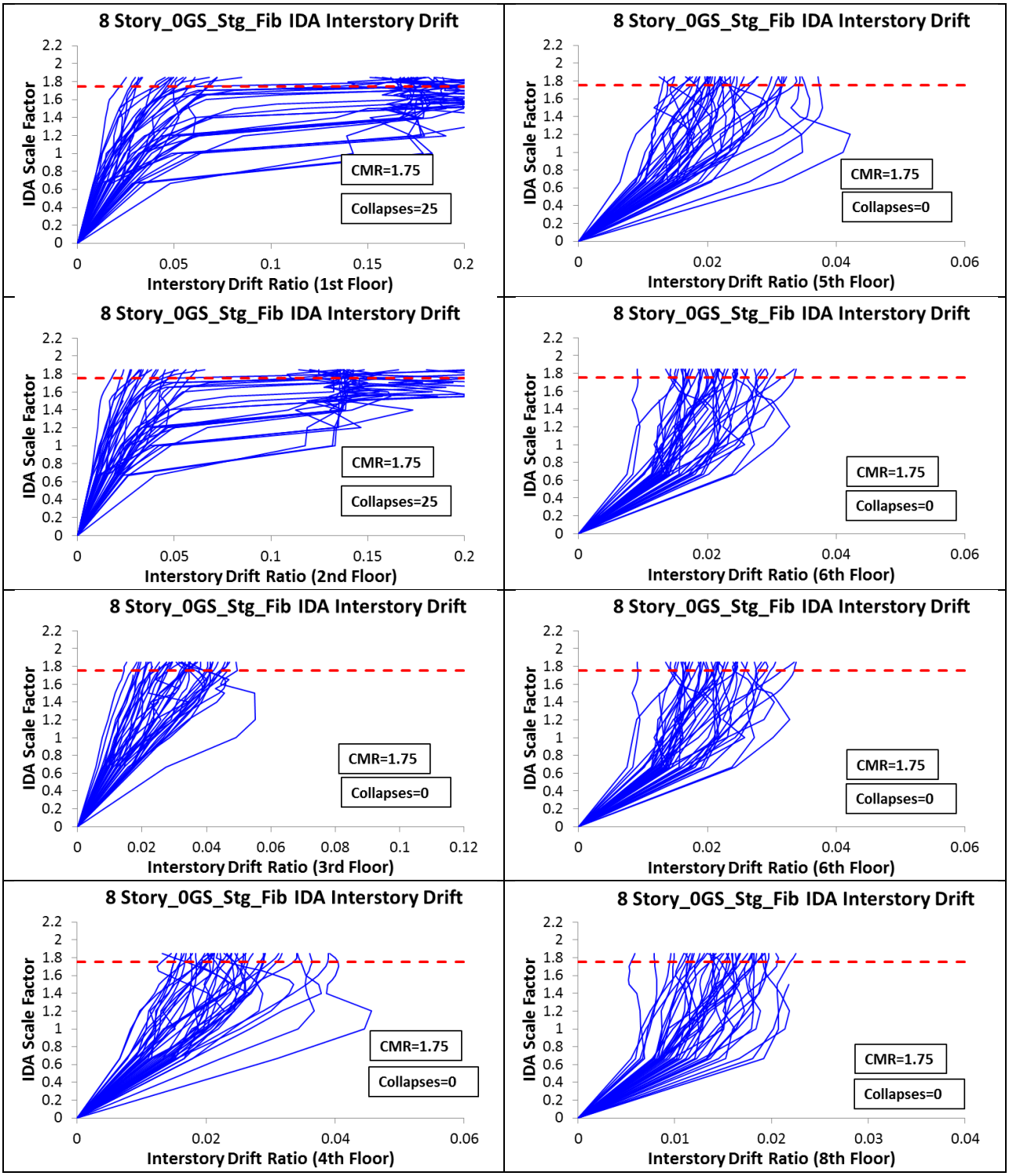

Model: 8Story_35GS_Staggered_Splices (Elastic)

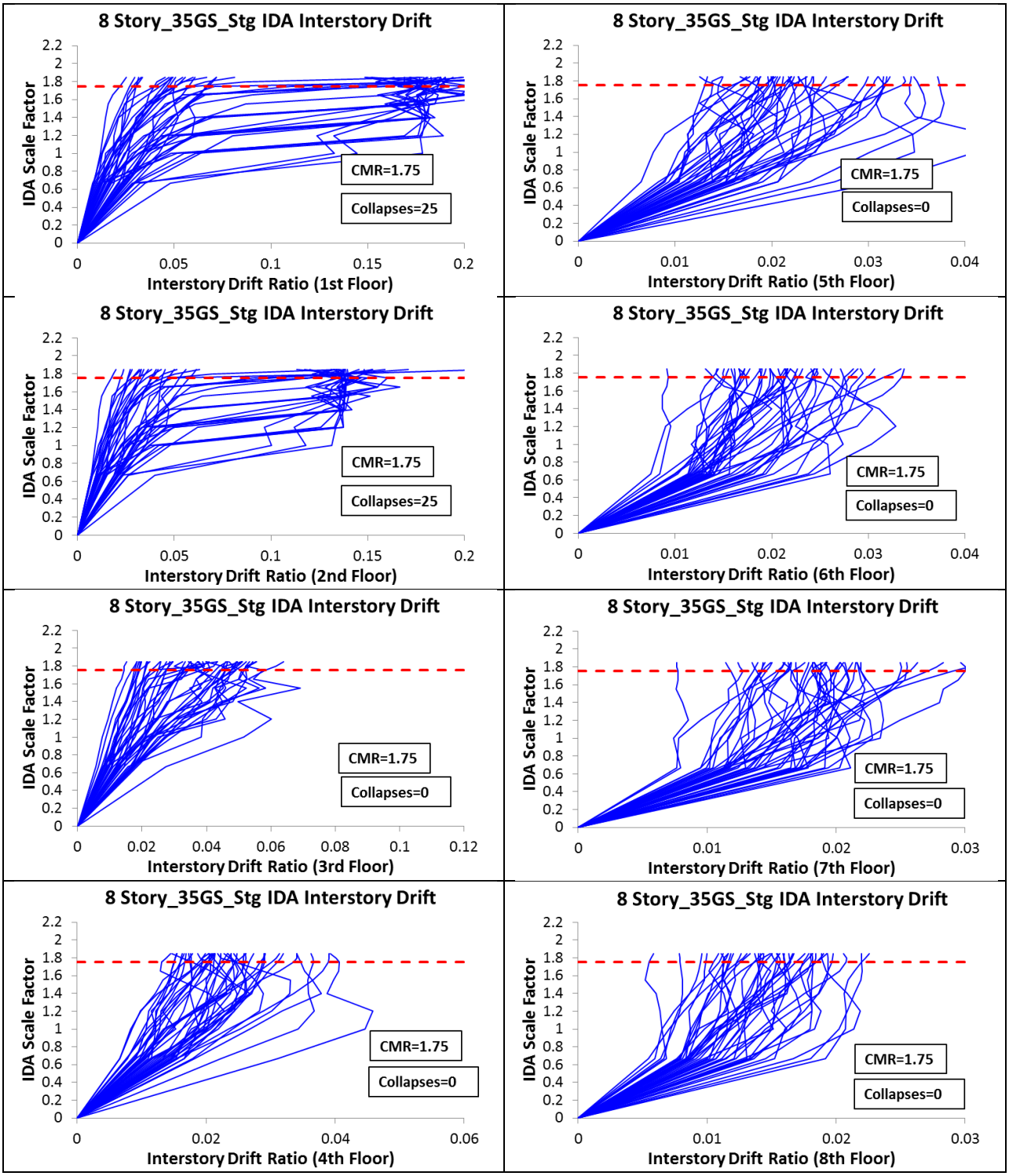

Model: 8Story_35GS_Staggered_Splices (Fibers)

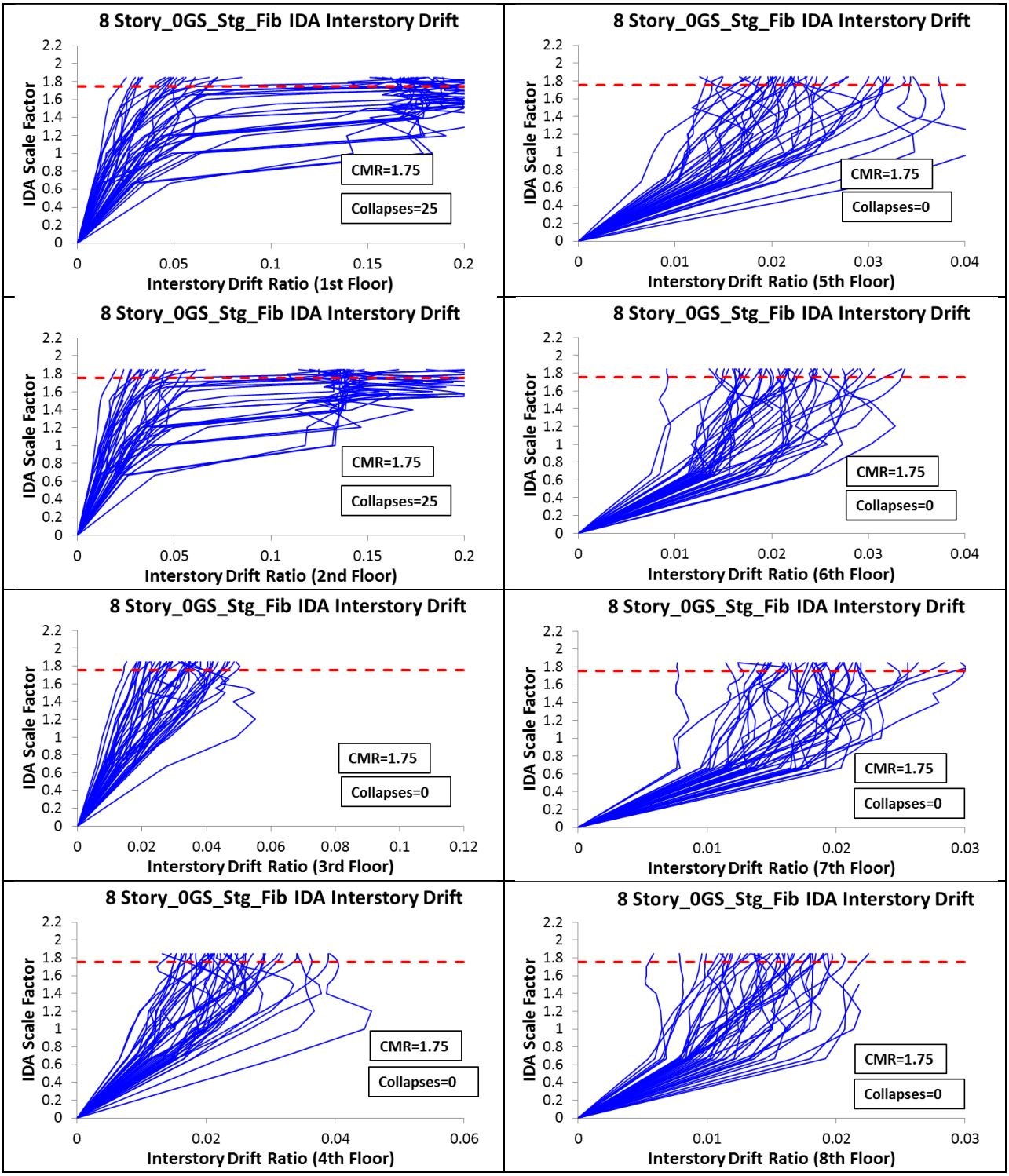

Model: 8Story_50GS_Staggered_Splices (Elastic)

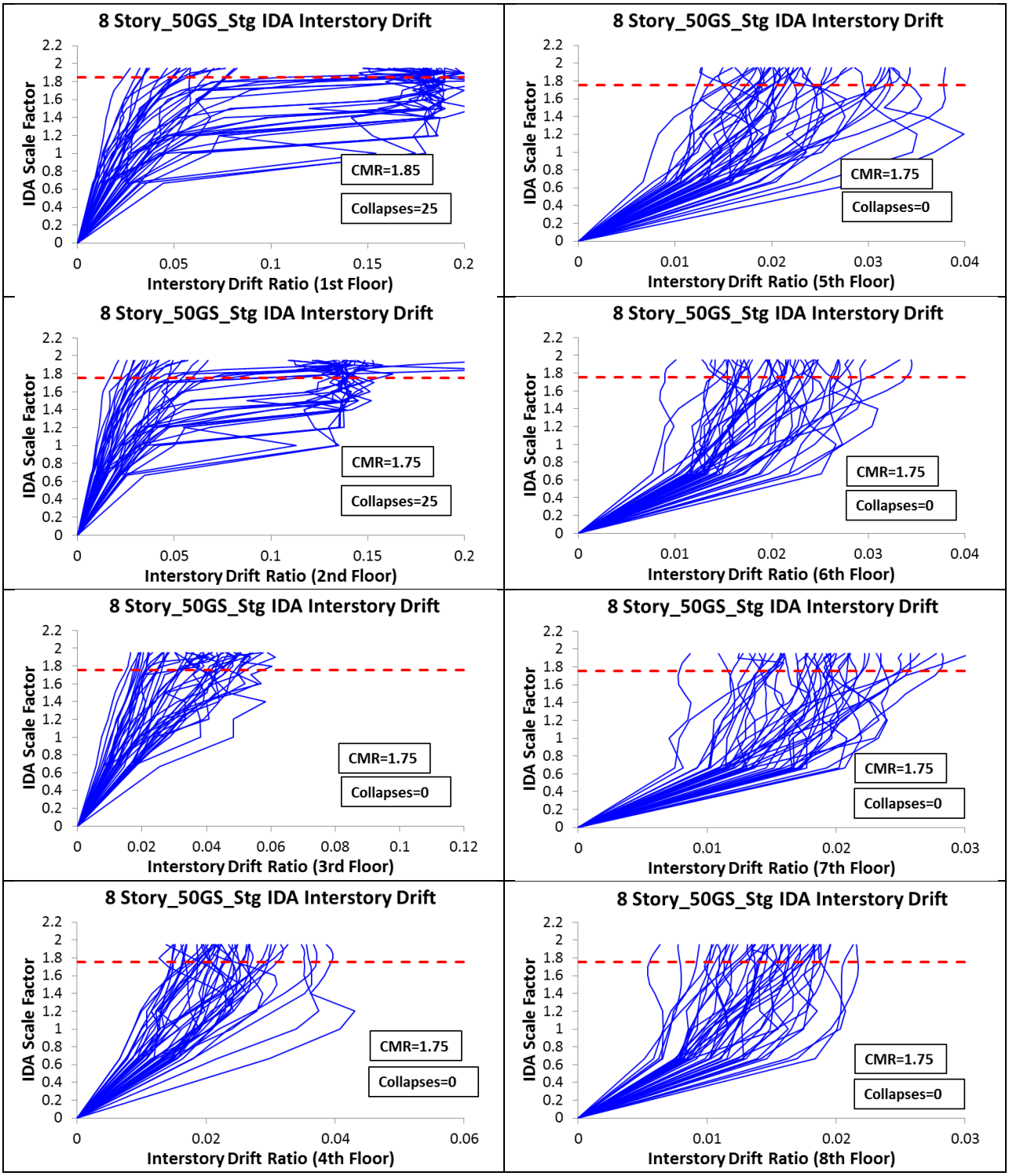

Model: 8Story_50GS_Staggered_Splices (Fibers)

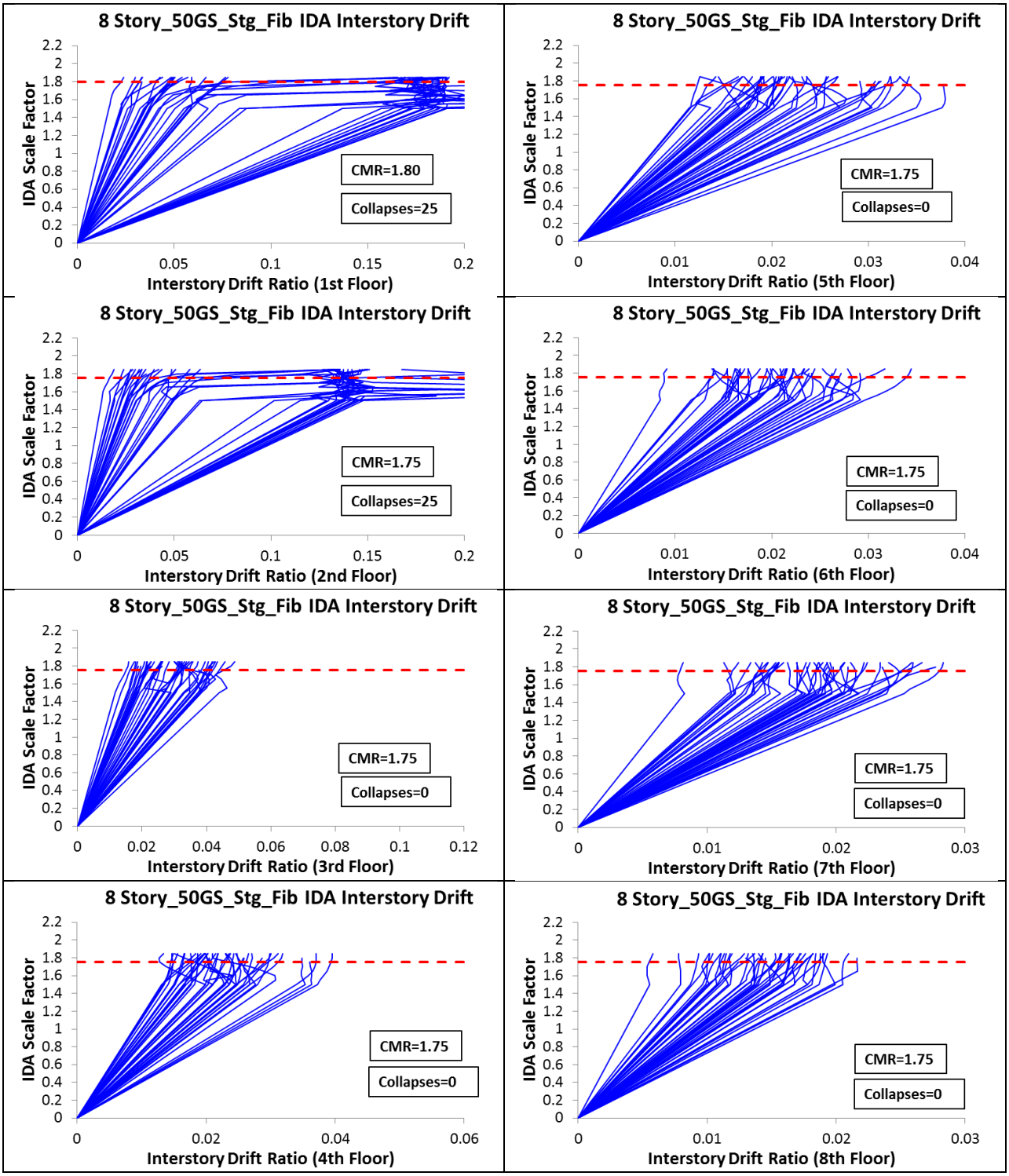

Model: 8Story_70GS_Staggered_Splices (Elastic)

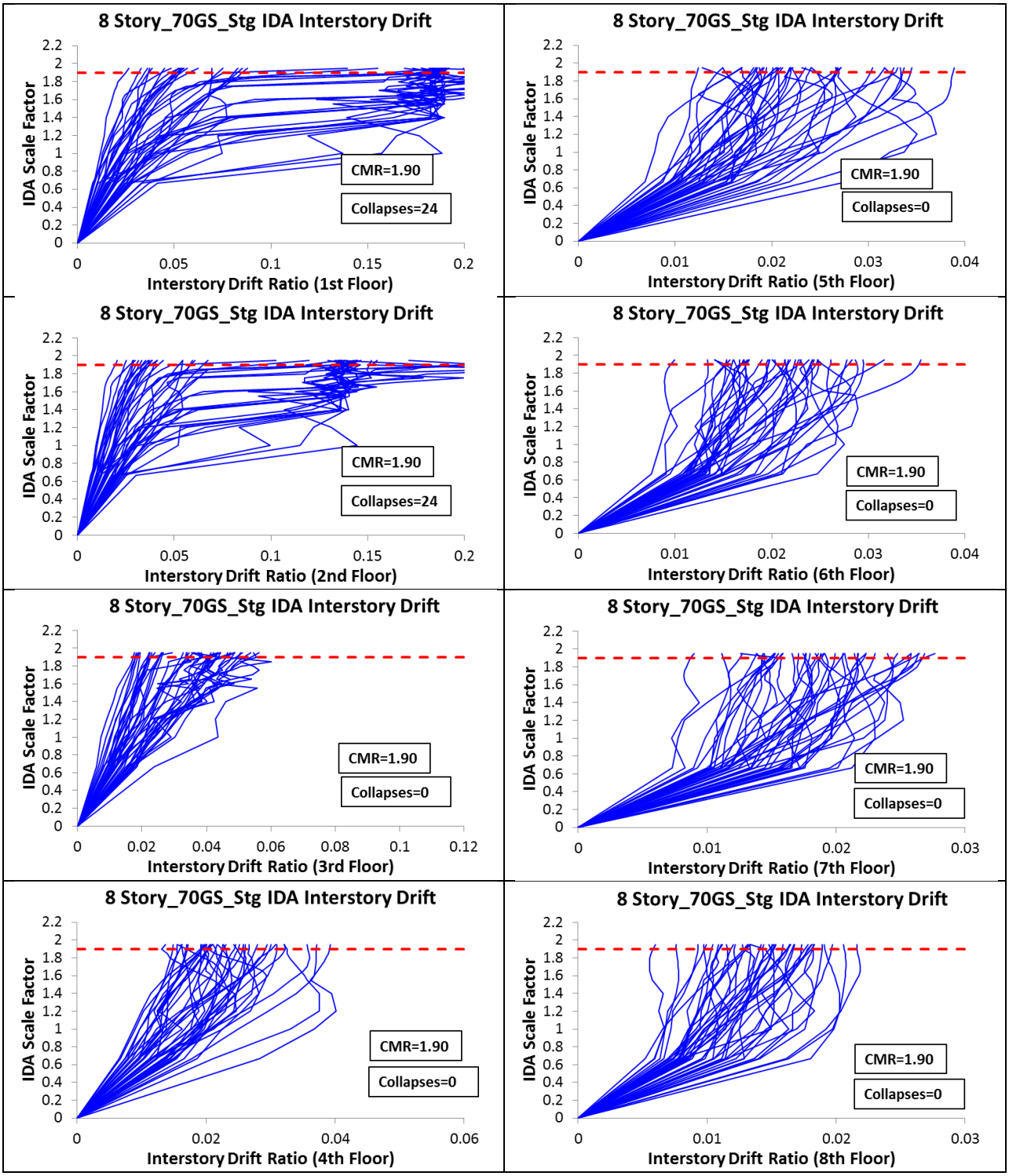

Model: 8Story_70GS_Staggered_Splices (Fibers)

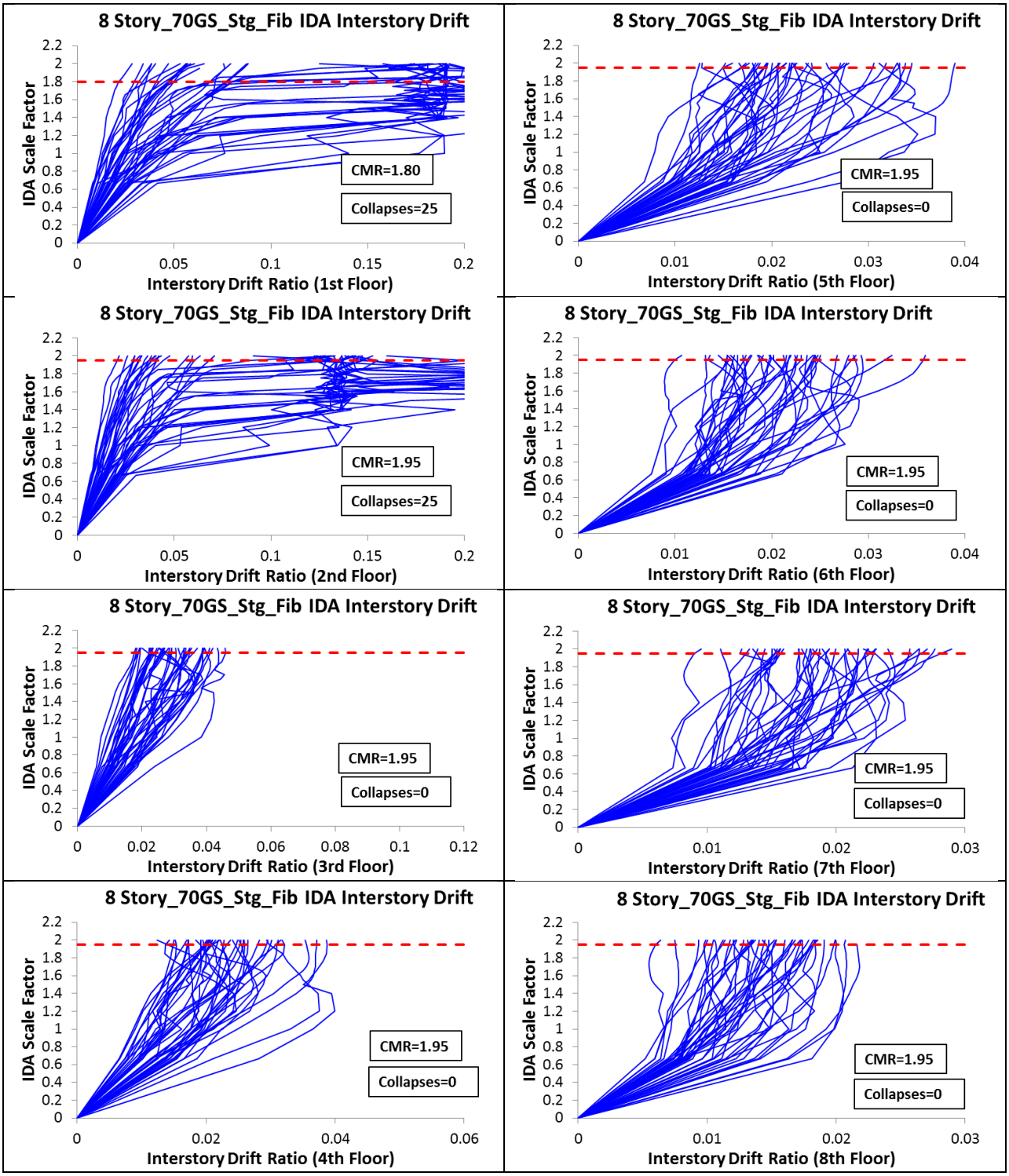

Scale Factors that Caused Collapse									
Far Field Ground Motions		Staggered Splices: Gravity Columns Elastic Sections				Staggered Splices: Gravity Columns with Fiber Sections			
		8 Story_0GS	8 Story_35GS	8 Story_50GS	8 Story_70GS	8 Story_0GS	8 Story_35GS	8 Story_50GS	8 Story_70GS
		CMR=1.70	CMR=1.75	CMR=1.85	CMR=1.90	CMR=1.75	CMR=1.75	CMR=1.80	CMR=1.95
Northridge-BH	MUL009								
Northridge-BH	MUL279								
Northridge-CC	LOS000	1.7	1.75	1.85	1.9	1.75	1.75	1.8	1.95
Northridge-CC	LOS270								
Duzce-Bolu	BOL000								
Duzce-Bolu	BOL090	1.4	1.65	1.8		1.55	1.55	1.7	1.95
Hector-Hector	HEC000								
Hector-Hector	HEC090								
Imperial Valley-Delta	H-DLT262	1	1	1	1	1	1	1.5	1
Imperial Valley-Delta	H-DLT352	0.666	1	1	1	1	1	1.5	1
Imperial Valley-EC	H-E11140	1.55	1.75	1.8	1.85	1.7	1.7	1.75	1.85
Imperial Valley-EC	H-E11230	1.6	1.75	1.8	1.9	1.75	1.75	1.8	1.85
Kobe-Nishi Akashi	NIS000	1.4	1.2	1.4	1.4	1.2	1.2	1.5	1.4
Kobe-Nishi Akashi	NIS090	1.7		1.85		1.75	1.75		1.95
Kobe-Shin Osaka	SHI000	1.4	1.4	1.4	1.55	1.4	1.4	1.5	1.5
Kobe-Shin Osaka	SHI090								
Kocaeli-Duzce	DZC180	1.2	1.4	1.4	1.4	1.4	1.4	1.5	1.4
Kocaeli-Duzce	DZC270	1.4	1.4	1.4	1.55	1.4	1.4	1.5	1.5
Kocaeli-Arcelik	ARC000								
Koaceli-Arcelik	ARC090	1.2	1.2	1.2	1.2	1.2	1.2	1.5	1.2
Landers-Yermo	YER270	1	1.4	1.4	1.4	1.4	1.4	1.5	2
Landers-Yermo	YER360				1.9				1.85
Landers-Coolwater	CLW-LN								
Landers-Coolwater	CLW-TR								
Loma Prieta-Capitola	CAP000	1.7							
Loma Prieta-Capitola	CAP090								
Loma Prieta-Gilroy	G03000								
Loma Prieta-Gilroy	G03090	1.6	1.75	1.7	1.8	1.65	1.65	1.7	1.8
Manjil-Abbar	ABBAR--L	1.6	1.55	1.6	1.65	1.5	1.5	1.6	1.6
Manjil-Abbar	ABBAR--T		1.55	1.5	1.55	1.5	1.5	1.5	1.5
Superstition Hills-EC	B-ICC000	1.4	1.55	1.6	1.6	1.5	1.5	1.55	1.6
Superstition Hills-EC	B-ICC090								
Superstition Hills-Poe	B-POE270	1.2	1.2	1.2	1.4	1.2	1.2	1.5	1.4
Superstition Hills-Poe	B-POE360	1.4	1.2	1.2	1.4	1.2	1.2	1.5	1.2
Cape Mendocino-Rio Dell	RIO270								
Cape Mendocino-Rio Dell	RIO360								
Chi Chi-CHY	CHY101-E	1.55	1.75	1.8	1.8	1.7	1.7	1.7	1.4
Chi Chi-CHY	CHY101-N	1.55	1.4	1.4	1.4	1.4	1.4	1.5	1.4
Chi Chi-TCU	TCU045-E	1.4	1.4	1.5	1.55	1.4	1.4	1.5	1.5
Chi Chi-TCU	TCU045-N								
San Fernando-LA	PEL180	1.4	1.4	1.5	1.55	1.4	1.4	1.55	1.5
San Fernando-LA	PEL090	1.2	1	1	1	1	1.7	1.5	1
Friuli-Tolmezzo	A-TMZ000								
Friuli-Tolmezzo	A-TMZ270								
Number of Colapses		24	23	24	23	24	24	23	25

Model: 4Story

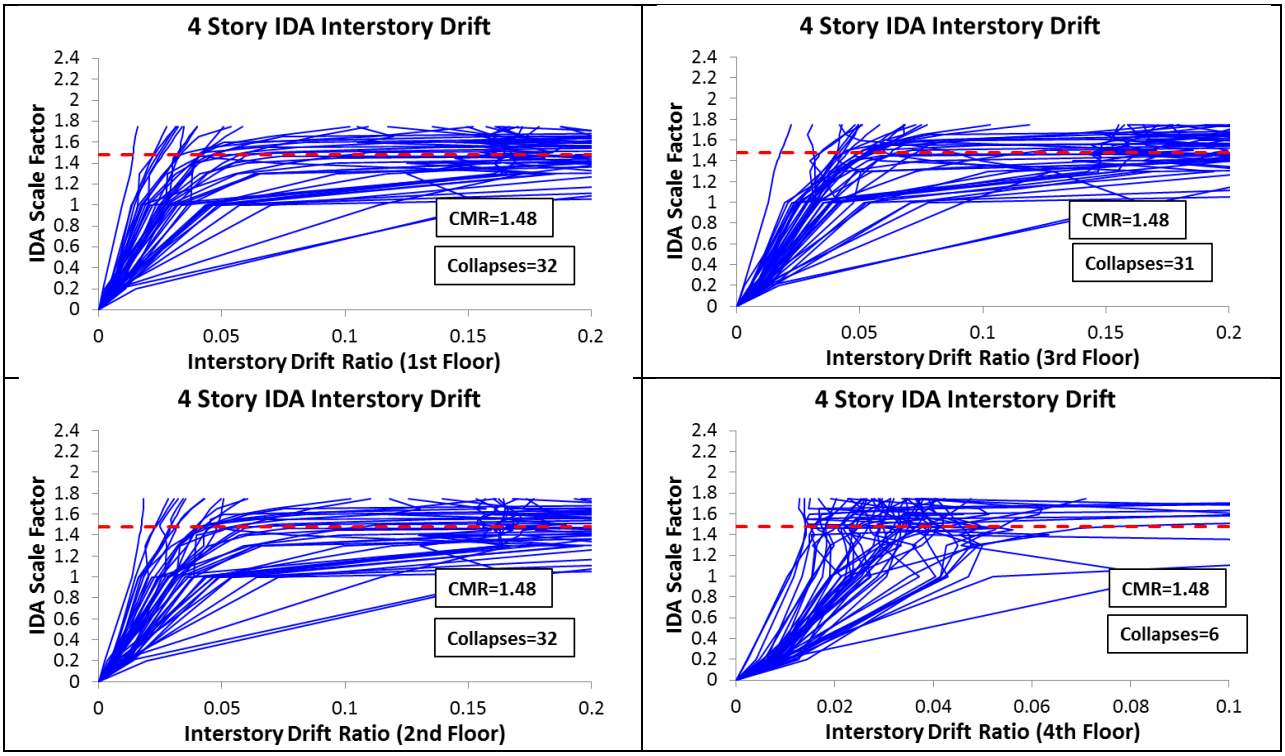

Model: 4Story_0GS (Elastic)

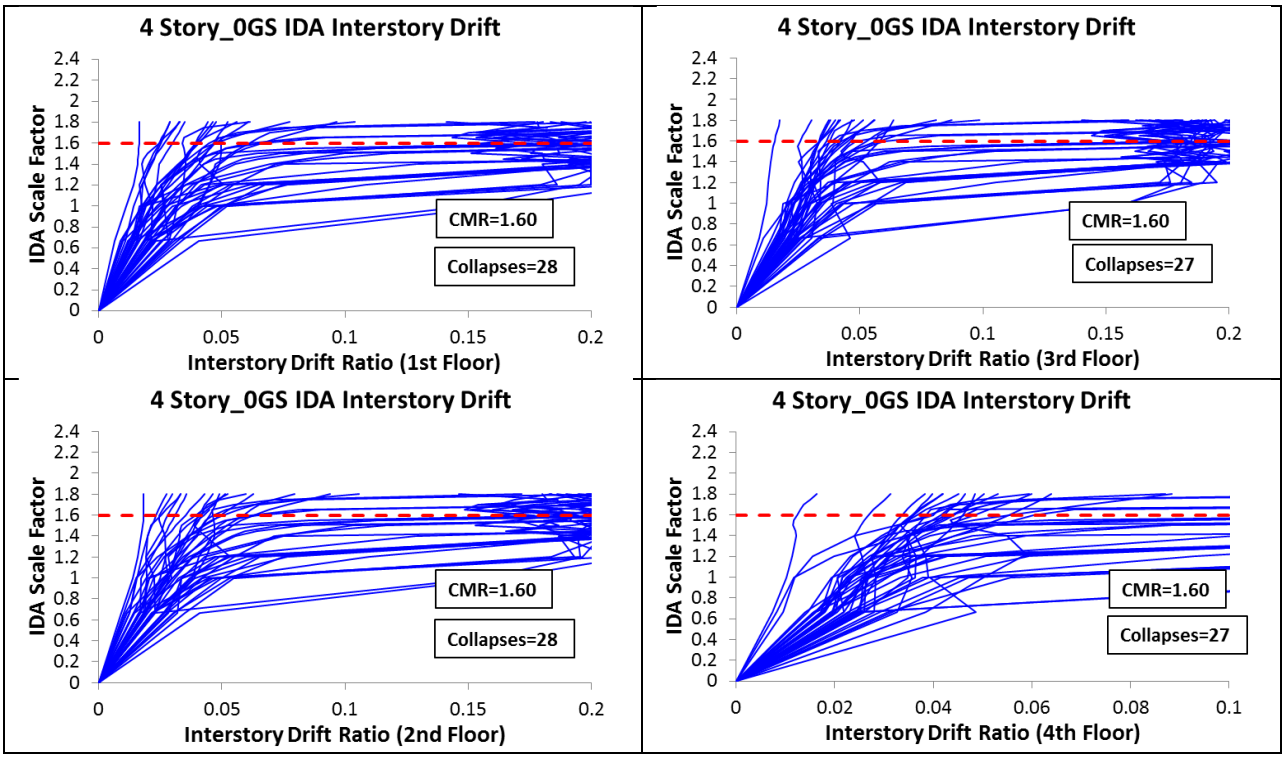

Model: 4Story_0GS (Fibers)

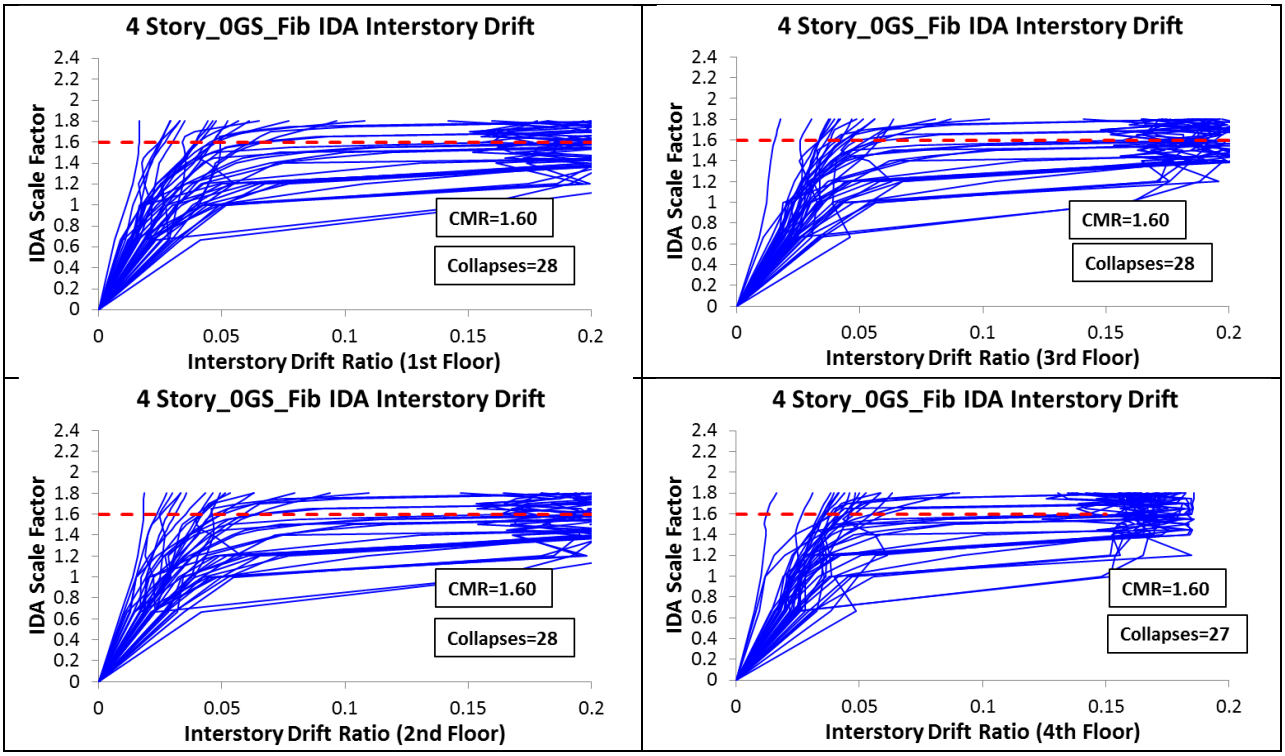

Model: 4Story_35GS (Elastic)

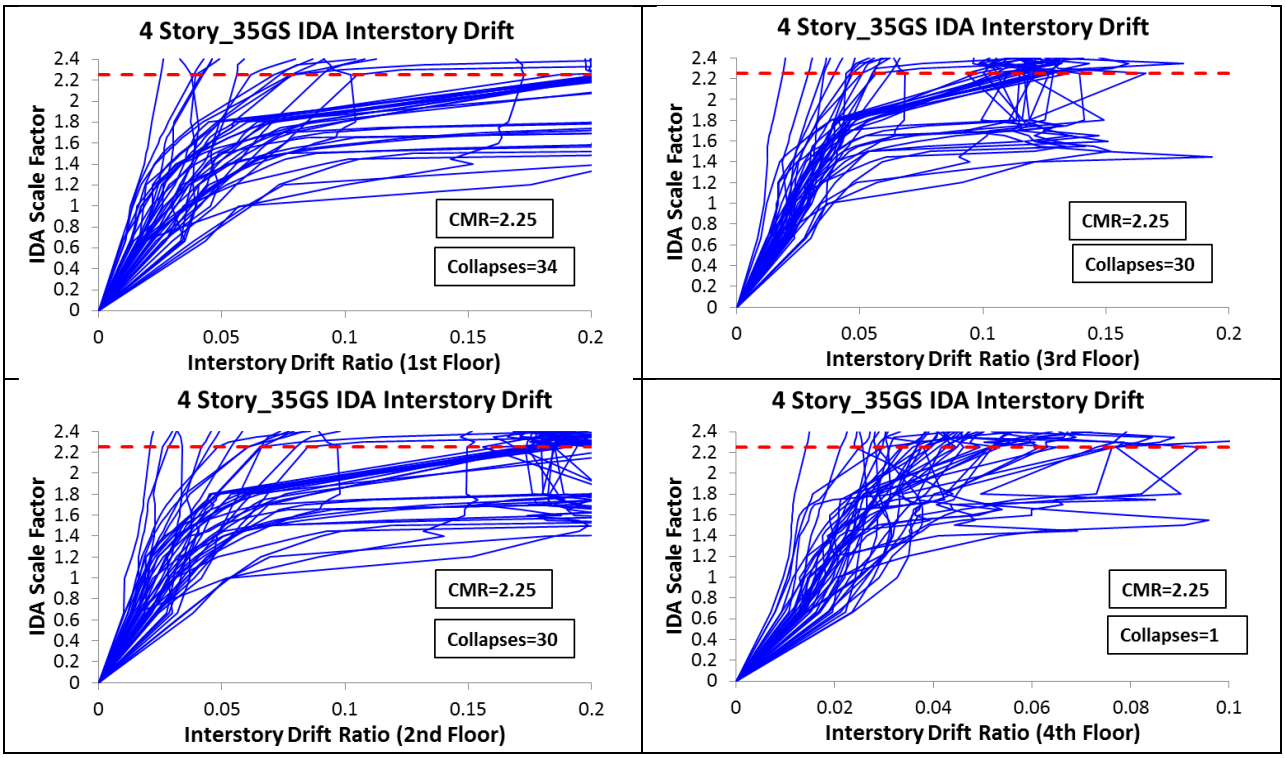

Model: 4Story_35GS (Fibers)

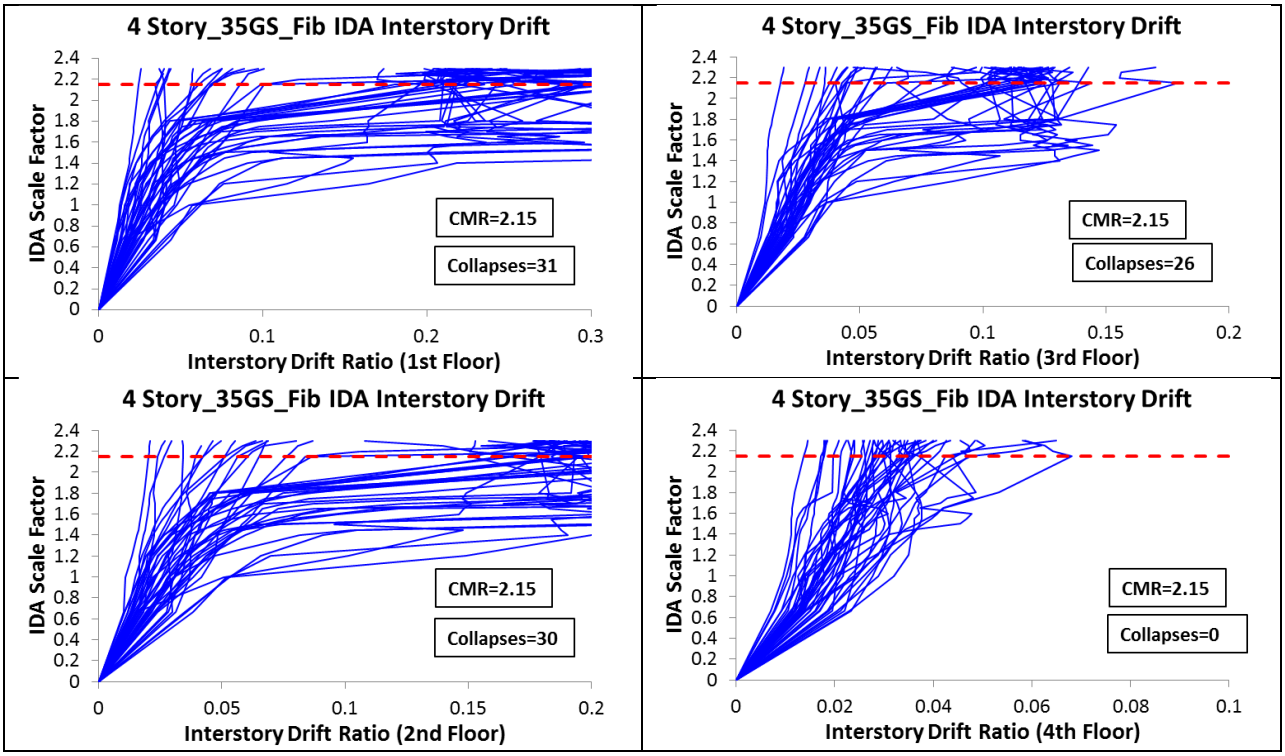

Model: 4Story_50GS (Elastic)

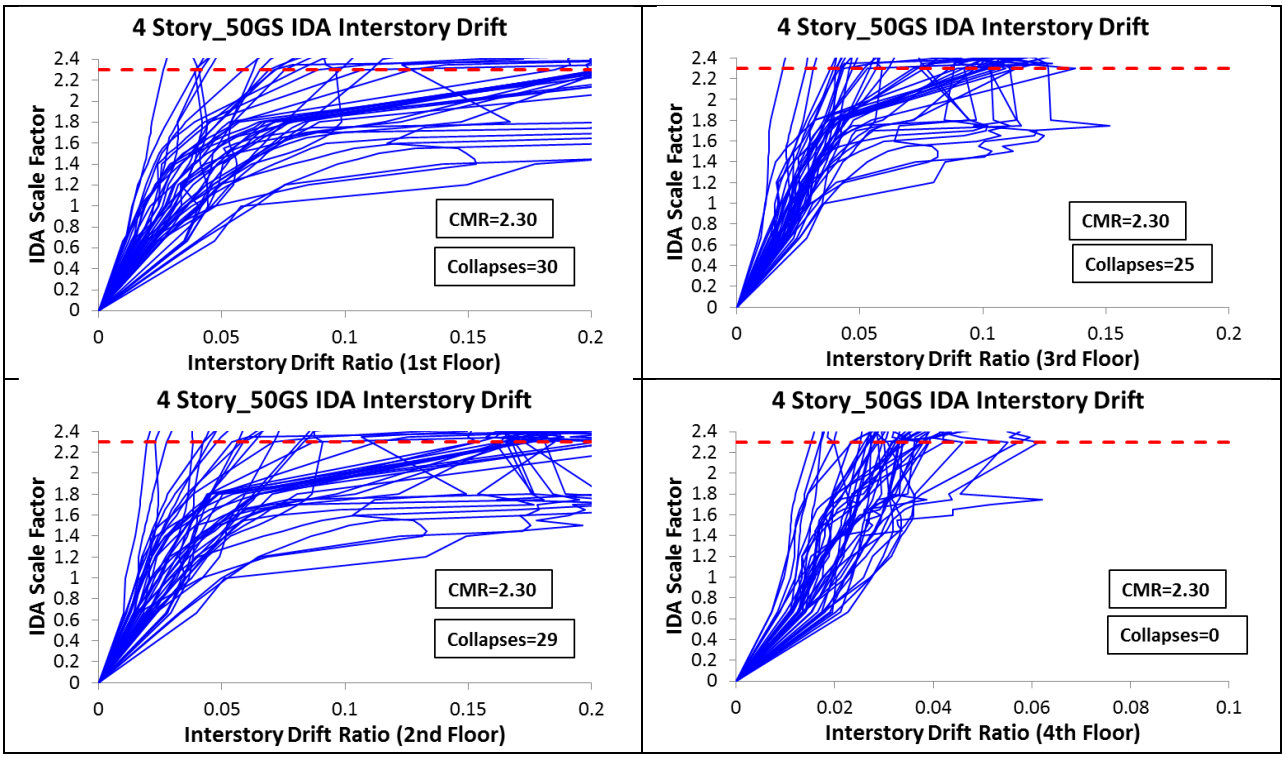

Model: 4Story_50GS (Fibers)

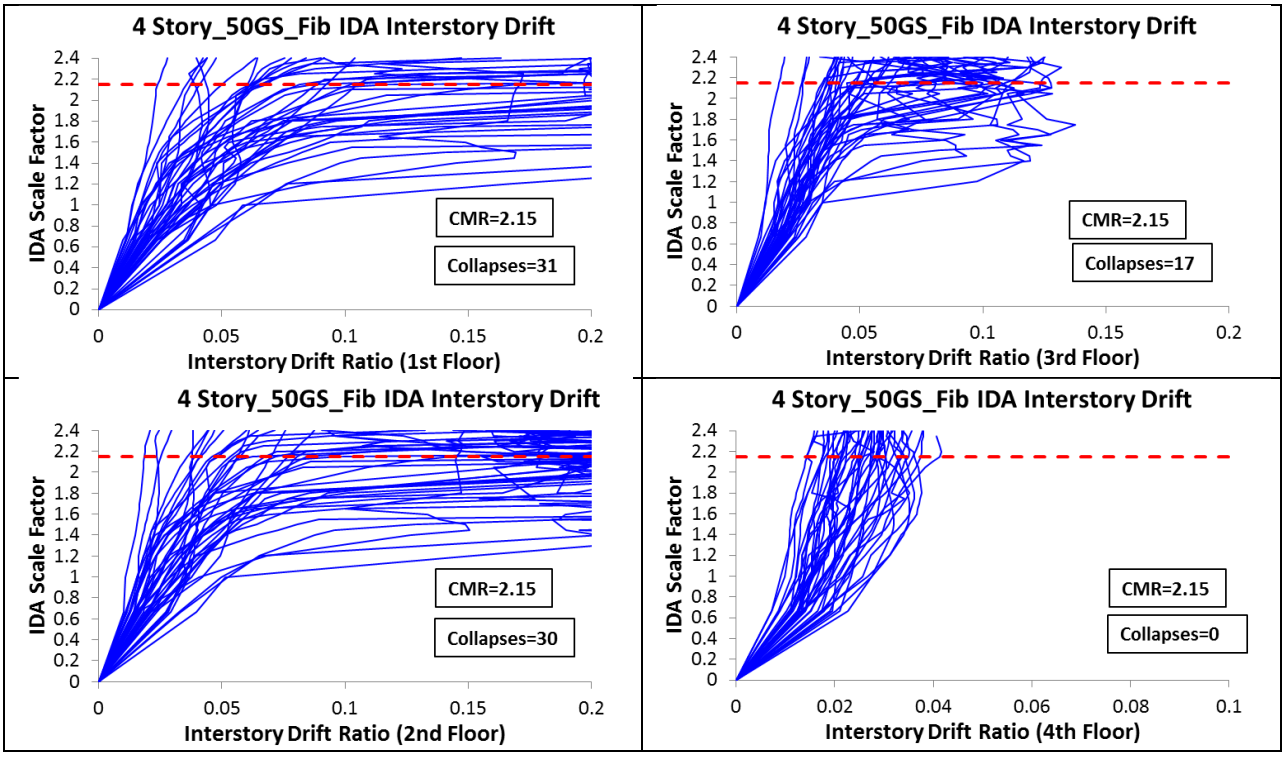

Model: 4Story_70GS (Elastic)

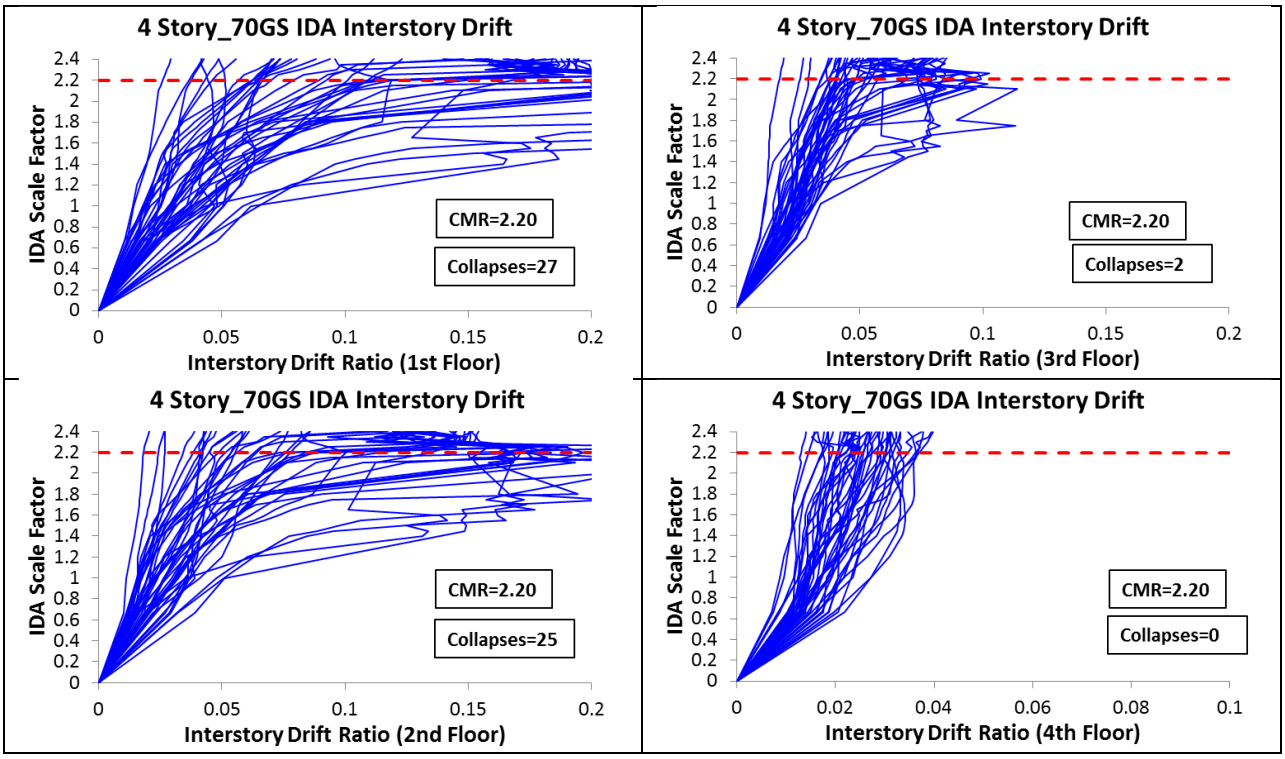

Model: 4Story_70GS (Fibers)

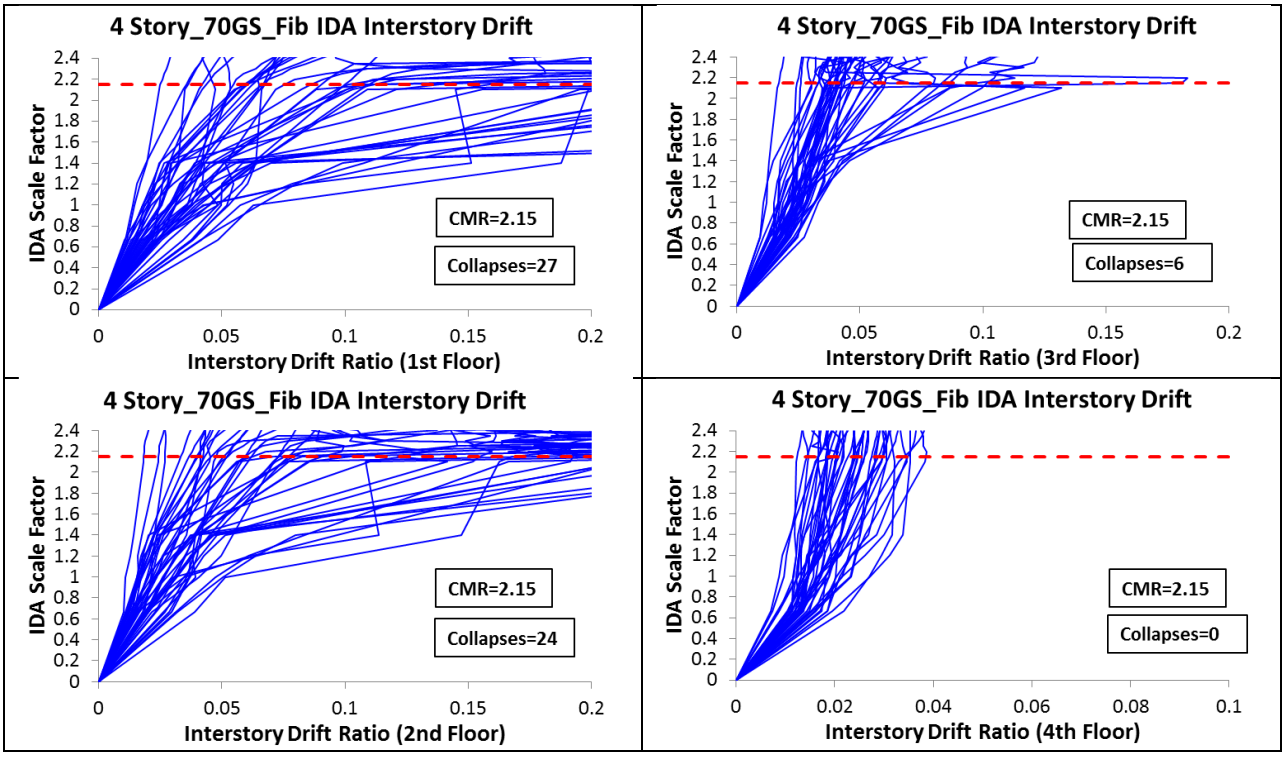

Scale Factors that Caused Collapse										
Far Field Ground Motions			Gravity Columns - Elastic Sections				Gravity Columns - Fiber Sections			
		4 Story	4 Story_0GS	4 Story_35GS	4 Story_50GS	4 Story_70GS	4 Story_0GS	4 Story_35GS	4 Story_50GS	4 Story_70GS
		CMR=1.48	CMR=1.60	CMR=2.25	CMR=2.30	CMR=2.20	CMR=1.60	CMR=2.15	CMR=2.15	CMR=2.15
Northridge-BH	MUL009									
Northridge-BH	MUL279									
Northridge-CC	LOS000	1.3	1.2	1.6	1.8	2.1	1.4	1.6	1.8	2.1
Northridge-CC	LOS270									
Duzce-Bolu	BOL000			2.25	2.3			2.15		
Duzce-Bolu	BOL090									
Hector-Hector	HEC000	1.48	1.55	2.25	2.3		1.55	2.15		
Hector-Hector	HEC090	1.4	1.4	2.25	2.3	2.2	1.4	2.15	2.05	2.15
Imperial Valley-Delta	H-DLT262	1	1	1.2	1.4	1.4	1	1.2	1.4	1.4
Imperial Valley-Delta	H-DLT352	1	1	1.2	1.45	1.45	1	1.2	1.2	1.4
Imperial Valley-EC	H-E11140	1.3	1.4	1.8		1.7	1.4	1.65	1.75	2.1
Imperial Valley-EC	H-E11230									
Kobe-Nishi Akashi	NIS000	1	1.2	1.55	1.75	2.1	1.2	1.55	1.75	2.1
Kobe-Nishi Akashi	NIS090		1.6	2.25	2.3		1.6	2.15		
Kobe-Shin Osaka	SHI000	1.3	1.4	1.6	1.75	2.1	1.4	1.6	1.7	2.1
Kobe-Shin Osaka	SHI090			2.25						
Kocaeli-Duzce	DZC180	1.3	1.4	1.65	1.75	2.1	1.4	1.65	1.75	2.1
Kocaeli-Duzce	DZC270	1.3	1.4	1.75	2.3	2.1	1.4	1.75	2.05	2.1
Kocaeli-Arcelik	ARC000									
Koaceli-Arcelik	ARC090			2.25	2.3	2.1		2.15	2.05	2.1
Landers-Yermo	YER270	1.3	1.2	1.4	1.4	1.4	1.2	1.4	1.4	1.4
Landers-Yermo	YER360	1.45	1.55	1.75	2.3	2.2	1.6	1.75	2.05	2.15
Landers-Coolwater	CLW-LN									
Landers-Coolwater	CLW-TR			2.25	2.3	2.1	1.8	2.15	2.05	2.1
Loma Prieta-Capitola	CAP000			2.25	2.3			2.15		
Loma Prieta-Capitola	CAP090	1.3	1.2	2.25			1.2	2.15		
Loma Prieta-Gilroy	G03000									
Loma Prieta-Gilroy	G03090	1.4	1.45	2.25	2.3	2.1	1.45	2.15	2.05	2.1
Manjil-Abbar	ABBAR--L		1.55	2.25	2.3		1.6	2.15	2.15	
Manjil-Abbar	ABBAR--T	1.3	1.4	1.7	1.8	2.1	1.4	1.7	1.8	2.1
Superstition Hills-EC	B-ICC000	1.46		2.25	2.3	2.1	1.7	1.8	2.05	2.1
Superstition Hills-EC	B-ICC090	1.3	1.5	2.4		2.2	1.55			2.15
Superstition Hills-Poe	B-POE270	1.4	1.4	1.55	1.65	1.7	1.4	1.55	1.65	2.15
Superstition Hills-Poe	B-POE360			2.25	2.3	2.1	1.8		2.15	2.1
Cape Mendocino-Rio Dell	RIO270									
Cape Mendocino-Rio Dell	RIO360									
Chi Chi-CHY	CHY101-E	1.48	1.55	2.25	2.3	2.15	1.55	2.15	2.1	2.1
Chi Chi-CHY	CHY101-N	1.4	1.4	1.45	1.65	1.65	1.4	1.45	1.55	2.1
Chi Chi-TCU	TCU045-E			2.25	2.3	2.1	1.7	2.15	2.05	2.1
Chi Chi-TCU	TCU045-N									
San Fernando-LA	PEL180	1.3	1.4	2.25	2.3	2.1	1.4	2.15	2.05	2.1
San Fernando-LA	PEL090	1.3	1.2	1.45	1.45	1.45	1.2	1.45	1.5	2.1
Friuli-Tolmezzo	A-TMZ000									
Friuli-Tolmezzo	A-TMZ270									
Number of Colapses		22	23	31	27	24	27	28	24	24

Model: 4Story_0GS_Levelled_Splices (Elastic)

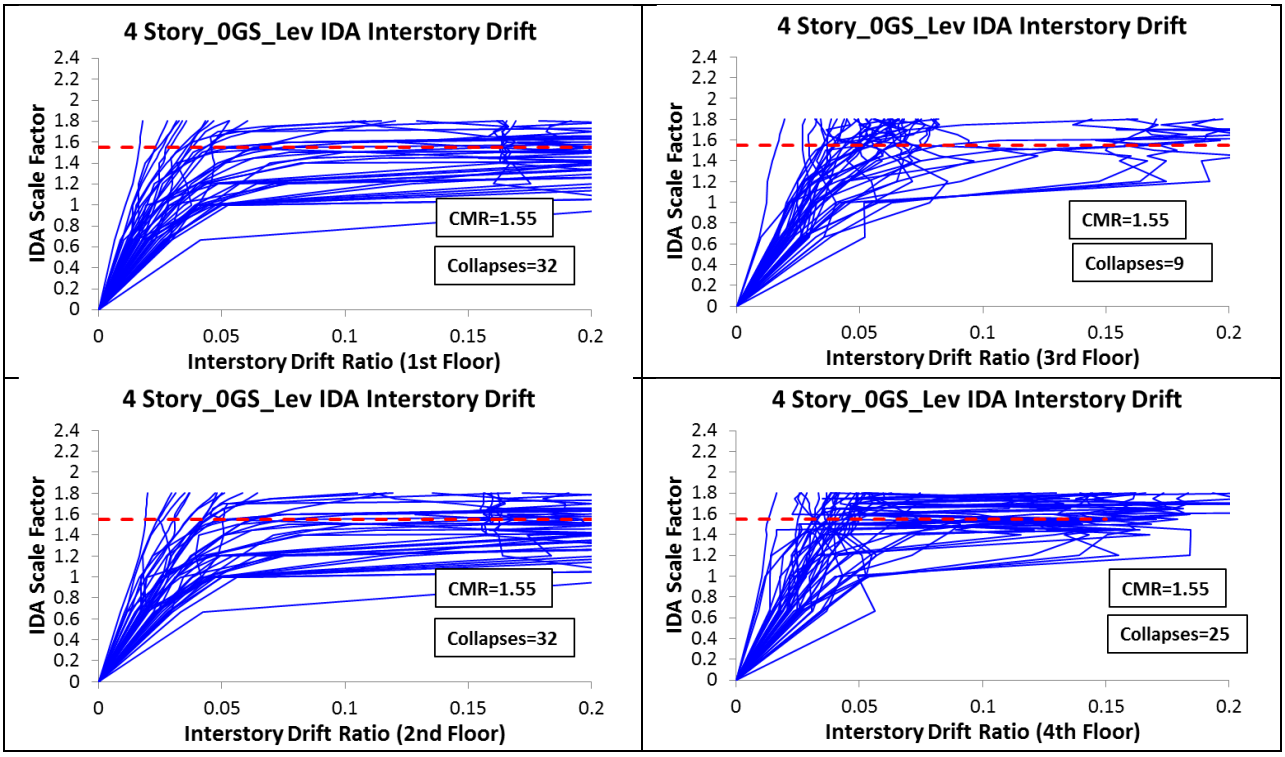

Model: 4Story_0GS_Levelled_Splices (Fibers)

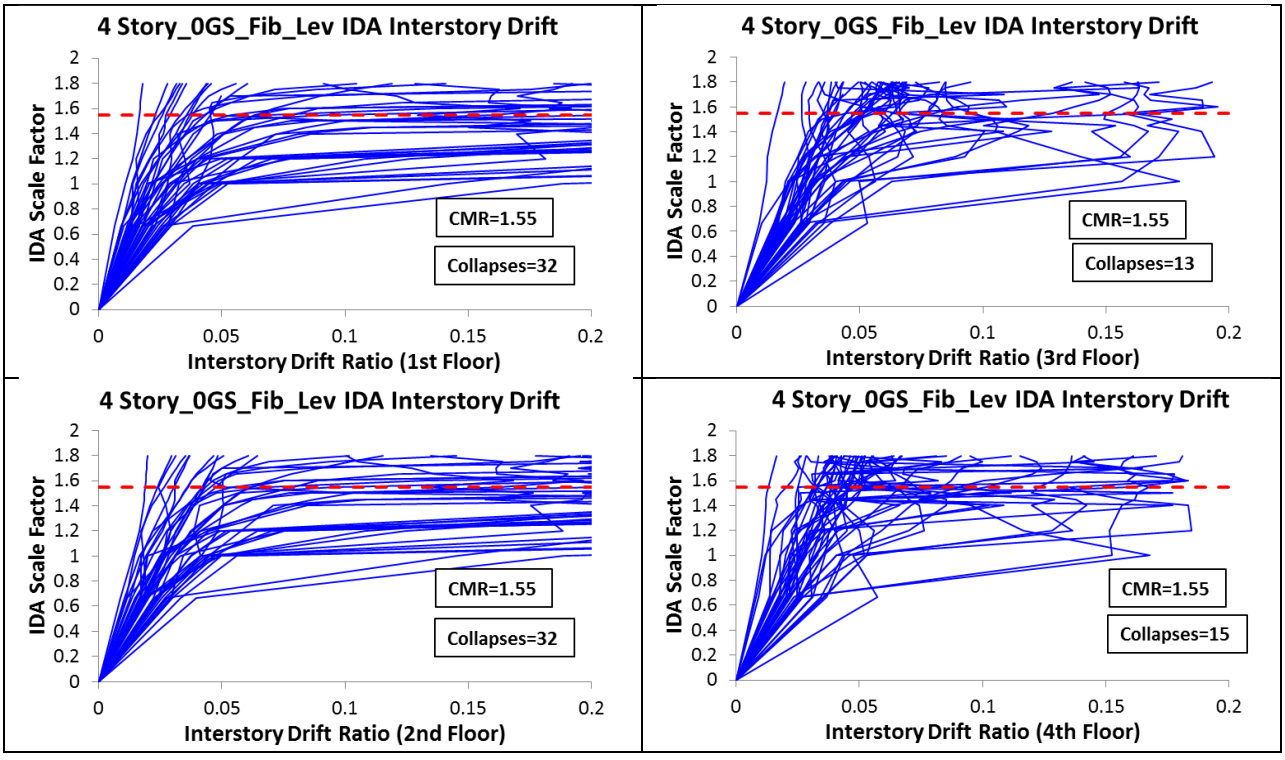

Model: 4Story_35GS_Levelled_Splices (Elastic)

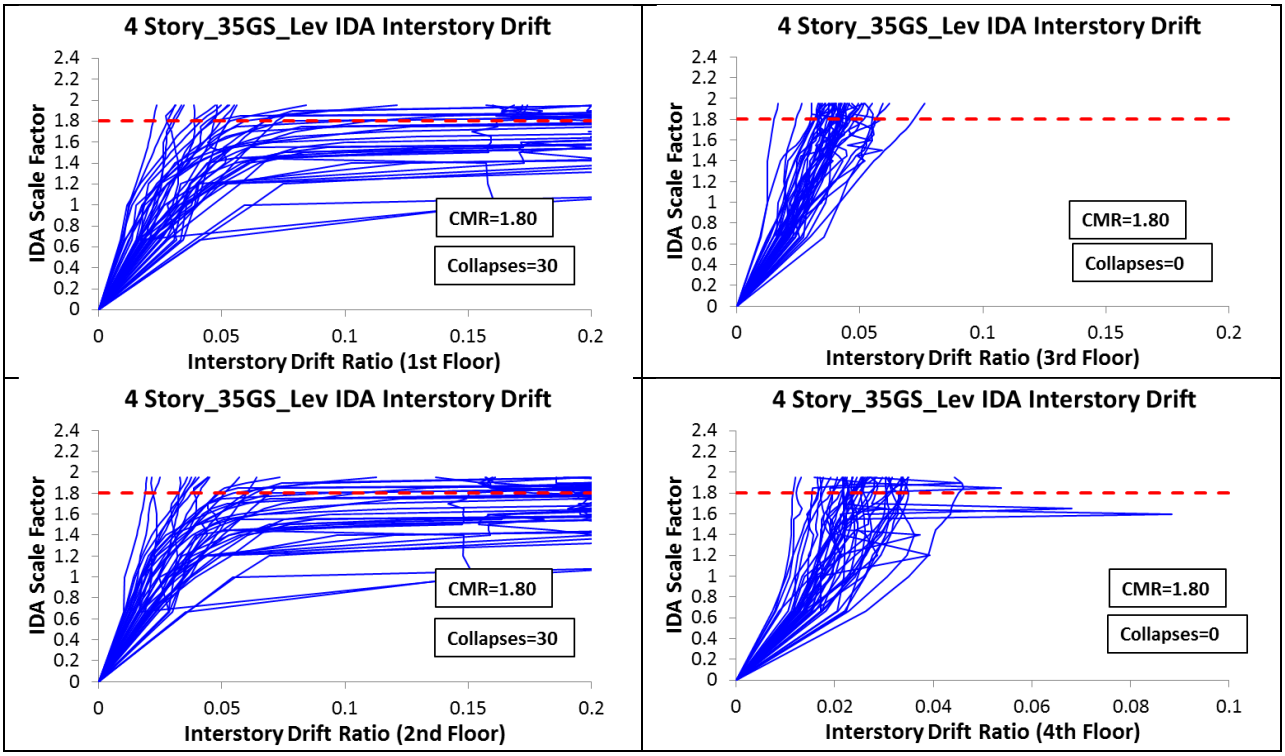

Model: 4Story_35GS_Levelled_Splices (Fibers)

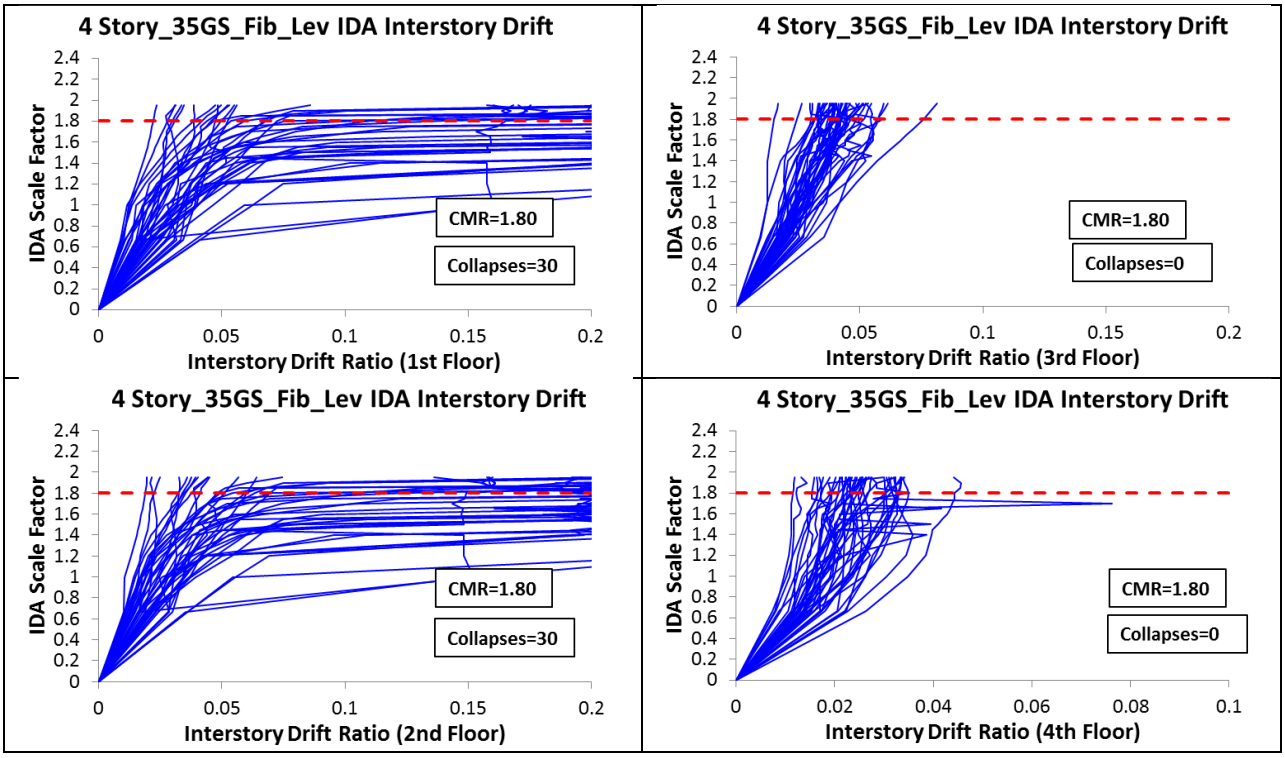

Model: 4Story_50GS_Levelled_Splices (Elastic)

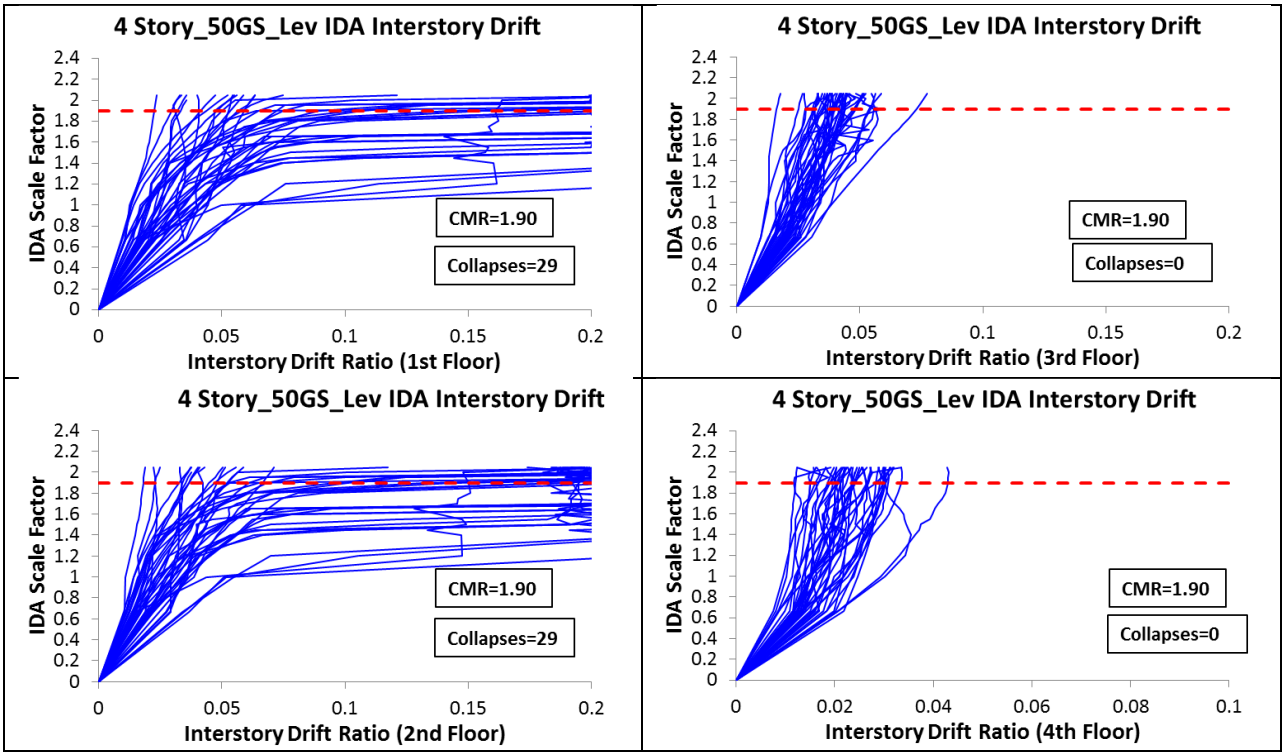

Model: 4Story_50GS_Levelled_Splices (Fibers)

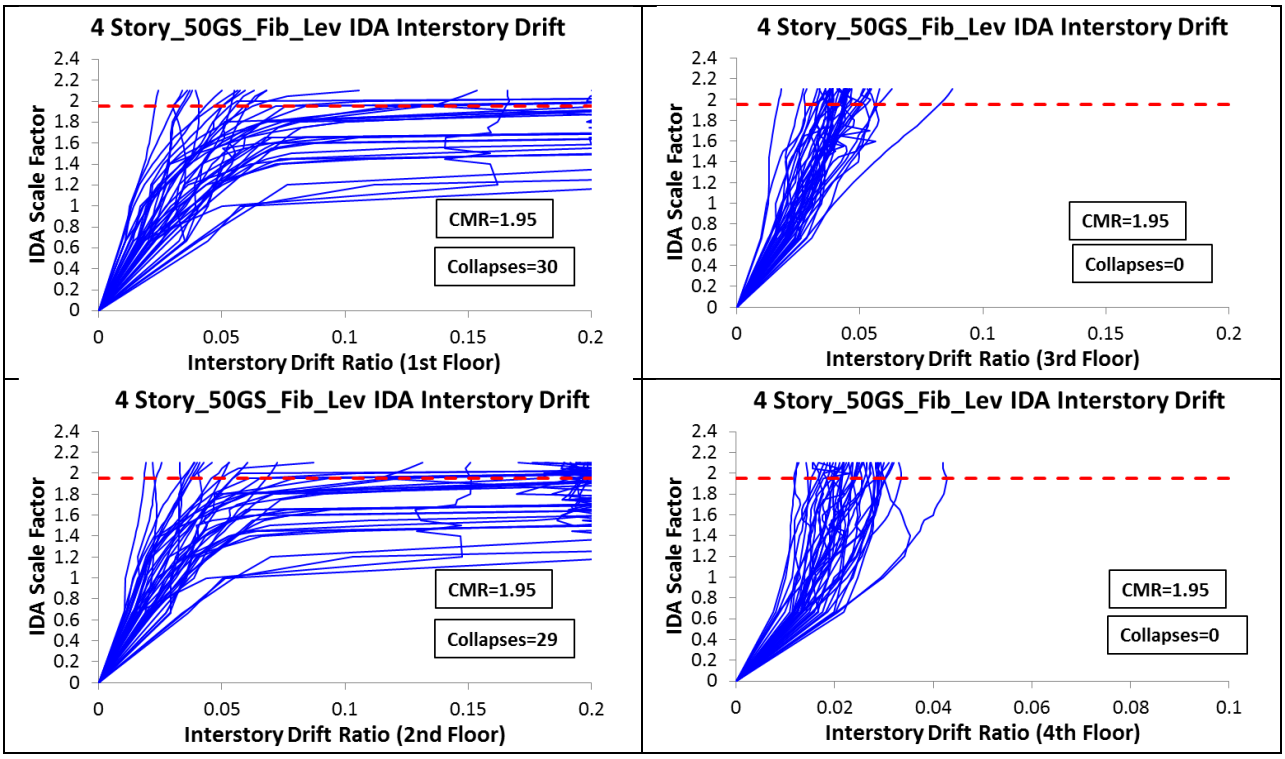

Model: 4Story_70GS_Levelled_Splices (Elastic)

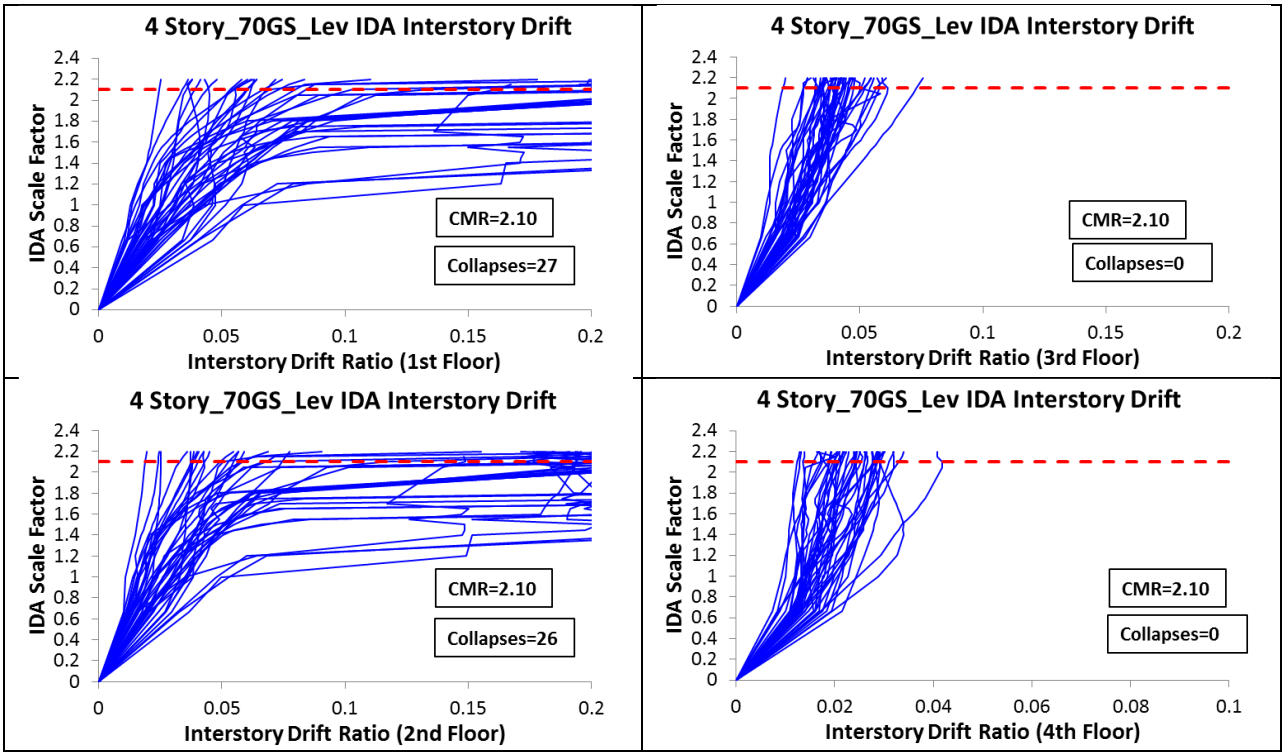

Model: 4Story_70GS_Levelled_Splices (Fibers)

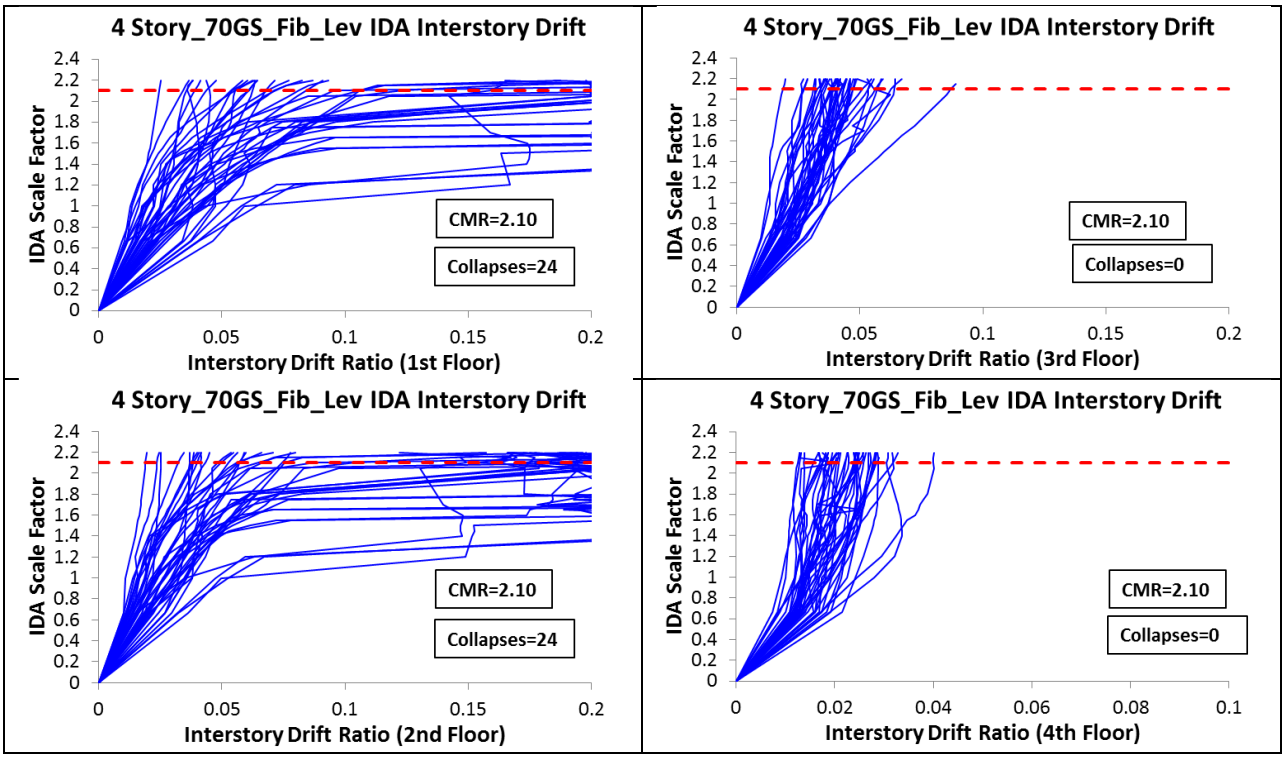

Scale Factors that Caused Collapse									
Far Field Ground Motions		Levelled Splices: Gravity Columns Elastic Sections				Levelled Splices: Gravity Columns with Fiber Sections			
		4 Story_0GS	4 Story_35GS	4 Story_50GS	4 Story_70GS	4 Story_0GS	4 Story_35GS	4 Story_50GS	4 Story_70GS
		CMR=1.55	CMR=1.80	CMR=1.90	CMR=2.10	CMR=1.65	CMR=1.80	CMR=1.95	CMR=2.10
Northridge-BH	MUL009								
Northridge-BH	MUL279								
Northridge-CC	LOS000	1.2	1.5	1.7	2.05	1.2	1.5	1.7	2.05
Northridge-CC	LOS270								
Duzce-Bolu	BOL000			2					
Duzce-Bolu	BOL090								
Hector-Hector	HEC000	1.55	1.7	1.9		1.55	1.7	1.95	
Hector-Hector	HEC090	1.4	1.65	1.9	2.1	1.4	1.65	1.95	2.1
Imperial Valley-Delta	H-DLT262	1.2	1.5	1.2	1.4	1	1.5	1.2	1.4
Imperial Valley-Delta	H-DLT352	1	1	1.2	1.2	1	1	1.2	1.2
Imperial Valley-EC	H-E11140	1.2	1.4	1.45	1.55	1.2	1.4	1.45	1.6
Imperial Valley-EC	H-E11230								
Kobe-Nishi Akashi	NIS000	1.2	1.4	1.5	1.7	1.2	1.4	1.5	1.7
Kobe-Nishi Akashi	NIS090								
Kobe-Shin Osaka	SHI000	1.4	1.4	1.55	1.75	1.4	1.4	1.55	1.8
Kobe-Shin Osaka	SHI090								
Kocaeli-Duzce	DZC180	1.4	1.6	1.7	2.05	1.4	1.6	1.7	2.05
Kocaeli-Duzce	DZC270	1.4	1.55	1.65	1.8	1.4	1.55	1.65	1.8
Kocaeli-Arcelik	ARC000								
Koaceli-Arcelik	ARC090		1.8	1.9	2.05		1.8	1.95	2.05
Landers-Yermo	YER270	1.2	1.2	1.2	1.4	1.2	1.2	1.2	1.4
Landers-Yermo	YER360	1.45	1.5	1.7	2.05	1.45	1.5	1.7	2.05
Landers-Coolwater	CLW-LN								
Landers-Coolwater	CLW-TR		1.65	1.9	2.05		1.65	1.95	2.05
Loma Prieta-Capitola	CAP000	1.2	1.8			1.2	1.8	1.95	
Loma Prieta-Capitola	CAP090	1.2	1.8			1.2	1.75		
Loma Prieta-Gilroy	G03000								
Loma Prieta-Gilroy	G03090	1.45	1.65	1.7	2.05	1.45	1.6	1.7	2.05
Manjil-Abbar	ABBAR--L			2					
Manjil-Abbar	ABBAR--T	1.4	1.5	1.65	1.8	1.4	1.55	1.65	1.8
Superstition Hills-EC	B-ICC000	1.55	1.55	1.65	2.05	1.55	1.55	1.65	2.05
Superstition Hills-EC	B-ICC090	1.5		1.9	2.05	1.45		1.95	2.05
Superstition Hills-Poe	B-POE270	1.4	1.4	1.5	1.7	1.4	1.4	1.5	1.7
Superstition Hills-Poe	B-POE360			2	2.1				
Cape Mendocino-Rio Dell	RIO270								
Cape Mendocino-Rio Dell	RIO360								
Chi Chi-CHY	CHY101-E	1.55		1.9	2.05	1.55		1.95	2.05
Chi Chi-CHY	CHY101-N	1.4	1.4	1.45	1.6	1.4	1.4	1.45	1.6
Chi Chi-TCU	TCU045-E		1.8		2.1		1.8	1.95	2.1
Chi Chi-TCU	TCU045-N								
San Fernando-LA	PEL180	1.4	1.7	1.8	2.05	1.4	1.7	1.95	2.05
San Fernando-LA	PEL090	1.2	1.4	1.4	1.4	1.2	1.4	1.4	1.4
Friuli-Tolmezzo	A-TMZ000								
Friuli-Tolmezzo	A-TMZ270								
Number of Colapses		23	24	26	24	23	24	25	23

Model: 4Story_0GS_Staggered_Splices (Elastic)

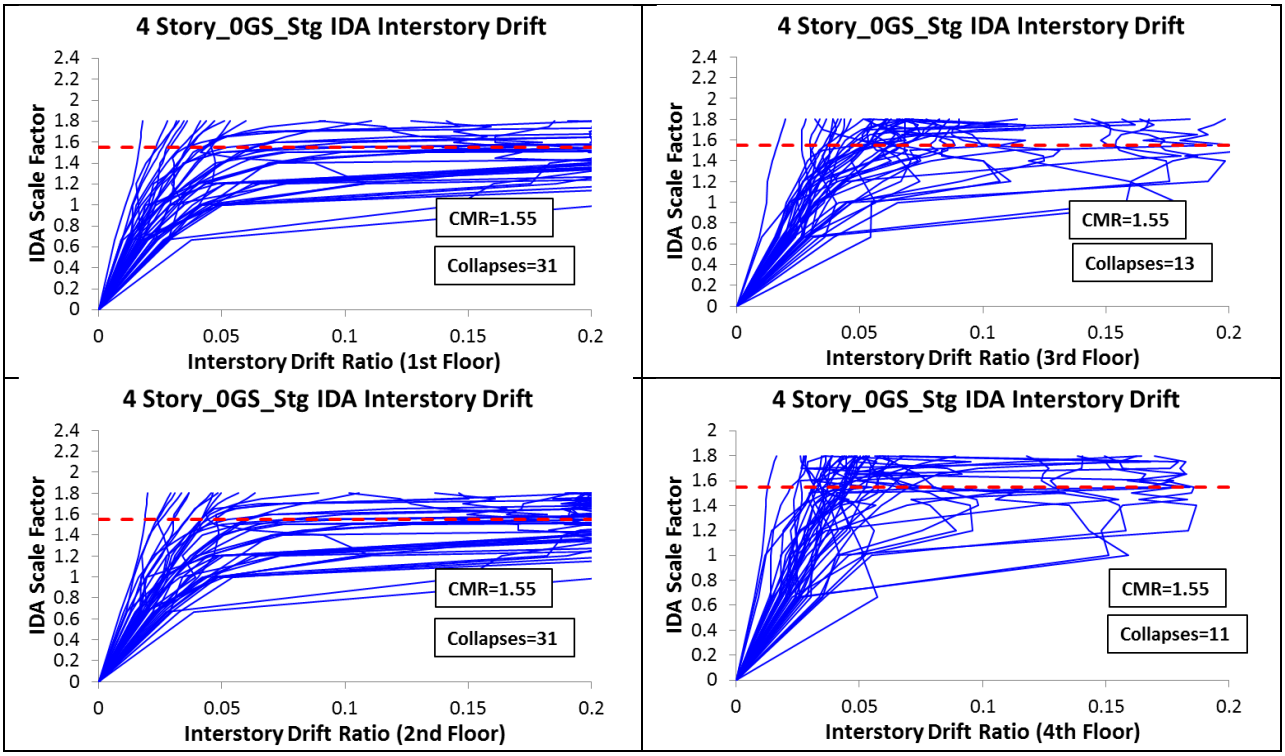

Model: 4Story_0GS_Staggered_Splices (Fibers)

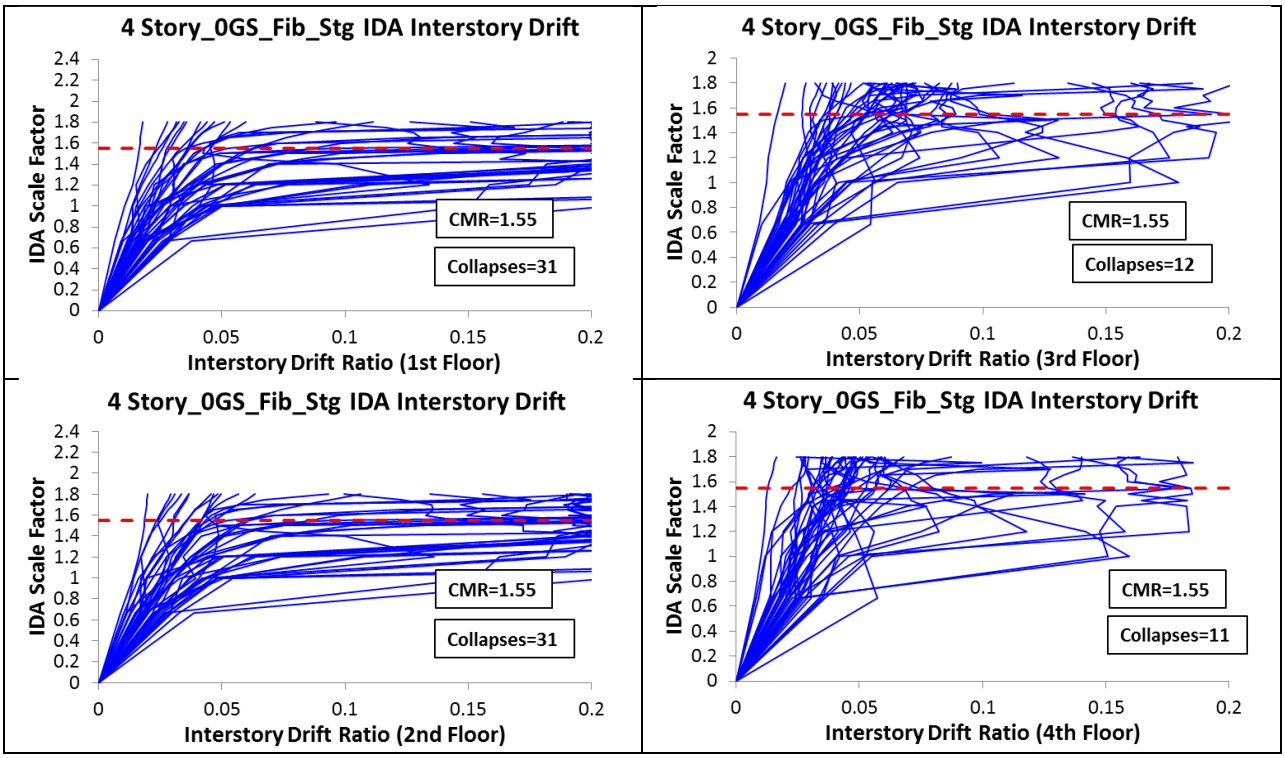

Model: 4Story_35GS_Staggered_Splices (Elastic)

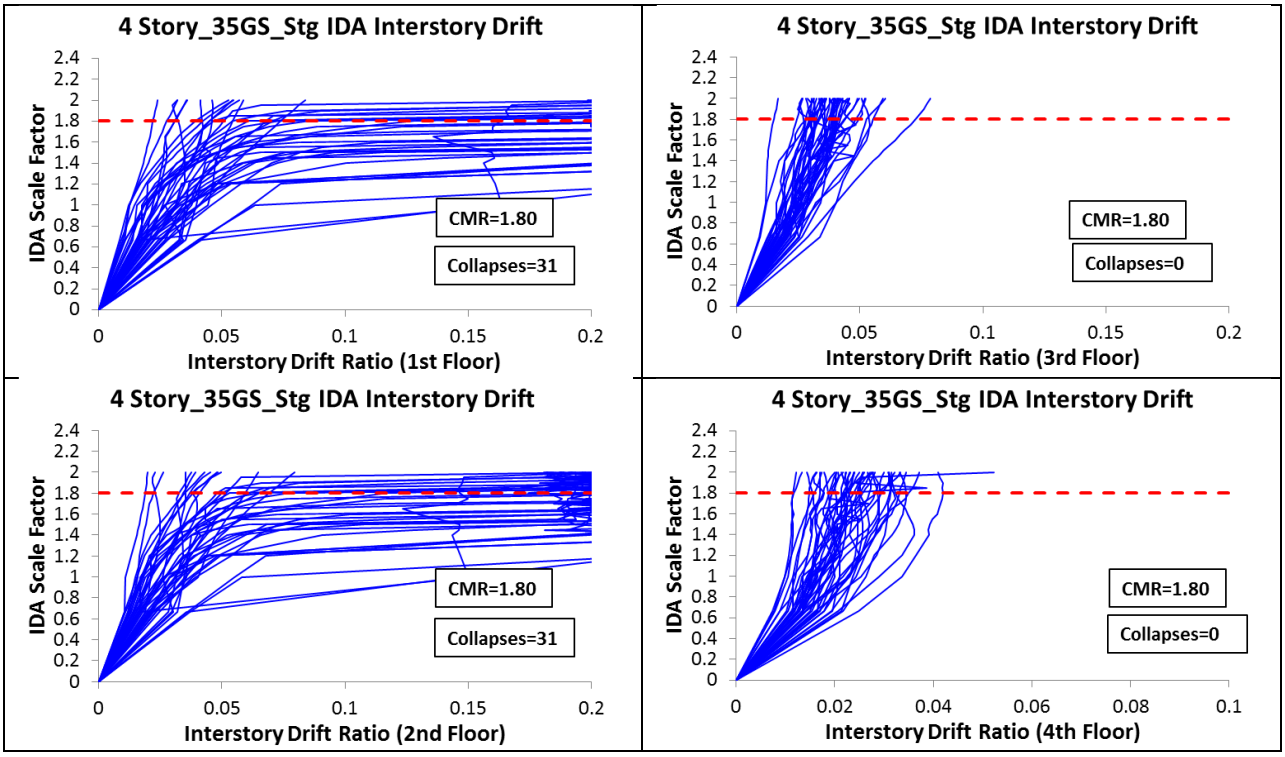

Model: 4Story_35GS_Staggered_Splices (Fibers)

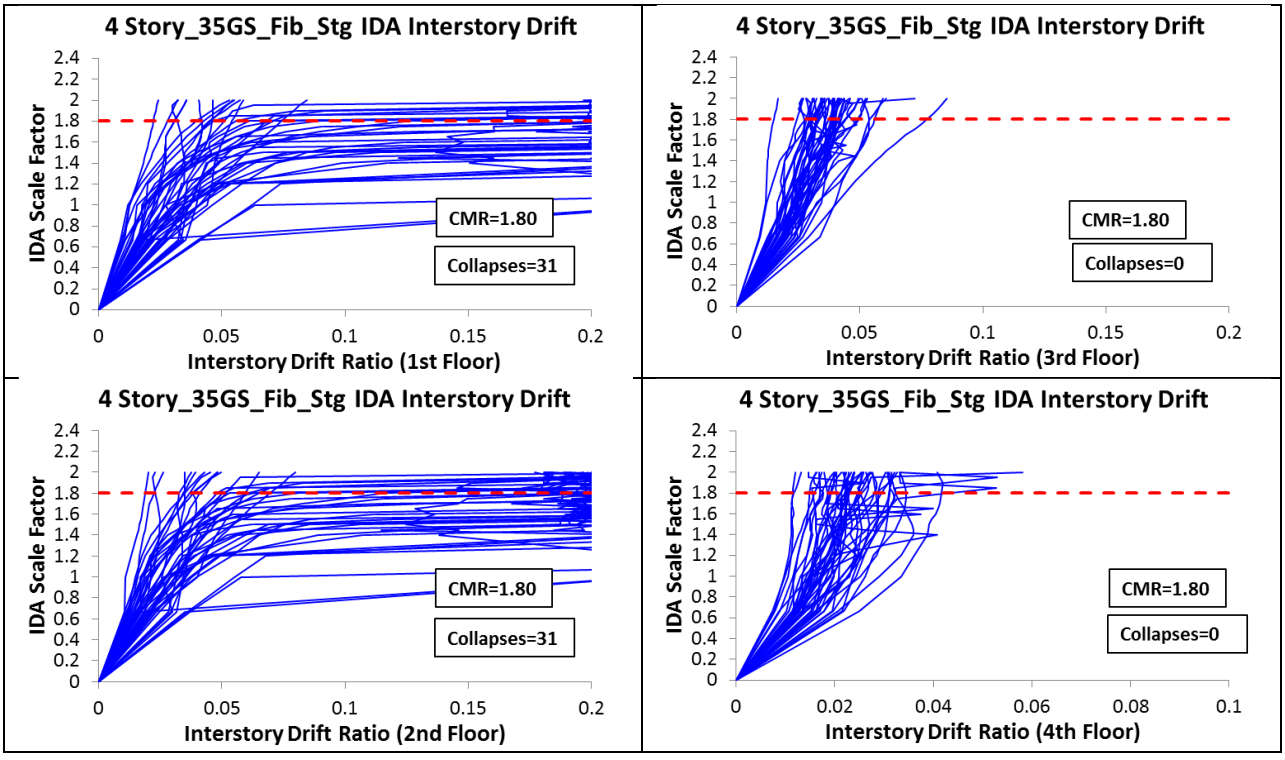

Model: 4Story_50GS_Staggered_Splices (Elastic)

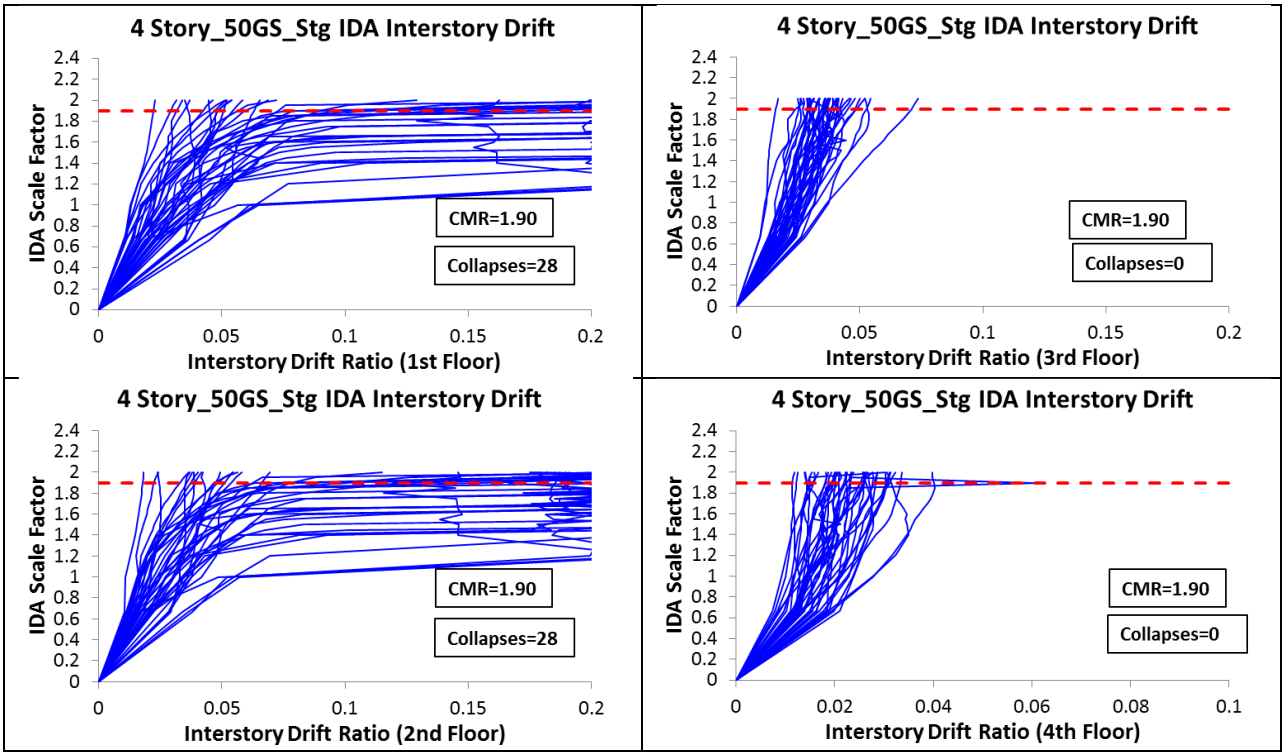

Model: 4Story_50GS_Staggered_Splices (Fibers)

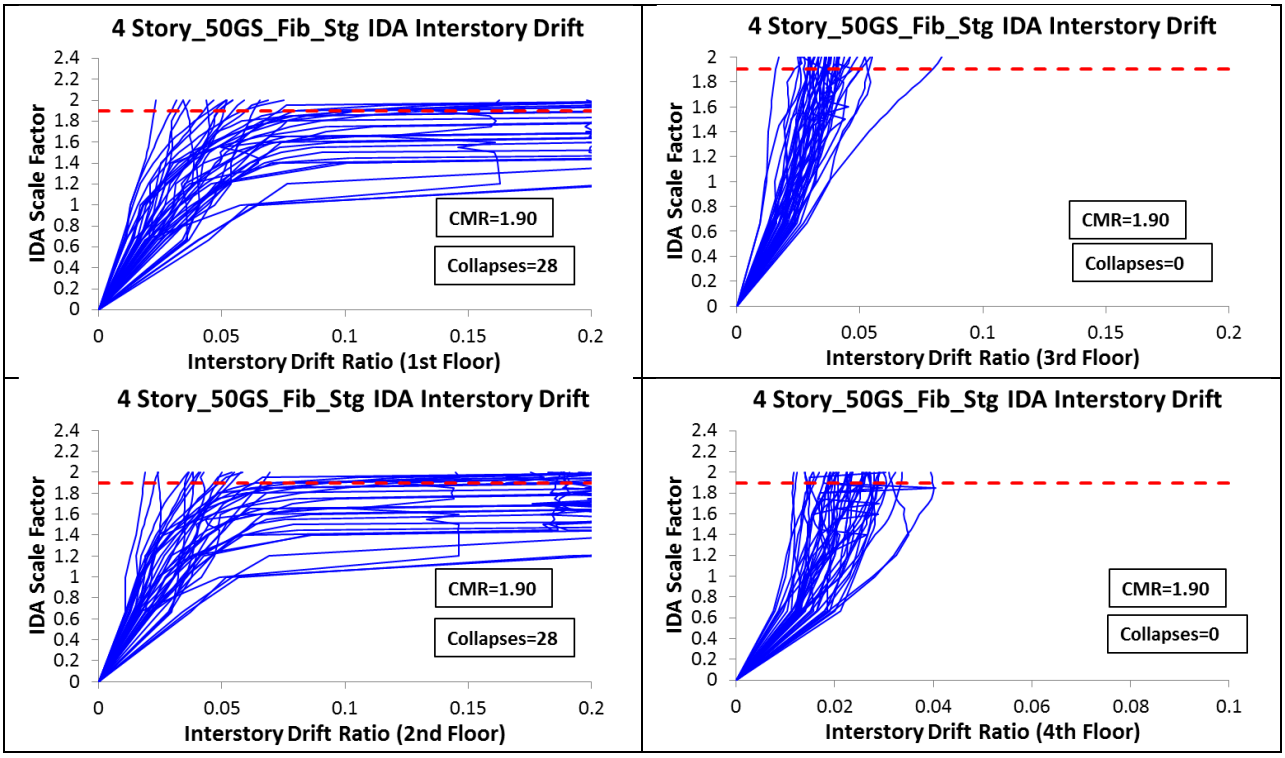

Model: 4Story_70GS_Staggered_Splices (Elastic)

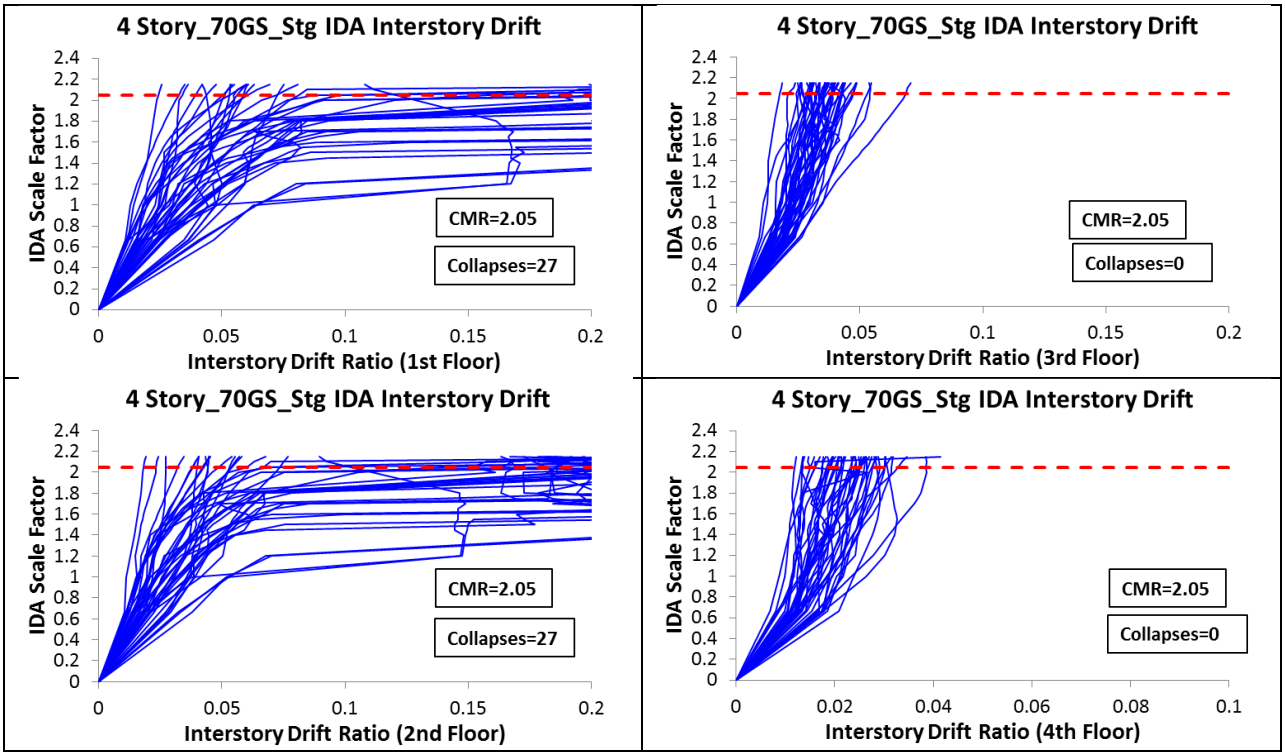

Model: 4Story_70GS_Staggered_Splices (Fibers)

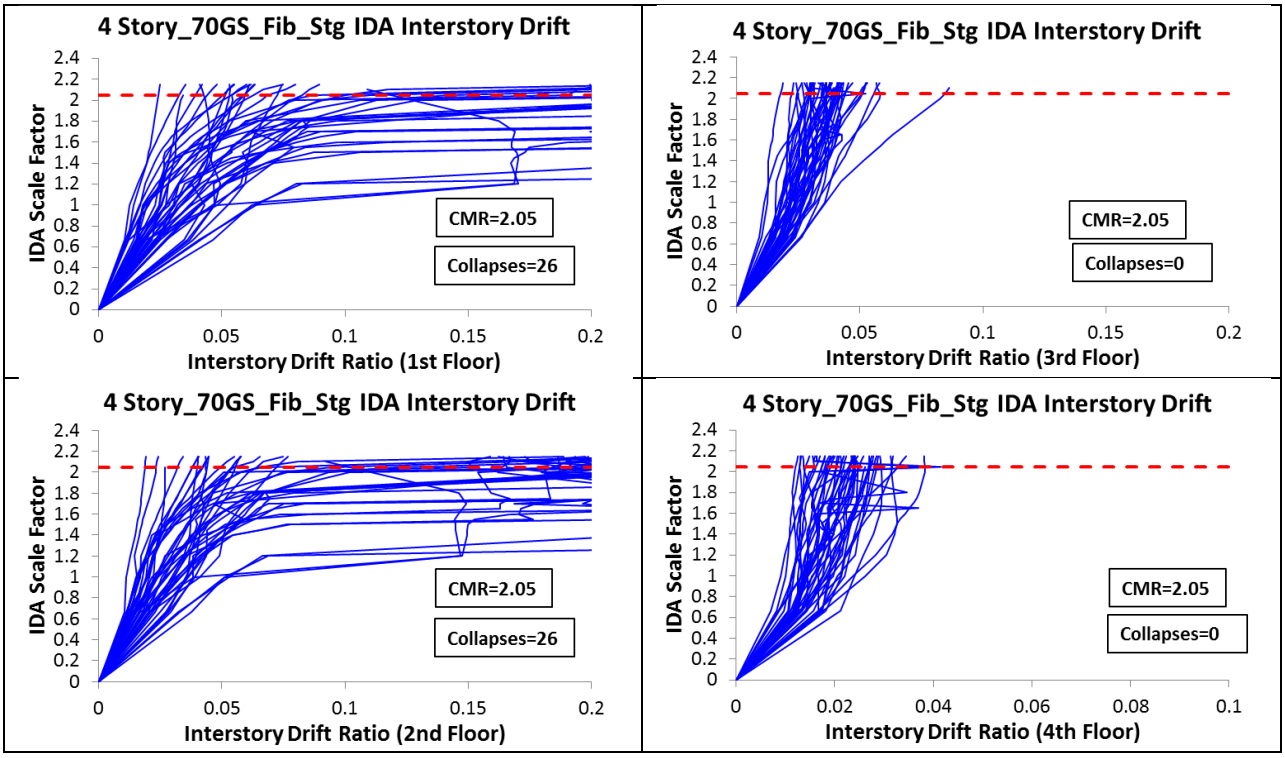

Scale Factors that Caused Collapse									
Far Field Ground Motions		Staggered Splices: Gravity Columns Elastic Sections				Staggered Splices: Gravity Columns with Fiber Sections			
		4 Story_0GS	4 Story_35GS	4 Story_50GS	4 Story_70GS	4 Story_0GS	4 Story_35GS	4 Story_50GS	4 Story_70GS
		CMR=1.55	CMR=1.80	CMR=1.90	CMR=2.05	CMR=1.55	CMR=1.80	CMR=1.90	CMR=2.05
Northridge-BH	MUL009								
Northridge-BH	MUL279								
Northridge-CC	LOS000		1.5	1.7	2	1.2	1.5	1.65	2
Northridge-CC	LOS270								
Duzce-Bolu	BOL000			2				2	
Duzce-Bolu	BOL090		2				2		
Hector-Hector	HEC000	1.55	1.7	1.9		1.55	1.7	1.9	
Hector-Hector	HEC090	1.4	1.65	1.85	2.05	1.4	1.65	1.85	2
Imperial Valley-Delta	H-DLT262	1	1	1.2	1.2	1	1	1.2	1.2
Imperial Valley-Delta	H-DLT352	1	1	1.2	1.2	1	1	1.2	1.2
Imperial Valley-EC	H-E11140	1.2	1.4	1.4	1.5	1.2	1.4	1.4	1.5
Imperial Valley-EC	H-E11230								
Kobe-Nishi Akashi	NIS000	1.2	1.4	1.45	1.65	1.2	1.4	1.45	1.65
Kobe-Nishi Akashi	NIS090	1.55							
Kobe-Shin Osaka	SHI000	1.4	1.4	1.55	1.7	1.4	1.45	1.55	1.7
Kobe-Shin Osaka	SHI090								
Kocaeli-Duzce	DZC180	1.4	1.55	1.7	2	1.4	1.55	1.7	2
Kocaeli-Duzce	DZC270	1.4	1.55	1.65	1.75	1.4	1.55	1.65	1.75
Kocaeli-Arcelik	ARC000								
Koaceli-Arcelik	ARC090		1.75	1.85	2		1.75	1.85	2
Landers-Yermo	YER270	1.2	1.2	1.2	1.4	1.2	1.2	1.2	1.4
Landers-Yermo	YER360	1.5	1.5	1.65	2	1.5	1.5	1.7	2
Landers-Coolwater	CLW-LN								
Landers-Coolwater	CLW-TR		1.6	1.8	2		1.6	1.75	2
Loma Prieta-Capitola	CAP000			1.9	2			1.9	2.05
Loma Prieta-Capitola	CAP090	1.2	1.7			1.2	1.7		
Loma Prieta-Gilroy	G03000								
Loma Prieta-Gilroy	G03090	1.45	1.6	1.7	2	1.45	1.6	1.7	2
Manjil-Abbar	ABBAR--L								
Manjil-Abbar	ABBAR--T	1.4	1.55	1.65	1.75	1.4	1.55	1.65	2
Superstition Hills-EC	B-ICC000	1.55	1.55	1.6	1.75	1.55	1.55	1.6	1.75
Superstition Hills-EC	B-ICC090	1.5			2	1.5		1.9	2
Superstition Hills-Poe	B-POE270	1.4	1.4	1.45	1.6	1.4	1.4	1.45	1.6
Superstition Hills-Poe	B-POE360				2.05				2.05
Cape Mendocino-Rio Dell	RIO270								
Cape Mendocino-Rio Dell	RIO360								
Chi Chi-CHY	CHY101-E	1.55		1.9	2	1.55		1.9	2
Chi Chi-CHY	CHY101-N	1.4	1.4	1.45	1.55	1.4	1.4	1.45	1.55
Chi Chi-TCU	TCU045-E		1.8				1.8	1.9	
Chi Chi-TCU	TCU045-N								
San Fernando-LA	PEL180	1.4	1.7	1.8	2	1.4	1.7	1.8	2
San Fernando-LA	PEL090	1.2	1.4	1.4	1.4	1.2	1.4	1.4	1.4
Friuli-Tolmezzo	A-TMZ000								
Friuli-Tolmezzo	A-TMZ270								
Number of Colapses		22	24	24	24	22	24	26	24

Model: 2Story

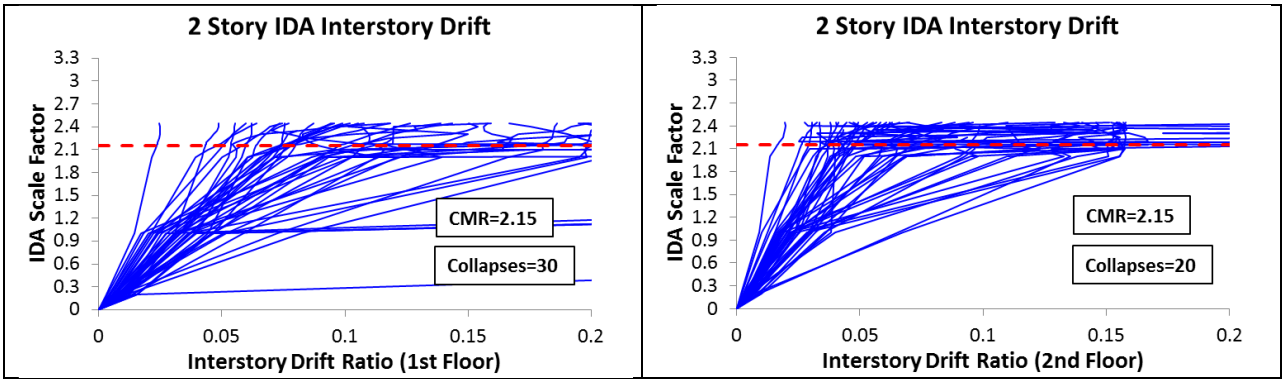

Model: 2Story_0GS (Elastic)

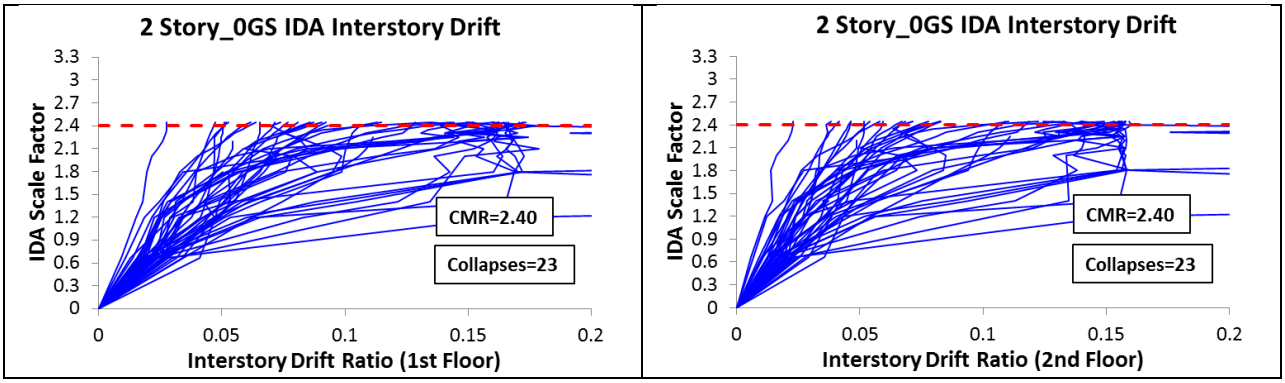

Model: 2Story_0GS (Fibers)

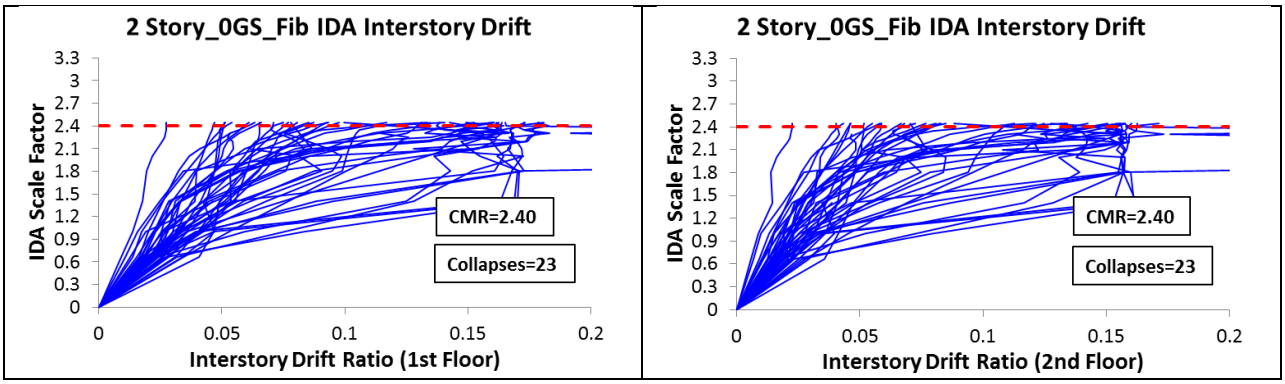

Model: 2Story_35GS (Elastic)

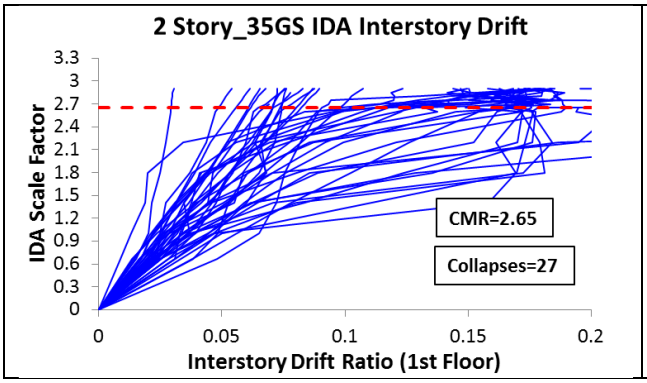

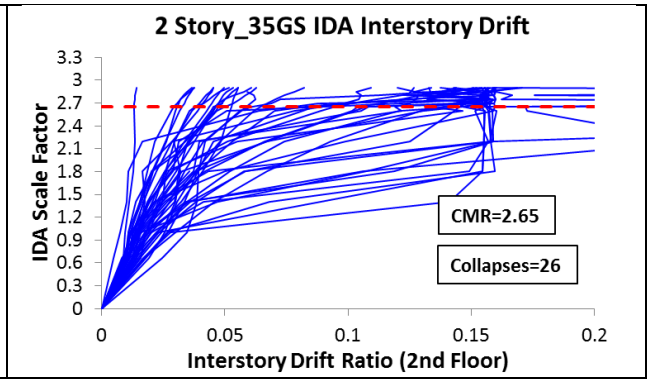

Model: 2Story_35GS (Fibers)

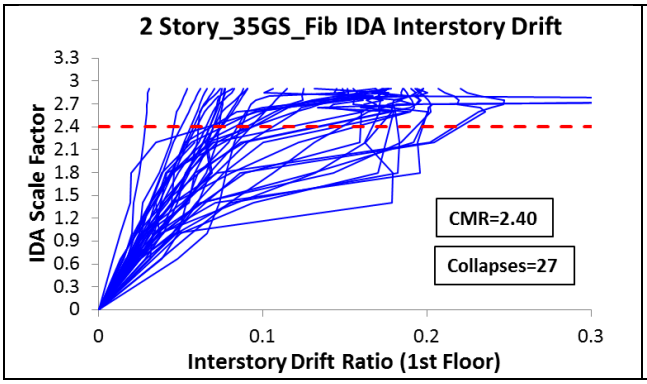

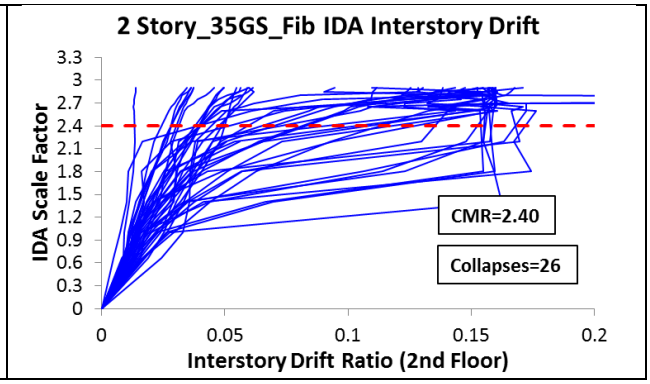

Model: 2Story_50GS (Elastic)

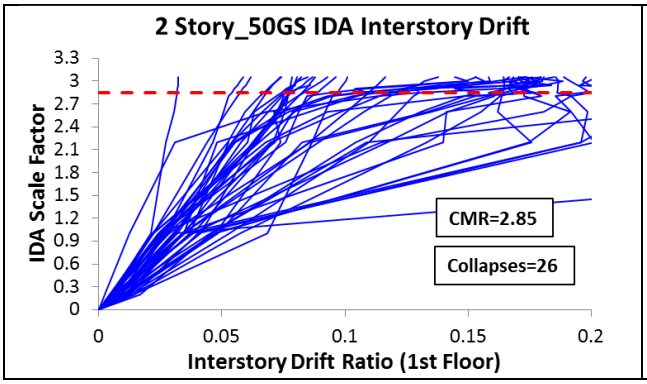

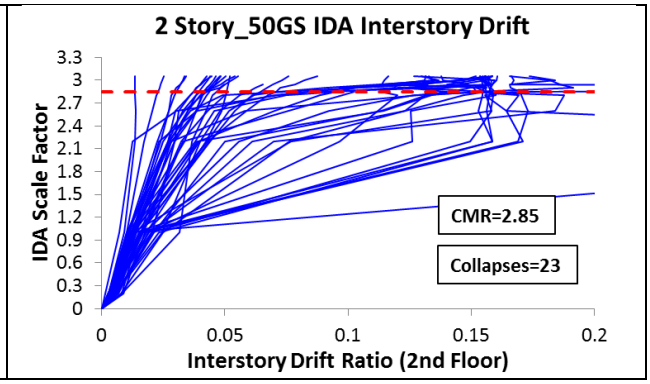

Model: 2Story_50GS (Fibers)

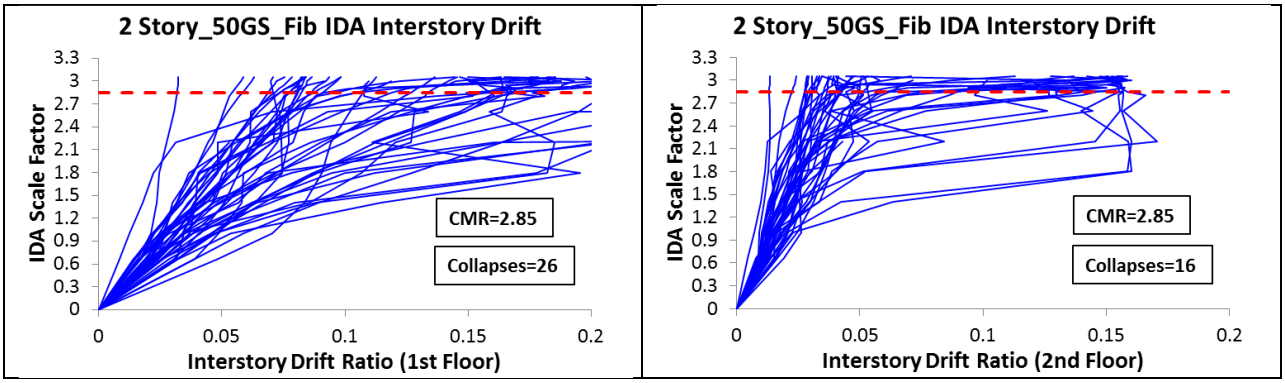

Model: 2Story_70GS (Elastic)

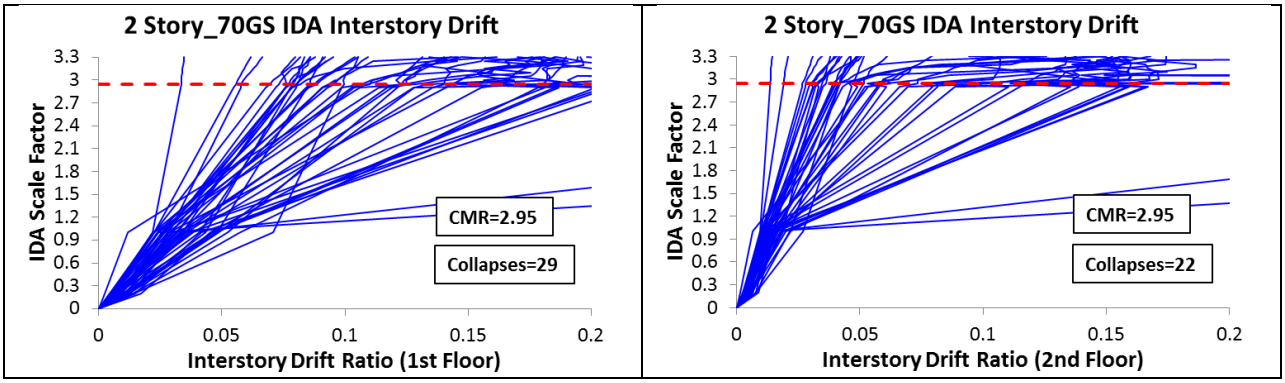

Model: 2Story_70GS (Fibers)

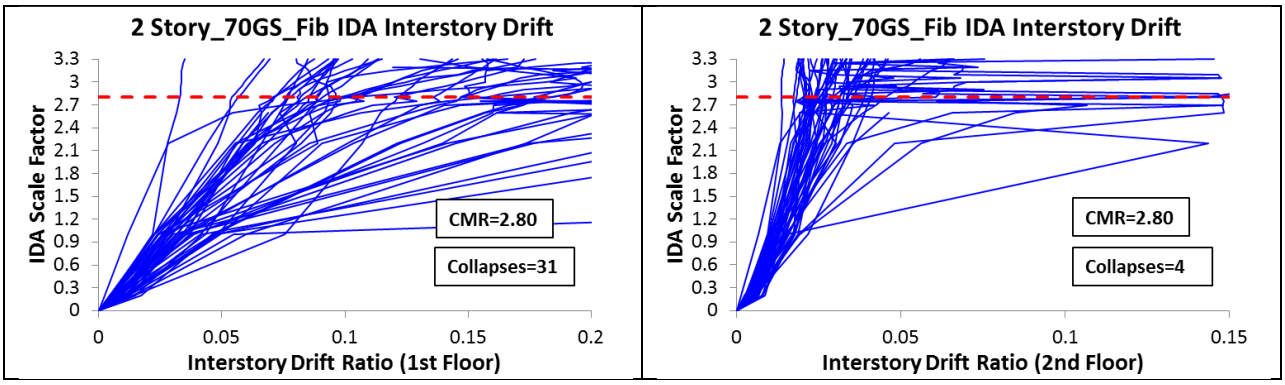

Scale Factors that Caused Collapse										
Far Field Ground Motions			Gravity Columns - Elastic Sections				Gravity Columns - Fiber Sections			
		2 Story	2 Story_0GS	2 Story_35GS	2 Story_50GS	2 Story_70GS	2 Story_0GS	2 Story_35GS	2 Story_50GS	2 Story_70GS
		CMR=2.15	CMR=2.40	CMR=2.65	CMR=2.85	CMR=2.95	CMR=2.40	CMR=2.65	CMR=2.85	CMR=2.80
Northridge-BH	MUL009	2	2.1	2.6	2.2	2.9		2.6	2.2	2.2
Northridge-BH	MUL279	2	2	1.8	2.2	2.9	1.8	1.8	1.8	2.2
Northridge-CC	LOS000	2	2.2	2.2	2.2	2.9	2	2.2	2.2	2.2
Northridge-CC	LOS270									
Duzce-Bolu	BOL000				2.6	2.9		2.6	2.6	2.2
Duzce-Bolu	BOL090		2.2			3.1	2.2		2.6	2.2
Hector-Hector	HEC000	2.1	2.2	2.6	2.8	2.9	2.2	2.6	2.85	2.8
Hector-Hector	HEC090	2	1.4	1.8	2.2	2.9	1.4	1.8	1.8	2.2
Imperial Valley-Delta	H-DLT262		2.25	2.65	2.85	2.9	2.3	2.65	2.6	2.6
Imperial Valley-Delta	H-DLT352	2	1.4	1.8	2.2	2.95	1.4	1.8	1.4	2.2
Imperial Valley-EC	H-E11140	2.1		2.6	2.8		2.4	2.6	2.8	2.6
Imperial Valley-EC	H-E11230	2.1	2.2				2.2			
Kobe-Nishi Akashi	NIS000									
Kobe-Nishi Akashi	NIS090									
Kobe-Shin Osaka	SHI000	2	2.2	2.6	2.6	2.9	2.1	2.6	2.6	2.6
Kobe-Shin Osaka	SHI090									
Kocaeli-Duzce	DZC180	2	2.25	2.65	2.85		2.2	2.65		
Kocaeli-Duzce	DZC270	2		2.2	2.2			2.2		2.2
Kocaeli-Arcelik	ARC000									
Koaceli-Arcelik	ARC090									
Landers-Yermo	YER270	2	1.8	2.2	2.2	2.9	1.8	2.2	2.2	2.2
Landers-Yermo	YER360									
Landers-Coolwater	CLW-LN									
Landers-Coolwater	CLW-TR	2	1.2	1.4	2.2	2.9	1.4	1.4	1.8	2.2
Loma Prieta-Capitola	CAP000	2	1.4	1.8	2.2	2.9	1.4	1.8	1.8	2.6
Loma Prieta-Capitola	CAP090	2								
Loma Prieta-Gilroy	G03000									
Loma Prieta-Gilroy	G03090	2	1.8	1.8	2.2	2.9	1.8	1.8	2.2	2.2
Manjil-Abbar	ABBAR--L									
Manjil-Abbar	ABBAR--T	2.1	2.1	2.6	2.6	3.05	2	2.6	2.6	2.6
Superstition Hills-EC	B-ICC000			2.2	2.2	2.9		2.2	2.2	2.2
Superstition Hills-EC	B-ICC090	2.1		2.65	2.8	2.9		2.65	2.8	2.8
Superstition Hills-Poe	B-POE270	2.1								
Superstition Hills-Poe	B-POE360	2.15	2.2			2.95	2.2		2.85	2.75
Cape Mendocino-Rio Dell	RIO270	2	1.8	1.8	2.2	2.9	1.4	1.8	1.8	2.2
Cape Mendocino-Rio Dell	RIO360	2.15	2.35				2.2			
Chi Chi-CHY	CHY101-E									
Chi Chi-CHY	CHY101-N		2.3	2.6	2.6	2.9	2.25	2.6	2.6	2.2
Chi Chi-TCU	TCU045-E		2.4	2.6	2.8	2.9	2.35	2.6	2.8	2.75
Chi Chi-TCU	TCU045-N									
San Fernando-LA	PEL180									
San Fernando-LA	PEL090	2	1.8	1.8	2.2	2.9	1.8	1.8	1.8	2.6
Friuli-Tolmezzo	A-TMZ000									
Friuli-Tolmezzo	A-TMZ270			2.65				2.6		
Number of Colapses		23	22	23	23	22	22	24	23	24

Appendix E: Partially Restrained Connections Designs

ORIGIN := 1

PARTIALLY RESTRAINED COMPOSITE CONNECTIONS

W14X38 (Ammerman Test)

$$\begin{pmatrix} d \\ t_w \\ b_f \\ t_f \\ t \\ b \\ Z_x \\ A_{ang} \end{pmatrix} :=$$

W, S, M, HP Shapes

Beam

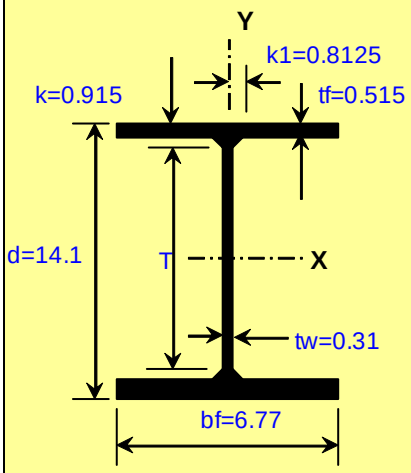

Single Angles

Seat angle

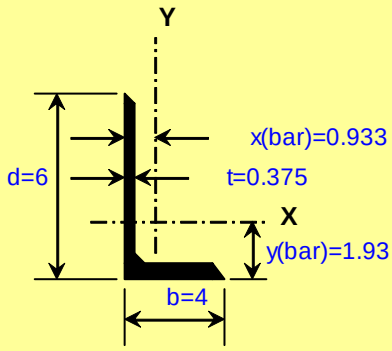

	W14x38	
A =	11.20	in.^2
d =	14.100	in.
tw =	0.310	in.
bf =	6.770	in.
tf =	0.515	in.
T =	11-5/8	in.
k =	0.9150	in.
k1 =	0.8125	in.
gage =	3-1/2	in.
rt =	1.770	in.
d/Af =	4.04	
Ix =	385.00	in.^4
Sx =	54.60	in.^3
rx =	5.870	in.
Iy =	26.70	in.^4

	L6x4x3/8	
d =	6	in.
b =	4	in.
t =	0.375	in.
k =	0.8750	in.
wt./ft. =	12.30	plf.
A =	3.61	in.^2
Ix =	13.40	in.^4
Sx =	3.30	in.^3
rx =	1.930	in.
y(bar) =	1.930	in.
Iy =	4.86	in.^4
Sy =	1.58	in.^3
ry =	1.160	in.
x(bar) =	0.933	in.
rz =	0.870	in.

("W14x38" "L6x4x3/8")

Beam: W14x38

$d = 14.1$

$t_w = 0.31$

$b_f = 6.77$

$t_f = 0.515$

Seat Angle (WT 15x90)

$t = 0.375$

$b = 4$

$A_{ang} = 3.61$

BEAM PLASTIC MOMENT

$Z_x = 61.5$

$Mp := Z_x \cdot 50 \cdot 1.1 = 3382.5$ **[Kips-in]**

DOUBLE WEB ANGLES:

2xL4x4x3/8 x8.5

$L_{web} := 8.5$ **[in]** Web angle length

$t_{web} := \frac{3}{8} = 0.375$ **[in]** Web angle thickness

$A_{wl} := L_{web} \cdot t_{web} \cdot 2 = 6.375$ **[in^2]** Gross area of double web angles for shear calculations.

$A_{wl} = 6.375$

COMPOSITE INTERACTION PROPERTIES:

$Y_3 := 2.75$ **[in]** Distance from the top flange of the girder to the centroid of the reinforcement. Total slab thickness = 5.25in (including deck)

$A_s := 1.6$ **[in^2]** Steel reinforcement area. Choose from prequalified connections: Type I,II,III,IV or V. (According to Steel Design Guide 8)

Type I	6 - #4	As=1.2in^2
Type II	8 - #4	As=1.6in^2
Type III	10 - #4	As= 2in^2
Type IV	12 - #4	As=2.4in^2
Type V	10 - #5	As=3.07in^2
	14- #5	As=4.298in^2
	10 - #6	As=4.442in^2

$F_{yrb} := 60$ **[ksi]** Yield stress of reinforcing.

BOTTOM ANGLE CONNECTION:

$F_y := 36$ **[ksi]** Yield stress of seat and web angles

$L := 8$ **[in]** Angle Length (6 in long alngle leg can normally accept 4 bolts (2 rows of 2) .

$\gamma := 1.2$ Recommended value: 1.2 - 1.25 **(6.5 Bottom Angle Connection)**

$$A_{Lreq} := \frac{\gamma \cdot A_s \cdot F_{yrb}}{F_y} = 3.2$$ **[in²]** Area of bottom angle

$$t_{req} := \frac{A_{Lreq}}{L} = 0.4$$ **[in]** Required bottom angle thickness

Angle Thickness: $t = 0.375$

Note: Has to be bigger than treq

$$\text{Thick\_angle} := \begin{cases} \text{"OK"} & \text{if } t > t_{req} \\ \text{"NOT OK"} & \text{otherwise} \end{cases}$$

Thick_angle = "NOT OK"

$A_L := t \cdot L = 3$ **[in²]** Area of bottom angle

$$\text{Req\_Area} := \begin{cases} \text{"OK"} & \text{if } A_L > A_{Lreq} \\ \text{"NOT OK"} & \text{otherwise} \end{cases}$$

Req_Area = "NOT OK"

M-θ CURVE UNDER NEGATIVE BENDING

$C1 := 0.18\left(4 \cdot A_s \cdot F_{yrb} + 0.857 \cdot A_L \cdot F_y\right) \cdot \left(d + Y_3\right) = 1445.394$

$C2 := 0.775$

$C3 := 0.007 \cdot \left(A_L + A_{wl}\right) \cdot F_y \cdot \left(d + Y_3\right) = 39.808$

$$Mneg_n(\theta) := C1 \cdot \left(1 - e^{-C2 \cdot \theta}\right) + C3 \cdot \theta \qquad \textbf{[kip-in]}$$

LINEARIZED M-θ CURVE UNDER NEGATIVE BENDING

LINEARIZED M-θ CURVE UNDER NEGATIVE BENDING

BILINEAR METHOD

$\theta 1_{BM} := 4$

$\theta 2_{BM} := 20$

$Mneg_n\left(\theta 2_{BM}\right) = 2241.557$ **[kip-in]**

$Mneg_n\left(\theta 1_{BM}\right) = 1539.513$

$\frac{Mneg_n\left(\theta 1_{BM}\right)}{12} = 128.293$ **[kip-ft]**

$\frac{Mneg_n\left(\theta 2_{BM}\right)}{12} = 186.796$ **[kip-ft]**

$Rot_{Bil_1} := 0$

$M_{Bilinear_1} := 0$

$Rot_{Bil_2} := \theta 1_{BM} = 4$

$M_{Bilinear_2} := Mneg_n\left(\theta 1_{BM}\right) = 1539.513$

$$SecantStiffness := \frac{M_{Bilinear_2}}{Rot_{Bil_2}} \cdot 1000 = 384878.246$$

$Rot_{Bil_3} := \theta 2_{BM} = 20$

$M_{Bilinear_3} := Mneg_n\left(\theta 2_{BM}\right) = 2241.557$

Partially Restrained Composite Connection Moment Rotation Backbone Curve Ammerman Test

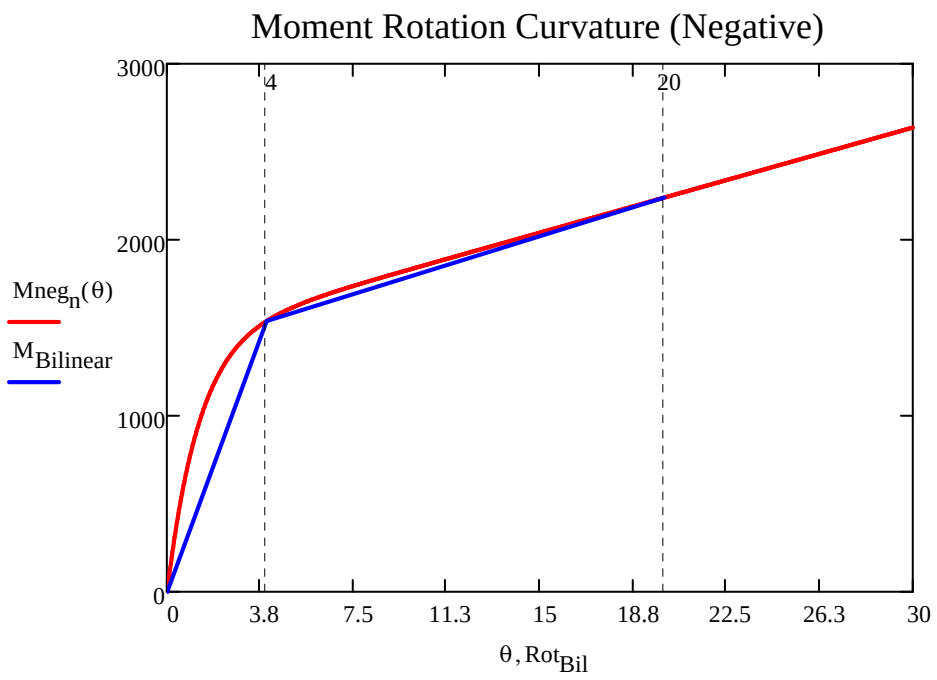

M-θ CURVE UNDER POSITIVE BENDING

$C1 := 0.2400 \cdot \left[\left(0.48 \cdot A_{wl} + A_L \right) \cdot \left(d + Y_3 \right) \cdot F_y \right] = 882.239$

$C2 := 0.021 \cdot \left(d + \frac{Y_3}{2} \right) = 0.325$

$C3 := 0.0100 \cdot \left(A_{wl} + A_L \right) \cdot \left(d + Y_3 \right) \cdot F_y = 56.869$

$C4 := 0.0065 \cdot A_{wl} \cdot \left(d + Y_3 \right) \cdot F_y = 25.136$

$$Mpos_n\left(\theta_p\right) := C1 \cdot \left(1 - e^{-C2 \cdot \theta_p} \right) + (C3 + C4) \cdot \theta_p \qquad \textbf{[kip-in]}$$

LINEARIZED M-θ CURVE UNDER POSITIVE BENDING

BILINEAR METHOD

$\theta 1_{BM} := 4$

$Mpos_n\left(\theta 1_{BM}\right) = 969.796$

$Rot_{Bil_1} := 0$

$Rot_{Bil_2} := \theta 1_{BM} = 4$

$\theta 2_{BM} := 20$

$Mpos_n\left(\theta 2_{BM}\right) = 2521.007$

$M_{Bilinear_1} := 0$

$M_{Bilinear_2} := Mpos_n\left(\theta 1_{BM}\right) = 969.796$

$$SecantStiffness := \frac{M_{Bilinear_2} \cdot 1000}{Rot_{Bil_2}} = 242448.939$$

$Rot_{Bil_3} := \theta 2_{BM} = 20$

$M_{Bilinear_3} := Mpos_n\left(\theta 2_{BM}\right) = 2521.007$

Partially Restrained Composite Connection Moment Rotation Backbone Curve Ammerman Test

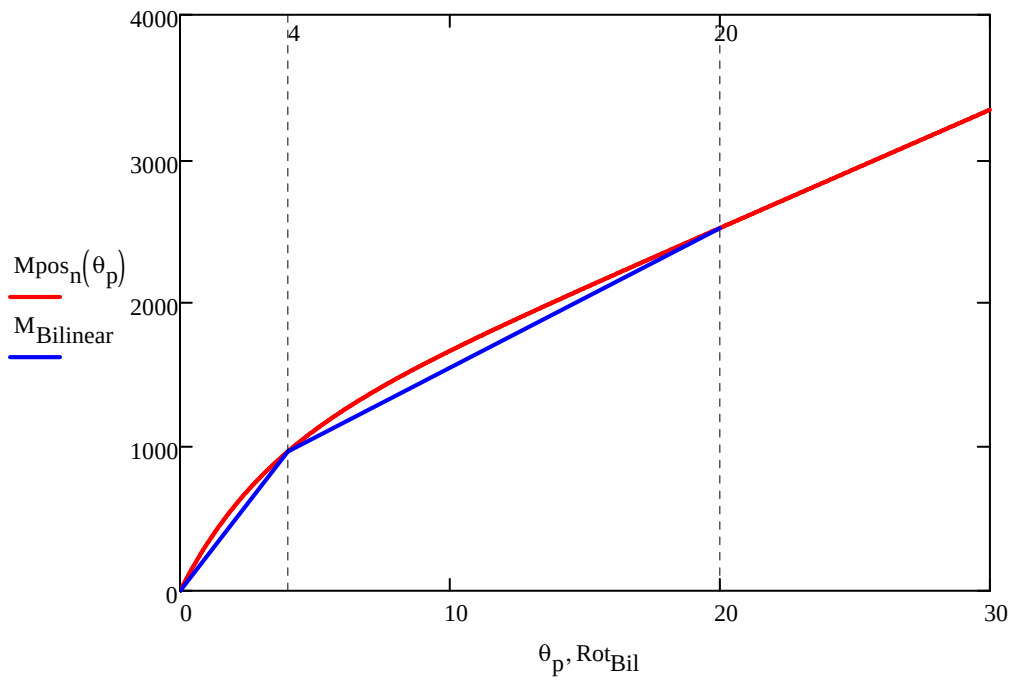

W16X36 CONNECTIONS

BEAM SECTION

W, S, M, HP Shapes

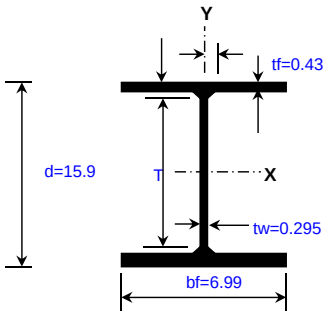

BEAM	W16x36	
A =	10.60	in.^2
d =	15.900	in.
tw =	0.295	in.
bf =	6.990	in.
tf =	0.430	in.
Ix =	448.00	in.^4
Sx =	56.50	in.^3
Iy =	24.50	in.^4
Sy =	7.00	in.^3
Zx =	64.00	in.^3
Zy =	10.80	in.^3

COLUMN SECTION

W, S, M, HP Shapes

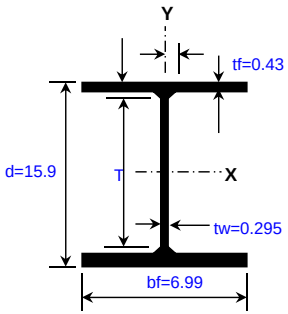

COLUMN	W14x61	
A =	17.90	in.^2
d =	13.900	in.
tw =	0.375	in.
bf =	9.990	in.
tf =	0.645	in.
Ix =	640.00	in.^4
Sx =	92.10	in.^3
Iy =	107.00	in.^4
Sy =	21.50	in.^3
Zx =	102.00	in.^3
Zy =	32.80	in.^3

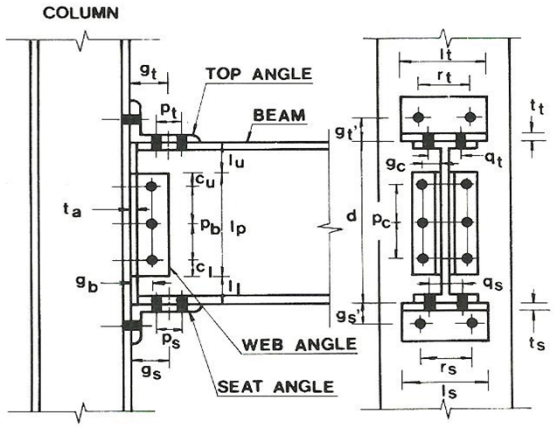

CONNECTION PROPERTIES AND DIMENSIONS

Top Angle	L6x4x3/4		Seat Angle	L6x4x3/4		Double Web angle	L4x4x1/4	
d =	6.000	in	d =	6.000	in	d =	4.000	in.
b=	4.000	in	b=	4.000	in	b=	4.000	in.
k=	1.250	in	k=	1.250	in	k=	0.625	in.
A=	6.940	in^2	A=	6.940	in^2	A=	1.930	in^2
t_t=	3/4	in	t_s=	3/4	in	t_a=	1/4	in.
L_t=	**6.000**	in	L_s=	6.000	in	L_p=	5.500	in
r_t=	**3.500**	in	r_s=	**3.500**	in	L_u=	1.375	in
g_t=	**3.500**	in	g_s=	**3.500**	in	L_l=	1.375	in
p_t=	**2.000**	in	p_s=	**2.000**	in	c_u=	1.250	in
g_t'=	**2.500**	in	g_s'=	**2.500**	in	p_b=	3.000	in
q_t=	**2.750**	in	q_s=	**2.750**	in	c_l=	1.250	in
I_t=	0.211	in^4	I_s=	0.211	in^4	g_b=	2.000	in
						p_c=	3.000	in
						g_c=	2.625	in

Bolts	Group A _ N	
Fnt=	90.00	ksi
Fnv=	54.000	ksi
db=	**3/4**	in.
D=	0.750	in.
Ab=	0.44	in.^2
ϕ=	0.750	
B=ϕRnt=	**29.8**	Tension Capacity
ϕRnv=	**17.9**	Shear capacity

MOMENT ROTATION CURVE

1) Initial Stiffness

E= 29000.000 ksi

Top angle:

I_t=	0.211	in^4
g_1=	1.750	in
d_1=	16.650	in
K_t=	830310.160	k/in

Double web angle:

I_w=	0.007	in^4
g_3=	2.125	in
d_3=	8.325	in
K_t=	8903.873	k/in

Seat Angle

I_s=	0.211	in^4
L_{s0}=	4.750	in
K_t=	5151.316	k/in

K= 844365.349 k/in

2) Prediction of Mechanism Moment Capacity

Top angle:

σ_y=	36.000	ksi
M_o=	30.375	kip-in
V_o=	81.000	kips
g_2=	0.875	in
V_{pt}=	**23.184**	Kips
equation	-0.659	Must be =0
d_2=	17.525	in
M_{pt}=	10.143	kip-in
M_{ut}=	416.452	kip-in

Double web angle:

σ_y=	36.000	ksi
M_o=		kip-in
V_o=	4.500	kips/in
V_{pl}=	**5.061**	Kips
y=	0.000	in
g_y=	0.392	in
equation	2.364	Must be =0
V_{pm}=	**2.680**	Kips
y=Lp/2	2.750	in
g_y=	1.009	in
equation	1.528	Must be =0
V_{pu}=	**1.681**	Kips
y=Lp	5.500	in
g_y=	1.625	in
equation	1.448	Must be =0
V_{pw}=	**16.640**	Kips
$\bar{Y}$=	2.238	in
d_4=	3.988	in
M_{uw}=	132.719	kip-in

Seat Angle

σ_y=	36.000	ksi
M_{os}=	30.375	kip-in

2.191666667

Mu= 579.546 kip-in

LOADS

Mu=	**73.33**	kip-ft
Ru=	9.4	kips

Structural Members Materials

Fy=	50	ksi
Fu=	65	ksi

Connecting Materials

Fy=	36	ksi
Fu=	58	ksi

Reduction Factors

Tension

ϕt=	0.9	yielding
ϕt=	0.75	rupture

Shear

ϕv=	0.9	yielding
ϕv=	0.75	rupture

Design Solution (Example 9-28 from AISC-LRFD 2nd Edition pg 9-255)

1) Check beam design flexural Strength

Zreq=	19.56	in.^3	Ok	pg_9-256 (AISC-LRFD 2nd edition)

F13 (pg16.1-64) Strength Reduction for Members with holes in tension flange

Afg=	3.01	in.^2		Gross area
n=	**2.00**			Assumed number of bolts in "**standard**" holes
Afn=	2.25	in.^2		Net Area
Yt=	1.00			_=1 if Fy/Fu<=0.8; =1.1 otherwise
Ze=	61.18	kip-in	Ok	Effective plastic Section Modulus (Must be larger than Zreq)

2) Design the double angle web connection

Bolt and Angle available strength: Table 10-1 (pg 10_13 to pg 10-45)

	Group A _ N			Bolt Group
N	2			Number of rows of bolts
	STD			Hole type
t=	1/4	in		Angle Thickness
ϕRn=	**48.90**	kip	Ok	**Value taken from table 10-1, (Must be bigger than Ru)**

Beam web available strength per inch thickness: Table 10-1 (pg 10_13 to pg 10-45)

	STD			Hole type
				Cope type
	Uncoped			
		in		
Leh=	**1 1/2**	in		
Lev=		in		
Zreq=		in.^3		
B. strength=	**176.00**	kip/in		**Value taken from table 10-1**
ϕRn=	51.92	kips	Ok	

Double web angle length

N=	2.00			Number of rows of bolts
s between bolts=	**3.00**	in		
Leh=	1.50	in		
Total Length=	**6.00**	in		Total Double Web Length

3) Design the tension flange angle and connection

Puf=	55.35	kips		
NboltsT=	**2.00**			Number of bolts required for tension
NboltsV=	**4.00**			Number of bolts required for shear

4)Determine flange angle thickness for flexure

Try angle length=	**6.00**	in		Trying an angle length

b=g't=	**1 1/4**	in		Distance from bolt centerline to centerline of angle length (g't or b) (Table 15-2a pg 15-12)
Trib load=	9.22	kip/in		
2 * Trib Load=	18.45	kip/in		Table 15-2a based upon a symmetrical connection, enter table with twice tributary load
Temp thickness=	**3/4**	in		Taken from table 15-2a pg 15-12. Available tensile strength must be bigger than 2*Trib Load. Note:AISC 13 Edition based on yelding strength and 14th edition based on ultimate strength
Avai tens strength	**23.50**	kip/in	**Ok**	
Selected angle	**L6x4x3/4**			
d=	6.00	in		Angle properties
b=	4.000	in.		Angle properties
t=	0.750	in.		Angle properties
A=	6.94	in^2		

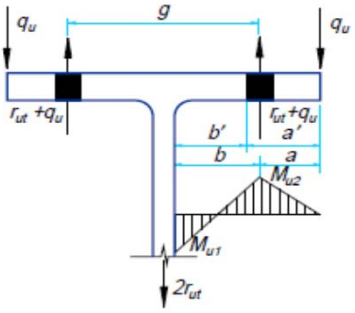

Fig. 11-2. Variables in prying action.

Check angle thickness for prying action assuming a gage

g=	**4.00**	in		Assumed gage
T=rut=	27.67	kips/bolt		Load bolts resist in tension
b=g't=	1 1/4	in		Distance from bolt centerline to centerline of angle length (Table 15-2a)
a=(b-g't)	2.00	in		Distance from bolt centerline to edge of fitting
b'=	0.88	in		Eq 9-21 (pg 9-11 AISC-LRFD 2010)
a'=	1.94	in		Eq 9-27 (pg 9-12 AISC-LRFD 2010)
ρ=	0.45			Eq 9-26 (pg 9-12 AISC-LRFD 2010)
B=ϕrn=	29.82	kips/bolt		Available tension per bolt (ϕrn)
β=	0.17			Eq 9-25 (pg 9-12 AISC-LRFD 2010)
d'=	0.81	in		Width of bolt hole parallel to the angle leg
s=	**3.00**	bolt spacing		
p=	**3.00**			Tributary length per pair of bolts, p, Figure 9-4 AISC Manual, less than bolt spacing s
δ=	0.73			ratio of the net length at bolt line to gross length at the face of the leg of angle
α'=	0.28			
tmin=	0.72	in	**OK**	Eq 9.23a. If tmin<=t preliminary fitting thickness is satisfactory. Otherwise, a fitting with a thicker flange or a change in geometry (i.e., b and p) is required.

Check tension yielding of the angle

Ag=	4.50	in^2		Angle area (length x t)
ϕRn=	145.80	kips	**OK**	

Check tension rupture of the angle

An=	3.19	in^2	
ϕRn=	138.66	kips	**OK**

Check shear yielding of the angle

ϕRn=	87.48	kips	**OK**

Check shear rupture of the angle

An=	3.19	in		Considers two bolts in flange (perpendicular to tension load)
ϕRn=	83.19	kips	**OK**	

Check block shear rupture of the angle

Ubs=	**1.00**			Ubs=1 where tension stress is uniform, otherwise 0.5
t=	3/4	in		
Agv=	**6.00**	in		
Anv=	**4.69**	Number of bolts		
Ant=	**2.34**			
0.6FuAnv=	163.13	kips /in		**Shear Rupture Component** per inch of thickness (Table 9-3c AISC 14th-pg 9-36)
FuAnt=	135.94	kips /in		**Tension Rupture Component** per inch of thickness (Table 9-3a AISC 14th -pg 9-33)
0.6FyAgv=	129.60	kips /in		**Shear Yielding Component** per inch of thickness (Table 9-3b AISC 14th-pg 9-34)
ϕRn=	199.15	kips	**OK**	min(0.6FuAnv+UbsFuAnt, 0.6FyAgv+UbsFuAnt)*t

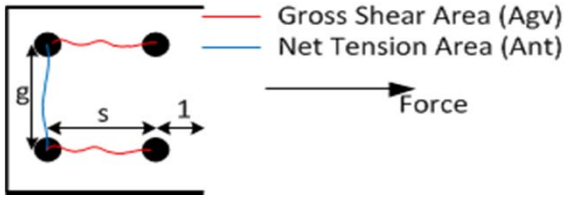

4)Design the compression flange angle and connection

For symmetry the same angle in tension is checked in compression.

Check design compressive strength of angle assuming K=0.65 and l=3in (normal gage)

K=	**0.65**			Unbraced length factor
L = (s)	3.00	in		Length (normal gage) = s
I=	0.21	in^4		Inertia
A=	4.50	in^2		Area
r=	0.22	in		radious of gyration
KL/r=	9.01	in		
ϕcFcr=	**32.20**	ksi		Available critical stress for compression Members (Table 4-22 pg 4-322)
ϕRn=	144.90	kips	**OK**	

Note: Example taken from AISC-LRFD manual 2nd Edition pg 9-258

ORIGIN := 1

PARTIALLY RESTRAINED COMPOSITE CONNECTIONS

W16X36

$$\begin{pmatrix} d \\ t_w \\ b_f \\ t_f \\ t \\ b \\ Z_x \\ A_{ang} \end{pmatrix} :=$$

W, S, M, HP Shapes

Beam

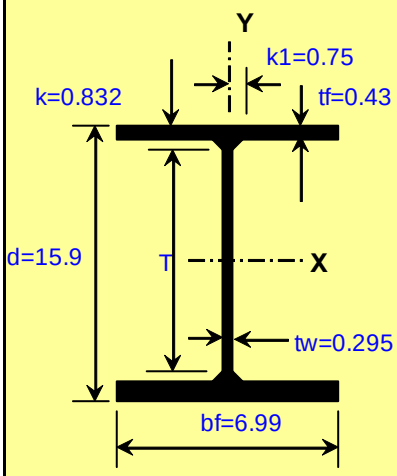

Single Angles

Seat angle

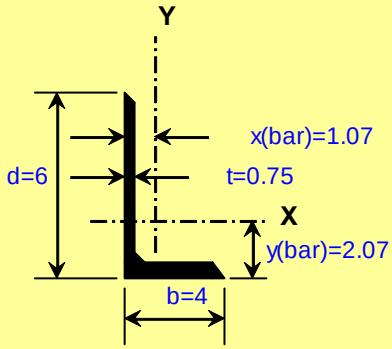

	W16x36	
A =	10.60	in.^2
d =	15.900	in.
tw =	0.295	in.
bf =	6.990	in.
tf =	0.430	in.
T =	13-5/8	in.
k =	0.8320	in.
k1 =	0.7500	in.
gage =	3-1/2	in.
rt =	1.790	in.
d/Af =	5.28	
Ix =	448.00	in.^4
Sx =	56.50	in.^3
rx =	6.510	in.
Iy =	24.50	in.^4

	L6x4x3/4	
d =	6	in.
b =	4	in.
t =	0.75	in.
k =	1.2500	in.
wt./ft. =	23.60	plf.
A =	6.94	in.^2
Ix =	24.50	in.^4
Sx =	6.23	in.^3
rx =	1.880	in.
y(bar) =	2.070	in.
Iy =	8.63	in.^4
Sy =	2.95	in.^3
ry =	1.120	in.
x(bar) =	1.070	in.
rz =	0.856	in.

("W16x36" "L6x4x3/4")

BEAM PLASTIC MOMENT

$Mp := Z_x \cdot 50 = 3200$ **[Kips-in]**

DOUBLE WEB ANGLES:

2xL4x3-1/2x1/4 x 6

$L_{web} := 6$ **[in]** Web angle length

$t_{web} := \frac{1}{4}$ **[in]** Web angle thickness

$A_{wl} := L_{web} \cdot t_{web} \cdot 2 = 3$ **[in^2]** Gross area of double web angles for shear calculations.

$A_{wl} = 3$

COMPOSITE INTERACTION PROPERTIES:

$Y_3 := 4$ **[in]** Distance from the top flange of the girder to the centroid of the reinforcement. Total slab thickness = 5.25in (including deck)

$A_s := 1.2$ **[in^2]** Steel reinforcement area. Choose from prequalified connections: Typ I,II,III,IV or V. (According to Steel Design Guide 8)

Type I	6 - #4	As=1.2in^2
Type II	8 - #4	As=1.6in^2
Type III	10 - #4	As= 2in^2
Type IV	12 - #4	As=2.4in^2
Type V	10 - #5	As=3.07in^2

$F_{yrb} := 60$ **[ksi]** Yield stress of reinforcing.

CONNECTION PROPERTIES:

BOTTOM ANGLE CONNECTION:

$F_y := 36$ **[ksi]** Yield stress of seat and web angles

$L := 6$ **[in]** Angle Length (6 in long alngle leg can normally accept 4 bolts (2 rows of 2) .

$\gamma := 1.2$ Recommended value: 1.2 - 1.25 **(6.5 Bottom Angle Connection)**

$A_{Lreq} := \frac{\gamma \cdot A_s \cdot F_{yrb}}{F_y} = 2.4$ **[in²]** Area of bottom angle

$t_{req} := \frac{A_{Lreq}}{L} = 0.4$ **[in]** Required bottom angle thickness

Angle Thickness: $t = 0.75$

Note: Has to be bigger than treq

$$Thick\_angle := \begin{cases} \text{"OK"} & \text{if } t > t_{req} \\ \text{"NOT OK"} & \text{otherwise} \end{cases}$$

Thick_angle = "OK"

$A_L := t \cdot L = 4.5$ **[in²]** Area of bottom angle

$$Req\_Area := \begin{cases} \text{"OK"} & \text{if } A_L > A_{Lreq} \\ \text{"NOT OK"} & \text{otherwise} \end{cases}$$

Req_Area = "OK"

M-θ CURVE UNDER NEGATIVE BENDING

$C1 := 0.18\left(4 \cdot A_s \cdot F_{yrb} + 0.857 \cdot A_L \cdot F_y\right) \cdot \left(d + Y_3\right) = 1528.919$

$C2 := 0.775$

$C3 := 0.007 \cdot \left(A_L + A_{wl}\right) \cdot F_y \cdot \left(d + Y_3\right) = 37.611$

$$Mneg_n(\theta) := C1 \cdot \left(1 - e^{-C2 \cdot \theta}\right) + C3 \cdot \theta \qquad \textbf{[kip-in]}$$

LINEARIZED M-θ CURVE UNDER NEGATIVE BENDING

BILINEAR METHOD

$\theta 1_{BM} := 4$

$Mneg_n\left(\theta 1_{BM}\right) = 1610.487$

$\frac{Mneg_n\left(\theta 1_{BM}\right)}{12} = 134.207$ **[kip-ft]**

$\theta 2_{BM} := 20$

$Mneg_n\left(\theta 2_{BM}\right) = 2281.139$ **[kip-in]**

$\frac{Mneg_n\left(\theta 2_{BM}\right)}{12} = 190.095$ **[kip-ft]**

$Rot_{Bil_1} := 0$

$M_{Bilinear_1} := 0$

$Rot_{Bil_2} := \theta 1_{BM} = 4$

$M_{Bilinear_2} := Mneg_n\left(\theta 1_{BM}\right) = 1610.487$

$SecantStiffness := \frac{M_{Bilinear_2}}{Rot_{Bil_2}} \cdot 1000 = 402621.697$

$Rot_{Bil_3} := \theta 2_{BM} = 20$

$M_{Bilinear_3} := Mneg_n\left(\theta 2_{BM}\right) = 2281.139$

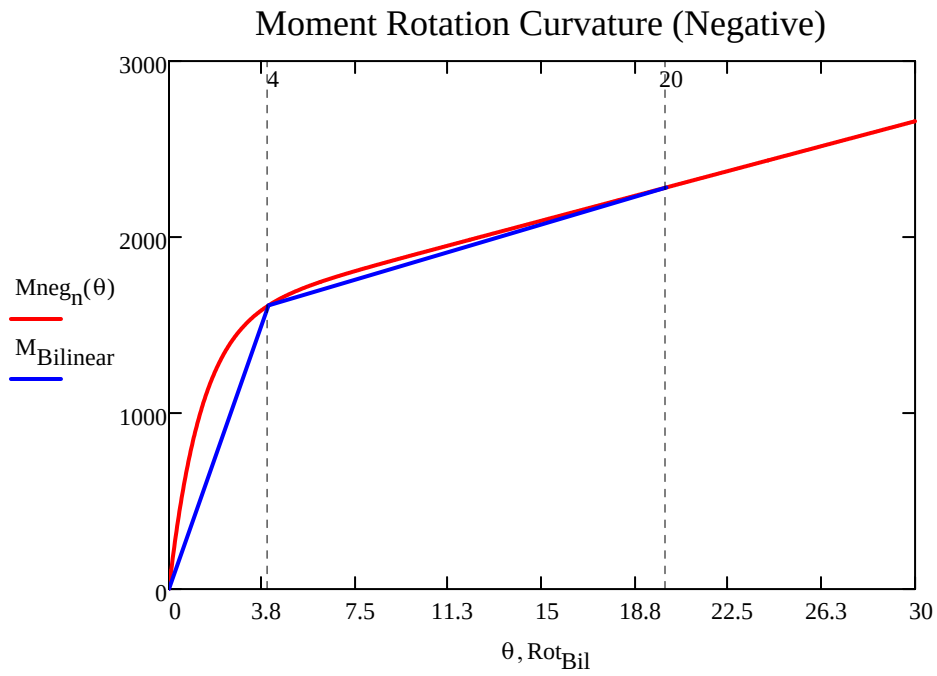
Moment Rotation Curvature (Negative)
3000
2000
1000
0
4
20
Mneg_n(θ)
M_Bilinear
0
3.8
7.5
11.3
15
18.8
22.5
26.3
30
θ, Rot_Bil

M-θ CURVE UNDER POSITIVE BENDING

$C1 := 0.2400 \cdot \left[\left(0.48 \cdot A_{wl} + A_L \right) \cdot \left(d + Y_3 \right) \cdot F_y \right] = 1021.3$

$C2 := 0.021 \cdot \left(d + \frac{Y_3}{2} \right) = 0.376$

$C3 := 0.0100 \cdot \left(A_{wl} + A_L \right) \cdot \left(d + Y_3 \right) \cdot F_y = 53.73$

$C4 := 0.0065 \cdot A_{wl} \cdot \left(d + Y_3 \right) \cdot F_y = 13.97$

$$Mpos_n\left(\theta_p\right) := C1 \cdot \left(1 - e^{-C2 \cdot \theta_p} \right) + (C3 + C4) \cdot \theta_p \qquad \textbf{[kip-in]}$$

LINEARIZED M-θ CURVE UNDER POSITIVE BENDING

BILINEAR METHOD

$\theta 1_{BM} := 4$

$Mpos_n\left(\theta 1_{BM}\right) = 1065.035$

$Rot_{Bil_1} := 0$

$Rot_{Bil_2} := \theta 1_{BM} = 4$

$\theta 2_{BM} := 20$

$Mpos_n\left(\theta 2_{BM}\right) = 2374.741$

$M_{Bilinear_1} := 0$

$M_{Bilinear_2} := Mpos_n\left(\theta 1_{BM}\right) = 1065.035$

$$SecantStiffness := \frac{M_{Bilinear_2} \cdot 1000}{Rot_{Bil_2}} = 266258.787$$

$Rot_{Bil_3} := \theta 2_{BM} = 20$

$M_{Bilinear_3} := Mpos_n\left(\theta 2_{BM}\right) = 2374.741$

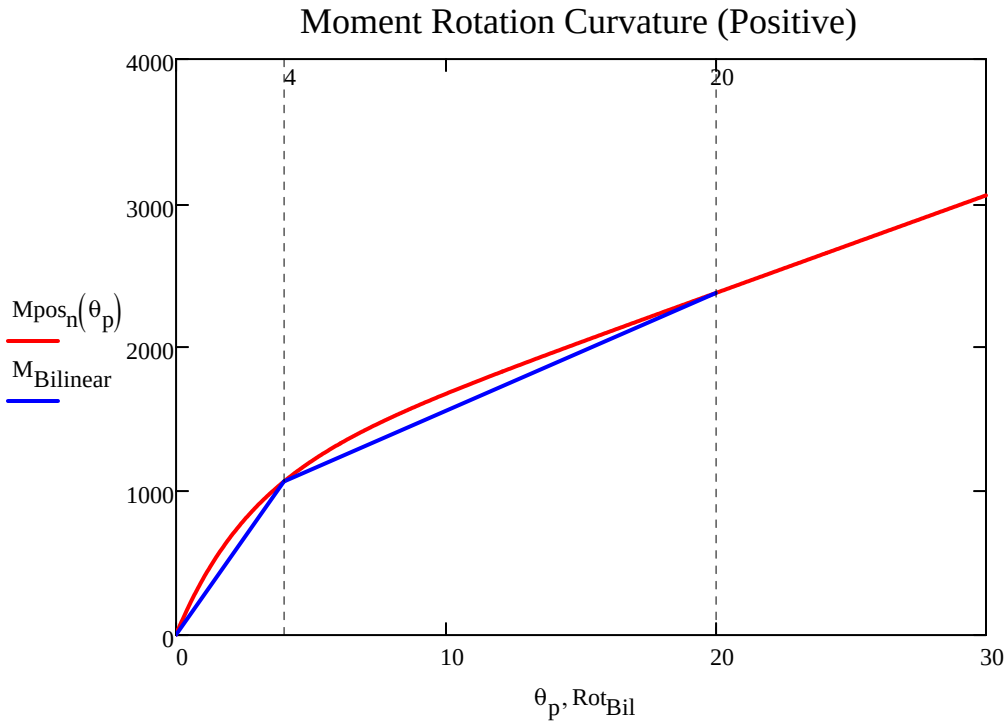
Moment Rotation Curvature (Positive)
4000
3000
2000
1000
0
4
20
0
10
20
30
Mpos_n(θ_p)
M_Bilinear
θ_p, Rot_Bil

W24X55 CONNECTIONS

BEAM SECTION

W, S, M, HP Shapes

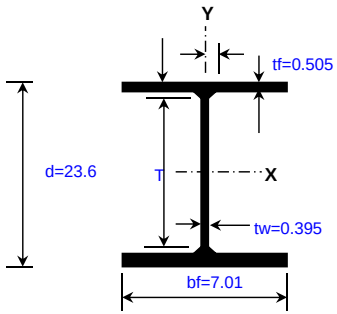

COLUMN SECTION

W, S, M, HP Shapes

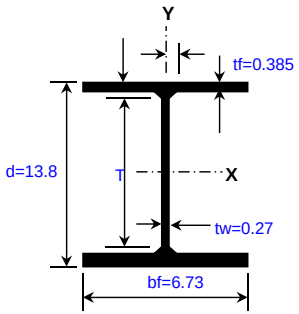

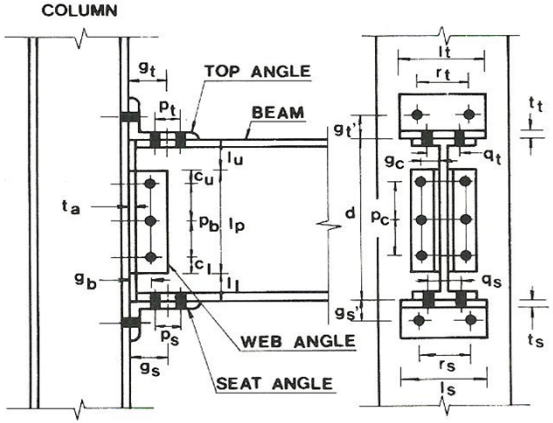

BEAM	W24x55	
A =	16.30	in.^2
d =	23.600	in.
tw =	0.395	in.
bf =	7.010	in.
tf =	0.505	in.
Ix =	1360.00	in.^4
Sx =	115.00	in.^3
Iy =	29.10	in.^4
Sy =	8.30	in.^3
Zx =	135.00	in.^3
Zy =	13.40	in.^3

COLUMN	W14x30	
A =	8.85	in.^2
d =	13.800	in.
tw =	0.270	in.
bf =	6.730	in.
tf =	0.385	in.
Ix =	291.00	in.^4
Sx =	42.00	in.^3
Iy =	19.60	in.^4
Sy =	5.82	in.^3
Zx =	47.30	in.^3
Zy =	8.99	in.^3

CONNECTION PROPERTIES AND DIMENSIONS

Top Angle	L8x4x3/4	
d =	8.000	in
b=	4.000	in
k=	1.250	in
A=	8.490	in^2
t_t=	3/4	in
L_t=	**6.000**	in
r_t=	**3.500**	in
g_t=	**3.500**	in
p_t=	**2.000**	in
g_t'=	**2.500**	in
q_t=	**2.750**	in
l_t=	0.211	in^4

Seat Angle	L8x4x3/4	
d =	8.000	in
b=	4.000	in
k=	1.250	in
A=	8.490	in^2
t_s=	3/4	in
L_s=	6.000	in
r_s=	**3.500**	in
g_s=	**3.500**	in
p_s=	**2.000**	in
g_s'=	**2.500**	in
q_s=	**2.750**	in
l_s=	0.211	in^4

Double Web angle	L4x4x1/4	
d =	4.000	in.
b=	4.000	in.
k=	0.625	in.
A=	1.930	in^2
t_a=	1/4	in.
L_p=	5.500	in
L_u=	1.375	in
L_l=	1.375	in
c_u=	1.250	in
p_b=	3.000	in
c_l=	1.250	in
g_b=	2.000	in
p_c=	3.000	in
g_c=	2.625	in

Bolts	Group A _ N	
Fnt=	90.00	ksi
Fnv=	54.000	ksi
db=	**3/4**	in.
D=	0.750	in.
Ab=	0.44	in.^2
ϕ=	0.750	
B=ϕRnt=	**29.8**	Tension Capacity
ϕRnv=	**17.9**	Shear capacity

MOMENT ROTATION CURVE

1) Initial Stiffness

E= 29000.000 ksi

Top angle:

I_t=	0.211	in^4
g_1=	1.750	in
d_1=	24.350	in
K_t=	1775864.427	k/in

Double web angle:

I_w=	0.007	in^4
g_3=	2.125	in
d_3=	12.175	in
K_t=	19043.572	k/in

Seat Angle

I_s=	0.211	in^4
L_{s0}=	6.750	in
K_t=	3625.000	k/in

K= 1798532.998 k/in

2) Prediction of Mechanism Moment Capacity

Top angle:

σ_y=	36.000	ksi
M_o=	30.375	kip-in
V_o=	81.000	kips
g_2=	0.875	in
V_{pt}=	**23.184**	Kips
equation	-0.659	Must be =0
d_2=	25.225	in
M_{pt}=	10.143	kip-in
M_{ut}=	594.972	kip-in

Double web angle:

σ_y=	36.000	ksi
M_o=		kip-in
V_o=	4.500	kips/in
V_{pl}=	**5.061**	Kips
y=	0.000	in
g_y=	0.392	in
equation	2.364	Must be =0
V_{pm}=	**2.680**	Kips
y=Lp/2	2.750	in
g_y=	1.009	in
equation	1.528	Must be =0
V_{pu}=	**1.681**	Kips
y=Lp	5.500	in
g_y=	1.625	in
equation	1.448	Must be =0
V_{pw}=	**16.640**	Kips
$\bar{Y}$=	2.238	in
d_4=	3.988	in
M_{uw}=	132.719	kip-in

Seat Angle

σ_y=	36.000	ksi
M_{os}=	30.375	kip-in

2.191666667

Mu= 758.066 kip-in

LOADS

Mu=	**154.69**	kip-ft
Ru=	24.9	kips

Structural Members Materials

Fy=	50	ksi
Fu=	65	ksi

Connecting Materials

Fy=	36	ksi
Fu=	58	ksi

Reduction Factors

Tension

ϕt=	0.9	yielding
ϕt=	0.75	rupture

Shear

ϕv=	0.9	yielding
ϕv=	0.75	rupture

Design Solution (Example 9-28 from AISC-LRFD 2nd Edition pg 9-255)

1) Check beam design flexural Strength

Zreq=	41.25	in.^3	Ok	pg_9-256 (AISC-LRFD 2nd edition)

F13 (pg16.1-64) Strength Reduction for Members with holes in tension flange

Afg=	3.54	in.^2		Gross area
n=	**2.00**			Assumed number of bolts in "**standard**" holes
Afn=	2.66	in.^2		Net Area
Yt=	1.00			_=1 if Fy/Fu<=0.8; =1.1 otherwise
Ze=	124.64	kip-in	Ok	Effective plastic Section Modulus (Must be bigger than Zreq)

2) Design the double angle web connection

Bolt and Angle available strength: Table 10-1 (pg 10_13 to pg 10-45)

	Group A _ N			Bolt Group
N	2			Number of rows of bolts
	STD			Hole type
t=	1/4	in		Angle Thickness
ϕRn=	**48.90**	kip	Ok	**Value taken from table 10-1, (Must be bigger than Ru)**

Beam web available strength per inch thickness: Table 10-1 (pg 10_13 to pg 10-45)

	STD			Hole type
				Cope type
	Uncoped			
		in		
Leh=	**1 1/2**	in		
Lev=		in		
Zreq=		in.^3		
B. strength=	**176.00**	kip/in		**Value taken from table 10-1**
ϕRn=	69.52	kips	Ok	

Double web angle length

N=	2.00			Number of rows of bolts
s between bolts=	**3.00**	in		
Leh=	1.50	in		
Total Length=	**6.00**	in		Total Double Web Length

3) Design the tension flange angle and connection

Puf=	78.65	kips		
NboltsT=	**4.00**			Number of bolts required for tension
NboltsV=	**6.00**			Number of bolts required for shear

4)Determine flange angle thickness for flexure

Try angle length=	**7.00**	in		Trying an angle length
b=g't=	**1 1/4**	in		Distance from bolt centerline to centerline of angle length (g't or b) (Table 15-2a pg 15-12)

Trib load=	11.24	kip/in		
2 * Trib Load=	22.47	kip/in		Table 15-2a based upon a symmetrical connection, enter table with twice tributary load
Temp thickness=	**3/4**	in		Taken from table 15-2a pg 15-12. Available tensile strength must be bigger than 2*Trib Load. Note:AISC 13 Edition based on yelding strength and 14th edition based on ultimate strength
Avai tens strength	**23.50**	kip/in	Ok	
Selected angle	**L8x4x3/4**			
d=	8.00	in		Angle properties
b=	4.000	in.		Angle properties
t=	0.750	in.		Angle properties
A=	8.49	in^2		

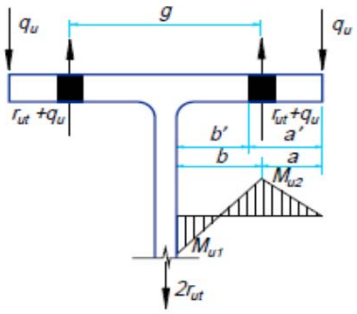

Fig. 11-2. Variables in prying action.

Check angle thickness for prying action assuming a gage

g=	**4.00**	in		Assumed gage
T=rut=	19.66	kips/bolt		Load bolts resist in tension
b=g't=	1 1/4	in		Distance from bolt centerline to centerline of angle length (Table 15-2a)
a=(b-g't)	2.00	in		Distance from bolt centerline to edge of fitting
b'=	0.88	in		Eq 9-21 (pg 9-11 AISC-LRFD 2010)
a'=	1.94	in		Eq 9-27 (pg 9-12 AISC-LRFD 2010)
ρ=	0.45			Eq 9-26 (pg 9-12 AISC-LRFD 2010)
B=ϕrn=	29.82	kips/bolt		Available tension per bolt (ϕrn)
β=	1.14			Eq 9-25 (pg 9-12 AISC-LRFD 2010)
d'=	0.81	in		Width of bolt hole parallel to the angle leg
s=	3.00	bolt spacing (in)		
p=	**3.00**			Tributary length per pair of bolts, p, Figure 9-4 AISC Manual, less than bolt spacing s
δ=	0.73			ratio of the net length at bolt line to gross length at the face of the leg of angle
α'=	1.00			
tmin=	0.50	in	OK	Eq 9.23a. If tmin<=t preliminary fitting thickness is satisfactory. Otherwise, a fitting with a thicker flange or a change in geometry (i.e., b and p) is required.

0.70711 3.535533906

Check tension yielding of the angle

Ag=	5.25	in^2		Angle area (length x t)
ϕRn=	170.10	kips	OK	

Check tension rupture of the angle

An=	3.94	in^2		
ϕRn=	171.28	kips	OK	

Check shear yielding of the angle

ϕRn=	102.06	kips	OK	

Check shear rupture of the angle

An=	3.94	in		Considers two bolts in flange (perpendicular to tension load)
ϕRn=	102.77	kips	OK	

Check block shear rupture of the angle

Ubs=	**1.00**			Ubs=1 where tension stress is uniform, otherwise 0.5
t=	3/4	in		
Agv=	**10.50**	in		
Anv=	**7.22**	Number of bolts		
Ant=	**2.34**			
0.6FuAnv=	251.21	kips /in		**Shear Rupture Component** per inch of thickness (Table 9-3c AISC 14th-pg 9-36)
FuAnt=	135.94	kips /in		**Tension Rupture Component** per inch of thickness (Table 9-3a AISC 14th -pg 9-33)
0.6FyAgv=	226.80	kips /in		**Shear Yielding Component** per inch of thickness (Table 9-3b AISC 14th-pg 9-34)
ϕRn=	272.05	kips	**OK**	min(0.6FuAnv+UbsFuAnt, 0.6FyAgv+UbsFuAnt)*t

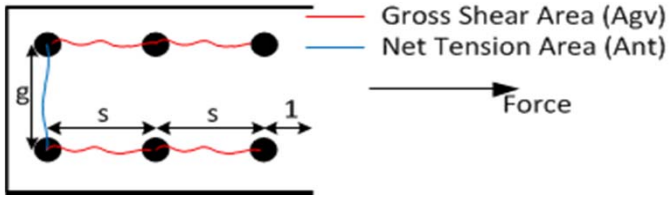

4)Design the compression flange angle and connection

For symmetry the same angle in tension is checked in compression.

Check design compressive strength of angle assuming K=0.65 and l=3in (normal gage)

K=	**0.65**			Unbraced length factor
L = (s)	3.00	in		Length (normal gage) = s
I=	0.25	in^4		Inertia
A=	5.25	in^2		Area
r=	0.22	in		radious of gyration
KL/r=	9.01	in		
ϕcFcr=	**32.20**	ksi		Available critical stress for compression Members (Table 4-22 pg 4-322)
ϕRn=	169.05	kips	**OK**	

Note: Example taken from AISC-LRFD manual 2nd Edition pg 9-258

ORIGIN := 1

PARTIALLY RESTRAINED COMPOSITE CONNECTIONS

W24X55

$$\begin{pmatrix} d \\ t_w \\ b_f \\ t_f \\ t \\ b \\ Z_x \\ A_{ang} \end{pmatrix} :=$$

W, S, M, HP Shapes

Beam

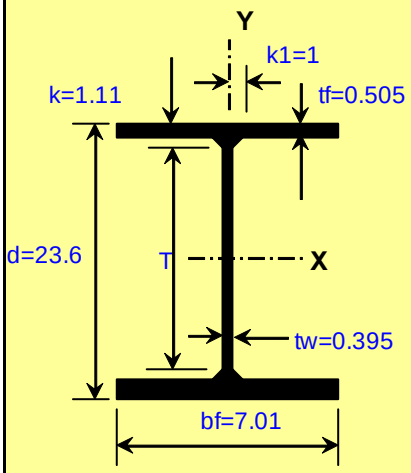

	W24x55	
A =	16.30	in.^2
d =	23.600	in.
tw =	0.395	in.
bf =	7.010	in.
tf =	0.505	in.
T =	20-3/4	in.
k =	1.1100	in.
k1 =	1.0000	in.
gage =	3-1/2	in.
rt =	1.680	in.
d/Af =	6.66	
Ix =	1360.00	in.^4
Sx =	115.00	in.^3
rx =	9.130	in.
Iy =	29.10	in.^4

Single Angles

Seat angle

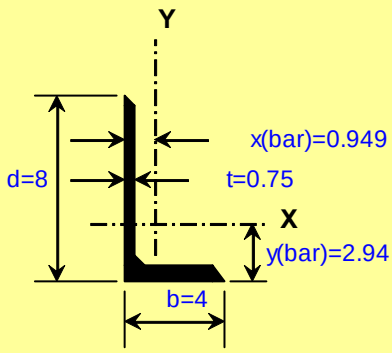

	L8x4x3/4	
d =	8	in.
b =	4	in.
t =	0.75	in.
k =	1.2500	in.
wt./ft. =	28.90	plf.
A =	8.49	in.^2
Ix =	55.00	in.^4
Sx =	10.90	in.^3
rx =	2.550	in.
y(bar) =	2.940	in.
Iy =	9.37	in.^4
Sy =	3.07	in.^3
ry =	1.050	in.
x(bar) =	0.949	in.
rz =	0.850	in.

("W24x55" "L8x4x3/4")

BEAM PLASTIC MOMENT

$Mp := Z_x \cdot 50 = 6750$ **[Kips-in]**

DOUBLE WEB ANGLES:

2xL4x4x1/4 x 6

$L_{web} := 6$ **[in]** Web angle length

$t_{web} := \frac{1}{4} = 0.25$ **[in]** Web angle thickness

$A_{wl} := L_{web} \cdot t_{web} \cdot 2 = 3$ **[in^2]** Gross area of double web angles for shear calculations.

$A_{wl} = 3$

COMPOSITE INTERACTION PROPERTIES:

$Y_3 := 4$ **[in]** Distance from the top flange of the girder to the centroid of the reinforcement. Total slab thickness = 5.25in (including deck)

$A_s := 1.2$ **[in^2]** Steel reinforcement area. Choose from prequalified connections: Type I,II,III,IV or V. (According to Steel Design Guide 8)

Type I	6 - #4	As=1.2in^2
Type II	8 - #4	As=1.6in^2
Type III	10 - #4	As= 2in^2
Type IV	12 - #4	As=2.4in^2
Type V	10 - #5	As=3.07in^2

$F_{yrb} := 60$ **[ksi]** Yield stress of reinforcing.

CONNECTION PROPERTIES:

BOTTOM ANGLE CONNECTION:

$F_y := 36$ **[ksi]** Yield stress of seat and web angles

$L := 7$ **[in]** Angle Length (6 in long alngle leg can normally accept 4 bolts (2 rows of 2) .

$\gamma := 1.2$ Recommended value: 1.2 - 1.25 **(6.5 Bottom Angle Connection)**

$A_{Lreq} := \frac{\gamma \cdot A_s \cdot F_{yrb}}{F_y} = 2.4$ **[in²]** Area of bottom angle

$t_{req} := \frac{A_{Lreq}}{L} = 0.343$ **[in]** Required bottom angle thickness

Angle Thickness: $t = 0.75$

Note: Has to be bigger than treq

$$Thick\_angle := \begin{cases} \text{"OK"} & \text{if } t > t_{req} \\ \text{"NOT OK"} & \text{otherwise} \end{cases}$$

Thick_angle = "OK"

$A_L := t \cdot L = 5.25$ **[in²]** Area of bottom angle

$$Req\_Area := \begin{cases} \text{"OK"} & \text{if } A_L > A_{Lreq} \\ \text{"NOT OK"} & \text{otherwise} \end{cases}$$

Req_Area = "OK"

M-θ CURVE UNDER NEGATIVE BENDING

$C1 := 0.18\left(4 \cdot A_s \cdot F_{yrb} + 0.857 \cdot A_L \cdot F_y\right) \cdot \left(d + Y_3\right) = 2235.466$

$C2 := 0.775$

$C3 := 0.007 \cdot \left(A_L + A_{wl}\right) \cdot F_y \cdot \left(d + Y_3\right) = 57.38$

$$Mneg_n(\theta) := C1 \cdot \left(1 - e^{-C2 \cdot \theta}\right) + C3 \cdot \theta \qquad \textbf{[kip-in]}$$

LINEARIZED M-θ CURVE UNDER NEGATIVE BENDING

The line is conformed by 4 points: (0,0) (θ1,M1), (θ2,M2), (θ3,M3).

BILINEAR METHOD

$\theta 1_{BM} := 4$

$Mneg_n\left(\theta 1_{BM}\right) = 2364.282$

$\dfrac{Mneg_n\left(\theta 1_{BM}\right)}{12} = 197.023$ **[kip-ft]**

$\theta 2_{BM} := 20$

$Mneg_n\left(\theta 2_{BM}\right) = 3383.073$ **[kip-in]**

$\dfrac{Mneg_n\left(\theta 2_{BM}\right)}{12} = 281.923$ **[kip-ft]**

$Rot_{Bil_1} := 0$

$M_{Bilinear_1} := 0$

$Rot_{Bil_2} := \theta 1_{BM} = 4$

$M_{Bilinear_2} := Mneg_n\left(\theta 1_{BM}\right) = 2364.282$

$SecantStiffness := \dfrac{M_{Bilinear_2}}{Rot_{Bil_2}} \cdot 1000 = 591070.377$

$Rot_{Bil_3} := \theta 2_{BM} = 20$

$M_{Bilinear_3} := Mneg_n\left(\theta 2_{BM}\right) = 3383.073$

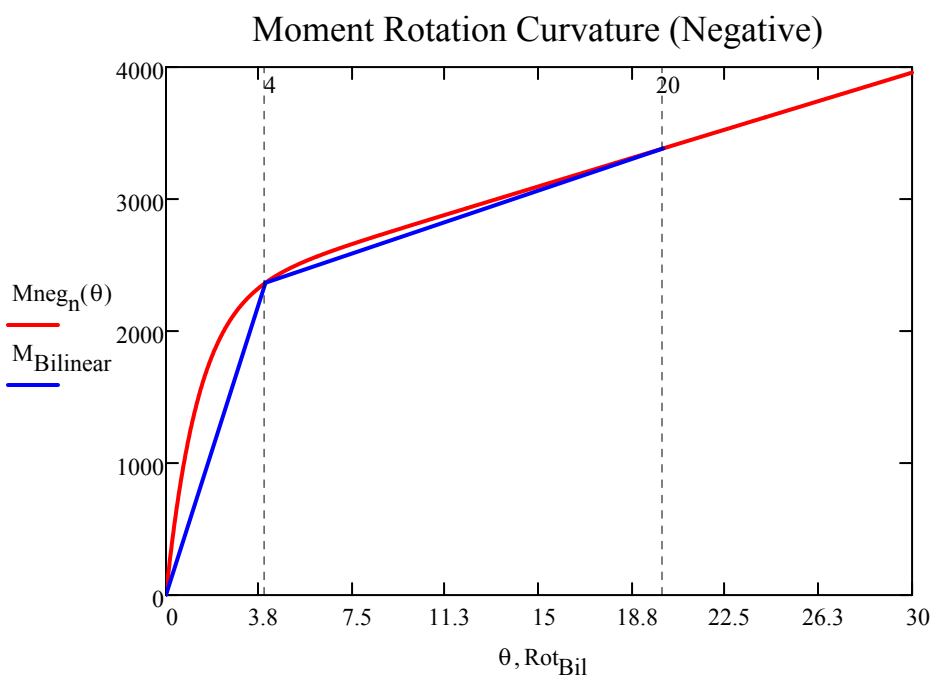
Moment Rotation Curvature (Negative)
4000
3000
2000
1000
0
4
20
Mneg_n(θ)
M_Bilinear
0
3.8
7.5
11.3
15
18.8
22.5
26.3
30
θ, Rot_Bil

M-θ CURVE UNDER POSITIVE BENDING

$$C1 := 0.2400\cdot\left[\left(0.48\cdot A_{wl} + A_L\right)\cdot\left(d + Y_3\right)\cdot F_y\right] = 1595.324$$

$$C2 := 0.021\cdot\left(d + \frac{Y_3}{2}\right) = 0.538$$

$$C3 := 0.0100\cdot\left(A_{wl} + A_L\right)\cdot\left(d + Y_3\right)\cdot F_y = 81.972$$

$$C4 := 0.0065\cdot A_{wl}\cdot\left(d + Y_3\right)\cdot F_y = 19.375$$

$$Mpos_n\left(\theta_p\right) := C1\cdot\left(1 - e^{-C2\cdot\theta_p}\right) + (C3 + C4)\cdot\theta_p \qquad \textbf{[kip-in]}$$

LINEARIZED M-θ CURVE UNDER POSITIVE BENDING

BILINEAR METHOD

$\theta 1_{BM} := 4$ $\qquad$ $\theta 2_{BM} := 20$

$Mpos_n\left(\theta 1_{BM}\right) = 1814.957$ $\qquad$ $Mpos_n\left(\theta 2_{BM}\right) = 3622.234$

$Rot_{Bil_1} := 0$ $\qquad$ $M_{Bilinear_1} := 0$

$Rot_{Bil_2} := \theta 1_{BM} = 4$ $\qquad$ $M_{Bilinear_2} := Mpos_n\left(\theta 1_{BM}\right) = 1814.957$

$$SecantStiffness := \frac{M_{Bilinear_2}\cdot 1000}{Rot_{Bil_2}} = 453739.321$$

$Rot_{Bil_3} := \theta 2_{BM} = 20$ $\qquad$ $M_{Bilinear_3} := Mpos_n\left(\theta 2_{BM}\right) = 3622.234$

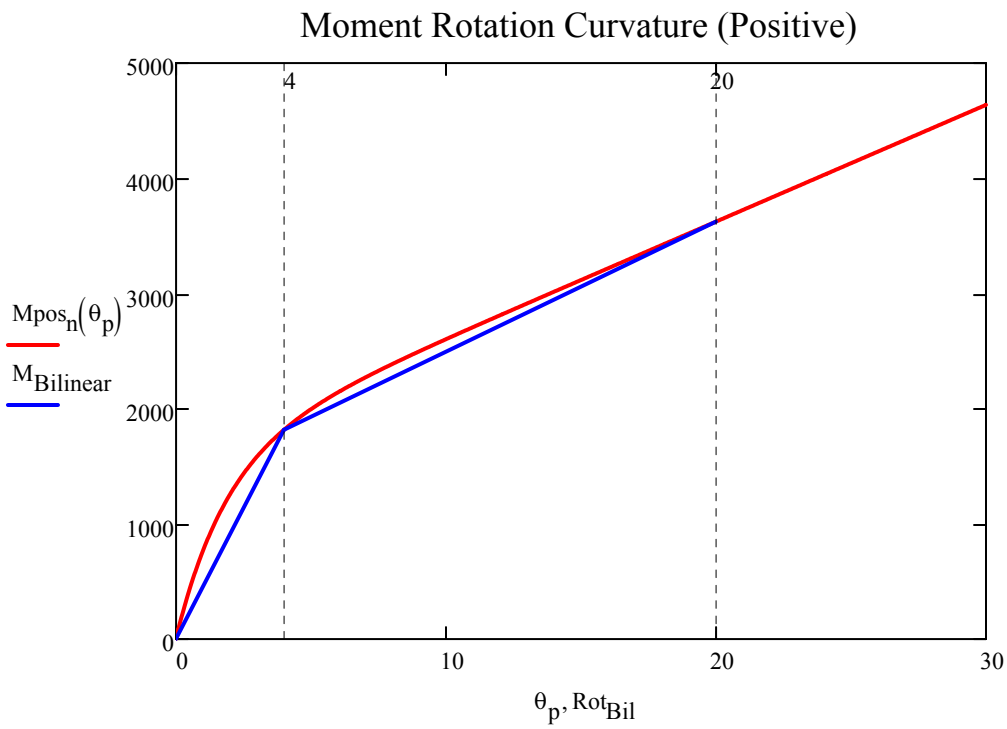
Moment Rotation Curvature (Positive)
5000
4000
3000
2000
1000
0
4
20
0
10
20
30
Mpos_n(θ_p)
M_Bilinear
θ_p, Rot_Bil

W24X62 CONNECTIONS

BEAM SECTION

W, S, M, HP Shapes

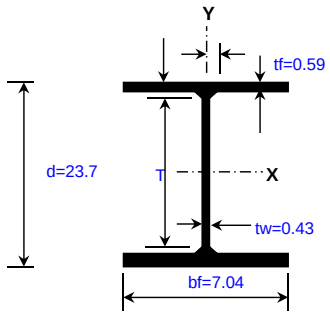

COLUMN SECTION

W, S, M, HP Shapes

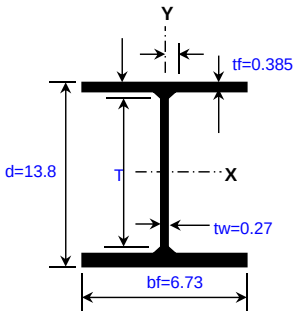

BEAM	W24x62	
A =	18.30	in.^2
d =	23.700	in.
tw =	0.430	in.
bf =	7.040	in.
tf =	0.590	in.
Ix =	1560.00	in.^4
Sx =	132.00	in.^3
Iy =	34.50	in.^4
Sy =	9.80	in.^3
Zx =	154.00	in.^3
Zy =	15.80	in.^3

COLUMN	W14x30	
A =	8.85	in.^2
d =	13.800	in.
tw =	0.270	in.
bf =	6.730	in.
tf =	0.385	in.
Ix =	291.00	in.^4
Sx =	42.00	in.^3
Iy =	19.60	in.^4
Sy =	5.82	in.^3
Zx =	47.30	in.^3
Zy =	8.99	in.^3

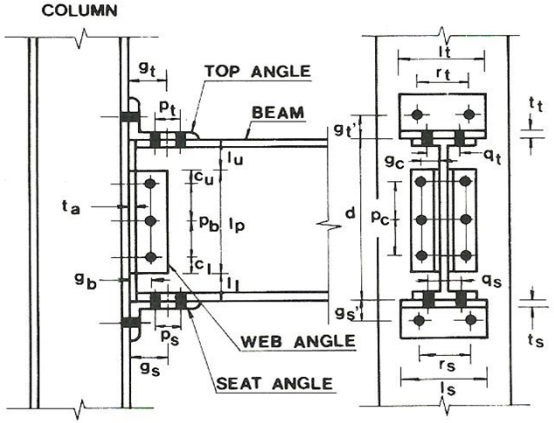

CONNECTION PROPERTIES AND DIMENSIONS

Top Angle	L8x4x3/4		Seat Angle	L8x4x3/4		Double Web angle	L4x4x1/4	
d =	8.000	in	d =	8.000	in	d =	4.000	in.
b=	4.000	in	b=	4.000	in	b=	4.000	in.
k=	1.250	in	k=	1.250	in	k=	0.625	in.
A=	8.490	in^2	A=	8.490	in^2	A=	1.930	in^2
t_t=	3/4	in	t_s=	3/4	in	t_a=	1/4	in.
L_t=	**6.000**	in	L_s=	6.000	in	L_p=	5.500	in
r_t=	**3.500**	in	r_s=	**3.500**	in	L_u=	1.375	in
g_t=	**3.500**	in	g_s=	**3.500**	in	L_l=	1.375	in
p_t=	**2.000**	in	p_s=	**2.000**	in	c_u=	1.250	in
g_t'=	**2.500**	in	g_s'=	**2.500**	in	p_b=	3.000	in
q_t=	**2.750**	in	q_s=	**2.750**	in	c_l=	1.250	in
I_t=	0.211	in^4	I_s=	0.211	in^4	g_b=	2.000	in
						p_c=	3.000	in
						g_c=	2.625	in

Bolts	Group A _ N	
Fnt=	90.00	ksi
Fnv=	54.000	ksi
db=	**3/4**	in.
D=	0.750	in.
Ab=	0.44	in.^2
ϕ=	0.750	
B=ϕRnt=	**29.8**	Tension Capacity
ϕRnv=	**17.9**	Shear capacity

MOMENT ROTATION CURVE

1) Initial Stiffness

E= 29000.000 ksi

Top angle:

I_t=	0.211	in^4
g_1=	1.750	in
d_1=	24.450	in
K_t=	1790480.533	k/in

Double web angle:

I_w=	0.007	in^4
g_3=	2.125	in
d_3=	12.225	in
K_t=	19200.308	k/in

Seat Angle

I_s=	0.211	in^4
L_{s0}=	6.750	in
K_t=	3625.000	k/in

K= 1813305.841 k/in

2) Prediction of Mechanism Moment Capacity

Top angle:

σ_y=	36.000	ksi
M_o=	30.375	kip-in
V_o=	81.000	kips
g_2=	0.875	in
V_{pt}=	**23.184**	Kips
equation	-0.659	Must be =0
d_2=	25.325	in
M_{pt}=	10.143	kip-in
M_{ut}=	597.291	kip-in

Double web angle:

σ_y=	36.000	ksi
M_o=		kip-in
V_o=	4.500	kips/in
V_{pl}=	**5.061**	Kips
y=	0.000	in
g_y=	0.392	in
equation	2.364	Must be =0
V_{pm}=	**2.680**	Kips
y=Lp/2	2.750	in
g_y=	1.009	in
equation	1.528	Must be =0
V_{pu}=	**1.681**	Kips
y=Lp	5.500	in
g_y=	1.625	in
equation	1.448	Must be =0
V_{pw}=	**16.640**	Kips
$\bar{Y}$=	2.238	in
d_4=	3.988	in
M_{uw}=	132.719	kip-in

Seat Angle

σ_y=	36.000	ksi
M_{os}=	30.375	kip-in

2.191666667

Mu= 760.385 kip-in

LOADS

Mu=	**176.46**	kip-ft
Ru=	36.6	kips

Structural Members Materials

Fy=	50	ksi
Fu=	65	ksi

Connecting Materials

Fy=	36	ksi
Fu=	58	ksi

Reduction Factors

Tension

ϕt=	0.9	yielding
ϕt=	0.75	rupture

Shear

ϕv=	0.9	yielding
ϕv=	0.75	rupture

Design Solution (Example 9-28 from AISC-LRFD 2nd Edition pg 9-255)

1) Check beam design flexural Strength

Zreq=	47.06	in.^3	Ok	pg_9-256 (AISC-LRFD 2nd edition)

F13 (pg16.1-64) Strength Reduction for Members with holes in tension flange

Afg=	4.15	in.^2		Gross area
n=	**2.00**			Assumed number of bolts in "**standard**" holes
Afn=	3.12	in.^2		Net Area
Yt=	1.00			_=1 if Fy/Fu<=0.8; =1.1 otherwise
Ze=	143.27	kip-in	Ok	Effective plastic Section Modulus (Must be bigger than Zreq)

2) Design the double angle web connection

Bolt and Angle available strength: Table 10-1 (pg 10_13 to pg 10-45)

	Group A _ N			Bolt Group
N	2			Number of rows of bolts
	STD			Hole type
t=	1/4	in		Angle Thickness
ϕRn=	**48.90**	kip	Ok	**Value taken from table 10-1, (Must be bigger than Ru)**

Beam web available strength per inch thickness: Table 10-1 (pg 10_13 to pg 10-45)

	STD			Hole type
				Cope type
	Uncoped			
		in		
Leh=	**1 1/2**	in		
Lev=		in		
Zreq=		in.^3		
B. strength=	**176.00**	kip/in		**Value taken from table 10-1**
ϕRn=	75.68	kips	Ok	

Double web angle length

N=	2.00			Number of rows of bolts
s between bolts=	**3.00**	in		
Leh=	1.50	in		
Total Length=	**6.00**	in		Total Double Web Length

3) Design the tension flange angle and connection

Puf=	89.35	kips		
NboltsT=	**4.00**			Number of bolts required for tension
NboltsV=	**6.00**			Number of bolts required for shear

4)Determine flange angle thickness for flexure

Try angle length=	**8.00**	in		Trying an angle length

b=g't=	**1 1/4**	in		Distance from bolt centerline to centerline of angle length (g't or b) (Table 15-2a pg 15-12)
Trib load=	11.17	kip/in		
2 * Trib Load=	22.34	kip/in		Table 15-2a based upon a symmetrical connection, enter table with twice tributary load
Temp thickness=	**3/4**	in		Taken from table 15-2a pg 15-12. Available tensile strength must be bigger than 2*Trib Load. Note:AISC 13 Edition based on yelding strength and 14th edition based on ultimate strength
Avai tens strength	**23.50**	kip/in	**Ok**	
Selected angle	**L8x4x3/4**			
d=	8.00	in		Angle properties
b=	4.000	in.		Angle properties
t=	0.750	in.		Angle properties
A=	8.49	in^2		

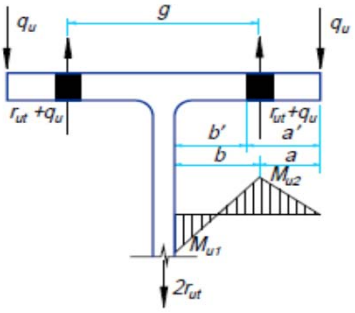

Fig. 11-2. Variables in prying action.

Check angle thickness for prying action assuming a gage

g=	**4.00**	in		Assumed gage
T=rut=	22.34	kips/bolt		Load bolts resist in tension
b=g't=	1 1/4	in		Distance from bolt centerline to centerline of angle length (Table 15-2a)
a=(b-g't)	2.00	in		Distance from bolt centerline to edge of fitting
b'=	0.88	in		Eq 9-21 (pg 9-11 AISC-LRFD 2010)
a'=	1.94	in		Eq 9-27 (pg 9-12 AISC-LRFD 2010)
ρ=	0.45			Eq 9-26 (pg 9-12 AISC-LRFD 2010)
B=ϕrn=	29.82	kips/bolt		Available tension per bolt (ϕrn)
β=	0.74			Eq 9-25 (pg 9-12 AISC-LRFD 2010)
d'=	0.81	in		Width of bolt hole parallel to the angle leg
s=	3.00	bolt spacing (in)		
p=	**3.00**			Tributary length per pair of bolts, p, Figure 9-4 AISC Manual, less than bolt spacing s
δ=	0.73			ratio of the net length at bolt line to gross length at the face of the leg of angle
α'=	1.00			
tmin=	0.54	in	**OK**	Eq 9.23a. If tmin<=t preliminary fitting thickness is satisfactory. Otherwise, a fitting with a thicker flange or a change in geometry (i.e., b and p) is required.

0.70711 3.535533906

Check tension yielding of the angle

Ag=	6.00	in^2		Angle area (length x t)
ϕRn=	194.40	kips	**OK**	

Check tension rupture of the angle

An=	4.69	in^2	
ϕRn=	203.91	kips	**OK**

Check shear yielding of the angle

ϕRn=	116.64	kips	**OK**

Check shear rupture of the angle

An=	4.69	in		Considers two bolts in flange (perpendicular to tension load)
ϕRn=	122.34	kips	**OK**	

Check block shear rupture of the angle

Ubs=	**1.00**			Ubs=1 where tension stress is uniform, otherwise 0.5
t=	3/4	in		
Agv=	**10.50**	in		
Anv=	**7.22**	Number of bolts		
Ant=	**2.34**			
0.6FuAnv=	251.21	kips /in		**Shear Rupture Component** per inch of thickness (Table 9-3c AISC 14th-pg 9-36)
FuAnt=	135.94	kips /in		**Tension Rupture Component** per inch of thickness (Table 9-3a AISC 14th -pg 9-33)
0.6FyAgv=	226.80	kips /in		**Shear Yielding Component** per inch of thickness (Table 9-3b AISC 14th-pg 9-34)
ϕRn=	272.05	kips	**OK**	min(0.6FuAnv+UbsFuAnt, 0.6FyAgv+UbsFuAnt)*t

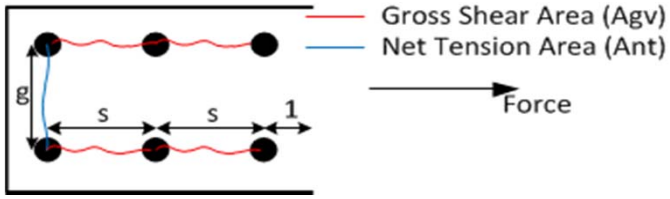

4)Design the compression flange angle and connection

For symmetry the same angle in tension is checked in compression.

Check design compressive strength of angle assuming K=0.65 and l=3in (normal gage)

K=	**0.65**			Unbraced length factor
L = (s)	3.00	in		Length (normal gage) = s
I=	0.28	in^4		Inertia
A=	6.00	in^2		Area
r=	0.22	in		radious of gyration
KL/r=	9.01	in		
ϕcFcr=	**32.20**	ksi		Available critical stress for compression Members (Table 4-22 pg 4-322)
ϕRn=	193.20	kips	**OK**	

Note: Example taken from AISC-LRFD manual 2nd Edition pg 9-258

ORIGIN := 1

PARTIALLY RESTRAINED COMPOSITE CONNECTIONS

W24X62

$$\begin{pmatrix} d \\ t_w \\ b_f \\ t_f \\ t \\ b \\ Z_x \\ A_{ang} \end{pmatrix} :=$$

W, S, M, HP Shapes

Beam

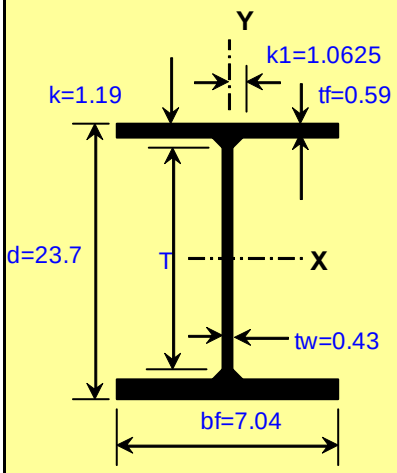

	W24x62	
A =	18.30	in.^2
d =	23.700	in.
tw =	0.430	in.
bf =	7.040	in.
tf =	0.590	in.
T =	20-3/4	in.
k =	1.1900	in.
k1 =	1.0625	in.
gage =	3-1/2	in.
rt =	1.710	in.
d/Af =	5.72	
Ix =	1560.00	in.^4
Sx =	132.00	in.^3
rx =	9.240	in.
Iy =	34.50	in.^4

Single Angles

Seat angle

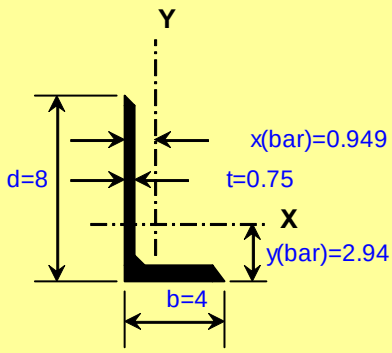

	L8x4x3/4	
d =	8	in.
b =	4	in.
t =	0.75	in.
k =	1.2500	in.
wt./ft. =	28.90	plf.
A =	8.49	in.^2
Ix =	55.00	in.^4
Sx =	10.90	in.^3
rx =	2.550	in.
y(bar) =	2.940	in.
Iy =	9.37	in.^4
Sy =	3.07	in.^3
ry =	1.050	in.
x(bar) =	0.949	in.
rz =	0.850	in.

("W24x62" "L8x4x3/4")

BEAM PLASTIC MOMENT

$Mp := Z_x \cdot 50 = 7700$ **[Kips-in]**

DOUBLE WEB ANGLES:

2xL4x4x1/4 x 12

$L_{web} := 6$ **[in]** Web angle length

$t_{web} := \frac{1}{4} = 0.25$ **[in]** Web angle thickness

$A_{wl} := L_{web} \cdot t_{web} \cdot 2 = 3$ **[in^2]** Gross area of double web angles for shear calculations.

$A_{wl} = 3$

COMPOSITE INTERACTION PROPERTIES:

$Y_3 := 4$ **[in]** Distance from the top flange of the girder to the centroid of the reinforcement. Total slab thickness = 5.25in (including deck)

$A_s := 1.2$ **[in^2]** Steel reinforcement area. Choose from prequalified connections: Type I,II,III,IV or V. (According to Steel Design Guide 8)

Type I	6 - #4	As=1.2in^2
Type II	8 - #4	As=1.6in^2
Type III	10 - #4	As= 2in^2
Type IV	12 - #4	As=2.4in^2
Type V	10 - #5	As=3.07in^2

$F_{yrb} := 60$ **[ksi]** Yield stress of reinforcing.

CONNECTION PROPERTIES:

BOTTOM ANGLE CONNECTION:

$F_y := 36$ **[ksi]** Yield stress of seat and web angles

$L := 8$ **[in]** Angle Length (6 in long alngle leg can normally accept 4 bolts (2 rows of 2) .

$\gamma := 1.2$ Recommended value: 1.2 - 1.25 **(6.5 Bottom Angle Connection)**

$$A_{Lreq} := \frac{\gamma \cdot A_s \cdot F_{yrb}}{F_y} = 2.4$$ **[in²]** Area of bottom angle

$$t_{req} := \frac{A_{Lreq}}{L} = 0.3$$ **[in]** Required bottom angle thickness

Angle Thickness: $t = 0.75$

Note: Has to be bigger than treq

$$\text{Thick\_angle} := \begin{cases} \text{"OK"} & \text{if } t > t_{req} \\ \text{"NOT OK"} & \text{otherwise} \end{cases}$$

Thick_angle = "OK"

$A_L := t \cdot L = 6$ **[in²]** Area of bottom angle

$$\text{Req\_Area} := \begin{cases} \text{"OK"} & \text{if } A_L > A_{Lreq} \\ \text{"NOT OK"} & \text{otherwise} \end{cases}$$

Req_Area = "OK"

M-θ CURVE UNDER NEGATIVE BENDING

$C1 := 0.18\left(4 \cdot A_s \cdot F_{yrb} + 0.857 \cdot A_L \cdot F_y\right) \cdot \left(d + Y_3\right) = 2358.936$

$C2 := 0.775$

$C3 := 0.007 \cdot \left(A_L + A_{wl}\right) \cdot F_y \cdot \left(d + Y_3\right) = 62.824$

$$Mneg_n(\theta) := C1 \cdot \left(1 - e^{-C2 \cdot \theta}\right) + C3 \cdot \theta \qquad \textbf{[kip-in]}$$

LINEARIZED M-θ CURVE UNDER NEGATIVE BENDING

BILINEAR METHOD

$\theta 1_{BM} := 4$

$Mneg_n\left(\theta 1_{BM}\right) = 2503.963$

$\theta 2_{BM} := 20$

$Mneg_n\left(\theta 2_{BM}\right) = 3615.408$ **[kip-in]**

$\frac{Mneg_n\left(\theta 1_{BM}\right)}{12} = 208.664$ **[kip-ft]**

$\frac{Mneg_n\left(\theta 2_{BM}\right)}{12} = 301.284$ **[kip-ft]**

$Rot_{Bil_1} := 0$

$M_{Bilinear_1} := 0$

$Rot_{Bil_2} := \theta 1_{BM} = 4$

$M_{Bilinear_2} := Mneg_n\left(\theta 1_{BM}\right) = 2503.963$

$SecantStiffness := \frac{M_{Bilinear_2}}{Rot_{Bil_2}} \cdot 1000 = 625990.657$

$Rot_{Bil_3} := \theta 2_{BM} = 20$

$M_{Bilinear_3} := Mneg_n\left(\theta 2_{BM}\right) = 3615.408$

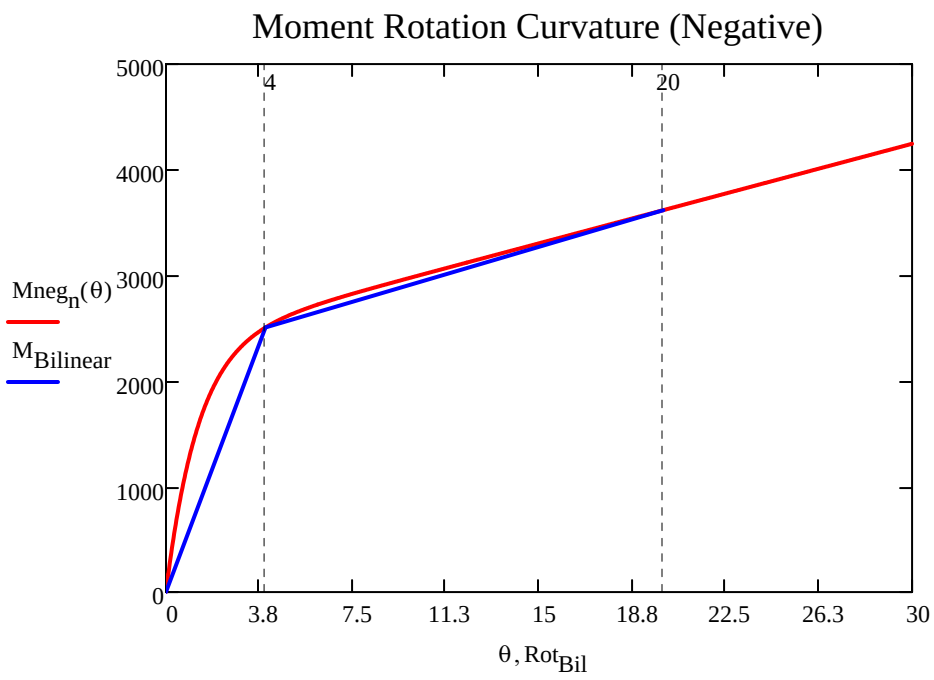
Moment Rotation Curvature (Negative)
5000
4000
3000
2000
1000
0
4
20
Mneg_n(θ)
M_Bilinear
0
3.8
7.5
11.3
15
18.8
22.5
26.3
30
θ, Rot_Bil

M-θ CURVE UNDER POSITIVE BENDING

$C1 := 0.2400 \cdot \left[\left(0.48 \cdot A_{wl} + A_L \right) \cdot \left(d + Y_3 \right) \cdot F_y \right] = 1780.6$

$C2 := 0.021 \cdot \left(d + \frac{Y_3}{2} \right) = 0.54$

$C3 := 0.0100 \cdot \left(A_{wl} + A_L \right) \cdot \left(d + Y_3 \right) \cdot F_y = 89.748$

$C4 := 0.0065 \cdot A_{wl} \cdot \left(d + Y_3 \right) \cdot F_y = 19.445$

$$Mpos_n\left(\theta_p\right) := C1 \cdot \left(1 - e^{-C2 \cdot \theta_p}\right) + (C3 + C4) \cdot \theta_p \qquad \textbf{[kip-in]}$$

LINEARIZED M-θ CURVE UNDER POSITIVE BENDING

BILINEAR METHOD

$\theta 1_{BM} := 4$ $\qquad$ $\theta 2_{BM} := 20$

$Mpos_n\left(\theta 1_{BM}\right) = 2011.779$ $\qquad$ $Mpos_n\left(\theta 2_{BM}\right) = 3964.432$

$Rot_{Bil_1} := 0$ $\qquad$ $M_{Bilinear_1} := 0$

$Rot_{Bil_2} := \theta 1_{BM} = 4$ $\qquad$ $M_{Bilinear_2} := Mpos_n\left(\theta 1_{BM}\right) = 2011.779$

$$SecantStiffness := \frac{M_{Bilinear_2} \cdot 1000}{Rot_{Bil_2}} = 502944.852$$

$Rot_{Bil_3} := \theta 2_{BM} = 20$ $\qquad$ $M_{Bilinear_3} := Mpos_n\left(\theta 2_{BM}\right) = 3964.432$

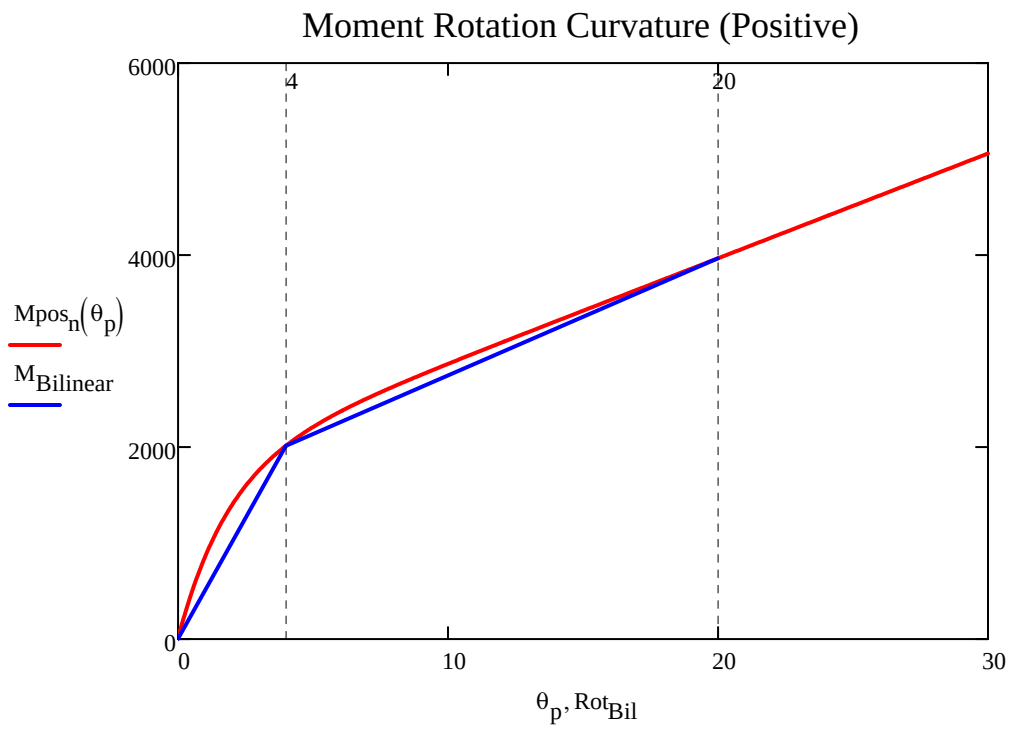
Moment Rotation Curvature (Positive)
6000
4000
2000
0
4
20
0
10
20
30
Mpos_n(θ_p)
M_Bilinear
θ_p, Rot_Bil

W24X94 CONNECTIONS

BEAM SECTION

W, S, M, HP Shapes

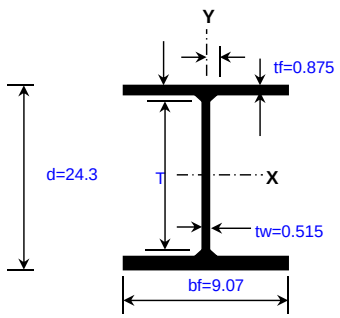

COLUMN SECTION

W, S, M, HP Shapes

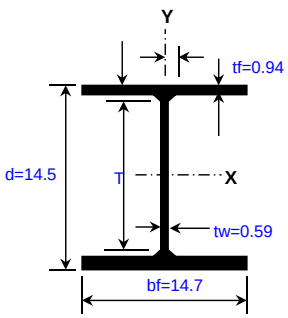

BEAM	W24x94	
A =	27.70	in.^2
d =	24.300	in.
tw =	0.515	in.
bf =	9.070	in.
tf =	0.875	in.
Ix =	2700.00	in.^4
Sx =	222.00	in.^3
Iy =	109.00	in.^4
Sy =	24.00	in.^3
Zx =	254.00	in.^3
Zy =	37.50	in.^3

COLUMN	W14x120	
A =	35.30	in.^2
d =	14.500	in.
tw =	0.590	in.
bf =	14.700	in.
tf =	0.940	in.
Ix =	1380.00	in.^4
Sx =	190.00	in.^3
Iy =	495.00	in.^4
Sy =	67.50	in.^3
Zx =	212.00	in.^3
Zy =	102.00	in.^3

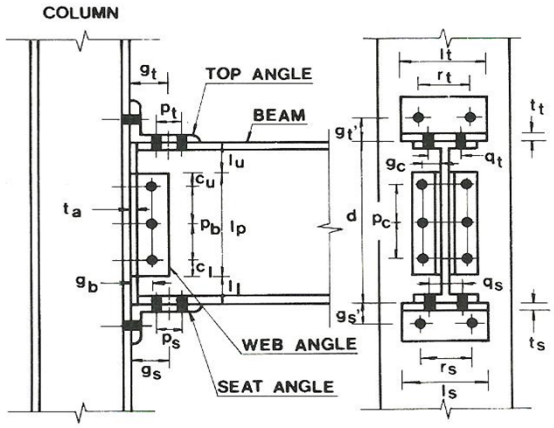

CONNECTION PROPERTIES AND DIMENSIONS

Top Angle	L8x4x7/8		Seat Angle	L8x4x7/8		Double Web angle	L4x4x1/4	
d =	8.000	in	d =	8.000	in	d =	4.000	in.
b=	4.000	in	b=	4.000	in	b=	4.000	in.
k=	1.375	in	k=	1.375	in	k=	0.625	in.
A=	9.790	in^2	A=	9.790	in^2	A=	1.930	in^2
t_t=	7/8	in	t_s=	7/8	in	t_a=	1/4	in.
L_t=	**6.000**			6.000	in	L_p=	5.500	in
r_t=	**3.500**			**3.500**	in	L_u=	1.375	in
g_t=	**3.500**			**3.500**	in	L_l=	1.375	in
p_t=	**2.000**			**2.000**	in	c_u=	1.250	in
g_t'=	**2.500**			**2.500**	in	p_b=	3.000	in
q_t=	**2.750**			**2.750**	in	c_l=	1.250	in
l_t=	0.335			0.335	in^4	g_b=	2.000	in
						p_c=	3.000	in
						g_c=	2.625	in

Bolts	Group A _ N	
Fnt=	90.00	ksi
Fnv=	54.000	ksi
db=	**7/8**	in.
D=	0.875	in.
Ab=	0.60	in.^2
ϕ=	0.750	
B=ϕRnt=	**40.6**	Tension Capacity
ϕRnv=	**24.4**	Shear capacity

MOMENT ROTATION CURVE

1) Initial Stiffness

E= 29000.000 ksi

Top angle:

I_t=	0.335	in^4
g_1=	1.625	in
d_1=	25.175	in
K_t=	3510324.893	k/in

Double web angle:

I_w=	0.007	in^4
g_3=	2.063	in
d_3=	12.588	in
K_t=	22248.415	k/in

Seat Angle

I_s=	0.335	in^4
L_{s0}=	6.625	in
K_t=	5864.976	k/in

K= 3538438.284 k/in

2) Prediction of Mechanism Moment Capacity

Top angle:

σ_y=	36.000	ksi
M_o=	41.344	kip-in
V_o=	94.500	kips
g_2=	0.688	in
V_{pt}=	**54.840**	Kips
equation	-0.431	Must be =0
d_2=	26.113	in
M_{pt}=	18.851	kip-in
M_{ut}=	1450.871	kip-in

Double web angle:

σ_y=	36.000	ksi
M_o=		kip-in
V_o=	4.500	kips/in
V_{pl}=	**2.565**	Kips
y=	0.000	in
g_y=	0.387	in
equation	-0.011	Must be =0
V_{pm}=	**1.111**	Kips
y=Lp/2	2.750	in
g_y=	0.975	in
equation	-0.033	Must be =0
V_{pu}=	**0.692**	Kips
y=Lp	5.500	in
g_y=	1.563	in
equation	-0.038	Must be =0
V_{pw}=	**7.535**	Kips
$\bar{Y}$=	2.123	in
d_4=	3.936	in
M_{uw}=	59.308	kip-in

Seat Angle

σ_y=	36.000	ksi
M_{os}=	41.344	kip-in

2.208333333

Mu= 1551.523 kip-in

LOADS

Mu=	**291.04**	kip-ft
Ru=	**54.00**	kips

Structural Members Materials

Fy=	50	ksi
Fu=	65	ksi

Connecting Materials

Fy=	36	ksi
Fu=	58	ksi

Reduction Factors

Tension

ϕt=	0.9	yielding
ϕt=	0.75	rupture

Shear

ϕv=	0.9	yielding
ϕv=	0.75	rupture

Design Solution Connection for Beam W24x94

1) Check beam design flexural Strength

Zreq=	77.61	in.^3	Ok	pg_9-256 (AISC-LRFD 2nd edition)

F13 (pg16.1-64) Strength Reduction for Members with holes in tension flange

Afg=	7.94	in.^2		Gross area
n=	**2.00**			Assumed number of bolts in "**standard**" holes
Afn=	6.19	in.^2		Net Area
Yt=	1.00			_=1 if Fy/Fu<=0.8; =1.1 otherwise
Ze=	254.00	kip-in	Ok	Effective plastic Section Modulus (Must be bigger than Zreq)

2) Design the double angle web connection

Bolt and Angle available strength: Table 10-1 (pg 10_13 to pg 10-45)

	Group A _ N			Bolt Group
N	3			Number of rows of bolts
	STD			Hole type
t=	1/4	in		Angle Thickness
ϕRn=	**76.40**	kip	Ok	**Value taken from table 10-1, (Must be bigger than Ru)**

Beam web available strength per inch thickness: Table 10-1 (pg 10_13 to pg 10-45)

	STD			Hole type
				Cope type
	Uncoped			
		in		
Leh=	**1 1/2**	in		
Lev=		in		
Zreq=		in.^3		
B. strength=	**263.00**	kip/in		**Value taken from table 10-1**
ϕRn=	135.45	kips	Ok	**(Must be bigger than Ru)**

Double web angle length

N=	3.00		
s between bolts=	**3.00**	in	Spacing between bolts
Leh=	1.50	in	
Total Length=	**9.00**	in	Total Double Web Length

3) Design the tension flange angle and connection

Puf=	143.72	kips	
NboltsT=	**4.00**		Number of bolts required for tension
NboltsV=	**6.00**		Number of bolts required for shear

4)Determine flange angle thickness for flexure

Try angle length=	**9.00**	in	Trying an angle length

b=g't=	**1 1/4**	in		Distance from bolt centerline to centerline of angle length (g't or b) (Table 15-2a pg 15-12)
Trib load=	15.97	kip/in		
2 * Trib Load=	31.94	kip/in		Table 15-2a based upon a symmetrical connection, enter table with twice tributary load
Temp thickness=	**7/8**	in		Taken from table 15-2a pg 15-12. Available tensile strength must be bigger than 2*Trib Load. Note:AISC 13 Edition based on yelding strength and 14th edition based on ultimate strength
Avai tens strength	**32.00**	kip/in	**Ok**	
Selected angle	**L8x4x7/8**			
d=	8.00	in		Angle properties
b=	4.000	in.		Angle properties
t=	0.875	in.		Angle properties
A=	9.79	in^2		

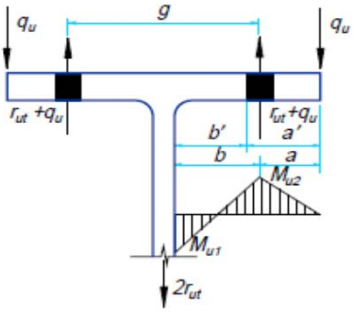

Fig. 11-2. Variables in prying action.

Check angle thickness for prying action assuming a gage

g=	**4.00**	in		Assumed gage
T=rut=	35.93	kips/bolt		Load bolts resist in tension
b=g't=	1 1/4	in		Distance from bolt centerline to centerline of angle length (Table 15-2a)
a=(b-g't)	1.88	in		Distance from bolt centerline to edge of fitting
b'=	0.81	in		Eq 9-21 (pg 9-11 AISC-LRFD 2010)
a'=	2.00	in		Eq 9-27 (pg 9-12 AISC-LRFD 2010)
ρ=	0.41			
B=ϕrn=	40.59	kips/bolt		Available tension per bolt
β=	0.32			Eq 9-25
d'=	0.94	in		Width of bolt hole parallel to the angle leg
s=	**3.00**	bolt spacing		
p=	**3.00**			Tributary length per pair of bolts, p, Figure 9-4 AISC Manual, less than bolt spacing s
δ=	0.69			ratio of the net length at bolt line to gross length at the face of the leg of angle
α'=	0.68			
tmin=	0.71	in	**OK**	Eq 9.23a. If tmin<=t preliminary fitting thickness is satisfactory. Otherwise, a fitting with a thicker flange or a change in geometry (i.e., b and p) is required.

Check tension yielding of the angle

Ag=	7.88	in^2		Angle area (length x t)
ϕRn=	255.15	kips	**OK**	

Check tension rupture of the angle

An=	6.13	in^2		
ϕRn=	266.44	kips	**OK**	

Check shear yielding of the angle

ϕRn=	153.09	kips	**OK**	

Check shear rupture of the angle

An=	6.13	in		Considers two bolts in flange (perpendicular to tension load)
ϕRn=	159.86	kips	**OK**	

Check block shear rupture of the angle

Ubs=	**1.00**			Ubs=1 where tension stress is uniform, otherwise 0.5
t=	7/8	in		
Agv=	**12.25**	in		
Anv=	**7.88**	Number of bolts		
Ant=	**2.63**			
0.6FuAnv=	274.05	kips /in		**Shear Rupture Component** per inch of thickness (Table 9-3c AISC 14th-pg 9-36)
FuAnt=	152.25	kips /in		**Tension Rupture Component** per inch of thickness (Table 9-3a AISC 14th -pg 9-33)
0.6FyAgv=	264.60	kips /in		**Shear Yielding Component** per inch of thickness (Table 9-3b AISC 14th-pg 9-34)
ϕRn=	364.74	kips	**OK**	min(0.6FuAnv+UbsFuAnt, 0.6FyAgv+UbsFuAnt)*t

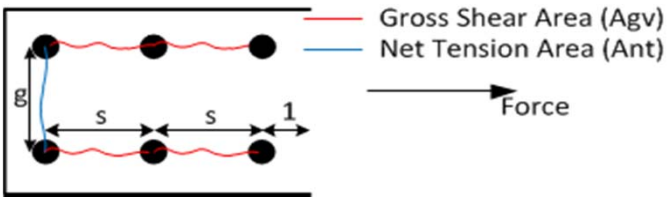

4)Design the compression flange angle and connection

For symmetry the same angle in tension is checked in compression.

Check design compressive strength of angle assuming K=0.65 and l=3in (normal gage)

K=	**0.65**			Unbraced length factor
L = (s)	3.00	in		Length (normal gage) = s
I=	0.50	in^4		Inertia
A=	7.88	in^2		Area
r=	0.25	in		radious of gyration
KL/r=	7.72	in		
ϕcFcr=	**32.20**	ksi		Available critical stress for compression Members (Table 4-22 pg 4-322)
ϕRn=	253.58	kips	**OK**	

Note: Example taken from AISC-LRFD manual 2nd Edition pg 9-258

ORIGIN := 1

PARTIALLY RESTRAINED COMPOSITE CONNECTIONS

W24X94

$$\begin{pmatrix} d \\ t_w \\ b_f \\ t_f \\ t \\ b \\ Z_x \\ A_{ang} \end{pmatrix} :=$$

W, S, M, HP Shapes

Beam

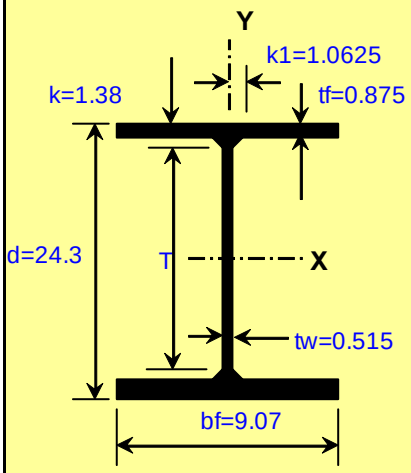

	W24x94	
A =	27.70	in.^2
d =	24.300	in.
tw =	0.515	in.
bf =	9.070	in.
tf =	0.875	in.
T =	20-3/4	in.
k =	1.3800	in.
k1 =	1.0625	in.
gage =	5-1/2	in.
rt =	2.330	in.
d/Af =	3.06	
Ix =	2700.00	in.^4
Sx =	222.00	in.^3
rx =	9.870	in.
Iy =	109.00	in.^4

Single Angles

Seat angle

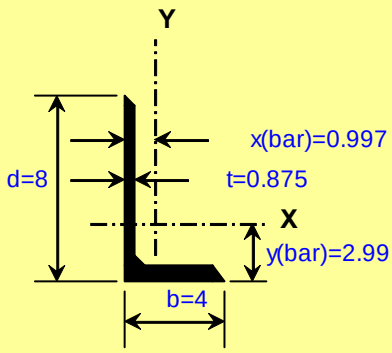

	L8x4x7/8	
d =	8	in.
b =	4	in.
t =	0.875	in.
k =	1.3750	in.
wt./ft. =	33.30	plf.
A =	9.79	in.^2
Ix =	62.60	in.^4
Sx =	12.50	in.^3
rx =	2.530	in.
y(bar) =	2.990	in.
Iy =	10.50	in.^4
Sy =	3.51	in.^3
ry =	1.040	in.
x(bar) =	0.997	in.
rz =	0.846	in.

("W24x94" "L8x4x7/8")

BEAM PLASTIC MOMENT

$Mp := Z_X \cdot 50 = 12700$ **[Kips-in]**

DOUBLE WEB ANGLES:

2xL4x4x1/4 x 9

$L_{web} := 9$ **[in]** Web angle length

$t_{web} := \frac{1}{4} = 0.25$ **[in]** Web angle thickness

$A_{wl} := L_{web} \cdot t_{web} \cdot 2 = 4.5$ **[in^2]** Gross area of double web angles for shear calculations.

$A_{wl} = 4.5$

COMPOSITE INTERACTION PROPERTIES:

$Y_3 := 4$ **[in]** Distance from the top flange of the girder to the centroid of the reinforcement. Total slab thickness = 5.25in (including deck)

$A_s := 1.2$ **[in^2]** Steel reinforcement area. Choose from prequalified connections: Type I,II,III,IV or V. (According to Steel Design Guide 8)

Type I	6 - #4	As=1.2in^2
Type II	8 - #4	As=1.6in^2
Type III	10 - #4	As= 2in^2
Type IV	12 - #4	As=2.4in^2
Type V	10 - #5	As=3.07in^2

$F_{yrb} := 60$ **[ksi]** Yield stress of reinforcing.

CONNECTION PROPERTIES:

BOTTOM ANGLE CONNECTION:

$F_y := 36$ **[ksi]** Yield stress of seat and web angles

$L := 9$ **[in]** Angle Length (6 in long alngle leg can normally accept 4 bolts (2 rows of 2) .

$\gamma := 1.2$ Recommended value: 1.2 - 1.25 **(6.5 Bottom Angle Connection)**

$$A_{Lreq} := \frac{\gamma \cdot A_s \cdot F_{yrb}}{F_y} = 2.4$$ **[in²]** Area of bottom angle

$$t_{req} := \frac{A_{Lreq}}{L} = 0.267$$ **[in]** Required bottom angle thickness

Angle Thickness: $t = 0.875$

Note: Has to be bigger than treq

$$\text{Thick\_angle} := \begin{cases} \text{"OK"} & \text{if } t > t_{req} \\ \text{"NOT OK"} & \text{otherwise} \end{cases}$$

Thick_angle = "OK"

$A_L := t \cdot L = 7.875$ **[in²]** Area of bottom angle

$$\text{Req\_Area} := \begin{cases} \text{"OK"} & \text{if } A_L > A_{Lreq} \\ \text{"NOT OK"} & \text{otherwise} \end{cases}$$

Req_Area = "OK"

M-θ CURVE UNDER NEGATIVE BENDING

$C1 := 0.18\left(4 \cdot A_s \cdot F_{yrb} + 0.857 \cdot A_L \cdot F_y\right) \cdot \left(d + Y_3\right) = 2704.708$

$C2 := 0.775$

$C3 := 0.007 \cdot \left(A_L + A_{wl}\right) \cdot F_y \cdot \left(d + Y_3\right) = 88.254$

$$Mneg_n(\theta) := C1 \cdot \left(1 - e^{-C2 \cdot \theta}\right) + C3 \cdot \theta \qquad \textbf{[kip-in]}$$

LINEARIZED M-θ CURVE UNDER NEGATIVE BENDING

BILINEAR METHOD

$\theta 1_{BM} := 4$

$Mneg_n\left(\theta 1_{BM}\right) = 2935.877$

$\dfrac{Mneg_n\left(\theta 1_{BM}\right)}{12} = 244.656$ **[kip-ft]**

$\theta 2_{BM} := 20$

$Mneg_n\left(\theta 2_{BM}\right) = 4469.778$ **[kip-in]**

$\dfrac{Mneg_n\left(\theta 2_{BM}\right)}{12} = 372.482$ **[kip-ft]**

$Rot_{Bil_1} := 0$

$Rot_{Bil_2} := \theta 1_{BM} = 4$

$Rot_{Bil_3} := \theta 2_{BM} = 20$

$M_{Bilinear_1} := 0$

$M_{Bilinear_2} := Mneg_n\left(\theta 1_{BM}\right) = 2935.877$

$M_{Bilinear_3} := Mneg_n\left(\theta 2_{BM}\right) = 4469.778$

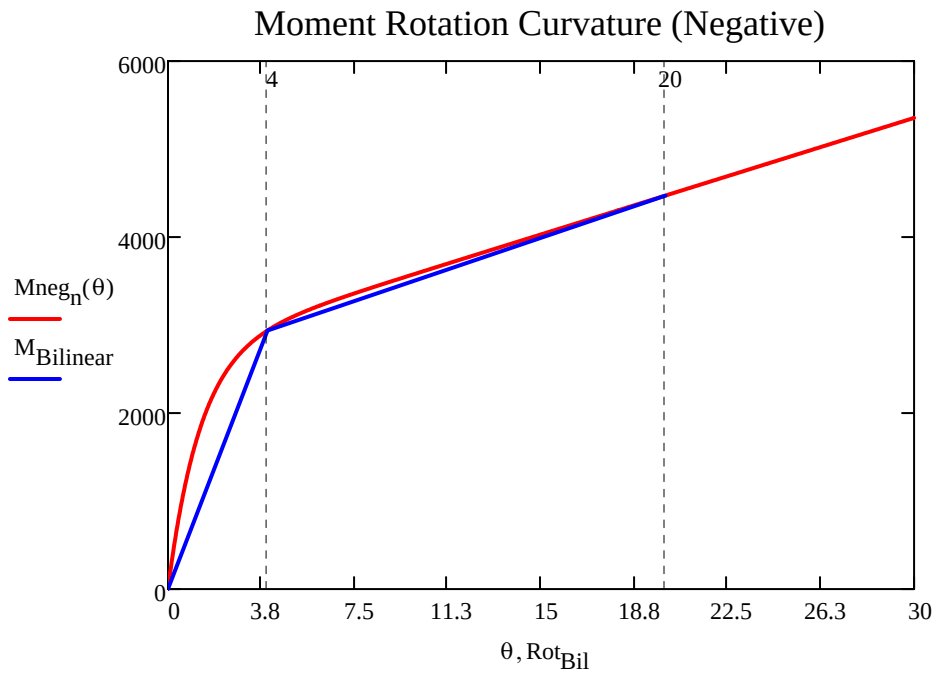
Moment Rotation Curvature (Negative)
6000
4000
2000
0
4
20
Mneg_n(θ)
M_Bilinear
0
3.8
7.5
11.3
15
18.8
22.5
26.3
30
θ, Rot_Bil

M-θ CURVE UNDER POSITIVE BENDING

$$C1 := 0.2400\cdot\left[\left(0.48\cdot A_{wl} + A_L\right)\cdot\left(d + Y_3\right)\cdot F_y\right] = 2453.678$$

$$C2 := 0.021\cdot\left(d + \frac{Y_3}{2}\right) = 0.552$$

$$C3 := 0.0100\cdot\left(A_{wl} + A_L\right)\cdot\left(d + Y_3\right)\cdot F_y = 126.076$$

$$C4 := 0.0065\cdot A_{wl}\cdot\left(d + Y_3\right)\cdot F_y = 29.8$$

$$Mpos_n\left(\theta_p\right) := C1\cdot\left(1 - e^{-C2\cdot\theta_p}\right) + (C3 + C4)\cdot\theta_p \qquad \textbf{[kip-in]}$$

LINEARIZED M-θ CURVE UNDER POSITIVE BENDING

BILINEAR METHOD

$\theta 1_{BM} := 4$

$Mpos_n\left(\theta 1_{BM}\right) = 2807.798$

$Rot_{Bil_1} := 0$

$Rot_{Bil_2} := \theta 1_{BM} = 4$

$Rot_{Bil_3} := \theta 2_{BM} = 20$

$\theta 2_{BM} := 20$

$Mpos_n\left(\theta 2_{BM}\right) = 5571.167$

$M_{Bilinear_1} := 0$

$M_{Bilinear_2} := Mpos_n\left(\theta 1_{BM}\right) = 2807.798$

$M_{Bilinear_3} := Mpos_n\left(\theta 2_{BM}\right) = 5571.167$

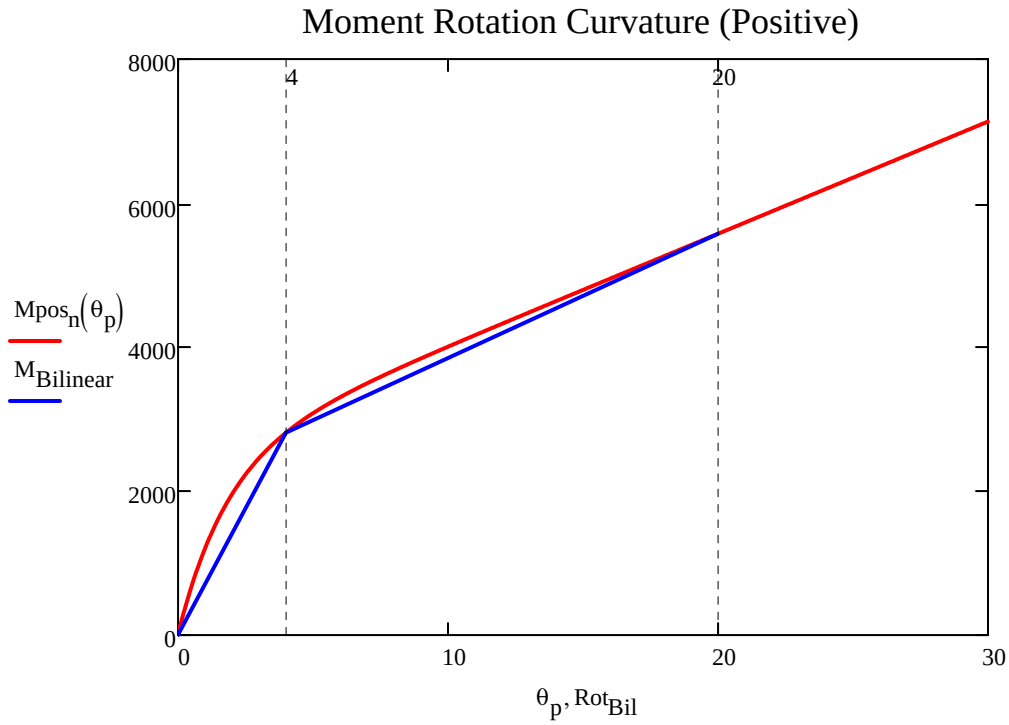
Moment Rotation Curvature (Positive)
8000
6000
4000
2000
0
4
20
0
10
20
30
Mpos_n(θ_p)
M_Bilinear
θ_p, Rot_Bil